UNIVERSITY OF CALIFORNIA,
IRVINE

Synthesis of Cytotoxic Haterumaimide and Lissoclimide Natural Products

DISSERTATION

submitted in partial satisfaction of the requirements
for the degree of

DOCTOR OF PHILOSOPHY

in Chemistry

by

Sharon Elizabeth Marie Michalak

Dissertation Committee:
Professor Christopher D. Vanderwal, Chair
Professor Larry E. Overman
Professor Scott Rychnovsky

2019

Portions of Chapter 2 have been adapted with permission from: Könst, Z. A.; Szklarski, A. R.; Pellegrino, S.; Michalak, S. E.; Meyer, M.; Zanette, C.; Cencic, R.; Nam, S.; Horne, D. A.; Pelletier, J.; Mobley, D.; Yusupov, M.; Vanderwal, C. D. *Nat. Chem.* **2017**, *9*, 1140-1149. © 2017 Springer Nature

Portions of Chapter 4 have been adapted with permission from: Michalak, S. E.; Nam, S.; Kwon, D. M.; Horne, D. A.; Vanderwal, C. D. *J. Am. Chem Soc.* **2019**. DOI: 10.1021/jacs.9b04702. © 2019 American Chemical Society

DEDICATION

For my family

TABLE OF CONTENTS

LIST OF FIGURES

LIST OF TABLES

LIST OF SCHEMES

LIST OF ABBREVIATIONS AND ACCRONYMS

μ	micro
λ	wavelength
π	pi
ν	frequency
°C	degree Celsius
Ac	acetyl
AIBN	azobisisobutyronitrile
Bn	benzyl
bp	boiling point
n-Bu	*n*-butyl
t-Bu	*tert*-butyl
ca.	about (Latin circa)
calcd	calculated
cat.	catalytic
CI	chemical ionization
cm^{-1}	wavenumber
Cy	cyclohexyl
DCE	dichloroethane
DCM	dichloromethane
DDQ	2,3-dichloro-5,6,-dicyano-1,4-benzoquinone
DMAP	4-dimethylaminopyridine
DME	1,2-dimethoxyethane
DMF	dimethylformamide
DMP	Dess-Martin periodinane
DMSO	dimethylsufloxide
DTBP	2,6-di-*tert*-butylpyridine
dr	diastereomeric ratio
EWG	electron-withdrawing group
EI	electron impact
equiv	equivalent
ee	enantiomeric excess
er	enantiomeric ratio
ESI	electrospray ionization
Et	ethyl
EtOAc	ethyl acetate

g	gram(s)
GC	gas chromatography
h	hour(s)
HAT	hydrogen atom transfer
HPLC	high-performance liquid chromatography
HRMS	high-resolution mass spectrometry
Hz	Hertz
IPA	isopropanol
i-Pr	*iso*-propyl
IC_{50}	half maximal inhibitory concentration
imid	imidazole
IR	infrared
J	coupling constant
K	Kelvin (absolute temperature)
kcal	kilocalorie
LDA	lithium diisopropylamide
lit.	literature value
M	molar; molecular ion
m/z	mass to charge ratio
m-CPBA	*meta*-chloroperoxybenzoic acid
Me	methyl
MHz	megahertz
min	minute(s)
mol	mole(s)
mp	melting point
Ms	methanesulfonyl (mesyl)
n	nano
NBS	*N*-bromosuccinimide
NCS	*N*-chlorosuccinimide
NMR	nuclear magnetic resonance
NOE	nuclear Overhauser effect
NOSEY	nuclear Overhauser enhancement spectroscopy
PDC	pyridinium dichromate
Ph	phenyl
PhMe	toluene
ppm	parts per million
Pr	propyl

pyr	pyridine
quant.	quantitative
rt	room temperature
SAR	structure–activity relationships
SI	selectivity index
TBAF	tetrbutylammonium fluoride
TBS	*tert*-butyldimethysilyl
TCA	trichloroacetic acid
TCCA	trichloroacetic anhydride
Tf	trifluoromethanesulfonyl
TFA	trfluoroacetoxy
THF	tetrhydrofuran
TLC	thin-layer chromatography
TMS	trimethylsilyl
TOF	time-of-flight
Ts	*p*-toluenesulfonyl (tosyl)
UV	ultraviolet

ACKNOWLEDGMENTS

I would first like to thank my supervisor Chris Vanderwal who has made my time in graduate school one of the most fun and educational experiences of my life. The education I received from him through classes, as a co-instructor for the synthesis course and as a research advisor, has been invaluable. His mentorship was critical to my growth as a scientist. He gave me complete independence on my research but was always there, with his door open, when I needed guidance, reassurance and the occasional pep talk. Chris inspires an excitement and curiosity for organic synthesis that I will carry with me throughout my career. Thank you for everything.

I would also like to thank Larry Overman, whom I have the greatest admiration for. Larry has been a mentor to me throughout my years in graduate school, from teaching heterocycles class to giving job interview advice. I always enjoyed our discussions, whether on chemistry, career paths or golf. It was an honor to work two doors down from such a distinguished professor, and I aspire to reach his level of modesty and selflessness in my future.

I need thank Liz Jarvo for always being there when I needed advice on chemistry problems, obtaining American visas, or the dorm quality at a Gordon conference. She has been someone I've connected with since my visitation weekend to UCI and I was extremely grateful to have her as a committee member throughout grad school. Additionally, I would like to thank Scott Rychnovsky, for so willingly subbing onto my dissertation committee last minute. His friendly smile in the hallways and our casual conversations always brighten my day.

Graduate school wouldn't have been such an enjoyable experience if it wasn't for the members of the Vanderwal lab, where I have made lasting friendships. Bryan Ellis has been a true friend throughout these five years. Without him, I wouldn't have kept my sanity during second year advancement, nor would I have had as much wine at the Lee dinners. The thoughtful manner in which he conducts research is something I've strived to emulate throughout our years together. I am forever grateful for Zef Könst's mentorship in my earlier years, his enthusiasm for science was contagious and working with him on the lissoclimide project was one of the most fun times in graduate school. Former group members, Alex Karns, Brian Atwood and Alex White were the hardest working guys I've ever met. Their work hard, play hard mentally cultured an extremely productive lab environment and the countless laughs we had made even the toughest days a fun time at work, I will be forever grateful for their friendship. I also need to thank my current bay members Ryan Kozlowski, Riley Mills and Sierra Nguyen, they've put up with my bay tyranny over the past two years and have always come into work with a genuine excitement for chemistry, which has uplifted my spirits throughout the past few months. And to the rest of the Vanderwal lab members, it's been a pleasure working with such brilliant chemists, thank you for making graduate school a fun and supportive environment over the years.

I am thankful for all the friendships I've made within my peers and cohort in graduate school, but I specifically need to thank Erika Lucas who has turned out to be one of my dearest friends. Her

unbreakable positive attitude, coupled with her selflessness and passion for organic chemistry inspires me, and I am a better person for having known her.

To Rylan Kautz, thank you for being my best bud, I could never imagine doing this all over again without you. He has been my biggest inspiration, even in the hardest times of grad school he's encouraged me to get back on my feet and keep persevering. His companionship has been critical for my happiness and success over these past five years.

I must end by thanking my family for their unwavering support and understanding. Despite being 3000 miles away my mom was always there for me when I needed her, whether it was hour long phone chats or trips to Palm Springs, she has been my rock and I wouldn't have made it through the tough times without her. My dad has instilled in me a love for knowledge and a drive for success, and I can only hope to one day be as smart as he is. My parents have always encouraged me to set high goals and strive to be the best version of myself, and without their confidence in me, I would not be in the position I am today.

CURRICULUM VITAE

Sharon E. Michalak

Education

University of California, Irvine , Irvine, California, USA
Doctor of Philosophy, Chemistry (Organic), Thesis Defense Date : June 20th, 2019
Courses: Organic Spectroscopy, Organic Reaction Mechanisms I and II, Biomacromolecules, Medicinal Chemistry, Organometallics, Organic Synthesis, Heterocycles
GPA: 3.982

Western University, London, Ontario, Canada
Bachelor of Science with Honours Specialization in Chemistry, May 2014
Overall Grade Average: 91%

Research Experience

University of California, Irvine 07/2014 – 06/2019
Summer research student and graduate student in the lab of Professor Christopher D. Vanderwal:
- complex scaffold formation through the use of dearomatizing Himbert cycloaddition reactions.
- total synthesis of biologically active terpenoid natural products.
- biological investigations into the origin of cytotoxicity of the lissoclimide family of natural products.

Western University 01/2013 – 06/2014
Research assistant and honours thesis student in the lab of Professor Michael A. Kerr:
- Synthesis of donor-acceptor cyclopropanes for cyclization to highly functionalized pyrroles.
- Studies towards the total synthesis of the indole alkaloid fargesine with method development to 3,4-fused indole scaffolds.

Publications

1) A Chlorine-Controlled Terminal-Epoxide-Initiated Bicyclization Cascade Enables a Synthesis of the Potent Cytotoxins Haterumaimides J and K. Michalak, S. E.; Nam, S.; Kwon, D. M.; Horne, D. A.; Vanderwal, C. D. *J. Am. Chem Soc.* **2019**, *141*, 9202–9206.

2) Synthesis Facilitates an Understanding of the Structural Basis for Translation Inhibition by the Lissoclimides. Könst, Z. A.; Szklarski, A. R.; Pellegrino, S.; Michalak, S. E.; Meyer, M.; Zanette, C.; Cencic, R.; Nam, S.; Horne, D. A.; Pelletier, J.; Mobley, D.; Yusupov, M.; Vanderwal, C. D. *Nat. Chem.* **2017**, *9*, 1140-1149.

3) Site-Selective Aliphatic C–H Chlorination Using *N*-Chloroamides Enables a Synthesis of Chlorolissoclimide. Quinn, R. K.; Könst, Z. A.; Michalak, S. E.; Schmidt, Y.; Szklarski, A. R.; Flores, A. R.; Nam, S.; Horne, D. A.; Vanderwal, C. D.; Alexanian, E. J. *J. Am. Chem. Soc.* **2016**, *138*, 696-702.

Presentations

Variations in the Syntheses of Haterumaimide and Lissoclimide Natural Products. *Gordon Research Seminar – Natural Products and Bioactive Compounds.* Proctor Academy, Andover, NH, 2018. *Oral Presentation.*

A Chlorine-Controlled Terminal-Epoxide-Initiated Bicyclization Cascade Enables a Synthesis of the Potent Cytotoxins Haterumaimides J and K. Gordon Research Conference – Natural Products and Bioactive Compounds. Proctor Academy, Andover, NH, 2018. Poster Presentation.

Synthesis and Biological Investigations of the Lissoclimide Family of Natural Products. *National Organic Chemistry Symposium.* UC Davis, CA, 2017. *Poster Presentation*

Synthesis of Lissoclimide Natural Products and Analogues with Studies on the Structural Basis for Translation Inhibition. *Moving Molecules from the Academic Lab to the Clinic Symposium.* UC Irvine, CA, 2017. *Poster Presentation.*

Synthesis and Biological Evaluation of Lissoclimide Natural Products. *Graduate and Post-Doctoral Research Colloquium.* UC Irvine, CA, 2016. *Oral Presentation.*

Progress Towards the Total Synthesis of Fargesine. *Southern Ontario Undergraduate Student Conference.* University of Windsor, ON, 2014. *Oral Presentation.*

Teaching Experience

2017–present: Mentoring two undergraduate student researchers on their own independent synthesis projects.
2017: Lecture teaching assistant for a graduate student level organic synthesis class.
2015–present: Lecture teaching assistant for general chemistry and advanced organic chemistry classes.
2015: Assistant lecturer for an organic chemistry 'flip-class'.
2014–2015: In lab teaching assistant for lower and upper division organic chemistry labs.

Awards and Honours

2018: Allergan Graduate Fellowship in Synthetic Organic Chemistry.
2018: Game MVP, Industry vs. Academics softball game, Natural Products Gordon Research Conference (Industry Team).

2016: Honourable Mention, National Sciences and Engineering Research Council of Canada PGS-D Fellowship.
2014: 1st Prize Oral Presentation in Organic Chemistry, Southern Ontario Undergraduate Student Chemistry Conference.
2013: Scholarship of Excellence, Western University.
2011–2014: Academic All-Canadian, Western University.
2011–2014: Dean's Honour List, Western University.

Co-Curricular Activities

2012–2014: Varsity Track and Field Women's Team Captain, Western University.
2014–present: Member of Iota Sigma Pi, a society based around volunteering, outreach and promoting women in chemistry, UC Irvine.
2015–present: Member of the Chemistry Outreach Committee, involved with organizing and conducting fun chemistry demonstrations at both elementary and high schools, UC Irvine.
2017–present: Volunteer Surf Instructor, City of Newport Beach Surfing Lessons.

ABSTRACT OF THE DISSERTATION

Synthesis of Cytotoxic Haterumaimide and Lissoclimide Natural Products

By

Sharon Elizabeth Marie Michalak

Doctor of Philosophy in Chemistry

University of California, Irvine, 2019

Professor Christopher D. Vanderwal, Chair

This dissertation describes synthetic strategies for the synthesis of lissoclimide and haterumaimide natural products. The development of both semi-synthesis and total synthesis routes will be highlighted. Chapter 1 provides a background on this family of cytotoxic diterpenoids including isolation, biological activity and general structure-activity-relationships. Previous efforts towards these products from the Vanderwal lab and other groups are described.

Chapter 2 focuses on the semi-synthesis of haterumaimide Q and chlorolissoclimide starting from commercially available sclareolide. An efficient and general strategy to for the elaboration of sclareolide to the lissoclimide scaffold was developed to access haterumaimide Q in high yields and was further implemented in synthesis of the potent chlorinated family member, chlorolissoclimide. These syntheses enabled investigations into the biological mode of action to gain further understanding into the key interactions that underly chlorolissoclimide's high potency. Through analysis of the structural biology and computationally generated binding poses, the hydroxyimide group was identified as the key

pharmacophore and the synthesis of hydroxyimide stereoisomers was pursued with the goal of generating potent analogues.

Chapter 3 describes our initial efforts towards the most potent members of the family, haterumaimide J and K. We envisioned accessing the pendent A-ring oxygenation of these products through a titanocene-mediated, radical bicyclization initiating on a 2,2-disubstituted epoxide. A model system synthesized from geranyl acetate was used to investigate this transformation.

Chapter 4 focuses on the development of a stereocontrolled, Lewis acid-mediated bicyclization of a 2,2-disubstutited epoxide to construct the core of haterumaimides J and K. A key finding was that the chlorine stereocenter could control the diastereoselectivity of this bicyclization regardless of the relative configuration of the epoxide. The completion of synthesis was achieved after optimization of a challenging Evans-auxiliary controlled aldol reaction to install the C12/C13 vicinal stereocenters and complete the formation of the succinimide motif.

Chapter 5 highlights the application of this chlorine-controlled, 2,2-disubstituted epoxide-initiated bicyclizations to access the C19-oxygenated scaffold of complex *ent*-kaurene natural products. Our efforts to develop rapid synthesis of enantioenriched 2,2-disubstituted epoxides for chiral -Lewis acid mediated cyclizations are described.

CHAPTER 1 : Introduction to the Haterumaimide and Lissoclimide Family of Labdane Diterpenoids

1.1 Introduction

The haterumaimide and lissoclimide family are marine derived labdane diterpenoids isolated from ascidians of the species *Lissoclinum voeltzkowi.* The first member, dichlorolissoclimide (DCL, **1.1**, Figure 1.1) was isolated in 1991 by Malochet-Grivois and co-workers off the coast of New Caledonia[1] and the isolation of a mono-chlorinated family member, chlorolissoclimide (CL, **1.3**, **Figure 1.1**) followed seven years later.[2] The structures were assigned through extensive NMR analysis and the absolute stereochemistry of DCL was confirmed through X-ray crystallography.[3] Since this initial work, the groups of Uemura and Schmitz have isolated 20 similar diterpenoids from ascidians and the mollusc *Pleurobranchus forskalii* that preys upon them, near Hateruma, Japan and named them haterumaimides.[4-7] Upon isolation, Uemura and coworkers tested 17 family members for anti-cancer activity against the P388 murine leukemia cancer cell line and many showed potent cytotoxic activity. With additional bioactivity data of synthetic analogues derived from **1.3**, preliminary structure activity relationships (SAR) were revealed.[7]

The haterumaimides contain several structurally unique functional groups and the data gathered from the P388 IC_{50} values have provided insight on the substituents that are important for biological activity. The pendent hydroxysuccinimide motif was found to be critical for activity as *N*-methylation (**1.6**) or C12-*O*-acetylation (**1.7**) resulted in significantly reduced potency; this data provides further understanding into the conserved nature of this group throughout all family members. Conversely, the

chlorination pattern varies; the haterumaimides can contain either mono, di or no chlorination on the A-ring. A C2-chlorine atom appears to be significant for cytotoxicity (**1.3** vs **1.4**) whereas the importance of a C3-chlorine is unclear (**1.1** vs **1.12**). Oxygenation has varying effects; a hydroxyl group at C7 or C6 is common among many of the sub-micromolar potent members (**1.**1, **1.3**, **1.8, 1.9**) but a ketone at C6 (**1.10, 1.11**) results in a complete loss of activity. Interestingly, the most potent members of the family, haterumaimide J (hatJ, **1.12**) and haterumaimide K (hatK, **1.13**) contain no B-ring oxygenation but are the only products with a C18-hydroxyl group (**Figure 1.1**).[7]

Several of the inititially isolated lissoclimidies—DCL (**1.1**), CL (**1.2**) and 3-β-hydroxychlorolissoclimide (**1.5**)—have also been tested on various other cancer cell lines. Screening against the NCI panel of 60 tumor cell lines revealed cytotoxic effects from DCL and CL, whereas **1.5** was fairly inactive; however it was the only lissoclimide to exhibit selectivity for solid tumors.[8] Additionally,

Figure 1.1 Representative members of the haterumaimide family of natural products

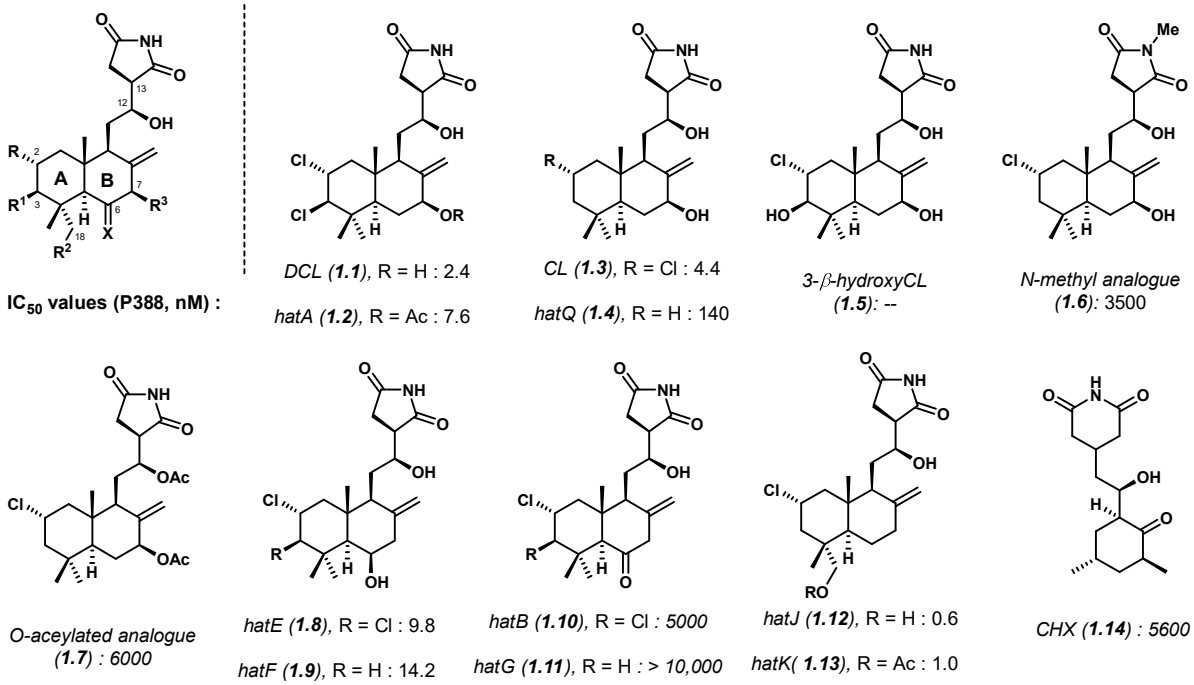

both CL and DCL were tested for *in vitro* effects on non-small-cell bronchopulmonary carcinoma cell line and resulted in complete cell death.[2]

Through biochemical experiments, Pelletier and coworkers established the haterumaimide's biological mode of action. In this study they screened extracts from the *Lissoclinum sp.* ascidians and the mollucs that prey upon them for protein synthesis inhibitory activity. Ascidians are shell-less sea squirts that have no physical means of self-defense, instead they use chemical defenses to ward off predators.[8] Consequently, they have become a valuable source of biologically active secondary metabolites. Pelletier and coworkers determined that DCL and CL target the eukaryotic ribosome, inhibiting the movement of the ribosome on the mRNA strand during the translation elongation process in protein synthesis. [9] This inhibition results in a buildup of ribosomes on the mRNA strand and eventual cell death. This irreversible effect was observed *in vitro* and *in vivo* for CL and DCL (IC_{50} = 0.7 μM and 1.25 μM, respectively). Additionally, Pelletier noted the structural similarities of the lissoclimides to the known translation inhibitor, cycloheximide (CHX, **1.14, Figure 1.1**) which is known to specifically target the E-site of the ribosome, possibly indicating a similar mechanism of action for the lissoclimides.

These studies on the biological activity of the haterumaimides and lissoclimides have only provided a preliminary understanding of their anti-cancer abilities. Moreover, there are several family members that have not yet been tested and a surprising lack of data remains for the most potent members, hatJ (**1.12**) and hatK (**1.13**). Isolation from the natural source is a tedious process and has only provided single-digit milligram quantities of these products. Efficient syntheses of the natural products would permit a more thorough evaluation of their antiproliferative effects and would enable identification of critical functionality required for high potency. Additionally, their challenging structural features such as

the varying chlorination/oxygenation patterns, as well as the pendent chiral imide, present an opportunity to develop new strategies for their chemical synthesis.

1.2 Previous Semi-Synthetic Approaches

This family of labdane diterpenoids showcases both interesting biological activities as well as unique structural motifs; therefore, it is not surprising that several synthetic groups have embarked on efforts towards the haterumaimides. The succinimide side chain attached to the B-ring of the decalin core through a C12-hydroxyl group linker is one of the more challenging functional groups of these molecules, containing two contiguous stereocenters and four heteroatoms. The Gonzaléz group set out to install the imide motif directly through a succinimide aldol addition on aldehyde **1.16**.[10] Commercially available *(+)*-sclareolide (**1.15**) was identified as a suitable starting material as the B-ring lactone could be elaborated in 3 steps to prepare **1.16**, which contains the decalin framework found in the haterumaimides. The aldol reaction between the succinimide dianion and **1.16** was successful in forging the critical C12–C13 bond, albiet in very poor diastereoselectivity (**Scheme 1.1**). The imide mixture of 4 stereoisomers (**1.17**, d.r. : 4.0 : 3.5 : 1.5 :1), likely favoring the anti-products owing to an E-enolate in a Zimmerman-Traxler addition, were inseparable by silica gel chromatography. While this approach accomplishes imide installation in a single step, it suffers from a lack of stereocontrol.

Scheme 1.1 González efforts towards a succinimide aldol

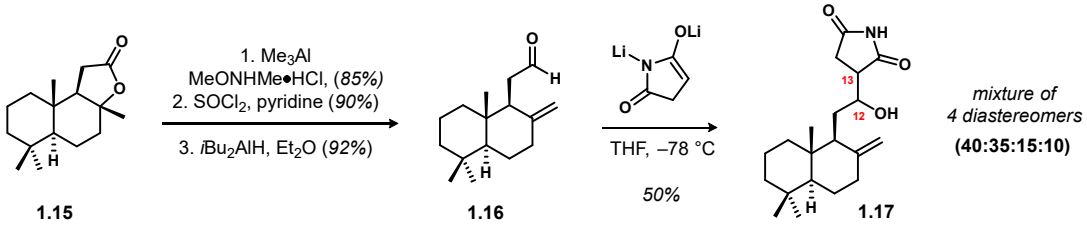

Scheme 1.2 Stereoselective construct of the C12-C13 hydroxyimide bond

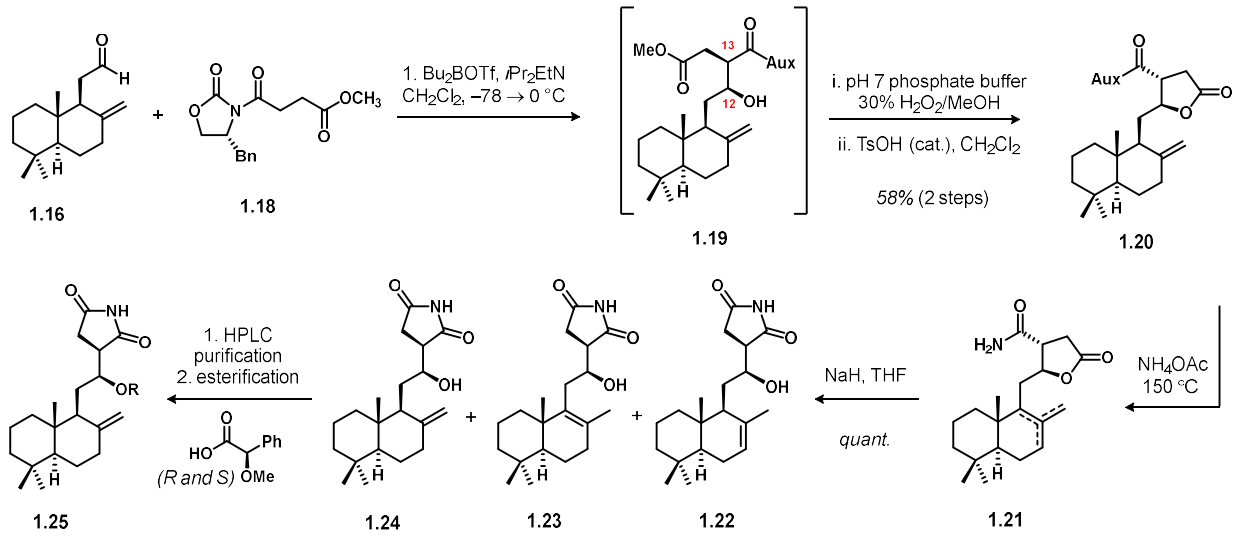

A year later Chai and coworkers reported a related strategy to access the hydroxysuccinimide using auxiliary control to set the C12-C13 stereocenters.[11] An Evans aldol addition between acylated oxazolidinone **1.18** and aldehyde **1.16** proceeded in high selectivity to yield aldol adduct **1.19** (**Scheme 1.2**). In order to cleave the oxygen-boron bond of the crude aldol adduct the reaction mixture was treated with hydrogen peroxide, but this resulted in partial formation of lactone **1.20**. In hopes of utilizing this undesired reactivity, *p*-TsOH was added to completely convert the aldol product mixture to **1.20**, which was isolated as a single diastereomer. Next, it was envisioned that a primary amide—formed by transamination of the auxiliary bond in **1.20**—could then undergo base-mediated imidation to install the hydroxysuccinimde motif. Unfortunately, cleavage of the oxazolidinone auxiliary proved challenging and was only achieved by heating **1.20** under microwave irradiation with NH_4OAc which resulted in migration of the exo-cyclic alkene into the ring. The inseparable mixture of alkene isomers (**1.21**) were then treated with NaH to effect succinimide formation. The imide products were formed in a 5.3 : 4.7 mixture of desired product to endo-alkene isomers (**1.24 : 1.22, 1.23**) and were only separable after iterative, preparatory HPLC purifications. The C12-hydroxyl group was acylated with both (*R*) and (*S*)-*O*-methyl

mandelic acid and NMR analysis of the resulting esters (**1.25**) confirmed the relative and absolute stereochemistry of the newly formed chiral centers. This work was not further pursued for the synthesis of a haterumaimide product. While this protocol was plagued with undesired reactivity, it showcased the power of auxiliary control to forge the challenging C12, C13 stereocenters with high selectivity; we adopted and optimized this strategy for our semi-synthesis which will be described in Chapter 2.

The reports from the Chai and Gonzaléz groups have provided useful insight to a semi-synthetic approach towards the haterumaimides. Even though they were never able make a natural product, their work addressed the challenges associated with installing the pendant succinimide motif. We eventually employed a similar strategy starting from *(+)*-sclareolide (**1.15**) to make hatQ (**1.4**) and CL (**1.3**, **Chapter 2**), but the lack of functionality in **1.15** limited its usefulness as a starting material for accessing A-ring dichlorinated and oxygenated family members. Therefore, the Vanderwal group initially set out to design a fully synthetic route which could allow for late stage diversification to access many naturally occurring haterumaimides and analogues.

1.3 Previous Fully Synthetic Approaches

Nature constructs the decalin core found in labdane diterpenoids through a polyene cyclization of linear polyprenyl precursors.[12] In a single step, this bicyclization cascade forms two new carbon-carbon bonds, in turn setting several stereocenters. The Vanderwal group has taken inspiration from natures ability to efficiently construct these scaffolds, as polyene cyclizations are a central theme of our fully synthetic approaches towards the haterumaimides.

1.3.1 A late stage succinimide coupling to furan-decalin core

The initial synthetic work on the haterumaimide project in our lab was done by former member, Anne Szklarski who targeted the core of DCL (**1.1**) through polyene bicyclizations.[13] To this end, a furan-terminated cationic cyclization was envisioned to construct decalin **1.27** from epoxide **1.26**. Taking a different approach from the Chai and Gonzalez groups, the imide installation was planned to occur through a coupling of **1.27** and a suitable maleimide partner (**1.28**). Subsequent oxidative furan opening of **1.29**, followed by selective alkene reduction could access dione **1.30**, an ideal candidate for a dynamic kinetic reduction to set the C12/C13 stereocenters. Functional group manipulations on the A and B rings as depicted in **1.31**, could then install the requisite chlorination and oxygenation patterns for DCL (**Scheme 1.3**).

Scheme 1.3 General strategy for a furan-fused decalin scaffold

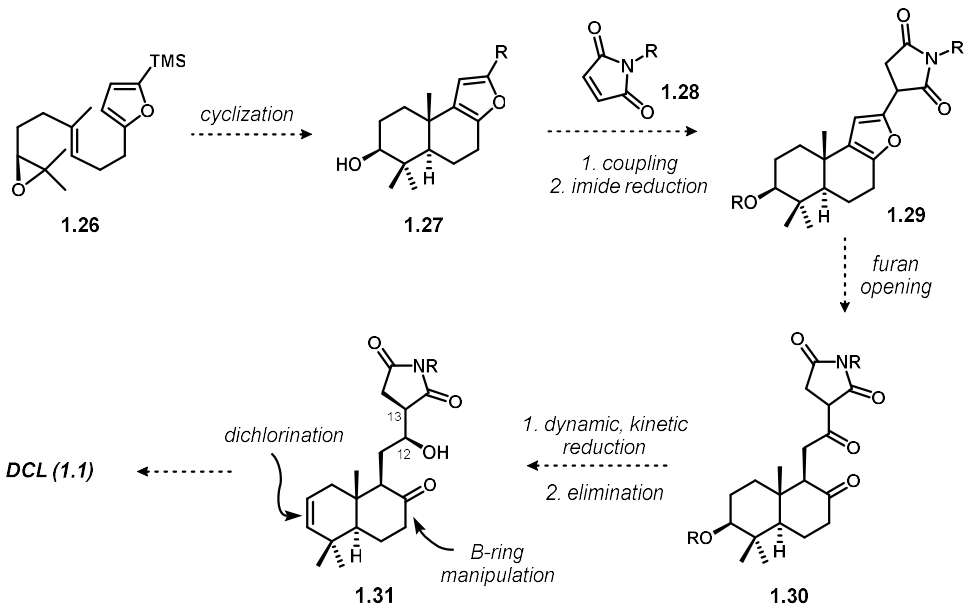

The synthesis of cyclization precursor **1.26**, involved a copper-mediated coupling between epoxygeranyl acetate **1.32** and **1.33**. The bicyclization of **1.26** was accomplished with iron trichloride and proceeded with concomitant protodesilylation to give **1.34** (**Scheme 1.4**). A variety of conditions to

Scheme 1.4 Efforts towards installing the hydroxysuccinimide motif

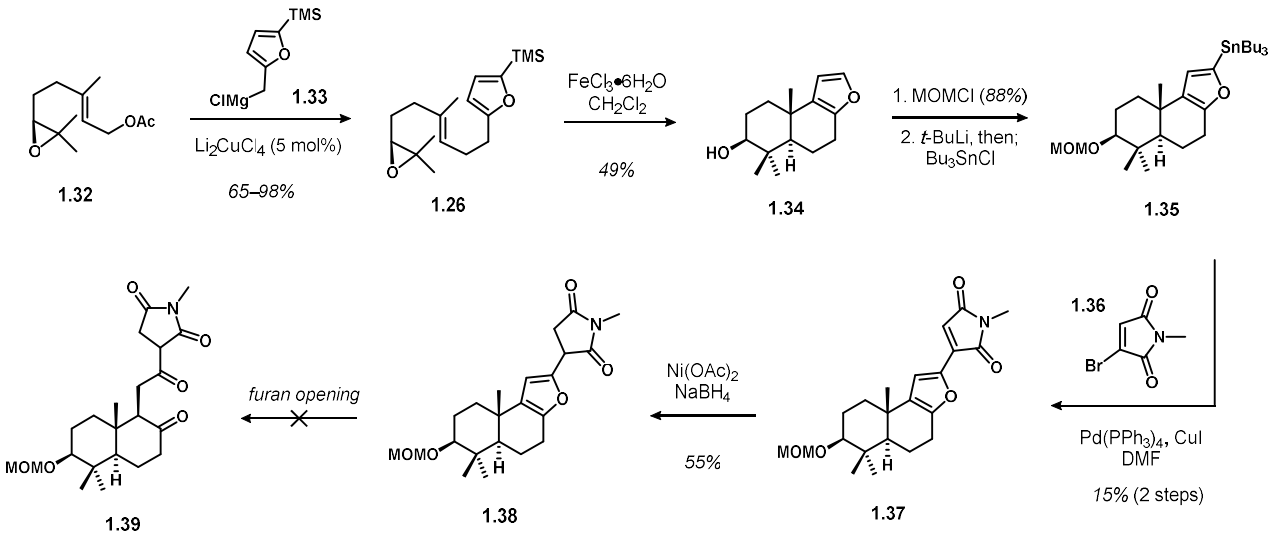

effect a conjugate addition of **1.34** to maleimide electrophiles were investigated and met with little success. An adequate solution involved conversion of **1.34** to stannane **1.35,** followed by a coupling with bromomaleimide (**1.36**) under Stille conditions to yield **1.37** in 15%. Despite the modest efficiency of this coupling, it presented a direct strategy for the installation of the succinimide group. Reduction of the maleimide was also a non-trivial task, but **1.38** was accessed in sufficient quantities to probe the furan ring opening step. Unfortunately, treatment of **1.38** with protic acids or oxidants only resulted in returned starting material or decomposition products.

The difficulty of material throughput was a main drawback of this strategy, but it demonstrated that an epoxide-initiated, furan-terminated cyclization is a viable entry to the desired decalin scaffold; this type of transformation was further pursued in a subsequent route (see section **1.3.2**). While the furan proved challenging to functionalize, it provides a critical handle for B-ring manipulation. A reverse order sequence, wherein oxidative furan ring opening unveils a 1,4-dicarbonyl motif—later utilized for imide installation—has been a successful protocol in our synthesis of hatJ and hatK (**Chapter 4**).

1.3.2 Diversifiable Intermediates for Natural Product and Analogue Production

An important aspect of the strategy described above was the opportunity for differential functionalization of the A and B rings post cyclization. The C3-hydroxyl group could be eliminated to provide an A-ring alkene for chlorination and as previously noted, the furan presents an opportunity for oxidative manipulation to the B-ring. The remarkable change in bioactivity based on the chlorination or oxygenation patterns on the decalin scaffold of these natural products can be seen from **Figure 1.1**. Specifically, dichlorination or pendant C18-oxygenation of the A-ring is featured in two of the most potent members of the family, DCL (**1.1**) and hatJ (**1.12**), respectively. These natural products would require different manipulations of the A and B-rings to install the corresponding chlorination or oxygenation, but they both possess the same decalin framework along with the conserved hydroxysuccinimide group. It was envisioned that construction of late stage intermediates **1.40** and **1.41** (**Figure 1.2**), containing an A-ring alkene and B-ring ketone, would allow for straightforward, differential functionalization of the decalin core for the synthesis of naturally occurring haterumaimides and analogues. The pendant acetal, masking an aldehyde, would be a key functional handle for installing the succinimide in a similar fashion to Chai[11] and Gonzaléz.[10]

Figure 1.2 Diversifiable intermediates

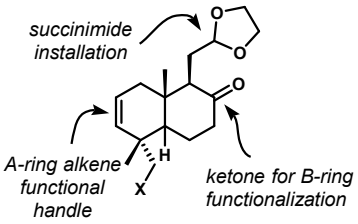

X = H : **1.40**

X = OH : **1.41**

Szklarski pursued the synthesis of **1.40** and aimed to use the A-ring alkene to address the challenging installation of diequatorial dichlorides.[13] The synthesis of **1.40** features an elegant polyene bicyclization developed by Corey and co-workers in their synthesis of scalarenedial[14] and α-onocerin.[15] Known acylsilane **1.42**[16] and lithiated sulfone **1.43** participated in a carbonyl addition followed by a Brook

Scheme 1.5 Enoxysilane-terminated cyclization for construction of the decalin core

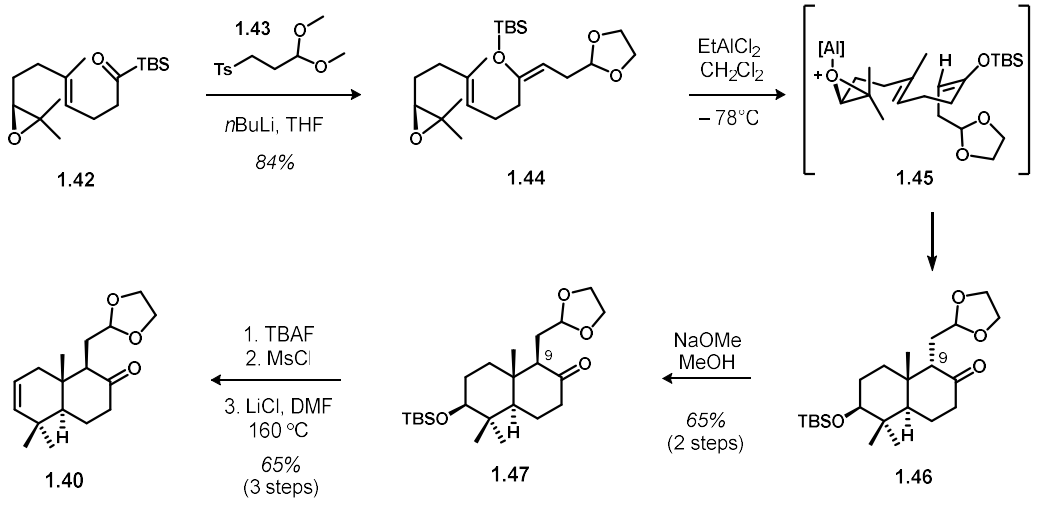

rearrangement/tolylsulfinate elimination. The resulting enoxysilane was formed with the appropriate regiochemistry to participate as the terminating group in a polyene cyclization. Treatment of **1.44** with $EtAlCl_2$ effected the bicyclization to trans decalin **1.46** via conformation **1.45**. Decalin **1.46** was formed with the undesired stereochemistry at C9 owing to the Z-enoxysilane geometry, but was corrected upon epimerization to yield **1.47** in 65% yield over two steps. The A-ring alkene of **1.40** was then installed in three steps; with this key intermediate in hand, Szklarski set out to install the two equatorial chlorides (**Scheme 1.6**). The use of Mioskowski's reagent (tetraethylammonium trichloride),[17] a bench alternative to Cl_2, exclusively afforded diaxialdichloride **1.48**. This result was not surprising as dichlorination of alkenes is known to proceed through a chloronium intermediate which is opened by a chloride anion

Scheme 1.6 A-ring alkene chlorination attempts

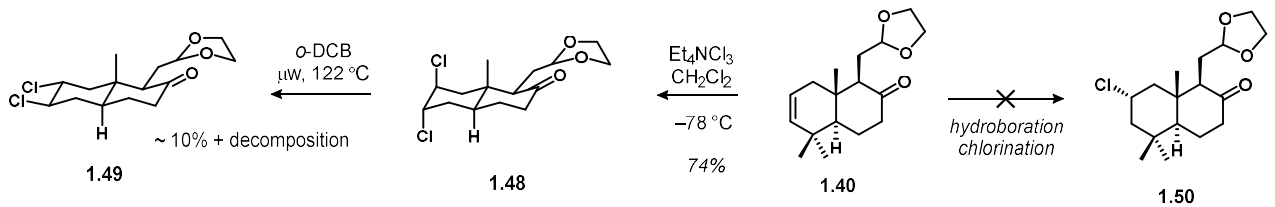

following the Fürst–Plattner model of addition. The Jung group reported that thermal isomerization of diaxial-1,2-dichlorides on a decalin system afforded the diequatorial dichlorides, but required high temperatures.[18] Following this protocol, **1.48** was isomerized under microwave irradiation to yield small amounts of **1.49** along with significant amounts of decomposition products. Szklarski then investigated the use of Lewis acid additives to permit the isomerization at lower temperatures, but these experiments only lead to ketal decomposition of **1.48.**[13] With the other option to hydrochlorinate alkene **1.40** for the synthesis of chlorolissoclimide (**1.3**), a hydroboration followed by a deborylative-chlorination reaction was attempted to make **1.50**, but this was also met with failure (**Scheme 1.6**). We later pursued a similar strategy using metal-mediated hydrochlorination procedures in our initial efforts towards hatJ (**1.12**), discussed in Chapter 3.

It was evident that chlorination of the A-ring alkene in **1.40** was not a viable way forward for the synthesis of chlorinated haterumaimides, but it still provided the necessary scaffold to synthesize non-chlorinated family members and analogues. Former lab member Zef Könst validated this route in the first synthesis of haterumaimide Q (**1.4, Scheme 1.7a**).[19] To this end, the A-ring alkene was hydrogenated, and the B-ring enolate was trapped as a vinyl triflate which then participated in a Kumada-Corriu coupling to give **1.51**.[20] This simple three step procedure differentiates the A and B rings, such that either could be selectivity functionalized. Additionally, the allysilane in **1.51** was designed to permit a variety of substitutions at the C7-position through electrophilic SE' reactions[21] while simultaneously installing the required exocyclic alkene. The aforementioned reaction, with several oxygen transfer reagents, exclusively gave the undesired configuration of the C7-alcohol. Instead, **1.51** was brominated to incorporate a good leaving group for a late stage displacement, and aldehyde **1.52** was obtained after ketal cleavage (**Scheme**

1.7a). Similar to previous reports,[10, 11] the pendent aldehyde was utilized to install the succinimide group through an aldol addition. The invaluable precedent from Chai on an Evans auxiliary controlled protocol[11] allowed Könst to optimize this chemistry and design a three-step sequence to selectively install the hydroxysuccinimide and access **1.53**. Much of the experimentation on this sequence was performed on sclareolide-derived aldehyde **1.16**. The success of the procedure relied on careful isolation of boron-aldol adduct **1.54**. The reaction was quenched at cold temperatures, and the work up was performed using pH 7 buffered solution, all to avoid the irreversible lactonization that thwarted the efforts of Chai and coworkers (see section **1.2**). We believe the C12-alcohol-boron bond is still intact in aldol adduct **1.54** owing to the neutral workup conditions. The crude aldol product **1.54** was immediately taken up in

Scheme 1.5 Synthesis of hatQ with optimization of the succinimide installation sequence

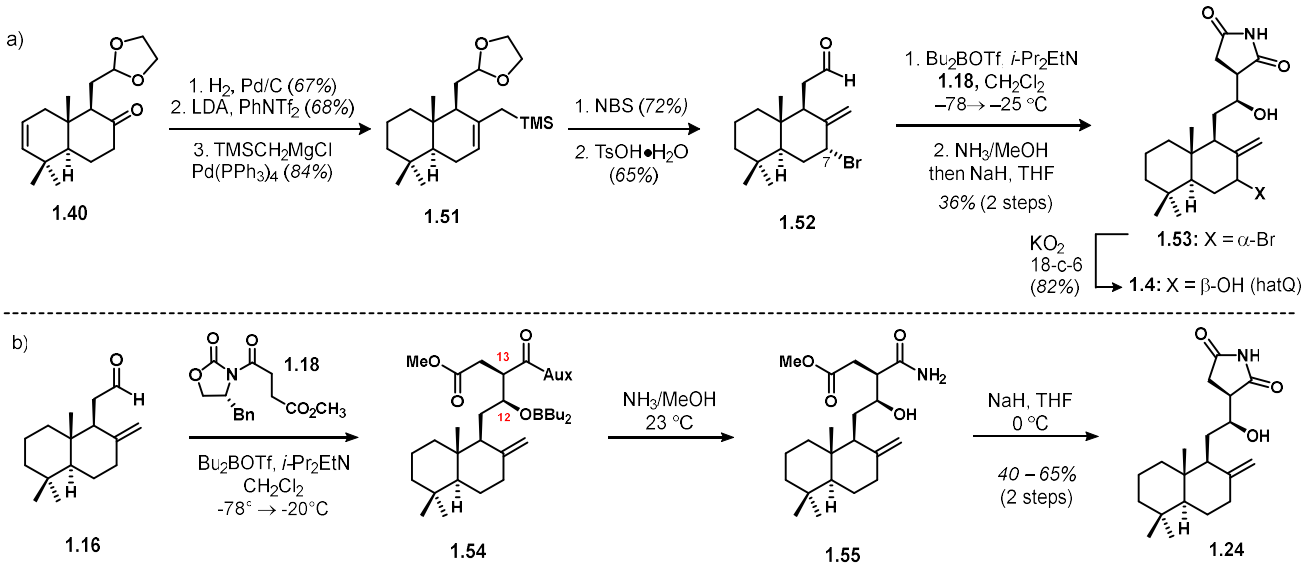

NH_3/MeOH solution to aminolyze the imide auxiliary. Under these conditions the resulting primary amide (**1.55**) partially cyclized onto the pendant methyl ester; however, to complete imide formation, crude **1.55** was treated with NaH in THF to yield **1.24** (**Scheme 1.7b**). To access hatQ (**1.4**), bromide

1.53 underwent a potassium-superoxide-mediated displacement to install the desired C7-hydroxyl group and complete the first total synthesis of a haterumaimide natural product (**Scheme 1.7**).

To expand upon this diversifiable route, Könst utilized intermediate **1.41** to construct uniquely potent analogues designed from the combination of features found in two of the most cytotoxic family members: the characteristic dichlorides of DCL, and the pendant A-ring C18-oxygenation of hatJ. As

Scheme 1.6 C18-oxygenation permits the synthesis of equatorial chlorinated analogues

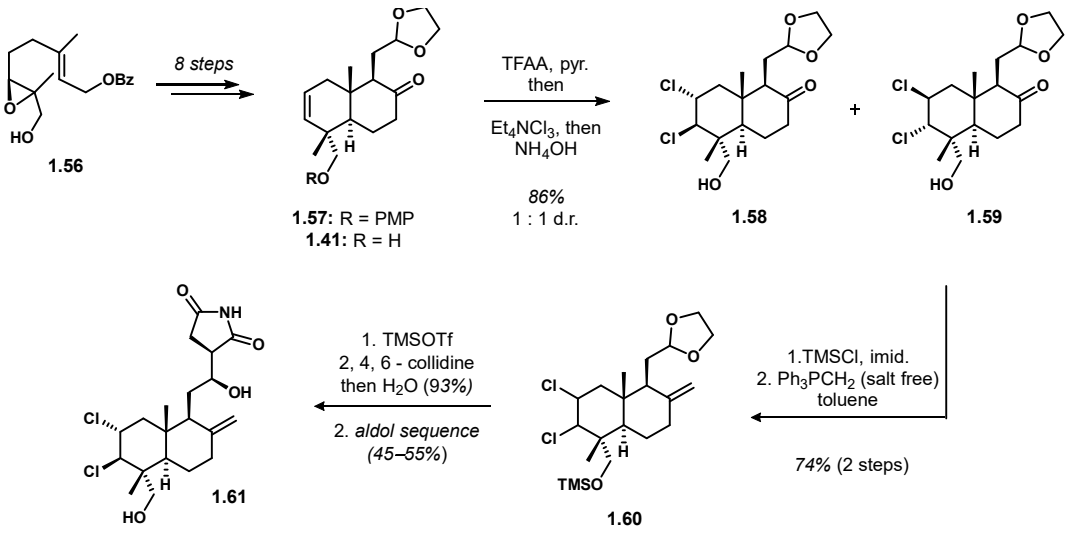

intermediate **1.41** differed from **1.40** by a single point of oxygenation, the strategy developed by Szklarski was applied with minor modifications (**Scheme 1.8**). Known chiral epoxide **1.56,** derived from geranyl acetate,[22] was advanced through a similar sequence of reactions[23, 24] to that outlined in **Scheme 1.5** to construct PMP-protected intermediate **1.57**. It was apparent that A-ring dichlorination would favor the diaxial addition product (see **Scheme 1.5**), but precedent from our lab had shown that alkenes bearing homoallylic oxygenation can greatly impact the stereoselectivity of a dichlorination event.[25, 26] Indeed, Könst observed mixtures of chlorinated products when **1.57** was treated with Et_4NCl_3, although the major component was chlorination of the PMP-protecting group. An investigation of different hydroxyl

protecting groups revealed that *in situ* protection of the C18-alcohol as its trifluoroacetate ester prior to addition of Et_4NCl_3,[26] resulted in a 1:1 mixture of equatorial (**1.58**) to axial (**1.59**) dichlorides. In spite of the low d.r. of this reaction, this was a significant accomplishment for the project as direct diequatorial dichlorination of the A-ring alkene had evaded our efforts up to this point. The diastereomers **1.58** and **1.59** were difficult to separate and were carried through as a mixture for purification at a later stage. The C18-hydroxyl groups were protected as the TMS-ethers, and a Wittig reaction using a salt-free ylide solution methylenated the hindered B-ring ketone (**1.60**). After ketal deprotection under Lewis acid conditions the diastereomeric dichlorides were separated, and Könst applied his optimized aldol sequence to access hybrid analogue **1.61**, named C3-chlorohaterumaimide J (**Scheme 1.8**).

This synthetic route, along with the C18-nonoxygenated series derived from **1.40**, facilitated access to a number of different haterumaimide analogues, all of which were tested against the P388 cell line, for comparison to the initial isolation data,[7] in addition to A2058 melanoma and DU145 prostate cancer cell lines. Surprisingly, the biological activity of **1.61** was underwhelming, with IC_{50} values only in the micromolar range. The diaxial analogue **1.63** was one of the most active compounds tested—differing from **1.62** by the lack of a C18-OH group—and was five times more potent (**Figure 1.3**). Through

Figure 1.3 DCL and dichlorinated analogues with IC_{50} values

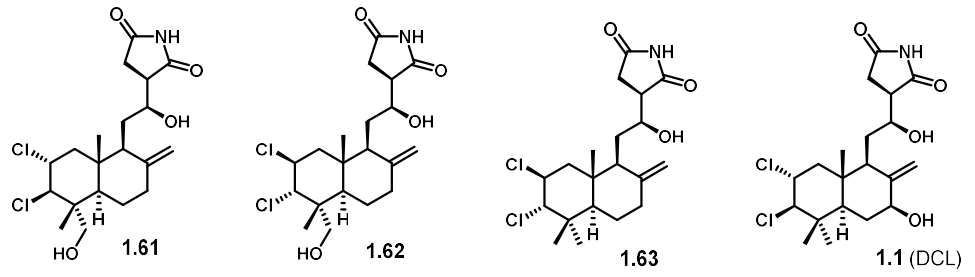

IC_{50} (μM)	**1.61**	**1.62**	**1.63**	**1.1** (DCL)
	P388: 0.33 **A2058:** 1.34 **DU145:** 2.19	**P388:** 0.70 **A2058:** 2.06 **DU145:** 9.42	**P388:** 0.14 **A2058:** 0.97 **DU145:** 0.37	**P388:** 0.4 (lit = 0.002) **A2058:** -- **DU145:** --

computational modeling of these analogues within the E-site of the ribosome, it was hypothesized that two A-ring chlorides in addition to a C18-hydroxyl group causes unfavorable crowding leading to disruption of other important binding interactions.[23] Additional bioactivity studies on a natural sample of DCL (**1.1**) found it to be significantly less potent than the initial reports,[2, 9] indicating that a C3-chloride may not be critical for high activity. These hypotheses were later validated through analysis of the binding conformations of various lissoclimides within the E-site pocket of the target ribosome (**Chapter 2**).[24]

1.4 Conclusion

Through the work of Szklarski and Könst, our research program on the haterumaimides expanded from target-oriented synthesis to include medicinal chemistry. The analogue-oriented synthesis allowed Könst to construct a library of differentially functionalized haterumaimide scaffolds and further developed our knowledge of the SAR.[24] As many of the analogues resulted in unexpected potencies against cancer cell lines, Könst was later able to rationalize this data through analysis of the binding conformation of CL and other analogues co-crystallized in the active site of the eukaryotic ribosome (presented in **Chapter 2**). While the enoxysilane cyclization strategy enabled the synthesis of 3-chlorohaterumaimide J, the challenge of synthesizing hatJ and hatK (**1.12, 1.13**) without the unnecessary C3-functionality still remained; access to these compounds will be critical to our understanding on the importance of C18-oxygenation for the anti-cancer activity of the haterumaimides. Lessons learned from the previous work including, Szklarski's furan-terminated cyclization approach,[13] informed our synthesis of hatJ (**Chapter 4**).

Even though the efforts of González[10] and Chai[11] never resulted in any haterumaimide natural product, features from their work have provided invaluable precedent for our research program.

González's identification of sclareolide as a starting material has inspired our semi-syntheses of hatQ and CL (**Chapter 2**). Chai's chiral auxiliary aldol approach for selectively forming the C12-C13 stereocenters has become a central theme in our syntheses for installing the hydroxysuccinimide.

1.5 References

1. Malochet-Grivois, C.; Cotelle, P.; Biard, J. F.; Henichart, J. P.; Debitus, C.; Roussakis, C.; Verbist, J. F., *Tetrahedron. Lett.* **1991,** *32* (46), 6701-6702.
2. Malochet-Grivois, C.; Roussakis, C.; Robillard, N.; Biard, J. F.; Riou, D.; Debitus, C.; Verbist, J. F., *Anti Can. Drug Des.* **1992,** *7* (6), 493-502.
3. Toupet, L.; Biard, J. F.; Verbist, J. F. *J. Nat. Prod.* **1996,** *59* (12), 1203-1204.
4. Uddin, M. J.; Kokubo, S.; Ueda, K.; Suenaga, K.; Uemura, D. *Chem. Lett.* **2002,** (10), 1028-1029.
5. Uddin, M. J.; Kokubo, S.; Ueda, K.; Suenaga, K.; Uemura, D. *J. Nat. Prod.* **2001,** *64* (9), 1169-1173.
6. Uddin, J.; Kokubo, S.; Suenaga, K.; Ueda, K.; Uemura, D., *Heterocycles* **2001,** *54* (2), 1039.

7. Uddin, J.; Ueda, K.; Siwu, E. R. O.; Kita, M.; Uemura, D., *Bioorg. Med. Chem.* **2006,** *14* (20), 6954-6961.

8. Fu, X.; Palomar, A. J.; Hong, E. P.; Schmitz, F. J.; Valeriote, F. A. *J. Nat Prod.* **2004,** *67* (8), 1415-1418.

9. Robert, F.; Gao, H. Q.; Donia, M.; Merrick, W. C.; Hamann, M. T.; Pelletier, J., *RNA* **2006,** *12* (5), 717-724.

10. Gonzalez, M. A.; Romero, D.; Zapata, B.; Betancur-Galvis, L. *Lett. Org. Chem.* **2009,** *6* (4), 289-292.

11. Tuan, M. N.; Nguyen, Q. V.; Youte, J. J.; Lau, J.; Cheong, A.; Ho, Y. S.; Tan, B. S. W.; Yoganathan, K.; Butler, M. S.; Chai, C. L. L., *Tetrahedron* **2010,** *66* (47), 9270-9276.

12. Peter, J. R. *Nat. Prod. Rep.* **2010**, *27*, 1521-1530.

13. Szklarski, A. R. PhD Dissertation, University of California, Irvine, 2013.

14. Corey, E. J.; Luo, G. L.; Lin, L. S. Z. *J. Am. Chem. Soc.* **1997,** *119* (41), 9927- 9928.

15. Mi, Y.; Schreiber, J. V.; Corey, E. J. *J. Am. Chem. Soc.* **2002,** *124* (38), 11290-11291.

16. Corey, E. J.; Lin, S. Z.; Luo, G. L. *Tetrahedron Lett.* **1997,** *38* (33), 5771-5774.

17. Schlama, T.; Gabriel, K.; Gouverneur, V.; Mioskowski, C. *Angew. Chem. Int. Ed. Engl.* **1997,** *36* (21), 2342-2344.

18. Jung, M. E.; Gomez, A. V. *Tet. Lett.* **1993,** *34* (18), 2891-2894.

19. Konst, Z. A. PhD Dissertation, University of California Irvine, 2017.

20. Takahashi, K.; Takeda, K.; Honda, T. *Tet. Lett.* **2010,** *51* (27), 3542-3544.

21. Dowling, M. S.; Vanderwal, C. D. *J. Org. Chem.* **2010,** *75* (20), 6908-6922.

22. Tanis, S. P.; Chuang, Y. H.; Head, D. B. *J. Org. Chem.* **1988,** *53* (21), 4929-4938.

23. Konst, Z. A. PhD Disstertation. University of California Irvine, 2017.

24. Konst, Z. A.; Szklarski, A. R.; Pellegrino, S.; Michalak, S. E.; Meyer, M.; Zanette, C.; Cencic, R.; Nam, S.; Voora, V. K.; Horne, D. A.; Pelletier, J.; Mobley, D. L.; Yusupova, G.; Yusupov, M.; Vanderwal, C. D., *Nat. Chem.* **2017,** *9*(11), 1140-1149.

25. Tartakoff, S. S.; Vanderwal, C. D., *Org. Lett.* **2014,** *16*(5), 1458-1461.

26. Vogel, C. V.; Pietraszkiewicz, H.; Sabry, O. M.; Gerwick, W. H.; Valeriote, F. A.; Vanderwal, C. D. *Angew. Chem. Int. Ed.* **2014,** *53*(45), 12205-12209.

CHAPTER 2 : Semi-Synthesis of Haterumaimide Q and Chlorolissoclimide

2.1 Introduction

A solid foundation had been set on the lissoclimide research program through the success of the enoxysilane-terminated cyclization to make haterumaimide Q (**2.1**, hatQ) and multiple analogues. This route was extremely diversifiable but required 15–21 steps to access the various lissoclimide products. We now aimed to investigate the utility of the plant-derived terpenoid (+)-sclareolide (**2.2**) as starting material for a highly efficient semi-synthesis of select haterumaimide and lissoclimide products. Several features of **2.2** make this scaffold an advantageous starting point (**Figure 2.1**): (1) In three steps the haterumaimide labdane core can be constructed with an appropriate carbonyl functional handle for installing the pendant imide;[1] (2) Under C–H activation methods, **2.2** is well-precedented for biased selectivity at either the C2, or C3 positions,[2-5] exactly where chlorination is observed in the haterumaimide products; (3) the average cost of $5/gram for **2.2** permits the synthesis to be conducted on multigram scale.

Figure 2.1 Sclareolide functionalization

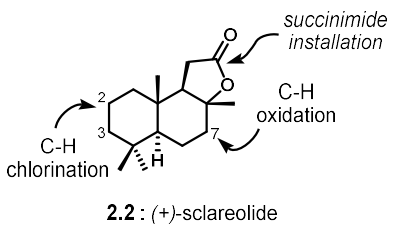

2.2 : *(+)*-sclareolide

A key accomplishment from our previous work was the development of a protocol for installing the hydroxysuccinimide group with high stereocontrol—an issue that no other previous group had solved. Könst initially evaluated this aldol sequence on sclareolide-derived aldehyde **2.3**,[1] and saw the potential to elaborate the imide product (**2.4**) to hatQ (**Scheme 2.1**).[6] All that remained was the installation of an equatorial C7-hydroxyl group, but this task was more difficult than anticipated. Direct allylic oxidation of **2.4** afforded solely the undesired axial C7-alcohol (**2.5**) and the sensitive functionality of the hydroxysuccinimide group (acidic N–H, free alcohol) limited experimentation on **2.4** due to the reagent

Scheme 2.1 First generation semi-synthesis of haterumaimide Q

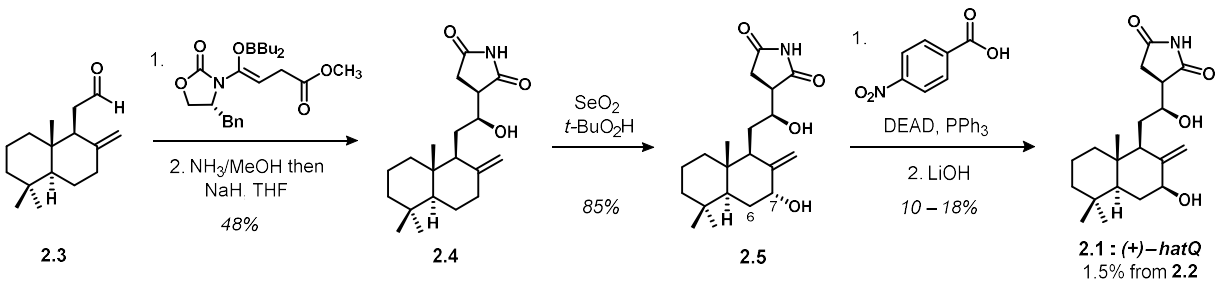

incompatibility. A Mitsunobu inversion corrected the stereochemistry at C7 (**2.1**), but this reaction was extremely low yielding due to facile elimination to a C6-C7 diene system. While this endeavor was successful in obtaining **2.1**, the overall yield was quite poor. A high yielding and general strategy to the haterumaimide scaffold from sclareolide (**2.2**) would improve the synthesis of hatQ and provide a reliable route for accessing C2-chlorinated family members, post C–H chlorination.

2.2 Semi-Synthesis of Haterumaimide Q

Based on the challenges encountered in first generation semi-synthesis of haterumaimide Q, we aimed to reverse the order of events for B-ring oxygenation and succinimide formation: incorporation of the C7-hydroxyl group before the hydroxysuccinimide would allow for a broader investigation of allylic oxidation procedures and save the difficult aldol sequence for the last step.

Following a similar procedure as González, the lactone of **2.2** was opened with the aluminate-Weinreb salt and the resulting tertiary alcohol was eliminated at cold temperatures with $SOCl_2$ and pyridine to access the kinetically favored exocyclic alkene **2.6** (**Scheme 2.2**). We elected to further investigate an allylic oxidation-inversion sequence to install the C7-hydroxyl group. As expected, allylic oxidation under SeO_2-mediated conditions afforded axial alcohol **2.7**. We surveyed a variety of activating

Scheme 2.2 Strategies for C7–oxidation

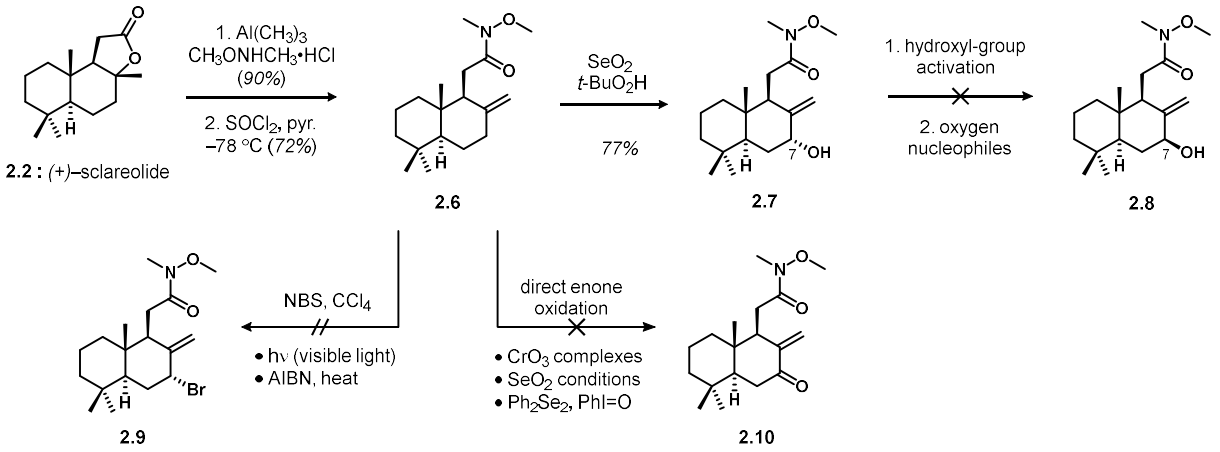

groups on the alcohol (mesyl, tosyl, acetyl, chloroformyl) in attempts to find a leaving group—that when paired with an oxygen nucleophile—would favor displacement (**2.8**) over elimination, but the latter was consistently the major pathway. Alternatively, we took inspiration from the previous total synthesis of hatQ, where Könst advanced an allylic bromide several steps before a final invertive displacement with KO_2. Unfortunately, subjecting **2.6** to radical bromination conditions afforded only minor amounts of **2.9** along with decomposition products that lacked the O–CH_3 group, likely owing to homolytically labile nature of the N–O bond. With limited success on the invertive-displacement strategy we then turned to an oxidation/reduction protocol; it was anticipated that reduction of a C7-ketone would preferentially install the desired alcohol stereochemistry. We surveyed a variety of reagents to effect direct oxidation of **2.6** to ketone **2.10**[7]—such as CrO_3-based complexes[8], Ph_2Se_2 with peroxides or hypervalent iodine oxidants[9] and stoichiometric SeO_2[10, 11];however, allylic alcohol **2.7** was consistently the major product and more forcing conditions resulted in over-oxidation of the B-ring. Eventually we conceded to the substrate's natural preference to give **2.7** and performed a subsequent oxidation under Swern-conditions to give enone **2.10** in high yields (**Scheme 2.3**). Treatment of **2.10** with di-*iso*-butylaluminum hydride reduced both the Weinreb amide to the aldehyde, and the ketone to the desired C7-alcohol to afford **2.12**

after trimethylsilyl protection. The high stereoselectivity of the reduction was attributed to the preference of the bulky reducing agent to approach the ketone from less-hindered bottom face (**2.11**). Although this reduction exclusively afforded one diastereomer, partial 1,4-reduction was observed. With aldehyde **2.12** in hand, the optimized aldol sequence was carried out to successfully install the C12, C13–hydroxysuccinimide. The yield of the aldol sequence was difficult to reproduce, averaging between 40–57% yield of **2.1** and a 6:1 d.r. of desired imide product to the other *syn*-diastereomer. This inconsistency could be a consequence of the Lewis basic C7-TMS ether competing for coordination with the boron Lewis acid. The acidic conditions used in the work up—post NaH-promoted imidation—presumably desilylated the C7-alcohol and haterumaimide Q (**2.1**) was obtained without any subsequent deprotection steps.

Scheme 2.3 End game strategy for the synthesis of haterumaimide Q

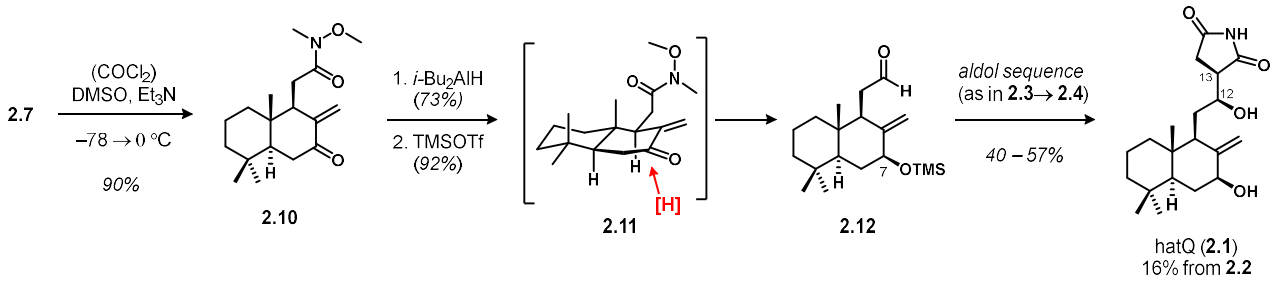

This optimized semi-synthesis addressed pertinent challenges in constructing the C7-oxygenated haterumaimide scaffold. The installation of the C7-hydroxyl group followed a high yielding and selective oxidation/reduction protocol and the sequence features the utility of the Weinreb-amide to mask the pendant aldehyde through most of the synthesis. Saving the arguably most difficult reaction—the boron-aldol addition—for the final step, increased the efficiency of material throughput and avoided subjecting the sensitive hydroxysuccinimide to incompatible reaction conditions. Altogether the strategy accessed hatQ in 16% yield from **2.2**, representing a ten-fold increase in yield from the previous semi-synthesis.

2.3 Application to the synthesis of chlorolissoclimide

During the optimization of the semi-synthesis, co-worker Zef Könst focused on the installation of a C2-chlorine on sclareolide (**2.2**) through C–H activation methods. He initially employed a protocol developed by Groves and coworkers[4] which used a porphyrin manganese catalyst with NaOCl as the chlorine source, but obtained only modest diastereoselectivity (4.5 : 1, Cl-α : Cl-β) and minimal yields of desired 2-chlorosclareolide (**2.14**). This inefficient reaction was a significant bottle-neck as the first step of the synthesis of chlorolissoclimide. A short time afterwards, the Alexanian group published a C2-selective C–H bromination of sclareolide (**2.2**) using *N*-bromoamides that proceeded in 65% yield with high diastereoselectivity.[5] A collaboration was initiated with Alexanian and coworkers to develop an analogous C–H chlorination of **2.2**. Through much optimization, Könst and collaborator Ryan Quinn developed conditions for a C–H chlorination of **2.2** with *N*-chloroamide **2.13** (**Scheme 2.4**). This transformation could be initiated under visible light or peroxide conditions to obtain **2.14** in high yields and with remarkable selectivity. It should be noted that **2.2** is a biased scaffold for C–H activation, although 21 C–H bonds available, there has been traditional selectivity for activation of the C2 or C3-methylene positions.[2, 5, 12, 13] The lactone withdraws electron density from the C–H bonds in the B-ring, leaving three sites for C–H abstraction in the A-ring. According to Houk, Baran and Eschenmoser, the

Scheme 2.4 Selective C–H chlorination permits the synthesis of chlorolissoclimide

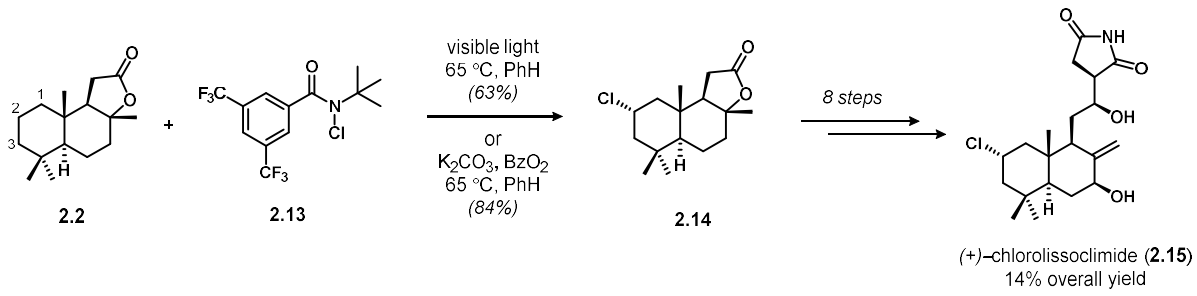

selectivity for a hydrogen atom abstraction from the C2 or C3 positions is in part due to strain relief between the axial C2-hydrogen and the C10/C4 angular methyl groups during the transition state.[14] The steric bulk incorporated in amide **2.13** is likely the source of the exquisite α-C2 selectivity, disfavoring abstraction from the neo-pentylic C3- and C1-methylene hydrogens.

With a reliable method for accessing sufficient quantities of **2.14,** we applied our optimized route for hatQ to the synthesis of chlorolissoclimide (CL, **2.15**). This strategy turned out to be extremely general for the C2-chlorinated series, requiring no modifications from the initial procedures. Additionally, we co-opted this route for the synthesis of C2-halogenated analogues of CL to investigate the biological effects of substituting the C2-chlorine with a fluorine and bromine (**Section 2.4**). Our work on the semi-synthesis from sclareolide permitted access to one of the most potent lissoclimide natural products (**2.15**) in 9 steps and 14% overall yield.[15] With the ability to synthesize large quantities of CL, we sought out collaborations that would help us further understand the biological mechanism of action of these natural products and probe the structural characteristics of CL that result in its high cytotoxicity.

2.4 Co-crystal structure of chlorolissoclimide in the E-site of the ribosome

Pelletier and co-workers established the general mechanism of action of CL (**2.15**) and dichlorolissoclimide through a protein inhibition screen[16] of the extracts of *Pleurobranchus forskalii*—a mollusk known to prey on the *Lissoclinum sp.* ascidians. In a screen for protein synthesis inhibitors, both of these lissoclimides were isolated from the extracts containing mRNA, encoding firefly (FF) or renilla (Ren) luciferases, that demonstrated a high fluorescent output, indicating ribosome inhibition.[17]

The eukaryotic ribosome is a complex molecular enzyme consisting of intertwined polypeptide fragments and ribosomal RNA (rRNA) responsible for the translation of mRNA into protein. To initiate

protein synthesis, initiation co-factors must bring the mRNA-bound small ribosomal subunit (40s) in proximity to the large ribosomal subunit (80s)[18]. The translation process of this mRNA strand into a polypeptide consists of four main steps. The first step, *activation,* is the aminoacylation of transfer RNAs (tRNA) and then the tRNA charged with amino acids (aa-tRNA) congregate around the complexed ribosome. The *initiation* step requires an aa-tRNA to bind to the start codon of the mRNA strand through base-pairing; this occurs at the acceptor site (A-site) on the small ribosomal subunit. Once this activation complex is formed, *elongation* occurs where another aa-tRNA binds to the peptidyl transferase site (P-site). During this process an aa-tRNA moves from the A-site to the P-site, and the polypeptide chain is transferred to the new P-site occupant while simultaneously forming a peptide bond with the amino acid. During this movement an empty tRNA has to move to the exit site (E-site, the translocation step) and that empty tRNA is ejected from the complex as a new aa-tRNA arrives at the A-site. *Termination* occurs when the ribosome encounters the stop codon on the translating mRNA strand.

In the study by the Pelletier group, they noted the similarity of the lissoclimides to the well-known protein synthesis inhibitor, cycloheximide (**2.16, Figure 2.2**). Both these naturally occurring small molecules inhibit the translation step of protein synthesis[16] and contain similar structural characteristics. Cellular extracts treated with CL or **2.16** contained mRNA stalled on the ribosome at all stages of translation. This phenotype is a characteristic of molecules that impede the translocation step, likely by interfering with ribosomal E-site

Figure 2.2 Naturally occurring translation inhibitors

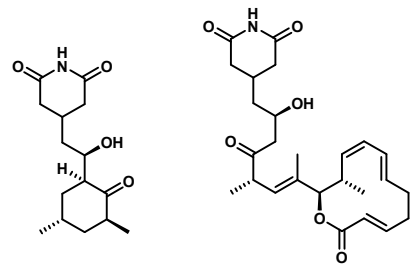

cycloheximide (**2.16**) lactimidomycin (**2.17**)

function and preventing deacylated tRNA in the P-site from moving into the E-site. A consequence of this interaction is ribosomal accumulation on the mRNA strand and eventual cell death.[17]

In 2014 the Yusupov group disclosed a co-crystal structure of **2.16**, as well as other naturally occurring small molecule translation inhibitors including lactimidomycin (**2.17, Figure 2.2**), bound to the E-site of the eukaryotic ribosome.[19] After the completion of our synthesis of CL (**2.15**), we initiated a collaboration with the Yusupov group and provided them with a synthetic sample of **2.15**. Yusupov and coworkers solved the crystal structure of the *S. cerevisiae* 80s ribosome in complex with inhibitor CL, located at the E-site (**Figure 2.3a**). As predicted by Pelletier,[17] CL shares the same binding site as **2.16**, and in turn **2.17**. These three molecules share a similar network of imide interactions, although the binding motif of **2.15** showed several novel features (**Figure 2.3b**): (1) The C12-hydroxyl group hydrogen bonds to a nucleotide of the phosphate-oxygen backbone; (2) The C7-hydroxyl group forms a hydrogen bond with a proline residue of the ribosomal protein, unique from other known inhibitors which

Figure 2.3 Ribosome co-crystal structure with chlorolissoclimide and binding pose

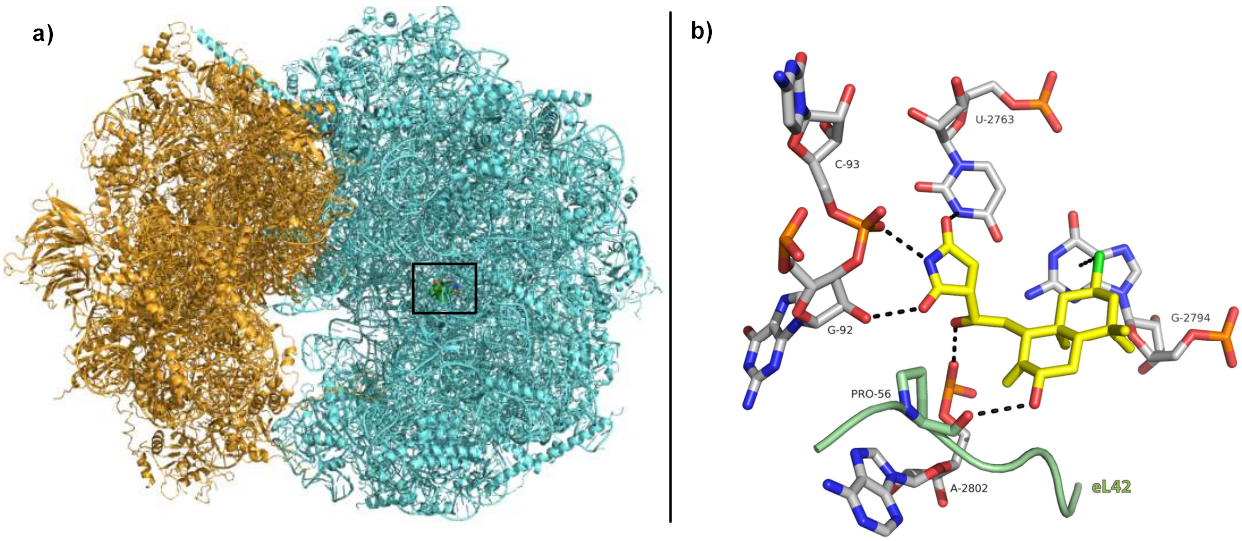

exclusively bind rRNA; (3) The C2-chlorine atom participates in a face-on halogen-π interaction with the pyrimidine ring of a guanine residue. The importance of the latter interaction is displayed in the significant difference of IC_{50} values between CL (**2.15**) and hatQ (**2.1**) for the same cancer cell lines. The Horne group assayed both natural products against the P338 murine leukemia cancer cell line and two other more aggressive tumor cell lines (DU145 prostate and A2058 melanoma). CL demonstrated sub-micro-molar activity against all cell lines, whereas hatQ was 2–3 fold less potent (**Figure 2.4**).[20] The only structural difference between these two family members is a C2-chlorine atom. Through analysis of the crystal structure we believe the chlorine in CL, positioned 3.2 Å away from the center of the guanine pyrimidine ring, shares its lone pair with this aromatic ring in a dispersion-based interaction. To investigate the energetic value for halogen-π interaction we collaborated with computational specialist Vamsee Voora from the Furche group at UCI. Voora, using the geometries from the solid-state structure, calculated a binding energy of 1.1 kcal/mol for a chlorine-π interaction of CL with the guanine moiety. While this value is small, Könst found that this beneficial interaction accounts for conformational changes in the binding poses of highly bioactive dichlorinated analogues.[20, 21] We were intrigued to exploit this halogen-π interaction, and hypothesized that the binding energy (and corresponding bioactivity) could be directly related to polarizability of the C2-halogen; substituting the C2-chlorine with a bromine and a fluorine could show an increase and decrease in binding energy respectively (i.e. Br > Cl > F). An on-going research project in our lab involves application of the hatQ semi-synthesis route, after C–H halogenation of sclareolide (**2.2**), for the synthesis of bromo- and fluoro-

Figure 2.4 IC_{50} values of hatQ and CL

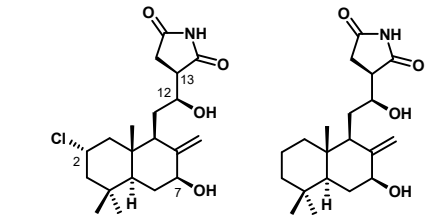

IC_{50} (μM)	CL, 2.15	hatQ, 2.1
P388:	0.059	0.20
A2058:	0.253	2.34
DU145:	0.488	1.34

lissoclimide. These efforts will further our understanding for the importance of the halogen-π interaction and have the potential to result in a uniquely potent lissoclimide analogue.

2.5 Efforts toward hydroxysuccinimide stereoisomers

The co-crystal structure confirmed that every hetero-atom in CL is interacting with the ribosome, and (most) importantly, that the hydroxysuccinimide motif is participating in four-hydrogen bonding events. This tetrad of hydrogen bonds likely constitutes the pharmacophore of the haterumaimides and provides insight into the conserved nature of this unusual group throughout the entire family. It is interesting to note the similarities between the haterumaimides and cycloheximide (CHX, **2.16**) and lactimidomycin (LTM, **2.17**)—these naturally occurring molecules bearing cyclic imides with proximal secondary hydroxyl groups demonstrate an interesting case of convergent evolution, as the bacterial-derived glutarimide compounds and the marine ascidian-derived haterumaimides have been developed by nature as ideal ligands for ribosomal E-site binding and ultimately protein synthesis inhibition.

Figure 2.5 Overlay of imide inhibitors in the ribosome E-site

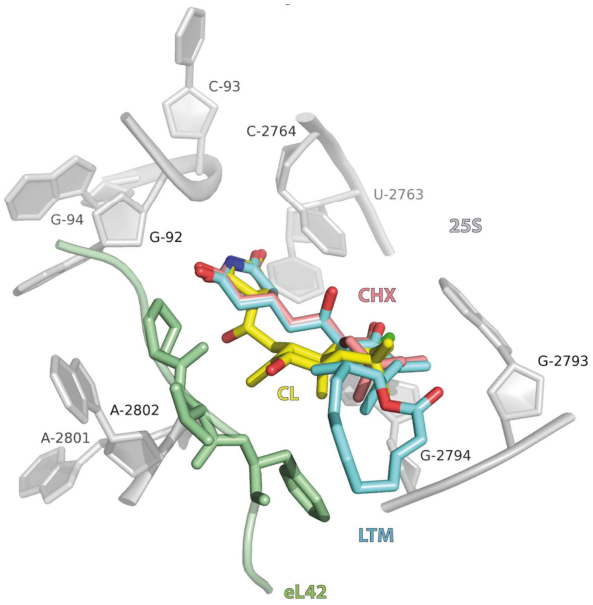

An overlay of the binding poses for CL (**2.15**, yellow), **2.16** (pink), and **2.17** (blue) shows that the pendent imide groups and hydrocarbon cores of the molecule occupy a similar space, but for CL, the secondary hydroxyl group is oriented differently (**Figure 2.5**). The hydroxyl group in the glutarimide compounds are oriented on the top-face of the molecule and participate in a hydrogen bond with a uracil

group (U2763, 3-NH). Even though the carbon chain length is slightly longer in the glutarimide compounds compared to CL, this presented an opportunity to probe new space in the binding pocket and investigate the ability to pick up different hydrogen bonding interactions through varying the configuration of the C12, C13-hydroxyimide stereocenters.

2.5.1 Auxiliary controlled aldol modifications

We set out to synthesize all four stereoisomers of the basic (A and B ring unfunctionalized) haterumaimide scaffold to then assess their relative bioactivities (**Figure 2.5**). From the sclareolide-derived aldehyde **2.3** the natural hydroxysuccinimide and its *syn*-C12, C13 stereoisomer (**2.4** and **2.18**)

Figure 2.6 Aldol additions for hydroxyimide stereoisomer analogues

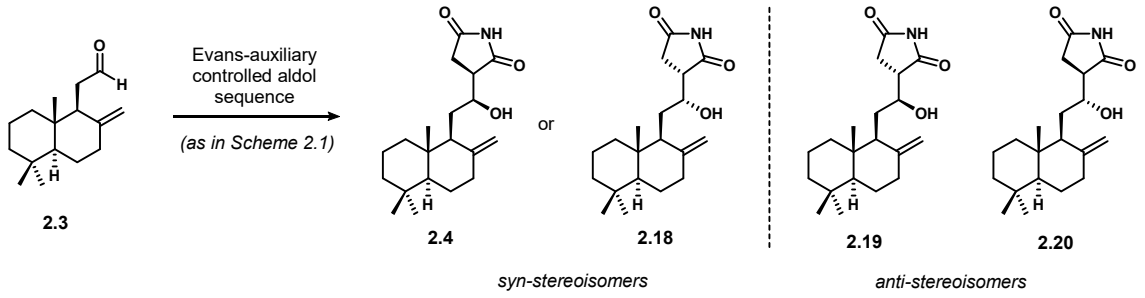

were obtained by using the *(R)* and *(S)*-enantiomers of the Evans auxiliary in the aldol step, respectively. The *anti*-stereoisomers (**2.19** and **2.20**) were significantly more challenging targets. While the *anti*-aldol product is thermodynamically favored,[22] the enolate geometry largely dictates the diastereoselectivity when the reaction proceeds under the kinetic control of the chelated Zimmerman-Traxler transition state.[23] The Evans-auxiliary approach inherently favors *syn*-aldol products due to the exclusive formation of the Z-enolate. This is dictated by the unfavorable $A_{1,3}$–strain between the oxazolidinone ring and the double bond substituent if adopting the E-enolate geometry .[24] We were apprehensive to deviate from the Evans oxazolidinone auxiliary as this potentially would require a new protocol for the imide formation.

Fortunately, there are known modifications to the Evans system for obtaining the other *syn*-aldol product (termed non-Evans-syn) and the *anti*-stereoisomers.[25]

Heathcock and coworkers reported that pre-complexation of the aldehyde with a Lewis acid prior to the reaction with the oxazolidinone enolate allowed access to non-Evans-*syn* and *anti*-aldol products. They proposed an open transition state model for their observed selectivities (**Scheme 2.5a**). In this system, gauche interactions around the forming C–C bond dictated the facial approach of the aldehyde. With an E-geometry maintained between the aldehyde and complexed Lewis acid, a small Lewis acid favored transition state-I (**TS-I**) to give the non-Evans-*syn* -product **2.21**. Conversely, when the exogenous Lewis acid was large the reaction proceeded through **TS-II** to avoid unfavorable gauche interactions between the large Lewis acid and the enolate substituent and resulted in *anti*-product **2.22**. We experimented with this tactic in our system and pre-coordinated a variety of bulky alkylaluminum or lanthanide Lewis acids to **2.3** before addition to a solution of boron enolate derived from **2.23**. While

Scheme 2.5 Heathcock method for non-Evans *syn* or *anti*-aldol products

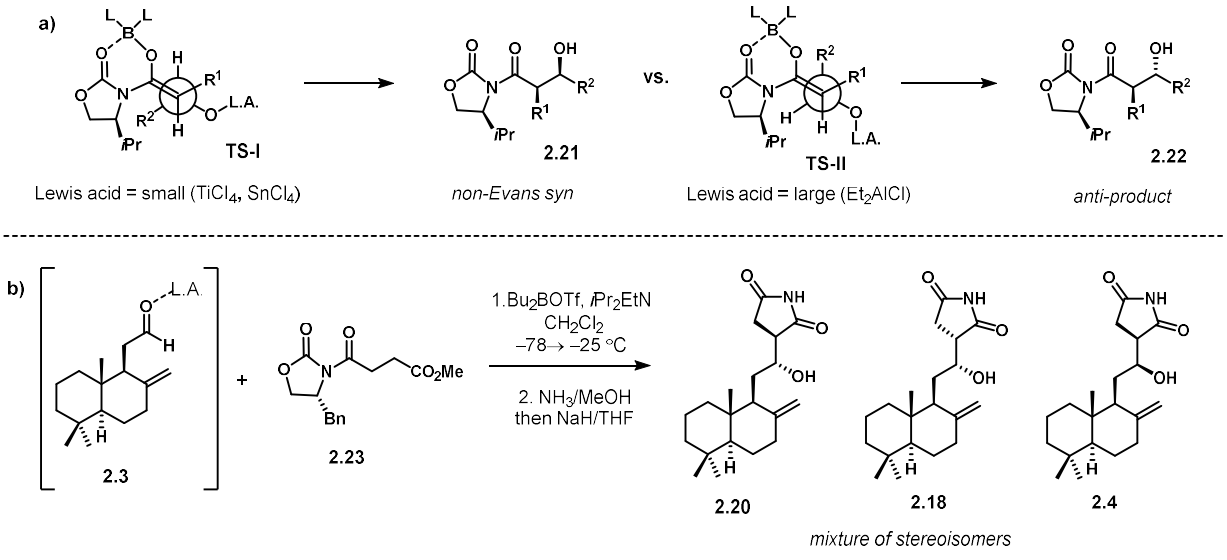

these conditions seemed to favor a new *anti*-diastereomer, the aldol products were consistently isolated as an inseparable mixture of 3 diastereomers (**Scheme 2.5b**). In the most successful case, which employed Et_2AlCl, the aldol adducts were isolated in a 3:1:1 ratio with **2.20** presumably as a the major product, along with the minor *syn*-diastereomers (**2.18** and **2.4**). Several other modifications were attempted with the Evans system such an inverse addition of reagents,[26] and the use of catalytic Mg-based Lewis acid conditions,[27] but these efforts also resulted in mixtures of aldol products.

The cause for the lack of selectivity with the modified aldol reactions was quickly elucidated by repeating several of the Heathcock experiments with the propionyl-substituted auxiliary **2.24** and aldehyde **2.3** (**Scheme 2.6**). The diastereomeric outcome was significantly less complicated and a dominant, isolable aldol product was consistently formed. We postulated this product possessed an anti-C12/C13-stereochemical relationship through ^{1}H NMR comparisons but this was never confirmed. Nevertheless, it was evident that the pendant methyl ester of acylated oxazolidinone **2.23** was the

Scheme 2.6 Control experiments with propionyl oxazolidinone

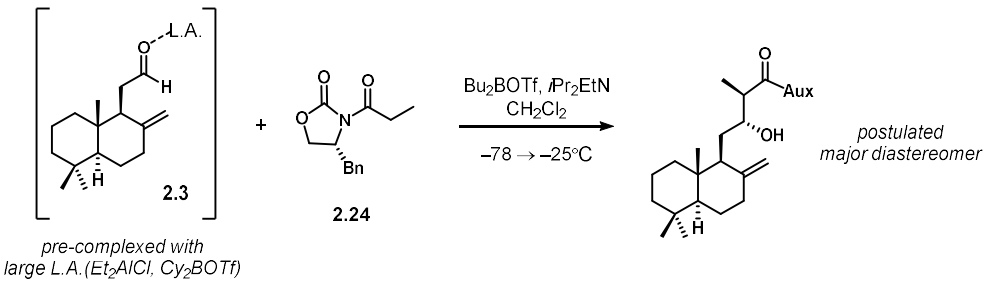

problematic variable in these procedures. The carbonyl group of the ester could undergo enolization in the presence of excess Lewis acid or simply coordinate to the imide-enolate metal center, which could disrupt the required pre-organization for a selective attack on the aldehyde substrate. Hajra and co-workers studied $TiCl_4$-mediated aldol reactions with the *iso*-propyl substituted Evans-acylated

oxazolidinone (**2.23** but with *i*-Pr instead of Bn) and found that either *syn*- or *anti*-aldol products could be produced depending on the sequence of reagent addition.[26] They rationalized that the unconventional selectivity was a result of a boat-like transition state (**TS-III**) where the pendent ester group coordinates to the Ti-metal center (**Figure 2.7**). In a final effort on aldol modifications we attempted this protocol, but $TiCl_4$ was not compatible with our aldehyde substrate (**2.3**) and resulted in decomposition products. Nevertheless, the Hajra precedent validated our hypothesis on the problematic pendent ester and suggested that reaction conditions would have a substantial effect on the efficiency of our auxiliary-controlled aldol addition. We never attempted to implement other chiral auxiliaries known to favor the *anti*-stereochemistry in an aldol reaction such as the Masamune norephedrine-derived auxiliary[28] or the Masamune/Reetz[29, 30] chiral boron Lewis acid; these methods are well-precedented to effect selective *anti*-aldol reaction and could be adapted for a subsequent imide cyclization.

Figure 2.7 Hajra postulated boat transition state

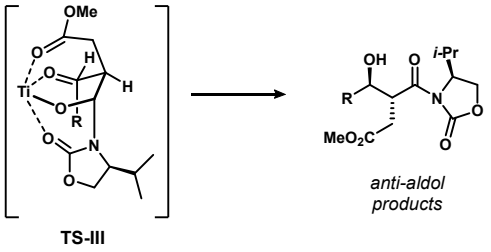

2.5.2 Dynamic-kinetic resolution strategy for anti-stereoisomers

It was evident that adaptation of our aldol sequence for direct formation of the C12/C13 hydroxysuccinimide stereocenters in an *anti*-configuration was unlikely to result in a selective synthesis of these analogues. We then opted for a more stepwise approach to the problem: the C12/C13 bond could be constructed through a simple succinimide aldol[1] with **2.3**, and subsequent oxidation to the β-keto imide (**2.25**) could allow for a selective reduction to the *anti*-β-hydroxy imide stereoisomers (**2.19**, **2.20, Scheme 2.7**). As there are limited methods for constructing stereodefined β-hydroxy succinimide motifs we hoped these efforts could result in a general strategy for accessing these unique functional groups.

Scheme 2.7 Dynamic-kinetic resolution hydrogenation strategy for *anti*-analogues

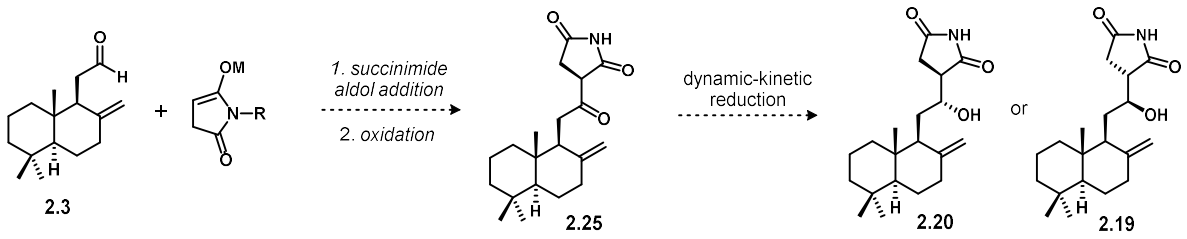

The Noyori group has pioneered the dynamic-kinetic resolution (DKR) and stereoselective reduction of β-keto ester and related systems. Since their seminal report[31] this asymmetric catalytic reduction been applied in a variety of systems to convert racemic starting materials to a single chiral product possessing stereodefined vicinal stereocenters. The efficiency of this transformation is highly dependent on the relative rates of substrate epimerization and catalyst-controlled hydrogenation. The rate of epimerization between A and B must be much faster than the rate of hydrogenation ($k_{H1} << k_{epim}$); in turn the rate of hydrogenation of one epimer over the other must be different ($k_{H1} >> k_{H2}$). The selective formation of either C or D is controlled by the facial selectivity of chiral ligand (i.e. *R*-BINAP) (**Scheme 2.8**). The hydrogenation occurs when the substrate is in the keto form, therefore the absolute configuration at the C3-center is governed by the catalyst while the C2-epimeric center is highly influenced by the steric environment of the substrate. The dependence on both substrate conformation and reaction conditions make it difficult to predict the stereochemical outcome.[32] Noyori and coworkers reported on the effect of substrate control, wherein cyclic β-keto esters provided either the syn or anti-products depending on the substitution (**Scheme**

Scheme 2.8 Dynamic-kinetic-resolution hydrogenation

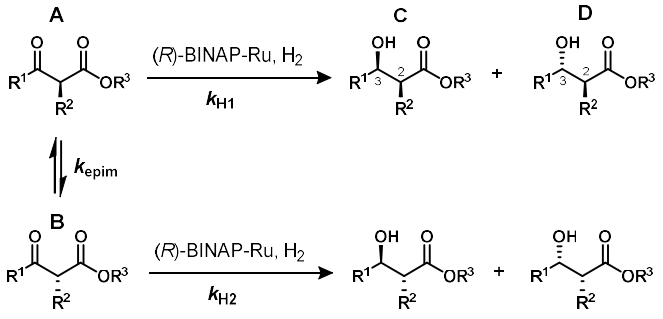

2.9a).[32] Additionally, scientists at Eli Lilly have shown that the solvent and ligand play a large role in determining the diastereoselectivity for dynamic-kinetic hydrogenations of β-keto-lactams (**Scheme 2.9b**).

Scheme 2.9 Substrate and reagent influence on DKR–hydrogenations

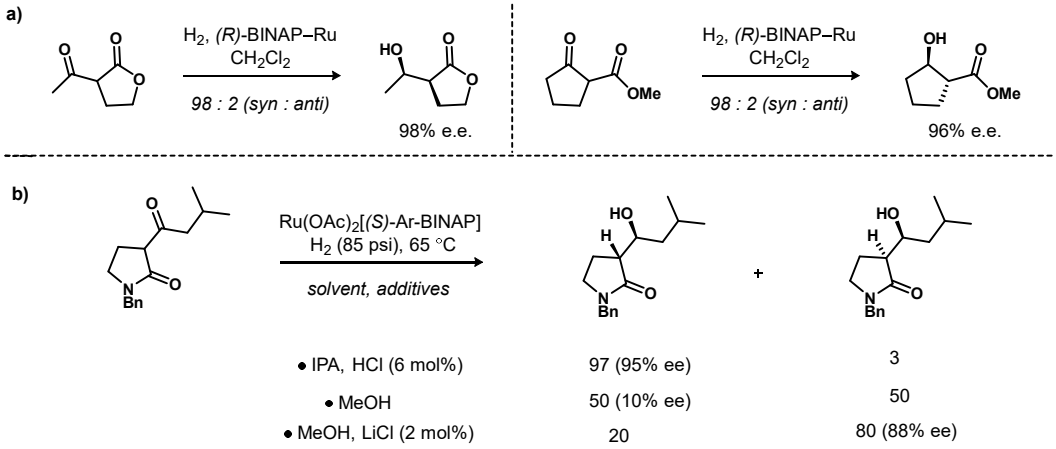

In Szklarski's route to dichlorolissoclimide, a DKR-hydrogenation was planned to set the C12/C13 hydroxyimide stereocenters after furan opening (**Chapter 1**, **section 1.4**). This strategy was never applied to the natural product scaffold (due to failed furan ring opening), but the reaction was investigated on a β-keto imide model system **2.26** by former undergraduate David Liu (**Table 2.1**).[33] These efforts uncovered an inherent selectivity to form the *anti*-β-hydroxy imide **2.27**, in high diastereoselectivity and enantiomeric excess (e.e.) over the *syn*-diastereomer (**2.28**) under both DKR hydrogenation and atom-transfer hydrogenation conditions. While this was the undesired configuration for the haterumaimide system, these results presented a promising strategy for obtaining the *anti*-configured analogues. It should be noted that Liu was later able to find conditions to favor the *syn*-hydroxy imide diastereomer (**2.28**) with catalyst system (*S*)-Ru(BINAP)$(OAc)_2$ and acid additives (**Table 2.1**).

Table 2.1 Szklarski and Liu's result on DKR-hydrogenation on imide model system

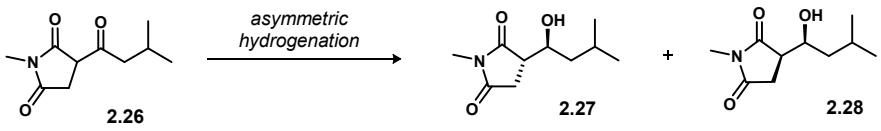

Ru-catalyst conditions/ additives	Anti	:	Syn
• $Ru(OAc)_2$[*(S)*-Ar-BINAP] H_2 (200 psi), MeCN	13 (95 %ee)	:	1
• Ru-TsDPEN-(*p*-cym) HCO_2H, Et_3N, DMF	7 (95 %ee)	:	1
• $Ru(OAc)_2$[*(S)*-Ar-BINAP] H_2 (200 psi), MeOH, HCl (5 mol%)	1	:	7 (78% ee)

We were able to reproduce Szklarski and Liu's results to selectively obtain either diastereomer on the *N*-methyl imide model system (**2.26**); however, application to the synthesis of haterumaimide analogues would require a removeable protecting group on the imide nitrogen. The selection of a suitable imide protecting group was not a trivial task as the deprotection conditions post DKR-hydrogenation would have to be compatible with the newly formed hydroxyimide. Additionally, while the ruthenium-based hydrogenation conditions should not affect the B-ring *exo*-cyclic alkene,[33] we had to avoid protecting groups that required highly reducing deprotection protocols (i.e. sulfonamide, benzyl protecting groups). We settled on a *para*-methoxybenzyl (PMB) protecting group as initial experiments resulted in smooth deprotection under oxidative conditions (CAN, DDQ). To recapitulate the reaction selectivities we first performed our hydrogenation experiments on PMB-model system **2.29** (**Figure 2.8**). Unfortunately, all attempts for a selective DKR hydrogenation of **2.29** resulted in minimal consumption of starting material or formation of a mixture of stereoisomers. Several catalyst systems were explored to improve the diastereoselectivity such as Ru-(BINAP)$(OAc)_2$, Ru-$(PPh_3)Cl_2$, and Ru-

Figure 2.8 Unsuccessful substrates for DKR hydrogenation

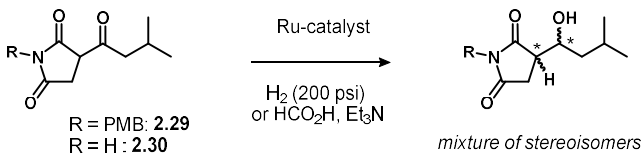

(SYNPHOS)Cl_2, but these efforts were also unsuccessful. We also implemented Noyori's atom-transfer-hydrogenation (ATH) method which employs formic acid and Et_3N as an H-transfer source to create an in-situ ruthenium-hydrido-complex,[34] but this resulted in minimal consumption of starting material. We hypothesized that the poor diastereoselectivity observed in our experiments could be attributed to subtle conformational effects from the PMB group that result in a slow rate of epimerization. If this rate is slow relative to the rate of hydrogenation, the kinetic resolution would be ineffective. Therefore, we deprotected **2.29** in hope that the free-imide would react in a more favorable manor. These efforts were met with little success as even high pressures of H_2 or atom-transfer hydrogenation conditions produced minimal reactivity of **2.30**, possibly due to *N*-coordination to the ruthenium center.

2.6 Computational binding poses for anti-analogues

Our synthetic pursuits towards *anti*-configured hydroxysuccinimide analogues proved more challenging than expected. We eventually decided to analyze the binding poses of these stereoisomers to rationalize whether this change in configuration would still result in adequate binding interactions in the E-site pocket. We enlisted the help of graduate researcher Camilia Zanette in the Mobley lab at UC Irvine. Our collaboration with the docking specialists in the Mobley lab originated before we obtained a co-crystal structure of CL in the ribosome. Zanette used known information on the eukaryotic ribosome structure[19] and pertinent residues present in the E-site domain, to computationally dock several haterumaimide structures—including CL—in the same binding site as cycloheximide and lactimidomycin. The predicted binding pose of CL was identical to the conformation later found in the co-crystal structure, validating these *in silico* experiments. Zanette used the high-resolution structural information from our co-crystal structure and performed docking studies on the C12/C13-*anti*-

stereoisomers of CL. Hundreds of poses were generated after parameterizing the binding site and likely conformations were chosen through collaborative analysis. The optimized poses were overlaid with natural 12*S,* 13*S*-CL (pink) for comparison purposes (**Figure 2.9**). We observed that changing one stereocenter of the hydroxysuccinimide group from the natural configuration resulted in the succinimide adopting a perpendicular orientation from the natural position but did not significantly perturb the decalin core and its substituents. The imide-NH consistently adopted a position to participate in a hydrogen bond with G92 ribose C2-OH. An interesting feature observed in the pose of imide diastereomer 12*S,* 13*S*-CL, was the potential for one of the imide carbonyls to participate in a hydrogen bond with the lysine residue (NH_2) of ribosomal protein eL42; no other inhibitors are known to interact with this residue which overhangs on the top face of the binding site. But in this optimized position, the other imide carbonyl is out of range for any hydrogen bonding contact. In the structure of 12*R,* 13*R*-CL

Figure 2.9 Computationally generated binding poses of *anti*-hydroxysuccinimide analogues

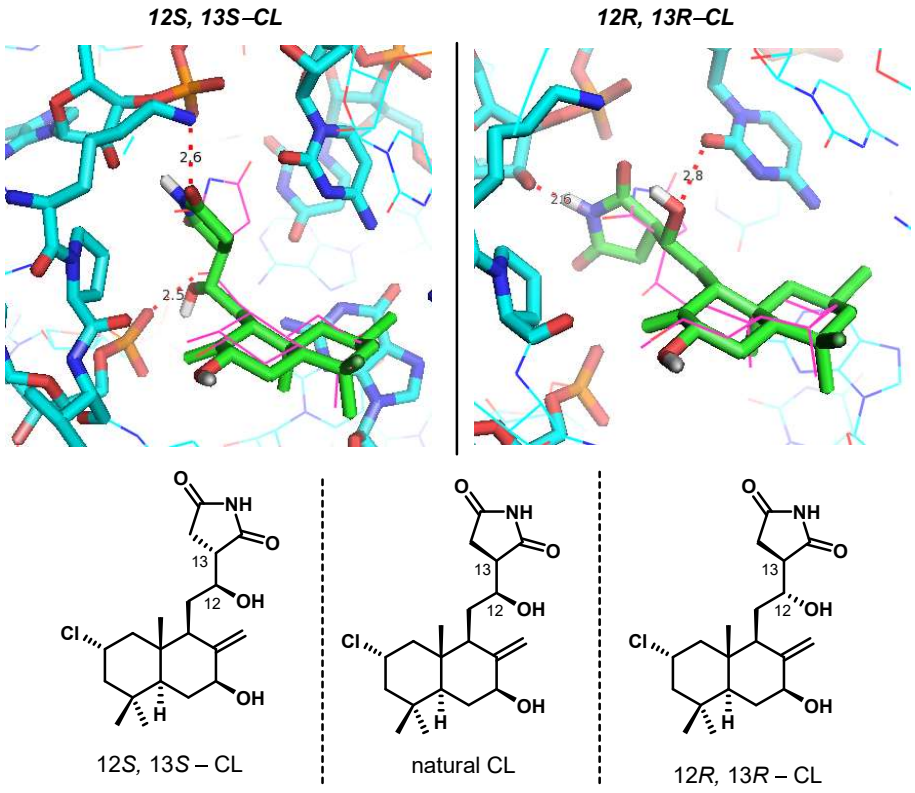

the C12-hydroxyl group linker is placed on the top face of the molecule, in position to hydrogen bond with U2763, similar to cycloheximide and lactimidomycin. Unfortunately, neither imide carbonyls are proximal to any hydrogen bond donor in this conformation. While these studies permitted us to probe potential interactions in the binding site, they confirmed that altering the critical hydroxysuccinimide could result in significantly poorer binding.

2.7 Conclusion

The optimized semi-synthesis of haterumaimide Q has provided a solid foundation for multiple endeavors on the haterumaimide project. This route enabled access to chlorolissoclimide, one of the most cytotoxic lissoclimides synthesized in the Vanderwal lab thus far. The combination of a highly selective C–H chlorination, a reliable protocol to install the C7-hydroxyl group and a late stage formation of the hydroxysuccinimide allowed us to obtain sufficient quantities of CL for biological investigations. The co-crystal structure of CL bound to the E-site of the eukaryotic ribosome validated the translation inhibitory action initially discovered in Pelletier's protein synthesis inhibition assays, and provided insight into the structural elements required for tight binding. Könst used this information to rationalize the bioactivity of several synthesized family members and numerous analogues, which has provided an invaluable understanding of the structure-activity relationships.[6] His work evolved into a thoughtful biology-driven synthesis project and showcased the therapeutic potential of the haterumaimides.

While our efforts to synthesize C12/C13-stereoisomic analogues were not entirely successful, we gained a further understanding of the limitations in our auxiliary-controlled aldol sequence and the difficulty involved with the selective formation of a β-hydroxysuccinimide motif. The (syn) 12, 13-di *epi*-stereoisomer (**2.18**) was tested against various cancer cell lines and showed a 100-fold decrease in potency

relative to the natural-configured analogue (**2.4**).[20] This data, along with the binding poses generated by Zanette for the *anti*-stereoisomers, suggest that altering this group from the natural configuration will decrease the binding affinity to the ribosome target. The imide group of CL and the glutarimide inhibitors adopt a specific orientation to form the exact same, (tight) hydrogen bonding network; therefore, rather than disruption of these critical interactions, a hybrid of the scaffolds could construct the ideal ligand. Simplifying the hydrocarbon core to a cyclohexanone (as in **2.16**) could allow for an investigation of substituent effects about the 6-membered ring. Moreover, the carbonyl group of cycloheximide occupies the same space as the C2-chlorine of CL (see overlay, **Figure 2.5**) and we are eager to see if incorporating a chlorine at this position will result in a halogen-π interaction with the proximal guanine residue. Alternatively, installing a pendent glutarimide to the CL decalin would likely result in the hydroxy group linker adopting a similar orientation to **2.16**; the extra bulk to this pendent imide could be optimal for space-filling in the E-site pocket.

2.8 Experimental Procedures

General Experimental Methods

All reactions were performed in oven-dried (120 °C) or flame-dried glassware under an atmosphere of dry argon unless otherwise noted. Reaction solvents including dichloromethane (CH_2Cl_2, Fisher, HPLC Grade), hexanes (Fisher, HPLC Grade), diethyl ether (Et_2O, Fisher, BHT stabilized, HPLC Grade), benzene (C_6H_6, Fisher, HPLC Grade), tetrahydrofuran (THF, Fisher, HPLC Grade), and toluene ($PhCH_3$, Fisher, HPLC Grade) were dried by percolation through a column packed with neutral alumina and a column packed with Q5 reactant, a supported copper catalyst for scavenging oxygen, under a positive pressure of argon.

Solvents for workup and chromatography were: acetone (Fisher, ACS grade), hexanes (Fisher or EMD, ACS Grade), EtOAc (EtOAc, Fisher, ACS Grade), dichloromethane (CH_2Cl_2, Fisher, ACS Grade), and methanol (MeOH, Fisher, ACS Grade). Column chromatography was performed using EMD Millipore 60 Å (0.040–0.063 mm) mesh silica gel (SiO_2). Analytical thin-layer chromatography was performed on Merck silica gel 60 F254 TLC plates. Visualization was accomplished with UV (254 or 210 nm), and p-anisaldehyde, ceric ammonium molybdate or potassium permanganate and heat as developing-agents.

^1H NMR and ^{13}C NMR spectra were recorded at 298 K on Bruker GN500 (500 MHz, ^1H; 125 MHz, ^{13}C), Bruker CRYO500 (500 MHz, ^1H; 125 MHz, ^{13}C), and Bruker AVANCE600 (600 MHz, ^1H; 125 MHz, ^{13}C) spectrometers. ^1H and ^{13}C spectra were referenced to residual $CHCl_3$ (7.26 ppm, ^1H or 77.0 ppm, ^{13}C). ^1H and ^{13}C spectra taken in DMSO-d_6 were referenced to residual DMSO-d_5 (2.49 ppm, ^1H or 39.5 ppm, ^{13}C). Chloroform-d ($CDCl_3$, D 99.8%, DLM-7) and dimethyl sulfoxide-d6 (CD_6SO, D 99.9%, DLM-10) were purchased from Cambridge Isotope Laboratories. Chemical shifts are reported in ppm and multiplicities are indicated by: app (apparent), s (singlet), d (doublet), t (triplet), q (quartet), m (multiplet), and br s (broad singlet). Coupling

constants, J, are reported in Hertz. Infrared (IR) spectra were recorded on a Perkin-Elmer spectrm RX1 FT-IR instrument or Varian 640-IR instrument on NaCl plates and peaks are reported in cm^{-1}. Mass spectrometry data were obtained from the University of California, Irvine Mass Spectrometry Facility. High-resolution mass spectra (HRMS) were recorded on a Waters LCT Premier spectrometer using ESI-TOF (electrospray ionization-time of flight) or CI-TOF (chemical ionization-time of flight) and data are reported in the form of (m/z). GC/FID analysis was performed on Agilent 7820A system with helium as carrier gas. HPLC analysis was performed on an Agilent 1100 series.

Citric acid (ACS grade, anhydrous, Fisher), potassium sodium tartrate (Oakwood), K_2CO_3 (anhydrous, 99%, Alfa Aesar), $NaHCO_3$ (ACS grade, Fisher), NaOH (ACS grade, Macron or Fisher), $Na_2S_2O_3$ (ACS grade, Fisher), *p*-anisaldehyde (99%, Acros Organics), selenium (IV) dioxide (SeO_2, 99.8% Acros Organics), tertbutylhydroperoxide (5.5 M in decane, Sigma-Aldrich), dimethylsulfoxide (DMSO, extra dry with molecular sieves, water <50 ppm, Acros Organics), trimethylaluminum ($Al(CH_3)_3$, Sure Pack™ reagent grade, Sigma Aldrich, diisobutylaluminum hydride (*i*-Bu_2AlH, Sure Pack™ reagent grade, Sigma Aldrich) and ammonia (2.0 M in methanol, Acros Organics), were used without further purification.

The following reagents were distilled from the indicated drying agents under argon prior to use: triethylamine (Et_3N, EMD, CaH_2), pyridine (Alfa Aesar, CaH_2 and *N,N*-diisopropylethylamine (*i*-Pr_2NEt, Alfa Aesar, CaH_2), thionyl chloride ($SOCl_2$, Sigma-Aldrich) oxalyl chloride ($(COCl_2)$, Sigma-Aldrich), trimethylsilyl triflate (TMSOTf, Acros Organics) and dibutylboron triflate (*n*-Bu_2BOTf, Acros Organics), were fractionally distilled prior to use.

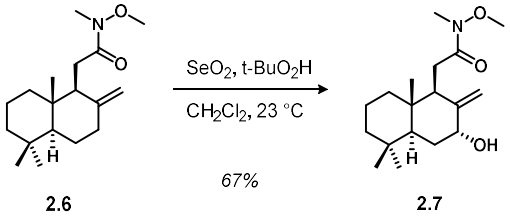

Allylic Alcohol 2.7:

A solution of *t*-butyl hydroperoxide (209 μL, 5.5 M in decane, 1.15 mmol, 4.4 equiv) was added to an ice cold stirring suspension of selenium dioxide (13.1 mg, 117 μmol, 0.3 equiv) in CH_2Cl_2 (7.8 mL, 0.05 M). After 30 min, a solution of Weinreb amide **2.6**[35] (115 mg, 392 μmol, 1.0 equiv) was added dropwise and the solution was allowed to warm to room temperature. TLC analysis indicated complete consumption of starting material after 8 h. The excess peroxide was quenched with sat. aq. Na_2SO_3. The biphasic solution was diluted with water (5 mL) and CH_2Cl_2 (5 mL) and the aqueous phase was extracted with CH_2Cl_2 (3 x 20 mL). The combined organic phases were dried ($MgSO_4$), and concentrated *in vacuo*. The crude white amorphous solid was purified by column chromatography (SiO_2, 70% EtOAc in hexanes) to give alcohol **2.7** as a thick oil (86.1 mg, 278 μmol, 67%).

^{1}H NMR (600 MHz, $CDCl_3$) δ 4.96 (s, 1H), 4.56 (s, 1H), 4.36 (t, J = 2.89 Hz, 1H), 3.72 (s, 3H), 3.15 (s, 3H), 2.98 (d, J = 10.7 Hz, 1H), 2.64 (t, J = 5.31 Hz, 1H), 2.45 (dd, J = 16.3, 3.41 Hz, 1H), 1.89 (dt, J = 13.9, 2.75 Hz, 1H), 1.77 (dd, J = 13.2, 2.81 Hz, 1H), 1.59–1.47 (m, 4H), 1.43 (d, J = 11.4 Hz, 1H) 1.27–1.18 (m, 2H), 0.904 (s, 3H), 0.818 (s, 3H), 0.714 (s, 3H); **^{13}C NMR** (125 MHz, $CDCl_3$) δ 150.9, 109.4, 73.8, 61.5, 47.5, 46.4, 42.2, 39.3, 38.8, 33.5, 33.3, 30.6, 27.1, 21.8, 19.5, 14.1; **IR** (Neat film NaCl) ν 3411.6, 2928.4, 1644.2, 1458.7, 1441.2, 1386.5 cm^{-1}; **HRMS** (ES+) *m/z* calc'd for $C_{18}H_{31}NO_3Na$ $[M+Na]^+$: 332.2202; found 332.2202; $[\alpha]_D^{25}$ –29.9 (c = 0.46, $CHCl_3$).

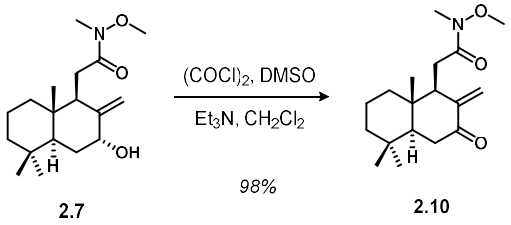

2.7 2.10

Enone 2.10:

A solution of oxalyl chloride (46.3 μL, 540 μmol, 1.2 equiv) in CH_2Cl_2 (2.7 mL) was cooled to –78℃ and DMSO (76.8 μL, 1.08 mmol, 2.4 equiv) was added. After 10 min alcohol **2.7** (140 mg in 900 μL CH_2Cl_2, 450 μmol, 1.0 equiv) was added dropwise over 10 min. The solution was stirred for 20 min and then Et_3N (314 μL, 2.25 mmol, 5 equiv) was added. The suspension was allowed to warm to 0 °C. After 40 min at 0 °C no starting material was present by TLC analysis and the mixture was diluted with hexanes (6 mL) and sat. aq. NH_4Cl (6 mL). The biphasic solution was further diluted with 1:1 hexanes in EtOAc (15 mL) and water. The organic phase was washed sequentially with brine (10 mL) and water (10 mL), dried ($MgSO_4$) and concentrated under reduced pressure. Flash column chromatography (SiO, 30% EtOAc in hexanes) gave **2.10** as a thick oil (137 mg, 445 μmol, 98% yield).

^{1}H NMR (600 MHz, $CDCl_3$) δ 5.94 (s, 1H), 5.05 (s, 1H), 3.71 (s, 3H), 3.15 (s, 3H), 2.92 (s, 1H), 1.71–1.66 (m, 2H), 1.60, (dt, J = 13.6, 3.16 Hz, 1H), 1.57 (m, 1H), 1.48 (d, J = 13.4 Hz, 1H), 1.27–1.19 (m, 3H), 0.886 (s, 6H), 0.852 (s, 3H); **^{13}C NMR** (125 MHz, $CDCl_3$) δ 202.0, 147.9, 119.7, 61.4, 50.7, 50.1, 41.5, 38.5, 38.1, 37.1, 33.4, 32.5, 28.7, 20.9, 18.8, 14.4; **IR** (Neat film NaCl) ν 2927.4, 1692.6, 1664.2, 1607.3, 1460.1, 1414.2, 1386.6 cm^{-1}; **HRMS** (ES+) *m/z* calc'd for $C_{18}H_{29}NO_3Na$ $[M+Na]^+$: 330.2045; found 330.2038; $[\alpha]_D^{23}$ –41.8 (c = 0.45, $CHCl_3$).

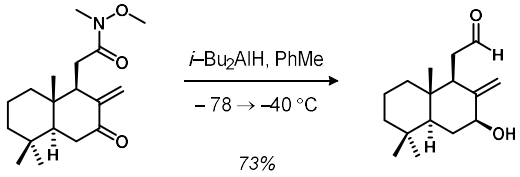

Hydroxy-aldehyde 2-S1:

Enone **2.10** (20 mg, 65 μmol, 1 equiv) was azeotroped in a 1 dram vial from benzene (30 μL) then taken up in toluene (650 μL, 0.1 M). The clear solution was cooled to –78 °C to give a cloudy white suspension. A solution of isobutylaluminum hydride (1M in toluene, 130 μmol, 130 μL, 2 equiv) was added dropwise down the side of the vial. After 3 h at –78 °C the reaction was warmed slowly to –40°C and EtOAc (50 μL) was added. The reaction mixture was warmed to –10 °C and water (10 μL) and 1M aq. NaOH (10 μL) were added sequentially followed by warming to room temperature. The reaction mixture was poured into ice water (5 mL) and extracted with (3 x 4 mL Et_2O). The combined organic phases were dried over $MgSO_4$, filtered, and concentrated. The crude substance was purified by flash column chromatography (SiO_2, 25% EtOAc in hexanes) to aldehyde give **2-S1** as a crystalline white solid (10.8 mg, 43 μmol, 66% yield).

^{1}H NMR (500 MHz, $CDCl_3$) δ 5.18 (s, 1H), 4.58 (s, 1H), 4.09 (m, 1H), 2.56 (ddd, *J* = 16.8, 10.6, 3.1 Hz, 1H), 2.48 (dd, *J* = 16.8, 4.0 Hz, 1H), 2.14–2.11 (m, 1H), 1.77 (d, *J* = 5.3 Hz, 1H), 1.76–1.59 (m, 1H), 1.54–1.50 (m, 1H), 1.45 (d, *J* = 13.0 Hz, 1H), 1.34–1.26 (m, 2H), 1.22 (td, *J* = 13.1, 4.0 Hz, 1H), 1.06 (td, *J* = 12.6, 3.9 Hz, 1H), 0.93 (s, 3H), 0.83 (s, 3H), 0.70 (s, 3H); **^{13}C NMR** (125 MHz, $CDCl_3$) δ 202.8, 150.5, 104.8, 73.4, 52.8, 49.0, 41.8, 39.6, 39.1, 38.6, 33.45, 33.42, 21.6, 19.1, 14.5; **IR** (film) ν 3422, 2924, 2846, 2721, 1722, 1649, 1460, 1388 cm^{-1}; **HRMS** (ES+) *m/z* calc'd for $C_{16}H_{26}O_2Na$ $[M + Na]^+$: 273.1830; found 273.1827; **$[\alpha]^{22}_D$** –15.3 (*c* = 0.2, $CHCl_3$).

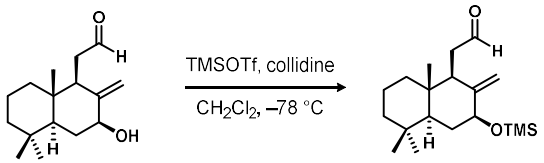

2-S1 2.12

TMS-Aldehyde 2.12:

Hydroxyaldehyde **2-S1** (9.0 mg, 36 μmol, 1.0 equiv) was dissolved in CH_2Cl_2 (375 μL, 0.09M) and cooled to –78 °C. To the reaction mixture were sequentially added 2,4,6-collidine (57 μL, 360 μmol, 10 equiv) and TMSOTf (40 μL, 216 μmol, 6.0 equiv). After 1 h at –78 °C, triethylamine (50 μL) and methanol (100 μL) were added and the flask was warmed to ambient temperature. The solution was diluted with 10% EtOAc in hexanes (5 mL) and washed consecutively with water, citric acid (10% aq.), and brine (4 mL each). The organic extract was dried over $MgSO_4$, filtered, and concentrated under reduced pressure. The residue was purified by flash column chromatography to give aldehyde **2.12** a thin clear film (9.2 mg, 28.3 μmol, 80% yield).

^{1}H NMR (600 MHz, $CDCl_3$) δ 9.63 (s, 1H), 5.21 (s, 1H), 4.54 (s, 1H), 4.02 (m, 1H), 2.53 (ddd, *J* = 19.9, 10.5, 3.12 Hz, 1H), 2.45 (dd, *J* = 16.7, 4.0 Hz, 1H), 2.28 (d, *J* = 10.5, 1H) 1.92 (app. d, *J* = 10, 1H) 1.59–1.56 (m, 1H), 1.55–1.48 (m, 2H), 1.44 (d, *J* = 13.2 Hz, 1H), 1.36 (q, *J* = 12.6 Hz, 1H), 1.25–1.16 (m, 2H), 1.04 (t, *J* = 12.9 Hz, 1H), 0.89 (s, 3H), 0.82 (s, 3H), 0.69 (s, 3H), 0.13 (s, 9H); **^{13}C NMR** (125 MHz, $CDCl_3$) δ 203.0, 149.7, 105.9, 73.9, 52.9, 49.2, 41.8, 39.6, 39.2, 38.6, 34.2, 33.4, 29.5, 21.6, 19.2, 14.5, –0.10; **IR** (film) ν 2951, 2845, 2712, 1727, 1649, 1459, 1389, 1250 cm^{-1}; **HRMS** (ES+) *m/z* calc'd for $C_{19}H_{34}O_2SiNa$ $[M + Na]^+$: 345.2226; found 345.2229; **$[\alpha]_D^{25}$** -10.4 (*c* = 0.38, $CHCl_3$).

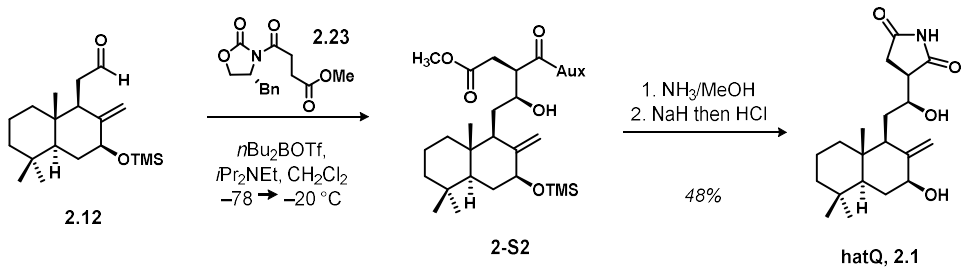

Haterumaimide Q (2.1)

Imide **2.23**[36] (15 mg, 57.4 μmol, 1.3 equiv.) was dried by azeotropic distillation from of benzene (20 μL) in a 1 dram vial and dissolved in CH_2Cl_2 (450 μL). The solution was cooled to –78 °C and *n*Bu_2BOTf (1.0 M in CH_2Cl_2, 60 μL, 60 μmol, 1.4 equiv.) was added along the side of the vial. The clear solution was stirred at –78 °C for 30 min. At that temperature, *i*Pr_2NEt (1.0 M in CH_2Cl_2, 78 μmol, 1.8 equiv.) was added and the mixture was stirred for 20 min. To ensure complete enolization, the vial was warmed to 0 °C for 30 sec and cooled back to –78 °C. The solution often becomes pale yellow upon warming but remained clear. A solution of aldehyde **2.12** (11.0 mg in 100 μL CH_2Cl_2, 34.5 μmol, 1.0 equiv.) was added at –78 °C and the reaction vial was warmed over 1.5 hours to –25 °C and a temperature between –30 and –25 °C was maintained for 20 h. The reaction mixture was quenched with methanol (50 μL) warmed to ambient temperature, and water (3 mL) and CH_2Cl_2 (3 mL) were added. The phases were separated and the aqueous phase was extracted with CH_2Cl_2 (2 x 3 mL). The combined organic extracts were dried ($MgSO_4$), filtered, and concentrated *in vacuo* to yield crude product aldol adduct as a yellow oil. The crude aldol product (**2-S2**)was transferred to a 1 dram vial, NH_3 (2.0 M in methanol, 800 μL) was added, and the reaction was stirred at 23 °Cfor 24 h. The solution was concentrated *in vacuo* to afford a thick yellow oil. To complete succinimide formation, the crude material was dissolved in dry THF (400 μL) and NaH (55% suspension in mineral oil, 5 mg, 145 μmol) was added at ambient temperature. The solution evolved bubbles for ~10 min. Water (200 μL) was added followed by 1 M HCl (100 μL). The

solution was quickly added to a mixture of brine (1 mL), and water (1 mL) and extracted with CH_2Cl_2 (4 x 4 mL CH_2Cl_2). The combined organic extracts were dried ($MgSO_4$) and concentrated under reduced pressure. Flash chromatography (SiO_2, 50%→65% EtOAc in hexanes) afforded a modestly (~80%) pure product. To further purify the product, this mixture was taken up in CH_2Cl_2 (250 μL) and hexanes were added until a white precipitate formed (~300 μL). The suspension was centrifuged for 1 min and the solvent was decanted with a pipette, leaving pure haterumaimide Q (**2.1**) as a white film in a 10:1 mixture with the minor diastereomer (5.7 mg, 16.4 μmol, 48% yield). The spectral data for this compound was in good agreement with those reported in the literature.[37]

For ^{1}HNMR and ^{13}CNMR data comparison to natural **2.1** in $(CD_3)_3SO$ see **Table 2.2**.

^{1}H NMR (600 MHz, $CDCl_3$) δ 7.94 (s, 1H), 5.28 (s, 1H), 4.86 (s, 1H), 4.34 (m, 1H),3.99 (app. dd, *J* = 11.1, 5.4 Hz, 1H), 2.92–2.89 (m, 1H), 2.86 (dd, *J* = 16.5, 5.5 Hz, 1H), 2.67 (dd, *J* = 16.5, 7.6 Hz, 1H), 2.13–2.10 (m, 1H), 2.06 (s, 1H), 1.82–1.77 (m, 2H), 1.69 (d, 12.3 Hz, 1H), 1.64, (dd, *J* = 14.2, 8.1 Hz, 1H), 1.59–1.56 (m, 1H), 1.53 (t, *J* = 3.5 Hz, 1H), 1.49 (d, *J* = 11.3 Hz, 1H), 1.44 (d, *J* = 13.3, 1H), 1.28–1.24 (m, 2H), 1.14 (td, *J* = 13.1, 2.4 Hz, 1H), 0.95–0.85 (m, 1H), 0.89 (s, 3H), 0.81 (s, 3H), 0.68 (s, 3H); **^{13}CNMR** (125 MHz, $CDCl_3$) δ 178.6, 176.4, 150.6, 104.2, 73.7, 69.0, 53.3, 51.9, 46.7, 41.8, 39.4, 39.0, 33.8, 33.5, 33.4, 29.3, 29.0, 21.5, 19.2, 14.4; m.p. = 197–200°C; **IR** (film) ν 3406.9, 2925.7, 1776.8, 1709.4, 1361.1, 1190.0 cm^{-1}; **HRMS** (ES+) m/z calc'd for $C_{20}H_{31}NO_4Na$ $[M + Na]^+$: 372.2151, found 372.2160. **$[\alpha]_D^{25}$** +30.2 (*c* = 0.03, $CHCl_3$ [lit: **$[\alpha]_D^{25}$** +36.0 (*c* = 0.19, $CHCl_3$).

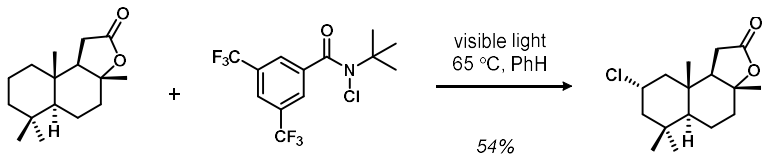

2.2 2.13 2.6

2-Chlorosclareolide (2.6):

(+)-Sclareolide **2.2** (200 mg, 0.8 mmol, 1.0 equiv), and chloroamide **2.13**[15] (3.5 g, 10.0 mmol, 2.5 equiv) were dissolved in benzene (13 mL) and the mixture was degassed for 20 min with an Ar balloon bearing a 22 gauge 4 inch needle. A reflux condenser was attached to the flask and the mixture was heated at reflux for 24 h, and irradiated with 2 X CFL bulbs (40W). The reaction mixture was cooled to ambient temperature and concentrated *in vacuo*. Direct chromatographic purification (SiO_2, 10% EtOAc in hexanes) afforded a white solid (124 mg, 0.44 mmol, 55% yield). Our data matches those previously reported by Groves.[4]

^{1}H NMR (500 MHz, $CDCl_3$) δ 4.22 (tt, *J*= 12.2, 4.2 Hz, 1H), 2.43 (dd, *J*=16.2, 14.8 Hz, 1H), 2.29 (dd, *J*= 16.2, 6.5 Hz, 1H), 2.13 (dt, *J*= 12.0, 3.3 Hz, 1H), 1.98–2.07 (m, 2H), 1.91 (dq, *J*= 14.4, 3.3 Hz, 1H), 1.70 (td, *J*= 12.4, 4.3 Hz, 1H), 1.54 (t, *J*= 12.7 Hz, 1H), 1.32–1.42 (m, 2H), 1.33 (s, 3H), 1.13 (dd, *J*= 12.7, 2.7 Hz, 1H), 0.972 (s, 3H), 0.968 (s, 3H), 0.90 (s, 3H); **^{13}C NMR** (125 MHz, $CDCl_3$) δ 176.0, 85.8, 58.6, 55.7, 53.8, 52.4, 49.7, 38.4, 38.2, 35.8, 32.9, 28.6, 21.6, 21.3, 20.1, 15.8; **IR** (film) 2951, 2871, 1773, 1387, 1197 cm^{-1}; **HRMS** (ES+) *m/z* calc'd for $C_{16}H_{25}O_2Cl$ $[M]^+$: 284.1543; found 284.1548; **$[\alpha]^{25}_D$** +48.2° (*c*= 1.00, $CHCl_3$).

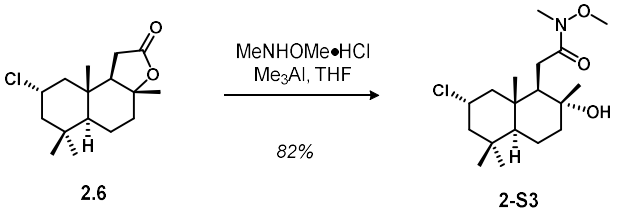

2.6 2-S3

Amide 2-S3:

Trimethylaluminum (2.0 M in toluene, 3.01 mmol, 2.1 equiv.) was added to a suspension of N,O-dimethylhydroxylamine hydrochloride (287 mg, 2.97 mmol, 2.0 equiv.) in CH_2Cl_2 (4.5 mL) at 0 °C. The suspension became a clear solution upon stirring for 10 min. The ice bath was removed and after 2h a solution of **2.6** (400 mg, 1.11 mmol, 1equiv.) in CH_2Cl_2 (4.5 mL) was added dropwise at room temperature. After stirring for 2 hours at room temperature the reaction was cooled to 0 °C and 5 mL of 10% H_2SO_4 was added. The ice bath was removed and the crude mixture was diluted with CH_2Cl_2 (15 mL) and 1 M HCl (10 mL). The organic phase was separated and the aqueous phase was extracted with CH_2Cl_2 (2 x 20 mL). The combined organic layers were dried over $MgSO_4$, filtered and concentrated *in vacuo*. The crude product was purified by flash chromatography (SiO_2, 80% EtOAc in hexanes) to afford amide **2-S3** as a thick oil (328 mg, 0.912 mmol, 82% yield).

^{1}H NMR (600 MHz, $CDCl_3$) δ 4.17 (tt, *J*= 12.3, 4.0 Hz, 1H), 3.74 (s, 1H), 3.20 (s, 1H), 2.58 (d, *J*= 16.1 Hz, 1H), 2.48 (dd, *J*= 16.4, 6.7 Hz, 1H), 2.08 (ap d, *J*= 10.9, 1H), 2.03 (dd, *J*= 6.5, 3.6 Hz, 1H), 1.92–1.98 (m, 2H), 1.69 (dq, *J*= 13.8, 2.4 Hz, 1H), 1.50 (t, *J*= 12.7 Hz, 1H), 1.47 (dd, *J*= 13.3, 3.9 Hz, 1H), 1.32 (t, *J*= 12.2 Hz, 1H), 1.26 (qd, *J*= 13.2, 3.2 Hz, 1H) 1.16 (s, 1H), 1.09 (dd, *J*= 12.3, 2.0 Hz, 1H), 0.95 (s, 3H), 0.88 (s, 3H), 0.85 (s, 3H); **^{13}C NMR** (125 MHz, $CDCl_3$) δ 175.5, 72.7, 61.3, 56.3, 55.8, 55.1, 54.9, 51.9, 49.6, 44.1, 41.0, 35.9, 33.1, 27.0, 23.4, 21.8, 20.1, 16.5; **IR** (film) ν 3500, 2966, 2927, 1655, 1454, 1340, 1158 cm^{-1}; **HRMS** (ES+) *m/z* calc'd for $C_{18}H_{32}O_3ClNa$ $[M+Na]^+$: 368.1968; found 368.1963; $[\alpha]^{25}_D$ +32.9 (*c*= 1.00, $CHCl_3$).

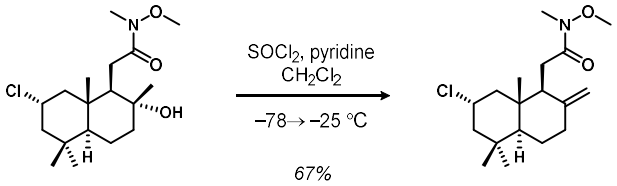

Alkene 2-S4:

Alcohol **2-S3** (510 mg, 1.46 mmol, 1.0 equiv.) was dissolved in CH_2Cl_2 (10 mL). Pyridine (236 μL, 2.92 mmol, 2.0 equiv.) was added, and the solution was cooled to –78 ˚C. Pyridine (969 μL, 12.0 mmol, 8.25 equiv.) was added to a conical flask containing $SOCl_2$ (530 μL, 7.30 mmol, 5 equiv.) and CH_2Cl_2 (15 mL) and this clear mixture was transferred via a Teflon cannula dropwise over 15 min to the flask containing alcohol **2-S3**. The reaction was complete after 45 min at –78 ˚C and sat. aq. $NaHCO_3$ (20 mL) was added. The product mixture was warmed to ambient temperature, the phases were separated and the aqueous phase was extracted (2 x 30 mL CH_2Cl_2). The combined organic extracts were dried ($MgSO_4$), filtered, and concentrated under reduced pressure. The pale yellow crude oil was purified by flash column chromatography (SiO_2, 8% EtOAc in hexanes) to afford alkene **8** as a white solid (319 mg, 0.971 mmol, 67% yield).

^{1}H NMR (600 MHz, $CDCl_3$) δ 4.78 (s, 1H), 4.48 (s, 1H), 4.17 (tt, *J* = 12.3, 3.9 Hz, 1H), 3.73 (s, 3H), 3.16 (s, 3H), 2.72 (dd, *J* = 15.0, 10.7 Hz, 1H), 2.58 (d, *J* = 10.1 Hz, 1H), 2.37–2.42 (m, 2H), 2.09–2.18 (m, 2H), 1.98 (ddd, *J* = 12.8, 3.7, 2.2 Hz, 1H), 1.70–1.76 (m, 1H), 1.55 (t, *J* = 12.6 Hz, 1H), 1.50 (t, *J* = 12.2 Hz, 1H), 0.97 (s, 3H), 0.85 (s, 3H), 0.79 (s, 3H); **^{13}C NMR** (125 MHz, $CDCl_3$) δ 174.1, 148.3, 107.0, 61.4, 55.8, 53.9, 52.0, 51.4, 49.3, 41.2, 37.1, 36.1, 33.3, 32.5, 24.1, 23.4, 22.2, 15.3; IR (film) ν 2939, 2852, 1776, 1667, 1461, 1385, 1004 cm^{-1}; **HRMS** (ESI) *m/z* calc'd for $C_{18}H_{30}O_2ClNNa$ $[M + Na]^+$ 350.1863, found 350.1866; $[\alpha]^{25}_D$ +7.38 (*c* = 1.00, $CHCl_3$).

Allylic alcohol 2-S5:

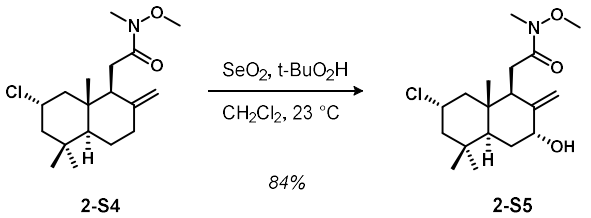

Alkene **2-S4** (336 mg, 1.02 mmol, 1 equiv.) was subjected to the same reaction conditions as **2.6** to make **2.7.** Allylic alcohol **2-S5** was purified by flash chromatography (SiO_2, 75 → 85% EtOAc in hexanes) and isolated as a white solid (293 mg, 0.856 mmol, 84% yield).

^{1}H NMR (500 MHz, $CDCl_3$) δ 5.01 (s, 1H), 4.61 (s, 1H), 4.37 (s, 1H), 4.17 (tt, *J* = 12.3, 3.9 Hz, 1H), 3.74 (s, 3H), 3.16 (s, 3H), 3.06 (d, *J* = 10.8 Hz, 1H), 2.68 (dd, *J* = 15.8, 10.9 Hz, 1H), 2.42 (dd, *J* = 16.1, 3.3 Hz, 1H), 2.13 (ap d, *J* = 12.1 Hz, 1H) 2.00 (ddd, *J* = 12.8, 3.8, 2.1 Hz, 1H), 1.91 (dt, *J* = 13.9, 2.7 Hz, 1H), 1.84 (dd, *J* = 12.9, 2.9 Hz, 1H), 1.60 (t, *J* = 12.6 Hz, 1H), 1.56 (t, *J* = 12.2 Hz, 1H), 1.48 (td, *J* = 13.4, 3.1 Hz, 1H), 0.98 (s, 3H), 0.87 (s, 3H), 0.76 (s, 3H); **^{13}C NMR** (125 MHz, $CDCl_3$) δ 177.5, 149.6, 110.2, 77.2, 73.1, 61.4, 55.7, 52.0, 49.0, 46.2, 46.0, 41.3, 35.7, 32.4, 33.0, 29.8, 26.7, 22.1, 14.4; **IR** (film) ν 3405, 2960, 2939, 2897, 1645, 1460, 1436, 1389, 766 cm^{-1}; **HRMS** (ES+) *m/z* calc'd for $C_{18}H_{30}O_3ClNNa$ [M + Na]$^+$: 366.1812, found 366.1818; **[α]$^{25}_D$** –25.7 (*c* = 0.60, $CHCl_3$).

Enone 2-S6:

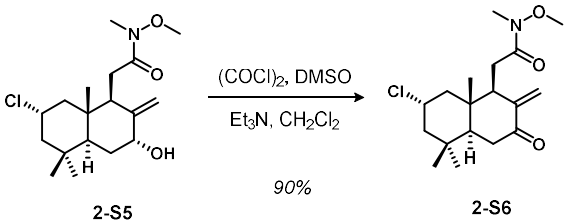

Allylic alcohol **2-S5** (110 mg, 0.320 mmol, 1 equiv.) was subjected to the same reaction conditions as **2.7** to make **2.10**. The crude product was purified by flash chromatography (SiO_2, 60% EtOAc in hexanes) to afford **2-S6** as a clear oil (98.2 mg, 0.288 mmol, 90 % yield).

^{1}H NMR (500 MHz, $CDCl_3$) δ 6.00 (d, *J* = 2.5 Hz, 1H), 5.11 (d, *J* = 2.4 Hz, 1H), 4.18 (tt, *J* = 12.4, 3.8 Hz, 1H), 3.74 (s, 3H), 3.19 (s, 3H), 2.97–3.03 (m, 1H), 2.58–2.72 (m, 3H), 2.28 (dd, *J* = 17.9, 14.1 Hz, 1H), 2.23 (ap d *J* = 12.5 Hz, 1H), 2.05 (ddd, *J* = 12.9, 3.7, 2.2 Hz, 1Hz), 1.73 (dd, *J* = 14.0, 4.6 Hz, 1H), 1.60 (t, *J* = 12.7 Hz, 1H), 1.56 (t, *J* = 12.3 Hz, 1H), 0.96 (s, 3H), 0.94 (s, 3H), 0.91 (s, 3H); **^{13}C NMR** (125 MHz, $CDCl_3$) δ 200.6, 146.8, 121.1, 72.1 61.5, 54.6, 51.6, 49.8, 49.6, 48.9, 39.5, 37.5, 36.0, 32.7, 32.3, 28.9, 21.4, 15.1; **IR** (film) ν 2963, 1693, 1662, 1608, 1461, 1415, 1388, 1264 cm^{-1}; **HRMS** (ES+) *m/z* calc'd for $C_{18}H_{28}O_3ClNNa$ $[M + Na]^+$: 364.1655, found 364.1658; **$[\alpha]^{22}_D$** –36.3 (*c* = 0.51, $CHCl_3$).

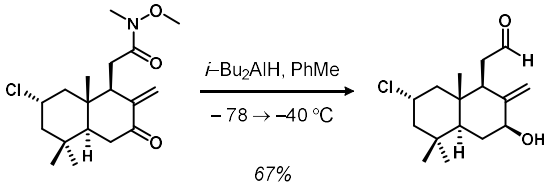

2-S6 2-S7

Hydroxyaldehyde 2-S7:

Enone **2-S6** (70 mg, 0.204 mmol, 1 equiv.) was subjected to the same reaction conditions as **2.10** to make **2-S1**. The crude residue was purified by flash chromatography (SiO_2, 35% EtOAc in hexanes) to afford **2-S7** as a colorless oil (47 mg, 0.165 mmol, 67% yield).

^{1}H NMR (500 MHz $CDCl_3$) δ 9.66 (d, *J* = 3.0 Hz, 1H) 5.23 (s, 1H), 4.62 (s, 1H), 4.16 (tt, *J* = 12.3, 4.0 Hz, 1H), 4.10 (br s, 1H), 2.63 (ddd, *J* = 17.0, 11.1, 3.0 Hz, 1H), 2.48 (dd, *J* = 17.0, 3.5 Hz, 1H), 2.41 (ap d, *J* = 11.0 Hz, 1H), 2.07–2.14 (m, 3H), 2.02 (ddd, *J* = 13.0, 3.9, 2.1 Hz, 1H), 1.86 (d, *J* = 4.1 Hz, 1H), 1.55 (t, *J* = 12.7 Hz, 1H), 1.41 (t, *J* = 12.2 Hz, 1H), 1.23–1.32 (m, 2H), 1.00 (s, 3H), 0.88 (s, 3H), 0.75 (s, 3H); **^{13}C NMR**(125 MHz, $CDCl_3$) δ 201.6, 149.3, 105.9, 72.97, 55.0, 51.84, 51.76, 49.4, 48.5, 40.7, 39.3, 35.9, 33.2, 32.7, 22.1, 15.1; **IR** (film) ν 3400, 2960, 2853, 2725, 1720, 1647, 1459, 1391 cm^{-1}; **HRMS**

(ES+) *m/z* calc'd for $C_{16}H_{25}O_2ClNH_4$ $[M+NH_4]^+$: 302.1887, found 302.1882. $[\alpha]^{22}_D$ –18.1(*c* = 1.0, $CHCl_3$).

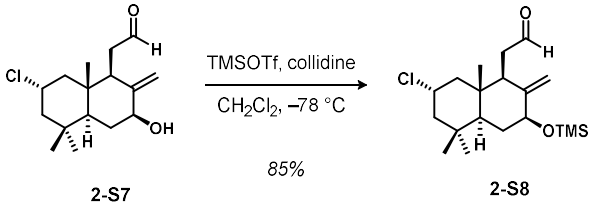

TMS-ether 2-S8:

Hydroxyaldehyde **2-S7** (45 mg, 0.158 mmol, 1 equiv.) was subjected to the same reaction conditions as **2-S1** to makes **2.12**. The crude residue as purified by flash chromatography (SiO_2, 5% → 10% EtOAc in hexanes) to afford **2-S8** as a pale yellow oil (48 mg, 0.134 mmol, 85% yield).

^{1}H NMR (500 MHz, $CDCl_3$) δ 9.64 (d, *J* = 2.8 Hz, 1H), 5.25 (s, 1H), 4.58 (s, 1H), 4.15 (tt, *J* = 12.2, 3.8 Hz, 1H), 4.02 (ap dd, *J* = 10.1, 5.2 Hz, 1H), 2.62 (ddd, *J* = 16.8, 10.9, 3.1 Hz, 1H), 2.46 (dd, *J* = 16.8, 3.5 Hz, 1H), 2.39 (ap d, *J* = 10.6 Hz, 1H), 2.08 (ap d, *J* = 12.1 Hz, 1H), 2.03 (ddd, *J* = 12.9, 3.9, 2.0 Hz, 1H), 1.93 (ddd, *J* = 11.9, 4.2, 1.7 Hz, 1H), 1.54 (t, *J* = 12.7 Hz, 1H), 1.39 (t, *J* = 11.9 Hz, 1H), 1.32 (ap t, *J* = 11.1 Hz, 1H), 1.29 (t, *J* = 15.1 Hz, 1H), 0.98 (s, 3H), 0.87 (s, 3H), 0.75 (s, 3H), 0.13 (s, 9H); **^{13}C NMR**(125 MHz, $CDCl_3$) δ 201.8, 148.5, 107.0, 73.5, 55.1, 51.9, 51.8, 49.5, 48.6, 40.7, 39.4, 35.8, 33.6, 33.1, 22.1, 15.1, –0.1; **IR** (film) ν 2956, 2851, 2718, 1726, 1650, 1460, 1393, 1251 cm^{-1}; **HRMS** (ES+) *m/z* calc'd for $C_{19}H_{33}O_2ClSiNH_4$ $[M+NH_4]^+$: 374.2282, found 374.2285; $[\alpha]_D^{22}$ –8.60 (*c* = 1.10, $CHCl_3$).

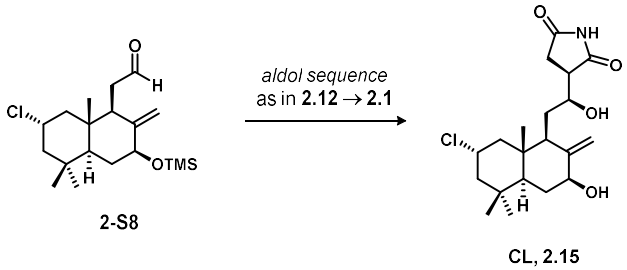

2-S8 CL, 2.15

(+)–chlorolissoclimide (2.15):

TMS-ether **2-S8** (13 mg, 36.5 μmol, 1 equiv.) was subjected to the same reaction conditions as **2.12** to make hatQ (**2.1**). The crude imide residue was purified by flash chromatography (SiO_2, 55% → 65% EtOAc in hexanes) to afford **2.15** as a white solid in a 7:1 mixture with a minor diastereomer. To further purify, the mixture was taken up in CH_2Cl_2 (200 μL), cooled to 0 °C and added hexanes dropwise until a precipitate formed. The mixture was centrifuged for 1 min, the solvent was decanted with a pipette, leaving pure chlorolissoclimide (**2.15**) as a white (5.1 mg, 13.5 μmol, 37% yield).

The data obtained for synthetic CL (**2.15**) matched those reported by Biard.[38] For ^{1}H HMR and ^{13}C NMR data comparison to natural **2.15** in CD_2Cl_2 see Table 2 below.

^{1}H NMR (500 MHz) δ 8.88 (br s, 1H), 5.30 (s, 1H), 4.90 (s, 1H), 4.29 (br s, 1H), 4.17 (tt, J = 12.2, 3.9 Hz, 1H), 4.00 (s, 1H), 3.03 (d, J = 3.2 Hz, 1H), 2.88–2.95 (m, 1H), 2.85 (dd, J = 18.0, 5.0 Hz, 1H), 2.68 (dd, J = 18.0, 9.2 Hz, 1H), 2.61 (br s, 1H), 2.20 (, J = 10.5 Hz, 1H), 2.09 (dd, J = 10.3, 4.8 Hz, 1H), 2.02 (d, J = 10.9 Hz, 1H), 1.82 (ddd, J = 13.2, 11.6, 5.3 Hz, 1H), 1.69 (s, 1H), 1.55–1.63 (m, 1H), 1.52 (t, J = 12.7 Hz, 1H), 1.23–1.28 (m, 2H), 1.20 (t, J = 14.2 Hz, 1H), 0.99 (s, 3H), 0.87 (s, 3H), 0.74 (s, 3H); **^{13}C NMR** (125 MHz, CDCl3) δ 178.4, 176.0, 149.6, 105.5, 73.3, 68.9, 55.0, 52.2, 51.9, 51.7, 49.4, 46.7, 41.6, 35.9, 33.2, 33.1, 29.3, 29.0, 22.0, 15.0; **IR** (film) ν 2972, 2951, 1773, 1709, 1647, 1538,

1461, 1368 cm–1; **HRMS** (ES+) m/z calc'd for C20H30O4ClNH4 [M + Na]+: 406.1761, found 406.1756; $[\alpha]^{22}_{D}$ +50 (c = 0.11, CH3OH), [lit.: $[\alpha]^{25}_{D}$ +119.3° (c = 1.59, CH3OH)].

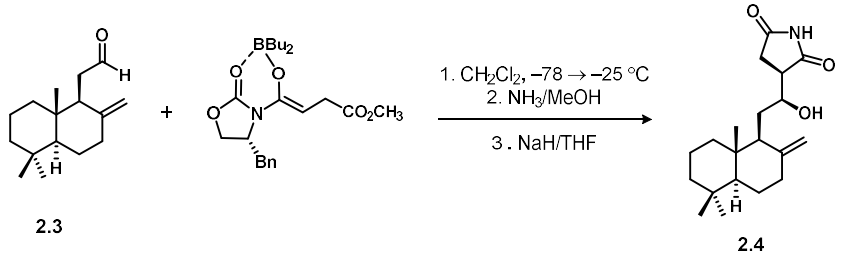

2.3 2.4

Hydroxyimide 2.4:

Aldehyde **2.3** (15 mg, 64.1 μmol, 1 equiv.) was subjected to the same reaction conditions as **2.12** to make **2.1**. The crude residue was purified by flash chromatography (SiO_2, 40% → 50% EtOAc in hexanes) to afford **2.4** as a white solid (11.2 mg, 35.2 μmol, 55% yield).

^{1}H NMR (600 MHz) δ 8.06 (br s, 1H), 4.91 (s, 1H), 4.67 (s, 1H), 4.35 (t, *J* = 6.5 Hz, 1H), 2.92–2.84 (m, 2H), 2.66 (dd, *J* = 17.7, 8.9 Hz, 1H), 2.42 (app d, *J* = 12.6 Hz, 1H), 1.98 (td, *J* = 12.9, 4.5 Hz, 1H), 1.77–1.68 (m, 3H), 1.62–1.55 (m, 4H), 1.54–1.49 (m, 2H), 1.41 (app d, *J* = 13.1 Hz, 1 H), 1.36–1.29 (qd, *J* = 12.9, 4.5 Hz, 1 H), 1.26–1.24 (m, 1H), 1.19–1.14 (M, 1H), 1.08 (dd, *J* = 12.9, 2.9 Hz, 1H), 0.94 (td, *J* = 12.9, 4.0 Hz, 1H), 0.87 (s, 3H), 0.80 (s, 3H), 0.68 (s, 3H); **^{13}C NMR** (125 MHz) δ 179.4, 176.9, 149.2, 10.5, 69.4, 55.6, 53.7, 46.6, 41.8, 39.7, 39.0, 38.1, 33.4, 33.3, 29.2, 28.9, 24.0, 21.4 19.1, 14.2; **HMRS** (ESI) *m/z* calc'd for $C_{20}H_{31}O_3NNa$ $(M+Na)^+$ 356.2203 found 356.2295.

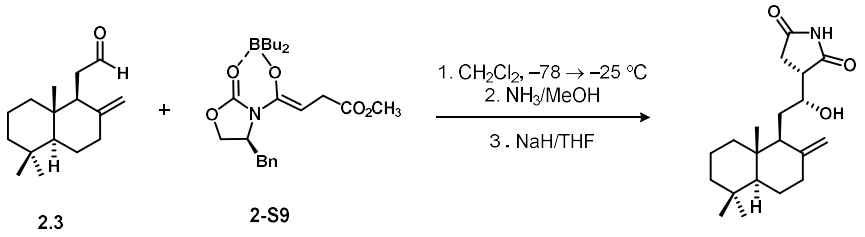

2.3 2-S9 2.18

C12, C13-epi-hydroxyimide 2.18:

Aldehyde **2.3** (15 mg, 64.1 μmol, 1 equiv.) was subjected to the same reaction conditions as **2.12** to make **2.1** but the *(S)*–enantiomer of the acylated oxazolidinone (**2-S9**) was used instead of the *(R)*–enantiomer (**2.23**). The crude residue was purified by flash chromatography (SiO_2, 40% → 50% EtOAc in hexanes) to afford **2.18** as a colorless oil (8.5 mg, 25.6 μmmol, 40% yield).

^{1}H NMR (500 MHz) δ 8.04 (br s, 1H), 4.86 (s, 1H), 4.41 (s, 1H), 4.27 (app d, *J* = 9.9 Hz, 1H), 2.90–2.83 (m, 2H), 2.69 (dd, *J* = 18.2, 9.3 Hz, 1H), 2.41 (app d, *J* = 12.7 Hz, 1H), 2.01–1.93 (m, 2H), 1.90 (d, *J* = 10.8 Hz, 1H), 1.77–1.73 (m, 1H), 1.69 (d, *J* = 12.8 Hz, 1H), 1.62–1.47 (m, 3H), 1.41–1.39 (m, 1H), 1.33 (dd, *J* = 12.8, 4.7 Hz, 1H), 1.21–1.14 (m 3H), 1.06 (td, *J* = 13.2, 4.4 Hz, 1H), 0.88 (s, 3H), 0.80 (s, 3H), 0.67 (s, 3H); **^{13}C NMR** (125 MHz) δ 178.8, 176.5, 148.3, 106.7, 67.8, 55.4, 52.3, 48.2, 41.9, 39.4, 38.9, 38.1, 33.5, 33.5, 29.9, 29.0, 24.3, 21.6, 19.3, 14.6.

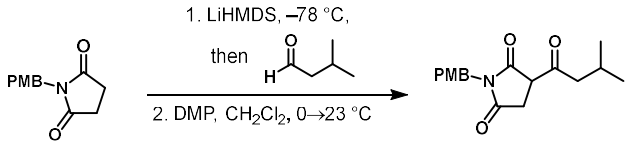

2-S10 *69%* 2.29

PMB-protected keto-imide 2.29:

A heterogeneous solution of PMB-succinimide (**2-S10**) (0.70 g, 3.19 mmol, 1 equiv.) in THF (27 mL,) was cooled to –78 °C and LiHMDS (4.15 mL, 1.3 equiv, 1 M in THF) was added dropwise over 10

mins upon which the slurry turned a bright orange color and was stirred at this temperature for 30 min. To ensure complete enolization, the flask was warmed to –10 °C for 1 min and then cooled back down to –78 °C. Isovaleraldehyde (490 μL, 4.47 mmol, 1.4 equiv) in THF (4.47 mL, 1 M) was added dropwise to the reaction mixture over 20 mins and was stirred at –78 °C for 2 h. The solution became homogenous and was warmed to –25 °C and stirred here for 1 h. The reaction was quenched with dropwise addition of saturated aqueous NH_4Cl (5 mL), warmed to ambient temperature, and water (25 mL) was added. The phases were separated and the aqueous phase was extracted with EtOAc (2 **x** 10 mL). The combined organic extracts were dried ($MgSO_4$), filtered and concentrated *in vacuo* to yield 0.92 g of sufficiently pure aldol product, which was carried onto the next step without purification. The crude aldol product was taken up in wet CH_2Cl_2 (60 mL, 0.05 M) and cooled to 0 °C. Dess-Martine Periodinane (1.78 g, ~1.4 equiv.) was added portion-wise and the heterogenous reaction mixture was stirred for 5 h as it warmed to ambient temperature. After no starting material was present by TLC analysis the reaction mixture was filtered through Celite washing with 25 mL Et_2O:pentane (1:10). The organic filtrate was concentrate *in vacuo* and the residue was taken up in 20 mL of the (1:10) Et_2O:pentane solution. The organic solution was washed with water (10 mL), brine (10 mL), then was dried (Mg_2SO_4), filtered and concentrated. The crude oil was purified by chromatography (SiO_2, 25% EtOAc in hexanes) to afford **2.29** as a thick oil (0.82 g, 2.69 mmol, 69%).

2.29 is in an 8:1 equilibrium mixture with the enol tautomer, the ^{1}H NMR ^{13}C NMR shifts are listed for major keto-tautomer.

^{1}H NMR (600 MHz, $CDCl_3$) δ 7.28 (d, *J* = 8.6 Hz, 2H), 6.82 (d, *J* = 8.6 Hz, 2H), 4.58 (d, *J* = 14.1 Hz, 1H), 4.53 (d, *J* = 14.1 Hz, 1H), 3.87 (dd, *J* = 8.90, 4.18 Hz, 1H), 3.77 (s, 3H), 3.29–3.26 (dd, *J* = 18.3, 4.2,

1H), 2.87–2.83 (dd, *J* = 17.4, 7.4 Hz, 1H), 2.65–2.60 (dd, *J* = 18.3, 8.9 Hz, 1H), 2.58–2.54 (dd, *J* = 17.4, 6.2 Hz, 1H), 2.20–2.12 (m, 1H), 0.96–0.95 (d, *J* = 6.6 Hz, 3H), 0.90–0.89 (d, *J* = 6.6 Hz, 3H); **^{13}CNMR** (125 MHz, $CDCl_3$) δ 201.3, 175.3, 172.4, 159.4, 130.3, 127.6, 114.0, 55.3, 53.3, 51.9, 42.3, 29.9, 24.1, 22.6, 22.2 ; **IR**(film) ν 3031.2, 2957.6, 1702.6, 1612.6, 1514.1 cm^{-1}; **HRMS** (ES+) m/z calc'd for $C_{17}H_{21}NO_4Na$ $[M+Na]^+$: 326.1368, found 326.1359.

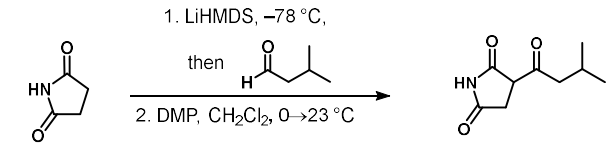

Free N-H keto-imide 2.30:

Succinimide (1.0 g, 10.1 mmol, 1 equiv.) was subjected to the reaction conditions with isovaleraldehyde describe above for **2.29** to provide crude aldol product. This was subjected to crude purification through a plug of SiO_2 eluting with 50% EtOAc in hexanes and concentrated under reduced pressure to afford aldol product of sufficient purity to carry on to the next step. The crude aldol product was subjected to the reaction conditions described above for **2.29** with Dess-Martin Periodinane to provide imide **2.30** (183 mg, 0.92 mmol, 19%) as a white solid (m.p. = 80–82 °C) after flash chromatography (SiO_2, 25% EtOAc in hexanes).

Imide **2.30** is in a 6:1 equilibrium mixture with the enol tautomer, the ^{1}H NMR ^{13}C NMR shifts are listed for major keto-tautomer.

^{1}H NMR (600 MHz, $CDCl_3$) δ 8.35 (s, 1H), 3.95 (dd, *J* = 9.0, 4.4 Hz, 1H) 3.35 (dd, *J* = 18.5, 4.4 Hz, 1H), 2.86 (dd, *J* = 17.5, 7.4 Hz, 1H), 2.69 (dd, *J* = 18.5, 9.0 Hz, 1H), 2.57 (dd, *J* = 17.5, 6.1 Hz, 1H), 2.23–2.18 (m, 1H), 0.97 (app. t, *J* = 6.1 Hz, 6H), 0.93 (d, *J* = 6.6 Hz, 3H); **^{13}CNMR** (125 MHz, $CDCl_3$) δ

200.7, 175.7, 172.6, 54.5, 51.7, 30.8, 24.1, 22.5, 22.2; **IR** (film) ν 2957.7, 1700.3, 1690.4 cm^{-1}; **HRMS** (ES+) m/z calc'd for $C_9H_{13}NO_3$ $[M+Na]^+$: 206.0793, found 206.0790.

Comparison Tables of Natural and Synthetic *(+)*–haterumaimide Q and *(+)*–chlorolissoclimide

Table 2.2 Synthetic and Natural[37] hatQ in d_6-DMSO

Atom	δ C nat. (ppm)	δ C syn. (ppm)	Δ	δ H nat. (ppm)	Multiplicity, *J* (Hz)	δH syn. (ppm)	Multiplicity, *J* (Hz)	Δ
1	38.0	38.0	-	1.60 0.91	ddd (3.0, 5.5, 13.5) dd (4.0, 13.5)	1.60 0.91	m td (10.7, 3.7)	- -0.02
2	18.9	18.9	-	1.50 1.42	m m	1.50	m m	-
3	41.5	41.5	-	1.36 1.11	ddd (3.5, 5.5, 13.0) m	1.36 1.53	d	-
4	33.1	33.1	-	-	-	-	-	-
5	52.2	52.2	-	1.12	dd (3.5, 12.0)	1.20		-
6	33.5	33.5	-	1.87 1.13	ddd (3.5, 4.4, 12.0) m	1.87 1.22	m m	0.01 -
7	72.0	71.9	-0.1	3.75	ddd (4.5, 5.5, 11.0)	3.76	dd (9.9, 4.8)	0.01
8	151.1	151.1	-	-	-	-	-	-
9	49.8	49.8	-	1.44	dd (10.0, 5.5)	1.63	dd (12.1)	-0.02
10	38.7	38.6	0.1	-	-	-	-	-
11	29.5	29.5	-	1.58 1.40	m m	1.58	m m	-
12	68.8	66.8	2.0	3.99	dddd (2.0, 5.0, 6.5, 9.0)	3.99	m	-
13	45.3	45.3	-	2.80	ddd (2.0, 5.0, 8.5)	2.80	ap t (6.3 Hz)	-
14	28.9	28.9	-	2.52 2.46	dd (5.0, 17.5) dd (8.5, 17.5)	2.45 – 2.61	m	-
15	181.1	181.1	-	-	-	-		-
16	178.8	178.8	-	-	-	-		-
17	103.6	103.6	-	5.18 4.76	s s	5.19 4.76	s s	0.01 -
18	33.3	33.3	-	0.85	s	0.85	s	-
19	21.5	21.5	-	0.75	s	0.75	s	-
20	14.2	14.2	-	0.57	s	0.58	s	0.01
NH				10.99	br s	10.98	br s	-0.01
7-OH				4.91	d (4.5)	4.89	s	-0.02
12-OH				4.92	d (5.0)	4.90	s	-0.02

Table 2.3 Synthetic and Natural[38] chlorolissoclimide in CD_2Cl_2

Atom	δ C nat. (ppm)	δ C syn. (ppm)	Δ	δ H nat. (ppm)	Multiplicity, *J* (Hz)	δ H syn. (ppm)	Multiplicity, *J* (Hz)	Δ
1	50.1	50.1	-	2.35 1.30	dd (12.5, 4.0) t (12.5)	2.23 1.28	br d (xx)	0.12 - 0.02
2	56.4	56.5	0.1	4.20	tt (12.5, 4.0)	4.20	tt (12.5, 4.0)	-
3	52.8	52.8	-	2.01 1.53	ddd (2.1, 4.0, 12.8) t (12.3)	2.01 1.53		-
4	36.8	36.7	-0.1	-	-	-		-
5	52.9	52.9	-	1.20	s	1.20	s	-
6	34.0	34.0	-	2.10 1.22	s s	2.09 1.22	s s	0.01 -
7	74.1	74.1	-	4.00	d (9.1)	4.00		-
8	150.9	150.9	-	-	-	-	-	-
9	52.3	52.3	-	1.65	dd (7.8, 11.3)	1.63		-0.02
10	42.4	42.4	-	-	-	-	-	-
11	29.9	30.0	0.1	1.80 1.60	ddd (5.6, 7.8, 11.3)	1.82 1.60		0.02 -
12	69.7	69.7	-	4.32	s	4.32	s	-
13	47.5	47.5	-	2.90	ddd (2.2, 5.2, 9.1)	2.89		0.01
14	30.1	30.2	0.1	2.85 2.65	dd (5.2, 17.7) dd (9.1, 17.7)	2.83 2.66		0.02 0.01
15	180.0	180.3	0.3	-	-	-	-	-
16	177.5	177.8	0.3	-	-	-	-	-
17	105.8	105.9	0.1	5.31 4.92	d (1.6) d (1.6)	5.32 4.91	s s	0.01 - 0.01
18	33.8	33.8	-	1.00	s	0.98	s	-0.02
19	22.6	22.7	0.1	0.85	s	0.87	s	0.02
20	15.5	15.6	0.1	0.75	s	0.74	s	-0.01
NH				8.31	br s	8.35	br s	0.04
7-OH				N.O.	-	2.14	-	-
12-OH				2.37	br s	2.42	br s	0.05

Note: synthetic sample in CD_2Cl_2 and comparison data was acquired and tabulated by Zef Könst

2.9 References

1. Gonzalez, M. A.; Romero, D.; Zapata, B.; Betancur-Galvis, L., *Lett. Org. Chem.* **2009,** *6* (4), 289-292.
2. Halperin, S. D.; Fan, H.; Chang, S.; Martin, R. E.; Britton, R., *Angew. Chem. Int. Ed.* **2014,** *53* (18), 4690-4693.
3. Chen, M. S.; White, M. C., *Science* **2010,** *327* (5965), 566-571.
4. Liu, W.; Groves, J. T., *J. Am. Chem. Soc.* **2010,** *132* (37), 12847-12849.
5. Schmidt, V. A.; Quinn, R. K.; Brusoe, A. T.; Alexanian, E. J., *J. Am. Chem. Soc.* **2014,** *136* (41), 14389-14392.
6. Konst, Z. A. PhD Disstertation, University of California Irvine, 2017.
7. Weidmann, V.; Maison, W., *Synthesis-Stuttgart* **2013,** *45* (16), 2201-2221.
8. Salmond, W. G.; Barta, M. A.; Havens, J. L., *J. Org. Chem.* **1978,** *43* (10), 2057-2059.
9. Barton, D. H. R.; Crich, D., *Tetrahedron* **1985,** *41* (19), 4359-4364.
10. Umbreit, M. A.; Sharpless, K. B., *J. Am. Chem. Soc.* **1977,** *99* (16), 5526-5528.
11. Coleman, R. S.; Walczak, M. C., *J. Org. Chem.* **2006,** *71* (26), 9841-9844.
12. Newhouse, T.; Baran, P. S., *Angew. Chem. Int. Ed.* **2011,** *50* (15), 3362-74.
13. Kawamata, Y.; Yan, M.; Liu, Z. Q.; Bao, D. H.; Chen, J. S.; Starr, J. T.; Baran, P. S., *J. Am. Chem. Soc.* **2017,** *139* (22), 7448-7451.
14. Zou, L. F.; Paton, R. S.; Eschenmoser, A.; Newhouse, T. R.; Baran, P. S.; Houk, K. N., *J. Org. Chem.* **2013,** *78* (8), 4037-4048.

15. Quinn, R. K.; Konst, Z. A.; Michalak, S. E.; Schmidt, Y.; Szklarski, A. R.; Flores, A. R.; Nam, S.; Horne, D. A.; Vanderwal, C. D.; Alexanian, E. J., *J. Am. Chem. Soc.* **2016,** *138* (2), 696-702.

16. Novac, O.; Guenier, A. S.; Pelletier, J., *Nucleic Acids Res.* **2004,** *32* (3), 902-915.

17. Robert, F.; Gao, H. Q.; Donia, M.; Merrick, W. C.; Hamann, M. T.; Pelletier, J., *RNA* **2006,** *12* (5), 717-724.

18. Jackson, R. J.; Hellen, C. U. T.; Pestova, T. V., *Nat. Rev. Molec. Cell Biol.* **2010,** *11* (2), 113-127.

19. de Loubresse, N. G.; Prokhorova, I.; Holtkamp, W.; Rodnina, M. V.; Yusupova, G.; Yusupov, M., *Nature* **2014,** *513* (7519), 517-+.

20. Konst, Z. A.; Szklarski, A. R.; Pellegrino, S.; Michalak, S. E.; Meyer, M.; Zanette, C.; Cencic, R.; Nam, S.; Voora, V. K.; Horne, D. A.; Pelletier, J.; Mobley, D. L.; Yusupova, G.; Yusupov, M.; Vanderwal, C. D., *Nat. Chem.* **2017,** *9* (11), 1140-1149.

21. Konst, Z. A. PhD Dissertation, University of California Irvine, 2017.

22. Mulzer, J.; Segner, J.; Bruntrup, G., *Tetrahedron Lett.* **1977,** (52), 4651-4654.

23. Zimmerman, H. E.; Traxler, M. D., *J. Am. Chem. Soc.* **1957,** *79* (8), 1920-1923.

24. Evans, D. A.; Bartroli, J.; Shih, T. L., *J. Am. Chem. Soc.* **1981,** *103* (8), 2127-2129.

25. Heravi, M. M.; Zadsirjan, V., *Tet. Asymm.* **2013,** *24* (19), 1149-1188.

26. Hajra, S.; Giri, A. K.; Karmakar, A.; Khatua, S., *Chem. Commun.* **2007,** (23), 2408-2410.

27. May, A. E.; Connell, N. T.; Dahlmann, H. A.; Hoye, T. R., *Synlett* **2010,** *13*, 1984-6.

28. Abiko, A.; Liu, J.-F.; Masamune, S., **1997**.

29. Masamune, S.; Sato, T.; Kim, B. M.; Wollmann, T. A., *J. Am. Chem. Soc.* **1986,** *108* (26), 8279-8281.

30. Reetz, M. T.; Kunisch, F.; Heitmann, P., *Tetrahedron Lett.* **1986,** *27* (39), 4721-4724.

31. Noyori, R.; Ikeda, T.; Ohkuma, T.; Widhalm, M.; Kitamura, M.; Takaya, H.; Akutagawa, S.; Sayo, N.; Saito, T.; Taketomi, T.; Kumobayashi, H., *J. Am. Chem. Soc.***1989,** *111* (25), 9134-9135.

32. Kitamura, M.; Ohkuma, T.; Tokunaga, M.; Noyori, R., *Tetrahedron Asymm.* **1990,** *1* (1), 1-4.

33. Szklarski, A. R. PhD Dissertation, University of California, Irvine, 2013.

34. Fujii, A.; Hashiguchi, S.; Uematsu, N.; Ikariya, T.; Noyori, R., *J. Am. Chem. Soc.* **1996,** *118* (10), 2521-2522.

35. Tuan, M. N.; Nguyen, Q. V.; Youte, J. J.; Lau, J.; Cheong, A.; Ho, Y. S.; Tan, B. S. W.; Yoganathan, K.; Butler, M. S.; Chai, C. L. L., *Tetrahedron* **2010,** *66* (47), 9270-9276.

36. Stoncius, A.; Nahrwold, M.; Sewald, N., *Synthesis-Stuttgart* **2005,** (11), 1829-1837.

37. Uddin, J.; Ueda, K.; Siwu, E. R. O.; Kita, M.; Uemura, D., *Bioorg. Med. Chem.* **2006,** *14* (20), 6954-6961.

38. Biard, J. F.; Malochet-Grivois, C.; Roussakis, C.; Cotelle, P.; Henichart, J. P.; Debitus, C.; Verbist, J.-F., *Nat. Prod. Lett.* **1994,** *4*, 43 - 57.

CHAPTER 3 : Initial Synthetic Efforts Towards Haterumaimide J and K

3.1 Introduction

In spite of our efforts to establish both a diversifiable synthetic approach and a direct semi-synthesis for many lissoclimides and haterumaimides, the two most potent members of the family—haterumaimide J (hatJ, **3.2**) and its acetylated congener-haterumaimide K (hatK, **3.3**)—have eluded synthesis by these initial designs. The decalin core is substituted with a familiar C2-chlorine but the characteristic C18-oxygenation defines the synthetic challenge and unique functional group arrangement of these two family members.

The chlorination and oxygenation patterns about the decalin A and B rings are the main source of diversity amongst the haterumaimides and lissoclimides, with the pendent succinimide and labdane carbon skeleton constant throughout all family members. While there is no explicit biosynthetic evidence for the haterumaimides, this single-group variation provides a plausible case for enzymatic C-H functionalization on a common labdane scaffold. The biosynthetic pathways for labdane related diterpenoids are widely studied and understood to proceed through a cyclase-mediated, electrophile-

Figure 3.1 Biogenetic synthesis of labdane diterpenoids

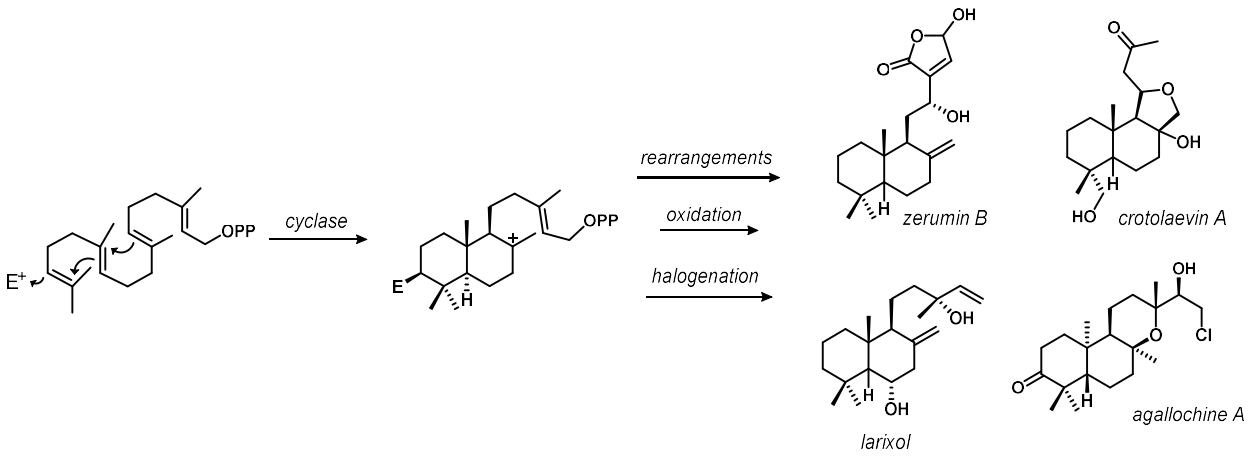

initiated, polyene cyclization of geranylgeranyl pyrophosphate precursors (**Figure 3.1**).[1, 2] These hydrocarbon scaffolds then undergo cation-induced rearrangements and enzymatic modifications to provide the substantial diversity of labdane diterpenes.[2, 3]

3.1.1 Postulated dual C–H activation of sclareolide

We speculated that a bioinspired strategy towards **3.2** and **3.3** could draw from aspects from our semi-synthesis approach. Two different C–H activation events on sclareolide (**3.1**) could install the A-ring chlorination and oxygenation; then our optimized sequence for elaboration of the B-ring lactone could access **3.2** and **3.3** (**Figure 3.2**). We have capitalized on the remarkable C2 selectivity for a C–H

Figure 3.2 Postulated dual C-H activation for the synthesis of hatJ and hatK

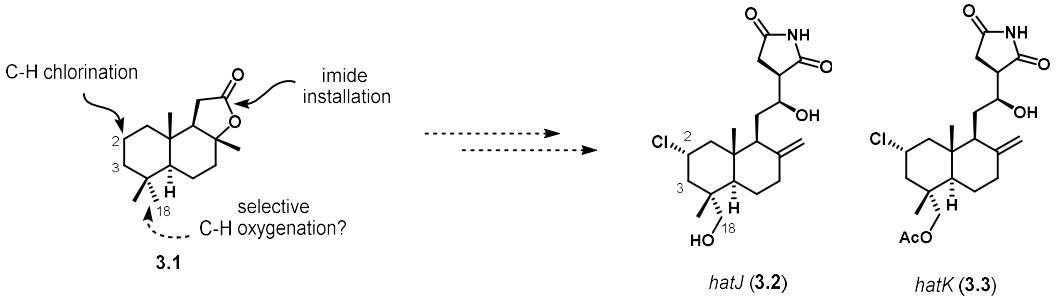

chlorination on sclareolide (**3.1**) but analogous methods for C–H oxidation of **3.1** are restricted to A-ring methylene sites.[4-7] Moreover, all known methods to effect a C–H hydroxylation specifically at C18-methyl group on steroidal scaffolds require a proximal functional handle at the C3 position.[8, 9] While synthetic methods are limited for this direct oxidation of sclareolide, many groups have studied *in vitro* biotransformations of labdane scaffolds with microorganisms containing various cytochrome P450 enzymes, the most abundant monooxygenases in nature.[2, 10] Experiments on the microbial oxidation of **3.1** resulted in mainly A-ring methylene hydroxylated products.[11] The biotransformation of naturally occurring sclareol (**3.4**)—commonly isolated with **3.1**—with several different fungal microorganisms

afforded three-major oxidized products (**3.5**, **3.6**, **3.7**, **Figure 3.3**).[12] Each of these points of oxidation are observed in different members of the haterumaimide family; while **3.4** may not be the biogenetic precursor to the haterumaimides, these studies support the hypothesis for post-cyclization, enzymatic

Figure 3.3 Biotransformations of sclareol

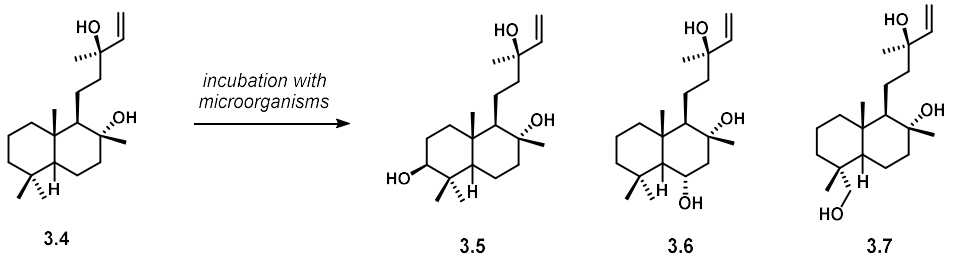

3.4 3.5 3.6 3.7

modifications for the origin of the varying oxidation patterns. Additionally, Diez and coworkers found that microbial-hydroxylation of **3.4** with fungi *Rhizopus Stolonifer* gave 18-hydroxysclareol (**3.7**) as the sole product in 74% yield.[13] It would be interesting to investigate whether or not this microorganism could impart the same C–H oxidation selectivity on 2-chloroscaleolide; therefore, we considered combining the use of synthetic methods and enzymology for the synthesis of hatJ (**3.2**). While this idea offers a unique dual C–H activation approach for the synthesis of C18-hydroxylated haterumaimides, it would rely significantly on collaborations with enzymology specialists. We believed this was a good opportunity to explore a purely synthetic strategy for the construction of this substitution pattern.

3.2 Alkene hydrochlorination attempts

The lack of C3-functionality in **3.1** is an underlying aspect to the synthetic challenge for accessing the C18-hydroxyl group. Hartwig and coworkers developed a robust C-H oxygenation protocol to install a C18-hydroxyl group from α-C3 alcohols on steroidal systems (**Scheme 3.1**). They appended a dihydrosilane as a directing group on the C3-alcohol of **3.8** and heated the substrate with an iridium-phenanthroline catalyst to effect a C–H insertion into the equatorial CH_3 group (**3.9**). A Tamao–Fleming

Scheme 3.1 Hartwig's strategy for directed C18-oxygenation

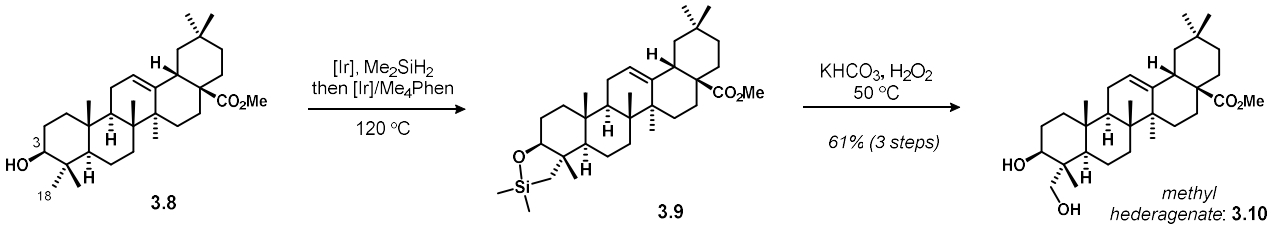

oxidation and silyl group removal afforded methyl hederagenate (**3.10**) in 61% yield.[14] Könst and Szklarski utilized an efficient Lewis acid-mediated polyene cyclization—initiated on internal epoxides of type **3.11**—to obtain decalin scaffolds with pre-installed C18-oxygenation (**3.12**, **Scheme 3.2a**, for details see Chapter 1).[15] The relative configuration of the newly formed C4/C5 (terpene numbering) bond is dictated by the stereochemistry of the internal epoxide and proceeds through **Conf-I** during the bicyclization. This 2,3-internal epoxide polyene manifold has been used to great effect for the synthesis of complex C3, C18-oxygenated diterpenoids.[16-18] In both examples presented, the products contain a C3-hydroxyl group that would require reductive excision for application to the hatJ synthesis. In Könst's analogue-oriented synthesis, the C3-hydroxyl group of **3.13** was eliminated to provide an A-ring alkene

Scheme 3.2 Polyene cyclization of internal epoxides for a C–H chlorination strategy

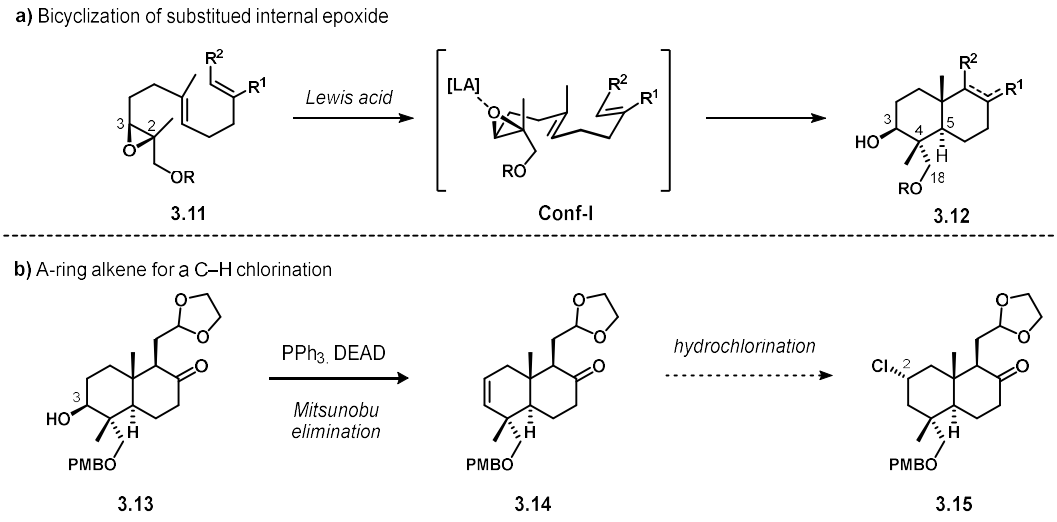

(**3.14**), necessary for subsequent dichlorination (**3.15**, **Scheme 3.2b**). We envisioned applying a similar strategy, but in this case utilize the A-ring alkene in a hydrochlorination reaction to install the C2-chlorine.

Classical conditions to carry out hydrochlorinations of alkenes involve the use of Brønsted acids (HCl) which have limited functional group tolerance. In recent years, the development of metal-catalyzed hydrogen atom transfer (HAT) to alkenes has broadened the scope and substrate compatibility of hydrofunctionalizations.[19] When these reaction conditions are paired with a chlorine-atom source, a robust hydrochlorination of unactivated alkenes can be accomplished. Carreira and coworkers developed a Markovnikov selective hydrochlorination procedure that employs a cobalt-salen cataylst (**3.16**), phenylsilane as the hydrogen atom donor, and tosyl chloride as the chlorine source (**Scheme 3.4a**).[20] They proposed a mechanism involving hydrocobaltlation of the alkene, followed by Co-C bond homolysis and subsequent radical trapping with tosylchloride. The Boger lab extended their iron(III)-mediated hydrofunctionalization method to the hydrochlorination of unactivated alkenes.[21] Treatment of β-citronellol with an iron(III)/$NaBH_4$ mixture and an arylsulfonyl chloride afforded the corresponding alkyl chloride in high yields with no interference from the free hydroxyl group (**Scheme 3.3b**).

Scheme 3.3 Representative methods for hydrochlorination of unactivated alkenes

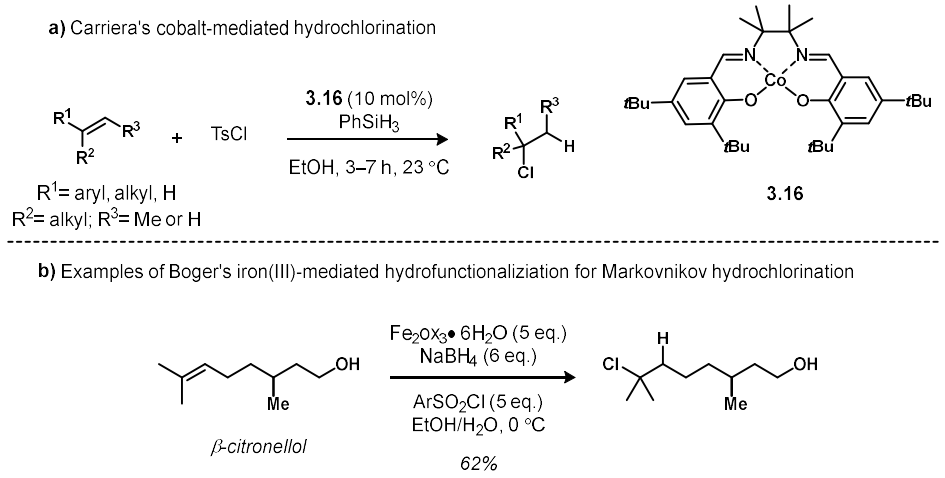

We began our investigations of hydrochlorinations reaction on intermediate **3.17** from Szklarski's synthesis toward dichlorolissoclimide (**Chapter 1**). We were unsure of the regioselectivity a HAT chlorination would afford on **3.14** since both A-ring alkene carbons are monosubstituted. According to Carreira's proposed mechanism,[20] an alkene-hydrometallation places the cobalt-complex in proximity to the more substituted carbon. Since both alkene carbons of **3.14** are equally substituted, we wondered whether a hydrometallation step would proceed in an anti-Markovnikov manner and disfavor placing the large cobalt complex at the neo-pentylic position (C3). If the H-atom addition occurred with the desired regioselectivity, a chloride- recombination at the C2-position would proceed from the α-face to avoid

Scheme 3.4 A-ring hydrochlorination efforts

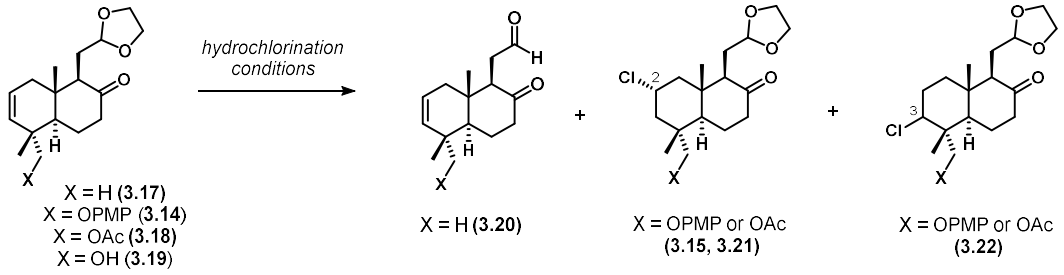

diaxial interactions. Initial experiments employing Carreira's conditions resulted in only acetal cleavage to unveil the pendant aldehyde (**3.20**) and no chlorination products were observed (**Scheme 3.4**). This undesired reactivity was presumed to be a result of the water present in the alcoholic solvent and trace amounts of HCl formed by the reaction of the silane reductant with tosyl chloride.[20] A syringe-pump addition of a solution of tosyl chloride in distilled EtOH tempered this side reaction and hydrochlorination of the A-ring alkene was realized, although a complex mixture of chlorinated products was isolated (**Scheme 3.4**). We speculated that homoallylic C18-oxygenation may impart some type of selectivity on the hydrochlorination. Unfortunately, C18-oxygenation did not improve the selectivity as both PMP and acetate protected substrates (**3.14** and **3.18**) afforded mixtures of 3 chlorinated products,

and the substrate with the unprotected hydroxyl group (**3.19**) gave minimal reactivity. Through ^{1}H NMR analysis the mixture was tentatively assigned to α-C3-chloro product (**3.15** or **3.21**) and C2-chloride diastereomers (**3.19**), indicating the hydrochlorination proceeded with low regioselectivity. We experimented with the Boger group's iron-oxalate-mediated protocol[21] as well as Herzon's hydrobromination procedure[22] with tosyl chloride as the chlorine-atom donor, but these efforts were also unsuccessful. It should be noted that Könst and Szklarski previously attempted a hydroboration followed by a deborylation-chlorination procedure[23] on alkene **3.17**,[24] but observed undesired reactivity with the B-ring functional groups. A hydroboration strategy should improve the desired regioselectivity for addition to the A-ring alkene, but optimization for a compatible substrate under these conditions was not pursued.

3.3 A titanocene-mediated radical bicyclization strategy

In spite of the undesired outcome for a cyclization/hydrochlorination strategy, we still believed that an epoxypolyene cyclization would provide the most efficient entry to the decalin core of hatJ (**3.2**), but it was apparent that selective installation of the C2-chlorine would need to precede decalin formation. We therefore pursed an alternative strategy utilizing a terminal epoxide with a pre-installed chlorine stereocenter as a cyclization substrate. We envisioned that a radical-mediated bicyclization of 2,2-disubstituted epoxide of type **3.23** would result in pendent A-ring oxygenation, avoiding the unnecessary

Scheme 3.5 A radical-mediated polyene cyclization for the synthesis of hatJ

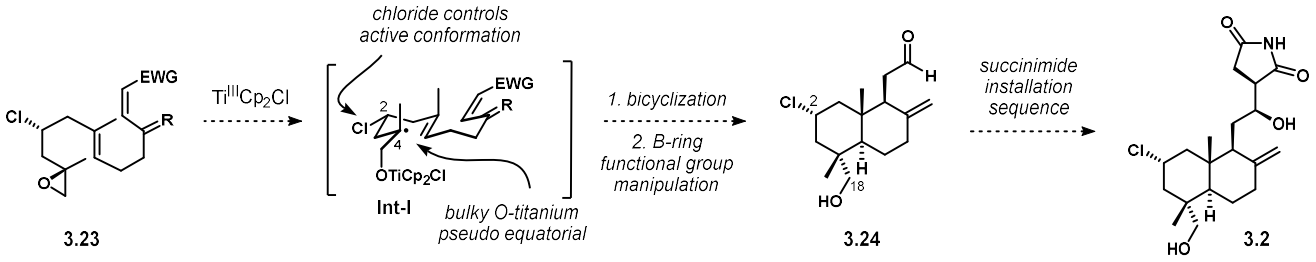

C3-hydroxyl that results from cyclization of internal epoxides (**Scheme 3.5**). Upon homolysis of the C-O epoxide bond, we speculated that the bulky O-Cp_2TiCl group would prefer to sit in an equatorial position and result in the desired C4 configuration (terpene numbering). The secondary chlorine would serve as an additional stereocontrol element, adopting a pseudo-equatorial position during the bicyclization (**Int-I**). The electron-deficient π-system used to terminate the bicyclization could be converted into pendent aldehyde **3.24.** This substrate could then undergo our optimized succinimide installation sequence to access **3.2**. While reagent control—for the iron and cobalt-mediated hydrochlorination attempts—gave minimal success in constructing the A-ring substitution pattern, this strategy would alternatively rely on substrate control to furnish the entire decorated core of hatJ (**3.2**).

Our motivation for a titanocene-mediated cyclization came from the work of Cuerva and coworkers, who have used the Nugent and RajanBabu method for reductive epoxide opening with Cp_2TiCl[25] to great effect for epoxypolyene cyclizations.[26-28] While Lewis acid-catalyzed cyclizations afford a thermodynamic distribution of B-ring alkene isomers, Ti(III)-mediated variants are selective for forming exo-alkenes.[29] Twenty years after the initial report by Nugent, the Gansäuer group developed a formal reductive catalytic approach,[30] and Cuerva subsequently expanded on this protocol to achieve an overall neutral catalytic cyclization (**Scheme 3.6**).[31] The Cuerva group has employed this catalytic Ti(III)–chemistry on polyunsaturated 2,3-disubstituted epoxides (**3.25**) to afford bicycles such as **3.26**. According to the proposed mechanism, bis(cyclopentadienyl)titanium dichloride ($Cp_2Ti^{IV}Cl_2$) is first reduced by Mn^0 to $Cp_2Ti^{III}Cl$; this species then homolytically opens the epoxide to a β-titanoxy radical which undergoes bicyclization to **3.27**. In Gansäuer's system, the tertiary radial in **3.27** is reduced by a

Scheme 3.6 Catalytic cycle for a titanocene-mediated polyene cyclization

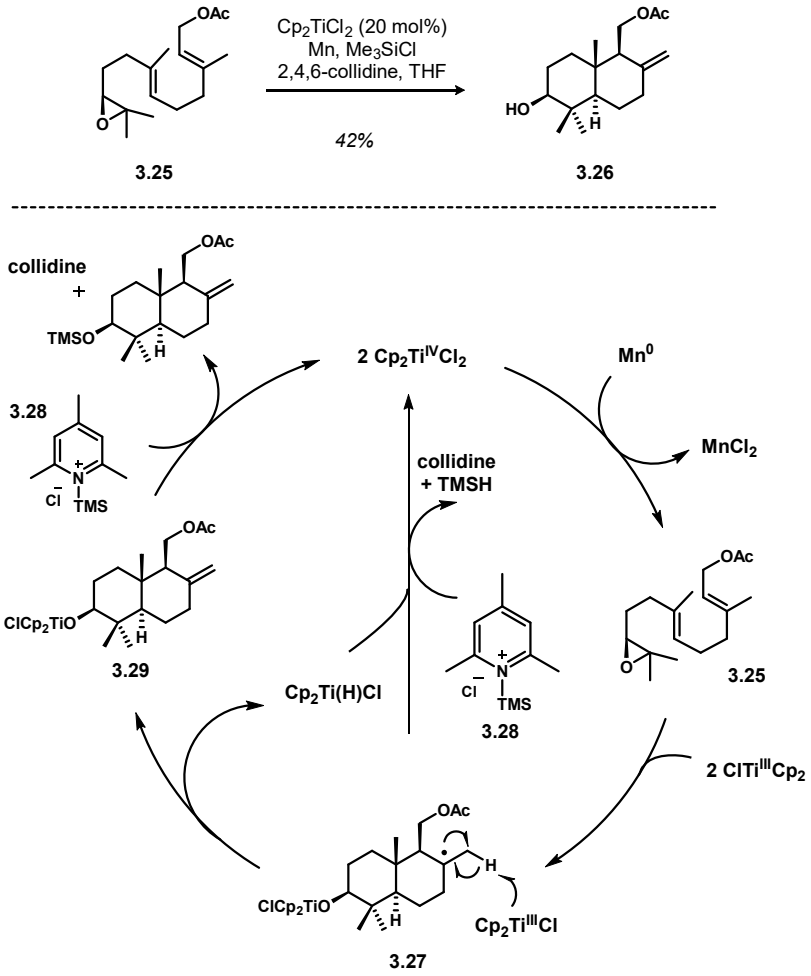

second equivalent of Cp_2TiCl and then protonation by HCl•collidine affords a C9-methyl group.[30] Cuerva's method substitutes the HCl salt with trimethylsilyl 2,4,6-collidinium chloride (**3.28**); by excluding acidic protons, the termination step predominantly proceeds through a formal β-hydride elimination affording exocyclic B-ring alkene (**3.29**). The resulting Cp_2TiHCl reduces **3.28** to collidine and trimethylsilane to reform Cp_2TiCl_2.

Cuerva and coworkers have also reported that under these conditions, 2,2-disubstituted epoxide **3.30** undergoes monocyclization onto an allylic carbonate to forge **3.31** possessing the desired

configuration of the C4/C5 stereocenters required for hatJ (**Scheme 3.7a**). While this constituted encouraging precedent for our strategy, the use of 2,2-disubstituted epoxides in a bicyclization manifold is surprisingly underexplored. Therefore, we began our investigations for this transformation on terminal

Scheme 3.7 Examples of titanocene-initiated cyclizations of 2,2-disubstituted epoxides

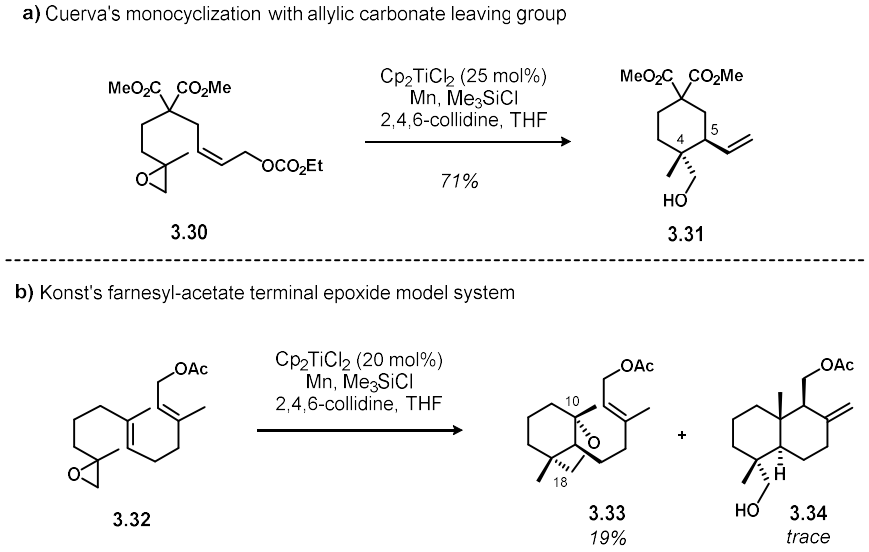

epoxide model system substrates. An important initial experiment was carried out by Könst who subjected farnesyl-acetate derived epoxide **3.32** to catalytic titanocene conditions (**Scheme 3.7b**). The reaction afforded oxabicycle **3.33** as the major product, and only trace amounts of the desired decalin (**3.34**) were isolated. After the first cyclization, the C10-radical is likely oxidized to the cation and then captured by the pendent C18-oxygen; this result indicated that a suitable radical acceptor is required to complete the second cyclization event.

We speculated that furan **3.38** could be a versatile intermediate for accessing a variety of electrophilic radical acceptors through oxidative furan ring openings. The synthesis of **3.38** commenced with a chlorination/alkene migration of geranyl acetate to afford **3.35** (**Scheme 3.8**).[32] The allylic chloride was reduced with $LiAlH_4$ and the resulting alcohol was protected as the trichloroacetate (**3.36**).

It should be noted that reduction of the chloride without acetate cleavage could be effected by heating **3.35** with Zn^0 dust in AcOH/THF, but epoxidation of the allylic acetate (deschloro-**3.35**) resulted in little chemoselectivity between the terminal and internal alkenes. The electron withdrawing properties of the trichloroacetate group proved essential to selectively form **3.37**. The furan fragment was then appended through a copper-mediated coupling of **3.37** with furfurol-derived Grignard **3.38**[24] to obtain diversifiable furan intermediate **3.39**.

Scheme 3.8 Synthesis of model system substrates for a radical bicyclization

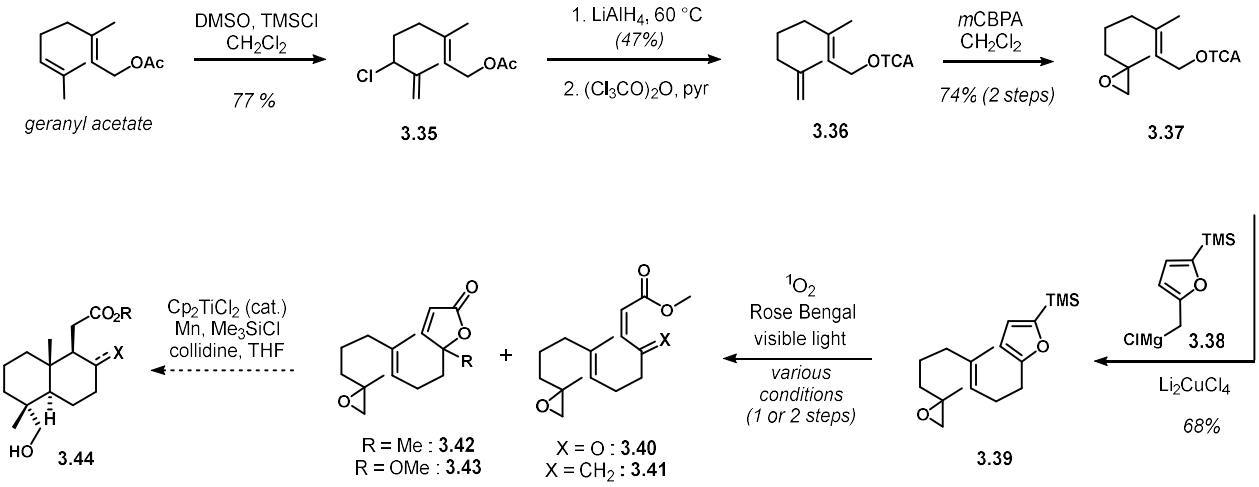

In collaboration with Könst, **3.39** was subjected to furan ring opening reactions with singlet-oxygen and by employing various work up conditions, we constructed enone and butenolide acceptor substrates (**3.40–3.43**) for Ti(III)-radical bicyclizations to decalins of type **3.44** (**Scheme 3.9**). Könst subjected highly electrophilic enoate **3.40** to Cuerva's conditions but only observed reduction of the C9/C10 alkene (**3.45**).[33] To lower the reduction potential of the acceptor group Könst converted the C8-ketone to alkene **3.41**, but this diene substrate did not result any desired bicyclization.[34] I treated enoate (**3.40**) with MeLi to form methyl butenolide **3.42**, but under Ti(III)-conditions the only discernable products isolated were monocyclized product **3.46** and oxabicycle **3.47**. The formation of

Scheme 3.9 Outcomes of a reductive radical opening of terminal epoxide substrates

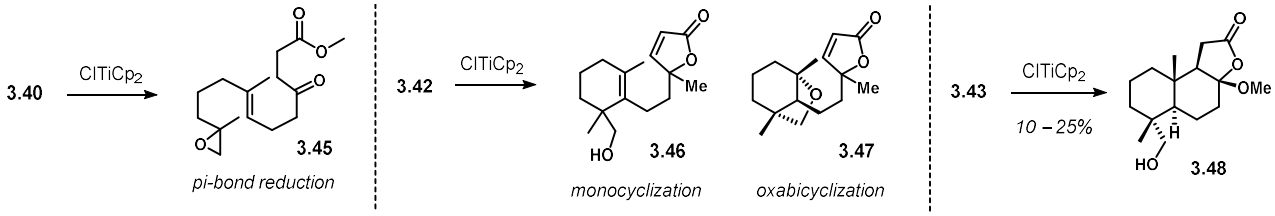

these undesired products was likely a result of the steric bulk imposed by the C8-methyl group which deterred the second cyclization; consequently unproductive radical quenching pathways prevailed. The most successful substrate was the analogous methoxy butenolide (**3.43**), which provided the desired product (**3.48**), albeit in low and inconsistent yields (10–25%).

3.4 Conclusion

During our initial efforts towards forming the C2-chlorinated, C18-oxygenated scaffold of haterumaimide J (**3.2**), we became aware of the unique challenge in constructing these remote stereocenters on the decalin core. A well precedented polyene cyclization initiating on a 2,3-disubstituted epoxide provided direct access to the C18-oxygenated decalin scaffold, but the resultant C3-hydroxyl group could not be utilized productively for installation of the C2-chlorine. A bicyclization initiated on a 2,2-disubstituted epoxide would afford the desired oxygenation pattern and a pre-installed chloride stereocenter could provide a unique mode of stereocontrol for this reaction. While we were not able to design a terminal epoxide substrate amenable for a high yielding titanocene(III)-catalyzed bicyclization, a polar-cationic manifold may overcome the challenges observed in the radical-mediated reactions.

3.5 Experimental Procedures

Materials and Methods:

All reactions were performed in oven-dried (120 °C) or flame-dried glassware under an atmosphere of dry argon unless otherwise noted. Reaction solvents including dichloromethane (CH_2Cl_2, Fisher, HPLC Grade), hexanes (Fisher, HPLC Grade), diethyl ether (Et_2O, Fisher, BHT stabilized, HPLC Grade), benzene (C_6H_6, Fisher, HPLC Grade), tetrahydrofuran (THF, Fisher, HPLC Grade), and toluene ($PhCH_3$, Fisher, HPLC Grade) were dried by percolation through a column packed with neutral alumina and a column packed with Q5 reactant, a supported copper catalyst for scavenging oxygen, under a positive pressure of argon.

Solvents for workup and chromatography were: acetone (Fisher, ACS grade), hexanes (Fisher or EMD, ACS Grade), EtOAc (EtOAc, Fisher, ACS Grade), dichloromethane (CH_2Cl_2, Fisher, ACS Grade), and methanol (MeOH, Fisher, ACS Grade). Column chromatography was performed using EMD Millipore 60 Å (0.040–0.063 mm) mesh silica gel (SiO_2). Analytical thin-layer chromatography was performed on Merck silica gel 60 F254 TLC plates. Visualization was accomplished with UV (254 or 210 nm), and p-anisaldehyde, ceric ammonium molybdate or potassium permanganate and heat as developing-agents.

^1H NMR and ^{13}C NMR spectra were recorded at 298 K on Bruker GN500 (500 MHz, ^1H; 125 MHz, ^{13}C), Bruker CRYO500 (500 MHz, ^1H; 125 MHz, ^{13}C), and Bruker AVANCE600 (600 MHz, ^1H; 125 MHz, ^{13}C) spectrometers. ^1H and ^{13}C spectra were referenced to residual $CHCl_3$ (7.26 ppm, ^1H or 77.0 ppm, ^{13}C). Chloroform-d ($CDCl_3$, D 99.8%, DLM-7) and dimethyl sulfoxide-d6 (CD_6SO, D 99.9%, DLM-10) were purchased from Cambridge Isotope Laboratories. Chemical shifts are reported in ppm

and multiplicities are indicated by: app (apparent), s (singlet), d (doublet), t (triplet), q (quartet), m (multiplet), and br s (broad singlet). Coupling constants, J, are reported in Hertz. Infrared (IR) spectra were recorded on a Perkin-Elmer spectrum RX1 FT-IR instrument or Varian 640-IR instrument on NaCl plates and peaks are reported in cm^{-1}. Mass spectrometry data were obtained from the University of California, Irvine Mass Spectrometry Facility. High-resolution mass spectra (HRMS) were recorded on a Waters LCT Premier spectrometer using ESI-TOF (electrospray ionization-time of flight) or CI-TOF (chemical ionization-time of flight) and data are reported in the form of (m/z). GC/FID analysis was performed on Agilent 7820A system with helium as carrier gas. HPLC analysis was performed on an Agilent1100series.

Citric acid (ACS grade, anhydrous, Fisher), potassium sodium tartrate (Oakwood), K_2CO_3 (anhydrous, 99%, Alfa Aesar), $NaHCO_3$ (ACS grade, Fisher), NaOH (ACS grade, Macron or Fisher), $Na_2S_2O_3$ (ACS grade, Fisher), *p*-anisaldehyde (99%, Acros Organics), borontrifluoride etherate (Alfa Aesa, 99%), diisobutylaluminum hydride (*i*-Bu_2AlH, Sure Pack™ reagent grade, Sigma Aldrich), *p*-toluenesulfonyl chloride (Sigma Aldrich, >99%), acetic anhydride (Acros Organic) trichloroacetic anhydride (Sigma Aldrich), lithium aluminum hydride (powder, Sigma Aldrich, 95%), *m*-CPBA (Sigma Aldrich) were used without subsequent purification.

The following reagents were distilled from the indicated drying agents under argon prior to use: triethylamine (Et_3N, EMD, CaH_2), pyridine (Alfa Aesar, CaH_2 and *N,N*-diisopropylethylamine (*i*-Pr_2NEt, Alfa Aesar, CaH_2), 2,4,6-collidine (Sigma Aldrich) and trimethylsilyl chloride ($(CH_3)_3SiCl$, Acros Organics) were fractionally distilled prior to use.

Experimental Procedures:

Alkene 3.17:

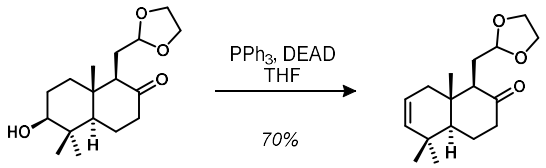

3S-1 3.17

Alcohol **3S-1**[15] (35 mg, 118 μmol, 1 equiv.) and Ph_3P (77.5 mg, 295 μmol, 2.5 equiv.) was dissolved in THF (800 μL). Diethyl azodicarboxylate (51.3 μL, 295 μmol, 2.5 equiv.) was added at room temperature and the reaction vessel was sealed and heated to 70 °C for 2 h. The reaction mixture was cooled to ambient temperature, diluted with hexanes (1 mL) and brine (2 mL) and extracted with hexanes (3 x 2 mL). The crude residue was purified by flash chromatography (SiO_2, 20% EtOAc in hexanes) to give **3.17** as a white solid (22.8 mg, 82.6 μmol, 70%).

Note: Alcohol **3S-1** was synthesized and provided by Anne Szklarski and Zef Könst.

^{1}H NMR (500 MHz, $CDCl_3$) δ 5.51–5.47 (m, 1H), 5.41 (br d, *J* = 10 Hz, 1H), 4.82 (dd, *J* = 2.9, 7.0 Hz, 1H), 3.97–3.89 (m, 2H), 3.84–3.76 (m, 2H), 2.48–2.42 (m, 3H), 2.36 (ddd, *J* = 2.8, 10.4, 13.2 Hz, 1H), 2.11–2.05 (m, 1H), 2.2 (app. s, 2H), 1.86 (dd, *J* = 2.8, 13.3 Hz, 1H), 1.81–1.73 (m, 1H), 1.41 (dd, *J* = 6.7, 13.3 Hz, 1H), 1.05 (s, 3H), 0.90 (s, 3H), 0.73 (s, 3H); **^{13}C NMR** (125 MHz, CDCl3) δ 211.1, 137.7, 120.7, 103.5, 64.8, 64.7, 57.2, 50.2, 42.3, 42.1, 38.9, 35.1, 31.9, 26.5, 25.2, 23.4, 14.6; **IR** (film) ν 2951, 2859, 1711, 1135, 725 cm^{-1}; **HRMS** (ES+) *m/z* calc'd for $C_{17}H_{26}O_3Na$ $[M + Na]^+$ 301.1780, found 301.1778; **$[\alpha]_{25}^{D}$** –23.1 (*c* = 0.61, $CHCl_3$).

Alkene 3.14:

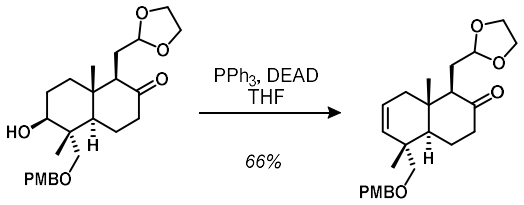

3S-2 3.14

Alcohol **3S-2**[15] (50 mg, 115 μmol, 1 equiv.) was subjected to the same reaction conditions as **3S-1** to make **3.17**. The crude alkene residue was purified by flash chromatography (SiO_2, 20% EtOAc in hexanes) to give **3.14** as a colorless oil (31.6 mg, 76.4 μmol, 66%).

Note: Alcohol **3S-2** was synthesized and provided by Zef Könst.

Allylic chloride 3.35:

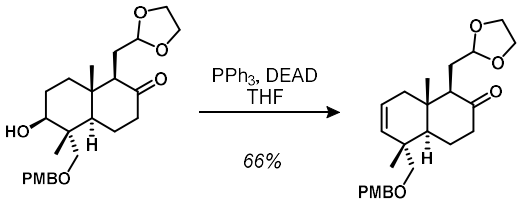

3S-2 3.14

A solution of DMSO (3.5 mL, 48.9 mmol, 8 equiv.) and TMSCl (12.4 mL, 97.9 mmol, 6 equiv.) in CH_2Cl_2 (61 mL) was cooled to 0 °C. The mixture was stirred for 10 mins before addition of geranyl acetate (1.20 g, 6.12 mmol, 1 equiv.). The reaction was stirred for 24 h maintaining the temperature at 10 °C in a cryo-cool bath. The reaction was quenched with $NaHCO_3$ (30 mL), then water (50 mL) and the mixture was extracted with CH_2Cl_2 (3 x 40 mL). The organic layers were combined, dried over $MgSO_4$, filtered and concentrated *in vacuo.* The crude residue was purified by flash chromatography (SiO_2, 5% EtOAc in hexanes) to give **3.35** as a colorless oil (1.08 g, 4.71 mmol, 77%).

The ^1H NMR and ^{13}C NMR matched the reported data for this compound.[32]

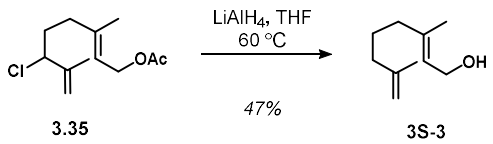

Allylic alcohol 3S-3

Allylic chloride **3.35** (150 mg, 0.650 mmol, 1 equiv.) was taken up in THF (2.6 mL, 0.25M) and $LiAlH_4$ (74 mg, 0.652 mmol, 3.0 equiv.) was added portion wise over 10 min at room temperature. The flask was equipped with a reflux condenser and the reaction mixture was then heated to 60 °C and stirred at this temperature for 10 h. The reaction mixture was cooled to 0 °C and 1 M NaOH (100 μL) was added, followed by H_2O (100 μL) and the mixture was stirred for 30 min. An additional 5 mL of NaOH (1M) was added and then the layers were separated. The aqueous layer was extracted with Et_2O (3 x 1 mL), the organic layers were combined and washed with aq. sat. $NaHCO_3$ (2 mL), brine (2 mL) then the organic layer was dried over Mg_2SO_4, filtered and concentrated *in vacuo* to give a brown oil. The crude product was purified by flash chromatography (SiO_2, 20% EtOAc in hexanes) to give allylic alcohol **3S-3** as a light yellow oil (47.3 mg, 0.305 mmol, 47%).

The ^{1}H NNR and ^{13}C NMR data agreed with the literature data.[35]

^{1}H NMR (500 MHz, $CDCl_3$) δ 5.42 (t, *J* = 6.54, 1H), 4.71 (br s, 1H), 4.67 (br s, 1H), 4.15 (d, *J* = 6.54 Hz, 2H), 2.03–1.96 (m, 4H), 1.71 (s, 3H), 1.67 (s, 3H), 1.61–1.52 (m, 3H), 1.71 (br s, 1H).

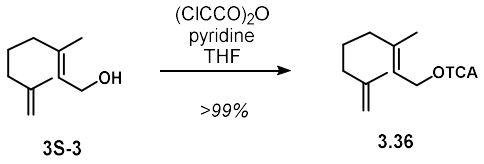

Trichloroacetate 3.36:

A solution of **3S-3** (43 mg, 0.278 mmol, 1 equiv.) in THF (5.5 mL) was cooled to 0 °C. Pyridine was added (45 μL, 0.556 mmol, 2 equiv) followed by trichloroacetic anhydride (61 μL, 0.334 mmol, 1.2 equiv). The reaction mixture was allowed to stir at room temperature for 1 h, hexanes was added (5 mL) to dilute the reaction mixture followed by the addition of H_2O (5 mL). The layers were separated and the organic layer was washed sequentially with H_2O (4 mL), sat. aq. $NaHCO_3$ (4 mL) then brine (4 mL). The organic layer was dried over $MgSO_4$, filtered and concentrated *in vacuo*. Trichloroacetate **3.36** was isolated as a bright yellow oil in quantitative yield (83.3 mg, 0.278 mmol, > 99%). The crude product was of sufficient purity and carried onto the next step without purification.

^{1}H NMR (500 MHz, $CDCl_3$) δ 5.43 (t, *J* = 7.1 Hz, 1H), 4.87 (d, *J* = 7.3 Hz, 2H), 4.71 (s, 1H) 4.66 (s, 1H), 2.09–2.04 (t, *J* = 7.5 Hz, 2H), 2.01–1.97 (t, *J* = 7.5 Hz, 2H) 1.76 (s, 3H), 1.67 (s, 3H), 1.60–1.54 (m, 2H). **^{13}CNMR** (125 MHz, $CDCl_3$) δ 162.0, 145.7, 145.5, 116.8, 116.3, 110.1, 66.1, 39.0, 37.2, 25.3, 22.4, 16.6; **IR** (film) ν 2935, 1764, 1603 cm^{-1}; **HRMS** (ES+) m/z calc'd for $C_{12}H_{17}O_2Cl_3Na$ $[M+Na]^+$: 321.0196, found 321.0188.

Epoxide 3.37:

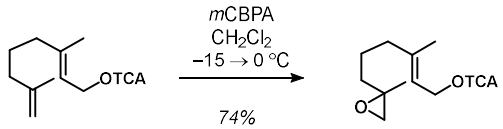

3.36 3.37

Trichloroacetate **3.36** (50 mg, 0.166 mmol, 1 equiv.) was taken up wet CH_2Cl_2 (1.7 mL, 0.08 M) and cooled to – 15 °C. *m*CBPA was added portion wise (32 mg, 0.166 mmol, 1 equiv.) to the reaction mixture and the reaction was monitored by TLC after each addition. The reaction was allowed to warm to 0 °C and upon consumption of starting material as indicated by TLC analysis the reaction was quenched with 0.5 mL of sat. aq. $Na_2S_2O_3$ and stirred for an additional 30 min. The mixture was subsequently diluted with H_2O (2 mL), the layers were separated and the aqueous layer was extracted with CH_2Cl_2 (3 x 3 mL). The organic layers were combined and dried over $MgSO_4$, filtered and concentrated *in vacuo* to give a yellow oil. The crude product was purified by flash chromatography (SiO_2, 30% EtOAc in hexanes) to give epoxide **3.37** as a pale yellow oil (0.123 mmol, 26 mg, 74%).

^{1}H NMR (500 MHz, $CDCl_3$) δ 5.38 (t, *J* = 7.2 Hz, 1H), 4.82 (d, *J* = 7.20 Hz, 2H), 2.57–2.53 (dd, *J* = 13.1, 4.7 Hz, 2H), 2.05 (br s, 2H), 1.63 (s, 3H), 1.51–1.45 (m 4H), 1.27 (s, 3H) **^{13}CNMR** (125 MHz, $CDCl_3$) δ 162.0, 145.3, 116.8,116.5, 66.0, 56.8, 39.4, 36.1, 30.4, 20.9, 18.8, 16.5 **IR** (film) ν 2941, 1764 cm^{-1}; **HRMS** (ES+) m/z calc'd for $C_{12}H_{17}O_3Cl_3Na$ $[M+Na]^+$: 337.0141, found 337.0137.

Furan 3.39:

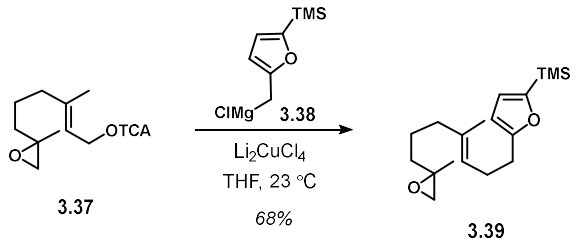

The furfuryl Grignard (**3.38**) was made through addition of the corresponding furfuryl chloride to a solution of excess Mg^0 in THF (1.7 mL), it should be noted that the Mg^0 pellets were initially flamed dried under vacuum. Dibromoethane was added (50 μL) and then the reaction mixture was warmed briefly to 60 °C to ensure Grignard formation. The grey-brown solution was titrated to 0.56 M. [24]

Epoxide **3.37** (10 mg, 0.032 mmol, 1 equiv.) was taken up in THF (200 μL, 0.2M). A solution of Li_2CuCl_4 was made by mixing LiCl (33.9 mg, 0.8 mmol, 2 equiv.) and $CuCl_2$ (53.8 mg, 0.4 mmol, 1 equiv.) in 2 mL of THF and sonicating the mixture until all solids were dissolved. The reddish-orange Li_2CuCl_4 solution was added to the epoxide mixture (6 μL, 0.04 equiv.). The reaction mixture was then cooled to 0 °C and 200 μL (0.095 mmol, 3 equiv.) of the **3.38** Grignard solution was added dropwise. The reaction was stirred at 0 °C for 45 mins and then quenched with 300 μL of sat. aq. NH_4Cl. The aqueous layer was extracted with EtOAc/hexanes (3:1, 2 x 3), washed with brine (1 mL), dried over $MgSO_4$, filtered and concentrated *in vacuo*. The crude product was purified by flash chromatography (SiO_2, 7% EtOAc in hexanes) to give **3.39** as a colorless oil (6.6 mg, 0.021 mmol, 68%).

^{1}H NMR (500 MHz, $CDCl_3$) δ 6.51 (d, *J* = 3.0 Hz, 1H), 5.95 (d, *J* = 3.0 Hz, 1H), 5.15 (t, *J* = 6.9Hz, 1H), 2.67 (t, *J* = 7.3, 2H), 2.60 – 2.56 (dd, *J* = 14.4, 4.9 Hz, 2H), 2.36–2.31 (dd, *J* = 14.4, 7.4 Hz, 2H), 1.97 (app. t, *J* = 6.9 Hz, 2H), 1.58 (s, 3H), 1.50–1.43 (m, 4H), 1.30 (s, 3H), 0.23 (s, 9H); **^{13}C NMR** (125 MHz, $CDCl_3$) δ 160.4, 158.3. 135.6, 123.4, 120.4, 105.0, 57.1, 54.0, 39.5, 39.3, 28.4, 26.5, 23.5, 21.0, 15.8, -1.45;

IR (film) ν 1635, 2952 cm^{-1}; **HRMS** (ES+) m/z calc'd for $C_{18}H_{30}O_2SiNa$ $[M + Na]^+$: 306.2015, found 306.2016.

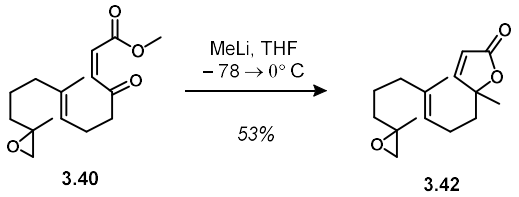

3.40 3.42

Methyl butenolide 3.42:

Enoate **3.40**[36] (15 mg, 53 μmol, 1 equiv.) was taken up in THF (800 μL) and cooled to –78 °C. MeLi (1.6 M in Et_2O, 156 μmol, 3 equiv.) was added dropwise and the solution was stirred for 1 h at –78 °C before gradual warming to 0 °C. The reaction was quenched with sat. aq. NH_4Cl (1 mL) and further diluted with water (1 mL). The aqueous layer was extracted with Et_2O (3 x 1 mL), the combined organic layers were washed with brine (2 mL), dried over $MgSO_4$, filtered and concentrated *in vacuo*. The crude product was purified by flash chromatography (SiO_2, 20% EtOAc in hexanes) to give **3.42** as a colorless oil (8.2 mg, 29.2 μmol, 55%).

Note: Enoate **3.40** was synthesized and provided by Zef Könst.[34]

^{1}H NMR (600 MHz, $CDCl_3$) δ 7.34 (d, *J* = 5.6 Hz, 1H), 6.00 (d, *J* = 5.6 Hz, 1H), 5.03 (t, *J* = 5.8 Hz, 1H), 2.58 (dd, *J* = 13.1, 5.0 Hz, 2H), 2.04–1.80 (m, 6H), 1.75–1.68 (m, 1H), 1.58 (s, 3H), 1.55–1.52 (m, 4H), 1.51–1.48 (m, 2H), 1.30 (s, 3H); **^{13}C NMR** (125 MHz, $CDCl_3$) 172.6, 160.2, 136.0, 123.1, 120.4, 88.8, 56.9, 53.9, 39.4, 38.2, 36.2, 24.0, 23.4, 22.3, 20.9, 15.8; **HRMS** (ES+) m/z calc'd for $C_{16}H_{28}O_3N$ $[M + NH_4]^+$: 282.2069, found 282.2058.

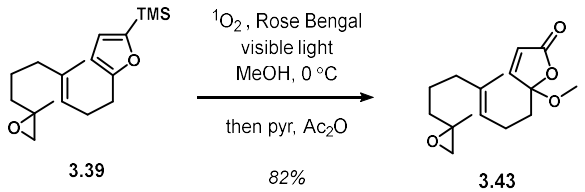

Methoxy butenolide 3.43:

Furan **3.39** (58 mg, 192 μmol. 1 equiv.) and Rose Bengal (2 mg, 0.192 μmol, 1 mol%) were dissolved in dry MeOH (2 mL) and cooled to 0 °C. The flask was sealed with a rubber septum and then equipped with a balloon of oxygen connected to a long needle to extend through the septum and reach the reaction solution. A short outlet needle was also added and O_2 was bubbled through the solution. The reaction was irradiated with 2 x CFL bulbs (40 W) while bubbling O_2 through the pink solution for 45 min. The solution was concentrated under reduced pressure and the resulting pink residue was redissolved in pyridine (1 mL). Ac_2O (23.5 μL, 250 μmol, 1.3 equiv.) was added and the reaction was stirred at room temperature for 3 h. At this point water (3 mL) was added, followed by Et_2O (3 mL). The layers were separated, the aqueous layer was further extracted with Et_2O (2 x 1 mL) and then the combined organic layers were washed sequentially with sat. aq. $CuSO_4$ (2 mL), water (2 mL) then brine (2 mL). The organic phase was dried over $MgSO_4$, filtered and concentrated *in vacuo.* The crude pink residue was purified by flash chromatography (SiO_2, 15% EtOAc in hexanes) to give **3.43** as a colorless oil (44 mg, 157 μmol, 82%).

^{1}H NMR (600 MHz, $CDCl_3$) δ 7.12 (d, *J* = 5.7 Hz, 1H), 6.20 (d, *J* = 5.7 Hz, 1H), 5.05 (t, *J* = 7.0 Hz, 1H), 3.21 (s, 3H), 2.57 (dd, *J* = 16.0, 4.7 Hz, 2H), 2.14–2.03 (m, 2H), 1.97–1.91 (m, 4H), 1.56 (s, 3H), 1.53–1.43 (m, 4H), 1.29 (s, 3H); **^{13}C NMR** (125 MHz, $CDCl_3$) δ 169.9, 153.4, 136.1, 124.7, 123.0, 110.9, 56.9, 53.9, 51.1, 39.4, 37.0, 36.2, 23.3, 21.9, 20.9, 15.8

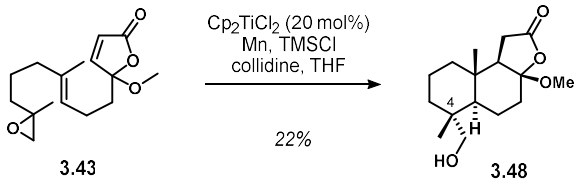

3.43 3.48

Decalin 3.48:

A 1 dram vial was charged with Cp_2TiCl_2 (2.5 mg, 10 μmol, 0.2 equiv.) and Mn^0 (23 mg, 424 μmol, 8 equiv.) and then the solids were dissolved in strictly deoxygenated THF (800 μL). The heterogeneous solution turned from reddish-brown to a dark forest green color after stirring at room temperature for 15 min. At this point 2,4,6–collidine (42 μL, 318 μmol, 6 equiv.) was added to the vial followed by methoxybutenolide **3.43** (15 mg, 53 μmol, 1 equiv.) as a solution in THF (100 μL) and TMSCl (27 μL, 212 μmol, 4 equiv.). The reaction mixture was stirred overnight at room temperature. The reaction was diluted with CH_2Cl_2 then poured into ice cold 1 M HCl (3 mL). The biphasic mixture was separated and then the aqueous layer was extracted with CH_2Cl_2 (3 x 1 mL). The combined organic layers were washed with brine (2 mL), dried over $MgSO_4$, filtered and concentrated *in vacuo.* The crude residue was purified by flash chromatography (SiO_2, 35% EtOAc in hexanes) to afford **3.48** as a colorless oil (3.3 mg, 11.6 μmol, 22%).

Note: cyclized product **3.48** was isolated as a ~ 9: 1 mixture with a minor diastereomer. We speculate this minor product is diastereomeric about the C4–carbon but this was not confirmed.

^{1}H NMR (600 MHz, $CDCl_3$) δ 3.42 (d, *J* = 10.6 Hz, 1H), 3.41 (s, 3H), 3.13 (d, *J* = 10.6 Hz, 1H), 2.63 (dd, *J* = 17.1, 13.5 H, 1H), 2.50 (dd, *J* = 17.1, 8.8 Hz, 1H), 2.38–2.34 (m, 1H), 2.31–2.26 (m, 1H), 1.73–1.64 (m, 1H), 1.59 (dd, *J* = 12.8, 2.5 Hz, 1H), 1.55–1.47 (m, 4H), 1.46–1.35 (m, 2H), 1.32–1.25 (m, 3H),

1.17 (s, 3H), 0.80 (s, 3H); **HRMS** (ES+) m/z calc'd for $C_{16}H_{24}O_4Na$ $[M + Na]^+$: 305.1631, found 305.1677.

3.6 References

1. Xu, M. M.; Hillwig, M. L.; Tiernan, M. S.; Peters, R. J. *J. Nat. Prod.* **2017,** *80* (2), 328-333.
2. Frija, L. M. T.; Frade, R. F. M.; Afonso, C. A. M. *Chem. Rev.* **2011,** *111* (8), 4418-4452.
3. Dewick, P. M. *Nat. Prod. Rep.* **2002,** *19* (2), 181-222.
4. Zou, L. F.; Paton, R. S.; Eschenmoser, A.; Newhouse, T. R.; Baran, P. S.; Houk, K. N. *J. Org. Chem.* **2013,** *78* (8), 4037-4048.
5. Kawamata, Y.; Yan, M.; Liu, Z. Q.; Bao, D. H.; Chen, J. S.; Starr, J. T.; Baran, P. S. *J. Am. Chem. Soc.* **2017,** *139* (22), 7448-7451.
6. Newhouse, T.; Baran, P. S. *Angew. Chem. Int. Ed. Eng.* **2011,** *50* (15), 3362-74.
7. Laudadio, G.; Govaerts, S.; Wang, Y.; Ravelli, D.; Koolman, H. F.; Fagnoni, M.; Djuric, S. W.; Noel, T. *Angew. Chem. Int. Ed.* **2018,** *57* (15), 4078-4082.
8. Hartwig, J. F. *J. Am. Chem. Soc.* **2016,** *138* (1), 2-24.
9. Desai, L. V.; Hull, K. L.; Sanford, M. S. *J. Am. Chem. Soc.* **2004,** *126* (31), 9542-9543.
10. Bathe, U.; Tissier, A. *Phytochemistry* **2019,** *161*, 149 - 162.
11. Choudhary, M. I.; Musharraf, S. G.; Sami, A.; Atta ur, R. *Helv. Chim. Act.* **2004,** *87* (10), 2685-2694.
12. Aranda, G.; Elkortbi, M. S.; Lallemand, J. Y.; Neuman, A.; Hammoumi, A.; Facon, I.; Azerad, R. *Tetrahedron* **1991,** *47* (39), 8339-8350.

13. Diez, D.; Sanchez, J. M.; Rodilla, J. M.; Rocha, P. M.; Mendes, R. S.; Paulino, C.; Marcos, I. S.; Basabe, P.; Urones, J. G. *Molecules* **2005,** *10* (8), 1005-1009.

14. Simmons, E. M.; Hartwig, J. F. *Nature* **2012,** *483* (7387), 70-73.

15. Konst, Z. A.; Szklarski, A. R.; Pellegrino, S.; Michalak, S. E.; Meyer, M.; Zanette, C.; Cencic, R.; Nam, S.; Voora, V. K.; Horne, D. A.; Pelletier, J.; Mobley, D. L.; Yusupova, G.; Yusupov, M.; Vanderwal, C. D. *Nat. Chem.* **2017,** *9* (11), 1140-1149.

16. Tanis, S. P.; Chuang, Y. H.; Head, D. B. *J. Org. Chem.* **1988,** *53* (21), 4929-4938.

17. Rajendar, G.; Corey, E. J. *J. Am. Chem. Soc.* **2015,** *137* (17), 5837-5844.

18. Cherney, E. C.; Green, J. C.; Baran, P. S. *Angew. Chem. Int. Ed.* **2013,** *52* (34), 9019-9022.

19. Crossley, S. W. M.; Obradors, C.; Martinez, R. M.; Shenvi, R. A. *Chem. Rev.* **2016,** *116* (15), 8912-9000.

20. Gaspar, B.; Carreira, E. M. *Angew. Chem. Int. Ed.* **2008,** *47* (31), 5758-5760.

21. Leggans, E. K.; Barker, T. J.; Duncan, K. K.; Boger, D. L. *Org. Lett.* **2012,** *14* (6), 1428-1431.

22. Ma, X. S.; Herzon, S. B. *Chem. Sci.* **2015,** *6* (11), 6250-6255.

23. Brown, H. C.; Delue, N. R. *Tetrahedron* **1988,** *44* (10), 2785-2792.

24. Szklarski, A. R. PhD Dissertation, University of California, Irvine, 2013.

25. Rajanbabu, T. V.; Nugent, W. A. *J. Am. Chem. Soc.* **1994,** *116* (3), 986-997.

26. Justicia, J.; Oltra, J. E.; Cuerva, J. M. *J. Org. Chem.* **2005,** *70* (21), 8265-8272.

27. Justicia, J.; Oltra, J. E.; Cuerva, J. M. *J. Org. Chem.* **2004,** *69* (17), 5803-5806.

28. Morcillo, S. P.; Miguel, D.; Resa, S.; Martin-Lasanta, A.; Millan, A.; Choquesillo-Lazarte, D.; Garcia-Ruiz, J. M.; Mota, A. J.; Justicia, J.; Cuerva, J. M. *J. Am. Chem. Soc.* **2014,** *136* (19), 6943-6951.

29. Barrero, A. F.; Cuerva, J. M.; Herrador, M. M.; Valdivia, M. V. *J. Org. Chem.* **2001,** *66* (11), 4074-4078.

30. Gansauer, A.; Bluhm, H.; Pierobon, M. *J. Am. Chem. Soc.* **1998,** *120* (49), 12849-12859.

31. Justicia, J.; Rosales, A.; Bunuel, E.; Oller-Lopez, J. L.; Valdivia, N.; Haidour, A.; Oltra, J. E.; Barrero, A. F.; Cardenas, D. J.; Cuerva, J. M. *Chem. Eur. J.* **2004,** *10* (7), 1778-1788.

32. Demertzidou, V. P.; Pappa, S.; Sarli, V.; Zografos, A. L. *J. Org. Chem.* **2017,** *82* (16), 8710-8715.

33. Fleury, L. M.; Ashfeld, B. L. *Org. Lett.* **2009,** *11* (24), 5670-5673.

34. Konst, Z. A. PhD Disstertation, University of California Irvine, 2017.

35. Xuan, M. Y.; Paterson, I.; Dalby, S. M. *Org. Lett.* **2012,** *14* (21), 5492-5495.

36. Konst, Z. A. PhD Dissertation, University of California Irvine, 2017.

CHAPTER 4 : A Chlorine-Controlled Bicyclization Enables the Synthesis of Haterumaimides J and K

4.1 Introduction

Our terminal epoxide-initiated bicyclization approach towards haterumaimide J (hatJ, **4.4**) and haterumaimide K (hatK, **4.5**) was reevaluated, and we speculated that switching from a radical to a polar (Lewis acid-initiated) cyclization manifold might afford a more promising outcome. Epoxide activation with a Lewis acid would create a partial positive charge at the more substituted epoxide center and trigger a *6-endo* ring closure for the first π-cyclization.[1] An electron-rich terminating group would then trap the incipient positive charge in a second *6-endo*-type ring closure to complete the bicyclization. Since the second ring forming event in a cation-π cyclization is considered to rapidly occur after the monocyclization,[1-4] this strategy may overcome the difficulties encountered with achieving the bicyclization in a stepwise radical-mediated system.

For a Lewis acid-initiated terminal epoxide cyclization, furan **4.1** was envisioned as an ideal candidate and we proposed a strategy adapted from our radical approach: a furan-terminated cation-π bicyclization of **4.1** with a secondary chloride as a stereocontrol element to construct the decalin core (**4.2**). Oxidative ring opening of the furan with B-ring functional group manipulation could lead to the

Scheme 4.1 Furan-terminated cationic cyclization for the synthesis of hatJ and hatK

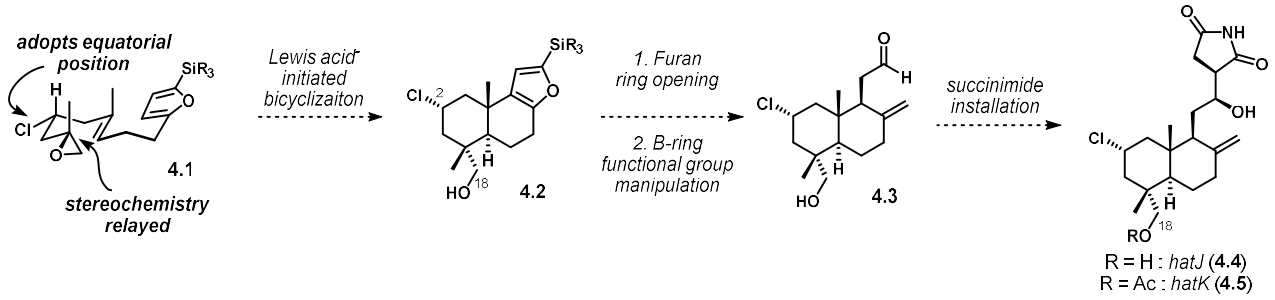

penultimate aldehyde intermediate **4.3**, where subsequent imide installation could access the desired natural products (**4.4** and **4.5**, **Scheme 4.1**).

4.1.1 Furans as terminators in cation-π cyclizations

As electron-rich aromatics, furans have proven quite useful as terminators in cationic cyclizations.[5-7] Their synthetic utility as precursors for unsaturated carbonyl functional groups has popularized their use in complex organic synthesis.[8-10] In 1983, Tanis and coworkers showcased furans as nucleophiles in epoxide-initiated cyclizations.[7] They demonstrated that six- and seven-membered rings could be generated when epoxides, tethered to a pendent furan, were treated with ZnI_2 or $ClTi(O\textit{i}\text{-}Pr)_3$. Additionally, they reported both *endo*- and *exo*-cyclization products could be formed, favoring bond formation at the more substituted carbon (**Scheme 4.2a**). The reaction outcome was dependent on the choice of Lewis acid, as more commonly employed reagents such as $BF_3{\cdot}OEt_2$, $TiCl_4$, and alkylaluminum

Scheme 4.2 Furans as terminators in Lewis acid-initiated cyclizations

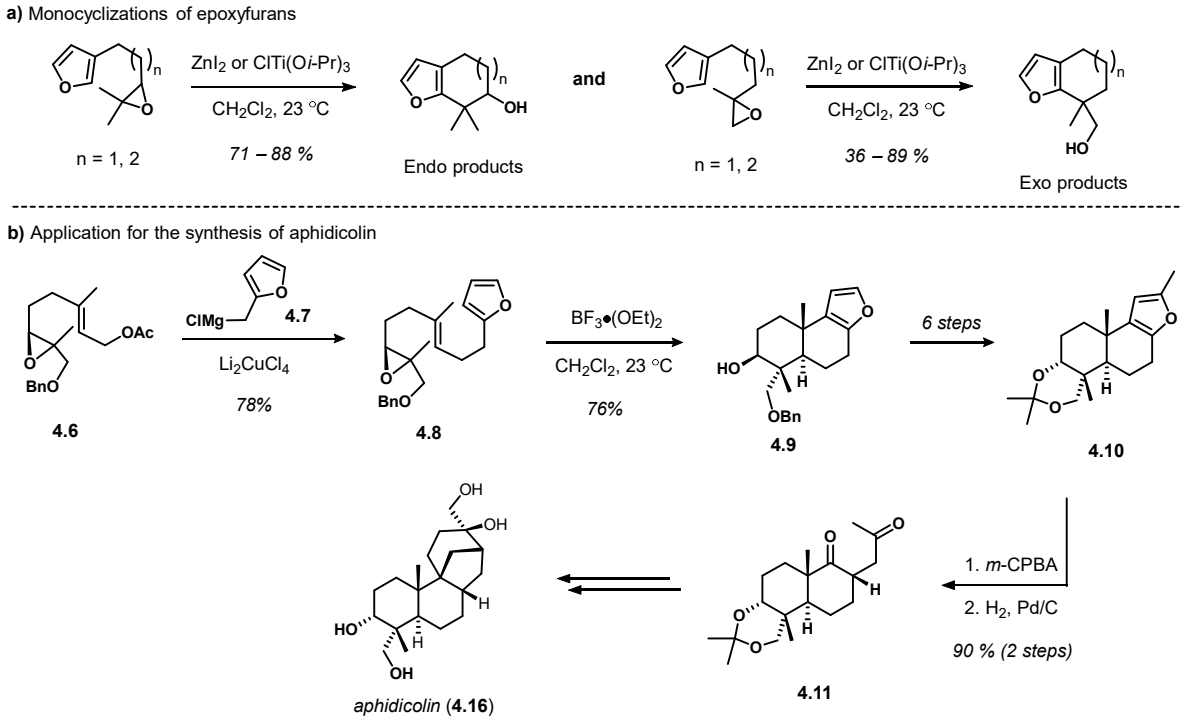

chlorides resulted in decomposition or non-productive epoxide opening. With a preliminary understanding of this reaction, Tanis and coworkers applied their methodology to the synthesis of aphidicolin (**Scheme 4.2b**).[9] Geranyl acetate-derived epoxide **4.6** underwent a copper-mediated coupling with furanyl methyl Grignard reagent **4.7** to afford cyclization precursor **4.8**. Upon treatment with $BF_3{\cdot}OEt_2$, the bicyclization was accomplished in a remarkable 76% yield. The *O*-benzyl protecting group was essential for the efficiency of the cyclization, as a bulkier TBS-protecting group resulted in poor yields of **4.9**. They rationalized that this was a consequence of the steric demand of the silyl ether in preventing the epoxide from adopting the required conformation for the cyclization. Treatment of **4.10** with *m*-CPBA effected an oxidative ring opening of the furan to an ene-dione motif, which was subsequently reduced under hydrogenation conditions to yield **4.11**. The furan provided a functional handle for unveiling the 1,4-dicarbonyl group, which was pertinent for constructing the bicyclic ring system in **4.16**. The pioneering work by the Tanis group on furan-terminated, epoxide-initiated cyclizations—in combination with the variety of conditions for oxidative furan ring opening (bromine, singlet oxygen, peroxides)—presents a powerful strategy for efficient access to terpene scaffolds.

4.2 Terminal epoxides in cationic bicyclizations

An important factor that needed to be addressed when switching from a radical to a cationic bicyclization was the stereocontrol in the formation of the C4–C5 bond. In a Cp_2TiCl-radical cyclization of 2,2-disbustituted epoxides (**4.17**), the conformation of a β-titanoxy radical (**4.18**)—formed by homolytic epoxide cleavage—presumably dictates the stereochemistry at C4 wherein the bulky *O*-$TiCp_2Cl$ group adopts an equatorial position to give **4.19** after bicyclization (**Scheme 4.3a**).[11] However, since a titanocene-mediated bicyclization of an unsubstituted terminal epoxide has not yet been reported,

Scheme 4.3 Stereochemical considerations for a radical- vs cationic-mediated bicyclization

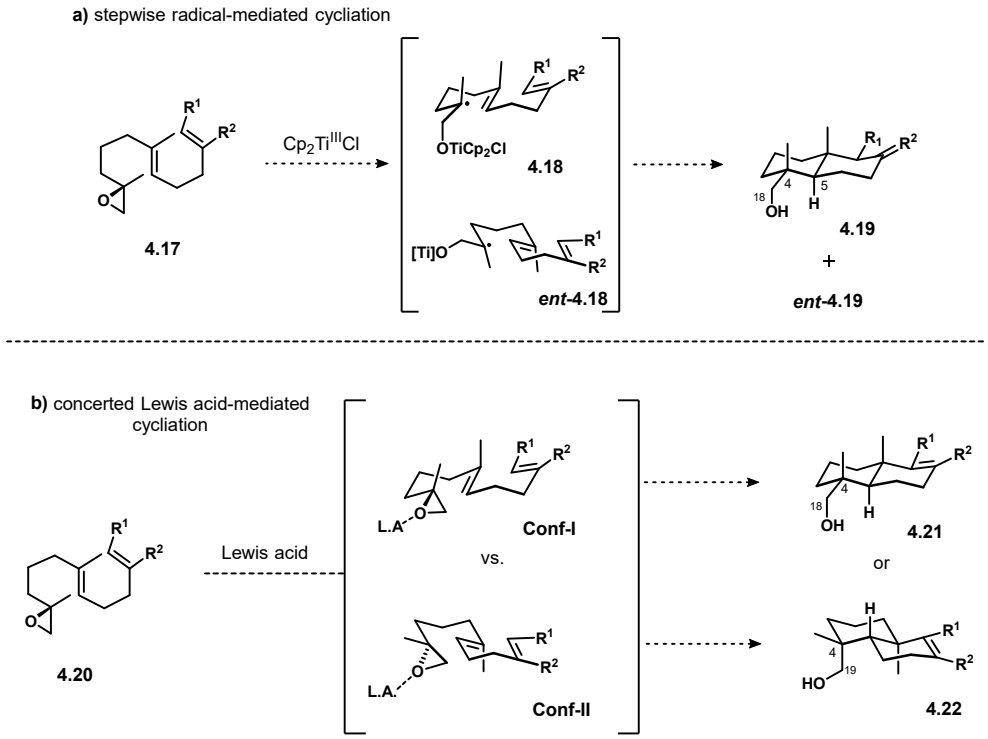

this rational for stereocontrol is only postulated. It should be noted that this step-wise radical cyclization is not stereospecific in regard to the epoxide configuration, upon homolysis of the epoxide bond, the absolute configuration is lost and the cyclization could also proceed through the intermediacy of ***ent*-4.18**. In a cationic Lewis acid-initiated manifold, no such intermediate species exists. Corey and Stass studied the kinetics of an acid-catalyzed cyclization of 5,6-unstaturated oxiranes and proposed that the heterolysis of the epoxide bond occurs with concerted formation of the C4–C5 bond;[1] therefore, the resulting configuration of the C4-center will result from stereospecific opening of the epoxide. The second cyclization event should occur in an concerted asynchronous manner—forming the *trans*-C5–C10 ring junction in accordance with the Stork–Eschenmoser hypothesis[4]—as the partial positive charge is propagated through the π–bonds.[2] The diastereomeric outcome for the bicyclization of 2,2-disbustituted epoxide of type **4.20** ultimately depends on the active conformation of the Lewis acid coordinated

epoxypolyene. If the cyclization proceeds through **Conf-I,** with the epoxide in an equatorial position, the outcome would be C18-oxygenated decalin **4.21**, while the chair flipped conformer **Conf-II** would give the axial C19-oxygenated product **4.22**. We anticipated that a secondary chloride bearing stereocenter on the epoxide substrate (**4.1**) would control the stereochemical outcome of the bicyclization (as shown in **Scheme 4.1**), but the inherent preference for an unsubstituted terminal epoxide to cyclize through **Conf-I** or **Conf-II** was vital information for our key step.

There are surprisingly only a few examples of Lewis acid-initiated bicyclizations of 2,2-disubstituted epoxides; moreover, the bicyclization of an unsaturated terminal-epoxide bearing no

Scheme 4.4 Goldsmith and Phillips example of a 2,2-disubstituted epoxide bicyclization

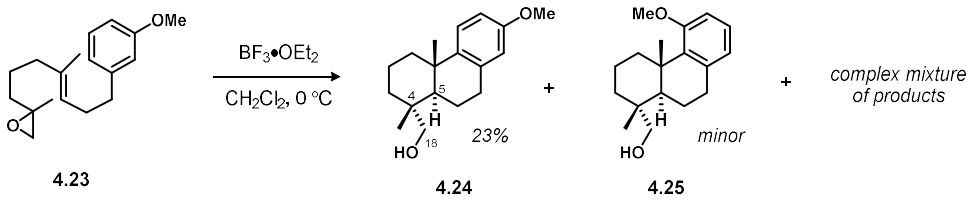

4.23 4.24 4.25

proximal functionality on the neighboring carbons to the epoxide center is essentially limited to a single report. In 1965 Goldsmith and Phillips studied the bicyclization of ***(±)*-4.23** under Lewis acid conditions. Treatment of **4.23** with $BF_3{\cdot}OEt_2$ at 0 °C generated the equatorial hydroxymethyl product (C18-oxygenated **4.24**) in 23% yield, along with the minor *ortho*-cyclized isomer **4.25**, as well as monocyclized and oxabicycled products of unconfirmed relative C4–C5 configuration (**Scheme 4.4**). There was no discussion regarding the diastereoselectivity of the bicyclization; as a result, we remained uncertain about the preferred cyclization conformation. Corey and Liu showed that benzyl ether-substituted terminal-epoxide **4.26** undergoes a high yielding and selective bicyclization to the equatorial C18-oxygenated

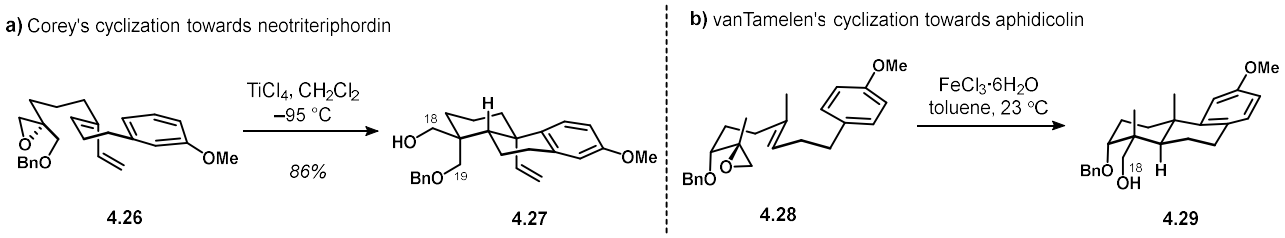

product **4.27** en route to neotripterifordin (**Scheme 4.5a**).[12] Bidendate coordination of the epoxide and benzylether to the titanium metal center likely stabilizes a preferred conformation for cyclization. van Tamelen and coworkers used a Lewis acid-initiated cyclization of terminal epoxide **4.28** in their biomimetic synthesis of aphidicolin.[13] While the isolated yield of **4.29** was not reported, the formation of stereoisomers was implied by reference to "repeated tedious HPLC separations" (**Scheme 4.5b**).

To assess the validity of the furan-terminated bicyclization, and to investigate the inherent cyclization preference, we performed initial experiments on epoxy-furan **4.30**—an intermediate we had readily at hand from our model system studies for the radical cyclization approach. The cyclization substrate (**4.30**) was treated with a variety of Lewis acids at cryogenic temperatures in CH_2Cl_2. The reactivity was consistently plagued with pinacol-type shifts to aldehyde **4.33**, unproductive epoxide opening to chlorohydrin **4.34** and minor amounts of oxabicylization (**4.35**) (**Scheme 4.6**). Eventually, it was found that treatment of **4.30** with $EtAlCl_2$ or $ClTi(O\textit{i}Pr)_3$ at –95 °C resulted in bicyclized products

as a major component of the crude reaction reaction, albeit as a mixture of silylated and desilylated furans. The crude mixture was subjected to $HF_{(x)}$·pyridine and decalin products **4.31** and **4.32** were isolated as a 5:1 diastereomeric mixture in 30–35% yields. These experiments not only provided insight into the critical

Scheme 4.4 Results from studies on des-chlorinated cyclization substrate

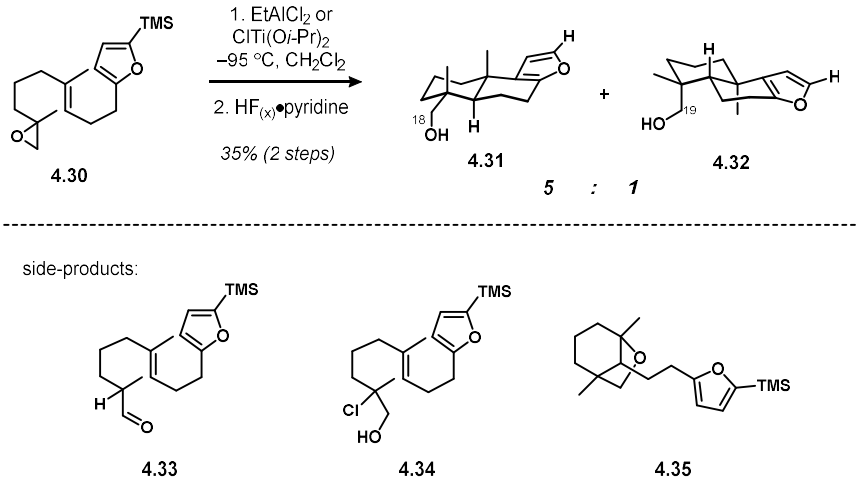

influence the Lewis acid and temperature had on reaction efficiency, but also demonstrated the inherent preference for the terminal epoxide cyclization. The carbon of the epoxide preferentially adopts a pseudo-equatorial position (as in **Conf-I**, **Scheme 4.3**) during the cyclization, over the pseudo-axial (as in **Conf-II**) to give C18-oxygenated product (**4.31**) as the major diastereomer, which coincides with the stereoselectivity reported by Goldsmith and Corey. With the chloride installed on the cyclization substrate, we believed this additional stereocontrol element would lead to a highly selective bicyclization to the C2-chlorinated, C18-hydroxylated core of hatJ.

4.3 Initial synthesis of cyclization precursor

With this promising result for our key bicyclization, we set out to synthesize the chlorinated cyclization substrate **4.36**. We envisioned a similar copper-mediated coupling as that employed in our

model system route to join epoxide (**4.37**) and furan (**4.38**) fragments in a convergent manner (**Scheme 4.7**). Inexpensive, (*S*)-epichlorohydrin (**4.39**) was utilized as a starting point for the synthesis. Addition of lithiated trimethylsilylacetylene to **4.39** opened the epoxide to the chlorohydrin, which subsequently underwent base-mediated epoxide formation to give **4.40**. Isopropenyl cuprate added to the less substituted position of the epoxide to afford known alcohol **4.41** in 55% yield over 3 steps (**Scheme 4.8**).[14, 15] While it was not ideal to start the synthesis of a C20 diterpenoid from a 3-carbon unit such as **4.39**, this three-step sequence was quite efficient and could be performed on a 50 g scale with only a single distillation of **4.41** required for purification. Next, the chloride was installed via a chlorinative displacement of the secondary hydroxyl group with $SOCl_2$/ pyridine; however **4.42** was difficult to obtain in high yields due to the propensity of the homoallylic alcohol (and resulting chloride)to eliminate under the reaction conditions to give

Scheme 4.5 Copper-coupling for the synthesis of cyclization substrate

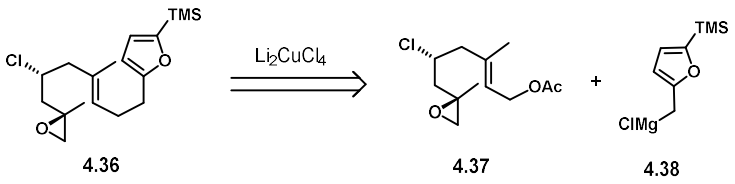

Scheme 4.6 First generation synthesis of chlorinated cyclization substrate

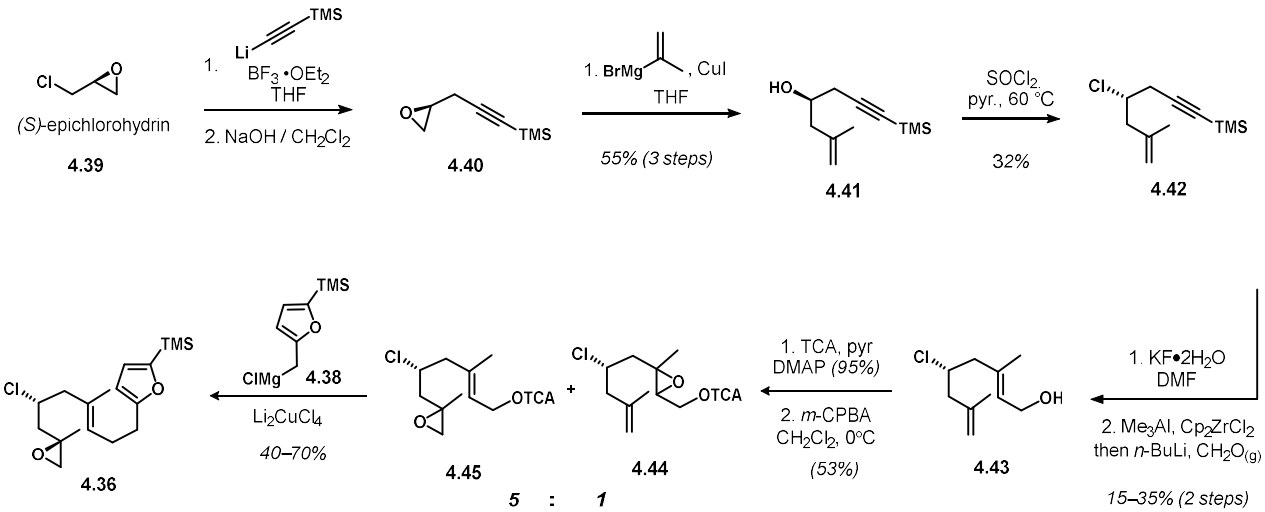

conjugated diene or enyne products. The alkyne desilylation of elimination-prone **4.42** was accomplished under mildly basic conditions with hydrated potassium fluoride, and the resulting alkyne was then subjected to a zirconocene-catalyzed methylalumination. The intermediate vinyl alane produced under these conditions was treated with *n*-BuLi to form the corresponding alanate, which underwent nucleophilic addition to gaseous paraformaldehyde to afford allylic alcohol **4.43**. The procedure for this step was difficult to carry out and the reaction low yielding, but this ultimately accomplished a *de novo* synthesis of a substituted geraniol-type intermediate (**4.43**). We next sought to install the terminal epoxide, and, while we anticipated that a trichloroacetate group would sufficiently deactivate the internal alkene towards epoxidation, a 5:1 mixture of terminal to internal epoxides (**4.45** and **4.44**) were isolated after reaction of trichloroacetate-protected **4.43** with *m*-CPBA. The terminal epoxide was formed as an equimolar mixture of diastereomers at the epoxide center; however, we planned on utilizing a more stereoselective variant for this oxidation during later optimization efforts. Nevertheless, the epoxides were separated and the *anti*-epoxychloride was advanced through the copper-mediated coupling with Grignard reagent **4.38** to obtain **4.36** in modest and inconsistent yields. At this point, initial investigations on the key bicyclization step were quickly deterred by our limited supplies of **4.36**. To construct the cyclization substrate, we encountered many low yielding steps and undesired reactivity. It was evident that trying to adapt our model system route to the synthesis of the chlorinated-epoxide fragment was not the most efficient way to access this intermediate.

4.4 A total synthesis of haterumaimides J and K

4.4.1 A revised synthesis of the cyclization substrate

We determined that the 3-step sequence to alcohol **4.41** did not require modification, but homologation of the alkyne with paraformaldehyde was an inconsistent reaction and a main bottleneck to material throughput. A reliable recourse to this step involved Negishi's well-precedented zirconocene-catalyzed methylalumination followed by iododealumination. Upon desilylation of **4.41,** this procedure

Scheme 4.7 Revised synthesis towards epoxide coupling fragment

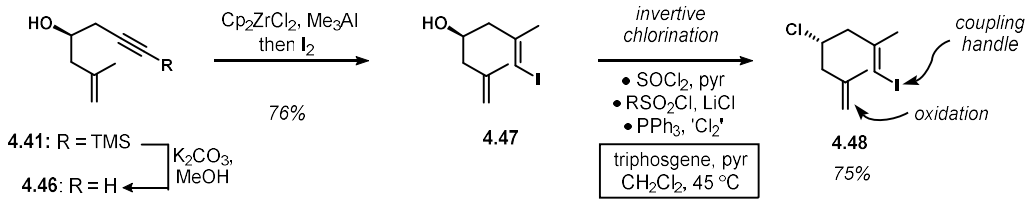

afforded vinyl iodide **4.47** in consistently high yields (**Scheme 4.9**).[16] By incorporating this reaction, the vinyl iodide would now be the functional handle for a convergent coupling to a homologated version of furan **4.38**. An invertive chlorination of alcohol **4.47** yet again proved challenging in the face of competing elimination pathways. We surveyed a variety of conditions for this seemingly trivial reaction ($SOCl_2$, RSO_2Cl and LiCl, PPh_3 with chloride donors) to obtain chloride **4.48** in only 20–35% yields. Eventually a uniquely effective procedure developed by the Kartika group prevailed, forming **4.48** in 75% yield without loss of enantiopurity. This protocol utilizes triphosgene and pyridine to activate the secondary alcohol as the chloroformate while generating a large concentration of chloride anions to complete the invertive displacement.[17] Finally, terminal epoxide installation was required to complete the construction of this coupling fragment. Two issues needed to be addressed for this desired reaction: (1) chemoselectivity with respect to the alkenyl iodide, and (2) the stereoselectivity of epoxide formation.

Table 4.1 Dihydroxylation studies for the stereoselective installation of the terminal epoxide

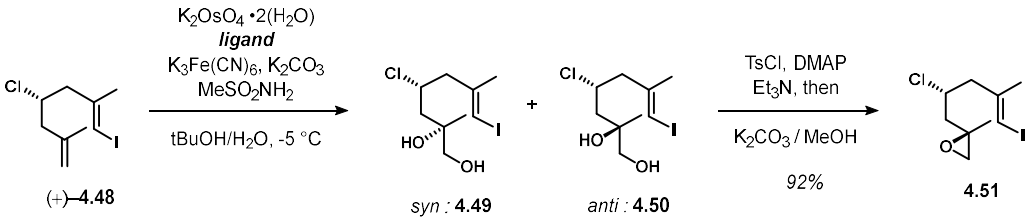

substrate	ligand	diastereomeric ratio (syn : anti)
(±)–**4.48**	none	**2** : **1**
(±)–**4.48**	$(DHQD)_2PHAL$	**1** : **1.3**
(+)–**4.48**	$(DHDQ)_2PHAL$	**1** : **1.7**
(+)–**4.48**	$(DHQ)_2PHAL$	**1.5** : **1**
(+)–**4.48**	**$(DHQD)_2PYR$**	**1** : **6.3** *(83% yield)*
(+)–**4.48**	**$(DHQ)_2PYR$**	**3.5** : **1**

Regarding the latter, the relative configuration between the epoxide stereocenter and the secondary chloride was paramount to the effectiveness of our hypothesized chloride-controlled cyclization, and chloride (**4.48**), posed as a challenging substrate for selective installation of this epoxide stereocenter. These types of 1,1-disubstituted alkenes, especially those bearing two unbranched alkyl groups, are notoriously poor substrates for asymmetric epoxidations and dihydroxylations.[18] The enantio- or in this case diastereotopic faces of the alkene presented to the chiral catalyst are quite similar. Our initial experiments evaluated racemic chloride ***(±)*-4.48** under epoxidation conditions, which resulted in partial reactivity of the trisubstituted alkene; however, a Sharpless dihydroxylation proceeded with complete chemoselectivity for the 2,2-disubstituted alkene. The native diastereoselectivity of a dihydroxylation of racemic ***(±)*-4.48** favored the undesired *syn*-product[1] (**4.49**, **Table 4.1**). The use of AD-mix-β (ligand = $(DHQD)_2PHAL$) imparted little improvement on this diastereoselectivity and the resulting diols were

[1] We colloquially refer to the diols and corresponding epoxides as syn or anti based on the relative configuration to the chlorine-stereocenter in the conformation presented in the schemes/figure/tables. But when these intermediates are in the linear (zigzag) conformation, the relative configuration of the stereocenters are opposite to how we refer to them in the written text.

found to be close to racemic. Similarly, starting from enantiopure **4.48**, the widely utilized phthalazine linked ligands of AD-mix-β and AD-mix-α (ligand = $(DHQ)_2PHAL$) resulted in a nearly equimolar ratio of the desired *anti*–chlorodiol (**4.50**) to the *syn*–diastereomer (**4.49**). We then evaluated other known chiral ligands and reaction conditions in attempts to improve this selectivity. The less frequently adopted pyrimidine-based ligands, $(DHQD)_2PYR$ and $(DHQ)_2PYR$, emerged as the superior option.[19] Employment of $(DHQD)_2PYR$ at –5 °C for 48 hours led to enhanced selectivity in the osmium-catalyzed dihydroxylation of **4.48**, to give **4.50** as the major product in a *ca.* 6:1 mixture. A report by Sharpless states that the alkene binding pocket created by the PHAL-ligands prefer flat aromatic groups, whereas the binding pocket of the PYR-ligands favor alkyl groups.[20] Moreover, the Lannou group investigated the asymmetric dihydroxylation of 2,2-disubstituted alkenes with a methylstereocenter in the homoallylic position (**4.52**) and found that the PYR-ligands gave better diastereomeric ratios (d.r.) of the resulting diols than any other ligand set. They also proposed matched or mis-matched cases for the diastereofacial preference of DHQD and DHQ ligands with the different enantiomers of **4.52** (**Table 4.2**). For example,

Figure 4.1 The Lannou group studies on SAD of 2,2-disubstituted alkenes

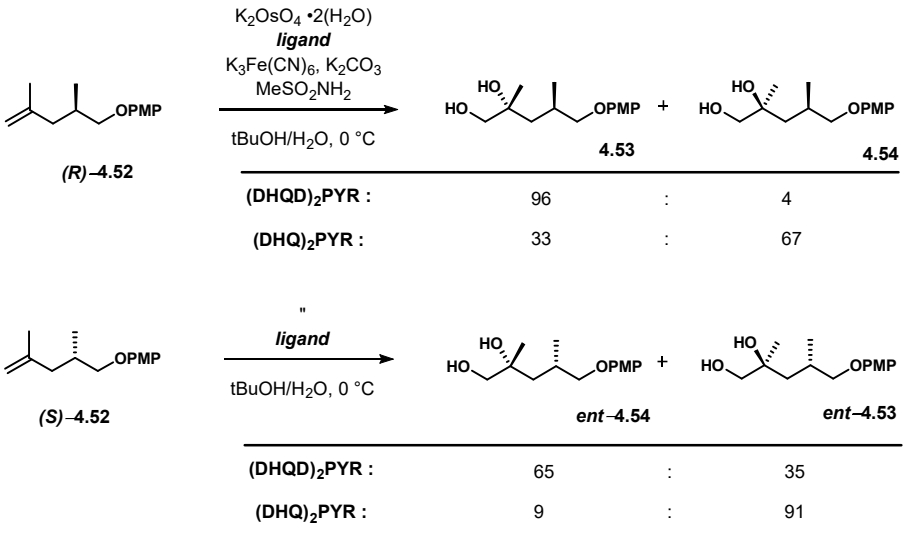

$(DHQD)_2PYR$ results in a stereoselective (d.r. = 96:4) dihydroxylation of **(*R*)-4.52** but gives a poor mixture of diastereomers (d.r. = 65:35) upon reaction with enantiomer **(*S*)-4.52**. The complimentary selectivity was observed with the $(DHQ)_2PYR$ ligand. These results indicate that a homoallylic stereocenter on an acyclic 2,2-disubstituted alkene may affect the diastereofacial preference of the chiral ligands during a Sharpless dihydroxylation. Nevertheless, a 6:1 d.r for the installation of this challenging stereocenter was a significant achievement for the synthesis. The desired diol **4.50** could be isolated by careful chromatography and advanced through epoxide formation to access the desired epoxide coupling fragment **4.51** (**Table 4.1**).

The synthesis of the furan coupling fragment was significantly less complicated. We opted to substitute the furan with a more robust TBS-group to negate the undesired desilylation that can occur during the Lewis acid-promoted cyclization. TBS-furan **4.54** was alkylated with 2-*t*-butyldimethylsilyloxyethyl iodide and the oxygen-silicon bond was selectively cleaved with a buffered TBAF solution to afford **4.55** in 72% yield over the two steps (**Scheme 4.10**). Alcohol **4.55** then underwent an Appel reaction to afford iodide **4.56**. The two fragments were joined together through a *B*-alkyl Suzuki reaction to construct cyclization precursor **4.57** in high yields. This Pd-catalyzed cross-coupling required minimal optimization; indeed, the fact that a general set of conditions have been widely employed in complex molecule synthesis[21, 22] speaks to the reliability and robust nature of this reaction.

Scheme 4.8 Synthesis of furan fragment for a B-alkyl Suzuki coupling

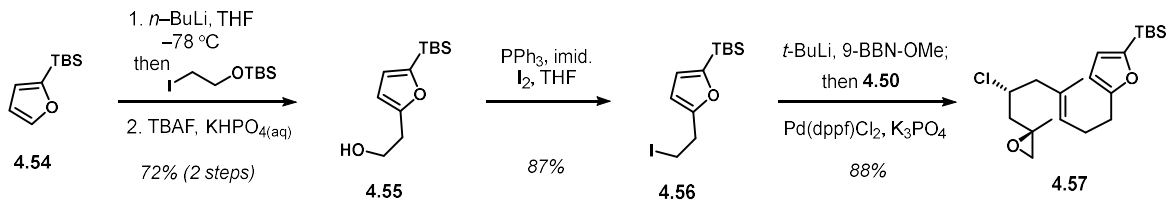

Additionally, this protocol was a substantial improvement upon the inconsistent Li_2CuCl_4-mediated coupling reaction, previously employed for this convergent step.

4.4.2 Optimization of the Lewis acid-mediated bicyclization

With substantial quantities of the cyclization precursor (**4.57**) in hand, a thorough evaluation of the Lewis acid-promoted epoxypolyene bicyclization was permitted. A commonality amongst almost all Lewis acids tested was minimal reactivity of **4.57** at temperatures colder than –80 °C. While cyclizations on our model system substrate were only productive at –95°C, we believe the chloride in **4.57** inductively withdraws electron density from the epoxide, necessitating warming for Lewis acid activation.

We initially tested $ClTi(O\textit{i}Pr)_3$—Tanis's preferred reagent for furan-terminated cyclizations—but this gave minimal reactivity on our system. Switching an *iso*-propoxide ligand with a chloride to make $Cl_2Ti(O\textit{i}Pr)_2$ created a more electron-deficient titanium center and upon reaction with **4.57** partial bicyclization to **4.58** was accomplished, but epoxide opening to halohydrin **4.61** was the predominant product; a similar case was observed for $TiCl_4$ (**Table 4.2**). $BF_3{\cdot}OEt_2$ resulted in modest yields (25–35%) of *trans*-decalin products, although this reaction was accompanied with complete desilylaltion of the furan to **4.59**. Consequently, these conditions were not suitable for our purposes as the TBS-group was vital for the furan ring opening step (discussed in Section 4.5). Employing lanthanide triflate Lewis acids such as $Sc(OTf)_3$, $Eu(OTf)_3$, $Yb(OTf)_3$ either returned starting material or gave minor desilylation of **4.57**; pronounced warming of the reactions resulted in decomposition. We then turned to alkylaluminum Lewis acids: Corey has popularized the use of $MeAlCl_2$ for epoxypolyene cyclizations, although all of his

Table 4.2 Lewis acid screen for desired bicyclization

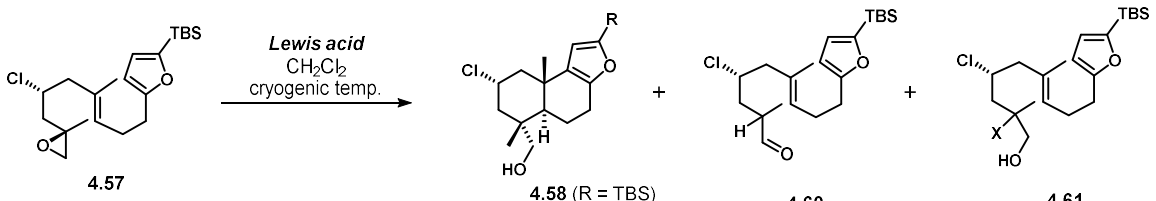

Lewis acid	4.58 (R = TBS) 4.59 (R = H)	4.60	4.61
$Cl_2Ti(O^iPr)_3$	minor	–	major (X = Cl)
$TiCl_4$	–	minor	major (X = Cl)
$BF_3{\bullet}OEt_2$	R = H (~30%)	major	–
$[M](OTf)_3$	–	–	–
$MeAlCl_2$	trace	major	minor
R_2AlCl	trace	minor	major (X = H)
$EtAlCl_2$	**R = TBS (~40%)**	minor	–

examples employ this Lewis acid on 2,3-disubstituted epoxide systems.[3, 23-25] When **4.57** was treated with $MeAlCl_2$, a complex mixture of products was formed with aldehyde **4.60** as the major isolable compound. As $MeAlCl_2$ is commonly used as the Lewis acid for carbonyl-ene/Prins reactions,[26] we speculated the complex mixture of products was likely a result of subsequent Prins-type cyclizations of the *in situ*-generated aldehyde **4.60**. It should be noted that **4.60** was a common side-product for most of our Lewis acid investigations and is a result of a Meinwald rearrangement of the terminal epoxide.[27] This reaction is well-documented in epoxypolyene literature and is a prevalent competing pathway for Lewis acid-initiated cyclizations.[28]

As we continued our screen of aluminum Lewis acids, we found that dialkylaluminum chlorides continued to promote the undesired Meinwald shift to **4.60**, or generated hydride addition products such as **4.61** (X= H). We eventually found $EtAlCl_2$ to be the superior Lewis acid and the desired C18-oxygenated bicyclization product **4.58** was formed as a single diastereomer in 37–45% yields. The

Scheme 4.9 Conformational analysis of cyclization diastereoselectivity

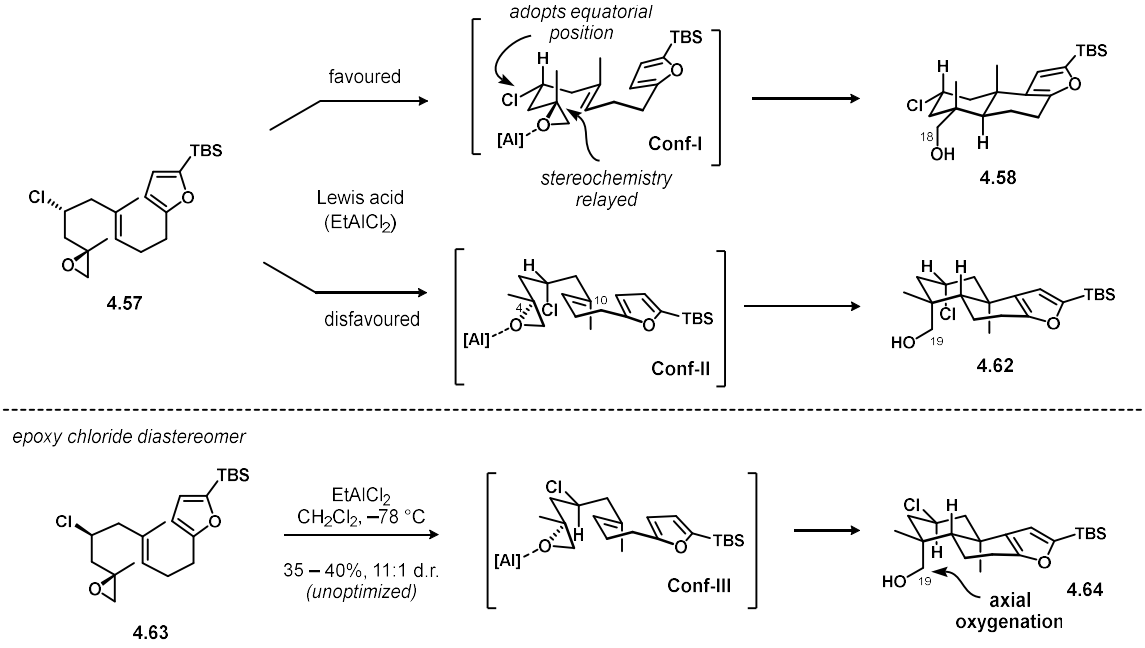

reaction proceeded exactly as we had hoped: both the secondary chloride and the epoxide adopted equatorial positions in the active conformation (**Conf-I**) to give **4.58** (**Scheme 4.11**). The undesired diastereomer **4.62** (which was undetected by ^{1}H NMR) would have to proceed through conformation **Conf-II**, where three axial substituents would create a sterically encumbered transition state. Even though the chlorine atom has a relatively small A-value (*ca.* 0.45), the exacerbation of non-bonded interactions resulting from the two other putative axial groups at C4 and C10 is likely the main contributing factor to the remarkable diastereocontrol.

The most interesting demonstration of chlorine-atom-control was observed in the experiments with *syn*-chloroepoxide **4.63**—derived from the undesired *syn*-chlorodiol **4.48**. Subjecting **4.63** to the same reaction conditions generated axial C19-oxygenated bicycle **4.64** in lower yields but an impressive 11:1 d.r. (**Scheme 4.11**). The bicyclization presumably proceeds through **Conf-III** where the epoxide is forced into a pseudo-axial orientation such that the chlorine can adopt an equatorial disposition. Clearly,

the chlorine atom can play a powerful role as a single atom auxiliary[29] for cationic epoxypolyene cyclizations, in this case overturning the intrinsic selectivity observed in the deschloro analogue (see **Scheme 4.6**). This result presents a novel mode of stereocontrol for accessing C19-oxygenated decalin scaffold from 2,2-disbustituted epoxide polyene substrates. Application of this reaction for the synthesis of complex, C19-oxygenated diterpenoids is ongoing in our lab and will be discussed in Chapter 5.

Once the optimal Lewis acid was discovered for the bicyclization, the reaction was further optimized by the following procedural changes: (1) slight warming from –80 to –70 °C was required for full consumption of starting material; (2) addition of 10 mol% of acid scavenger 2,6-di-*tert*-butylpyridine (DTBP) repressed furan proto-desilylation; and (3) doping a non-polar constituent (toluene) into the solvent mixture with CH_2Cl_2 reduced the amount of aldehyde **4.60** produced through Meinwald shifts. Altogether, these conditions for our key bicyclization increased the isolated yields of **4.58** to 55–65%.

4.4.3 End game sequence

Once we had constructed the decalin core, and ultimately the entire A-ring substituent pattern, we next focused on elaborating the B-ring. Taking inspiration from the strategy developed by Tanis,[9] the furan was oxidatively cleaved by the addition of singlet oxygen after TBS-protection of the C18-hydroxyl group (**Scheme 4.12a**). *In situ* addition of TBAF (1.0 equiv.) and MeI in the furan ring-opening step afforded methyl enoate **4.66** in 85% yield together with minor amounts of hydroxybutenolide **4.67**. Under these conditions,[10] furan **4.65** participates in a Diels–Alder cycloaddition with oxygen—in its excited singlet state—to give endo peroxide **4.68** (**Scheme 4.12b**). This unstable intermediate rearranges to silyl ester **4.69**, which is then methylated through the intermediacy of carboxylate **4.70**. We speculated the furan TBS-group was critical for the formation of silyl ester **4.69**, as similar conditions performed on the

Scheme 4.10 Furan terminating group as a functional handle for a 1,4-dicarbonyl motif

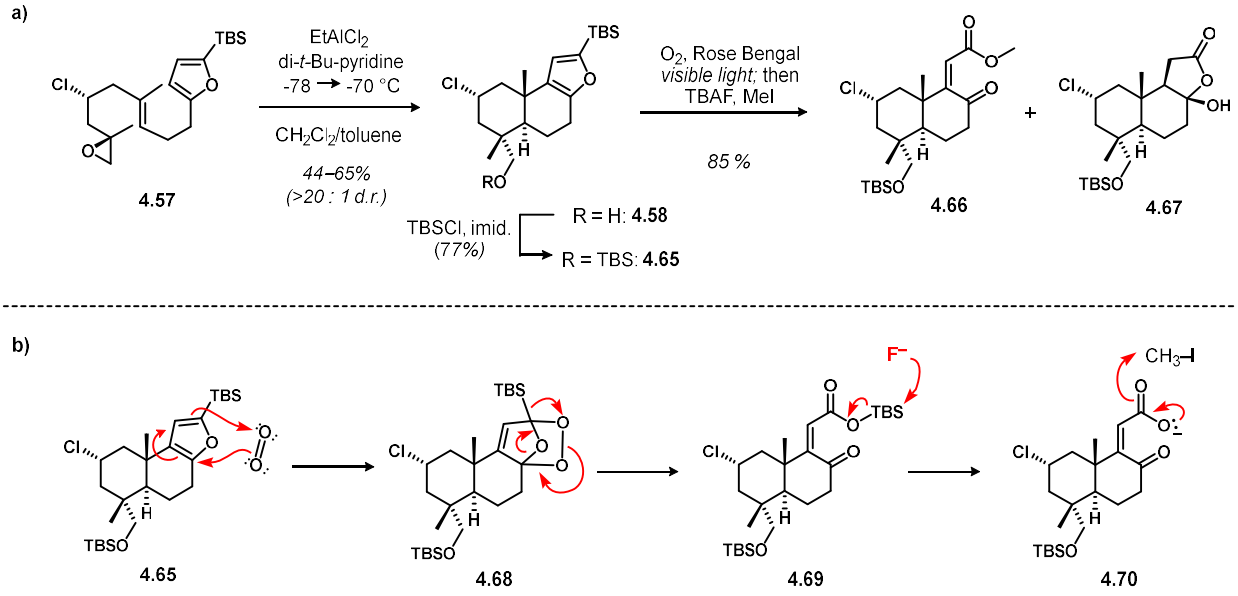

non-silylated furan (**4.59**) solely afforded hydroxybutenolide **4.67**, even in the presence of excess MeI. While **4.67** could be converted to methyl enoate **4.66** (see Experimental Procedures, Section 4.6), the TBS-group allowed for a one-pot procedure. The hydrogenation of **4.66** proceeded selectively from the face opposite of the angular C10-methyl group to afford **4.71** (**Scheme 4.11**). The aforementioned conditions for the oxidative furan ring-opening were strategically implemented such that the resulting 1,4-dicarbonyl motif would be sufficiently differentiated to allow for a selective, salt-free Wittig reaction on the B-ring carbonyl to give **4.72**. Finally, the methyl ester was carefully reduced with *i*-Bu_2AlH to access the aldehyde **4.73**, leaving only succinimide installation to complete the synthesis of hatJ.

Scheme 4.11 B-ring functional group manipulation

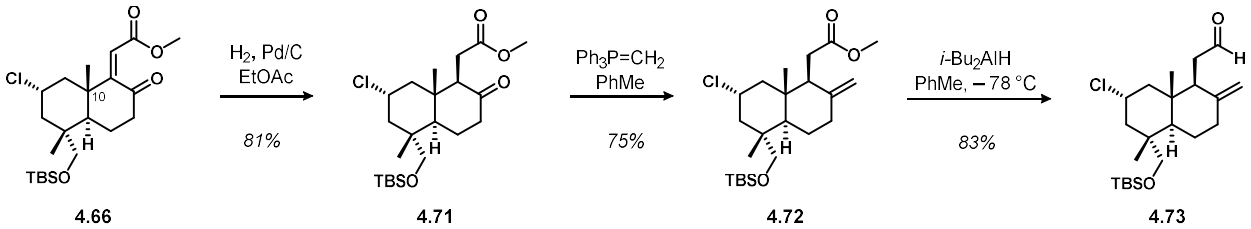

We optimistically employed our Evans-auxiliary controlled aldol sequence to find that the boron-mediated aldol reaction was inconsistent, and, at many times, completely inefficient on small quantities (3–7 mg) of **4.73**. We concluded that the moisture-sensitive Bu_2BOTf Lewis acid was the cause of the

Scheme 4.12 Undesirable reactivity of a Bu_2BOTf-mediated aldol addition

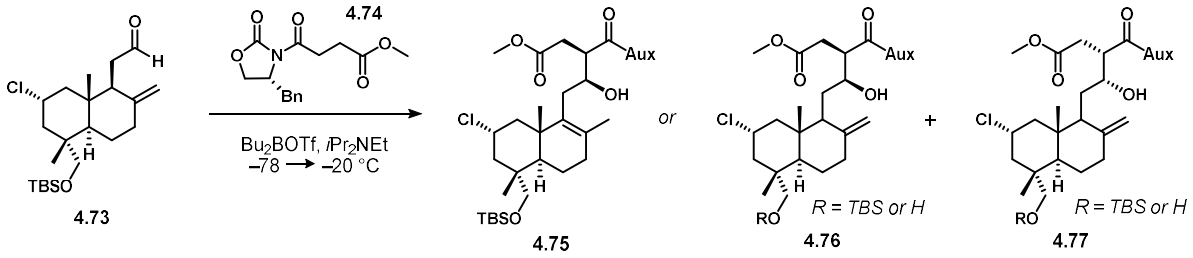

undesired reactivity (**Scheme 4.12**). Even after freshly distilling the reagent, we observed exocyclic-alkene isomerization (**4.75**) on <5 mg quantities of **4.73**, presumably from endogenous TfOH. When reactions were conducted on 10 mg portions of **4.73**, the aldol addition would proceed without alkene isomerization, but the aldol adducts were formed as a mixture of desired **4.76** with the non-Evans-syn diastereomer **4.77**. Furthermore, the TBS-ether was sometimes deprotected under the aldol reaction conditions, and in these cases the major aldol product was the other syn diastereomer (**4.77**). We have currently have no explanation for this undesired result.

It was evident that the aldol addition on **4.73** required a different Lewis acid. Thankfully, our efforts quickly uncovered Cy_2BOTf for this purpose. Enolization of **4.74** with Cy_2BOTf and Et_3N and subsequent addition to **4.73** accomplished a highly selective aldol addition. Following aminolysis/imide formation, **4.78** was formed in a consistent 12: 1 d.r. with the minor syn diastereomer and subsequently

Scheme 4.13 Optimized aldol reaction conditions for the synthesis of hatJ and hatK

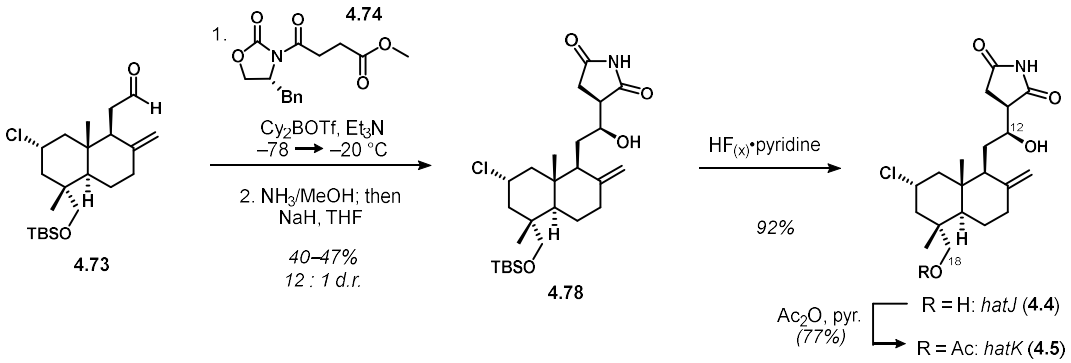

isolated in 40–47 % yields (**Scheme 4.13**). The revised aldol conditions would only consume ~75% of starting material on most attempts; however, **4.73** could be cleanly recovered after the three-step sequence. We speculate that the bulky cyclohexyl ligands on the boron center—which traditionally have been used to selectively form the *E*-enolate on acyclic substrates[30]— impose some steric hinderance when forming the *Z*-enolate on acylated-oxazolidinone which may result in incomplete enolization of **4.74**. With this reliable aldol sequence implemented, **4.73** could be elaborated to **4.78** on a variety of starting material quantities (5 – 20 mg), and further isolated as a pure diastereomer. Imide **4.78** was then treated with $HF_{(x)}$·pyridine to deprotect the C18-TBS-ether and complete the synthesis of hatJ (**4.4**). The primary hydroxyl group of **4.4** was acetylated with decent selectivity (7:1, C18-OAc : C12-OAc) to then afford hat K (**4.5**).

These synthetic products were re-tested against the P388-leukemia cancer cell line and several other human cancer cell lines—HUT78 (cutaneous T-cell lymphoma), A2058 (aggressive melanoma), and DU145 (aggressive prostate cancer) (**Figure 4.2**). The IC_{50} values for the P388 cell line were significantly less potent than those reported by Uemura;[31] however, this discrepancy has been a consistent trend between our synthesized compounds and the reported isolation values. Even so, haterumaimides J

and K are the most potent compounds that we have yet made—natural or unnatural—in the haterumaimide series at *ca.* 30 nM each. For this reason, we tested them against the human hematological cancer HUT78, and again found nanomolar activities. Consistent with our previous work,[32] **4.4** and **4.5** were less active against the solid tumor cell lines A2058 and DU145.

Figure 4.2 Bioactivities of hatJ and hatK against various cancer cell lines

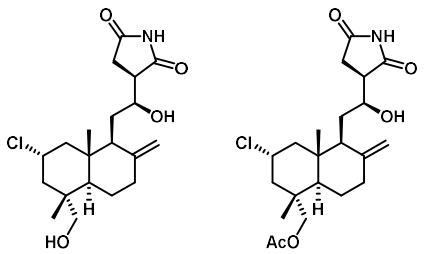

	4.4: *haterumaimide J*	**4.5**: *haterumaimide K*
P388	26 nM (lit = 0.5 nM)	33 nM (lit = 1.0 nM)
HUT78	0.16 μM	0.20 μM
A2058	1.4 μM	1.1 μM
DU145	0.57 μM	0.53 μM

4.5 Conclusion

Our synthetic work towards hatJ and hatK encountered—and subsequently overcame—issues regarding substrate control, asymmetric catalysis and auxiliary control. The initial synthetic efforts revealed inherent difficulties for selectively installing the chloride and epoxide stereocenters. This has been an underlying challenge throughout the entirety of our work on the C18-oxygenated, C2-chlorinated haterumaimides. Through extensive route optimization, we developed a stereoselective and convergent synthesis of the chloride-containing cyclization precursor (**4.57**). The scarcity of synthetic work on polyene cyclizations of simple 2,2-disbustitued epoxides required us to engage in a thorough evaluation for this reaction. Optimized conditions were developed—minimizing side-product formation—to accomplish the key bicyclization to the core of the natural products in good yields and high diastereoselectivity. While the hydroxysuccinimide proved yet again one of more synthetically challenging motifs in the haterumaimides, a reliable protocol was developed to complete the synthesis of hatJ (**4.4**) and hatK (**4.5**). This work allowed us to confirm **4.4** and **4.5** as the most potent cytotoxins of the haterumaimide family and we are eager to co-crystallize **4.4** with the eukaryotic ribosome to investigate the key interactions that underlie its unique cytotoxicity.

In our synthetic studies we revealed the utility of a chlorine-stereocenter as a single-atom auxiliary to control the stereochemical outcome of epoxypolyene cyclizations. Owing to the facile incorporation and excision of chlorine atoms, ongoing work in our lab aims to generalize this strategy for the synthesis of C18/C19-oxygenated, C3-unoxygenated diterpenoids.

4.6 Experimental Procedures

Materials and Methods:

All reactions were performed in oven-dried (120 °C) or flame-dried glassware under an atmosphere of dry argon unless otherwise noted. Reaction solvents including dichloromethane (CH_2Cl_2, Fisher, HPLC Grade), hexanes (Fisher, HPLC Grade), diethyl ether (Et_2O, Fisher, BHT stabilized, HPLC Grade), benzene (C_6H_6, Fisher, HPLC Grade), tetrahydrofuran (THF, Fisher, HPLC Grade), and toluene ($PhCH_3$, Fisher, HPLC Grade) were dried by percolation through a column packed with neutral alumina and a column packed with Q5 reactant, a supported copper catalyst for scavenging oxygen, under a positive pressure of argon.

Solvents for workup and chromatography were: acetone (Fisher, ACS grade), hexanes (Fisher or EMD, ACS Grade), EtOAc (EtOAc, Fisher, ACS Grade), dichloromethane (CH_2Cl_2, Fisher, ACS Grade), and methanol (MeOH, Fisher, ACS Grade). Column chromatography was performed using EMD Millipore 60 Å (0.040–0.063 mm) mesh silica gel (SiO_2). Analytical thin-layer chromatography was performed on Merck silica gel 60 F254 TLC plates. Visualization was accomplished with UV (254 or 210 nm), and p-anisaldehyde, ceric ammonium molybdate or potassium permanganate and heat as

developing-agents.

^{1}H NMR and ^{13}C NMR spectra were recorded at 298 K on Bruker GN500 (500 MHz, ^{1}H; 125 MHz, ^{13}C), Bruker CRYO500 (500 MHz, ^{1}H; 125 MHz, ^{13}C), and Bruker AVANCE600 (600 MHz, ^{1}H; 125 MHz, ^{13}C) spectrometers. ^{1}H and ^{13}C spectra were referenced to residual $CHCl_3$ (7.26 ppm, ^{1}H or 77.0 ppm, ^{13}C). ^{1}H and ^{13}C spectra taken in DMSO-d_6 were referenced to residual DMSO-d_5 (2.49 ppm, ^{1}H or 39.5 ppm, ^{13}C). Chloroform-d ($CDCl_3$, D 99.8%, DLM-7) and dimethyl sulfoxide-d6 (CD_6SO, D 99.9%, DLM-10) were purchased from Cambridge Isotope Laboratories. Chemical shifts are reported in ppm and multiplicities are indicated by: app (apparent), s (singlet), d (doublet), t (triplet), q (quartet), m (multiplet), and br s (broad singlet). Coupling constants, J, are reported in Hertz. Infrared (IR) spectra were recorded on a Perkin-Elmer spectrum RX1 FT-IR instrument or Varian 640-IR instrument on NaCl plates and peaks are reported in cm^{-1}. Mass spectrometry data were obtained from the University of California, Irvine Mass Spectrometry Facility. High-resolution mass spectra (HRMS) were recorded on a Waters LCT Premier spectrometer using ESI-TOF (electrospray ionization-time of flight) or CI-TOF (chemical ionization-time of flight) and data are reported in the form of (m/z). GC/FID analysis was performed on Agilent 7820A system with helium as carrier gas. HPLC analysis was performed on an Agilent 1100 series.

Citric acid (ACS grade, anhydrous, Fisher), potassium sodium tartrate (Oakwood), K_2CO_3 (anhydrous, 99%, Alfa Aesar), $NaHCO_3$ (ACS grade, Fisher), NaOH (ACS grade, Macron or Fisher), $Na_2S_2O_3$ (ACS grade, Fisher), *p*-anisaldehyde (99%, Acros Organics), isopropenylmagnesium bromide (0.5 M in THF, Sigma-Aldrich), tetrabutylammonium fluoride (TBAF, 1 M in THF, Sigma Aldrich), trimethylaluminum ($Al(CH_3)_3$, Sure Pack™ reagent grade, Sigma Aldrich), B-methoxy-9BBN solution (1 M in hexanes, Sigma Aldrich), ethylaluminum dichloride solution (1 M in hexanes, $EtAlCl_2$, Acros Organic), 2,6-di-*t*-butylpyridine (99%, Alfa Aesar), diisobutylaluminum hydride (*i*-Bu_2AlH, Sure Pack™ reagent grade, Sigma Aldrich), ammonia (2.0 M in methanol, Acros Organics), dicyclohexylboron trifluoromethansulfonate (Cy_2BOTf, Sigma Aldrich) were used without further purification. The following reagents were distilled from the indicated drying agents under argon prior to use:

triethylamine (Et_3N, EMD, CaH_2), pyridine (Alfa Aesar, CaH_2 and *N,N*-diisopropylethylamine (*i*-Pr_2NEt, Alfa Aesar, CaH_2). Trimethylsilyl chloride ($(CH_3)_3SiCl$, Acros Organics) and dibutylboron triflate (*n*-Bu_2BOTf, Acros Organics), were fractionally distilled prior to use.

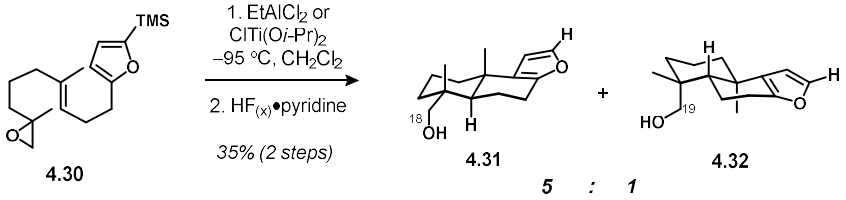

Des-chloro decalins 4.31 and 4.32:

A solution of des-chloro cyclization precursor **4.30** (15 mg, 49 μmol, 1 equiv. see Chapter 3 experimentals) in CH_2Cl_2 (0.05 M, 980 μL) was cooled to –90 °C. $EtAlCl_2$ (0.9 M in heptane, 93 μmol, 2 equiv.) was added dropwise down the side of the vial. After 45 min, Et_3N (100 μL) was added and the solution was warmed to 0 °C. Sat. aq. potassium sodium tartrate solution (1 mL) was added and the mixture was stirred vigorously. The biphasic mixture was further diluted with water (1 mL), the phases were separated and the aqueous phase was extracted with Et_2O/hexanes (1:1, 3 x 1 mL). The organic extracts were combined, washed with brine, dried over anhydrous $MgSO_4$, filtered, and concentrated *in vacuo.* The crude residue contained a mixture of cyclized, silylated and desilylated diastereomers. To simplify the crude diastereomeric analysis the mixture was taken up in THF (400 μL) and HF *(*x*)*•pyridine (50 μL) was added. The mixture was stirred at room temperature for 7 h and then diluted with water (1 mL), EtOAc (1 mL) and the excess acid was quenched with sat. aq. K_2CO_3 (500 μL). The layers were separated and the aqueous layer was extracted with EtOAc (2 x 0.5 mL), the organic extracts were washed

with brine, dried over anhydrous $MgSO_4$, filtered, and concentrated *in vacuo.* The crude residue was analyzed by ^1H NMR and a diastereomeric ratio of 5:1 was observed for **S9** and **S10**, respectively. The crude product residue was purified by flash chromatography (SiO_2, 10% EtOAc in hexanes) to obtain the purified mixture of decalin diastereomers (**4.31** & **4.32**, 5.1 mg, 35% and the same diastereomeric ratio was observed by comparing the resonances at 3.47 ppm, 3.26 ppm for C18-oxygenated product and 3.80 ppm, 3.55 ppm for C19-oxygenated product in the ^1H NMR (see spectra for details).

HRMS (ESI+) *m/z* calc'd for $C_{15}H_{22}O_2Na$ $[M+H]^+$: 235.1698; found 235.1707.

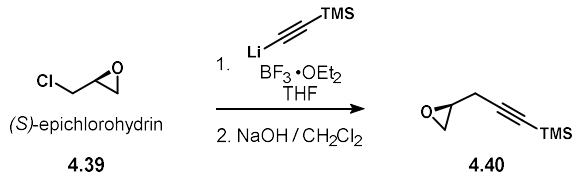

Epoxide 4.40:

A 1 L-three neck round bottom flask was charged with trimethylsilyl acetylene (23 mL, 162.1 mmol, 1.5 equiv.) in dry THF (188 mL) and the solution was cooled to −78 °C. *n*-BuLi (2.5 M in hexanes, 64 mL, 162.1 mmol, 1.5 equiv.) was added through an addition funnel followed by $BF_3.OEt_2$ (20 mL, 162.1 mmol, 1.5 equiv.). The yellow solution was stirred for 10 min at –78 °C before a solution of *(S)*-epichlorohydrin (10.0 g, 100.8 mmol, 1 equiv.) in dry THF (100 mL) was added dropwise. The reaction mixture was maintained at this temperature for 30 min, warmed to 0 °C over a period of 2 h, and then held at 0 °C for 1 h. The resulting suspension was diluted with sat. aq. NH_4Cl (800 mL) and Et_2O (100 mL). The layers were separated, the aqueous layer was extracted with Et_2O (3 x 50 mL), the combined organic extracts were washed with brine, dried over anhydrous $MgSO_4$, filtered, and concentrated *in vacuo*. The crude chlorohydrin was taken up in CH_2Cl_2 (300 mL), NaOH (~3 equiv.) was added, the mixture was

stirred at ambient temperature for 14 h. The reaction was diluted sequentially with sat. aq. NH_4Cl (100 mL) and water (200 mL). The layers were separated and the aqueous layer was extracted with CH_2Cl_2 (2 x 25 mL), the organic phases were combined, washed with brine, dried over anhydrous $MgSO_4$, filtered, and concentrated *in vacuo.* The resulting crude oil was purified by fractional distillation (80 °C, 40 mmHg) to give epoxide **4.40**, contaminated with minor amounts of THF, as a clear, colorless oil (11.1 g, 72.5 mmol, 72%). This intermediate was immediately advanced to the next step.

The ^1H MR and ^{13}C NMR spectra agreed with the literature data.[33]

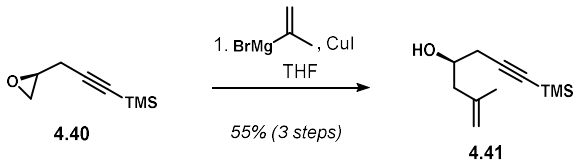

TMS-alkyne 4.41:

A 3-neck round bottom flask was charged with a solution of **4.40** (8.50 g, 55.1 mmol, 1 equiv.) in dry THF (110 mL, 0.5 M), followed by the addition of CuI (734 mg, 3.85 mmol, 0.07 equiv.) and the suspension was cooled to –78 °C. A solution of isopropenylmagnesium bromide (0.5 M in THF, 200 mL, 2 equiv.) was added dropwise through an addition funnel. The temperature was maintained at –78 °C for 30 min, the reaction mixture was allowed to warm to –25 °C over 4 h and then sat. aq. NH_4Cl (100 mL) was added. The biphasic mixture was stirred at 0 °C for 20 min, further diluted with water (100 mL) and Et_2O/hexanes (1:4, 50 mL), and the layers were separated. The aqueous layer was further extracted with Et_2O/hexanes (1:4, 3 x 50 mL), the organic layers were combined, washed with brine, dried over anhydrous $MgSO_4$, filtered, and concentrated *in vacuo.* The crude residue was purified by

distillation in a Kugelrohr apparatus (90 °C, 15 mmHg) to afford **4.41** as a clear oil (5.60 g, 36.3 mmol, 55% over 3 steps).

The ^{1}H MR and ^{13}C NMR spectra agreed with the literature data.[15]

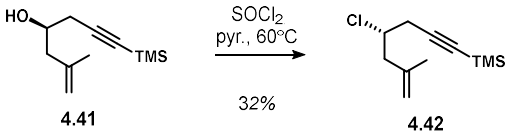

4.41 4.42

Propargylic chloride 4.42:

Alcohol **4.41** (150 mg, 0.764 mmol, 1 equiv.) was taken up in dry THF (5 mL) and then pyridine (306 µL, 3.82 mmol, 5 equiv.) was added. Freshly distilled $SOCl_2$ (166 µL, 2.29 mmol, 3 equiv.) was added dropwise to the reaction. The flask was equipped with a reflux condenser, the reaction was heated to 65 °C and vigorously stirred at this temperature for 8 h. The brown reaction mixture was cooled to 0 °C and sat. aq. NH_4Cl (5 mL) was added dropwise. The biphasic mixture was extracted with hexanes (3 x 5 mL) and washed sequentially with water (3 mL) and brine (3 mL). The organic extracts were combined, dried over $MgSO_4$, filtered, and concentrated *in vacuo.* The crude residue was purified by flash chromatography (SiO_2, hexanes) to afford **4.42** (52.3 mg, 0.244 mmol, 32% yield) as a yellow oil.

^{1}H NMR (500 mHz, $CDCl_3$) δ 4.89 (s, 1H), 4.83 (s, 1H), 4.09 (q, J = 6.5 Hz, 1H), 2.72–2.65 (m, 3H), 2.43 (dd, J = 14.2, 8.5 Hz, 1H), 1.77 (s, 3H), 0.16 (s, 9H); **^{13}C NMR** (125 mHz, $CDCl_3$) δ 141.2, 114.1, 102.1, 87.9, 57.3, 45.4, 29.5, 22.1, -0.05.

Chloride 4-S1:

4.42 4-S1

TMS-alkyne **4.42** (110 mg, 0.502 mmol, 1 equiv.) was taken up in wet DMF (2 mL), the solution was cooled to 0 °C and then $KF•2H_2O$ (161 mg, 1.71 mmol, 3.5 equiv.) was added. The reaction was allowed to warm to ambient temperature and stirred for an additional 12 h. The resulting suspension was diluted sequentially with sat. aq. NH_4Cl (3 mL), water (1 mL) and hexanes (3 mL). The biphasic mixture was extracted with hexanes (3 x 3 mL) and washed sequentially with water (2 x 3 mL) and brine (2 x 3 mL). The organic extracts were combined, dried over $MgSO_4$, filtered, and concentrated *in vacuo.* The crude residue was sufficiently pure and carried onto the next step without purification.

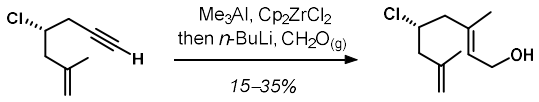

4-S1 4.43

Allylic Alcohol 4.43:

A 3-neck round bottom flask was charged with Cp_2ZrCl_2 (42.5 mg, 0.145 mmol, 0.5 equiv.), this was dissolved in dry CH_2Cl_2 (1 mL) and the solution was cooled to –20 °C. Me_3Al (217 µL, 0.435 mmol, 2 equiv.) was added dropwise to the reaction and the resulting solution was stirred at –20 °C for 1 h. A solution of alkyne **4-S1** (31 mg, 0.29 mmol, 1 equiv.) in CH_2Cl_2 (300 µL) was added dropwise to yellow solution and the reaction was allowed to warm to ambient temperature over 3 h. The reaction was cooled –30 °C and *n*-BuLi (1M in hexanes, 1.2 equiv.) was added dropwise, after 20 mins of stirring the alanate solution was warmed to 0 °C. The reaction flask was equipped with a septum which was pierced with a glass cannula, the other end of the cannula was connected to a septum sealed over a round

bottom flask containing ~1.0 g of *p*-formaldehyde. The solid *p*-formaldehyde flask was heated to 200 °C and the resulting formaldehyde gas was bubbled into the alanate solution. Once the solution appeared saturated the glass cannula was removed, and the reaction was quenched with 1N HCl (2 mL). The solution was further diluted with CH_2Cl_2 (2 mL) and the layers were separated. The aqueous layer was extracted once with CH_2Cl_2 (1 mL) and the organic layers were then combined, washed with brine (2 mL), dried over $MgSO_4$, filtered and concentrated *in vacuo.* The crude residue was purified by flash chromatography (SiO_2, 10% EtOAc in hexanes) to afford allylic alcohol **4.43** (19.3 mg, 101 mmol, 35% yield) as a white foam. The yield of this reaction varied between 15–35%.

^{1}H NMR (500 mHz, $CDCl_3$) δ 5.51 (t, *J* = 6.9 Hz, 1H), 4.88 (s, 1H), 4.80 (s, 1H), 4.19 (d, *J* = 6.9 Hz, 2H), 4.17–4.13 (m, 1H), 2.55–2.35 (m, 4H), 1.76 (s, 3H), 1.71 (s, 3H), 1.32 (br s, 1H); **^{13}C NMR** (125 mHz, $CDCl_3$) δ 141.5, 135.3, 127.2, 113.7, 59.2, 58.1, 48.1, 46.7, 22.1, 16.1; **HRMS** (ES+) *m/z* calc'd for $C_{10}H_{17}OClNa$ $[M + Na]^+$: 210.9968; found 210.9982.

Trichloroacetate 4-S2:

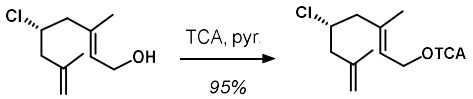

4.43 4-S2

Allylic alcohol **4.43** (7.5 mg, 38 μmol, 1 equiv.) was dissolved in THF (750 μL) and resulting solution was cooled to 0 °C. Pyridine (74 μmol, 2 equiv.) was added as a solution in THF (1M) followed by trichloroacetic anhydride (44 μmol, 1.5 equiv.) as a solution in THF (1M). The reaction was allowed to warm to ambient temperature and stirring was continued for 4 h. The reaction was diluted with water (1 mL) and the aqueous layer was extracted with Et_2O (3 x 1 mL). The combined organic layers were washed with brine (1 mL), dried over $MgSO_4$, filtered and concentrated *in vacuo.* The crude residue was

purified by flash chromatography (SiO_2, 3% EtOAc in hexanes) to afford trichloroacetate **4-S2** (10 mg, 33 μmol, 90% yield) as a clear oil.

^{1}H NMR (500 mHz, $CDCl_3$) δ 5.53 (t, *J* = 7.33, 1H), 4.92–4.85 (m, 3H), 4.80 (s, 1H), 4.15 (m, 1H), 2.55 (dd, *J* = 14.2, 4.9 Hz, 1H), 2.44 (app d, *J* = 7.2 Hz, 2H), 2.41 (dd, *J* = 14.2, 5.3 Hz, 1H), 1.81 (3H), 1.75 (3H); **HRMS** (ES+) *m/z* calc'd for $C_{12}H_{16}O_2Cl_4Na$ $[M + Na]^+$: 354.9704; found 354.9755.

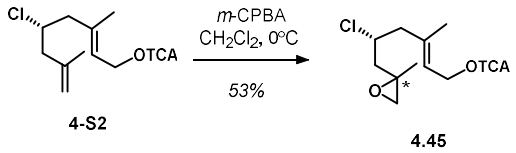

4-S2 4.45

Epoxide 4.45:

Trichloroacetate **4-S2** (10 mg, 26 μmol, 1 equiv.) was taken up in CH_2Cl_2 (800 μL) and the solution was cooled to 0°C. In a single portion, *m*-CPBA (12 mg, 53 μmol, 1.5 equiv) was added, the reaction was monitored by TLC and a subsequent addition of *m*-CPBA (1 equiv.) was required for consumption of starting material. The reaction was quenched by the addition of sat. aq. $NaHCO_3$ (1 mL) and then diluted sequentially with water (1 mL) and Et_2O (1 mL). The biphasic mixture was separated and the aqueous layer was extracted with Et_2O (2 x 1 mL). The organic layers were combined, washed with brine (1 mL), dried over $MgSO_4$, filtered and concentrated *in vacuo.* The crude residue contained a mixture of regioisomeric epoxides **4.45** and **4.44** in a 5:1 ratio. The mixture purified by flash chromatography (SiO_2, 10% EtOAc in hexanes) and the desired terminal epoxide **4.45** was isolated as a 1:1 mixture of diastereomers (8 mg, 22.8 μmol, 53% yield). The desired anti-chloroepoxide was isolated after subsequent flash chromatography (SiO_2, 5% EtOAc in hexanes) to afford 3.8 mg of anti-chloroepoxide **4-S3**.

*The ^{1}H NMR tabulated is a mixture of **4.45** diastereomers at the epoxide stereocenter.

^{1}H NMR (500 mHz, $CDCl_3$) δ 5.30 (m, 2H), 4.89 (app d, *J* = 7.2 Hz, 4H), 4.16 (m, 1H), 3.99 (m, 1H), 2.88 (d, *J* = 4.4 Hz, 1H), 2.72 (dd, *J* = 22, 4.7 Hz, 4H), 2.62 (d *J* = 4.4 Hz, 1H), 2.5 (dd, *J* = 14.2, 5.4 Hz, 2H), 2.52–2.44 (m, 4H), 2.13 (dd, *J* = 14.6, 4.2 Hz, 2H), 2.07 (d, *J* = 6.5 Hz, 2 H), 1.82 (s, 3H), 1.80 (s, 3H), 1.71 (dd, *J* = 14.5, 10.4 Hz, 4H), 1.39 (s, 3H), 1.38 (s, 3H); **HRMS** (ES+) *m/z* calc'd for $C_{12}H_{16}O_3Cl_4Na$ $[M + Na]^+$: 372.9723; found 372.9801.

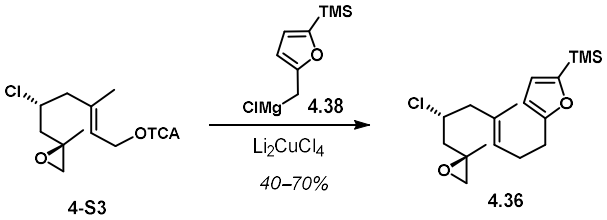

4-S3 4.36

Epoxypolyene 4.36:

The furfuryl Grignard (**4.38**) was made through addition of the corresponding furfuryl chloride to a solution of excess Mg^0 in THF (1.7 mL), it should be noted that the Mg^0 pellets were initially flamed dried under vacuum. Dibromoethane was added (50 μL) and then the reaction mixture was warmed briefly to 60 °C to ensure Grignard formation. The grey-brown solution was titrated to 0.56 M. [34]

Epoxide **4-S3** (5 mg, 14 μmol, 1 equiv.) was taken up in THF (200 μL). A solution of Li_2CuCl_4 was made by mixing LiCl (18.4 mg, 28 μmol, 2 equiv.) and $CuCl_2$ (12 mg, 14 μmol, 1 equiv.) in 1 mL of THF and sonicating the mixture until all solids were dissolved. The reddish-orange Li_2CuCl_4 solution was added to the epoxide solution (6 μL, 0.04 equiv.). The reaction mixture was then cooled to 0 °C and the **4.38** Grignard solution (42 mmol, 3 equiv.) was added dropwise. The reaction was stirred at 0 °C for 45 mins and then quenched with 300 μL of sat. aq. NH_4Cl. The aqueous layer was extracted with EtOAc/hexanes (3:1, 2 x 3), washed with brine (1 mL), dried over $MgSO_4$, filtered and concentrated *in*

vacuo. The crude product was purified by flash chromatography (SiO_2, 7% EtOAc in hexanes) to give **4.36** as a colorless oil (3.5 mg, 9.55 μmol, 68%).

^{1}H NMR (600 MHz, $CDCl_3$) δ 6.54 (d, *J* = 3.0 Hz, 1H), 5.92 (d, *J* = 3.0, 1H), 5.25 (t, *J* = 7.0 Hz, 1H), 3.98–3.95 (m, 1H), 2.77 (d, *J* = 4.6, 1H), 2.69 (app t, *J* = 7.4 Hz, 2H), 2.60 (d, *J* = 4.7 Hz, 1H), 2.39–2.37 (m, 4H), 2.06 (dd, *J* = 15.2, 4.1 Hz, 1H), 1.97 (dd, *J* = 15.2, 8.9 Hz, 1H), 0.19 (s, 9H); **^{13}C NMR** (125 MHz, $CDCl_3$) δ 160.0, 156.8, 131.6, 127.8, 121.5, 105.1, 56.2, 55.1, 52.9, 49.1, 44.0, 28.1, 26.5, 26.3, 21.9, 16.7, 15.7, –6.25; **HRMS** (ES+) *m/z* calc'd for $C_{18}H_{29}ClO_2SiNa$ $[M+Na]^+$: 340.1625; found 340.1633.

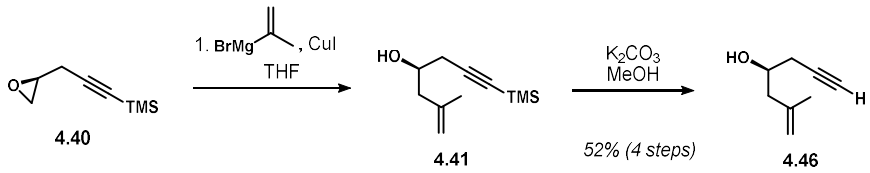

Alkyne 4.46:

A 3-neck round bottom flask was charged with a solution of **4.40** (8.50 g, 55.1 mmol, 1 equiv.) in dry THF (110 mL, 0.5 M), followed by the addition of CuI (734 mg, 3.85 mmol, 0.07 equiv.) and the suspension was cooled to –78 °C. A solution of isopropenylmagnesium bromide (0.5 M in THF, 200 mL, 2 equiv.) was added dropwise through an addition funnel. The temperature was maintained at –78 °C for 30 min, the reaction mixture was allowed to warm to –25 °C over 4 h and then sat. aq. NH_4Cl (100 mL) was added. The biphasic mixture was stirred at 0 °C for 20 min, further diluted with water (100 mL) and Et_2O/hexanes (1:4, 50 mL), and the layers were separated. The aqueous layer was further extracted with Et_2O/hexanes (1:4, 3 x 50 mL), the organic layers were combined, washed with brine, dried over anhydrous $MgSO_4$, filtered, and concentrated *in vacuo.*

The crude orange oil was immediately taken up in dry MeOH (220 mL, ~0.25 M) and cooled to 0 °C. K_2CO_3 (~3 equiv.) was added to the solution and the resulting suspension was allowed to warm to ambient temperature and stirred for 3 h. The MeOH was evaporated *in vacuo* to half the volume, Et_2O/hexanes (3:1, 50 mL) was added and the suspension was diluted with sat. aq. NH_4Cl (100 mL) followed by water to solubilize particulates. The biphasic mixture was separated and the aqueous phase was extracted with Et_2O/hexanes (3:1, 3 x 30 mL). The combined organic extracts were washed with brine, dried over anhydrous $MgSO_4$, filtered, and the organic solution was concentrated *in vacuo* to remove almost all of the solvent (25 °C, 200 mmHg). The resulting yellow oil was purified by Kugelrohr short path distillation (100 °C, 10 mmHg) to provide **4.46** as a colorless oil (4.51 g, 36.4 mmol, 66%).

^{1}H NMR (500 mHz, $CDCl_3$) δ 4.89 (s, 1H), 4.82 (s, 1H), 3.94–3.90 (m, 1H), 2.46–2.37 (m, 2H), 2.34 (dd, *J* = 13.7, 4.6 Hz, 1H), 2.23 (dd, *J* = 14.0, 8.5 Hz, 1 H), 2.06 (t, *J* = 2.5 Hz, 1H), 2.00 (br s, 1H) 1.77 (s, 3H); **^{13}C NMR** (125 mHz, $CDCl_3$) δ 142.0, 113.8, 80.6, 70.8, 67.3, 44.7, 26.7, 22.4; **IR** (film) ν 3299, 3075, 2934, 1646 cm^{-1}; **HRMS** (ES+) *m/z* calc'd for $C_8H_{12}O$ [M + Na]$^+$: 147.0786; found 147.0890; **[α]$^{22}_D$** –1.56 (*c* = 1.00, $CHCl_3$).

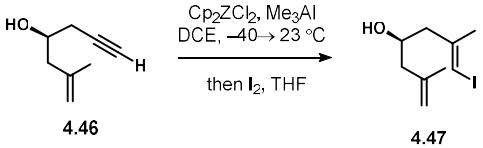

4.46 4.47

Vinyl Iodide 4.47:

$Al(CH_3)_3$ (11.0 mL, 115 mmol, 2.1 equiv.) was added dropwise to a suspension of Cp_2ZrCl_2 (8.41 g, 28.5 mmol, 0.25 equiv.) in DCE (150 mL) at –30 °C; this temperature was carefully maintained over the course of the addition. H_2O (98 μL, 5.47 mmol, 0.1 equiv.) was added very slowly and the reaction was warmed to 0 °C; the suspension became a clear yellow solution. After stirring for 1.5 h at 0 °C, the

mixture was cooled to –50 °C and a solution of **4.46** (6.80 g, 54.7 mmol, 1 equiv.) in DCE (55 mL) was added dropwise. The reaction was warmed to room temperature and stirred for 18 h. After TLC analysis indicated consumption of starting material, the reaction was cooled to –50 °C. A solution of I_2 (29.1 g, 114.8 mmol, 2.1 equiv.) in THF (27 mL) was cannulated into the reaction flask. The reaction mixture was allowed to warm to room temperature over 5 h at which time the deep red solution turned to yellow. The reaction was diluted at 0 °C with sat. aq. potassium sodium tartrate (20 mL), and the biphasic mixture was stirred for an additional 1 h at room temperature. The phases were separated, the aqueous phase was diluted with sat. aq. potassium sodium tartrate (200 mL) and was extracted with Et_2O (3 x 50 mL). The organic phases were combined, washed sequentially with sat. aq. $NaHCO_3$ (100 mL), brine (50 mL) then dried over anhydrous $MgSO_4$, filtered, and concentrated *in vacuo*. The residue was purified by flash chromatography (SiO_2, 20% EtOAc in hexanes) to afford **4.47** as a thick colorless oil (11.2 g, 42.1 mmol, 77%).

^{1}H NMR (500 mHz, $CDCl_3$) δ 6.02 (s, 1H), 4.89 (s, 1H), 4.80 (s, 1H), 3.89–3.87 (m, 1H), 2.37–2.36 (m, 2H), 2.19–2.09 (m, 2H), 1.89 (s, 3H), 1.76 (s, 3H), 1.70 (br s, 1H); **^{13}C NMR** (125 mHz, $CDCl_3$) δ 145.0, 142.2, 113.8, 77.2, 66.4, 47.0, 45.6, 24.2, 22.4; **IR** (film) ν 3410, 2990, 2900, 2855 cm^{-1}; **HRMS** (ES+) *m/z* calc'd for $C_9H_{15}IONa$ $[M+Na]^+$: 289.0065; found 275.1471; **$[\alpha]^{23}_D$** –13.2 (*c* = 1.00, $CHCl_3$).

Chloride 4.48:

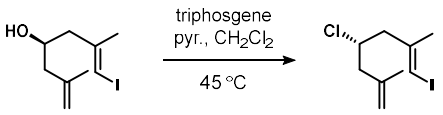

4.47 — *75%* — 4.48

Triphosgene (4.2 g, 14.3 mmol. 1 equiv.) was added to a pressure vessel, the vessel was evacuated and refilled with argon, and CH_2Cl_2 (20 mL) was added. The clear solution was cooled to 0 °C before

slowly adding pyridine (4.61 mL, 57.1 mmol, 4 equiv.), followed by **4.47** (3.8 g, 14.3 mmol, 1 equiv.) in a solution of CH_2Cl_2 (10 mL) under an atmosphere of argon. The pressure vessel was sealed and stirred at 45 °C for 12 h. The reaction mixture was cooled to 0 °C and 1 M HCl (5 mL) was slowly added. The mixture was diluted with hexanes (50 mL) and stirred for 30 min. Water (100 mL) and more hexanes (50 mL) were added to the diluted product mixture and the layers were separated. The aqueous layer was extracted with hexanes (2 x 20 mL), the organic phases were combined, washed with brine, dried over anhydrous $MgSO_4$, filtered, and concentrated *in vacuo*. The crude residue was purified by flash chromatography (SiO_2, hexanes) to afford **4.48** as a light yellow oil (2.83 g, 10.1 mmol, 70% yield, 95 % e.e.). This protocol was based on a procedure developed by Kartika and coworkers.[i]

^{1}H NMR (600 mHz, $CDCl_3$) δ 6.07 (s, 1H), 4.89 (s, 1H), 4.80 (s, 1H), 4.14–4.11 (m, 1H), 2.65 (dd, J = 14.3, 4.8 Hz, 1 H), 2.57 (dd, J = 14.3, 9.0 Hz, 1H), 2.43 (app. d, J = 7.3 Hz, 2H), 1.87 (s, 3H), 1.75 (s, 3H); **^{13}C NMR** (125 mHz, $CDCl_3$) δ 143.8, 141.3, 78.4, 57.3, 47.6, 46.4, 23.4, 21.8; **IR** (film) ν 2980, 2910, 1640 cm^{-1}; **HRMS** (CI+) *m/z* calc'd for $C_9H_{14}ClI$ [CI+]$^+$: 283.9829; found 283.9825; **[α]$^{23}_D$** 18.9 (c = 1.10, $CHCl_3$); GC/FID (HP – Chiral – 20B; 6.88 psi; 0.5 mL/min; column temperature 50 °C for 1 min, then 0.5 °C/min to 135 °C hold for 20 mins); t_R = 175.795, 176.491.

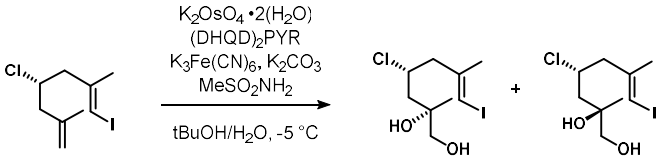

4.48 → *syn :* **4.49** + *anti :* **4.50** (1 : 6.3)

Diol 4.50:

$K_3Fe(CN)_6$ (5.10 g, 15.5 mmol, 2.1 equiv.), K_2CO_3 (2.56 g, 18.4 mmol, 2.5 equiv.), $MeSO_2NH_2$ (325 mg, 0.367 mmol, 1.1 equiv.), $K_2OsO_4{\cdot}2H_2O$ (54.0 mg, 0.147 mmol, 2 mol%) and $(DHQD)_2PYR$

(325 mg, 0.317 mmol, 4 mol%) were mixed together and then taken up in *t*-BuOH/H_2O (90 mL, 1:1). The slurry was stirred vigorously, cooled to 0 °C and then **4.48** (2.11 g, 7.39 mmol, 1 equiv.) was added. The reaction mixture was stirred at 0 °C until the reaction was complete, indicated by TLC analysis (24–36 h). The reaction slurry was stirred with sat. aq. Na_2SO_3 (30 mL) for 1 h. EtOAc (20 mL) was added and the layers were separated. The aqueous layer was extracted with EtOAc (2 x 20 mL), the organic extracts were combined, washed sequentially with sat. aq. Na_2SO_3 and brine, and dried over anhydrous $MgSO_4$, filtered, and concentrated *in vacuo.* The crude oil was eluted through a plug of silica gel (70% EtOAc in hexanes) and concentrated *in vacuo* to afford **4.50** and **4.49** as a 6 : 1 mixture of diastereomers (2.03 g, 6.43 mmol, 87%). The diastereomers could be separated by flash chromatography eluting with a gradient of EtOAc in hexanes (SiO_2, 30% EtOAc in hexanes → 50% EtOAc in hexanes) to give **4.50** as a colorless oil (1.53 g, 4.81 mmol, 65% overall yield).

Note: Diol diastereomer **4.49** was isolated as a white solid and an X-ray crystal structure of **4.49** was obtained to confirm the relative configuration. See pages 22–31 for crystallographic data.

Diol 4.50: **^{1}H NMR** (500 mHz, $CDCl_3$) δ 6.09 (s, 1H), 4.30–4.27 (m, 1H), 3.50 (dd, *J* = 18.8, 10.8 Hz, 2H), 2.69–2.61 (m, 2H), 2.48 (br s, 1H), 2.03 (dd, *J* = 15.4, 9.8 Hz, 1H), 1.99 (br s, 1H), 1.90 (dd, *J* = 15.5, 2.6 Hz, 1 H), 1.87 (s, 3H), 1.26 (s, 3H); **^{13}C NMR** (125 mHz, $CDCl_3$) δ 143.2, 79.1, 72.3, 69.9, 55.9, 49.5, 45.6, 24.3, 23.5; **IR** (film) ν 3373, 2969, 2923, 1616 cm^{-1}; **HRMS** (ES+) *m/z* calc'd for $C_9H_{16}ClIO_2$ $[M+Na]^+$: 340.9781; found 340.9773; **$[\alpha]^{21}_D$** –2.44 (*c* = 1.10, $CHCl_3$).

Diol 4.49: **^{1}H NMR** (500 mHz, $CDCl_3$) δ 6.08 (s, 1H), 4.29–4.27 (m, 1H), 3.55 (d, *J* = 10.8 Hz, 1H), 3.47 (d, *J* = 10.8 Hz, 1H), 2.71–2.61 (m, 2H), 2.39–2.08 (br s, 1 H), 2.03 (dd, *J* = 15.3, 3.1 Hz, 1H), 1.89

(dd, J = 15.3, 8.9 Hz, 1H), 1.87 (s, 3H), 1.27 (s, 3H); **^{13}C NMR** (125 mHz, $CDCl_3$) δ 143.3, 79.1, 72.3, 69.8, 55.9, 49.4, 45.6, 24.2, 23.5; **IR** (film) ν 3389, 2960, 2903, 1632 cm^{-1}; **HRMS** (ES+) *m/z* calc'd for $C_9H_{16}ClIO_2$ $[M+Na]^+$: 340.9781; found 340.9771; **$[\alpha]^{22}_D$** –0.95 (c = 0.6, $CHCl_3$).

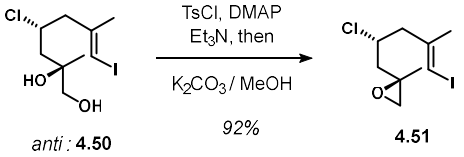

anti : **4.50** **4.51**

Epoxide 4.51:

Toluenesulfonyl chloride (500 mg, 2.61 mmol, 1.3 equiv.) and DMAP (170 mg, 4.00 mmol, 0.75 equiv.) were dissolved in CH_2Cl_2 (10 mL) and the solution was cooled to 0 °C. Diol **4.50** (640 mg, 2.00 mmol, 1 equiv.) was added as a solution in CH_2Cl_2 (3 mL). The reaction was allowed to warm to ambient temperature and stirred for 5 h. The solvent was concentrated *in vacuo*, and the resulting residue was taken up in MeOH (15 mL) followed by the addition of K_2CO_3 (830 mg, 6.00 mmol, 3 equiv.). The slurry was stirred for 3 h, the solvent was concentrated *in vacuo* to one third the initial volume, and the resulting mixture was diluted with EtOAc:pentanes (20 mL, 3:1). The remaining base was quenched with sat. aq. NH_4Cl (50 mL). The layers were separated, and the aqueous layer was extracted with EtOAc:pentanes (3:1, 3 x 15 mL). The organic layers were combined, washed with brine, dried over anhydrous $MgSO_4$, filtered, and concentrated *in vacuo*. The crude residue was purified by flash chromatography (SiO_2, 10% EtOAc in hexanes) to afford **4.51** (538 mg, 1.80 mmol, 90%) as a colorless oil.

^{1}H NMR (600 MHz, $CDCl_3$) δ 6.07 (s, 1H), 3.97 (quint, J = 6.42, 1H), 2.63–2.60 (m, 3H), 2.09–2.04 (m, 2H), 1.85 (s, 3H), 1.39 (s, 3H); **^{13}C NMR** (125 mHz, $CDCl_3$) δ 143.3, 78.9, 72.3, 55.0, 54.8, 52.8,

48.5, 44.0, 23.6, 22.0; **IR** (film) ν 2925, 2853, 1214 cm^{-1}; **HRMS** (CI+) *m/z* calc'd for $C_9H_{14}ClIONH_4$ $[M+NH_4]^+$: 318.0122; found 318.0119; $[\alpha]^{21}_D$ –10.5 (*c* = 0.95, $CHCl_3$).

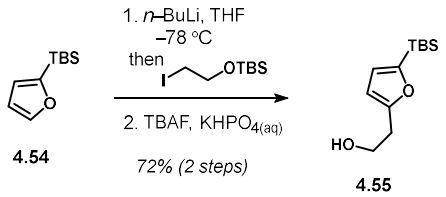

Furan alcohol 4.55:

2-*t*-Butyldimethylsilylfuran[35] (3.5 g, 19.2 mmol, 1.4 equiv.) was dissolved in THF (155 mL) and cooled to –78 °C, followed by the addition of *n*-BuLi (2.5 M in hexanes, 19.2 mmol, 1.4 equiv.). The solution was stirred for 2.5 h while warming to –25 °C, and it turned a deep red color. The lithiated furan solution was cooled back to –78 °C and 2-*t*-butyldimethylsilyloxyethyl iodide (4.30 g, 15.9 mmol, 1 equiv.) was added dropwise as a 1 M solution in THF. The reaction was slowly warmed to ambient temperature and stirred for an additional 3 h before diluting with sat. aq. NH_4Cl (100 mL). The biphasic mixture was further diluted with water (50 mL). The layers were separated, and the aqueous phase was extracted with hexanes (3 x 50 mL). The combined organic phases were washed with brine, dried over anhydrous $MgSO_4$, filtered, and concentrated *in vacuo.* The crude residue was then taken up in THF (70 mL), cooled to 0 °C, sat. aq. K_2HPO_4 (400 μL) was added followed by TBAF (1 M in THF, 1.2 equiv.). The solution was warmed to ambient temperature and stirred for 4 h. Sat. aq. NH_4Cl (50 mL) was added, followed by Et_2O (30 mL), then the layers were separated and the aqueous layer was further extracted with Et_2O/hexanes (1:1, 3 x 30 mL). The organic layers were combined, washed with brine, dried over anhydrous $MgSO_4$, filtered, and concentrated *in vacuo*. The crude residue was purified by flash

chromatography (SiO_2, 30% Et_2O in hexanes) to afford **4.55** (2.47 g, 10.7 mmol, 67%) as a pale yellow oil.

^{1}H NMR (500 MHz, $CDCl_3$) δ 6.56 (d, *J* = 3.0 Hz, 1H), 6.09 (d, *J* = 3.0, 1H), 3.88 (t, *J* = 3.2 Hz, 2H), 2.93 (t, *J* = 3.2 Hz, 2H), 1.56 (br s, 1H), 0.90 (s, 9H), 0.20 (s, 6H); **^{13}C NMR** (125 MHz, $CDCl_3$) δ 157.8, 157.1, 121.6, 106.4, 61.2, 31.8, 26.3, 16.8, –6.30; **IR** (film) ν 3353, 2953, 2927, 2856, 1675 cm^{-1}; **HRMS** (ES+) *m/z* calc'd for $C_{12}H_{22}O_2SiNa$ $[M+Na]^+$: 249.1287; found 249.1291.

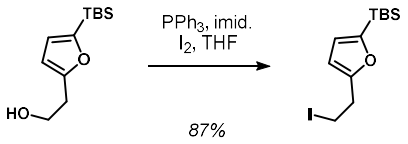

4.55 4.56

Furan iodide 4.56:

Triphenylphosphine (2.56 g, 9.76 mmol, 1.3 equiv.) and imidazole (2.50 g, 37.5 mmol, 5 equiv.) were dissolved in CH_2Cl_2 (52 mL) and the solution was cooled to 0 °C before I_2 (2.47 g, 9.76 mmol, 1.3 equiv.) was added portion-wise. Upon dissolution of the reaction mixture, **4.55** (1.70 g, 7.51 mmol, 1 equiv.) was added as a solution in CH_2Cl_2 (1 M). The reaction was allowed to warm to ambient temperature and stirring was continued for 5 h. The solution was diluted with hexanes (50 mL) and water (35 mL), and was stirred vigorously. The layers were separated, the organic layer was washed sequentially with sat. aq. $Na_2S_2O_3$, brine and then dried over anhydrous $MgSO_4$, filtered, and concentrated *in vacuo*. The crude residue contained significant amounts of $Ph_3P{=}O$ and was extracted with hexanes (10 mL) and filtered (x2). The collected filtrate was concentrated under reduced pressure and the resulting crude oil was purified by flash chromatography (SiO_2, hexanes → 5% Et_2O in hexanes) to afford **4.56** (2.04 g, 6.10 mmol, 81%) as a pale yellow liquid. The compound was stored at –18 °C in a foil-wrapped vial and shielded from light when in use.

^{1}H NMR (500 MHz, $CDCl_3$) δ 6.54 (d, *J* = 3.0 Hz, 1H), 6.10 (d, *J* = 3.0, 1H), 3.36 (t, *J* = 7.5 Hz, 2H), 3.23 (t, *J* = 7.5 Hz, 2H), 0.91 (s, 9H), 0.20 (s, 6H); **^{13}C NMR** (125 mHz, $CDCl_3$) δ 158.1, 157.9, 121.5, 106.2, 32.8, 26.4, 16.8, 1.98, –6.33; **IR** (film) ν 2942, 2917, 1658 cm^{-1}; **HRMS** (CI+) *m/z* calc'd for $C_{12}H_{21}OISi$ $[M]^+$: 336.0406; found 336.0416.

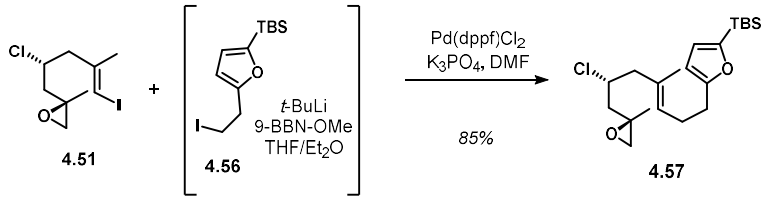

Cyclization substrate 4.57:

A solution of **4.56** (581 mg, 1.73 mmol, 1.3 equiv.) in Et_2O (4 mL) was cooled to –78 °C and *t*-BuLi (1.7 M in pentane, 3.20 mL, 4 equiv.) was added quickly followed by 9-BBN-OMe (1 M in hexanes, 6.0 mL, 4.5 equiv.). THF (2 mL) was added and the reaction was warmed to ambient temperature over 1 h. After stirring for an additional 3 h the white slurry became homogeneous. Aq. K_3PO_4 (3M, 1.1 mL, 2.5 equiv.) and $Pd(dppf)Cl_2{\cdot}CH_2Cl_2$ (162 mg, 0.199 mmol, 0.15 equiv.) were added sequentially under an atmosphere of argon, followed by the addition of **4.51** (400 mg, 1.33 mmol, 1.0 equiv.) as a solution in DMF (5 mL). The reaction mixture was shielded from light and stirred vigorously at ambient temperature for 12 h. The biphasic mixture was diluted with brine (20 mL), hexanes (30 mL) and the layers were separated. The aqueous phase was extracted with Et_2O/hexanes (1:3, 3 x 10 mL), the organic phases were combined, washed sequentially with water (2 x 10 mL) and brine (2 x 10 mL), and then dried over anhydrous $MgSO_4$, filtered, and concentrated under reduced pressure. The crude product residue was purified by flash chromatography (SiO_2, 5% EtOAc in hexanes) to afford **4.57** (440 mg, 1.13 mmol, 85%) as a colorless oil.

^{1}H NMR (600 MHz, $CDCl_3$) δ 6.52 (d, *J* = 3.0 Hz, 1H), 5.96 (d, *J* = 3.0, 1H), 5.25 (t, *J* = 7.0 Hz, 1H), 3.98–3.95 (m, 1H), 2.77 (d, *J* = 4.6, 1H), 2.69 (app t, *J* = 7.4 Hz, 2H), 2.60 (d, *J* = 4.7 Hz, 1H), 2.39–2.37 (m, 4H), 2.06 (dd, *J* = 15.2, 4.1 Hz, 1H), 1.97 (dd, *J* = 15.2, 8.9 Hz, 1H), 1.58 (s, 3H), 1.38 (s, 3H), 0.91 (s, 9H), 0.19 (s, 6H); **^{13}C NMR** (125 MHz, $CDCl_3$) δ 160.0, 156.8, 131.6, 127.8, 121.5, 105.1, 56.2, 55.1, 52.9, 49.1, 44.0, 28.1, 26.5, 26.3, 21.9, 16.7, 15.7, –6.25; **IR** (film) ν 2962, 2854, 1249 cm^{-1}; **HRMS** (ES+) *m/z* calc'd for $C_{21}H_{35}ClO_2SiNa$ $[M+Na]^+$: 405.1992; found 405.1996; **$[\alpha]^{23}_D$** –15.8 (*c* = 1.10, $CHCl_3$).

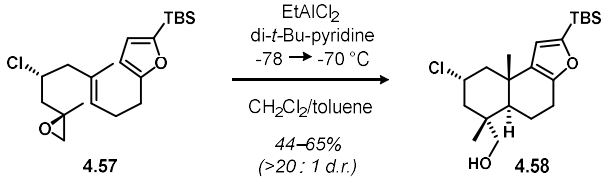

C18-oxygenated decalin 4.58:

To a solution of **4.57** (50 mg, 0.131 mmol, 1 equiv.) in dry CH_2Cl_2/toluene (6:1, 2.7 mL, 0.05 M) was added 2,6-di-*t*-butylpyridine (6.55 μmol, 5 mol%). The solution was cooled to –78 °C and $EtAlCl_2$ (0.9 M in heptane, 0.230 mmol, 1.7 equiv.) was added very slowly down the side of flask. The reaction was slightly warmed to –70 °C over 30 min while the solution turned a pale yellow color, and then Et_3N (100 μL) and MeOH (200 μL) were added sequentially. The mixture was allowed to warm to 0 °C then a sat. aq. solution of potassium sodium tartrate (3 mL) was added and the biphasic mixture was vigorously stirred for 20 min. The layers were separated and the aqueous layer was extracted with Et_2O/hexanes (1:3, 3 x 1 mL). The organic phases were combined, washed with brine, and then dried over anhydrous $MgSO_4$, filtered, and concentrated under reduced pressure. The crude product residue was purified by flash chromatography (SiO_2, 10% → 20% EtOAc in hexanes) to afford **4.58** (31 mg, 78.6 μmol, 60%) as a

colorless foam. This reaction was extremely moisture and temperature sensitive, the yield varied between 45–65% depending on the reaction scale (>200 mg resulted in the lower percent yield range).

^{1}H NMR (600 MHz, $CDCl_3$) δ 6.41 (s, 1H), 4.36 (tt, *J* = 12.3, 4.3 Hz, 1H), 3.49 (d, *J* = 10.8 Hz, 1H), 3.22 (d, *J* = 10.8 Hz, 1H), 2.72 (dd, *J* = 15.7, 5.9 Hz, 1H), 2.66–2.60 (m, 1H), 2.48 (app d, *J* = 12.5 Hz, 1H), 1.93 (ddd, *J* = 13.0, 4.6, 2.3 Hz, 1H), 1.87–1.81 (m, 2H), 1.71–1.63 (m, 3H), 1.51 (br s, 1H), 1.19 (s, 3H), 0.90 (s, 9H), 0.89 (s, 3H), 0.18 (app s, 6H); **^{13}C NMR** (125 MHz, $CDCl_3$) δ 156.9, 152.7, 129.1, 117.8, 71.3, 55.1, 48.3, 46.2, 44.3, 40.0, 36.6, 26.3, 24.4, 24.3, 18.4, 17.5, 16.7, –6.17, –6.19; **IR** (film) ν 3390, 2955, 2925, 2854, 1745 cm^{-1}; **HRMS** (CI+) *m/z* calc'd for $C_{21}H_{35}ClO_2Si$ $[M]^+$: 382.2095; found 382.2086; **$[\alpha]^{25}_D$** 19.6 (*c* = 1.0, $CHCl_3$).

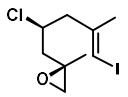

4-S4

Epoxide 4-S4:

Epoxide **4-S4** was synthesized from *(R)*-epichlorohydrin following the same sequence of steps to make **4.49** and **4.50** although the *syn*-chlorodiol diastereomer (the enantiomer of **4.49**) was isolated and advanced through to epoxide formation.

^{1}H NMR (600 MHz, $CDCl_3$) δ 6.08 (app. s, 1H), 4.14 (dddd, *J* = 20.0, 8.3, 5.7, 4.1 Hz, 1H), 2.72–2.61 (m, 4H), 2.11 (ddd, *J* = 14.4, 4.1, 1.3 Hz, 1H), 1.88 (app. d, *J* = 1.3 Hz, 3H), 1.69 (dd, *J* = 14.4, 10.1 Hz, 1H), 1.37 (s, 3H); **^{13}C NMR** (125 MHz, $CDCl_3$) δ 143.2, 78.9, 56.6, 55.1, 48.5, 45.4, 23.6, 22.2; **IR** (film) ν 2957, 2893, 1237 cm^{-1}; **HRMS** (MS+) *m/z* calc'd for $C_9H_{14}ClIONH_4$ $[M+NH_4]^+$: 318.0122; found 318.0120; **$[\alpha]^{23}_D$** 19.2 (*c* = 0.80, $CHCl_3$).

Cyclization precursor 4.63:

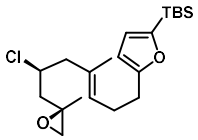

4.63

Cyclization precursor **4.63** was obtained from epoxide **4-S4** (50.0 mg, 0.166 mmol, 1 equiv.) and furan **16** (83.8 mg, 0.249 mmol, 1.5 equiv.) as a clear oil (49.9 mg, 0.141 mmol, 85%) after column chromatography (SiO_2, 10% EtOAc in hexanes). For experimental details, refer to the procedure to make **4.57**.

^{1}H NMR (600 MHz, $CDCl_3$) δ 6.52 (d, *J* = 3.0 Hz, 1H), 5.96 (d, *J* = 3.0, 1H), 5.26 (t, *J* = 7.4 Hz, 1H), 4.11 (dddd, *J* = 14.3,10.5, 7.1, 3.5 Hz, 1H), 2.73–2.67 (m, 4H), 2.44–2.34 (m, 4H), 2.17 (dd, *J* = 14.3, 3.2 Hz, 1H), 1.60 (s, 3H), 1.55 (dd, *J* = 14.3, 10.5, 1H), 1.35 (s, 3H), 0.91 (s, 9H), 0.19 (s, 6H); **^{13}C NMR** (125 MHz, $CDCl_3$) δ160.0, 156.8, 131.5, 127.8, 121.6, 105.1, 57.8, 55.4, 55.2, 49.3, 45.2, 28.1, 26.5, 26.3, 20.3, 16.7, 15.8, –6.25; **IR** (film) *ν* 2973, 2833, 1251 cm^{-1}; **HRMS** (MS+) *m/z* calc'd for $C_{21}H_{35}ClO_2SiNa$ $[M+Na]^+$: 405.1992; found 405.1999; **$[\alpha]^{23}_D$** 4.02 (*c* = 0.90, $CHCl_3$).

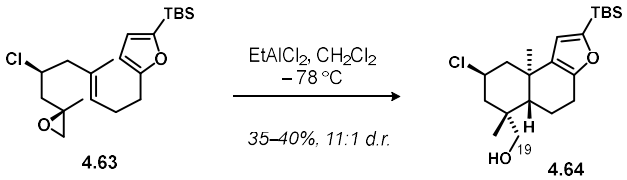

4.63 4.64

C19-oxygenated decalin 4.64:

A solution of **4.63** (30 mg, 88.2 μmol, 1 equiv.) in CH_2Cl_2 (0.05 M, 1.7 mL) was cooled to –78 °C. $EtAlCl_2$ (0.9 M in heptane, 176 μmol, 2 equiv.) was added dropwise down the side of the vial. After 45 min Et_3N (100 μL) was added and the solution was warmed to 0 °C. Sat. aq. potassium sodium tartrate solution (1 mL) was added and the mixture was stirred vigorously. The biphasic mixture was further

diluted with water (2 mL), the phases were separated, and the aqueous phase was extracted with Et_2O/hexanes (1:1, 2 x 2 mL). The organic extracts were combined, washed with brine, dried over anhydrous $MgSO_4$, filtered, and concentrated *in vacuo.* The crude residue was purified by column chromatography (SiO_2, 10 →15% EtOAc in hexanes) to afford **4.64** (12.8 mg, 36.1 μmol, 41%) as a colorless oil. The minor impurity in the ^1H and ^{13}C NMR is desilylated-**4.64**, which co-elutes with **25** during flash chromatography.

^1H NMR (600 MHz, $CDCl_3$) δ 6.40 (s, 1H), 4.27 (tt, *J* = 12.3, 4.0 Hz, 1H), 3.74 (d, *J* = 10.8 Hz, 1H), 3.55 (d, *J* = 10.8 Hz, 1H), 2.74 (dd, *J* = 16.7, 5.8 Hz, 1H), 2.59 (ddd, *J* = 17.6, 11.5, 7.0 Hz, 1H), 2.50 (ddd, *J* = 12.4, 3.7, 2.2 Hz, 1H), 2.43 (ddd, *J* = 13.3, 4.0, 2.2 Hz, 1H), 2.04 (dd, *J* = 13.3, 7.0 Hz, 1H), 1.70–1.67 (m, 2H), 1.49 (app d, *J* = 12.4 Hz, 1H), 1.37 (app t, 13.3 Hz, 1H), 1.23 (br s, 1H), 1.16 (s, 3H), 1.10 (s, 3H), 0.90 (s, 9H), 0.18 (s, 6H); **^{13}C NMR** (125 MHz, $CDCl_3$) δ 157.2, 152.68, 129.08, 117.8, 65.2, 54.4, 51.6, 48.7, 46.0, 41.1, 36.5, 26.9, 26.3, 25.0, 24.4, 19.0, 16.7, –6.18, –6.20; **HRMS** (CI+) *m/z* calc'd for $C_{21}H_{35}ClO_2Si$ $[M]^+$: 382.2088; found 382.2080; **$[\alpha]^{24}_D$** 5.44 (*c* = 1.0, $CHCl_3$).

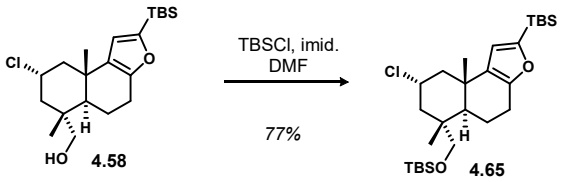

TBS-ether 4.65:

TBSCl (165 mg, 1.09 mmol, 3.5 equiv.) and imidazole (127 mg, 1.87 mmol, 6 equiv.) were dissolved in DMF (2.5 mL). The solution was cooled to 0 °C and **4.58** (120 mg, 0.313 mmol, 1 equiv.) was added as a solution in DMF (500 μL). The reaction was warmed to room temperature and stirred for 3 h. The reaction was diluted with water (5 mL) and the layers were separated. The aqueous layer was

extracted with Et_2O/hexanes (1:10, 3 x 1 mL). The organic extracts were combined, washed with water (2 mL), brine, and dried over anhydrous $MgSO_4$, filtered, and concentrated under reduced pressure. The resulting crude residue was filtered through a plug of silica gel eluting with 5% Et_2O in hexanes to afford **4.65** (120 mg, 0.241 mmol, 77%) as a colorless oil.

^{1}H NMR (600 MHz, $CDCl_3$) δ 6.41 (s, 1H), 4.38–4.33 (m, 1H), 3.40 (d, *J*= 9.7 Hz, 1H), 3.1 (d, *J*= 10.8 Hz, 1H), 2.69 (dd, *J*= 16.4, 6.1 Hz, 1H), 2.66–2.60 (m, 1H), 2.45 (dd, *J*= 12.5 Hz, 3.4 Hz, 1H), 1.80 (d, *J*= 8.6 Hz, 2H), 1.80 (dd, *J* =13.2, 6.8,1H), 1.64 (app t, *J*= 12.5 Hz, 1H), 1.61–1.57 (m, 1H), 1.17 (s, 3H), 0.90 (s,9H), 0.88 (s, 9H), 0.83 (s, 3H), 0.19 (s, 6H), 0.04 (s, 6H); **^{13}C NMR** (125 MHz, $CDCl_3$) δ 156.7, 152.9, 129.2, 118.0, 71.2, 55.5, 48.5, 46.4, 44.2, 40.1, 36.5, 26.3, 25.9, 24.5, 24.4, 18.4, 18.3 17.6, 16.7, –5.56, –6.15, –6.17; **IR** (film) ν 2935, 2902, 2873, 1747 cm^{-1}; **HRMS** (CI+) *m/z* calc'd for $C_{27}H_{49}ClO_2Si_2$ $[M]^+$: 496.2960; found 496.2967; **$[\alpha]^{25}_D$** 15.9 (*c*= 1.0, $CHCl_3$).

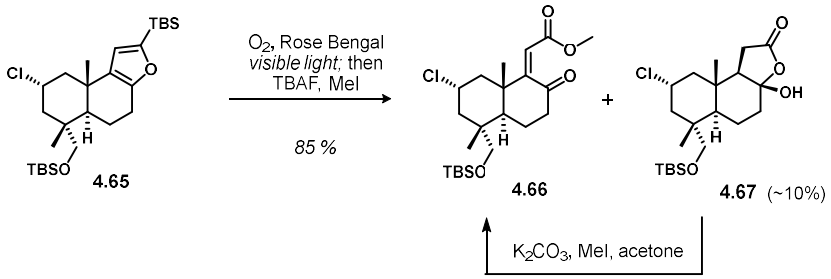

Enoate 4.66:

To a solution of **4.65** (180 mg, 0.362 mmol, 1 equiv.) in CH_2Cl_2 (4 mL) was added Rose Bengal (10 mg, 5 mol %) and the pink mixture was cooled to –10 °C. The reaction flask was equipped with a balloon of O_2 with long needle through the septum and an outlet needle in order to bubble O_2 through the solution. The reaction was irradiated with 2 x CFL bulbs (20 W), while bubbling O_2 through the

solution and the dry ice/acetone bath was maintained between –10→0 °C. Once TLC analysis confirmed consumption of starting material (1–2 h) the remaining solvent was evaporated under reduced pressure and the residue was immediately taken up in dry THF and cooled to –20 °C. TBAF (1 M in THF, 0.543 mmol. 1.5 equiv.) was added slowly and the mixture was stirred for 10 mins. Iodomethane (112 μL, 1.81 mmol, 5 equiv.) was added and the reaction was allowed to warm to room temperature and stirred for 2 h at that temperature. The reaction was diluted with sat. aq. NH_4Cl (2 mL) and the layers were separated. The aqueous layer was extracted with EtOAc/hexanes (1:5, 3 x 1 mL) and the organic phases were combined, washed with brine, and dried over anhydrous $MgSO_4$, filtered, and concentrated *in vacuo*. The pink residue was purified by flash chromatography (SiO_2, 15% → 20% EtOAc in hexanes) to afford **4.66** (134 mg, 0.311 mmol, 86%) as a white solid. The remaining mass balance (~10%) consisted of undesired hydroxy-butenolide **4.67** which could be converted to **4.66** (in 80% yield) by stirring with K_2CO_3 (1 equiv.), iodomethane (3 equiv.) in acetone (0.10 M) .

^{1}H NMR (600 MHz, $CDCl_3$) δ 5.57 (s, 1H), 4.25 (tt, *J* = 12.1, 3.8 Hz, 1H), 3.69 (s, 3H), 3.37 (d, *J* = 10.0 Hz, 1H), 3.06 (d, *J* = 10.0 Hz, 1H), 2.66 (dd, *J* = 13.1, 4.2 Hz, 1H), 2.56 (app td, *J* = 13.1, 6.8 Hz, 1H), 2.13 (app d, *J* = 12.1 Hz, 1H), 1.98–1.93 (m, 2H), 1.90–1.75 (m, 3H), 1.66 (ddd, *J* = 18.1, 13.2, 4.7 Hz, 1H), 1.07 (s, 3H), 0.89 (s, 9H), 0.84 (s, 3H), 0.04 (s, 3H), 0.03 (s, 3H); **^{13}C NMR** (125 MHz, $CDCl_3$) δ 205.1, 166.5, 164.7, 113.0, 70.5, 54.2, 51.9, 46.6, 46.2, 45.9, 44.9, 42.8, 41.1, 25.8, 22.4, 19.3, 18.4, 18.2, –5.52, –5.60; **IR** (film) ν 2952, 2926, 2854, 1727, 1711 cm^{-1}; **HRMS** (ESI+) *m/z* calc'd for $C_{22}H_{37}ClO_4SiNa$ $[M+Na]^+$: 451.2047; found 451.2042; **$[\alpha]^{25}_D$** 4.09 (*c* = 0.5, $CHCl_3$).

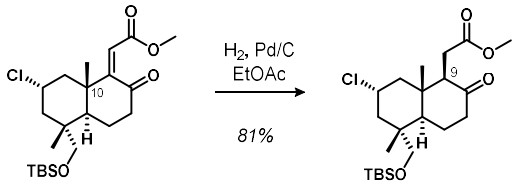

4.66 4.71

Ketone 4.71:

Enoate **4.66** (115 mg, 0.268 mmol, 1 equiv.) and Pd/C (10% Pd by weight, 43 mg, 0.04 mmol, 15 mol%) were taken up in EtOAc (3.5 mL). The flask was flushed with argon before bubbling H_2 through the reaction mixture for 5 min. The reaction was vigorously stirred under balloon pressure of H_2 for 4 h. The mixture was filtered through a pad of Celite, rinsing with EtOAc. The solvent was concentrated under reduced pressure and the crude residue was purified by flash chromatography (SiO_2, 20% EtOAc in hexanes) to afford **4.71** (98 mg, 0.252 mmol, 94%) as a colorless oil. The C9-epimer of **4.71** (9.0 mg) was also isolated and could be converted to **4.71** (85% yield) by stirring with freshly prepared NaOMe (0.5 equiv.) in MeOH (0.05 M) for 3 h.

^{1}H NMR (500 MHz, $CDCl_3$) δ 4.15 (tt, *J* = 12.3, 3.5 Hz, 1H), 3.67 (s, 3H), 3.40 (d, *J* = 10.0 Hz, 1H), 3.06 (d, *J* = 10.0 Hz, 1H), 2.84 (app d, *J* = 10.1 Hz, 1H), 2.71 (dd, *J* = 16.0, 10.1 Hz, 1H), 2.45 (dd, *J* = 14.0, 3.5 Hz, 1H), 2.36 (app td, *J* = 13.4, 7.1 Hz, 1H), 2.22 (dd, *J* = 16.0, 3.1 Hz, 1H), 2.09 (app d, *J* = 12.8 Hz, 2H), 1.95–1.91 (m, 2H), 1.80 (d, *J* = 12.8 Hz, 1H), 1.58–1.53 (m, 2H), 0.9 (s, 9H), 0.79 (s, 6H), 0.07 (s, 3H), 0.06 (s, 3H); **^{13}C NMR** (125 MHz, $CDCl_3$) δ 210.1, 173.7, 70.5, 59.4, 54.4, 51.7, 48.8, 45.8, 44.9, 43.0, 40.9, 40.3, 27.3, 25.7, 22.2, 18.1, 18.0, 15.9, –5.80, –5.86; **IR** (film) ν 2939, 2920, 1718, 1692 cm^{-1} ; **HRMS** (ESI+) *m/z* calc'd for $C_{22}H_{39}ClO_4SiH$ $[M+H]^+$: 431.2384; found 431.2395; **$[\alpha]^{23}_D$** –13.0 (*c* = 0.8, $CHCl_3$).

Exo-alkene 4.72:

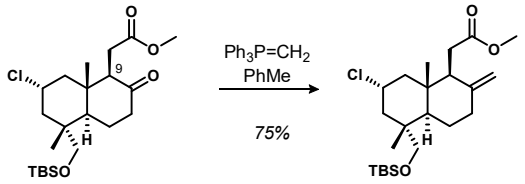

Methyltriphenylphosphonium bromide (660 mg, dried at 110 °C at ~ 20 mmHg overnight, 1.84 mmol, 1 equiv.) and $NaNH_2$ (180 mg, 50% w/v in toluene, 2.31 mmol, 1.25 equiv.) were dissolved in toluene (6 mL) and heated at reflux (~110 °C) for 3 h. The resulting yellow suspension was allowed to cool to room temperature over 1 h while the solids settled to the bottom of the flask. The clear yellow, salt free solution of $Ph_3P{=}CH_2$ (2.55 mL, 0.752 mmol, 3 equiv.) was transferred to a flask containing **4.71** (108 mg, 0.251 mmol, 1 equiv.) in toluene (2.5 mL) at 0 °C. After addition of the ylide, the reaction was allowed to warm to ambient temperature and stir for 1 h. The solution was diluted with brine (3 mL) and the biphasic mixture was extracted with hexanes (3 x 1 mL). The combined organic extracts were washed sequentially with water (2 mL), and brine (2 mL), and then dried over anhydrous $MgSO_4$, filtered, and concentrated *in vacuo*. The crude residue was purified by flash chromatography (SiO_2, 5% → 10% EtOAc in hexanes) to afford **4.72** (80.7 mg, 0.188 mmol, 75%) as a colorless oil.

^{1}H NMR (600 MHz, $CDCl_3$) δ 4.79 (s, 1H), 4.52 (s, 1H), 4.19 (tt, *J* = 12.4, 3.8 Hz, 1H), 3.65 (s, 3H), 3.34 (d, *J* = 9.8 Hz, 1H), 3.00 (d, *J* = 9.8 Hz, 1H), 2.48–2.41 (m, 2H), 2.36, (app d, *J* = 13.0 Hz, 1H), 2.11–2.05 (m, 2H), 1.86 (app t, *J* = 12.4 Hz, 1H), 1.78 (app d, *J* = 12.4 Hz, 1H), 1.68 (dd, *J* = 12.8, 2.4 Hz, 1H), 1.59–1.57 (m, 1H), 1.47 (t, *J* = 12.0 Hz, 1H), 1.27–1.20 (m, 2H), 0.91 (s, 9H), 0.76 (s, 3H), 0.75 (s, 3H), 0.04 (app s, 6H); **^{13}C NMR** (125 MHz, $CDCl_3$) δ 173.8, 147.8, 107.3, 70.7, 55.8, 52.2, 51.6, 49.1, 46.4, 40.8, 40.6, 37.0, 30.7, 25.9, 23.3, 18.2, 18.1, 15.4, –5.54, –5.58; **IR** (film) ν 2948, 2927, 2854, 1738, 1682

cm^{-1}; **HRMS** (CI+) *m/z* calc'd for $C_{23}H_{41}ClO_3SiNH_4$ $[M+NH_4]^+$: 446.2857; found 446.2867; $[\alpha]^{23}_D$ 2.66 (c = 0.5, $CHCl_3$).

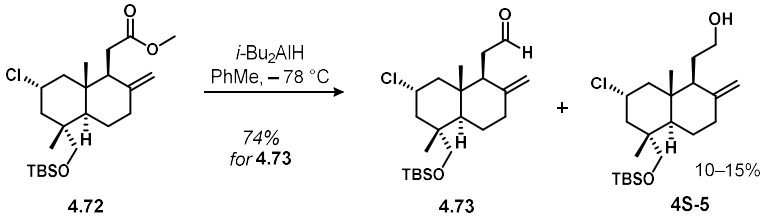

4.72 4.73 4S-5

Aldehyde 4.73:

To a solution of **4.72** (90 mg, 0.209 mmol, 1 equiv.) in toluene (1.3 mL) at –78 °C was added a freshly prepared solution of *i*-Bu_2AlH (1 M in toluene, 0.440 mmol, 2.1 equiv.) slowly down the side of the flask. The reaction mixture was stirred at –78 °C for 45 min and MeOH (100 µL) was added dropwise down the side of the flask. The reaction mixture was allowed to warm to room temperature and then further diluted with 0.5 M HCl (2 mL). The phases were separated and the aqueous phase was extracted with Et_2O/hexanes (1:5, 2 x 1 mL). The organic extracts were combined, washed with a sat. aq. potassium sodium tartrate (2 mL), brine (2 mL) and then dried over anhydrous $MgSO_4$, filtered, and concentrated *in vacuo*. The crude product residue was purified by flash chromatography (SiO_2, hexanes → 5% EtOAc in hexanes) to afford **4.73** (62 mg, 0.154 mmol 74%) as a colorless oil. A significant portion of the mass balance isolated was the over reduced alcohol product **4S-5** (10-15%) which could be converted to the aldehyde (in 90% yield) by stirring with Dess–Martin Periodinane (3 equiv.) in CH_2Cl_2 (0.1 M) for 45 min.

^{1}H NMR (500 MHz, $CDCl_3$) δ 9.64 (d, J = 3.38 Hz, 1H), 4.88 (s, 1H), 4.42 (s, 1H), 4.20 (tt, J = 12.4, 3.8 Hz, 1H), 3.36 (d, J = 9.8 Hz, 1H), 3.00 (d, J = 9.8 Hz, 1H), 2.54–2.50 (m, 1H), 2.46–2.38 (m, 3H), 2.13–2.04 (m, 2H), 1.89 (app t, J = 12.7 Hz, 1H), 1.78 (ddd, J = 12.7, 4.3, 2.0 Hz, 1H), 1.71 (dd, J = 12.6, 2.6

Hz, 1H), 1.60 (ddd, J = 13.0, 5.0, 2.6 Hz, 1H), 1.42 (t, J= 12.0 Hz, 1H), 1.31–1.22 (m, 1H), 0.91 (s, 9H), 0.78 (s, 3H), 0.75 (s, 3H), 0.05 (s, 3H), 0.04 (s, 3H); **^{13}C NMR** (125 MHz, $CDCl_3$) δ 202.8, 147.4, 109.3, 70.4, 55.5, 50.5, 49.2, 46.2, 46.0, 40.6, 40.4, 39.4, 36.7, 25.6, 22.7, 17.9, 17.9, 15.3, –5.90, –5.94; **IR** (film) ν 2921, 2855, 1727 cm^{-1}; **HRMS** (CI+) *m/z* calc'd for $C_{22}H_{39}ClO_2SiH$ $[M+H]^+$: 399.2486; found 399.2498; **$[\alpha]^{22}_D$** 17.3 (c = 0.6, $CHCl_3$).

Imide 4.78:

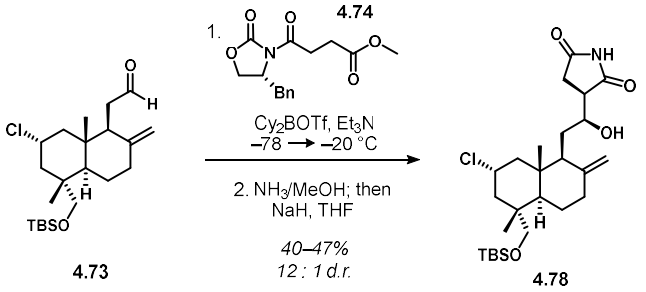

Acylated oxazolidinone[36] (**4.74**, 16.5 mg, 57 μmol, 1.5 equiv) was dried by azeotropic distillation from benzene (50 μL) in a 1 dram vial and dissolved in CH_2Cl_2 (350 μL). The solution was cooled to –78 °C and a freshly prepared solution of Cy_2BOTf (1.0 M in CH_2Cl_2, 37 μmol, 1.7 equiv.) was added along the side of the vial. The clear solution was stirred at –78 °C for 30 min. At that temperature, Et_3N (1.0 M in CH_2Cl_2, 111 μmol, 2.5 equiv.) was added and the mixture was stirred for 20 min. To ensure complete enolization the solution was allowed to warm to 0 °C over 1 h and stirred at this temperature for an additional 30 min, then cooled back to –78 °C. The enolate solution changed from clear to pale yellow during this warming. A solution of **4.73** (14 mg in 100 μL CH_2Cl_2, 37 μmol, 1.0 equiv.) was added at –78 °C and the reaction vial was warmed over 1.5 h to –10 °C and was maintained at this temperature for 20 h. The reaction mixture was diluted with methanol (50 μL) and warmed to ambient temperature. Aq. pH7 buffer solution (2 mL) was added. The phases were separated and the aqueous phase was extracted with

CH_2Cl_2 (3 x 1 mL). The combined organic extracts were dried over anhydrous $MgSO_4$, filtered, and concentrated *in vacuo*.

The crude aldol product was immediately transferred to a 1 dram vial, NH_3 (2.0 M in methanol, 800 μL) was added, and the reaction was stirred at 23 °C for 24 h. The solution was concentrated *in vacuo* to afford a mixture of desired imide (**4.78**), and the primary amide. To complete succinimide formation, the crude material was dissolved in dry THF (800 μL), the solution was cooled to 0 °C, and NaH (55% suspension in mineral oil, 7.0 mg, 80 μmol, 5 equiv.) was added. After bubbling subsided (~10 mins), 1 M HCl (500 μL) was added dropwise, followed by water (2 mL). The layers were separated and the aqueous phase was extracted with EtOAc (3 x 1 mL) then the combined organic phases were washed with brine, dried over anhydrous $MgSO_4$, filtered, and concentrated *in vacuo.* The crude yellow oil was purified by flash chromatography (SiO_2, 35 → 45% EtOAc in hexanes) to afford **4.78** (8.6 mg, 17.4 μmol, 47%) as an oil and its *syn*-aldol diastereomer in a 12:1 diastereomer ratio. The reaction sequence proceeds to 75% consumption of starting material, and unreacted aldehyde **4.73** can be recovered. The diastereomers could be separated by column chromatography or purified after TBS-ether deprotection.

Note: This procedure was optimized and adapted from a similar procedure used in our previous syntheses of haterumaimide and lissoclimide products.[37]

^{1}H NMR (500 MHz, $CDCl_3$) δ 7.96 (br s, 1H), 4.96 (s, 1H), 4.73 (s, 1H), 4.35 (app t, J = 6.2 Hz, 1H), 4.20 (tt, J = 12.0, 3.8 Hz, 1H), 3.34 (d, J = 10.0 Hz), 2.98 (d, J = 10.0 Hz, 1H), 2.93–2.86 (m, 2H), 1.72–2.66 (m, 1H), 2.41 (d, J = 12.2 Hz, 1H), 2.21 (d, J = 12.2 Hz, 1H), 2.00–1.94 (m, 1H), 1.85 (app t, J = 12.5 Hz, 1H), 1.78–1.67 (m, 2H), 1.61–1.55 (m, 2H), 1.27–1.20 (m, 2H), 0.91 (s, 9H), 0.75 (s, 3H), 0.73

(s, 3H), 0.04 (s, 3H), 0.03 (s, 3H); **^{13}C NMR** (125 MHz, $CDCl_3$) δ 178.7, 176.3, 147.9, 108.5, 70.5, 69.5, 55.7, 53.9 49.3, 46.9, 46.8, 46.1, 41.7, 40.5, 37.6, 29.4, 29.2, 25.9, 23.4, 18.2, 18.1, 15.4, –5.55, –5.59; **IR** (film) ν 2921, 2855, 1727 cm^{-1}; **HRMS** (ESI+) *m/z* calc'd for $C_{26}H_{44}ClNO_4SiNa$ $[M+Na]^+$: 520.2626; found 520.2608.

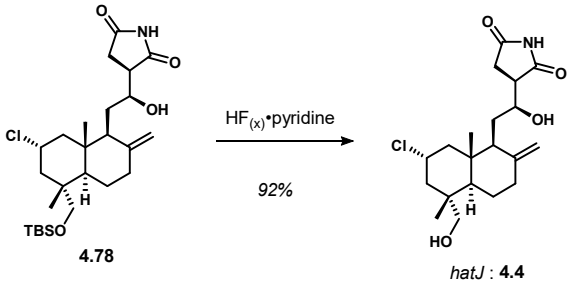

4.78 *hatJ* : **4.4**

***(+)*-haterumaimide J (4.4):**

Imide **4.78** (6.7 mg, 13.4 μmol) was dissolved in THF (500 μL) in a 1 dram vial and the mixture was cooled to 0 °C. A solution of HF(x)·pyridine (100 μL) was added dropwise and the reaction was allowed to warm to room temperature. After several min a white precipitate formed and the reaction was stirred vigorously for an additional 10 h at ambient temperature. The slurry was diluted with water (1 mL), EtOAc (1 mL) was added and excess acid was quenched with K_2CO_3 (500 μL). The biphasic mixture was separated, the aqueous layer was extracted with EtOAc (2 x 1 mL) and the combined organic extracts were washed with brine, dried over anhydrous $MgSO_4$, filtered, and concentrated *in vacuo* to afford a fairly pure (~90%) product. The crude residue was purified by column chromatography (SiO_2, 60% EtOAc in hexanes) to give pure haterumaimide J (**4.4**) (4.6 mg, 12.0 μmol, 90%) as a white solid.

The data obtained for our synthetic sample of **4.4** matched those reported by Uemura et al.[31] For ^{1}H NMR and ^{13}C NMR data comparison to natural **4.4** in d_6-DMSO see Table 3. Note: ^{1}H and ^{13}C NMR contains residual CH_2Cl_2, H_2O and benzene from azeotropic distillation in attempts to remove excess H_2O.

^{1}H NMR (500 MHz, $CDCl_3$) δ 8.03 (br s, 1H), 4.97 (s, 1H), 4.72 (s, 1H), 4.35 (br s, 1H), 4.20 (tt, *J* = 12.0, 4.0 Hz, 1H), 3.46 (d, *J* = 10.7 Hz), 3.12 (d, *J* = 10.7 Hz, 1H), 2.93–2.89 (m, 1H), 2.86 (d, *J* = 5.2 Hz, 1H), 2.69 (dd, *J* = 17.4, 8.8 Hz, 1H), 2.42 (ddd, *J* = 13.0, 4.5, 2.2 Hz, 1H), 2.23 (dd, *J* = 12.2, 3.8 Hz, 1H), 2.07–2.00 (m, 2H), 1,86–1.84 (m, 1H), 1.76–1.73 (m, 2H), 1.66 (ddd, *J* = 13.0, 4.7, 2.2 Hz, 1H), 1.62–2.59 (m, 1H), 1.55–1.52 (m, 1H), 1.34–1.23 (m, 3H), 0.78 (s, 3H), 0.77 (s, 3H); **^{13}C NMR** (125 MHz, $CDCl_3$) δ 178.7, 176.4, 147.5, 108.6, 70.7, 69.2, 55.3, 53.5, 49.0, 47.0, 46.7, 45.9, 41.7, 40.4, 37.5, 29.3, 29.2, 23.4, 18.1, 15.4; **IR** (film) *ν* 3680, 3340, 2966, 2864, 2843, 1709 cm^{-1}; **HRMS** (ESI-) *m/z* calc'd for $C_{20}H_{29}ClNO_4$ $[M-H]^-$: 382.1785; found 382.106; **$[\alpha]^{22}_D$** 60.4 (*c* = 0.7, $CHCl_3$), [lit: **$[\alpha]^{29}_D$** 68 (*c* = 0.92, $CHCl_3$)].

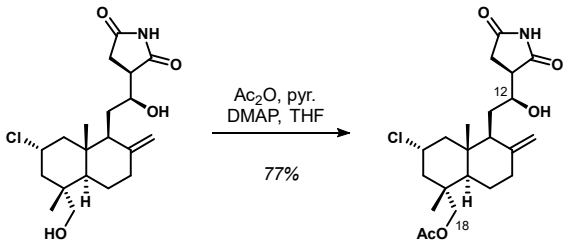

hatJ : **4.4** *hatJ* : **4.5**

***(+)*-haterumaimide K (4.5):**

In a 1 dram vial, **4.4** (2.0 mg, 5.22 μmol, 1 equiv.) was dissolved in CH_2Cl_2 (300 μL) and pyridine (0.5 M in CH_2Cl_2, 26.2 μmol, 5 equiv.), acetic anhydride (0.3 M in CH_2Cl_2, 7.10 μmol, 1.2 equiv.) and DMAP (0.1 M in CH_2Cl_2, 1.33 μmol, 0.25 equiv.) were sequentially added at 0 °C. The solution was stirred for 3 h maintaining the temperature below 10 °C, and water (500 μL) was added. The layers were separated and the aqueous layer was extracted with CH_2Cl_2 (3 x 500 μL) then the combined organic extracts were washed with brine, dried over anhydrous $MgSO_4$, filtered, and concentrated *in vacuo.* The crude residue contained haterumaimide K (**4.5**) and the undesired bisacetylated (C18, C12-OAc)

product in a 6:1 ratio. The desired product was purified by flash chromatography (SiO_2, 40% EtOAc in hexanes) to give **5** (1.7 mg, 4.01 μmol, 77%).

The data obtained for our synthetic sample of **4.5** matched those reported by Uemura.[31] For ^{1}H NMR and ^{13}C NMR data comparison to natural **4.5** in $CDCl_3$ see Table 4. The ^{1}H NMR contains a residual H_2O signal.

Note: $CDCl_3$ calibrated to 7.24 ppm for ^{1}H NMR and 77.2 ppm for ^{13}C NMR according to reported literature data. **^{1}H NMR** (600 MHz, $CDCl_3$) δ 7.65 (br s, 1H), 4.97 (s, 1H), 4.73 (s, 1H), 4.34 (br s, 1H), 4.17 (tt, *J* = 12.0, 4.0 Hz, 1H), 3.85 (d, *J* = 11.1 Hz, 1H), 3.63 (d, *J* = 11.1 Hz, 1H), 2.92–2.89 (m, 1H), 2.87 (dd, *J* = 17.5, 5.0 Hz, 1H), 2.68 (dd, *J* = 17.5, 8.7 Hz, 1H), 2.42 (app dt, *J* = 13.0, 3.2 Hz, 1H), 2.23 (app d, *J* = 12.5 Hz, 1H), 2.08 (s, 3H), 1.97–1.94 (m, 2H), 1.75–1.68 (m, 3H), 1.62–1.56 (m, 2H), 1.39 (dd, *J* = 12.8, 2.0 Hz, 1H), 1.34–1.23 (m, 2H), 0.85 (s, 3H), 0.79 (s, 3H); **^{13}C NMR** (125 MHz, $CDCl_3$) δ 178.8, 176.4, 171.4, 147.6, 109.2, 71.8, 69.5, 54.7, 53.7, 49.1 48.5, 46.9, 46.3, 41.8, 39.1, 37.5, 30.9, 29.4, 29.2, 23.5, 20.9, 18.0, 15.4; **IR** (film) ν 3480, 3221, 2936, 1774, 1712 cm^{-1}; **HRMS** (ES+) *m/z* calc'd for $C_{22}H_{32}ClNO_5Na$ $[M+Na]^+$: 448.1867; found 448.1877; **$[\alpha]^{22}_D$** 43.9 (*c* = 0.7, $CHCl_3$), [lit: **$[\alpha]^{29}_D$** 59.6 (*c* = 0.19, $CHCl_3$)].

Table 4.3 Comparison data for synthetic hatJ to natural in d_6-DMSO

Atom	δ C nat. (ppm)	δ C syn. (ppm)	Δ	δ H nat. (ppm)	Multiplicity, J (Hz)	δ H syn. (ppm)	Multiplicity, J (Hz)	Δ
1	48.4	48.4	–	2.12 1.27	ddd (12.5, 4.0, 1.5) t (12.5)	2.13 1.28	d (11.5 Hz) t (12.5)	+ 0.01 + 0.01
2	57.3	57.3	–	4.38	(tt, 12.5, 4.0)	4.39	tt (12.4, 4.0)	+ 0.01
3	45.9	45.9	–	1.67 1.78	ddd (12.5, 4.0, 1.5) t (12.5)	1.69 1.79	dd (13.0, 3.5) t (12.8)	+ 0.02 + 0.01
4	40.3	40.2	0.1	–				
5	46.0	46.0	–	1.52	dd (12.5, 2.5)	1.53	d (12.5)	+ 0.01
6	22.9	22.7	0.2	1.57 1.15	dddd (12.5, 5.0, 3.5, 2.5) dq (12.5, 4.0)	1.56–1.58 1.13–1.16	m (overlapping) m	– –
7	37.0	36.9	0.1	2.30 1.96	ddd (13.0, 4.0, 3.5) dt (13.0, 5.0)	2.31 1.95	app d (13.0) dt (13.0, 4.5)	+0.01 – 0.01
8	147.6	147.8	0.2	–				
9	51.4	51.3	0.1	1.65	m	1.65	app d (11.0)	–
10	41.3	41.3	–	–				
11	30.0	29.8	0.2	1.58 1.40	m ddd (13.0, 9.5, 5.0)	1.56–1.59 1.41	m app t (13.0)	– + 0.01
12	66.9	66.9	–	3.99	m	3.98–4.00	m	–
13	45.5	45.4	0.1	2.89	ddd (9.0, 5.0, 1.5)	2.89	dd (8.5, 5.0)	–
14	29.0	28.9	0.1	2.54 2.46	dd (17.5, 5.0) dd (17.0, 9.5)	2.54 2.46	dd (17.5, 5.0) overlapping	– –
15	181.1	181.4	0.3	–				
16	178.8	179.2	0.4	–				
17	107.7	107.7	–	4.87 4.69	br s br s	4.87 4.71		– + 0.02
18	69.3	69.3	–	3.20 2.84	dd (11.0, 5.5) dd (11.0, 5.5)	3.20 2.85	dd (11.0, 5.5) dd (11.0, 5.5)	– + 0.01
19	17.9	17.7	0.2	0.68	s	0.69	s	+ 0.01
20	15.0	14.8	0.2	0.67	s	0.68	s	+ 0.01
NH				11.01	s	11.00		– 0.01
12-OH				4.94	d (5.0)	4.93	d (4.8)	– 0.01
18-OH				4.74	t (5.5)	4.73	t (5.4)	– 0.01

Reported natural shifts: Uddin, M. J.; Kokubo, S.; Ueda, K.; Suenaga, K.; Uemura, D. *Chem. Lett.* **2002**, 1028–1029.

Table 4.4 Comparison data for synthetic hatK to natural in $CDCl_3$

Atom	δ C nat. (ppm)	δ C syn. (ppm)	Δ	δ H nat. (ppm)	Multiplicity, *J* (Hz)	δ H syn. (ppm)	Multiplicity, *J* (Hz)	Δ
1	49.0	49.1	–	2.22 1.23	ddd (13.0, 4.0, 2.0) dd (12.5)	2.23 1.22–1.24	d (12.5) m	+ 0.01 –
2	54.7	54.7	–	4.17	(tt, 13.0, 12.0*)	4.17	tt (12.0, 4.0)	–
3	46.2	46.3	0.1	1.97 1.68	ddd (12.0, 4.0, 2.0) m	1.96–1.98 1.67–1.69	m (overlapping) m	– –
4	39.1	39.1	–					
5	48.4	48.4	–	1.39	dd (12.5, 6.0)	1.39	dd (12.8, 2.0)	–
6	23.6	23.6	–	1.60 1.30	m dddd (13.0,12.5, 12.0, 6.5)	1.60–1.62 1.29–1.32	m m	– –
7	37.5	37.5	–	2.41 1.92	ddd (13.0, 6.5, 2.5) ddd (13.0, 12.0, 6.4)	2.42 1.94	dt (13.0, 3.0) m (overlapping)	+ 0.01 + 0.02
8	147.1	147.6	0.5					
9	53.5	53.7	0.1	1.70	m	1.69–1.71	m	–
10	41.7	41.8	0.1					
11	29.3	29.2	0.1	1.75 1.55	m m	1.73–1.75 1.56–1.58	m m	– 0.01 + 0.02
12	69.2	69.5	0.3	4.33	dt (7.5, 2.0)	4.34	br s	+ 0.01
13	46.8	46.9	0.1	2.89	ddd (8.5, 5.0, 2.0)	2.90	m (overlapping)	+ 0.01
14	29.4	29.5	–	2.85 2.68	dd (17.5, 5.0) dd (17.4, 8.5)	2.87 2.68	dd (12.0, 4.0) dd (17.5, 8.5)	+ 0.02 –
15	178.8	178.8	–					
16	176.4	176.4	–					
17	109.0	109.2	0.2	4.96 4.73	br s br s	4.97 4.73	s s	+ 0.01 –
18	71.7	71.8	0.1	3.85 3.63	d (11.0) d (11.0)	3.85 3.64	d (11.1 Hz) d (11.1 Hz)	– + 0.01
19	18.0	18.0	–	0.85	s	0.85	s	
20	15.4	15.4	–	0.67*	s	0.76	s	+ 0.09
21	171.0	171.4	0.4					
22	21.0	20.9	0.1	2.1	s	2.08	s	– 0.02
NH				8.05	s	7.65	s	– 0.4

* Note: Reported resonance is the same as that for C20–CH_3 for haterumaimide J (Table 1). We cannot rule out a possible transcription error.

Reported natural shifts: Uddin, M. J.; Kokubo, S.; Ueda, K.; Suenaga, K.; Uemura, D. *Chem. Lett.* **2002**, 1028–1029.

4.7 References

1. Corey, E. J.; Staas, D. D. *J. Am. Chem. Soc.* **1998,** *120* (14), 3526-3527.
2. Johnson, W. S.; Vanderge.A; Swoboda, J. J. *J. Am. Chem. Soc.* **1967,** *89* (1), 170-&.
3. Yoder, R. A.; Johnston, J. N. *Chem. Rev.* **2005,** *105* (12), 4730-4756.
4. Stadler, P. A.; Eschenmoser, A.; Schinz, H.; Stork, G. *Helv. Chim. Acta* **1957,** *40* (7), 2191-1298.
5. Tanis, S. P.; Deaton, M. V.; Dixon, L. A.; McMills, M. C.; Raggon, J. W.; Collins, M. A. *J. Org. Chem.* **1998,** *63* (20), 6914-6928.
6. Tanis, S. P.; Chuang, Y. H.; Head, D. B. *J. Org. Chem.* **1988,** *53* (21), 4929-4938.
7. Tanis, S. P.; Herrinton, P. M. *J. Org. Chem.* **1983,** *48* (24), 4572-4580.
8. Piancatelli, G.; Dauria, M.; Donofrio, F. *Synthesis-Stuttgart* **1994,** (9), 867-889.
9. Tanis, S. P.; Chuang, Y. H.; Head, D. B. *Tetrahedron Lett.* **1985,** *26* (50), 6147-6150.
10. Yoshimura, F.; Sasaki, M.; Hattori, I.; Komatsu, K.; Sakai, M.; Tanino, K.; Miyashita, M. *Chem. Eur. J.* **2009,** *15* (27), 6626-6644.
11. Millan, I.; Campana, A. G.; Cuerva, J. M. *Org. Chem. Front.* **2014,** *1* (4), 373-381.
12. Corey, E. J.; Liu, K. *J. Am. Chem. Soc.* **1997,** *119* (41), 9929-9930.
13. Vantamelen, E. E.; Zawacky, S. R.; Russell, R. K.; Carlson, J. G. *J. Am. Chem. Soc.* **1983,** *105* (1), 142-143.
14. Tang, W. F.; Prusov, E. V. *Angew. Chem. Int. Ed.* **2012,** *51* (14), 3401-3404.
15. Dai, M. J.; Krauss, I. J.; Danishefsky, S. J. *J. Org. Chem.* **2008,** *73* (24), 9576-9583.
16. Negishi, E.; Vanhorn, D. E.; Yoshida, T. *J. Am. Chem. Soc.* **1985,** *107* (23), 6639-6647.
17. Villalpando, A.; Ayala, C. E.; Watson, C. B.; Kartika, R. *J. Org. Chem.* **2013,** *78* (8), 3989-3996.
18. Kolb, H. C.; Vannieuwenhze, M. S.; Sharpless, K. B. *Chem. Rev.* **1994,** *94* (8), 2483-2547.

19. Crispino, G. A.; Jeong, K. S.; Kolb, H. C.; Wang, Z. M.; Xu, D. Q.; Sharpless, K. B. *J. Org. Chem.* **1993,** *58* (15), 3785-3786.

20. Vanhessche, K. P. M.; Sharpless, K. B. *J. Org. Chem.***1996,** *61* (23), 7978-7979.

21. Corbu, A.; Aquino, M.; Pratap, T. Y.; Retailleau, P.; Arseniyadis, S. *Org. Lett.* **2008,** *10* (9), 1787-1790.

22. Marshall, J. A.; Schaaf, G. M. *J. Org. Chem.* **2003,** *68* (19), 7428-7432.

23. Mi, Y.; Schreiber, J. V.; Corey, E. J. *J. Am. Chem. Soc.* **2002,** *124* (38), 11290-11291.

24. Surendra, K.; Corey, E. J. *J. Am. Chem. Soc.* **2008,** *130* (27), 8865-8869.

25. Corey, E. J.; Lin, S. Z. *J. Am. Chem. Soc.* **1996,** *118* (36), 8765-8766.

26. Mikami, K.; Shimizu, M. *Chem. Rev.* **1992,** *92* (5), 1021-1050.

27. Meinwald, J. S.; Singhcha.M; Labana, S. S. *J. Am. Chem. Soc.***1963,** *85* (5), 582-&.

28. Rickborn, B., The Meinwald Rearrangement. In *Comprehensive Organic Synthesis*, Trost, B. M.; Fleming, I.; Pattenden, G., Eds. Pergamon, Oxford: 1991; Vol. 3, p 733.

29. Halperin, S. D.; Britton, R., *Org. Biomol. Chem.* **2013,** *11* (10), 1702-1705.

30. Goodman, J. M.; Paterson, I. *Tetrahedron Lett.* **1992,** *33* (47), 7223-7226.

31. Uddin, M. J.; Kokubo, S.; Ueda, K.; Suenaga, K.; Uemura, D. *Chem. Lett.* **2002,** (10), 1028-1029.

32. Konst, Z. A.; Szklarski, A. R.; Pellegrino, S.; Michalak, S. E.; Meyer, M.; Zanette, C.; Cencic, R.; Nam, S.; Voora, V. K.; Horne, D. A.; Pelletier, J.; Mobley, D. L.; Yusupova, G.; Yusupov, M.; Vanderwal, C. D. *Nat. Chem.* **2017,** *9* (11), 1140-1149.

33. Kjeldsen, N. D.; Funder, E. D.; Gothelf, K. V. *Org. Biomol. Chem.* **2014,** *12* (22), 3679-3685.

34. Szklarski, A. R. PhD Dissertation, University of California, Irvine, 2013.

35. Hashmi, A. S. K.; Kurpejovic, E.; Frey, W.; Bats, J. W. *Tetrahedron* **2007,** *63* (26), 5879-5885.

36. Stoncius, A.; Nahrwold, M.; Sewald, N. *Synthesis-Stuttgart* **2005,** (11), 1829-1837.

37. Quinn, R. K.; Konst, Z. A.; Michalak, S. E.; Schmidt, Y.; Szklarski, A. R.; Flores, A. R.; Nam, S.; Horne, D. A.; Vanderwal, C. D.; Alexanian, E. J. *J. Am. Chem. Soc.* **2016,** *138* (2), 696-702.

CHAPTER 5: Studies on Stereoselective Terminal Epoxide Polyene Cyclizations for the Synthesis of C18/C19-oxygenated Diterpenes

5.1. Application of a chlorine-controlled terminal epoxide cyclization

Epoxide-initiated cationic-π cyclizations are among the most powerful transformations in both biosynthesis and chemical synthesis. Despite extensive work in this field, the bi- and poly-cyclization of terminal epoxides is significantly underdeveloped. This reaction provides rapid entry into the C3-deoxygenated, C18/C19-oxygenated trans-decalin scaffold. A simple Reaxys search of these scaffolds returns hundreds of diterpene natural products, many of which are bioactive.

Stereochemical control of the cyclization is imperative for the selective formation of products bearing either an equatorial C18-hydroxymethyl group or an axial C19-hydroxymethyl group (**Scheme 5.1a**). The intrinsic diastereoselectivity of this bicyclization was not explicitly known until our studies on **5.1**. These experiments unveiled the preference for an unsubstituted terminal epoxide, under Lewis acid-initiated conditions, to undergo cyclization to the equatorial C18-oxygenated decalin (**5.2, Scheme 5.1a**). This result coincided with the few literature examples for a cation-π cyclization initiated on terminal epoxides—both unsubstituted[1] and benzylether-substituted[2, 3]—which terminated to give equatorial hydroxymethyl decalin products. While the disparity between **5.2** and **5.3** was not large (5:1), we screened multiple Lewis acids and varied the terminating groups from the furan to alkyl substituted methoxyarenes, but these reactions never afforded the C19-oxygenated product as the major diastereomer. During our work on the synthesis of haterumaimide J (hatJ) and haterumaimide K (hatK) (**Chapter 4**) we discovered that a Lewis acid-initiated cyclization of *syn*-chloroepoxide **5.4** produced decalin **5.5** in high

Scheme 5.1 Preference of unsubstituted terminal epoxide vs chlorine-controlled cyclization

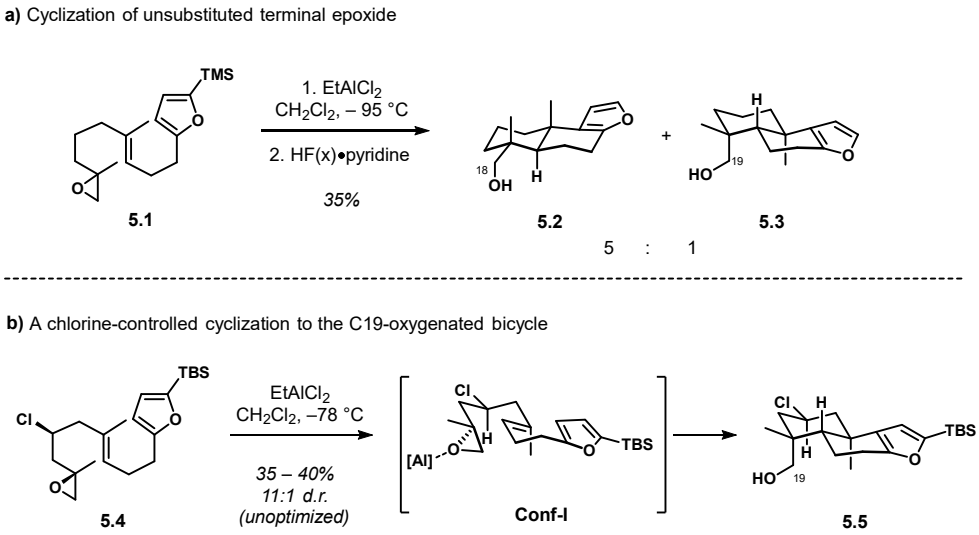

diastereoselectivity (**Scheme 5.1b**). This was the first example of a bicyclization initiated on a 2,2-disbustituted epoxide that favored the axial C19-hydroxymethyl product. Moreover, this reaction demonstrated the remarkable ability of a single chlorine atom to overturn the intrinsic preference of a polyene cyclization and dictate the stereochemical outcome.

The utility of chlorine as a single atom auxiliary for terminal epoxypolyene cyclizations could be widely applicable to the synthesis of C3-deoxygeanted, C19-oxygenated diterpenes. Cyclization substrates of type **5.6** could allow for rapid construction of polycyclic scaffolds bearing axial hydroxymethyl groups (**5.7**). Owing to the facile reductive excision of alkyl chloride substituents, we envisioned this strategy would permit access to a variety of *ent*-kaurene natural products (**Scheme 5.2**).

Scheme 5.2 Application of chlorine as an internal auxiliary for epoxypolyene cyclizations

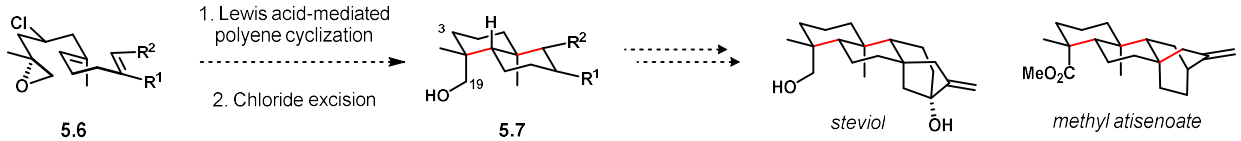

5.1.1. Examples of single atom/substituents as internal auxiliaries

The utility of a chlorine-bearing stereocenter to control the stereochemical outcome of a reaction has been has been demonstrated in a variety of nucleophilic 1,2-additions to chiral α-chloroaldehydes.[4-6] Specifically, Britton and coworkers have made extensive use of chlorine as an atom economical auxiliary for asymmetric aldol additions. The incorporation of an α-chlorine stereocenter to an aldehyde via organocatalysis[7,8] establishes a substrate that follows the Conforth model[6] for nucleophilic 1,2-additions to the carbonyl group. Britton and coworkers utilized the stereodirecting ability of these chiral α-chloroaldehydes (**5.8**) to accomplish a stereoselective methyl ketone aldol addition; arguably one of the more challenging aldol additions to render asymmetric.[9] Radical reduction of the chloromethine group in **5.9** with tris(trimethylsilyl)silane (TTMS) and AIBN proceeded smoothly to provide the corresponding β-hydroxyketones (**5.10**) in decent yields over two steps with high enantiopurity (**Scheme 5.3**).[10] The Britton group has applied this strategy to the stereoselective synthesis of many natural products.[11]

Scheme 5.3 Britton's chlorine directed aldol additions

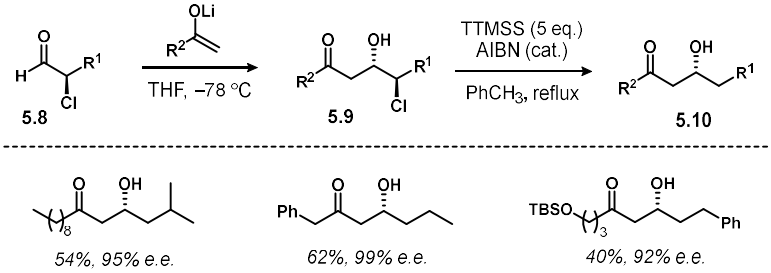

The use of a chlorine stereocenter as an internal auxiliary for polyene cyclizations had not been reported before our work;[12] however, there are a few examples of asymmetric induction by remote substituents during a polycyclization event. On route to 11α-methylprogesterone (**5.14**), Johnson and coworkers showcased a diastereoselective Brønsted acid-initiated polyene cyclization of **5.11** to give tetracycle **5.12** in 66% yield as a 10:1 mixture of epimers at C17 (**Scheme 5.4**).[13] They attributed the high

Scheme 5.4 Johnson's polyene cyclization with internal substituent control

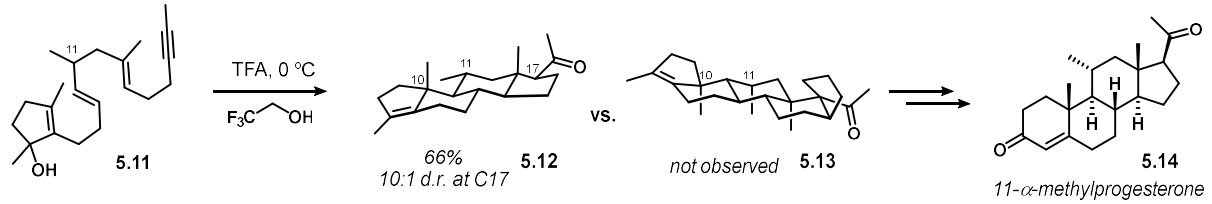

stereoselectivity of the cyclization to a conformational preference imposed by the C11-methyl bearing stereocenter. The non-bonded, 1,3-diaxial interactions between the C11-CH_3 and C10-CH_3 in the transition state leading to **5.13** disfavors the formation of the axial C11-CH_3 product. The Johnson group observed a similar mode of stereocontrol for the C11-hydroxyl substituted variant of **5.11**.[14] More recently, Liu and coworkers reported a stereoselective radical bicyclization of **5.15** triggered by hydrogen atom transfer (HAT), in their synthesis of hispidanin A (**Scheme 5.5**). The polyene cyclization was initiated on the 2,2-disubstituted alkene of **5.15**, which featured the least steric hindrance and greatest electron density. The polyene substrate **5.15**, bearing an OTBS-stereocenter, presumably adopts an equatorial disposition and consequently controls the relative stereochemistry through the bicyclization to afford **5.16** in 45% yield after silyl group deprotection. Similar to Britton's strategy, they reductively removed the C2-hydroxyl group (**5.17**) after the stereodefining step for elaboration to the western portion of hispidanin A (**5.18**).

Scheme 5.5 Liu's stereoselective HAT-initiated radical cyclization

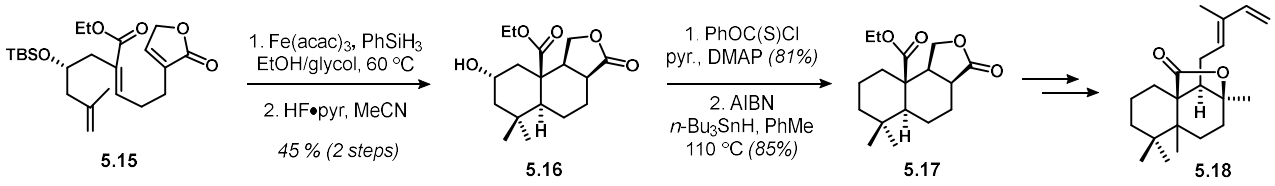

5.1.2. A formal synthesis of steviol

The chlorine-controlled cyclization was uniquely appropriate for our synthesis of haterumaimide J (**Chapter 4**), as the target product contained a C2-chlorine. While most naturally occurring terpenoids are not chlorinated, we aimed to utilize the C2-chlorine as removable auxiliary for polycyclizations. For this purpose, we set out to apply this novel mode of stereocontrol for rapid access to A-ring unsubstituted, C19-oxygenated polycyclic products by implementing a post-cyclization, reductive-dechlorination. We saw the opportunity to showcase this strategy in a formal synthesis of steviol (**5.23**). Baran and coworkers developed a practical synthesis of the *ent*-kaurene natural product **5.23** featuring an arene-terminated, Lewis-acid initiated bicyclization of internal epoxide **5.19** to for the construction of decalin **5.20**, bearing C3- and C19-oxygenation (**Scheme 5.6a**).[15] The authors noted the lack of methods available for obtaining the A-ring axial hydroxymethyl group through polyene cyclizations, and therefore relied on the *Z*-stereochemistry of the internal epoxide (with respect to the benzyl ether) to furnish bicycle **5.20** in high

Scheme 5.6 Baran's synthesis of steviol and our formal synthesis strategy

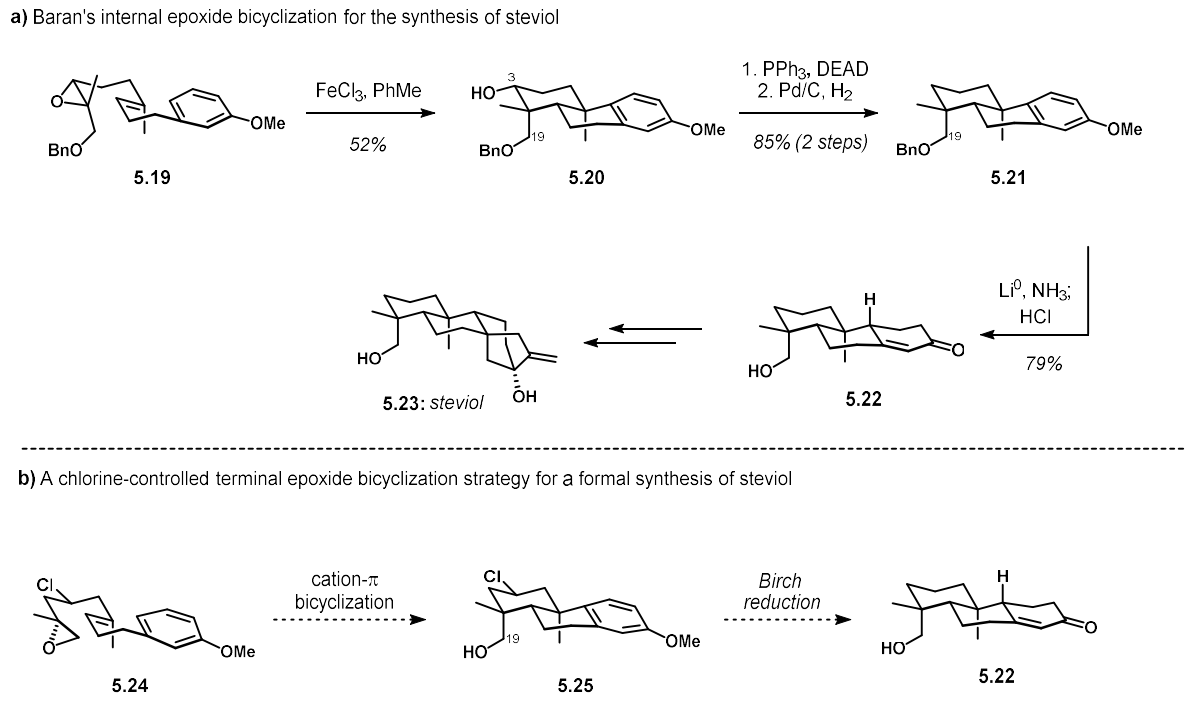

diastereoselectivity. Consequently, a 2-step reduction procedure was required to remove the C3-hydroxyl group of **5.20** to access the C3-deoxygenated core (**5.21**). They subsequently carried out a Birch reduction of the methoxyarene to yield **5.22**. The internal, trisubstituted enone—which resisted all attempts at conjugate additions and Diels–Alder reactions—was the key functional handle for the formation of the [3.2.1] bicyclic system of steviol (**5.23**). For an alternative strategy to enone **5.22**, we envisioned that a chlorine-controlled, terminal epoxide cyclization of **5.24** would permit direct access to C-19 oxygenated decalin **5.25**. Owing to the highly reducing nature of dissolving metal reactions, it was postulated that both the alkyl chloride and the methoxyarene would be reduced under Birch conditions to give enone **5.22** after acidic workup (**Scheme 5.6b**).

The success of the chlorine-controlled cyclization relies on the selective construction of the chlorine and epoxide stereocenters, in this case, in a relative syn arrangement. Since the *ent*-kaurene natural products are in the enantiomeric configuration as the haterumaimides, chloride **5.26** was synthesized from (*R*)-epichlorohydrin, following the same 6-step procedure outlined in Chapter 4 (**Scheme 5.7**).[12] Our thorough investigation on the dihydroxylation of *ent*–**5.26** (**Chapter 4**) allowed for

Scheme 5.7 Synthesis of the cyclization substrate

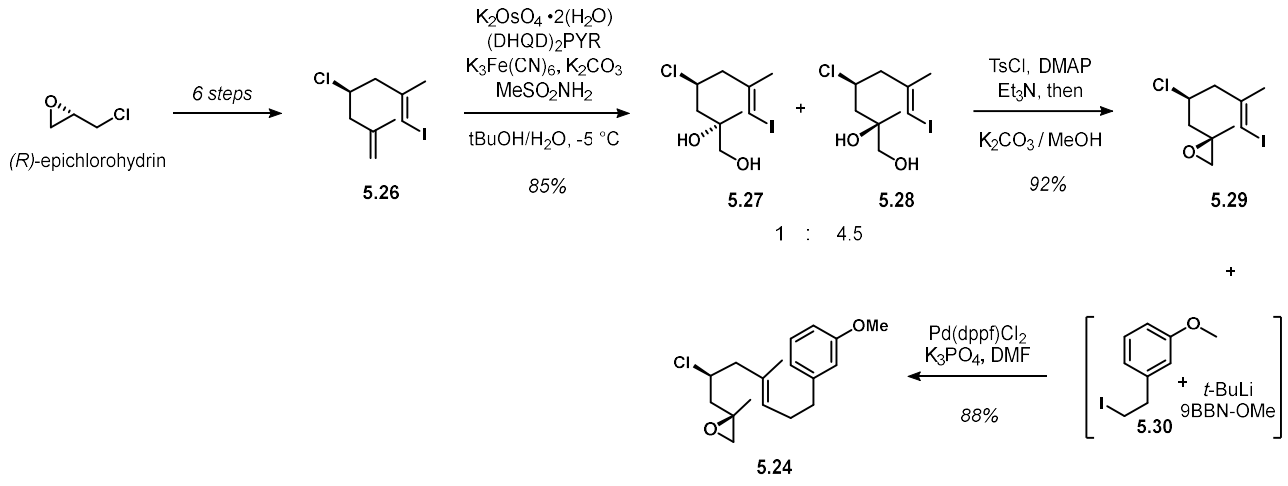

a quick selection of reaction conditions. Employment of the $(DHQD)_2PYR$ ligand set for the Sharpless dihydroxylation of **5.26** proceeded in slightly lower diastereoselectivity (4.5:1 d.r.) than observed for *ent*–**5.26** (6.3:1 d.r.). While the DHQD-based ligand imparted the expected diastereofacial preference for the osmylation of the 2,2-disbustituted alkene,[16] the different reaction outcomes between the chloride enantiomers suggests that the homoallylic stereocenter in **5.26** may have an effect on the dihydroxylation selectivity.[17] Nevertheless, the desired *syn*-diastereomer (**5.28**) was isolated and advance through epoxide formation to yield **5.29**. A *B*-alkyl Suzuki coupling between the *in situ* generated borate of **5.30** and vinyl iodide **5.29** constructed the cyclization substrate **5.24** in 88% yield.

We anticipated a facile bicyclization of **5.24** under our highly optimized conditions ($EtAlCl_2$, DTBP); however these initial experiments revealed particular challenges for the desired reaction (**Scheme 5.8**). Under $EtAlCl_2$-intiating conditions, the C2-chlorinated, C19-oxygenated decalin (**5.24**) was formed in 28% yield in a 10:1 ratio with the C18-oxygenated diastereomer; a similar diastereoselectivity was observed with the furan substrate (**5.4**). An inherent consequence associated with the *meta*-methoxylphenyl terminating group was the formation of the ortho-cyclized isomer **5.31**;[1] this isomer was isolated as the minor component in a 5:1 ratio with **5.25**. Aldehyde **5.32** was a recognizable side product; however, it constituted much more of the mass balance (25%) as compared to the reactions

Scheme 5.8 Initial results for the methoxyarene-terminated bicyclization and major side-products

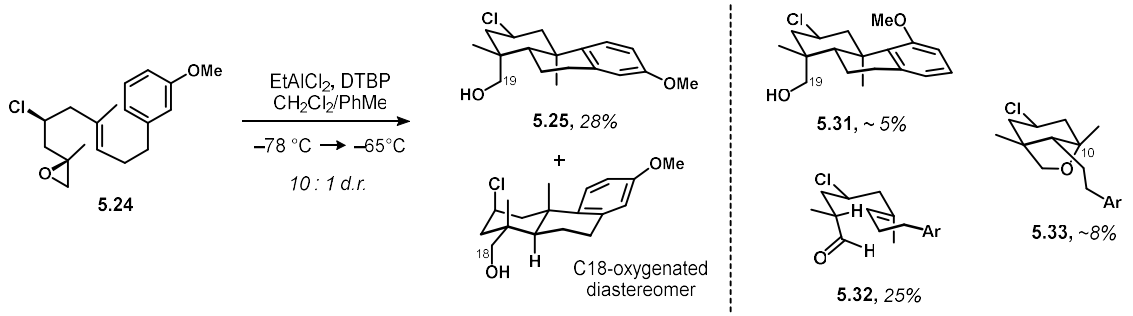

for the equatorial hydroxymethyl products. Additionally, oxabicycle **5.33** was also a more prevalent side product for this reaction than previously observed for the furan systems. We assume that when the epoxide is placed in a pseudo-axial position the oxygen-aluminate bond is posed to trap the positive charge formed at C10 during the A-ring cyclization; conversely, an equatorial oxyaluminate bond is conformationally constrained from interacting with the C10-position. Interestingly, in the furan-terminated cyclization of **5.4** (**Scheme 5.1b**), oxabicyclization was essentially a non-issue. We speculated that the furan-terminating group—possessing greater electron density than the methoxyarene—could effectively outcompete C19-oxygen ring closure for the second cyclization event. A survey of several Lewis acids found that $BF_3{\cdot}OEt_2$ could effect the desired cyclization to give **5.25** in a 42% isolated yield and a consistent 10:1 d.r. It should be noted that we could not employ this Lewis acid for our furan-terminated bicyclizations due to the tendency of this reagent to cause furan desilylation. While a broad investigation of Lewis acids for the conversion of **5.24** to **5.25** was not conducted, we believe that the optimal reagent/conditions for these 2,2-dibsubstituted epoxypolyene cyclizations may vary between substrates with different terminating groups.

With sufficient quantities of bicycle **5.25** in hand, this intermediate was subjected to a Birch reduction to complete the formal synthesis. To our satisfaction, enone **5.22**—a late-stage intermediate in Baran's synthesis[15]—was isolated after stirring the crude Birch reduction mixture with etherial HCl. While reductive dehalogenations commonly employ silane- or stannane-based reagents, the highly reducing Li^0/NH_3 mixture is an effective alternative for this reaction.[18] Notably, when the Birch reduction was not

warmed to reflux (–40 °C), deschloro-**5.25** was isolated along with **5.22**, indicating that alkyl chlorine reduction precedes reduction of the methoxyarene.

Scheme 5.9 Completion of the formal synthesis of steviol

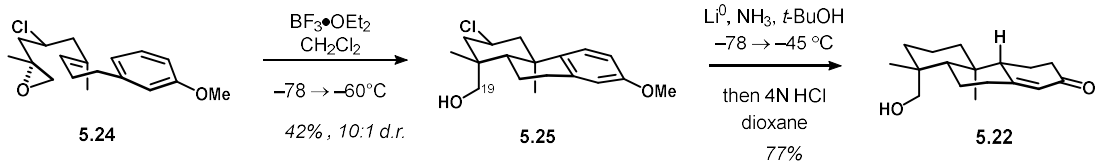

The formal synthesis of steviol showcased the utility of our chlorine-controlled terminal epoxide bicyclization. In terms of step count, our synthesis of **5.22** is essentially on-par with the previous report (11 steps vs. 13 steps[15]); however, our strategy is more convergent and presents a new-mode of epoxypolyene stereocontrol for installing the challenging C19-hydroxymethyl group. Ongoing work in our lab aims to utilize chlorine as a single-atom auxiliary in terminal epoxide cyclizations for the synthesis of ceylonamide B and methyl atisenote (**Figure 5.1**). These efforts have also encountered challenges associated with the cyclization of the *syn*-chloroepoxide substrates, as this configuration results in the terminal epoxide adopting axial-orientation during the cyclization transition state. It is evident that biasing the epoxide to the inherently undesired (axial) conformation results in a less desirable outcome than in the cases where both the chloride and the epoxide can adopt equatorial position in the transition state. Hopefully our ongoing work in this area can develop reliable and high-yielding protocols for the cyclization to C19-oxygenated products, as this would be widely applicable to terpenoid synthesis.

Figure 5.1 Ongoing-projects utilizing a chlorine-controlled, terminal epoxide cyclization

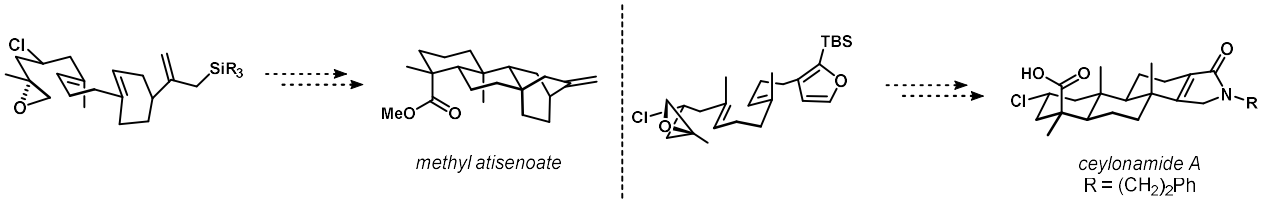

5.2. Initial efforts towards a chiral Lewis acid-mediated bicyclization of terminal epoxides

Despite the prevalence of C3-unsubsistuted, C18/19-oxygenated terpene natural products, the polyene cyclizations of 2,2-disubstituted epoxides have rarely been utilized for the synthesis of these common scaffolds, likely owing to lack of stereocontrol for these cyclizations. While we have shown that a secondary chlorine stereocenter is a novel solution to this issue of stereocontrol, the incorporation of this group governs the synthesis of the epoxide fragment. Alternatively, the ability to control the stereochemical outcome of the cyclization with a chiral reagent would negate the need for an internal auxiliary on the polyene substrate. Therefore, we are eager to investigate whether or not chiral Lewis acids could impart some energetic preference, between **Conf-I** and **Conf-II**, during a terminal epoxide bicyclization, such that either C18- or C19-oxygenated decalins (**5.35** and **5.36**) could be selectively formed from enantioenriched epoxides of type **5.34** (**Figure 5.2**).

Figure 5.2 Chiral Lewis acids for the stereocontrol of unsubstituted terminal epoxypolyenes

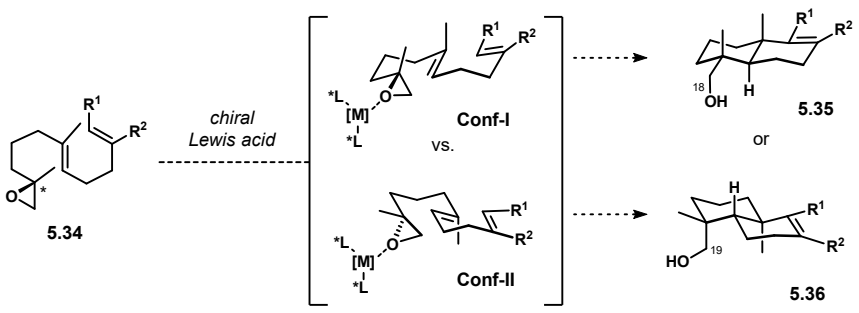

5.2.1. Select examples of enantioselective cationic polyene cyclizations

The cationic ionization of linear polyene substrates has been the dominant method for initiating biomimetic polycyclizations. The use of chiral Brønsted acids for alkene protonation and chiral Lewis acids for the activation of leaving groups, has rendered this transformation enantioselective from pro-chiral substrates.[19] While these methods have not yet been applied to a terminal epoxypolyene system,

there have been an number of examples of enantioselective, cationic polyene cyclizations that terminate to give an A-ring pendant alkene; in some cases this has provided a functional handle for accessing C18 or C19-oxygenation.

The first enantioselective, proton-initiated, polyene cyclization was reported by Yamamoto and coworkers. This method relied on a Lewis acid-assisted activation of a Brønsted acid (LBA), wherein the Lewis acid increases Brønsted acid reactivity through coordination.[20] The Corey group expanded upon Yamamoto's initial LBA systems and utilized $SbCl_5$-BINOL complex **5.37** for proton-initiated polyene cyclizations. Specifically, they employed this method for the cyclization of **5.38** which afforded **5.39** in high enantiomeric excess. The pendent isoprene group was oxidatively cleaved to give C18-oxygenated products, dehydroabietic (**5.40**) acid or 4-epipodocarpic acid (**5.41**) (**Scheme 5.10**).

Scheme 5.10 Corey's LBA-mediated enantioselective polyene cyclization

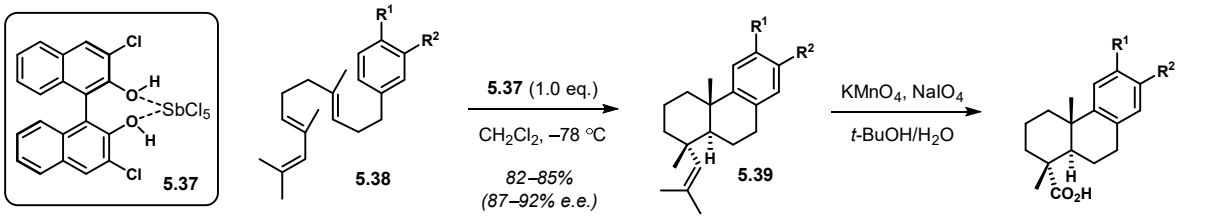

5.40: *(+)*-dehydroacietic acid
R^1 = H, R^2 = *i*-Pr; *62% (2 steps)*

5.41: *(+)*-4-epipodocarpic acid
R^1= OMe, R^2= H; *63% (2 steps)*

Rather than proton-initiation, transition metals have been utilized as π-acids or Lewis acids to initiate a cyclization on a π-system or an allylic leaving group. Carreira and coworkers developed an iridium(I)-phosporamidite (**5.44**) catalyst for a polyene cyclization initiated on allylic alcohols (**Scheme 5.12a**).[21] Exposure of a branched allylic alcohol (**5.42**) to $Zn(OTf)_2$ and the iridium catalyst generates an iridium π-allyl species (**TS-I**) which serves as the initiating electrophile for an enantioselective cyclization.

The reaction terminates to give a bicyclic product with a pendant A-ring alkene (**5.43**) after protodemetallation. The Carreira group applied this method—utilizing an allylsilane terminating group—to accomplish the bicyclization of **5.45** to decalin **5.46** (**Scheme 5.12b**).[22] The pendent alkene of **5.46** was ultimately used to construct the A-ring quaternary center for the synthesis of C19-oxygenated asperolide C (**5.47**).

Scheme 5.11 Carreira's iridium-mediated enantioselective polyene cyclizations of allylic alcohols

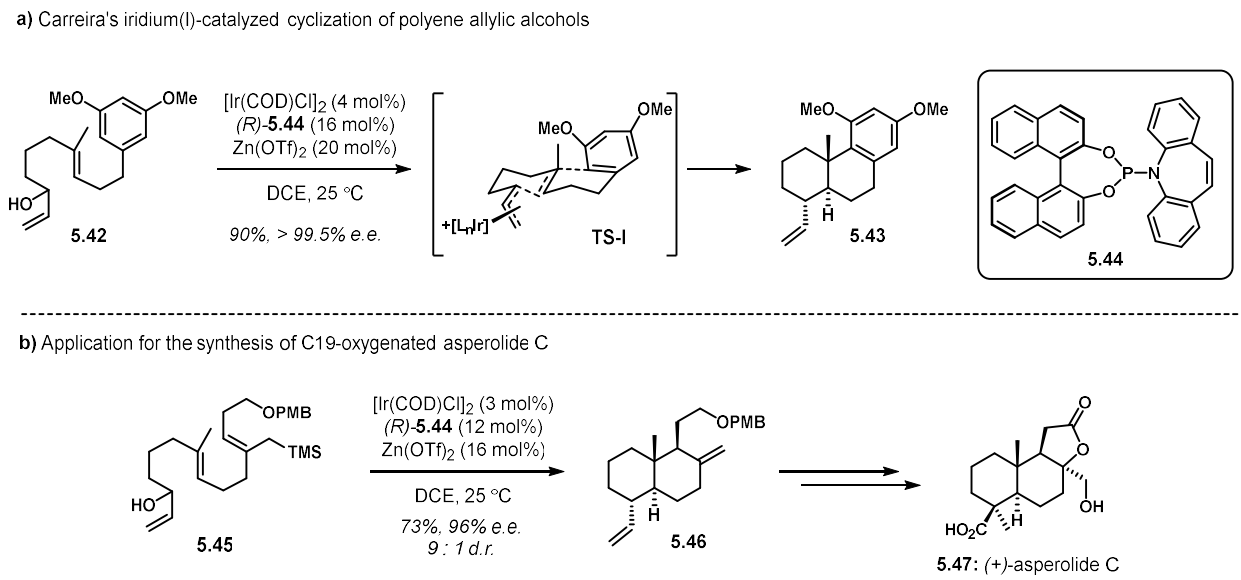

5.2.2. Development of a synthesis of enantiopure terminal epoxide cyclization substrates

It is evident that the chiral ligands on a Brønsted acid donor or Lewis acid metal center can impart high levels of enantiocontrol through polycyclizations of achiral substrates. In our proposed system the chiral Lewis acid activation of a 2,2-disubstituted epoxide is a diastereomeric complexation; therefore, to fully assess the stereocontrol imparted by the Lewis acid during the cyclization, the epoxide substrate

Scheme 5.12 Known methods for asymmetric oxidations of 2,2-disubstituted alkenes

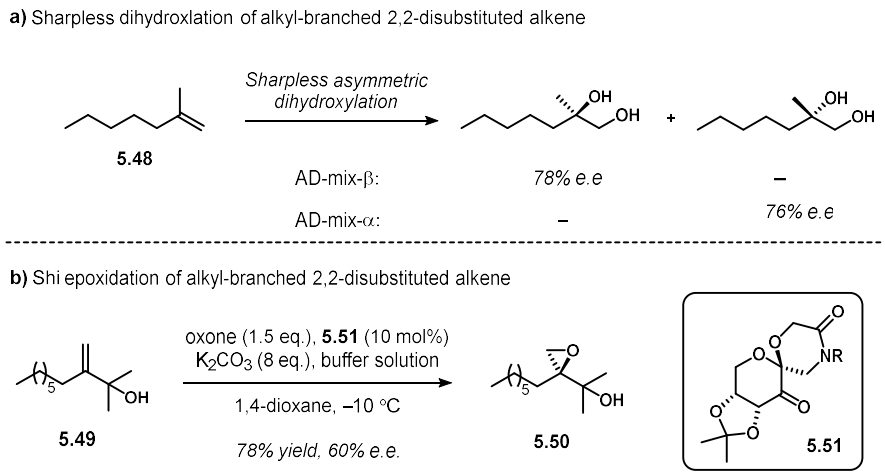

needs to be enantiopure. As we set out to synthesize enantioenriched, unsubstituted, terminal epoxide substrates, we were fully aware of the challenges associated with accessing these intermediates through asymmetric oxidations of alkyl branched 2,2-disubstitued alkenes. Sharpless reported a dihydroxylation of **5.48** under AD-mix-β and AD-mix-α conditions but only moderate e.e. values were obtained for the resulting diols (**Scheme 5.12a**).[23] Shi developed a catalyst system (**5.51** with oxone) to improve the enantioselectivity for epoxidations of 2,2,-disbustituted alkenes. While this method was successful on the styrenyl-substrates, providing the corresponding terminal epoxides with high enantiopurity (87–95% e.e.), the epoxidation of alkyl-branched alkene **5.49** proceeded with much lower enantioselectivity to give **5.50** in only 60% e.e (**Scheme 5.12b**).[24] Alternatively, we considered a Corey–Chaykovsky epoxidation

Scheme 5.13 Shibisaki's methods for an asymmetric Corey-Chaykovsky epoxidation

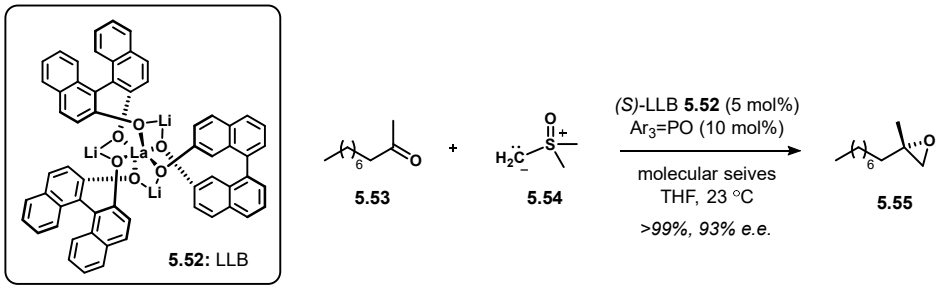

of an acyclic methyl ketone. Shibasaki and coworkers reported a catalytic asymmetric variant of this reaction utilizing a La-Li_3-tris(binaphthoxide) (LLB, **5.52**) as a chiral Lewis acid for an asymmetric sulfoxonium ylide-mediated epoxidation of ketones. With this protocol, they were able to achieve high yields and excellent enantioselectivities for a Corey–Chaykovsky epoxidation of a variety of substituted ketones with **5.54**; notably, 2-decanone **5.53** was converted to epoxide **5.55** in quantitative yield and a remarkable 93 % e.e. (**Scheme 5.13**).

With this precedent, we aimed to develop a rapid synthesis of a general methyl ketone fragment—that after an asymmetric Corey–Chaykovsky epoxidation—would afford enantiopure 2,2-disubsituted

Scheme 5.14 Ideas for the synthesis of an unsubstituted methyl ketone fragment

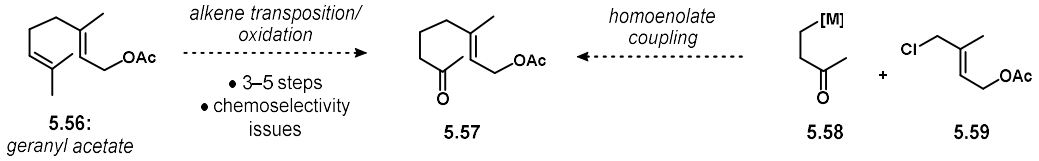

epoxides. A suitable coupling handle on the epoxide substrate to install the terminating groups would allow for a convergent and diversifiable synthesis of unsubstituted cyclization substrates. We considered starting the synthesis from geranyl acetate (**5.56**), as this monoterpene provides the appropriate carbon-scaffold for the epoxide fragment as well as an allylic acetate coupling handle. However, converting **5.56** to methyl ketone **5.57** would require an alkene transposition/oxidation sequence, similar to the route utilized to construct our model system substrates (**Chapter 3**) which was fairly tedious and encountered chemoselectivity issues with the alkene oxidation. We instead focused on a strategy that would directly install the methyl ketone and negate the need for an oxidation step. For this purpose, we pursued homoenolate-type couplings of **5.58** with functionalized isoprene unit **5.59** (**Scheme 5.14**). This unique

building block was originally developed by Bäckvall and Nyström[25] for 1,4-difunctionalizations of isoprene.[26] In a similar sense, a selective homoenolate coupling to the allylic chloride could install the methyl ketone (**5.57**), and following epoxidation, the allylic acetate in **5.60** would serve as an electrophile for a copper-mediated coupling with a variety of arene-terminating groups (**5.61**). This three-step sequence would allow for rapid construction of enantioenriched cyclization substrates (**5.62**) (**Scheme 5.15**).

Scheme 5.15 Strategy for the synthesis of unsubstituted cyclization substrates

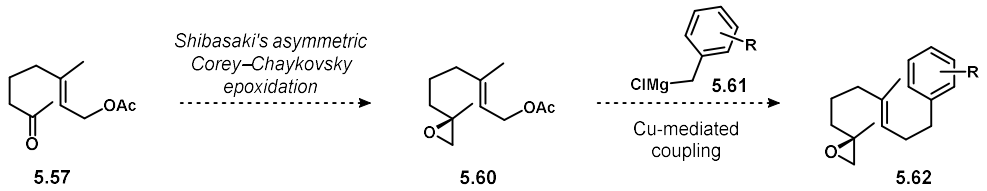

For the homoenolate coupling, we turned to the extensive work done by Nakamura and coworkers on the coupling of zinc homoenolates. Their seminal report in this area describes the utility of homoenolates derived from a zinc Lewis acid coordination with siloxycyclopropane **5.63**. They propose this mixture forms a dialkylzinc homoenolate (**5.64**); the authors have shown that this species can be intercepted by transition metals such as copper or nickel for productive couplings with allylic halides.[27] The regioselectivity of this coupling was significantly influenced by the transition metal. The reaction between homoenolate **5.64** and allylic chloride **5.65** with catalytic amounts of $CuBr{\cdot}Me_2S$ proceeded in

Scheme 5.16 Nakamura's zinc homoenolate couplings with allylic chloride

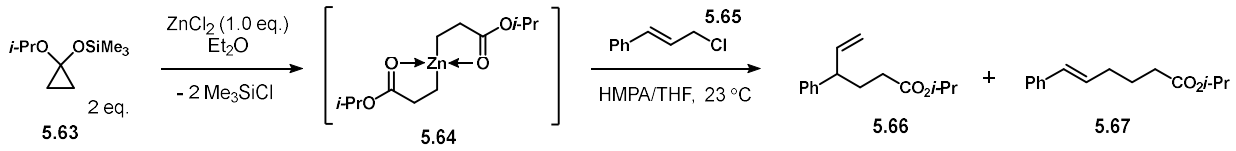

an S_N2' fashion to afford **5.66** as the major product. However, when $NiCl_2$(dppe) was employed as the catalyst, the regioselectivity of this coupling followed an S_N2-type addition to give linear product **5.67** as the major isomer (**Scheme 5.16**). This Ni-catalyzed protocol was encouraging precedent for the desired S_N2-type coupling with allylic chloride **5.59**. Conversely, the methyl ketone zinc homoenolate equivalent of **5.58** has rarely been used for nucleophilic couplings in comparison to the widely employed ester-variant.[27, 28] For the coupling of ketone-based homoenolates, palladium has emerged as the transition metal of choice. However, these conditions tend to favor the S_N2' product on reaction with a branched allylic leaving groups;[27] moreover, we were uncertain about the chemoselectivity for a palladium-homoenolate coupling between an allylic chloride or an allylic acetate.

We believed an investigation of zinc Lewis acids could uncover an optimal reagent to effect a nickel-catalyzed homoenolate coupling of **5.68** with allylic chloride **5.59**. Gratifyingly, upon pre-coordination of **5.68** with Et_2Zn, this complex underwent $NiCl_2$(dppe)-mediated coupling with **5.59** to provide small quantities of the desired linear methyl ketone **5.57**. Through a non-exhaustive survey of Ni(II)catalysts we found that the combination $NiCl_2$(dme) with the unsubstituted-PyBOX ligand afforded **5.57** in 40% yield as a single regioisomer (**Scheme 5.17**). Further optimization of the reaction conditions will likely result in a highly efficient homoenolate coupling for a *de novo* synthesis of geranyl acetate type fragment **5.57**. With quick access to ketone **5.57**, the Shibasaki-protocol for an asymmetric Corey-Chaykovsky epoxidation will be evaluated. This strategy has the potential to construct

Scheme 5.17 Successful conditions for a nickel-catalyzed coupling of keto-homoenolate

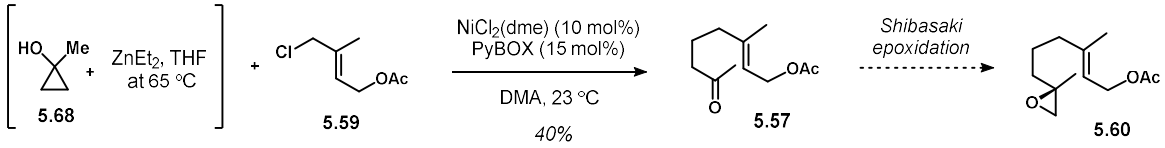

enantioenriched, terminal epoxide polyene substrates in only three steps, and will allow for a thorough investigation of chiral Lewis acids for a selective bicyclization.

5.2.3. Potential application towards a second generation synthesis of haterumaimide J

The development of a chiral Lewis acid-controlled bicyclization of 2,2-disubsituted epoxides would serve as a general method for selectively accessing C18 or C19-oxygenated trans-decalins, and this transformation could be applied for a second-generation synthesis of haterumaimide J. We know that the cyclization of racemic **5.69**—initiated with $EtAlCl_2$—provides a 5:1 mixture of C18- to C19-oxygenated decalins, respectively (**Scheme 5.1a**). This selectively potentially could be enhanced by the use of chiral

Scheme 5.18 A postulated second generation synthesis of haterumaimide J

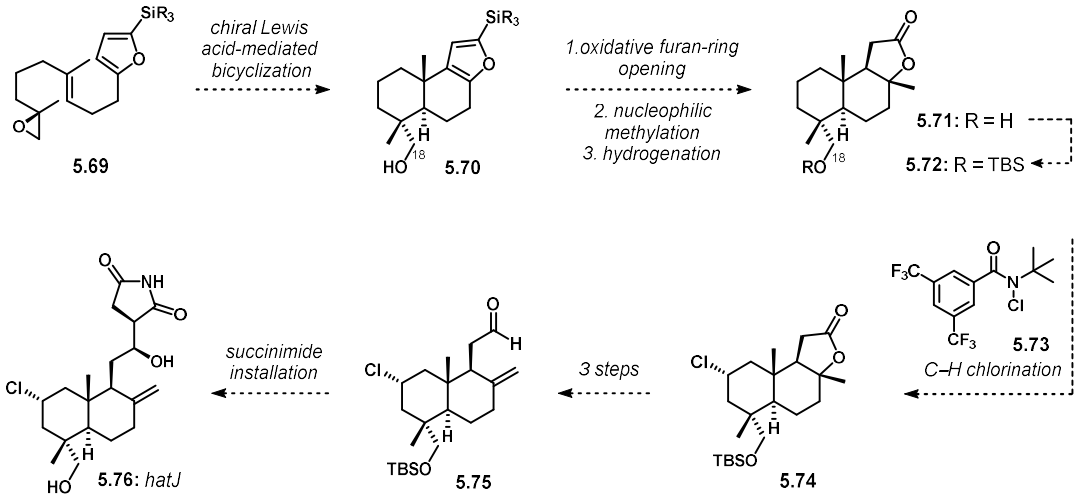

ligands on a Lewis acid metal center to deliver **5.70** in high enantiopurity from **5.69**. A three-step reaction sequence could elaborate the furan to the methyl lactone and ultimately construct C18-hydroxy sclareolide (**5.71**). With a bulky silyl protecting group on the neo-pentylic alcohol (**5.72**), we believe that *N*-chloroamide **5.73** stands a good chance at imparting the same C–H chlorination selectivity on **5.72** as it does on sclareolide.[29] With the A-ring substituents installed, **5.74** could be advanced through a similar

sequence of events as our semi-synthesis route: elaboration of the B-ring lactone to aldehyde **5.75** and installation of the hydroxysuccinimide motif to access hatJ (**5.76**). The success of this second generation strategy would combine two key elements from our previous syntheses of haterumaimide products: a stereocontrolled terminal epoxide bicyclization[12] (hatJ, **Chapter 4**), and a selective C–H chlorination[30](chlorolissoclimide, **Chapter 2**).

5.3. Conclusion

Our work on Lewis acid-initiated, terminal epoxide bicyclizations has addressed solutions for the stereocontrol, as well as provided a further understanding of the inherent challenges for this underdeveloped transformation. We successfully applied our chlorine-controlled manifold to access the intrinsically unfavored, C19-oxygenated decalin and in a subsequent step, complete a formal synthesis of steviol (**5.23**). This work showcased how a simple configurational change of the chlorine stereocenter on the cyclization substrate can permit access to the oxygenation pattern present in either labdane- or *ent*-kaurene-type scaffolds. Ongoing efforts in our lab work towards developing a more general method for a stereoselective terminal epoxide bicyclization through the use of chiral Lewis acids. Direct cyclization to construct unfunctionalized polycyclic frameworks bearing C18- or C19-oxygenation will be widely applicable for the synthesis of terpenoid natural products.

5.4. Experimentals

Materials and Methods:

All reactions were performed in oven-dried (120 °C) or flame-dried glassware under an atmosphere of dry argon unless otherwise noted. Reaction solvents including dichloromethane (CH_2Cl_2, Fisher, HPLC Grade), hexanes (Fisher, HPLC Grade), diethyl ether (Et_2O, Fisher, BHT stabilized, HPLC Grade), benzene (C_6H_6, Fisher, HPLC Grade), tetrahydrofuran (THF, Fisher, HPLC Grade), and toluene ($PhCH_3$, Fisher, HPLC Grade) were dried by percolation through a column packed with neutral alumina and a column packed with Q5 reactant, a supported copper catalyst for scavenging oxygen, under a positive pressure of argon.

Solvents for workup and chromatography were: acetone (Fisher, ACS grade), hexanes (Fisher or EMD, ACS Grade), EtOAc (EtOAc, Fisher, ACS Grade), dichloromethane (CH_2Cl_2, Fisher, ACS Grade), and methanol (MeOH, Fisher, ACS Grade). Column chromatography was performed using EMD Millipore 60 Å (0.040–0.063 mm) mesh silica gel (SiO_2). Analytical thin-layer chromatography was performed on Merck silica gel 60 F254 TLC plates. Visualization was accomplished with UV (254 or 210 nm), and p-anisaldehyde, ceric ammonium molybdate or potassium permanganate and heat as developing-agents.

^1H NMR and ^{13}C NMR spectra were recorded at 298 K on Bruker GN500 (500 MHz, ^1H; 125 MHz, ^{13}C), Bruker CRYO500 (500 MHz, ^1H; 125 MHz, ^{13}C), and Bruker AVANCE600 (600 MHz, ^1H; 125 MHz, ^{13}C) spectrometers. ^1H and ^{13}C spectra were referenced to residual $CHCl_3$ (7.26 ppm, ^1H or 77.0 ppm, ^{13}C). Chloroform-d ($CDCl_3$, D 99.8%, DLM-7) and dimethyl sulfoxide-d6 (CD_6SO, D 99.9%, DLM-10) were purchased from Cambridge Isotope Laboratories. Chemical shifts are reported in ppm

and multiplicities are indicated by: app (apparent), s (singlet), d (doublet), t (triplet), q (quartet), m (multiplet), and br s (broad singlet). Coupling constants, J, are reported in Hertz. Infrared (IR) spectra were recorded on a Perkin-Elmer spectrum RX1 FT-IR instrument or Varian 640-IR instrument on NaCl plates and peaks are reported in cm^{-1}. Mass spectrometry data were obtained from the University of California, Irvine Mass Spectrometry Facility. High-resolution mass spectra (HRMS) were recorded on a Waters LCT Premier spectrometer using ESI-TOF (electrospray ionization-time of flight) or CI-TOF (chemical ionization-time of flight) and data are reported in the form of (m/z). GC/FID analysis was performed on Agilent 7820A system with helium as carrier gas. HPLC analysis was performed on an Agilent1100series.

Citric acid (ACS grade, anhydrous, Fisher), potassium sodium tartrate (Oakwood), K_2CO_3 (anhydrous, 99%, Alfa Aesar), $NaHCO_3$ (ACS grade, Fisher), NaOH (ACS grade, Macron or Fisher), $Na_2S_2O_3$ (ACS grade, Fisher), *p*-anisaldehyde (99%, Acros Organics), isopropenylmagnesium bromide (0.5 M in THF, Sigma-Aldrich), borontrifluoride etherate (Alfa Aesa, 99%), B-methoxy-9BBN solution (1 M in hexanes, Sigma Aldrich), ethylaluminum dichloride solution (1 M in hexanes, $EtAlCl_2$, Acros Organic), 2,6-di-*t*-butylpyridine (99%, Alfa Aesar), diisobutylaluminum hydride (*i*-Bu_2AlH, Sure Pack™ reagent grade, Sigma Aldrich), dimethyl zinc (Me_2Zn, 2M in toluene, Sigma Aldrich) were used without further purification.

The following reagents were distilled from the indicated drying agents under argon prior to use: triethylamine (Et_3N, EMD, CaH_2), pyridine (Alfa Aesar, CaH_2 and *N,N*-diisopropylethylamine (*i*-Pr_2NEt, Alfa Aesar, CaH_2), trimethylsilyl chloride ($(CH_3)_3SiCl$, Acros Organics) and dimethylacetamide (Alfa Aesar, CaH_2) were fractionally distilled prior to use.

Experimental Procedures:

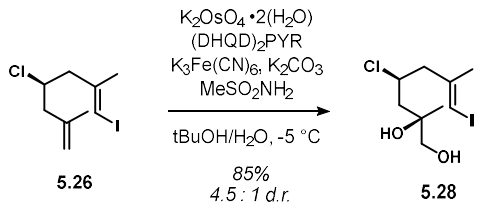

5.26 5.28

Diol 5.28:

$K_3Fe(CN)_6$ (2.55 g, 7.75 mmol, 2.1 equiv.), K_2CO_3 (1.28 g, 9.20 mmol, 2.5 equiv.), $MeSO_2NH_2$ (162 mg, 0.184 mmol, 1.1 equiv.), $K_2OsO_4•2H_2O$ (27.0 mg, 87 μmol, 2 mol%) and $(DHQD)_2PYR$ (162 mg, 0.158 mmol, 4 mol%) were mixed together and then taken up in *t*-BuOH/H_2O (45 mL, 1:1). The slurry was stirred vigorously, cooled to 0 °C and then **5.26** (1.05 g, 3.69 mmol, 1 equiv.) was added. The reaction mixture was stirred at 0 °C until the reaction was complete, indicated by TLC analysis (24–36 h). The reaction slurry was stirred with sat. aq. Na_2SO_3 (30 mL) for 1 h. EtOAc (20 mL) was added and the layers were separated. The aqueous layer was extracted with EtOAc (2 x 20 mL), the organic extracts were combined, washed sequentially with sat. aq. Na_2SO_3 and brine, and dried over anhydrous $MgSO_4$, filtered, and concentrated *in vacuo.* The crude oil was eluted through a plug of silica gel (70% EtOAc in hexanes) and concentrated *in vacuo* to afford **5.28** and **5.27** as a 4.5 : 1 mixture of diastereomers (1.02 g, 3.21 mmol, 85%). The diastereomers could be separated by flash chromatography eluting with a gradient of EtOAc in hexanes (SiO_2, 30% EtOAc in hexanes → 50% EtOAc in hexanes) to give **5.28** as a colorless oil (703 mg, 2.21 mmol, 60% overall yield).

^{1}H NMR (500 mHz, $CDCl_3$) δ 6.08 (s, 1H), 4.29–4.27 (m, 1H), 3.55 (d, *J* = 10.8 Hz, 1H), 3.47 (d, *J* = 10.8 Hz, 1H), 2.71–2.61 (m, 2H), 2.39–2.08 (br s, 1 H), 2.03 (dd, *J* = 15.3, 3.1 Hz, 1H), 1.89 (dd, *J* = 15.3, 8.9 Hz, 1H), 1.87 (s, 3H), 1.27 (s, 3H); **^{13}C NMR** (125 mHz, $CDCl_3$) δ 143.3, 79.1, 72.3, 69.8, 55.9,

49.4, 45.6, 24.2, 23.5; **IR** (film) ν 3389, 2960, 2903, 1632 cm^{-1}; **HRMS** (ES+) *m/z* calc'd for $C_9H_{16}ClIO_2$ $[M+Na]^+$: 340.9781; found 340.9771; $[\alpha]^{22}_D$ 1.45 (*c* = 0.8, $CHCl_3$).

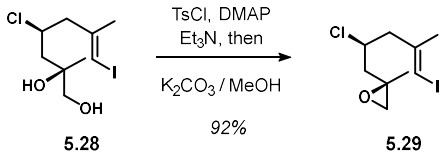

5.28 5.29

Epoxide 5.29:

Toluenesulfonyl chloride (500 mg, 2.61 mmol, 1.3 equiv.) and DMAP (170 mg, 4.00 mmol, 0.75 equiv.) were dissolved in CH_2Cl_2 (10 mL) and the solution was cooled to 0 °C. Diol **5.28** (640 mg, 2.00 mmol, 1 equiv.) was added as a solution in CH_2Cl_2 (3 mL). The reaction was allowed to warm to ambient temperature and stirred for 5 h. The solvent was concentrated *in vacuo*, and the resulting residue was taken up in MeOH (15 mL) followed by the addition of K_2CO_3 (830 mg, 6.00 mmol, 3 equiv.). The slurry was stirred for 3 h, the solvent was concentrated *in vacuo* to one third the initial volume, and the resulting mixture was diluted with EtOAc:pentanes (20 mL, 3:1). The remaining base was quenched with sat. aq. NH_4Cl (50 mL). The layers were separated, and the aqueous layer was extracted with EtOAc:pentanes (3:1, 3 x 15 mL). The organic layers were combined, washed with brine, dried over anhydrous $MgSO_4$, filtered, and concentrated *in vacuo*. The crude residue was purified by flash chromatography (SiO_2, 10% EtOAc in hexanes) to afford **5.29** (538 mg, 1.80 mmol, 90%) as a colorless oil.

^{1}H NMR (600 MHz, $CDCl_3$) δ 6.08 (app. s, 1H), 4.14 (dddd, *J* = 20.0, 8.3, 5.7, 4.1 Hz, 1H), 2.72–2.61 (m, 4H), 2.11 (ddd, *J* = 14.4, 4.1, 1.3 Hz, 1H), 1.88 (app. d, *J* = 1.3 Hz, 3H), 1.69 (dd, *J* = 14.4, 10.1 Hz, 1H), 1.37 (s, 3H); **^{13}C NMR** (125 MHz, $CDCl_3$) δ 143.2, 78.9, 56.6, 55.1, 48.5, 45.4, 23.6, 22.2; **IR** (film)

ν 2957, 2893, 1237 cm^{-1}; **HRMS** (CI+) *m/z* calc'd for $C_9H_{14}ClIONH_4$ $[M+NH_4]^+$: 318.0122; found 318.0120; $[\alpha]^{23}_D$ –15.7 (*c* = 1.0, $CHCl_3$).

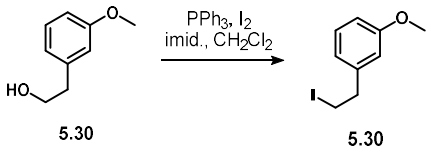

5.30 5.30

Iodide 5.30:

A solution of PPh_3 (1.04 g, 3.97 mmol, 1.3 equiv.) and imidazole (1.03 g, 15.3 mmol, 5 equiv.) in CH_2Cl_2 (10 mL) was cooled to 0 °C. Iodine (1.0g, 3.97 mmol, 1.3 equiv.) was added portion-wise to the mixture. Commercially available **5-S1** (500 mg, 3.05 mmol, 1 equiv.) in CH_2Cl_2 (2 mL) was then added to the dark red reaction mixture. The reaction was allowed to warm to ambient temperature and stirring was continued for 8 hr. After this time the reaction had turned slightly yellow and then the mixture was diluted with sat. aq. Na_2SO_3 (7 mL); the biphasic mixture was stirring vigorously for 5 min. The layers were separated and aqueous layer was diluted with water (10 mL) and extracted with hexanes (2 x 10 mL). The organic layers were combined and washed sequentially with water (2 x 10 mL) and brine (2 x 10 mL) and then dried over $MgSO_4$, filtered and concentrated *in vacuo.* The crude residue was extracted with hexanes and filtered (x2) to remove the excess Ph_3P=O. The hexanes filtrate was collected and concentrated *in vacuo.* The crude residue was purified by flash chromatography (SiO_2, hexanes → 2% EtOAc in hexanes) to afford **5.30** (795 mg, 3.03 mmol, 97%) as a pale yellow oil.

^{1}H NMR (500 MHz, $CDCl_3$) δ 7.23 (t, *J* = 7.7 Hz, 1 H), 6.81 (d, *J* = 6.8 Hz, 1H), 6.79 (d, *J* = 7.7 Hz, 1H), 6.73 (s, 1H), 3.80 (s, 3H), 3.34 (t, *J* = 7.8 Hz, 2H), 3.15 (t, *J* = 7.8 Hz, 2H); **^{13}C NMR** (125 MHz, $CDCl_3$) δ 159.8, 142.2, 129.6, 120.6, 114.1, 112.1, 55.2, 40.4, 5.23

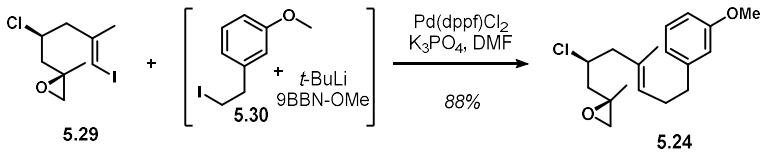

Cyclization substrate 5.24:

A solution of **5.30** (323 mg, 1.99 mmol, 1.3 equiv.) in Et_2O (4 mL) was cooled to –78 °C and *t*-BuLi (1.7 M in pentane, 5.32 mL, 4 equiv.) was added quickly followed by 9-BBN-OMe (1 M in hexanes, 5.96 mL, 4.5 equiv.). THF (2 mL) was added and the reaction was warmed to ambient temperature over 1 h. After stirring for an additional 3 h the white slurry became homogeneous. Aq. K_3PO_4 (3M, 1.1 mL, 2.5 equiv.) and $Pd(dppf)Cl_2 \bullet CH_2Cl_2$ (87 mg, 0.106 mmol, 0.15 equiv.) were added sequentially under an atmosphere of argon, followed by the addition of **5.29** (400 mg, 1.33 mmol, 1.0 equiv.) as a solution in DMF (5 mL). The reaction mixture was shielded from light and stirred vigorously at ambient temperature for 12 h. The biphasic mixture was diluted with brine (15 mL), hexanes (15 mL) and the layers were separated. The aqueous phase was extracted with Et_2O/hexanes (1:3, 3 x 10 mL), the organic phases were combined, washed sequentially with water (2 x 10 mL) and brine (2 x 10 mL), and then dried over anhydrous $MgSO_4$, filtered, and concentrated under reduced pressure. The crude product residue was purified by flash chromatography (SiO_2, 10% EtOAc in hexanes) to afford **5.24** (361 mg, 1.17 mmol, 88%) as a colorless oil.

^{1}H NMR (500 MHz, $CDCl_3$) δ 7.20 (t, *J* = 7.7 Hz, 1H), 6.78 (d, *J* = 7.7 Hz, 1H) 6.75–6.72 (m, 2H), 5.27 (t, *J* = 7.6 Hz, 1H), 4.10 (m, 1H), 3.79 (s, 3H), 2.73 (d, *J* = 4.7 Hz, 1H), 2.68 (d, *J* = 4.7 Hz, 1H), 2.64 (app q, *J* = 7.3 Hz, 2H), 2.47–2.38 (m, 2H), 2.33 (dd, *J* = 14.8, 7.3, 2H), 2.16 (dd, *J* = 14.8, 3.2 Hz, 1H), 1.59 (s, 3H), 1.53 (dd, *J* = 14.2, 10.8 Hz, 1H), 1.35 (s, 3H); **^{13}C NMR** (125 MHz, $CDCl_3$) δ 159.5, 143.5,

131.3, 129.2, 128.1, 120.8, 114.1, 110.9, 57.8, 55.4, 55.2, 55.1, 49.3, 45.2, 35.7, 29.6, 20.2, 15.8; **HRMS** (ES+) *m/z* calc'd for $C_{18}H_{25}ClO_2Na$ $[M+Na]^+$: 331.1441; found 331.1439.

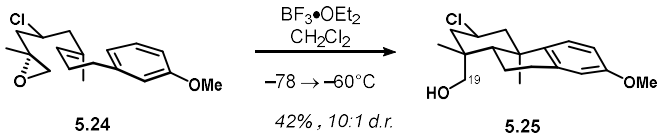

5.24 **5.25**

Decalin 5.25:

A solution of **5.24** (25 mg, 89 μmol, 1 equiv.) in CH_2Cl_2/toluene (6: 1, 1.4 mL) was cooled to –78 °C. A solution of $BF_3.OEt_2$ in CH_2Cl_2 (1M, 168 μmol, 2 equiv.) was added slowly down the side of the flask. The reaction was allowed to warm to –65 °C over 25 min and then Et_3N (50 μL) was added slowly down the side of the flask. The reaction was allowed to warm to 0 °C and sat. aq. $NaHCO_3$ (1 mL) was added. The biphasic solution was extracted with CH_2Cl_2 (3 x 1 mL), the organic layers were combined and washed with brine (1 mL), dried over $MgSO_4$, filtered and concentrated *in vacuo.* The crude residue contained a complex mixture of products, by eluting the mixture through a small plug of silica (25% EtOAc in hexanes) a more discernable mixture of products could be analyzed by ^{1}HNMR. The mixture contained desired **5.25** in an ~10:1 d.r. with the C18-hydroxylated diastereomer and the ortho-cyclized isomer (**5.31**), in a 5:1 ratio. This mixture was further purified by flash chromatography (SiO_2, 15% EtOAc in hexanes) to afford **5.25** (11.4 mg, 37.4 μmol, 42%).

^{1}H NMR (500 MHz, $CDCl_3$) δ 7.14 (d, *J*= 8.8 Hz, 1H), 6.72 (dd, *J*= 8.9, 2.8 Hz, 1H), 6.57 (app d, *J*= 2.8 Hz, 1H), 4.30 (tt, *J*= 12.2, 3.9 Hz, 1H), 3.78 (d, *J*= 11.2 Hz, 1H), 3.77 (s, 3H), 3.55 (d, *J*= 11.2 Hz, 1H), 2.94–2.80 (m, 3H), 2.48 (m, 1H), 1.96 (dd, *J*= 13.2, 7.1 Hz, 1H), 1.76–1.63 (m, 2H), 1.59–1.55

(m, 1H), 1.37 (dd, *J* = 24.9, 12.0 Hz, 1H), 1.20 (s, 3H), 1.11 (s, 3H); **^{13}C NMR** (125 MHz, $CDCl_3$) δ ** ; HRMS ***

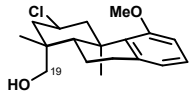

5.31

Ortho-cyclized decalin 5.31:

^{1}H NMR (500 MHz, $CDCl_3$) δ 7.06 (t, *J* = 7.5 Hz, 1H), 6.67 (dd, *J* = 7.5, 3.8 Hz, 2H), 4.30 (tt, 12.8, 4.4 Hz, 1H), 3.80 (s, 3H), 3.75 (m, 1H), 3.57 (d, *J* = 11.2 Hz, 1H), 2.86 (dd, *J* = 7.8, 3.4 Hz, 2H), 2.44–2.40 (m, 1H), 1.95–1.91 (m, 1H), 1.52–1.36 (m, 5H), 1.32 (s, 3H), 1.12 (s, 3H).

Oxabicycle 5.33:

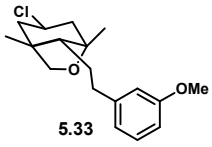

5.33

^{1}H NMR (500 MHz, $CDCl_3$) δ 7.21 (t, *J* = 7.8 Hz, 1H), 6.78–6.73 (m, 3H), 4.33–4.29 (m, 1H), 3.81 (s, 3H), 3.64 (d, *J* = 8.0 Hz, 1H), 3.54 (dd, *J* = 8.0, 1,5 Hz), 2.75–2.69 (m, 1H), 2.65–2.56 (m, 1H), 2.28 (dd, *J* = 12.8, 6.5 Hz, 1H), 2.13 (dd, *J* = 12.8, 6.5 Hz, 1H), 1.82–1.75 (m, 2H), 1.73–1.67 (m, 1H), 1.59–1.57 (m, 1H), 1.50–1.47 (m, 1H), 1.32 (s, 3H), 1.07 (s, 3H).

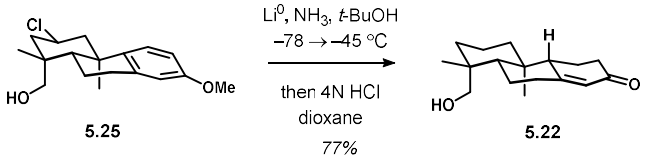

Enone 5.22:

Liquid ammonia (~1.6 mL) was condensed into a 25 mL, 3-neck round bottom flask at –78 °C with a dry ice condenser equipped to the middle neck of the flask. One side neck was sealed with a septum equipped with a balloon of argon and the other was sealed with a plastic yellow cap. The oxidized

surface of Li^0 wire was removed by shaving the edges with a with a razor and a piece weighing approximately 10 mg was added through the side neck of the flask with a plastic cap and following the addition, the cap was resealed. Alcohol **5.25** (15 mg, 48 μmol , 1 equiv.) was added as a solution in THF (0.5 M). The dark blue reaction was stirred at –78 °C for 30 min and then *t*-BuOH (500 μL) was added dropwise. The reaction was warmed to –45 °C and vigorously stirred for an additional 1 hr after which time, MeOH (500 μL) was added and the solution became clear. The mixture was slowly warmed to room temperature and sequentially diluted with sat. aq. NH_4Cl (500 μL) and EtOAc (1 mL). The layers were separated and the aqueous layer was extracted with EtOAc (2 x 1 mL), the organic layers were combined, washed with brine (1 mL), dried over $MgSO_4$, filtered and concentrated *in vacuo.* The crude residue was immediately taken up in 4N HCl in dioxane (2 mL) at 0 °C. The solution was allowed to warm to ambient temperature and stir for an additional 45 min before the dropwise addition of sat. aq. $NaHCO_3$ (1 mL). The layers were separated, the organic phase was washed with brine (1 mL), dried over $MgSO_4$, filtered and concentrated *in vacuo*. The resulting residue which still contained some 1,4-dioxane was purified by flash chromatography (SiO_2, 40% EtOAc in hexanes) to afford **5.22** (9.6 mg, 36 μmol, 77%) as a clear oil.

The ^1H and ^{13}C NMR match the reported literature data.[15]

^1H NMR (500 MHz, $CDCl_3$) δ 5.87 (s, 1H), 8.81 (d, J = 11.0 Hz, 1H), 3.47 (d, J= 11.0 Hz, 1H), 2.54 (dd, J= 16.5, 5.2 Hz, 1H), 2.39 (dt, J= 15.6, 3.9 Hz, 1H), 2.28–2.18 (m, 2H), 2.11–2.08 (m, 1H), 2.04–1.98 (m, 1H), 1.91–1.84 (m, 2H), 1.79 (app d, J= 12.5 Hz, 1H), 1.75–1.71 (m, 2H), 1.53–1.46 (m, 2H), 1.35 (dd, J= 13.0, 3.1 Hz, 1H), 1.15 (td, J= 12.5, 5.0 Hz, 1H), 1.03 (s, 3H), 0.99 (dd, J= 13.5, 5.0 Hz, 1H), 0.78 (s, 3H); **^{13}C NMR** (125 MHz, $CDCl_3$) δ 199.8, 164.9, 126.0, 65.1, 54.9, 51.7, 39.3, 38.9, 38.6,

36.7, 35.9, 35.2, 27.1, 21.9, 20.6, 18.4, 16.3; **HRMS** (SI+) *m/z* calc'd for $C_{17}H_{26}O_2Na$ $[M+Na]^+$: 285.1830; found 285.1838.

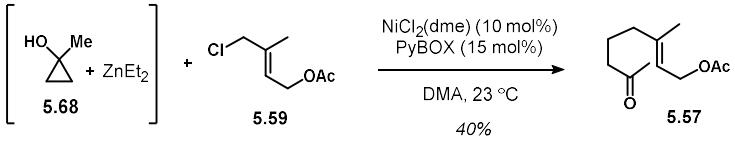

Methyl Ketone 5.57:

Cyclopropanol **5S-1**[31] (50 mg, 0.694 mmol) was taken up in dry THF (2.3 mL). The solution was cooled to 0 °C and $ZnEt_2$ (1M in hexanes, 700 µL, 1 equiv. to **5S-1**) was added dropwise. The reaction was then heated to 50 °C for 1 hr. A different round-bottom flask was charged with $NiCl_2$(dme) (10mg, 45 µmol, 0.25 equiv.) and PyBOX (21 mg, 91 µmol, 0.5 equiv.) and these solids were taken up freshly distilled DMA (950 µL). The nickel pre-catalyst and ligand were allowed to stir at room temperature for 30 min upon which the solution turned from green to yellow. The allylic chloride **5.59** (30 mg, 0.184 mmol, 1 equiv.) was added to the catalyst solution followed the zinc homoenolate solution (~0.3 M in THF, 0.396 mmol, 2 equiv.). The reaction mixture was then heated to 45 °C for 3 hr. After this time the murky yellow reaction was cooled to 0 °C and sat. aq. $NaHCO_3$ (500 µL) was added dropwise. The biphasic mixture was further diluted with water (1 mL) and EtOAc (1 mL). The layers were separated and the aqueous layer was extracted with EtOAc (2 x 1 mL). The combined organic layers were washed sequentially with water (1 mL) and brine (2 mL) then dried over $MgSO_4$, filter and concentrated *in vacuo.* The crude residue was purified by flash chromatography (SiO_2, 10% EtOAc in hexanes) to afford **5.57** (14.5 mg, 73.6 µmol, 40%) as a clear oil.

^{1}H NMR (500 MHz, $CDCl_3$) δ 5.33 (t, *J* = 7.32 Hz, 1H), 4.58 (d, *J* = 7.0 Hz, 2H), 2.40 (t, *J* = 7.3 Hz, 2H), 2.14 (s, 3H), 2.05 (s, 3H), 2.05–2.01 (m, 2H), 1.71 (q, *J* = 7.7 Hz, 2H), 1.68 (s, 3H); **HRMS** (ES+) *m/z* calc'd for $C_{11}H_{18}O_3Na$ $[M+Na]^+$: 221.1154; found 221.1155.

5.5. References

1. Goldsmith, D. J.; Phillips, C. F., *J. Am. Chem. Soc.* **1969,** *91* (21), 5862

2. Corey, E. J.; Liu, K., *J. Am. Chem. Soc.* **1997,** *119* (41), 9929-9930.

3. Vantamelen, E. E.; Zawacky, S. R.; Russell, R. K.; Carlson, J. G., *J. Am. Chem. Soc.* **1983,** *105* (1), 142-143.

4. Brinkmann, H.; Hoffmann, R. W., *Chem. Ber.* **1990,** *123* (12), 2395-2401.

5. Yasuda, M.; Ohhata, T.; Shibata, I.; Baba, A.; Matsuda, H., *J. Chem. Soc. Per. Trans. 1* **1993,** (7), 859-865.

6. Cornforth, J. W.; Cornforth, R. H.; Matthew, K. K., *J. Am. Chem. Soc.* **1959,** *81*, 112.

7. Brochu, M. P.; Brown, S. P.; MacMillan, D. W. C., *J. Am. Chem. Soc.* **2004,** *126* (13), 4108-4109.

8. Halland, N.; Braunton, A.; Bachmann, S.; Marigo, M.; Jorgensen, K. A., *J. Am. Chem. Soc.* **2004,** *126* (15), 4790-4791.

9. Goodman, J. M.; Paton, R. S., *Chem. Comm.* **2007,** (21), 2124-2126.

10. Kang, B.; Mowat, J.; Pinter, T.; Britton, R., *Org. Lett.* **2009,** *11* (8), 1717-1720.

11. Halperin, S. D.; Britton, R., *Org. Biomol. Chem.* **2013,** *11* (10), 1702-1705.

12. Michalak, S. E.; Nam, S.; Kwon, D. M.; Horne, D. A., *J. Am. Chem. Soc.* **2019,** *Just Accepted.*

13. Johnson, W. S.; Dubois, G. E., *J. Am. Chem. Soc.* **1976,** *98* (4), 1038-1039.

14. Johnson, W. S.; Escher, S.; Metcalf, B. W., *J. Am. Chem. Soc.* **1976,** *98* (4), 1039-1041.

15. Cherney, E. C.; Green, J. C.; Baran, P. S., *Angew. Chem. Int. Ed.* **2013,** *52* (34), 9019-9022.

16. Crispino, G. A.; Jeong, K. S.; Kolb, H. C.; Wang, Z. M.; Xu, D. Q.; Sharpless, K. B., *J. Org. Chem.* **1993,** *58* (15), 3785-3786.

17. Mohammad, S.; Dhambri, S.; Gori, D.; Vacelaire, C.; Sorin, G.; Ardisson, J.; Lannou, S. I., *Synlett* **2013,** *24*, 2581-2585.

18. Alonso, F.; Beletskaya, I. P.; Yus, M., *Chem. Rev.* **2002,** *102* (11), 4009-4091.

19. Ungarean, C. N.; Southgate, E. H.; Sarlah, D., *Org. Biomol. Chem.* **2016,** *14* (24), 5454-5467.

20. Ishihara, K.; Nakamura, S.; Yamamoto, H., *J. Am. Chem. Soc.* **1999,** *121* (20), 4906-4907.

21. Schafroth, M. A.; Sarlah, D.; Krautwald, S.; Carreira, E. M., *J. Am. Chem. Soc.* **2012,** *134* (50), 20276-20278.

22. Jeker, O. F.; Kravina, A. G.; Carreira, E. M., *Angew. Chem. Int. Ed.* **2013,** *52* (46), 12166-12169.

23. Sharpless, K. B.; Amberg, W.; Bennani, Y. L.; Crispino, G. A.; Hartung, J.; Jeong, K. S.; Kwong, H. L.; Morikawa, K.; Wang, Z. M.; Xu, D. Q.; Zhang, X. L., *J. Org. Chem.* **1992,** *57* (10), 2768-2771.

24. Wang, B.; Wong, O. A.; Zhao, M. X.; Shi, Y., *J. Org. Chem.* **2008,** *73* (24), 9539-9543.

25. Nystrom, J. E.; Backvall, J. E., *J. Org. Chem.* **1983,** *48* (22), 3947-3950.

26. Backvall, J. E.; Sellen, M.; Grant, B., *J. Am. Chem. Soc.* **1990,** *112* (18), 615-6621.

27. Nakamura, E.; Aoki, S.; Sekiya, K.; Oshino, H.; Kuwajima, I., *J. Am. Chem. Soc.* **1987,** *109* (26), 8056-8066.

28. Mills, L. R.; Rousseaux, S. A. L., *Eur. J. Org. Chem.* **2019,** (1), 8-26.

29. Quinn, R. K.; Konst, Z. A.; Michalak, S. E.; Schmidt, Y.; Szklarski, A. R.; Flores, A. R.; Nam, S.; Horne, D. A.; Vanderwal, C. D.; Alexanian, E. J., *J. Am. Chem. Soc.* **2016,** *138* (2), 696-702.

30. Konst, Z. A.; Szklarski, A. R.; Pellegrino, S.; Michalak, S. E.; Meyer, M.; Zanette, C.; Cencic, R.; Nam, S.; Voora, V. K.; Horne, D. A.; Pelletier, J.; Mobley, D. L.; Yusupova, G.; Yusupov, M.; Vanderwal, C. D., *Nat. Chem.* **2017,** *9* (11), 1140-1149.

31. Kulinkovich, O. G.; Sviridov, S. V.; Dmitry, A. V., *Synthesis* **1990**, 234.

APPENDIX

1H spectrum

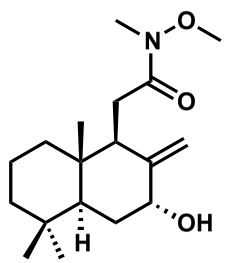

2.7


```
Current Data Parameters
USER              michal
NAME          SEM-1-272
EXPNO                 4
PROCNO                1

F2 - Acquisition Parameters
Date_          20150817
Time              18.26
INSTRUM           av600
PROBHD   5 mm BBO BB-1H
PULPROG            zg30
TD                38460
SOLVENT           CDCl3
NS                   16
DS                    2
SWH            9615.385 Hz
FIDRES         0.250010 Hz
AQ             1.9999700 sec
RG                  575
DW               52.000 usec
DE               14.33 usec
TE               298.2 K
D1            0.10000000 sec
TD0                   1

======== CHANNEL f1 ========
SFO1         600.1342009 MHz
NUC1                 1H
P1                9.00 usec

F2 - Processing parameters
SI                65536
SF           600.1300343 MHz
WDW                  EM
SSB                   0
LB                 0.30 Hz
GB                    0
PC                 1.00

1D NMR plot parameters
CX                22.80 cm
CY                15.00 cm
F1P               8.000 ppm
F1              4801.04 Hz
F2P               0.000 ppm
F2                0.00 Hz
PPMCM          0.35088 ppm/cm
HZCM         210.57195 Hz/cm
```

Z-restored spin-echo 13C spectrum with 1H decoupling

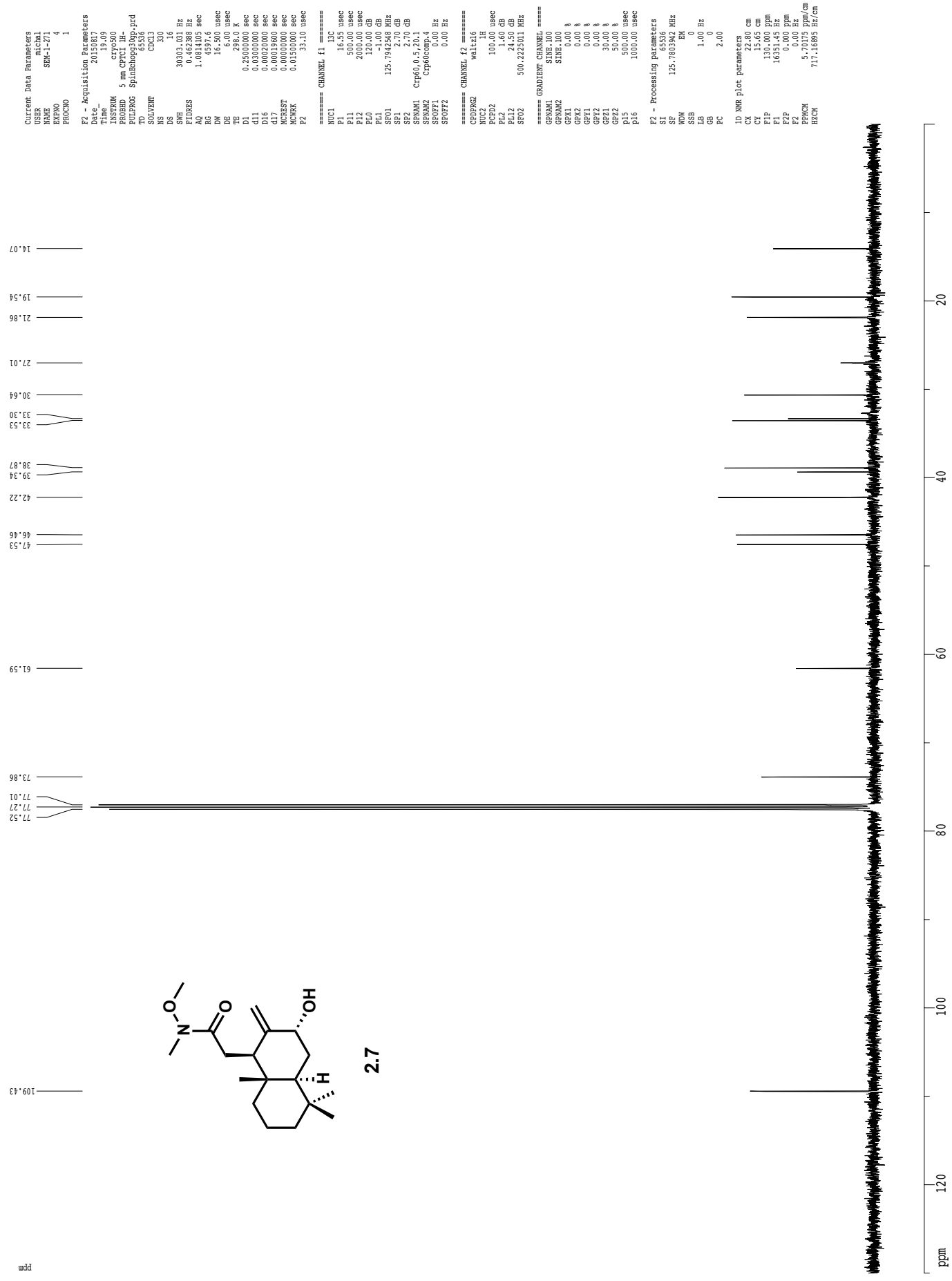

2.7

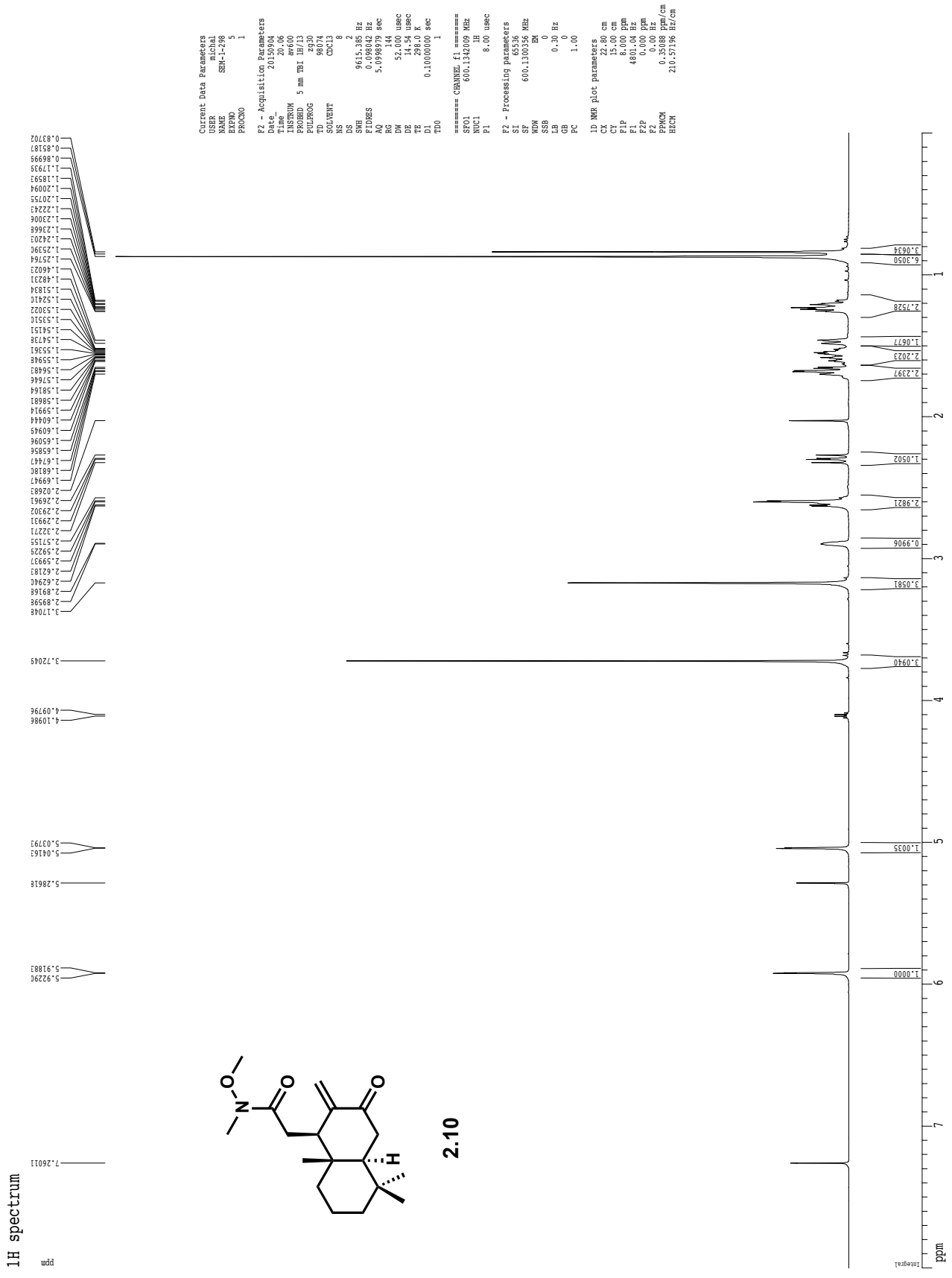
1H spectrum
2.10
Current Data Parameters
USER michal
NAME SEM-1-298
EXPNO 5
PROCNO 1
F2 - Acquisition Parameters
Date_ 20150904
Time 20.06
INSTRUM av600
PROBHD 5 mm TBI 1H/13
PULPROG zg30
TD 98074
SOLVENT CDCl3
NS 8
DS 2
SWH 9615.385 Hz
FIDRES 0.098042 Hz
AQ 5.0998979 sec
RG 144
DW 52.000 usec
DE 14.34 usec
TE 298.0 K
D1 0.10000000 sec
TD0 1
======== CHANNEL f1 ========
SFO1 600.1342009 MHz
NUC1 1H
P1 8.00 usec
F2 - Processing parameters
SI 65536
SF 600.1300356 MHz
WDW EM
SSB 0
LB 0.30 Hz
GB 0
PC 1.00
1D NMR plot parameters
CX 20.00 cm
CY 15.00 cm
F1P 8.000 ppm
F1 4801.04 Hz
F2P 0.000 ppm
F2 0.00 Hz
PPMCM 0.35088 ppm/cm
HZCM 210.57196 Hz/cm
ppm
Integral

Z-restored spin-echo 13C spectrum with 1H decoupling

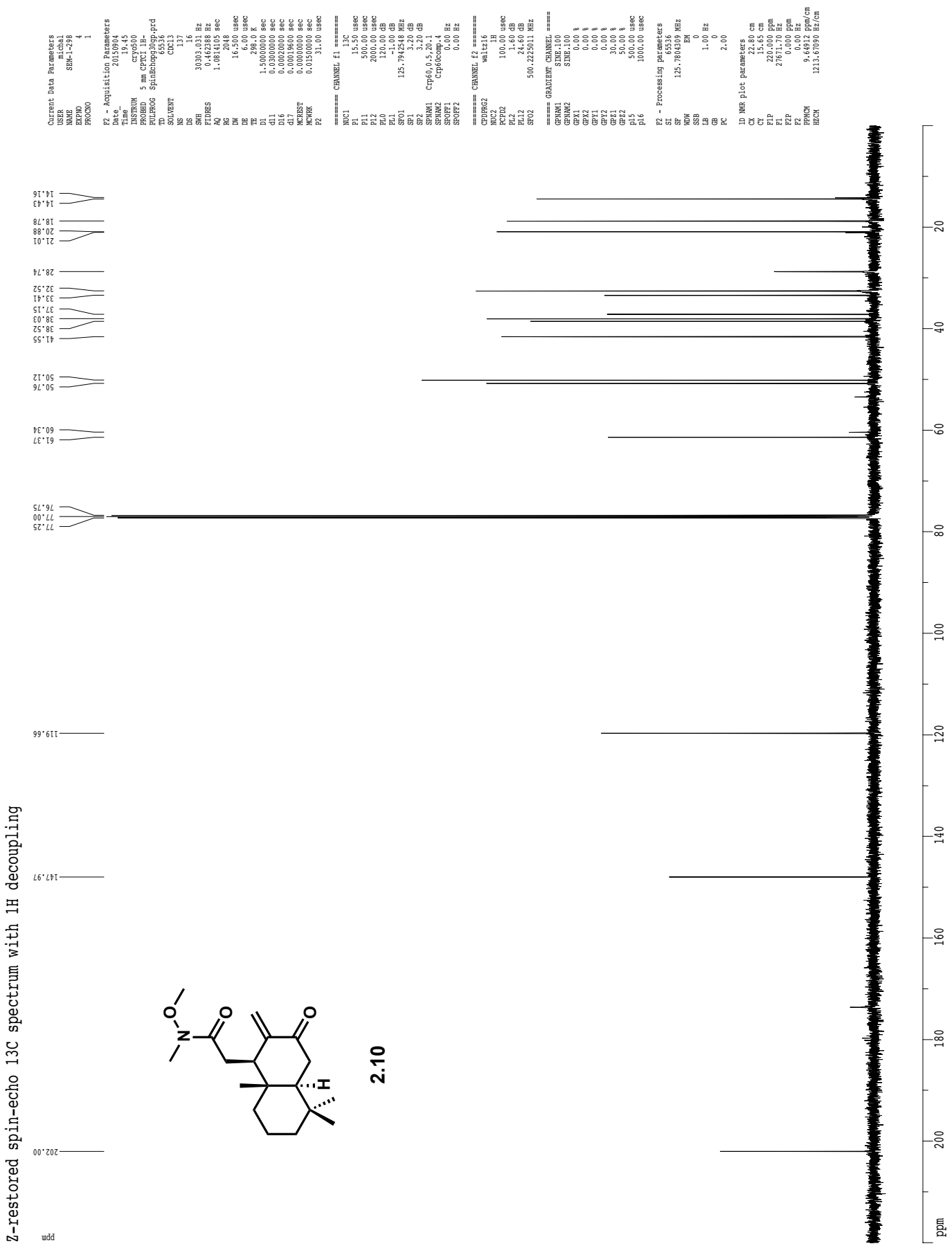

2.10

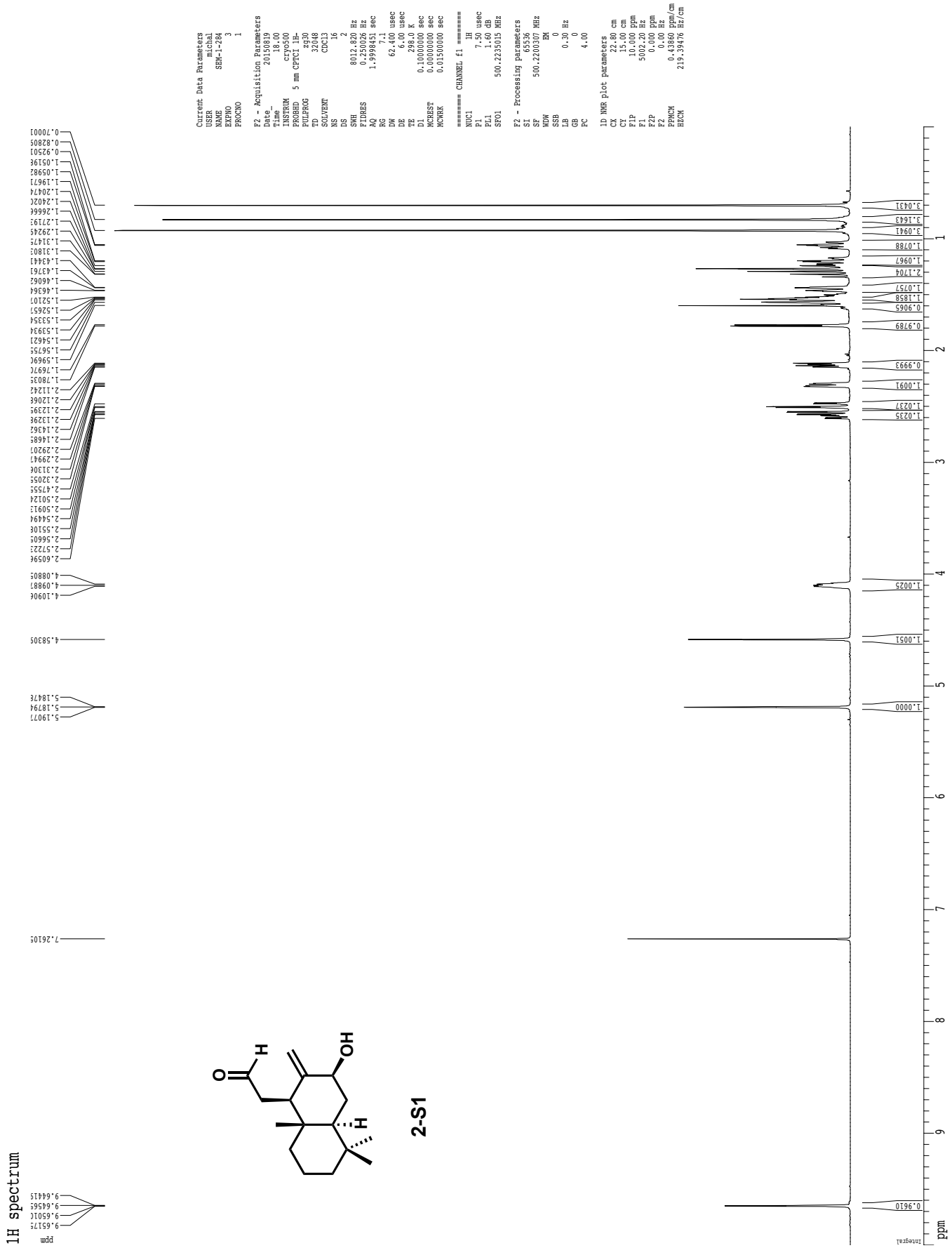
1H spectrum
2-S1

Z-restored spin-echo 13C spectrum with 1H decoupling

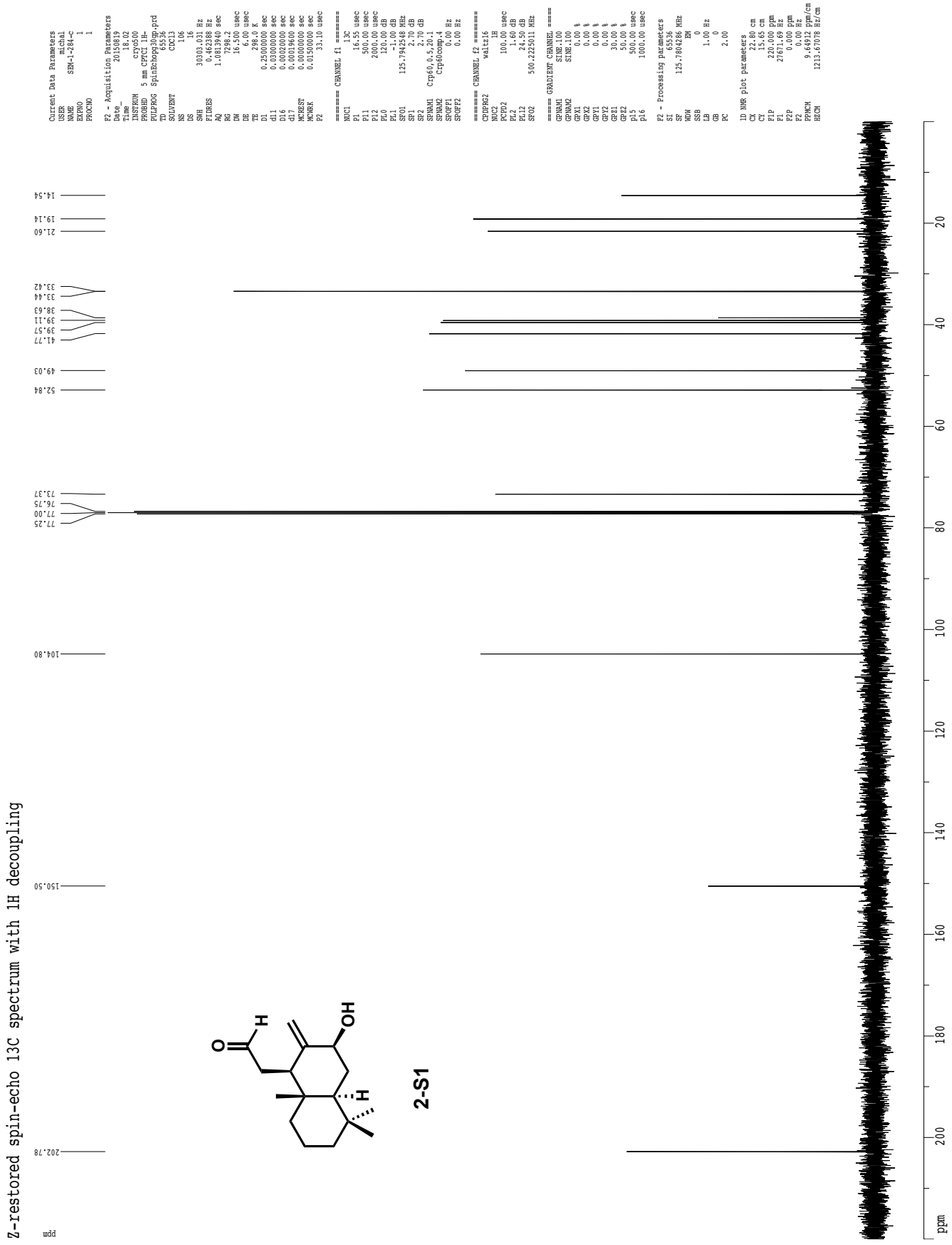

2-S1

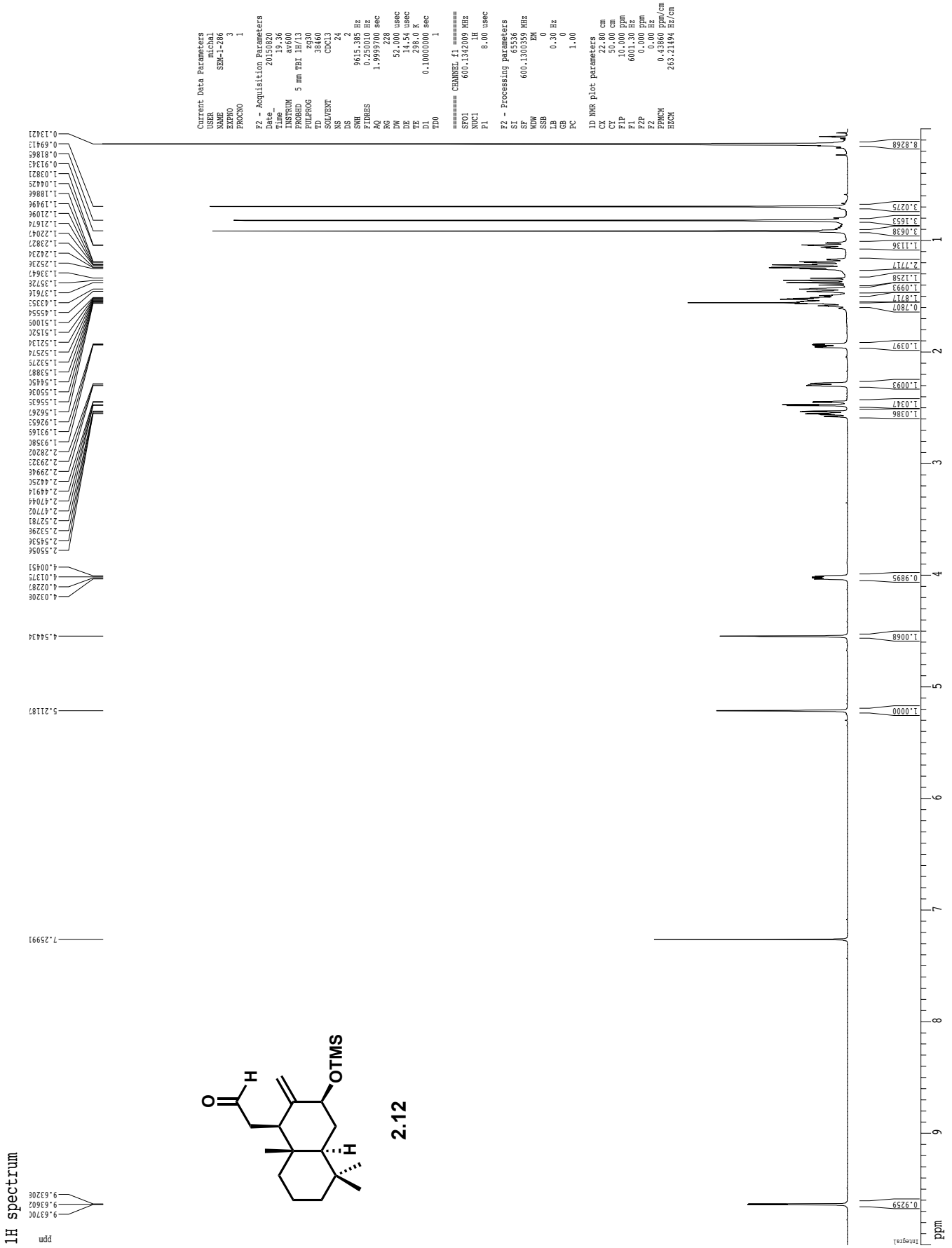

2.12

Z-restored spin-echo 13C spectrum with 1H decoupling

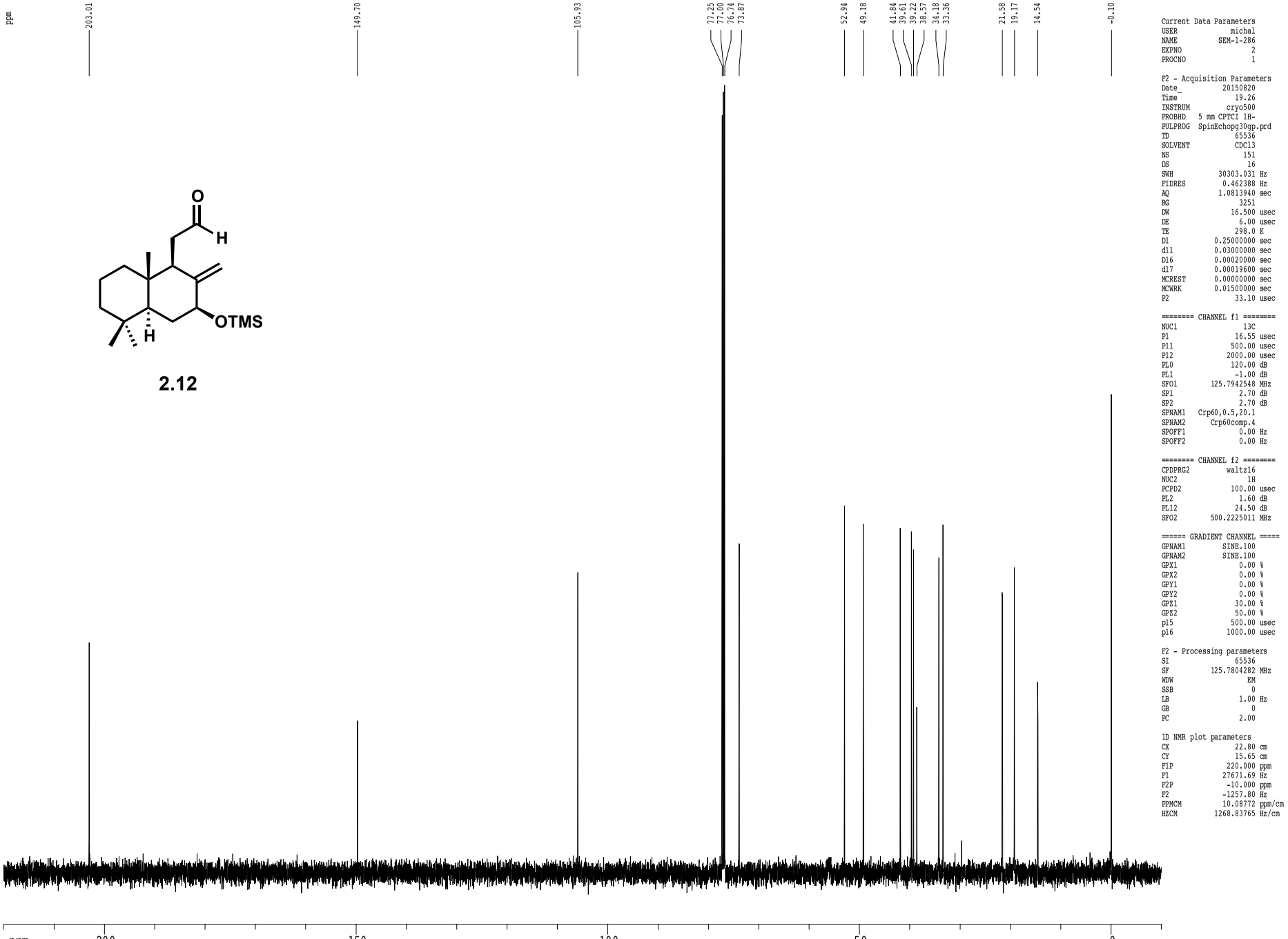

188

Current Data Parameters
USER michal
NAME SEM-1-286
EXPNO 2
PROCNO 1

F2 - Acquisition Parameters
Date_ 20150820
Time 19.26
INSTRUM cryo500
PROBHD 5 mm CPTCI 1H-
PULPROG SpinEchopg30gp.prd
TD 65536
SOLVENT CDCl3
NS 151
DS 16
SWH 30303.031 Hz
FIDRES 0.462388 Hz
AQ 1.0813940 sec
RG 3251
DW 16.500 usec
DE 6.00 usec
TE 298.0 K
D1 0.25000000 sec
d11 0.03000000 sec
D16 0.00020000 sec
d17 0.00019600 sec
MCREST 0.00000000 sec
MCWRK 0.01500000 sec
P2 33.10 usec

======== CHANNEL f1 ========
NUC1 13C
P1 16.55 usec
P11 500.00 usec
P12 2000.00 usec
PL0 120.00 dB
PL1 -1.00 dB
SFO1 125.7942548 MHz
SP1 2.70 dB
SP2 2.70 dB
SPNAM1 Crp60,0.5,20.1
SPNAM2 Crp60comp.4
SPOFF1 0.00 Hz
SPOFF2 0.00 Hz

======== CHANNEL f2 ========
CPDPRG2 waltz16
NUC2 1H
PCPD2 100.00 usec
PL2 1.60 dB
PL12 24.50 dB
SFO2 500.2225011 MHz

====== GRADIENT CHANNEL =====
GPNAM1 SINE.100
GPNAM2 SINE.100
GPX1 0.00 %
GPX2 0.00 %
GPY1 0.00 %
GPY2 0.00 %
GPZ1 30.00 %
GPZ2 50.00 %
p15 500.00 usec
p16 1000.00 usec

F2 - Processing parameters
SI 65536
SF 125.7804282 MHz
WDW EM
SSB 0
LB 1.00 Hz
GB 0
PC 2.00

1D NMR plot parameters
CX 22.80 cm
CY 15.65 cm
F1P 220.000 ppm
F1 27671.69 Hz
F2P -10.000 ppm
F2 -1257.80 Hz
PPMCM 10.08772 ppm/cm
HZCM 1268.83765 Hz/cm

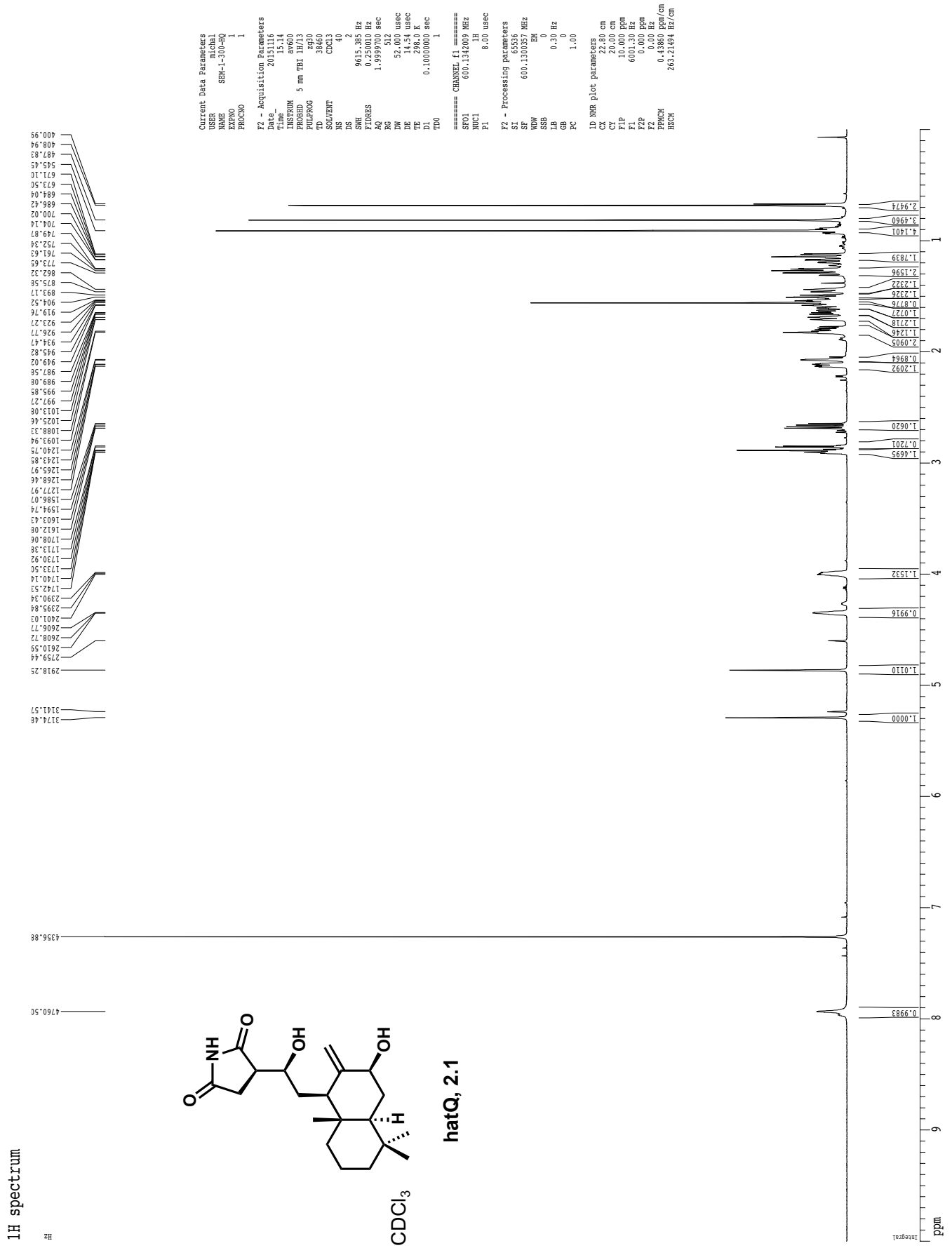
1H spectrum
CDCl3
hatQ, 2.1
Current Data Parameters
F2 - Acquisition Parameters
F2 - Processing parameters
1D NMR plot parameters
ppm

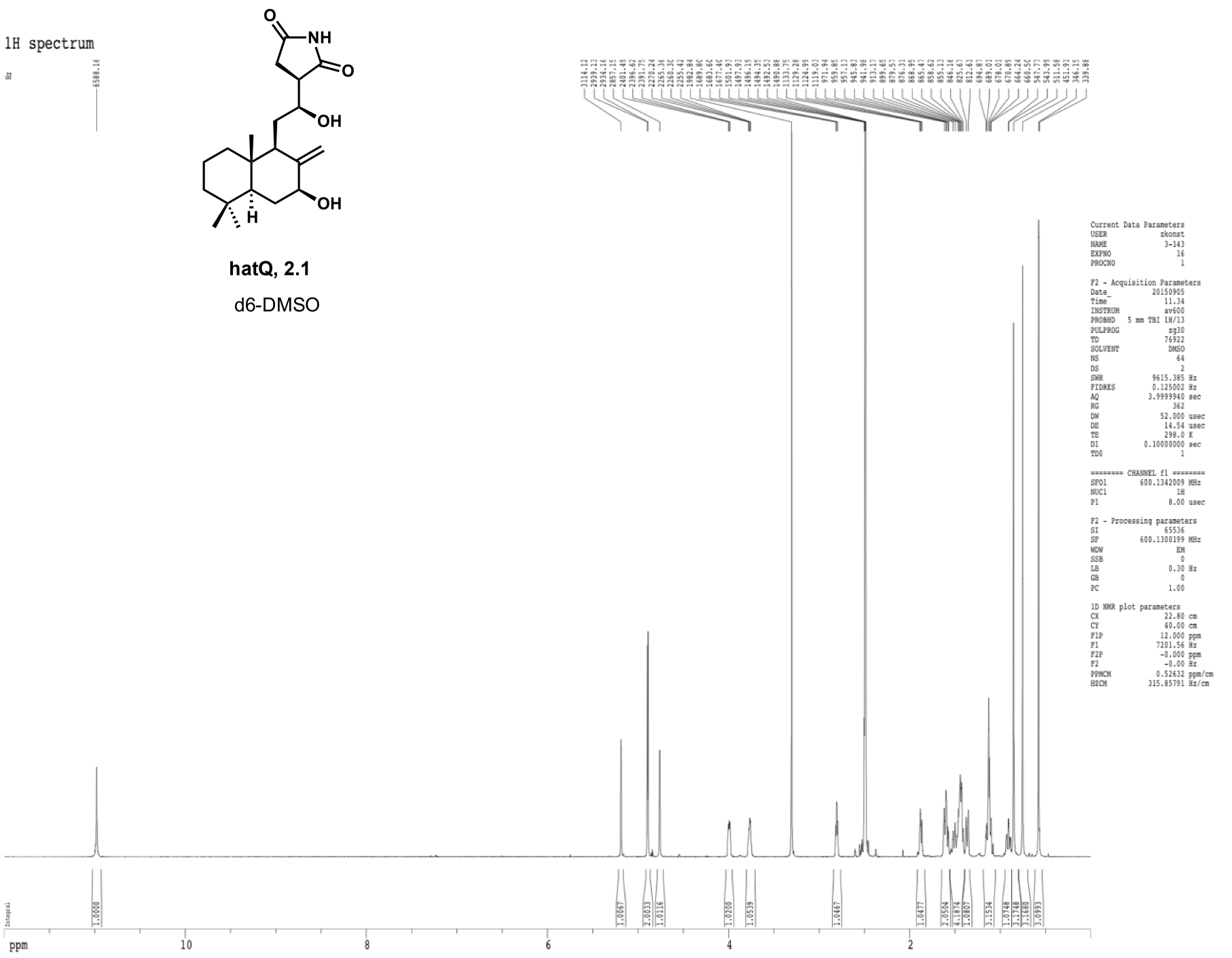
1H spectrum
Hz
6588.14
O
NH
O
OH
OH
H
hatQ, 2.1
d6-DMSO
3114.12
2939.13
2934.16
2857.15
2401.46
2396.62
2391.75
2270.24
2265.38
2260.51
2255.64
1982.84
1689.86
1683.66
1677.46
1501.93
1497.93
1496.35
1494.35
1492.53
1490.88
1133.75
1129.28
1124.99
1119.03
971.94
959.85
957.13
945.83
941.98
913.17
899.65
879.57
876.31
868.95
865.47
858.62
855.13
846.14
825.67
812.61
694.87
689.01
678.01
670.85
664.24
660.56
547.77
543.99
511.58
451.91
346.15
339.88
Current Data Parameters
USER zkonst
NAME 3-143
EXPNO 16
PROCNO 1
F2 - Acquisition Parameters
Date_ 20150905
Time 11.34
INSTRUM av600
PROBHD 5 mm TBI 1H/13
PULPROG zg30
TD 76922
SOLVENT DMSO
NS 64
DS 2
SWH 9615.385 Hz
FIDRES 0.125002 Hz
AQ 3.9999940 sec
RG 362
DW 52.000 usec
DE 14.54 usec
TE 298.0 K
D1 0.10000000 sec
TD0 1
======== CHANNEL f1 ========
SFO1 600.1342009 MHz
NUC1 1H
P1 8.00 usec
F2 - Processing parameters
SI 65536
SF 600.1300199 MHz
WDW EM
SSB 0
LB 0.30 Hz
GB 0
PC 1.00
1D NMR plot parameters
CX 22.80 cm
CY 40.00 cm
F1P 12.000 ppm
F1 7201.56 Hz
F2P -0.000 ppm
F2 -0.00 Hz
PPMCM 0.52632 ppm/cm
HZCM 315.85791 Hz/cm
Integral
1.0000
1.0067
2.0033
1.0116
1.0200
1.0539
1.0467
1.0477
2.0504
4.1874
1.0807
3.1534
1.0748
3.1748
3.1680
3.0993
ppm
10
8
6
4
2

Z-restored spin-echo 13C spectrum with 1H decoupling

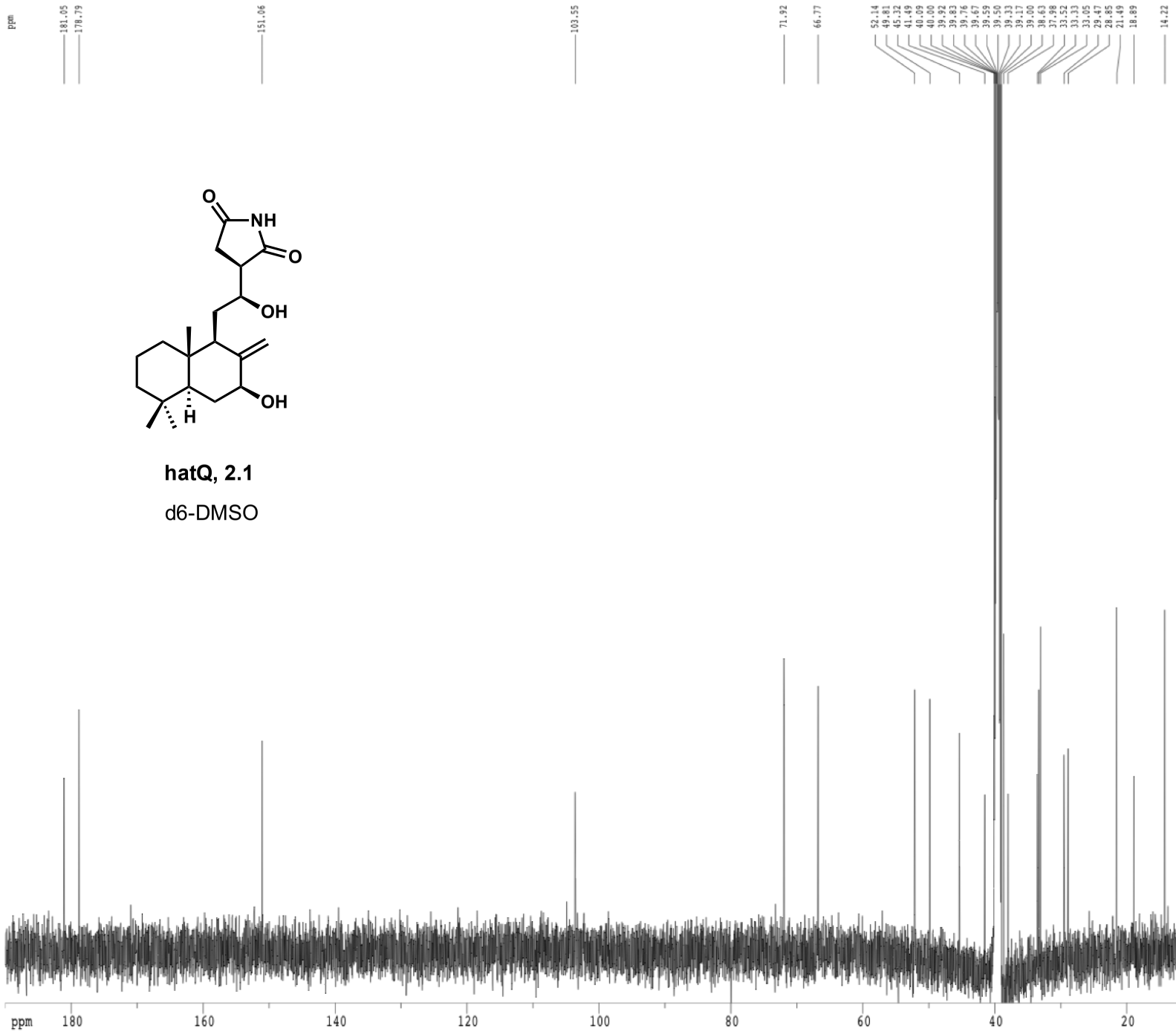

hatQ, 2.1

d6-DMSO

191

```
Current Data Parameters
USER                zkonst
NAME                 3-143
EXPNO                   13
PROCNO                   1

F2 - Acquisition Parameters
Date_             20150903
Time                 16.26
INSTRUM           cryo500
PROBHD   5 mm CPTCI 1H-
PULPROG  SpinEchopg30gp.prd
TD                   65536
SOLVENT               DMSO
NS                     680
DS                      16
SWH             30303.031 Hz
FIDRES          0.462388 Hz
AQ              1.0813940 sec
RG                 7298.2
DW                16.500 usec
DE                 6.00 usec
TE                298.0 K
D1             1.00000000 sec
d11            0.03000000 sec
D16            0.00020000 sec
d17            0.00019600 sec
MCREST         0.00000000 sec
MCWRK          0.01500000 sec
P2                31.00 usec

======== CHANNEL f1 ========
NUC1                   13C
P1                  15.50 usec
P11                500.00 usec
P12               2000.00 usec
PL0                120.00 dB
PL1                 -1.00 dB
SFO1          125.7942548 MHz
SP1                 3.20 dB
SP2                 3.20 dB
SPNAM1    Crp60,0.5,20.1
SPNAM2      Crp60comp.4
SPOFF1                0.00 Hz
SPOFF2                0.00 Hz

======== CHANNEL f2 ========
CPDPRG2           waltz16
NUC2                   1H
PCPD2              100.00 usec
PL2                 1.60 dB
PL12               24.60 dB
SFO2          500.2225011 MHz

====== GRADIENT CHANNEL =====
GPNAM1           SINE.100
GPNAM2           SINE.100
GPX1                  0.00 %
GPX2                  0.00 %
GPY1                  0.00 %
GPY2                  0.00 %
GPZ1                 30.00 %
GPZ2                 50.00 %
p15                500.00 usec
p16               1000.00 usec

F2 - Processing parameters
SI                    65536
SF            125.7804817 MHz
WDW                     EM
SSB                      0
LB                    1.00 Hz
GB                       0
PC                    2.00

1D NMR plot parameters
CX                   22.80 cm
CY                  300.00 cm
F1P                190.000 ppm
F1                23898.29 Hz
F2P                  0.000 ppm
F2                   0.00 Hz
PPMCM              8.33333 ppm/cm
HZCM            1048.17065 Hz/cm
```

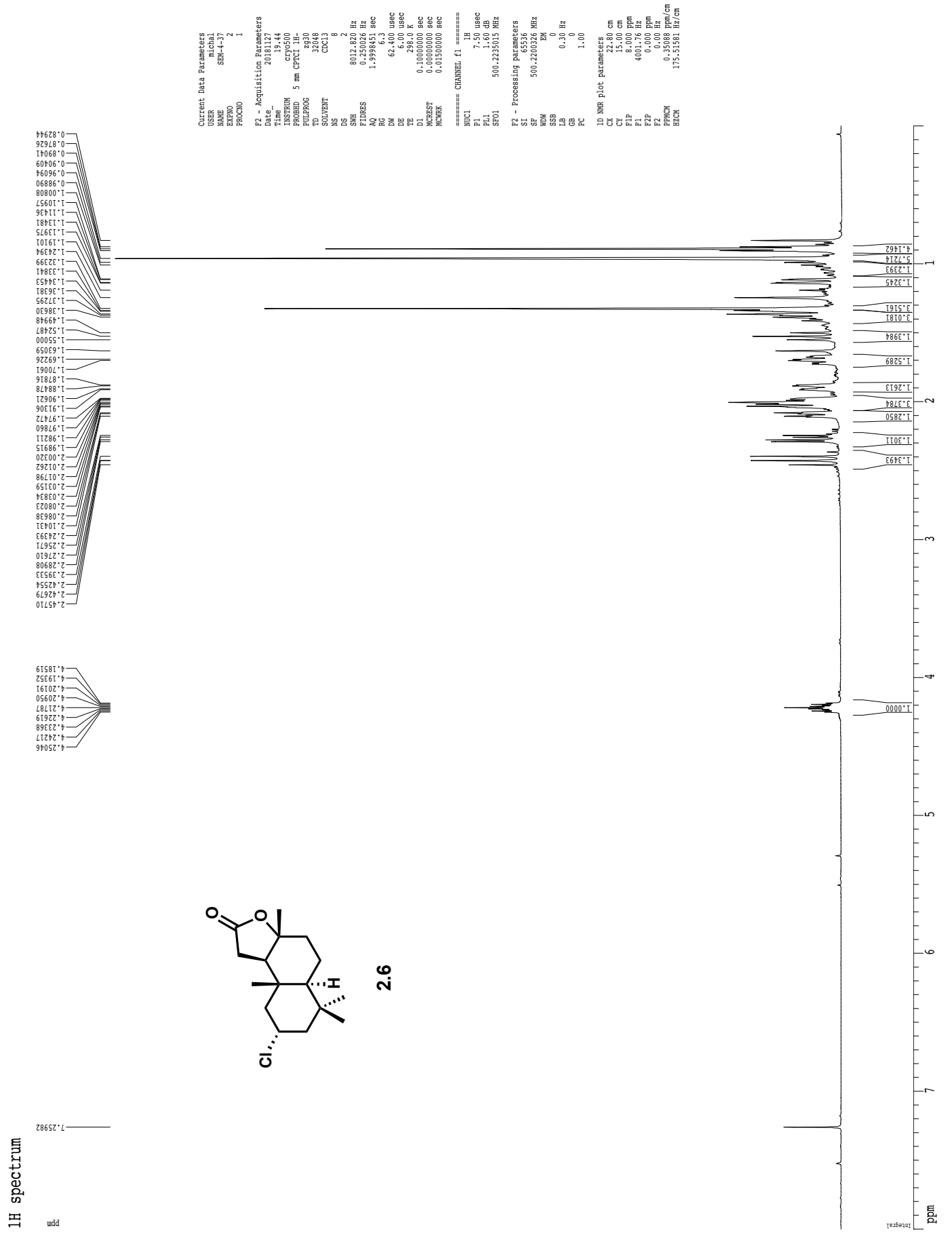
1H spectrum
Current Data Parameters
USER michal
NAME SEM-4-37
EXPNO 2
PROCNO 1
F2 - Acquisition Parameters
Date_ 20181127
Time 19.44
INSTRUM cryo500
PROBHD 5 mm CPTCI 1H-
PULPROG zg30
TD 32048
SOLVENT CDCl3
NS 8
DS 2
SWH 8012.820 Hz
FIDRES 0.250026 Hz
AQ 1.9998451 sec
RG 6.3
DW 62.400 usec
DE 6.00 usec
TE 298.0 K
D1 0.10000000 sec
MCREST 0.00000000 sec
MCWRK 0.01500000 sec
======== CHANNEL f1 ========
NUC1 1H
P1 7.50 usec
PL1 1.60 dB
SFO1 500.2235015 MHz
F2 - Processing parameters
SI 65536
SF 500.2200326 MHz
WDW EM
SSB 0
LB 0.30 Hz
GB 0
PC 1.00
1D NMR plot parameters
CX 22.80 cm
CY 15.00 cm
F1P 8.000 ppm
F1 4001.76 Hz
F2P 0.000 ppm
F2 0.00 Hz
PPMCM 0.35088 ppm/cm
HZCM 175.51581 Hz/cm
2.6
Cl
H
O
O
ppm
Integral

13C spectrum with 1H decoupling

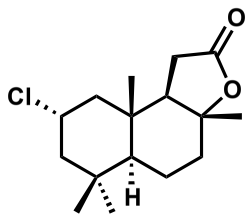

2.6

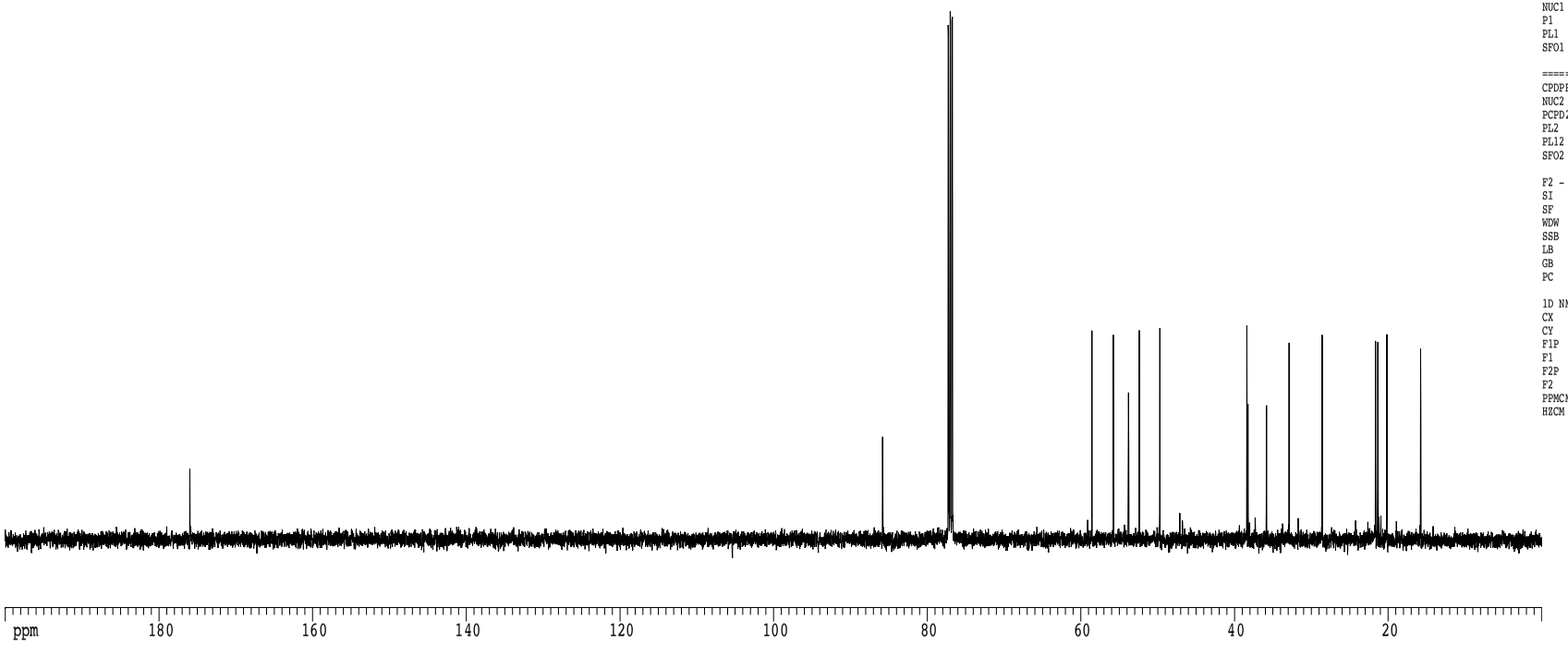


```
Current Data Parameters
USER              michal
NAME                2-39
EXPNO                 26
PROCNO                 1

F2 - Acquisition Parameters
Date_           20140222
Time                0.54
INSTRUM            gn500
PROBHD   5 mm broadband
PULPROG          zgdc30
TD                65536
SOLVENT           CDCl3
NS                  228
DS                    4
SWH           30303.031 Hz
FIDRES        0.462388 Hz
AQ            1.0813940 sec
RG               4597.6
DW               16.500 usec
DE                4.50 usec
TE               298.0 K
D1            0.25000000 sec
d11           0.03000000 sec
MCREST        0.00000000 sec
MCWRK         0.01500000 sec

======== CHANNEL f1 ========
NUC1               13C
P1                7.70 usec
PL1               0.00 dB
SFO1        125.5603801 MHz

======== CHANNEL f2 ========
CPDPRG2         waltz16
NUC2               1H
PCPD2            80.00 usec
PL2              -3.00 dB
PL12              13.20 dB
SFO2        499.2924964 MHz

F2 - Processing parameters
SI                65536
SF          125.5465793 MHz
WDW                  EM
SSB                   0
LB                1.00 Hz
GB                    0
PC                2.00

1D NMR plot parameters
CX                22.80 cm
CY                 8.00 cm
F1P             200.000 ppm
F1             25109.32 Hz
F2P               0.000 ppm
F2                0.00 Hz
PPMCM          8.77193 ppm/cm
HZCM        1101.28577 Hz/cm
```

1H spectrum

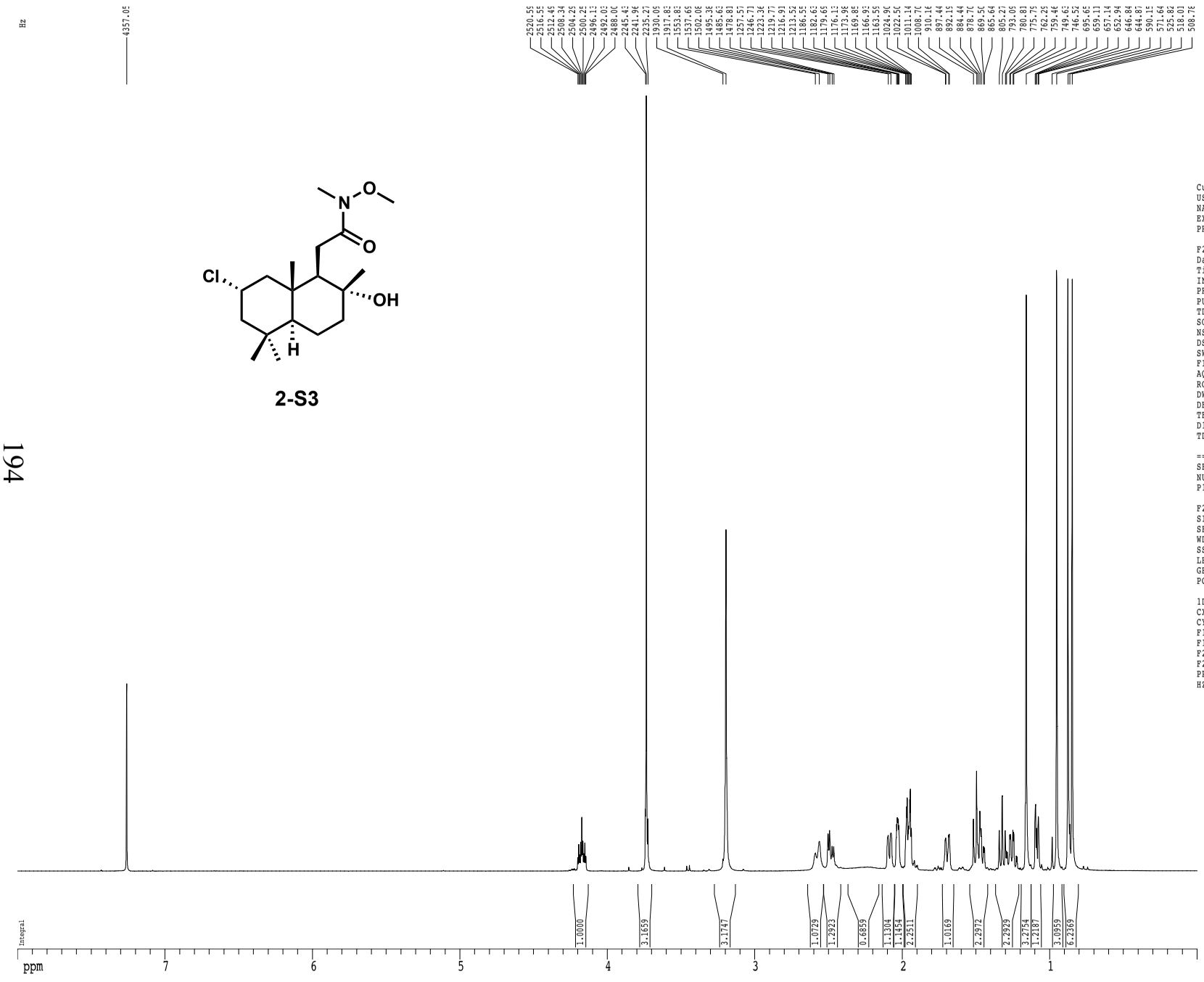
Hz
4357.05
2520.55
2516.55
2512.45
2508.34
2504.25
2500.25
2496.11
2492.03
2488.00
2245.43
2241.96
2235.27
1930.05
1917.83
1553.83
1537.65
1502.08
1495.38
1485.63
1478.81
1257.51
1246.71
1223.36
1219.77
1216.91
1213.52
1186.55
1182.65
1179.65
1176.11
1173.96
1169.88
1166.93
1163.55
1024.90
1022.50
1011.14
1008.70
910.18
897.44
892.15
884.44
878.70
869.50
865.64
805.27
793.05
780.81
775.75
762.26
759.46
749.63
746.52
695.65
659.11
657.14
652.94
646.84
644.87
590.15
571.64
525.82
518.01
508.78
Cl
N
O
O
OH
H
2-S3
Current Data Parameters
USER michal
NAME 2-43
EXPNO 15
PROCNO 1
F2 - Acquisition Parameters
Date_ 20140226
Time 20.57
INSTRUM av600
PROBHD 5 mm TBI 1H/13
PULPROG zg30
TD 57690
SOLVENT CDCl3
NS 16
DS 1
SWH 9615.385 Hz
FIDRES 0.166673 Hz
AQ 2.9999299 sec
RG 161
DW 52.000 usec
DE 14.54 usec
TE 298.0 K
D1 0.10000000 sec
TD0 1
======== CHANNEL f1 ========
SFO1 600.1342009 MHz
NUC1 1H
P1 8.00 usec
F2 - Processing parameters
SI 65536
SF 600.1300351 MHz
WDW EM
SSB 0
LB 0.30 Hz
GB 0
PC 1.00
1D NMR plot parameters
CX 22.80 cm
CY 15.00 cm
F1P 8.000 ppm
F1 4801.04 Hz
F2P 0.000 ppm
F2 0.00 Hz
PPMCM 0.35088 ppm/cm
HZCM 210.57195 Hz/cm
Integral
1.0000
3.1659
3.1747
1.0729
1.2923
0.6859
1.1304
1.1454
2.2511
1.0169
2.2972
2.2929
3.2754
1.2187
3.0959
6.2369
ppm
7
6
5
4
3
2
1

13C spectrum with 1H decoupling

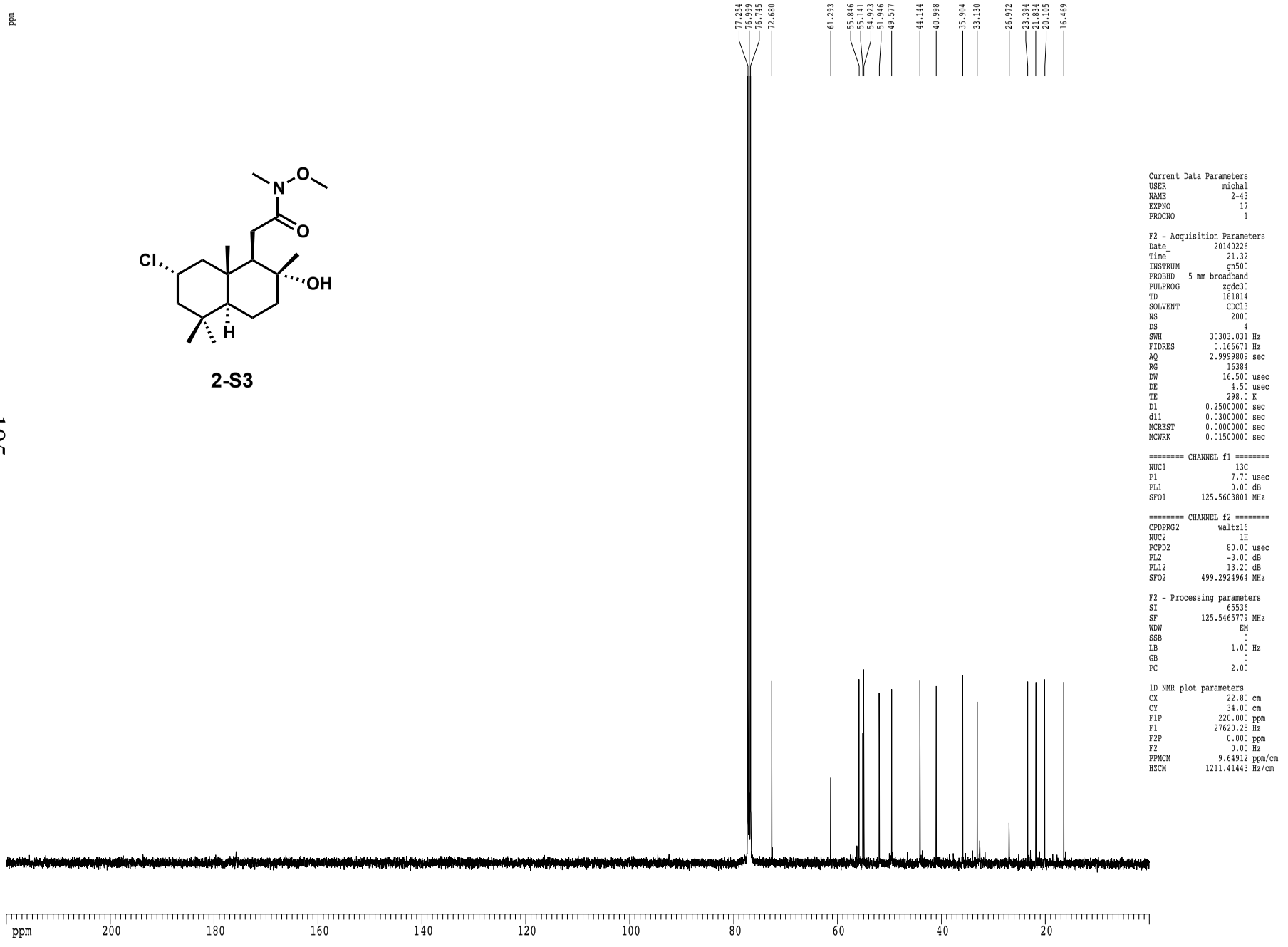

Current Data Parameters
USER michal
NAME 2-43
EXPNO 17
PROCNO 1

F2 - Acquisition Parameters
Date_ 20140226
Time 21.32
INSTRUM gn500
PROBHD 5 mm broadband
PULPROG zgdc30
TD 181814
SOLVENT CDCl3
NS 2000
DS 4
SWH 30303.031 Hz
FIDRES 0.166671 Hz
AQ 2.9999809 sec
RG 16384
DW 16.500 usec
DE 4.50 usec
TE 298.0 K
D1 0.25000000 sec
d11 0.03000000 sec
MCREST 0.00000000 sec
MCWRK 0.01500000 sec

======== CHANNEL f1 ========
NUC1 13C
P1 7.70 usec
PL1 0.00 dB
SFO1 125.5603801 MHz

======== CHANNEL f2 ========
CPDPRG2 waltz16
NUC2 1H
PCPD2 80.00 usec
PL2 -3.00 dB
PL12 13.20 dB
SFO2 499.2924964 MHz

F2 - Processing parameters
SI 65536
SF 125.5465779 MHz
WDW EM
SSB 0
LB 1.00 Hz
GB 0
PC 2.00

1D NMR plot parameters
CX 22.80 cm
CY 34.00 cm
F1P 220.000 ppm
F1 27620.25 Hz
F2P 0.000 ppm
F2 0.00 Hz
PPMCM 9.64912 ppm/cm
HZCM 1211.41443 Hz/cm

1H spectrum

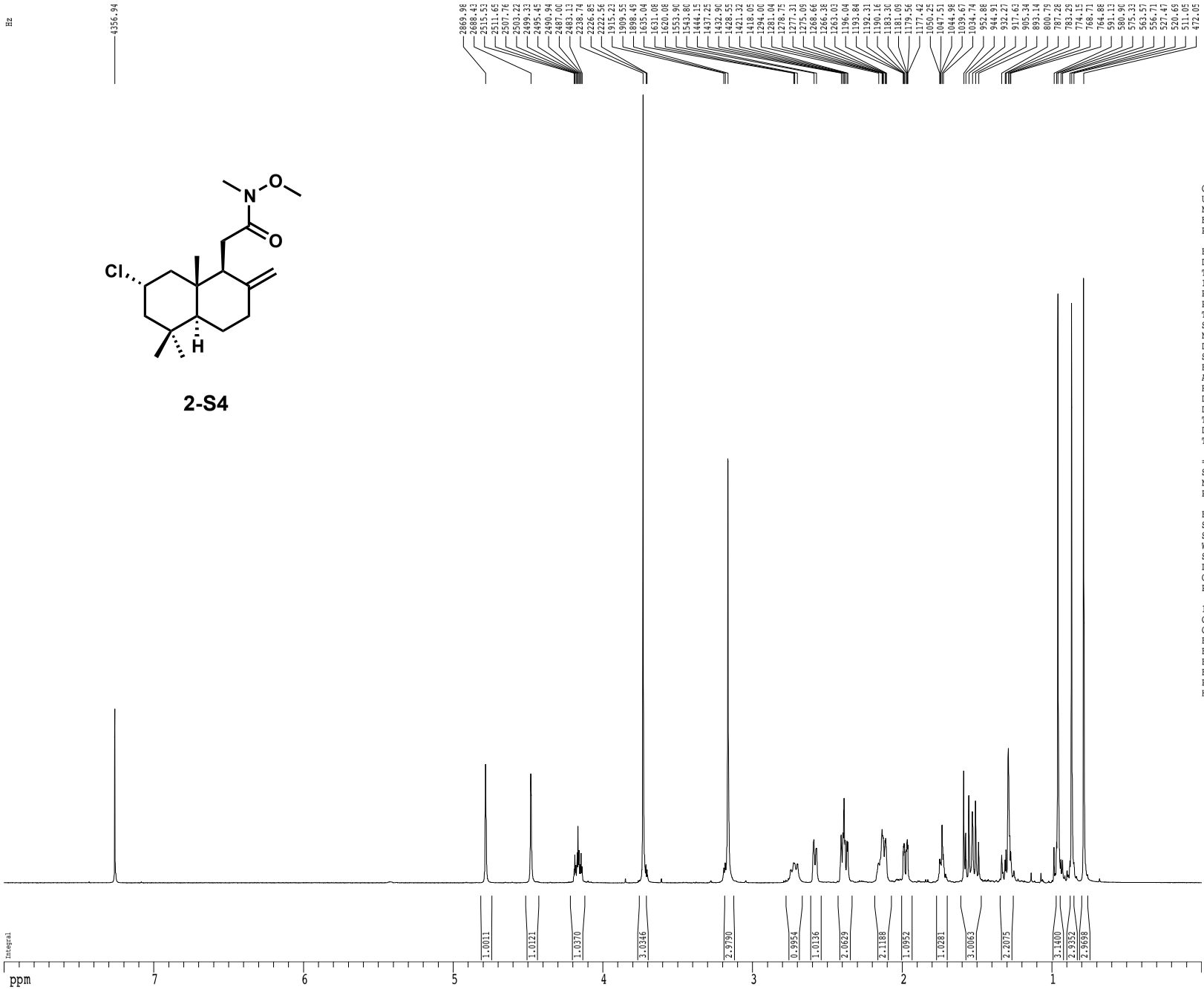
Hz
4356.94
2869.98
2688.43
2515.53
2511.65
2507.76
2503.22
2499.33
2495.45
2491.94
2487.06
2483.13
2230.74
2226.85
2221.56
1913.23
1909.55
1898.49
1635.04
1631.08
1620.08
1553.90
1543.80
1444.15
1437.25
1432.90
1428.55
1421.32
1418.05
1294.00
1281.04
1278.75
1277.31
1275.09
1268.66
1266.38
1263.03
1196.04
1193.84
1192.31
1190.16
1183.30
1181.09
1179.56
1177.42
1050.25
1047.51
1044.98
1039.67
1034.74
952.88
944.91
932.27
917.63
905.34
893.14
800.79
787.28
783.29
774.15
768.71
764.88
591.13
580.90
575.33
563.57
556.71
527.47
520.69
511.05
472.05
Cl
N
O
O
H
2-S4
Current Data Parameters
USER michal
NAME 2-46
EXPNO 11
PROCNO 1
F2 - Acquisition Parameters
Date_ 20140228
Time 18.37
INSTRUM av600
PROBHD 5 mm TBI 1H/13
PULPROG zg30
TD 57690
SOLVENT CDCl3
NS 16
DS 2
SWH 9615.385 Hz
FIDRES 0.166673 Hz
AQ 2.9999299 sec
RG 161
DW 52.000 usec
DE 14.54 usec
TE 298.1 K
D1 0.10000000 sec
TD0 1
======== CHANNEL f1 ========
SFO1 600.1342009 MHz
NUC1 1H
P1 8.00 usec
F2 - Processing parameters
SI 65536
SF 600.1300340 MHz
WDW EM
SSB 0
LB 0.30 Hz
GB 0
PC 1.00
1D NMR plot parameters
CX 22.80 cm
CY 15.00 cm
F1P 8.000 ppm
F1 4801.04 Hz
F2P 0.000 ppm
F2 0.00 Hz
PPMCM 0.35088 ppm/cm
HZCM 210.57195 Hz/cm
Integral
1.0011
1.0121
1.0370
3.0346
2.9790
0.9954
1.0136
2.0629
2.1188
1.0952
1.0281
3.0063
2.2075
3.1400
2.9352
2.9698
ppm
7
6
5
4
3
2
1

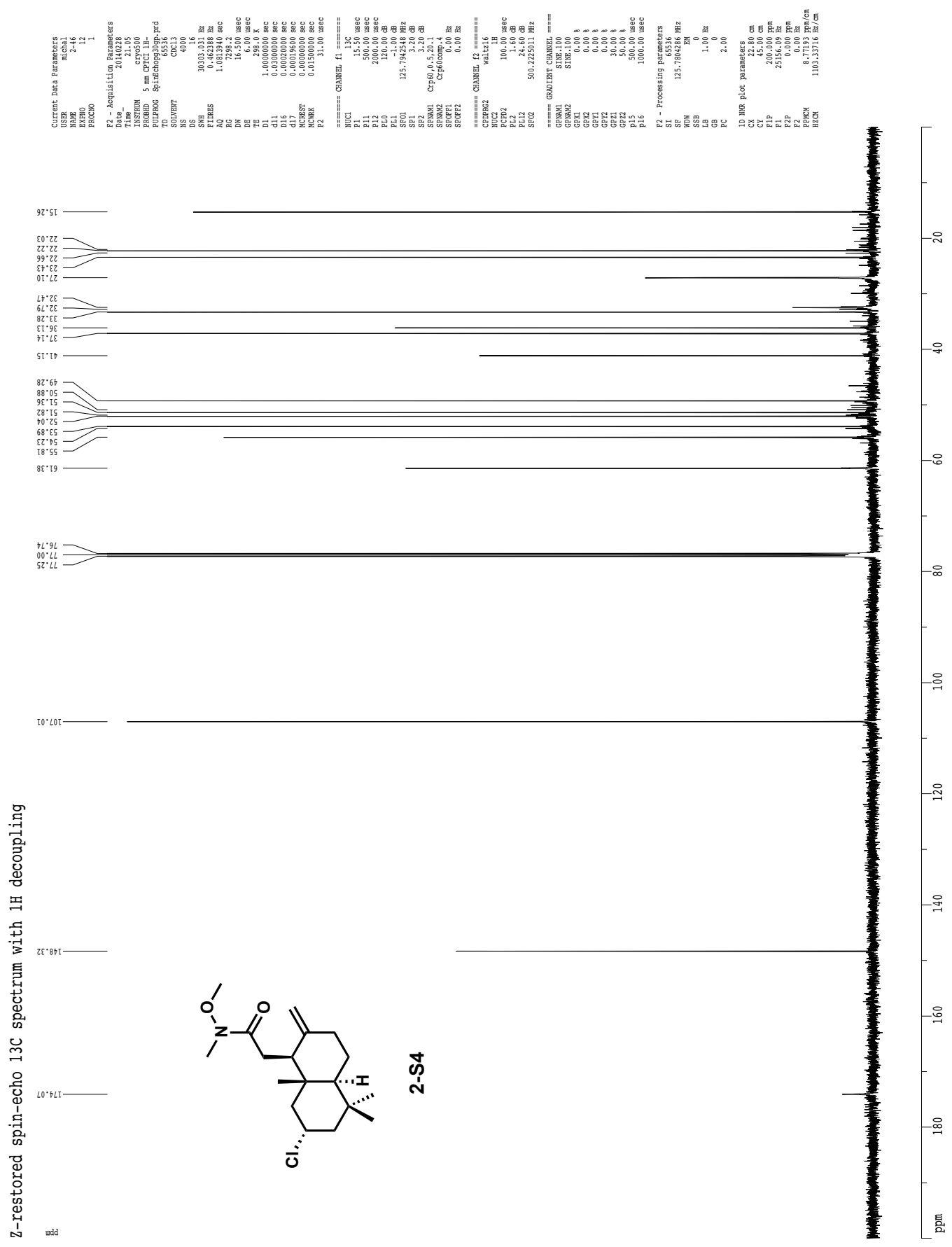
Z-restored spin-echo 13C spectrum with 1H decoupling
2-S4
Cl
H
ppm

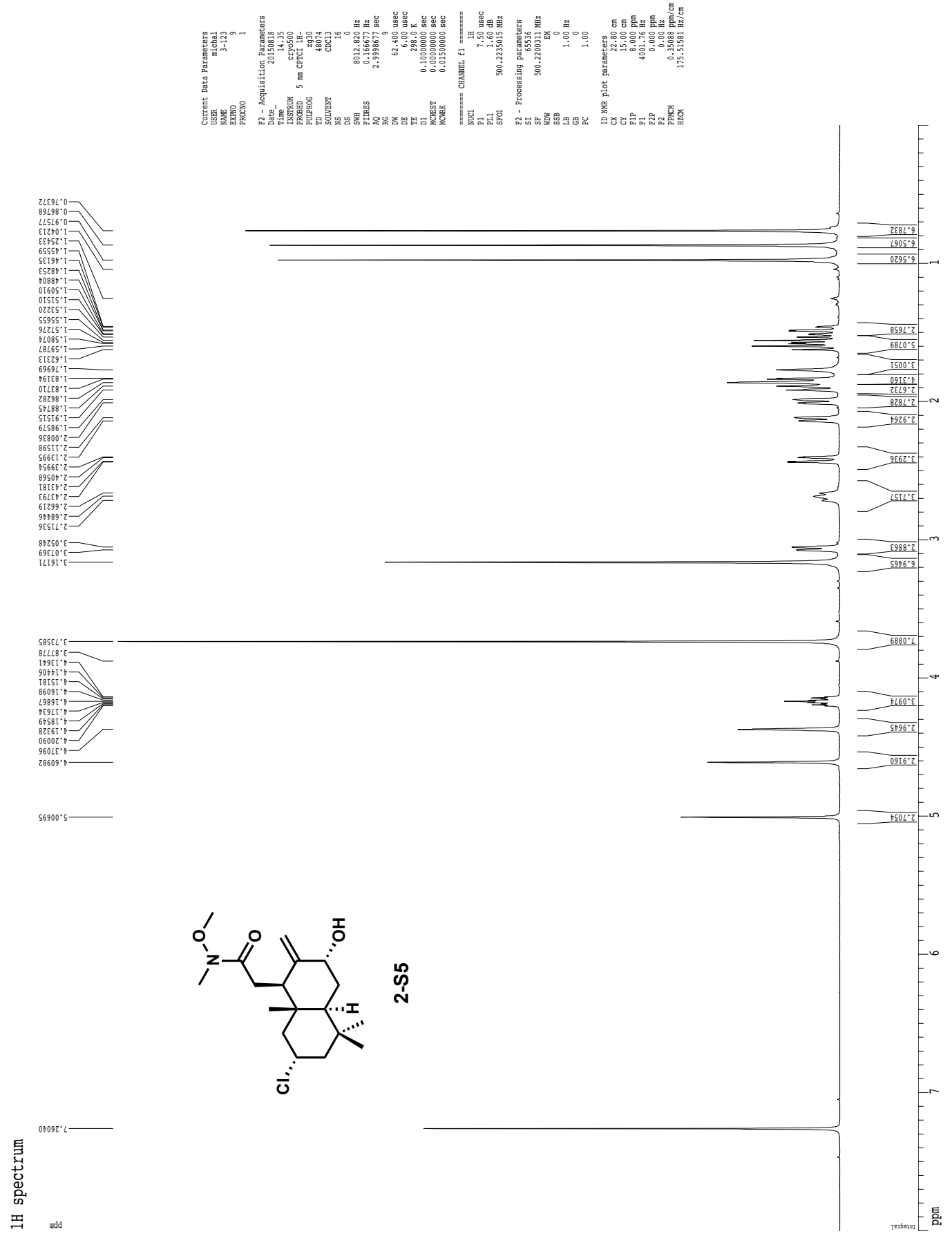
1H spectrum
2-S5
Cl
OH
H
ppm

Z-restored spin-echo 13C spectrum with 1H decoupling

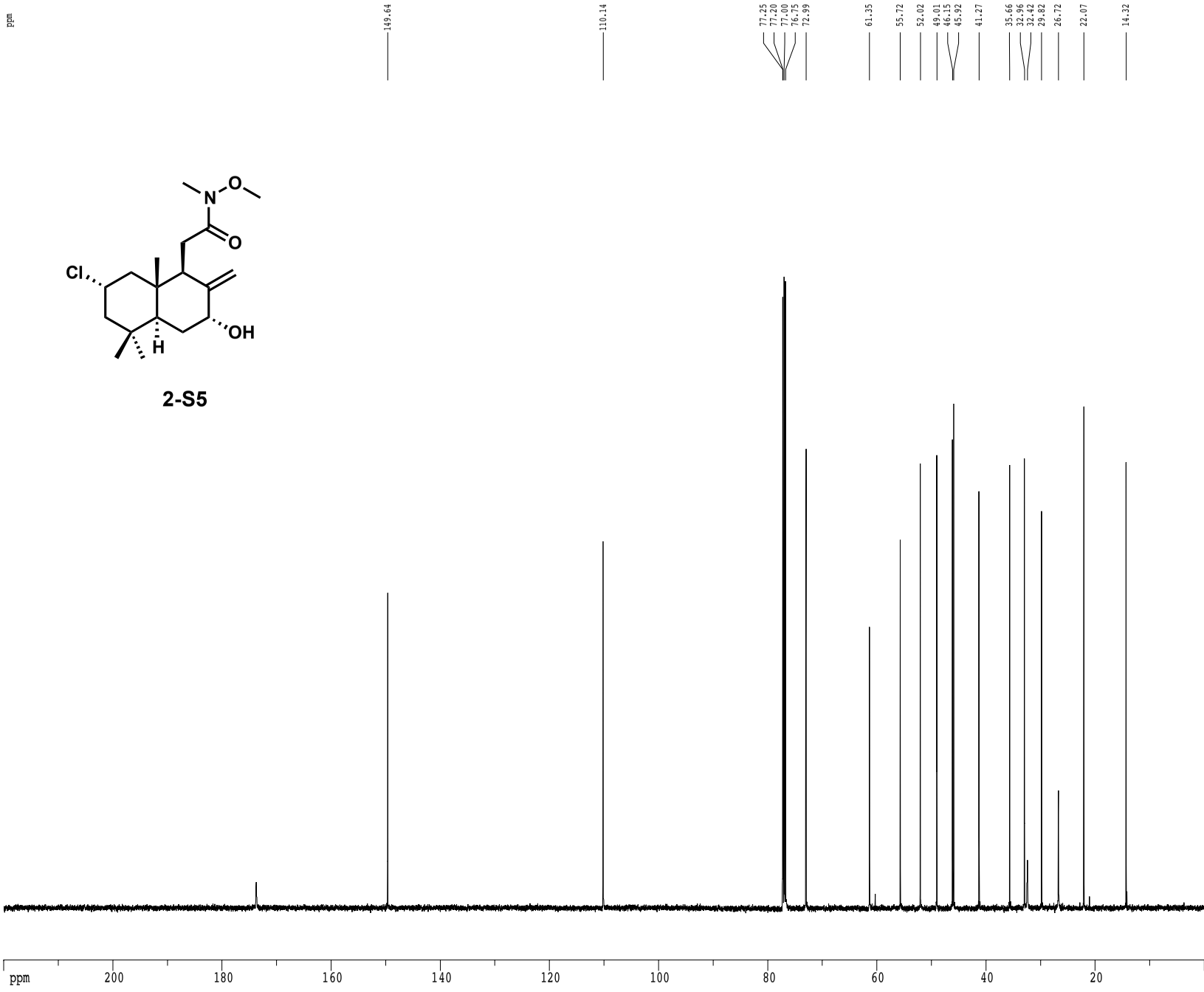

Current Data Parameters
USER michal
NAME 3-123
EXPNO 11
PROCNO 1

F2 - Acquisition Parameters
Date_ 20150905
Time 11.49
INSTRUM cryo500
PROBHD 5 mm CPTCI 1H-
PULPROG SpinEchopg30gp.prd
TD 65536
SOLVENT CDCl3
NS 480
DS 16
SWH 30303.031 Hz
FIDRES 0.462388 Hz
AQ 1.0813940 sec
RG 4096
DW 16.500 usec
DE 6.00 usec
TE 298.0 K
D1 1.50000000 sec
d11 0.03000000 sec
D16 0.00020000 sec
d17 0.00019600 sec
MCREST 0.00000000 sec
MCWRK 0.01500000 sec
P2 31.00 usec

======== CHANNEL f1 ========
NUC1 13C
P1 15.50 usec
P11 500.00 usec
P12 2000.00 usec
PL0 120.00 dB
PL1 -1.00 dB
SFO1 125.7942548 MHz
SP1 3.20 dB
SP2 3.20 dB
SPNAM1 Crp60,0.5,20.1
SPNAM2 Crp60comp.4
SPOFF1 0.00 Hz
SPOFF2 0.00 Hz

======== CHANNEL f2 ========
CPDPRG2 waltz16
NUC2 1H
PCPD2 100.00 usec
PL2 1.60 dB
PL12 24.60 dB
SFO2 500.2225011 MHz

====== GRADIENT CHANNEL =====
GPNAM1 SINE.100
GPNAM2 SINE.100
GPX1 0.00 %
GPX2 0.00 %
GPY1 0.00 %
GPY2 0.00 %
GPZ1 30.00 %
GPZ2 50.00 %
p15 500.00 usec
p16 1000.00 usec

F2 - Processing parameters
SI 65536
SF 125.7804314 MHz
WDW EM
SSB 0
LB 1.00 Hz
GB 0
PC 2.00

1D NMR plot parameters
CX 22.80 cm
CY 12.00 cm
F1P 220.000 ppm
F1 27671.70 Hz
F2P 0.000 ppm
F2 0.00 Hz
PPMCM 9.64912 ppm/cm
HZCM 1213.67090 Hz/cm

1H spectrum

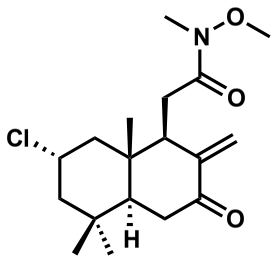

2-S6

Current Data Parameters
USER michal
NAME SEM-1-266-pr
EXPNO 1
PROCNO 1

F2 - Acquisition Parameters
Date_ 20150721
Time 18.18
INSTRUM av600
PROBHD 5 mm BBO BB-1H
PULPROG zg30
TD 38460
SOLVENT CDCl3
NS 16
DS 2
SWH 9615.385 Hz
FIDRES 0.250010 Hz
AQ 1.9999700 sec
RG 161
DW 52.000 usec
DE 14.33 usec
TE 298.6 K
D1 0.10000000 sec
TD0 1

======== CHANNEL f1 ========
SFO1 600.1342009 MHz
NUC1 1H
P1 9.00 usec

F2 - Processing parameters
SI 65536
SF 600.1300345 MHz
WDW EM
SSB 0
LB 0.30 Hz
GB 0
PC 1.00

1D NMR plot parameters
CX 22.80 cm
CY 15.00 cm
F1P 8.000 ppm
F1 4801.04 Hz
F2P 0.000 ppm
F2 0.00 Hz
PPMCM 0.35088 ppm/cm
HZCM 210.57195 Hz/cm

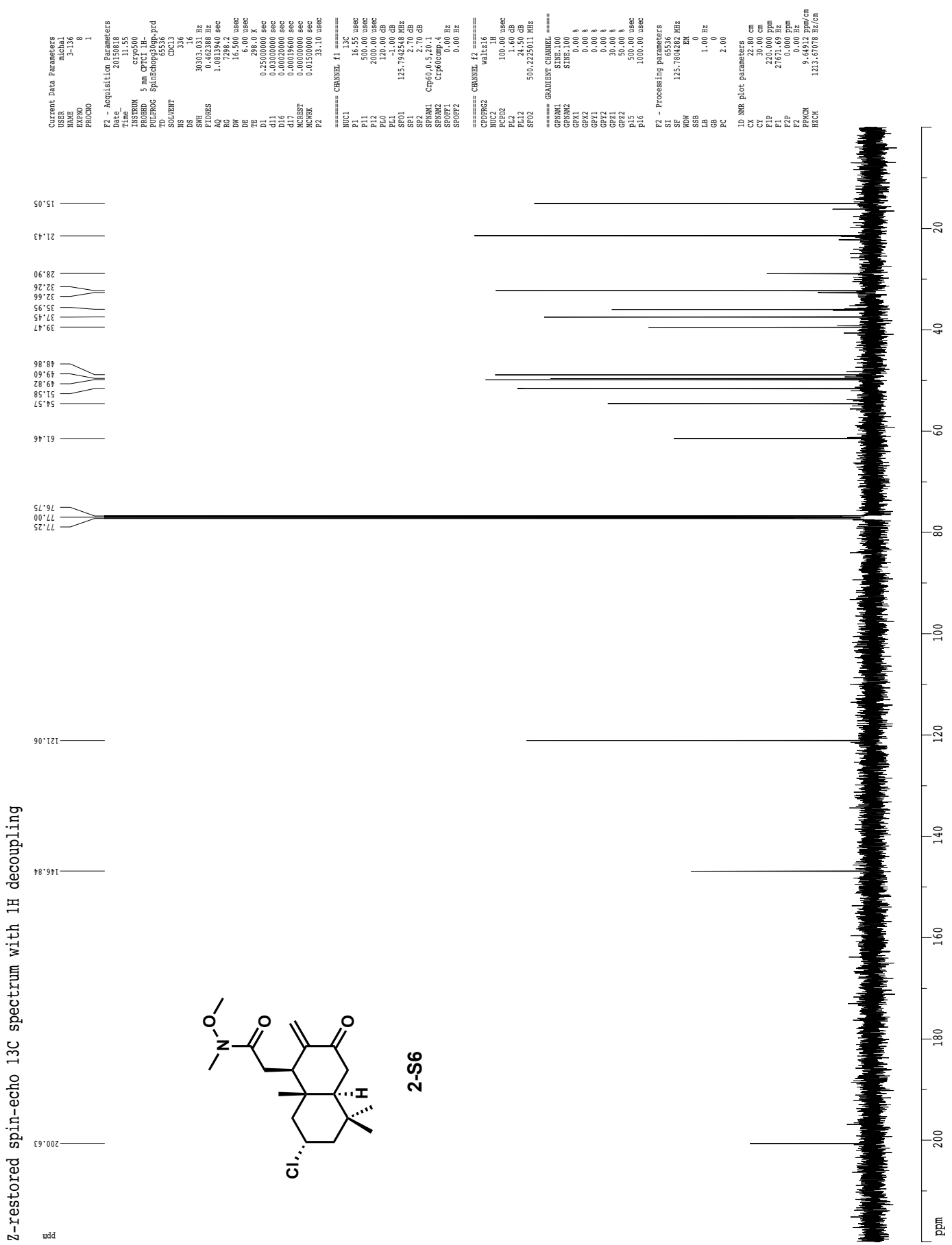
Z-restored spin-echo 13C spectrum with 1H decoupling
2-S6
Cl
H
O
N
ppm

1H spectrum

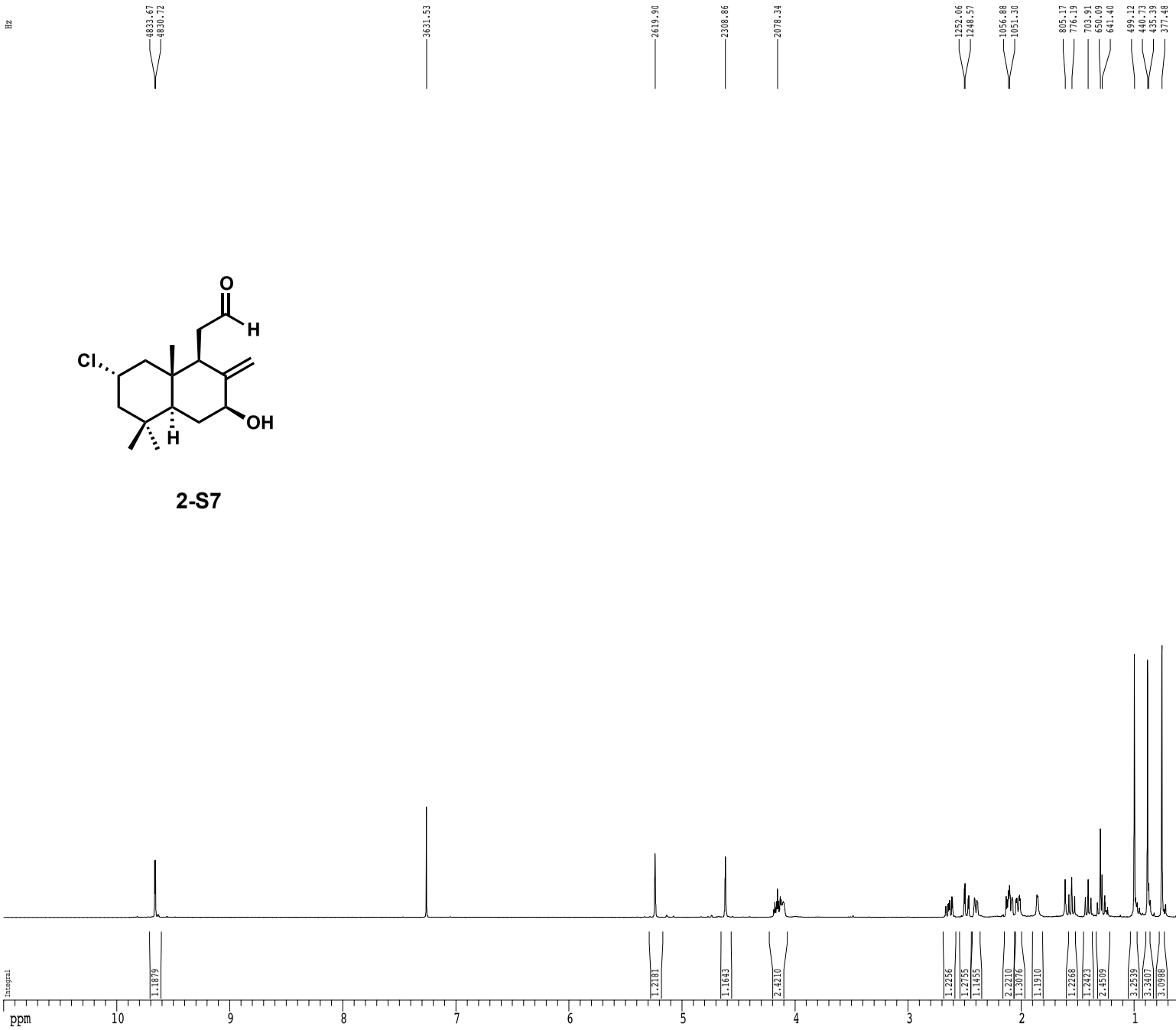

2-S7

Current Data Parameters
USER michal
NAME 3-137
EXPNO 17
PROCNO 1

F2 - Acquisition Parameters
Date_ 20150819
Time 13.44
INSTRUM cryo500
PROBHD 5 mm CPTCI 1H-
PULPROG zg30
TD 48074
SOLVENT CDCl3
NS 16
DS 0
SWH 8012.820 Hz
FIDRES 0.166677 Hz
AQ 2.9998677 sec
RG 8
DW 62.400 usec
DE 6.00 usec
TE 298.0 K
D1 0.10000000 sec
MCREST 0.00000000 sec
MCWRK 0.01500000 sec

======== CHANNEL f1 ========
NUC1 1H
P1 7.50 usec
PL1 1.60 dB
SFO1 500.2235015 MHz

F2 - Processing parameters
SI 65536
SF 500.2200312 MHz
WDW EM
SSB 0
LB 0.30 Hz
GB 0
PC 4.00

1D NMR plot parameters
CX 22.80 cm
CY 5.00 cm
F1P 11.000 ppm
F1 5502.42 Hz
F2P 0.000 ppm
F2 0.00 Hz
PPMCM 0.48246 ppm/cm
HZCM 241.33423 Hz/cm

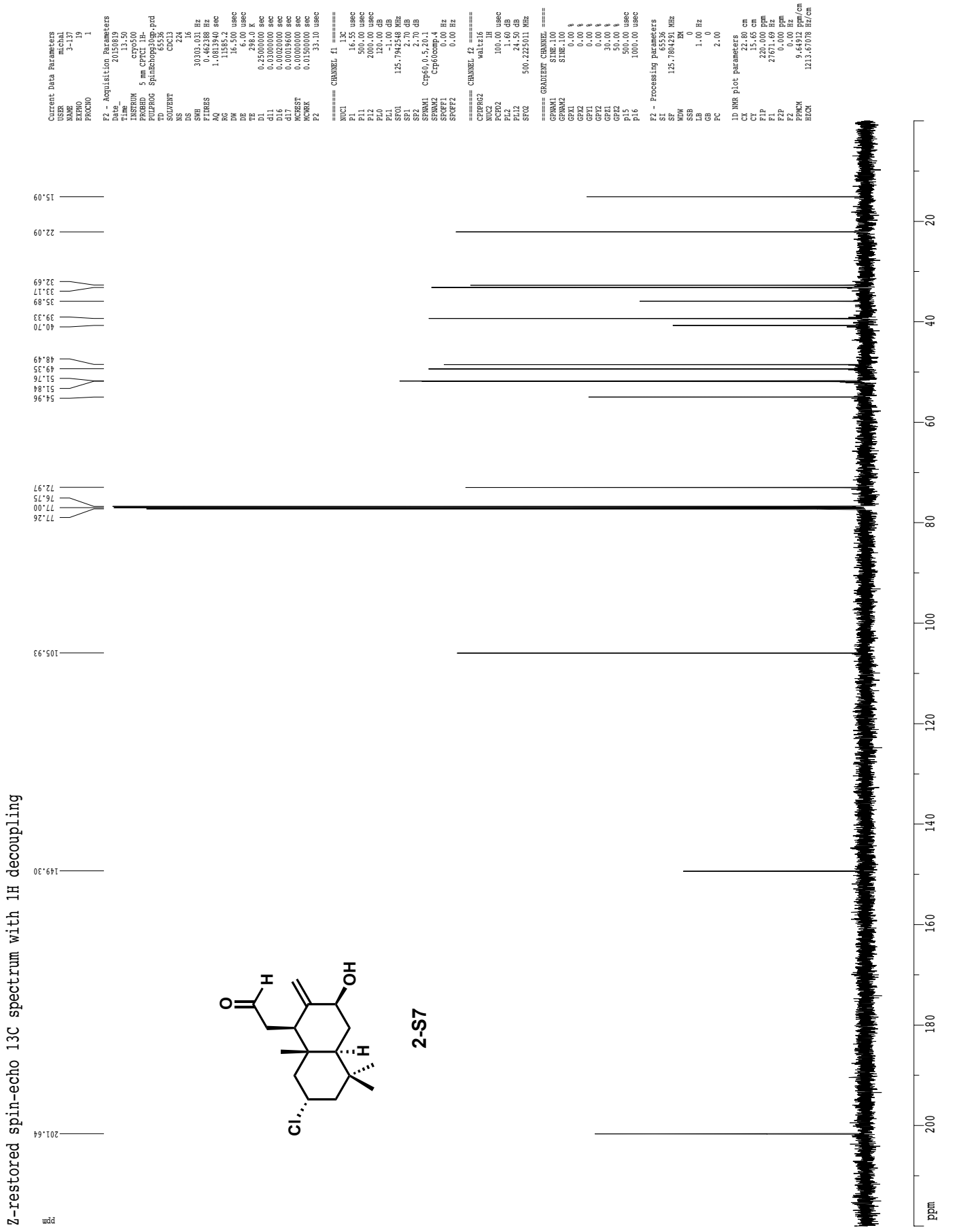
Z-restored spin-echo 13C spectrum with 1H decoupling
ppm
Current Data Parameters
USER michal
NAME 3-137
EXPNO 19
PROCNO 1
F2 - Acquisition Parameters
Date_ 20150819
Time 13:50
INSTRUM cryo500
PROBHD 5 mm CPTCI 1H-
PULPROG spinEchoDec13gp.ppd
TD 65536
SOLVENT CDCl3
NS 224
DS 16
SWH 30303.031 Hz
FIDRES 0.462388 Hz
AQ 1.0813940 sec
RG 11585.2
DW 16.500 usec
DE 6.00 usec
TE 298.0 K
D1 0.25000000 sec
d11 0.03000000 sec
D16 0.00020000 sec
d17 0.00019600 sec
MCREST 0.00000000 sec
MCWRK 0.01500000 sec
P2 33.10 usec
======== CHANNEL f1 ========
NUC1 13C
P1 16.55 usec
P11 500.00 usec
P12 2000.00 usec
PL1 1.00 dB
PL11 121.00 dB
SFO1 125.7942548 MHz
SF1 2.70 dB
SF2 2.70 dB
SPNAM1 Crp60,0.5,20.1
SPNAM2 Crp60comp.4
SFOFF1 0.00 Hz
SFOFF2 0.00 Hz
======== CHANNEL f2 ========
CPDPRG2 waltz16
NUC2 1H
PCPD2 100.00 usec
PL2 1.60 dB
PL12 24.50 dB
SFO2 500.2225011 MHz
===== GRADIENT CHANNEL =====
GPNAM1 SINE.100
GPNAM2 SINE.100
GPX1 0.00 %
GPX2 0.00 %
GPY1 0.00 %
GPY2 0.00 %
GPZ1 30.00 %
GPZ2 50.00 %
p15 500.00 usec
p16 1000.00 usec
F2 - Processing parameters
SI 65536
SF 125.7804291 MHz
WDW EM
SSB 0
LB 1.00 Hz
GB 0
PC 2.00
1D NMR plot parameters
CX 22.80 cm
CY 15.65 cm
F1P 220.000 ppm
F1 27671.69 Hz
F2P 0.000 ppm
F2 0.00 Hz
PPMCM 9.64912 ppm/cm
HZCM 1213.67078 Hz/cm
15.09
22.09
32.69
33.17
35.89
39.33
40.70
48.49
49.35
51.76
51.84
54.96
72.97
76.75
77.00
77.26
105.93
149.30
201.64
ppm
O
H
OH
H
Cl
2-S7

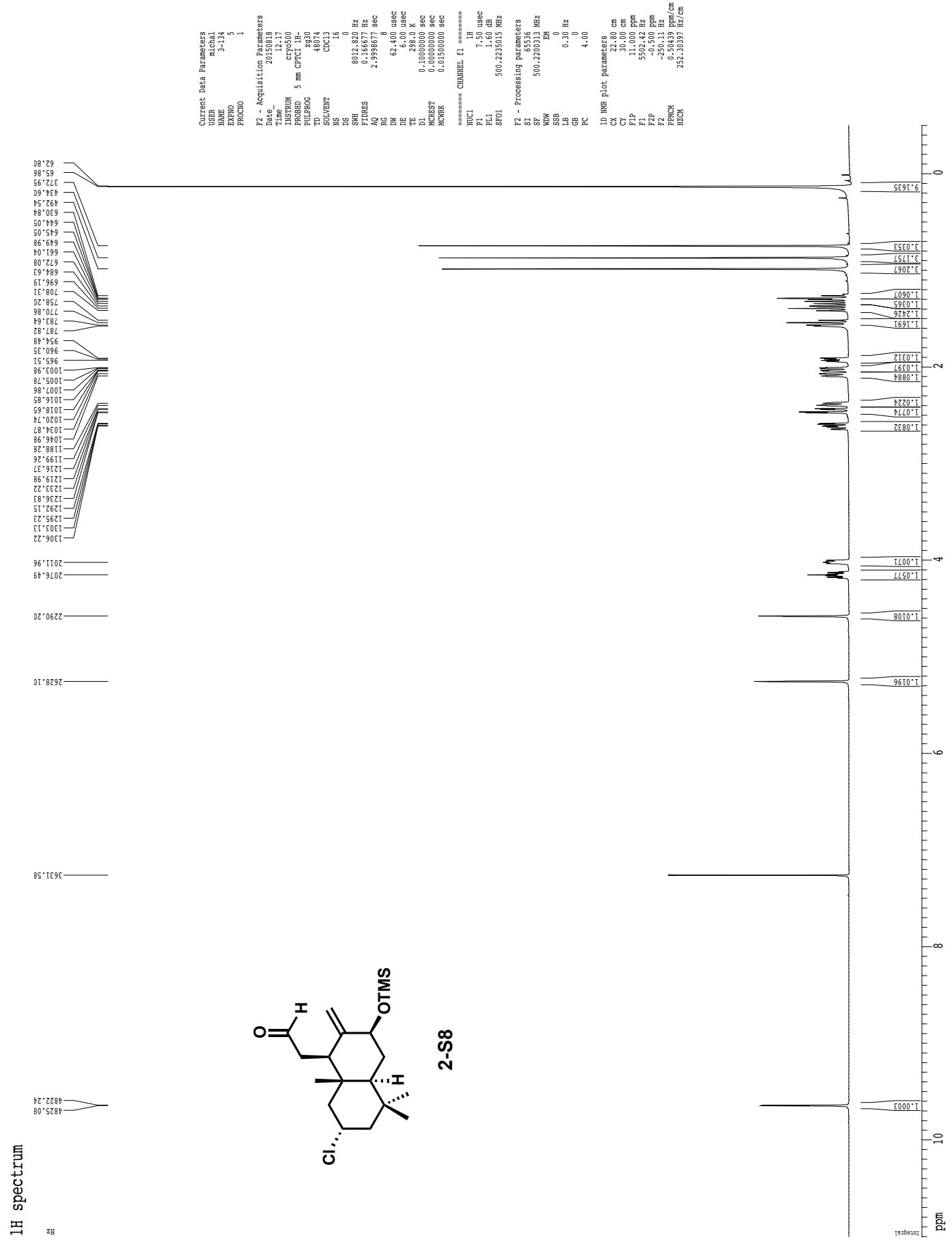
1H spectrum
Current Data Parameters
USER michai
NAME 3-134
EXPNO 5
PROCNO 1
F2 - Acquisition Parameters
Date_ 20150818
Time 12.17
INSTRUM cryo500
PROBHD 5 mm CPTCI 1H-
PULPROG zg30
TD 48074
SOLVENT CDCl3
NS 16
DS 0
SWH 8012.820 Hz
FIDRES 0.166677 Hz
AQ 2.9998677 sec
RG 8
DW 62.400 usec
DE 6.00 usec
TE 298.0 K
D1 0.10000000 sec
MCREST 0.00000000 sec
MCWRK 0.01500000 sec
======== CHANNEL f1 ========
NUC1 1H
P1 7.50 usec
PL1 1.60 dB
SFO1 500.2235015 MHz
F2 - Processing parameters
SI 65536
SF 500.2200313 MHz
WDW EM
SSB 0
LB 0.30 Hz
GB 0
PC 4.00
1D NMR plot parameters
CX 22.00 cm
CY 30.00 cm
F1P 11.000 ppm
F1 5502.42 Hz
F2P -0.500 ppm
F2 -250.11 Hz
PPMCM 0.50439 ppm/cm
HZCM 252.30397 Hz/cm
62.80
65.86
372.95
434.60
492.54
630.84
644.05
645.05
649.98
661.04
672.08
684.63
696.19
708.31
758.20
770.86
783.64
787.82
954.48
960.35
965.51
1003.98
1005.78
1007.86
1016.85
1018.65
1020.74
1034.87
1046.98
1188.28
1199.26
1216.37
1219.98
1233.22
1236.83
1292.15
1295.23
1303.13
1306.22
2011.96
2076.49
2290.20
2628.10
3631.58
4825.08
4822.24
9.1635
3.0353
3.1757
3.2067
1.0607
1.0365
1.2426
1.1691
1.0312
1.0397
1.0884
1.0224
1.0774
1.0832
1.0071
1.0577
1.0108
1.0196
1.0003
Integral
ppm
Hz
O
H
OTMS
H
Cl
2-S8

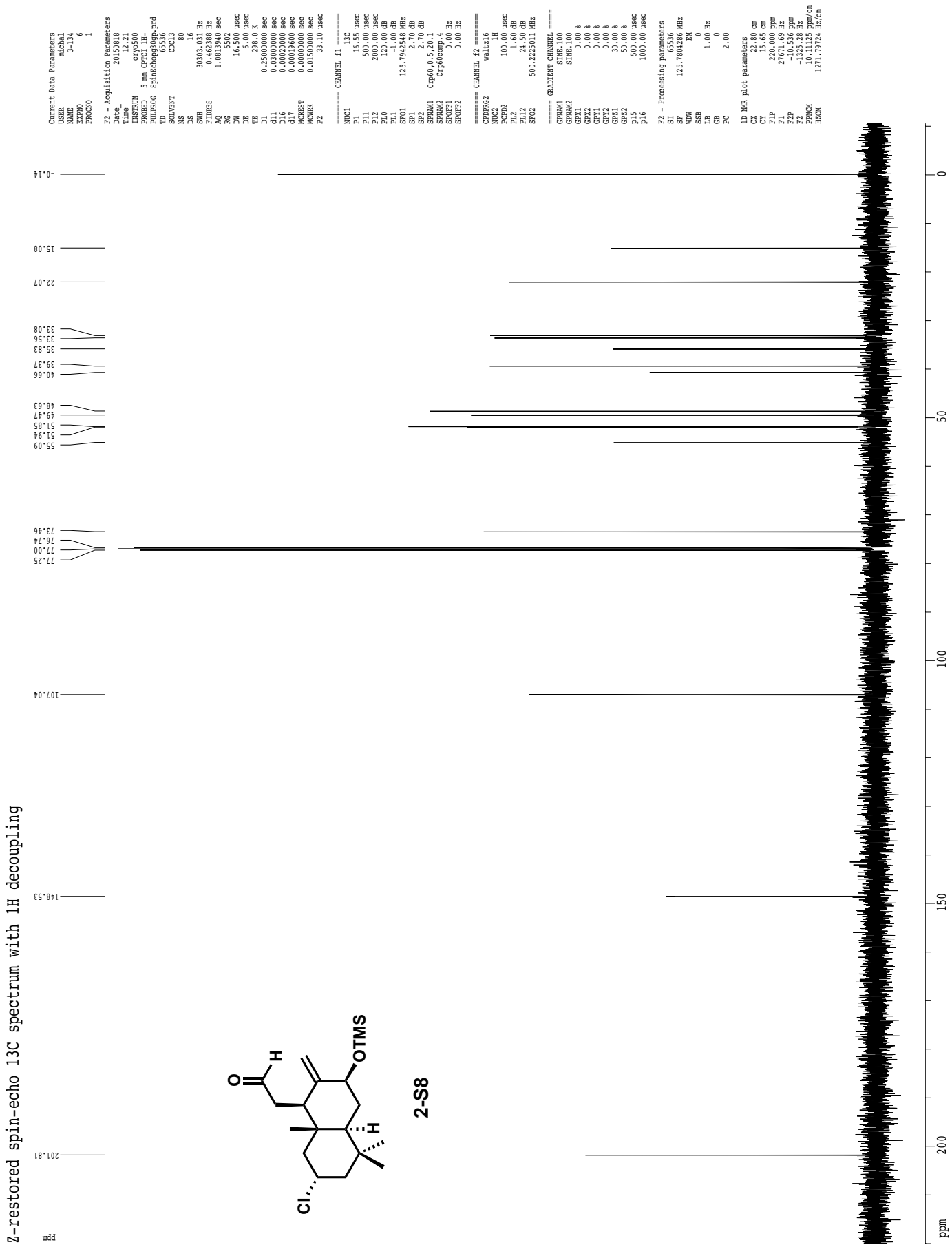
Z-restored spin-echo 13C spectrum with 1H decoupling
ppm
201.81
148.53
107.04
77.25
76.74
77.00
73.46
55.09
51.94
51.85
49.47
48.63
40.66
39.37
35.83
33.56
33.08
22.07
15.08
-0.14
Current Data Parameters
USER michal
NAME 3-134
EXPNO 6
PROCNO 1
F2 - Acquisition Parameters
Date_ 20150818
Time 12.21
INSTRUM cryo500
PROBHD 5 mm CPTCI 1H-
PULPROG SpinEchopg30gp.prd
TD 65536
SOLVENT CDCl3
NS 80
DS 16
SWH 30303.031 Hz
FIDRES 0.462388 Hz
AQ 1.0813940 sec
RG 6502
DW 16.500 usec
DE 6.00 usec
TE 298.0 K
D1 0.25000000 sec
D11 0.03000000 sec
D16 0.00020000 sec
d17 0.00019600 sec
MCREST 0.00000000 sec
MCWRK 0.01500000 sec
P2 33.10 usec
======== CHANNEL f1 ========
NUC1 13C
P1 16.55 usec
P11 500.00 usec
P12 2000.00 usec
PL0 120.00 dB
PL1 -1.00 dB
SFO1 125.7942548 MHz
SP1 2.70 dB
SP2 2.70 dB
SPNAM1 Crp60,0.5,20.1
SPNAM2 Crp60comp.4
SPOFF1 0.00 Hz
SPOFF2 0.00 Hz
======== CHANNEL f2 ========
CPDPRG2 waltz16
NUC2 1H
PCPD2 100.00 usec
PL2 1.60 dB
PL12 24.50 dB
SFO2 500.2225011 MHz
====== GRADIENT CHANNEL ====
GPNAM1 SINE.100
GPNAM2 SINE.100
GPX1 0.00 %
GPX2 0.00 %
GPY1 0.00 %
GPY2 0.00 %
GPZ1 30.00 %
GPZ2 50.00 %
P15 500.00 usec
P16 1000.00 usec
F2 - Processing parameters
SI 65536
SF 125.7604286 MHz
WDW EM
SSB 0
LB 1.00 Hz
GB 0
PC 2.00
1D NMR plot parameters
CX 22.80 cm
CY 15.65 cm
F1P 220.000 ppm
F1 27671.69 Hz
F2P -10.536 ppm
F2 -1325.28 Hz
PPMCM 10.11125 ppm/cm
HZCM 1271.79724 Hz/cm
ppm
200
150
100
50
0
O
H
OTMS
H
Cl
2-S8

1H spectrum

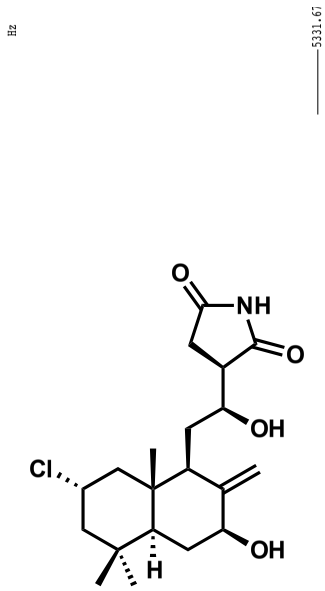

CL, 2.15

Current Data Parameters
USER michal
NAME 3-141
EXPNO 10
PROCNO 1

F2 - Acquisition Parameters
Date_ 20150903
Time 9.06
INSTRUM av600
PROBHD 5 mm TBI 1H/13
PULPROG zg30
TD 57690
SOLVENT CDCl3
NS 16
DS 2
SWH 9615.385 Hz
FIDRES 0.166673 Hz
AQ 2.9999299 sec
RG 256
DW 52.000 usec
DE 14.54 usec
TE 298.0 K
D1 0.10000000 sec
TD0 1

======== CHANNEL f1 ========
SFO1 600.1342009 MHz
NUC1 1H
P1 8.00 usec

F2 - Processing parameters
SI 65536
SF 600.1300357 MHz
WDW EM
SSB 0
LB 0.30 Hz
GB 0
PC 1.00

1D NMR plot parameters
CX 22.80 cm
CY 15.00 cm
F1P 11.000 ppm
F1 6601.43 Hz
F2P 0.000 ppm
F2 0.00 Hz
PPMCM 0.48246 ppm/cm
HZCM 289.53644 Hz/cm

Z-restored spin-echo 13C spectrum with 1H decoupling

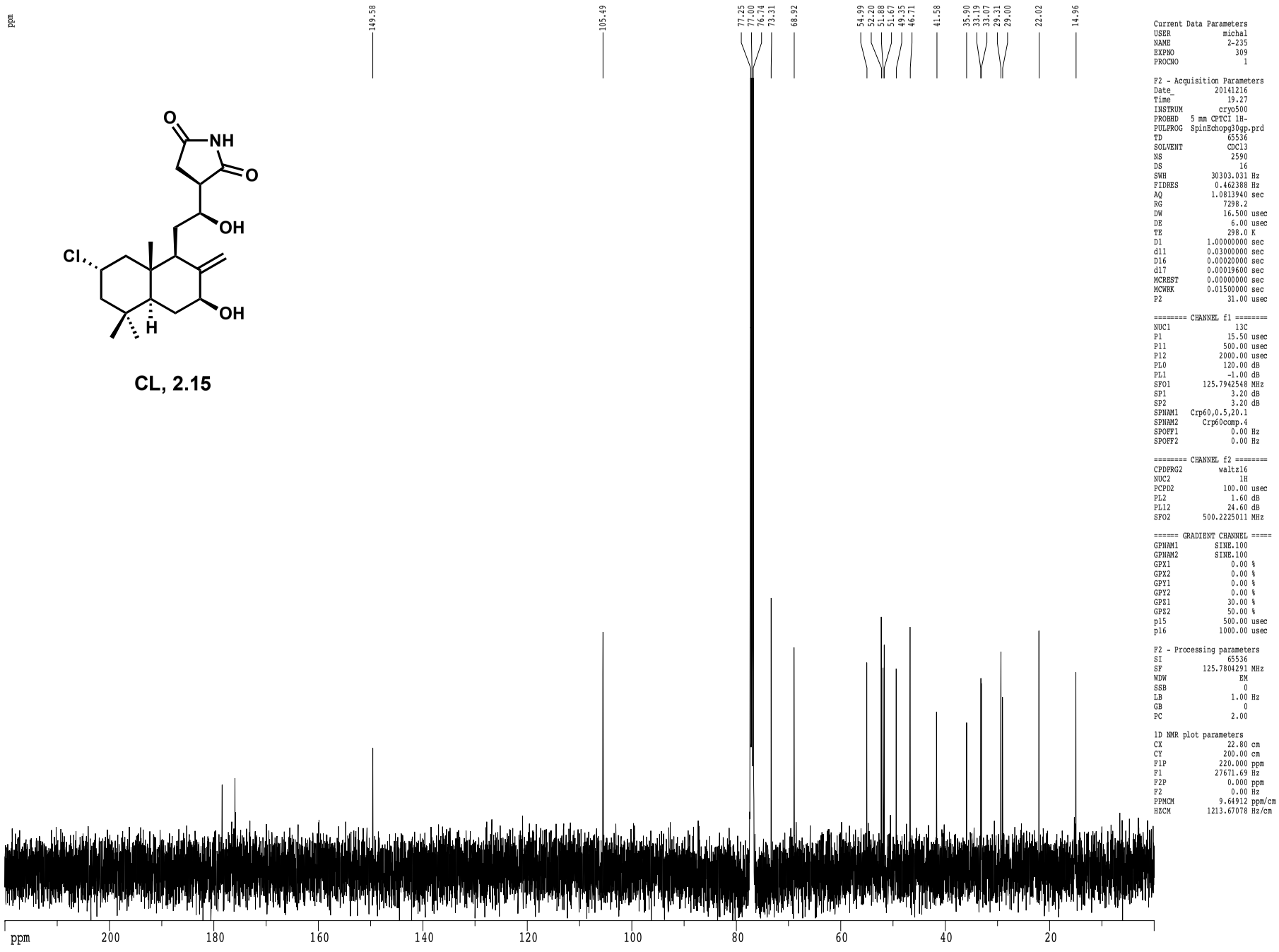

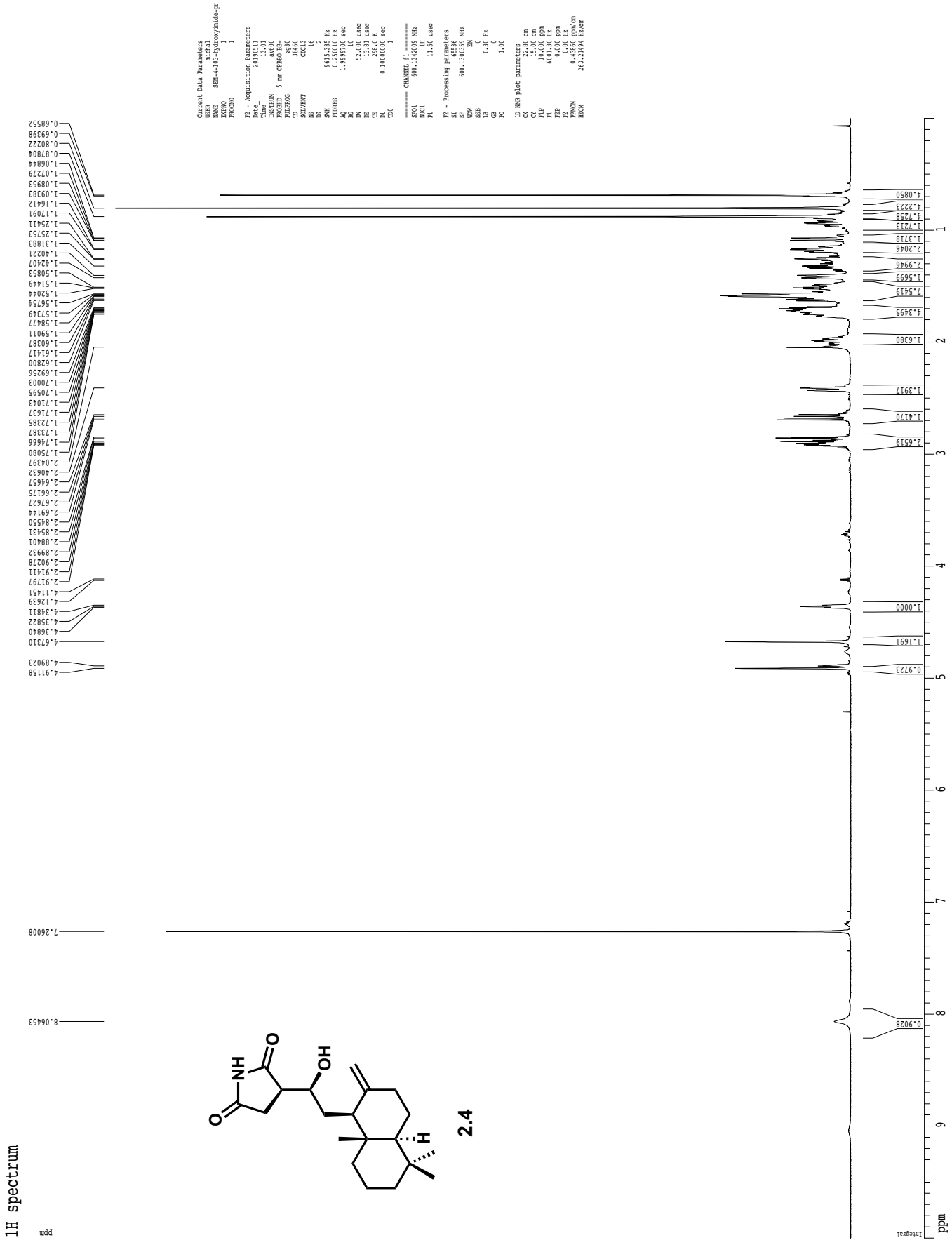
1H spectrum
Current Data Parameters
USER michal
NAME SEM-4-103-hydroxylmide-pr
EXPNO 1
PROCNO 1
F2 - Acquisition Parameters
Date_ 20190511
Time 13.01
INSTRUM spect
PROBHD 5 mm CPBBO BB-
PULPROG zg30
TD 38460
SOLVENT CDCl3
NS 16
DS 2
SWH 9615.385 Hz
FIDRES 0.250010 Hz
AQ 1.9999700 sec
RG 10
DW 52.000 usec
DE 13.81 usec
TE 298.0 K
D1 0.10000000 sec
TD0 1
======== CHANNEL f1 ========
SFO1 600.1342009 MHz
NUC1 1H
P1 11.50 usec
F2 - Processing parameters
SI 65536
SF 600.1300359 MHz
WDW EM
SSB 0
LB 0.30 Hz
GB 0
PC 1.00
1D NMR plot parameters
CX 23.40 cm
CY 15.10 cm
F1P 10.000 ppm
F1 6001.30 Hz
F2P 0.000 ppm
F2 0.00 Hz
PPMCM 0.43860 ppm/cm
HZCM 263.21494 Hz/cm
ppm
integral
2.4

Z-restored spin-echo 13C spectrum with 1H decoupling

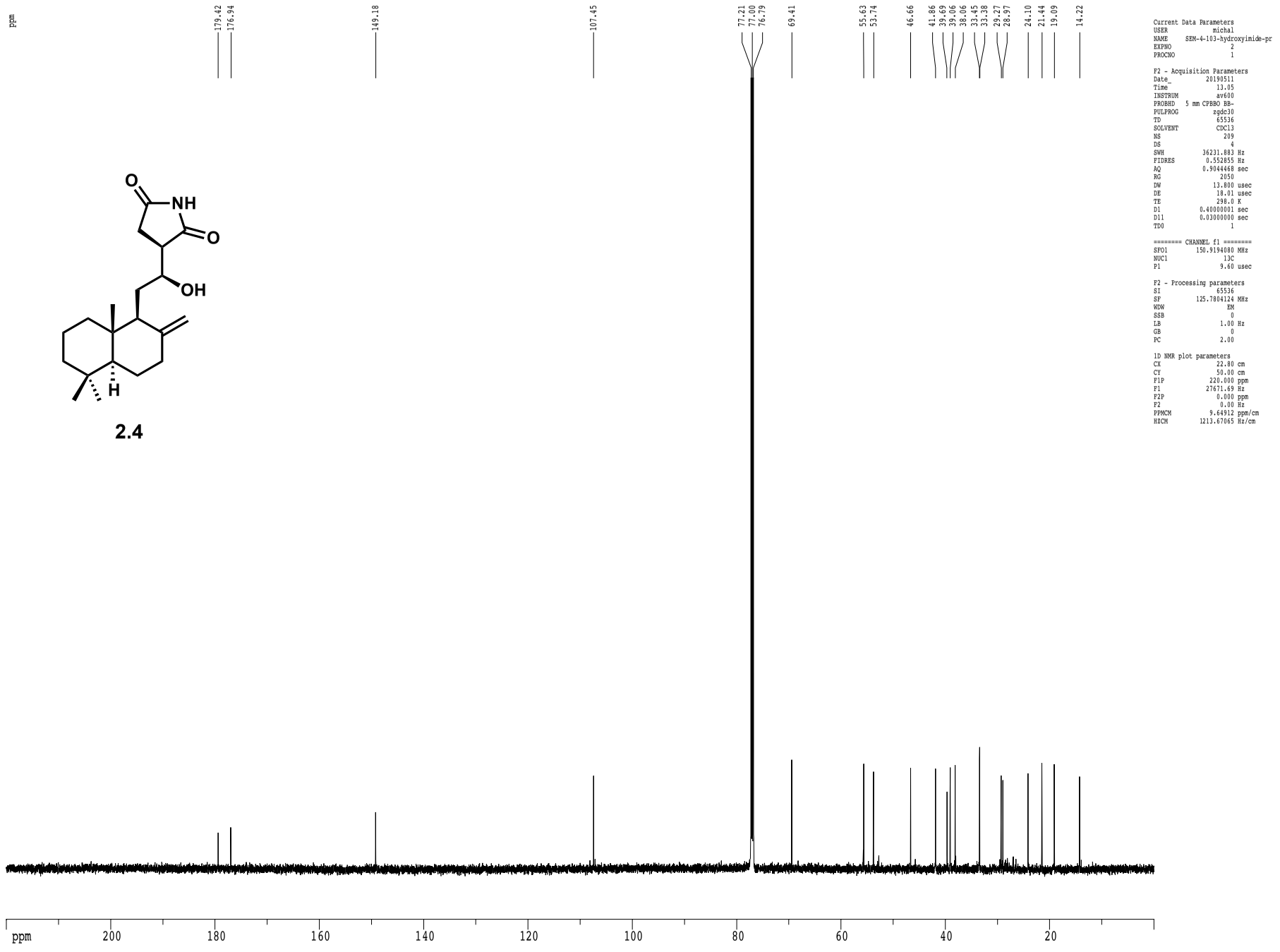

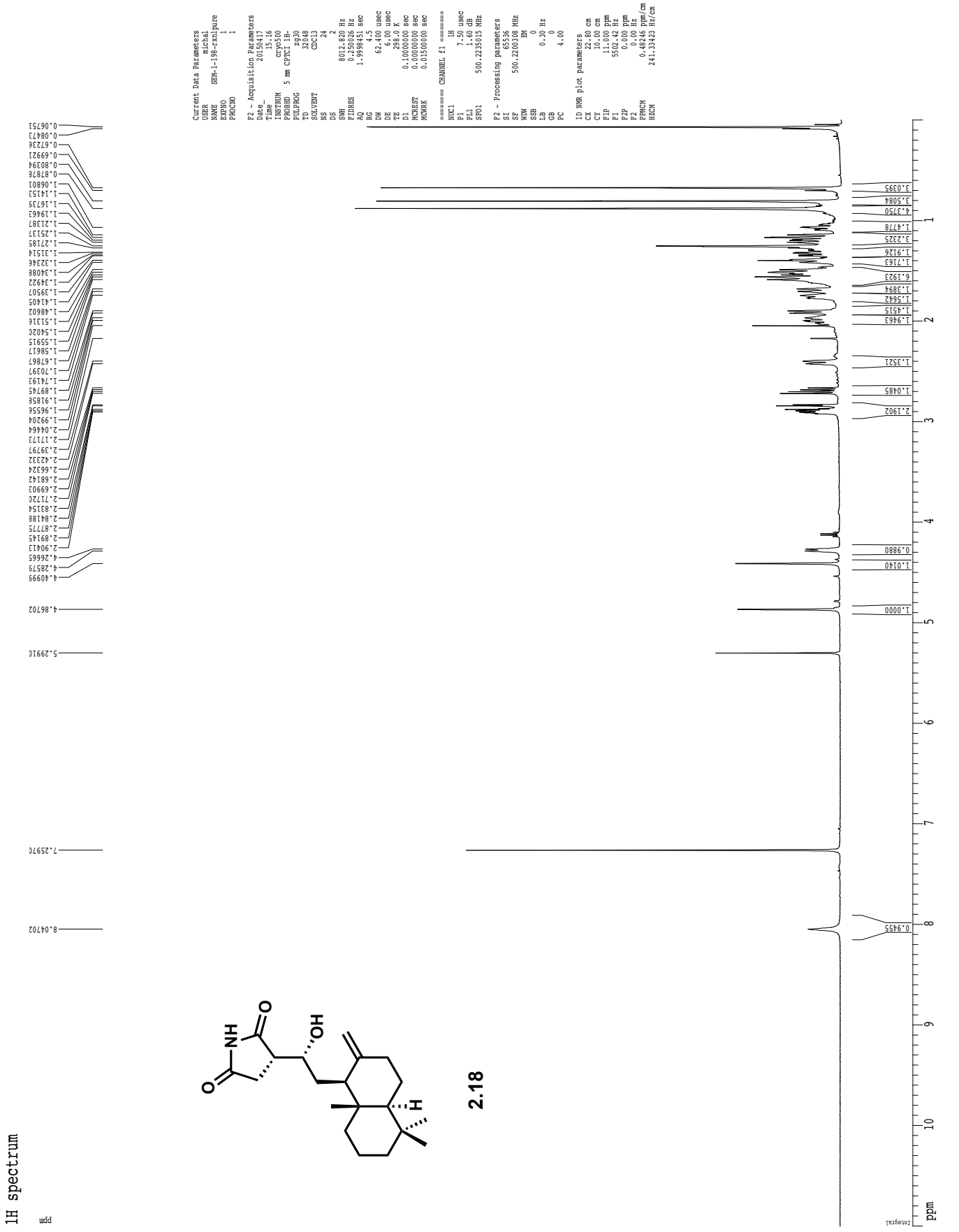
1H spectrum
Current Data Parameters
F2 - Acquisition Parameters
F2 - Processing parameters
1D NMR plot parameters
integral
ppm
2.18

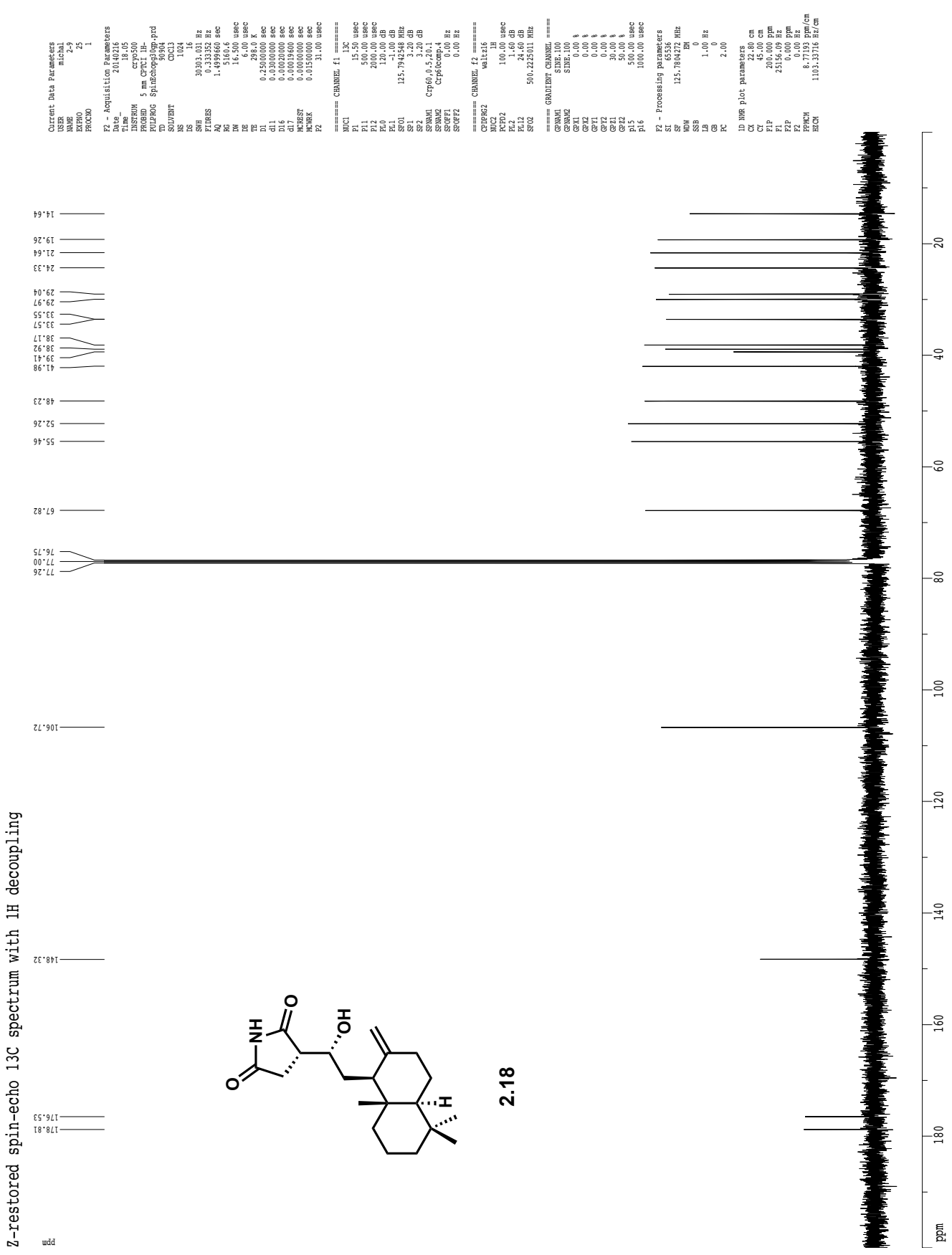
Z-restored spin-echo 13C spectrum with 1H decoupling
ppm
2.18
NH
O
O
OH
H
Current Data Parameters
USER michal
NAME 2-9
EXPNO 25
PROCNO 1
F2 - Acquisition Parameters
Date_ 20140216
Time_ 18.05
INSTRUM ccryo500
PROBHD 5 mm CPCCI 1H-
PULPROG SpinEchopg30gp.pxd
TD 90904
SOLVENT CDCl3
NS 1024
DS 16
SWH 30303.031 Hz
FIDRES 0.332552 Hz
AQ 1.4999668 sec
RG 5160.6
DW 16.500 usec
DE 6.00 usec
TE 298.0 K
D1 0.25000000 sec
d11 0.03000000 sec
D16 0.00020000 sec
d17 0.00019600 sec
MC_REST 0.00000000 sec
MC_WRK 0.01500000 sec
P2 31.00 usec
======== CHANNEL f1 ========
NUC1 13C
P1 15.50 usec
P11 500.00 usec
P12 2000.00 usec
PL0 120.00 dB
PL1 -1.00 dB
SFO1 125.7942548 MHz
SF1 3.20 dB
SF2 3.20 dB
SPNAM1 Crp60,0.5,20.1
SPNAM2 Crp60comp.4
SFOFP1 0.00 Hz
SFOFP2 0.00 Hz
======== CHANNEL f2 ========
CPDPRG2 waltz16
NUC2 1H
PCPD2 100.00 usec
PL2 1.60 dB
PL12 24.60 dB
SFO2 500.2225011 MHz
===== GRADIENT CHANNEL =====
GPNAM1 SINE.100
GPNAM2 SINE.100
GPX1 0.00 %
GPX2 0.00 %
GPY1 0.00 %
GPY2 0.00 %
GPZ1 30.00 %
GPZ2 50.00 %
p15 500.00 usec
p16 1000.00 usec
F2 - Processing parameters
SI 65536
SF 125.7804272 MHz
WDW EM
SSB 0
LB 1.00 Hz
GB 0
PC 2.00
1D NMR plot parameters
CX 22.80 cm
CY 45.00 cm
F1P 201.000 ppm
F1 25156.09 Hz
F2P 0.000 ppm
F2 0.00 Hz
PPMCM 8.77193 ppm/cm
HZCM 1103.33716 Hz/cm
14.64
19.26
21.64
24.33
29.04
29.97
33.55
33.57
38.17
38.92
39.41
41.98
48.23
52.26
55.46
67.82
76.75
77.00
77.26
106.72
148.32
176.53
178.81
ppm

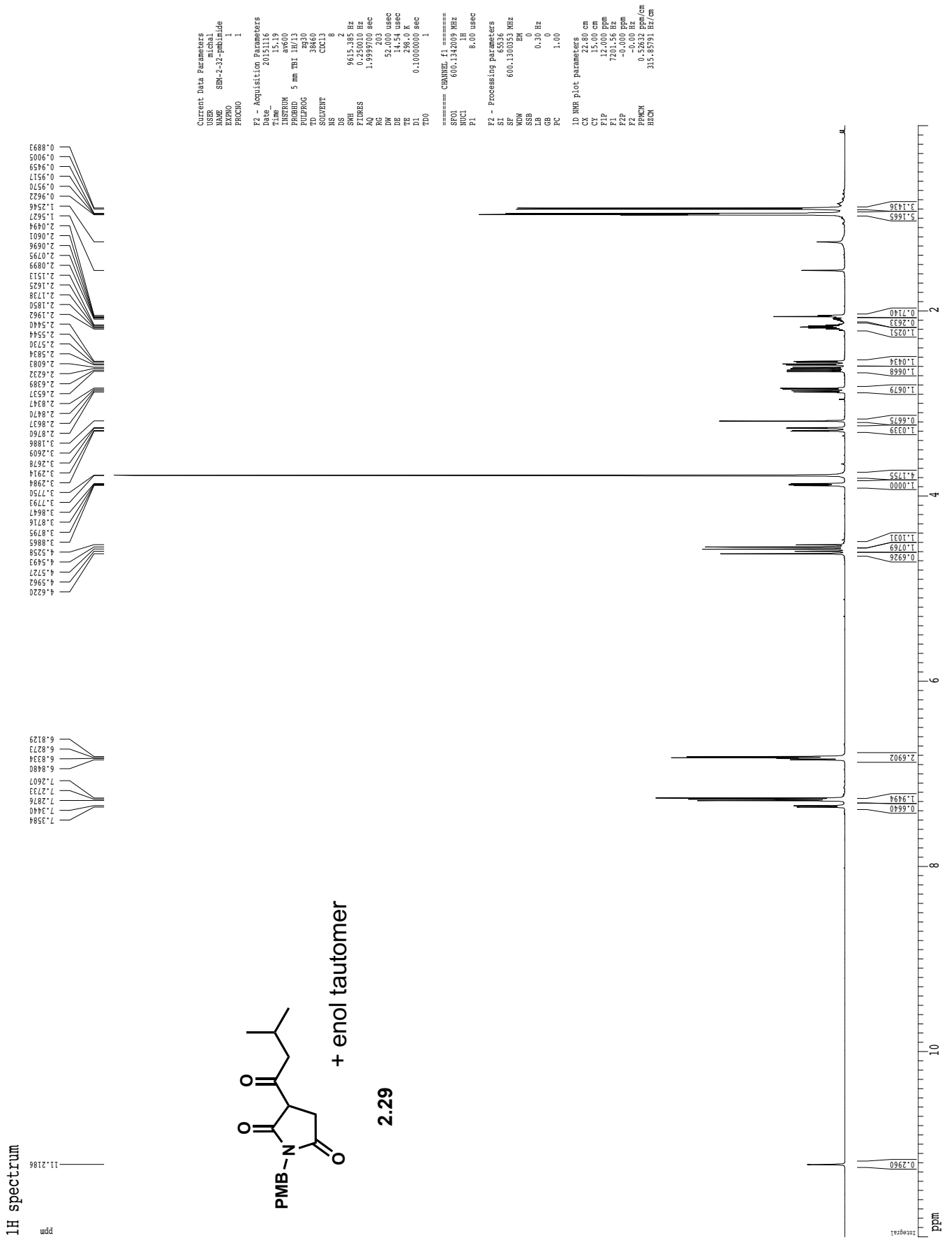
1H spectrum
PMB
N
O
O
O
+ enol tautomer
2.29

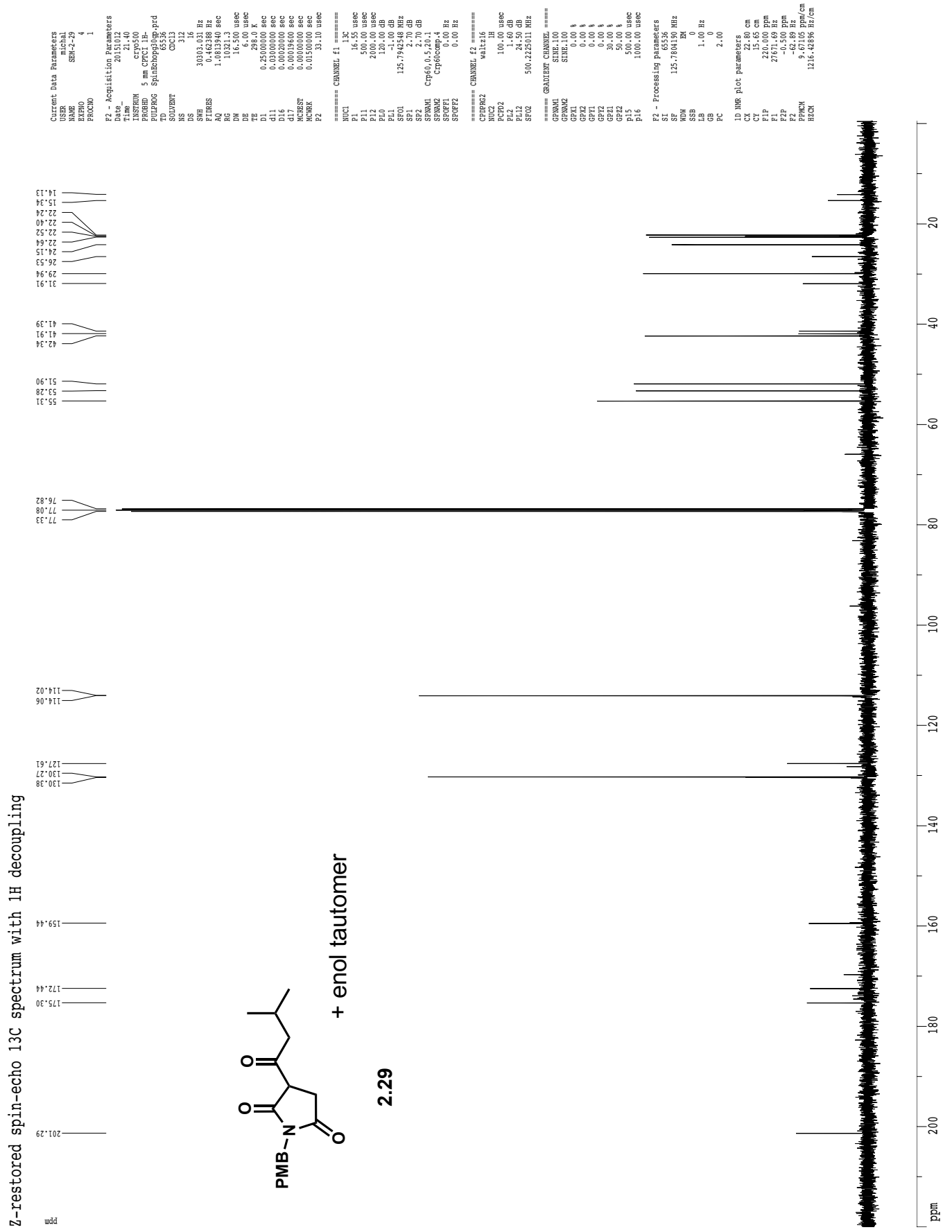
Z-restored spin-echo 13C spectrum with 1H decoupling
+ enol tautomer
2.29
PMB
ppm

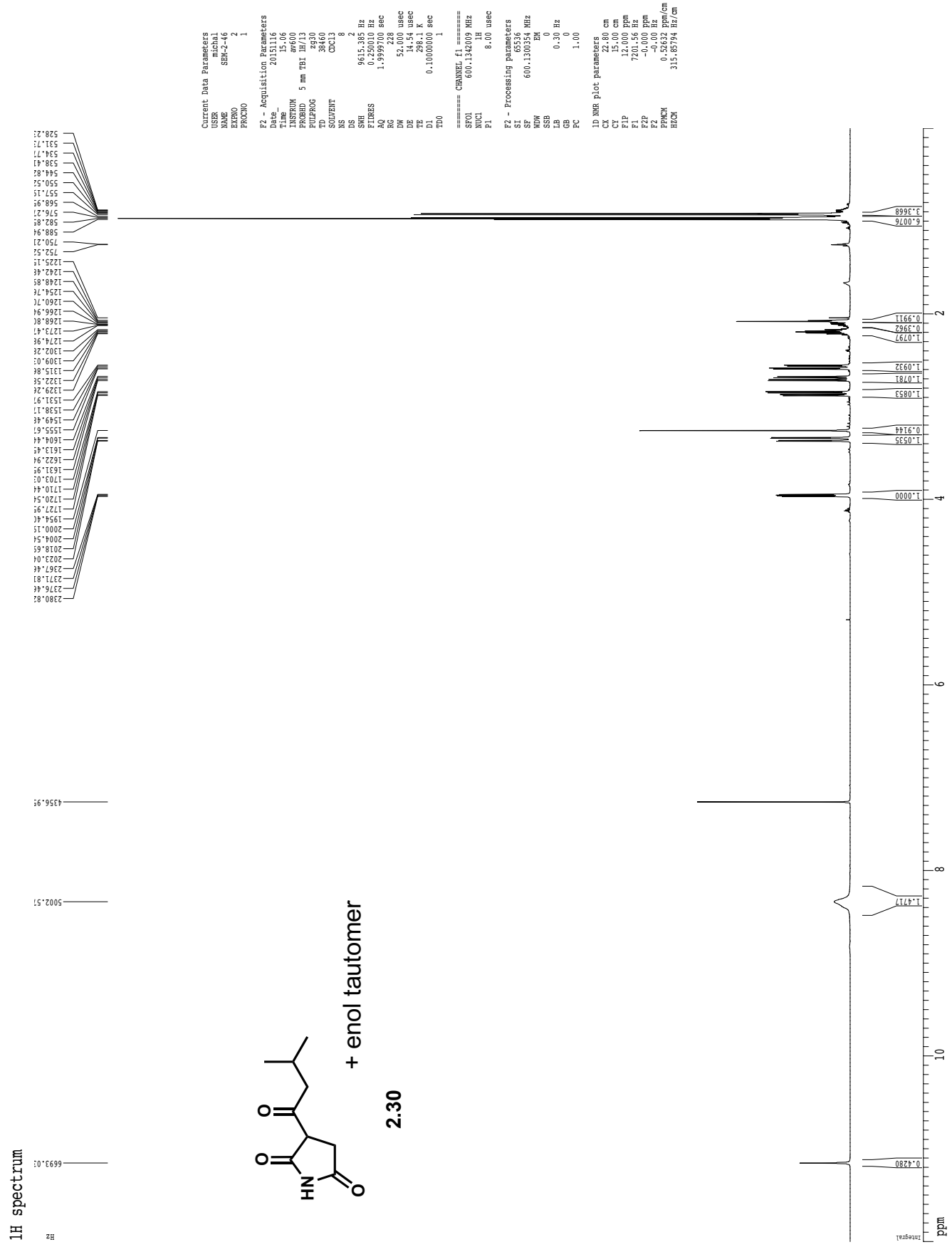
1H spectrum
+ enol tautomer
2.30
O
O
HN
O
ppm
integral

Z-restored spin-echo 13C spectrum with 1H decoupling

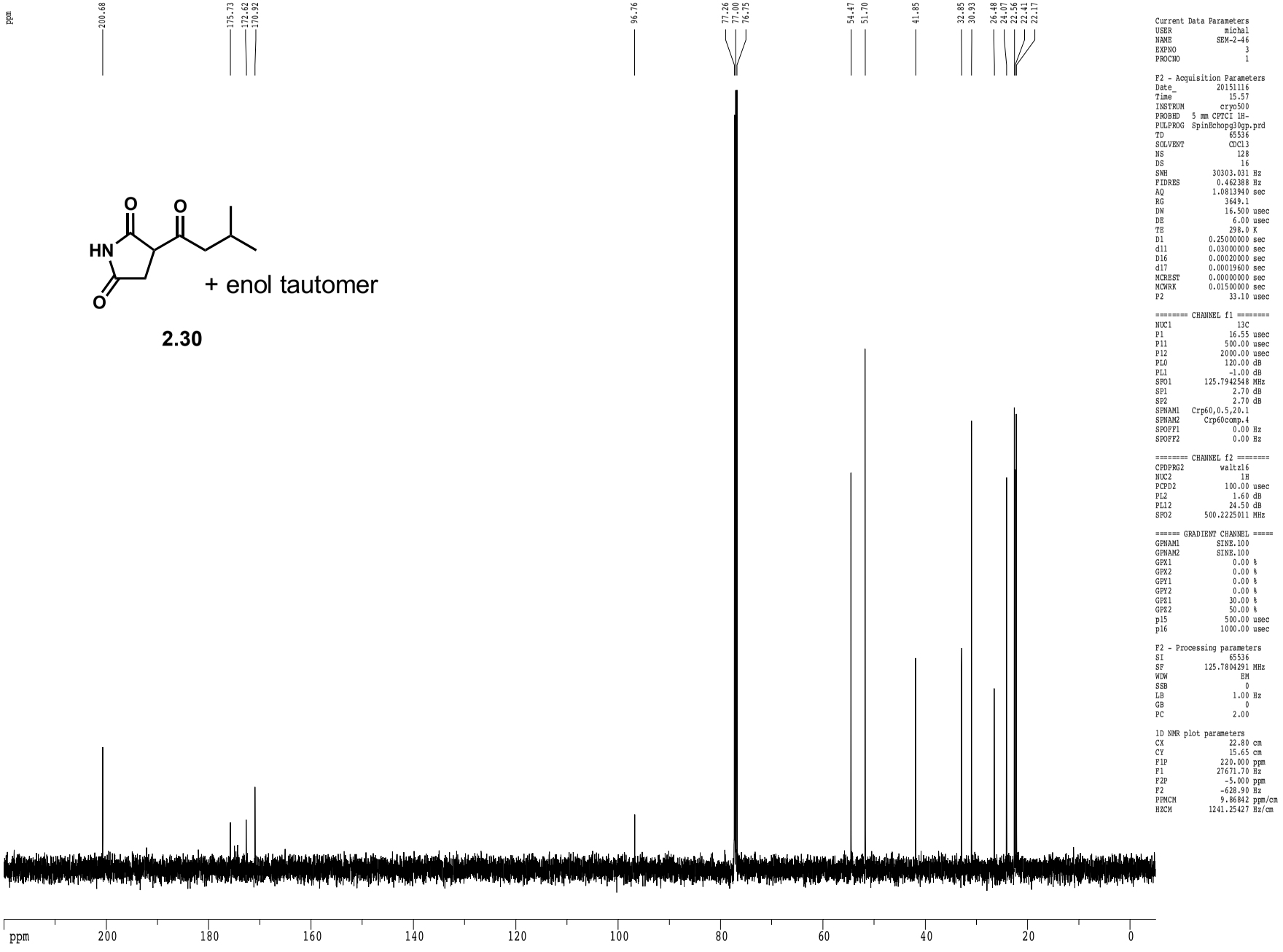

Current Data Parameters
USER michal
NAME SEM-2-46
EXPNO 3
PROCNO 1

F2 - Acquisition Parameters
Date_ 20151116
Time 15.57
INSTRUM cryo500
PROBHD 5 mm CPTCI 1H-
PULPROG SpinEchopg30gp.prd
TD 65536
SOLVENT CDCl3
NS 128
DS 16
SWH 30303.031 Hz
FIDRES 0.462388 Hz
AQ 1.0813940 sec
RG 3649.1
DW 16.500 usec
DE 6.00 usec
TE 298.0 K
D1 0.25000000 sec
d11 0.03000000 sec
D16 0.00020000 sec
d17 0.00019600 sec
MCREST 0.00000000 sec
MCWRK 0.01500000 sec
P2 33.10 usec

======= CHANNEL f1 =======
NUC1 13C
P1 16.55 usec
P11 500.00 usec
P12 2000.00 usec
PL0 120.00 dB
PL1 -1.00 dB
SFO1 125.7942548 MHz
SP1 2.70 dB
SP2 2.70 dB
SPNAM1 Crp60,0.5,20.1
SPNAM2 Crp60comp.4
SPOFF1 0.00 Hz
SPOFF2 0.00 Hz

======= CHANNEL f2 =======
CPDPRG2 waltz16
NUC2 1H
PCPD2 100.00 usec
PL2 1.60 dB
PL12 24.50 dB
SFO2 500.2225011 MHz

===== GRADIENT CHANNEL =====
GPNAM1 SINE.100
GPNAM2 SINE.100
GPX1 0.00 %
GPX2 0.00 %
GPY1 0.00 %
GPY2 0.00 %
GPZ1 30.00 %
GPZ2 50.00 %
p15 500.00 usec
p16 1000.00 usec

F2 - Processing parameters
SI 65536
SF 125.7804291 MHz
WDW EM
SSB 0
LB 1.00 Hz
GB 0
PC 2.00

1D NMR plot parameters
CX 22.80 cm
CY 15.65 cm
F1P 220.000 ppm
F1 27671.70 Hz
F2P -5.000 ppm
F2 -628.90 Hz
PPMCM 9.86842 ppm/cm
HZCM 1241.25427 Hz/cm

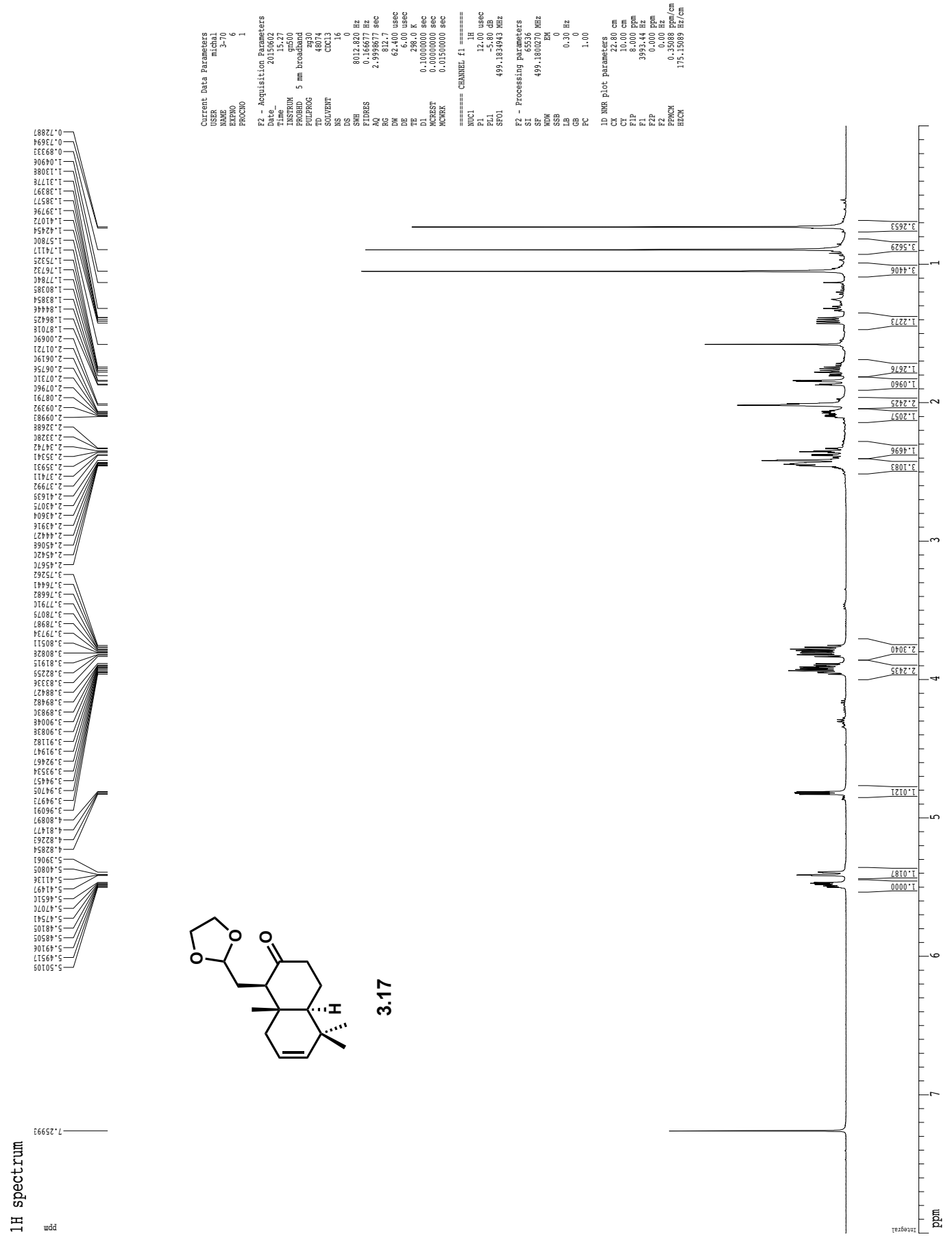
1H spectrum
Current Data Parameters
USER michal
NAME 3-70
EXPNO 6
PROCNO 1
F2 - Acquisition Parameters
Date_ 20150602
Time 15:27
INSTRUM qnp500
PROBHD 5 mm broadband
PULPROG zg30
TD 48074
SOLVENT CDCl3
NS 16
DS 0
SWH 8012.820 Hz
FIDRES 0.166677 Hz
AQ 2.9996677 sec
RG 812.7
DW 62.400 usec
DE 6.00 usec
TE 298.0 K
D1 0.10000000 sec
MCREST 0.00000000 sec
MCWRK 0.01500000 sec
======== CHANNEL f1 ========
NUC1 1H
P1 12.00 usec
PL1 5.00 dB
SFO1 499.1834943 MHz
F2 - Processing parameters
SI 65536
SF 499.1800270 MHz
WDW EM
SSB 0
LB 0.30 Hz
GB 0
PC 1.00
1D NMR plot parameters
CX 22.80 cm
CY 10.00 cm
F1P 8.000 ppm
F1 3993.44 Hz
F2P 0.000 ppm
F2 0.00 Hz
PPMCM 0.35088 ppm/cm
HZCM 175.15089 Hz/cm
3.2653
3.5629
3.4406
1.2273
1.2676
1.0960
2.2425
1.2057
1.4696
3.1083
2.3040
2.2435
1.0121
1.0187
1.0000
Integral
ppm
3.17

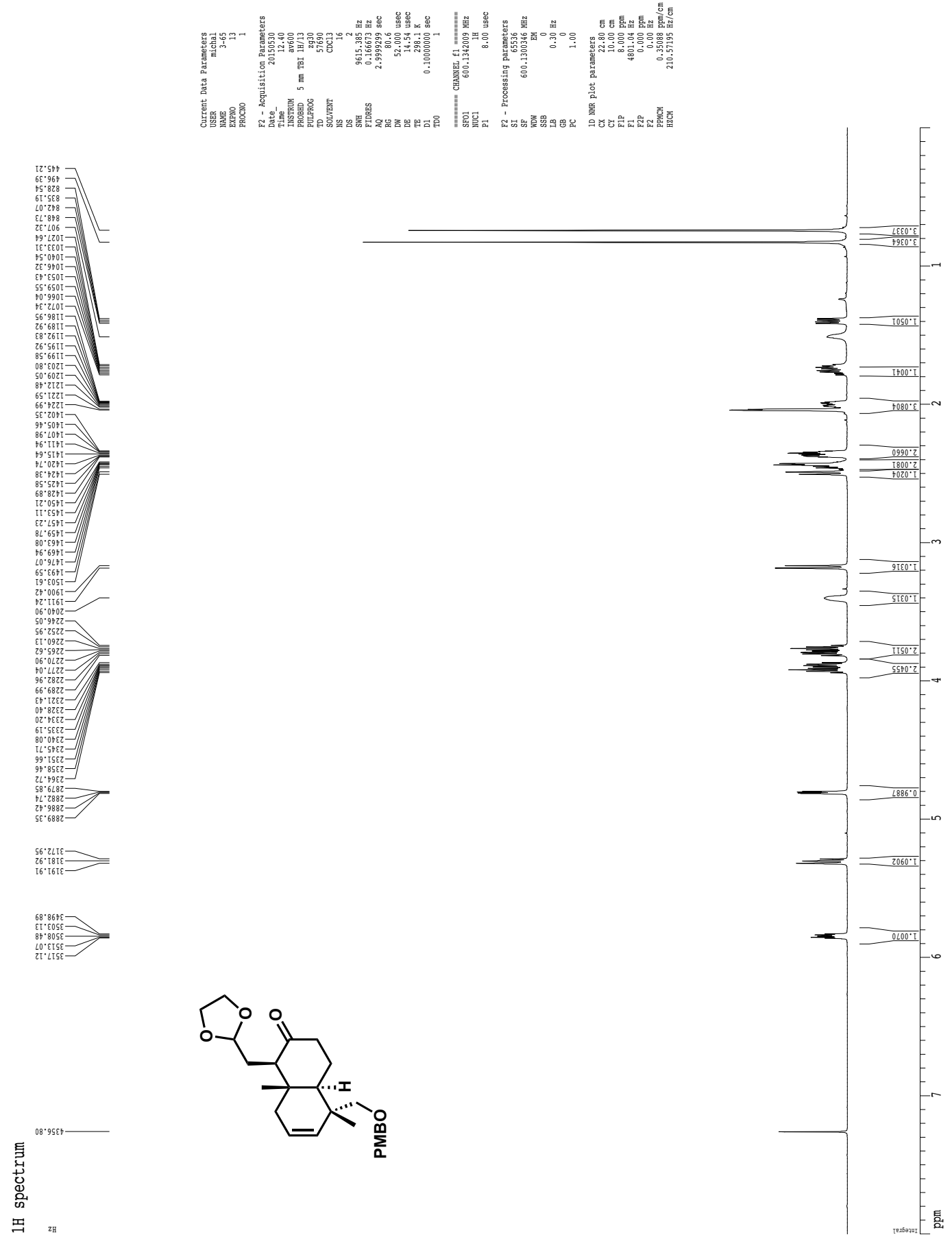
1H spectrum
Current Data Parameters
USER michal
NAME 3-65
EXPNO 13
PROCNO 1
F2 - Acquisition Parameters
Date_ 20150530
Time 12.40
INSTRUM av600
PROBHD 5 mm TBI 1H/13
PULPROG zg30
TD 57690
SOLVENT CDCl3
NS 16
DS 2
SWH 9615.385 Hz
FIDRES 0.166673 Hz
AQ 2.9999299 sec
RG 80.6
DW 52.000 usec
DE 14.54 usec
TE 298.1 K
D1 0.10000000 sec
TD0 1
======== CHANNEL f1 ========
SFO1 600.1342009 MHz
NUC1 1H
P1 8.00 usec
F2 - Processing parameters
SI 65536
SF 600.1300346 MHz
WDW EM
SSB 0
LB 0.30 Hz
GB 0
PC 1.00
1D NMR plot parameters
CX 22.80 cm
CY 10.00 cm
F1P 8.000 ppm
F1 4801.04 Hz
F2P 0.000 ppm
F2 0.00 Hz
PPMCM 0.35088 ppm/cm
HZCM 210.57195 Hz/cm
PMBO
H
O
O
O
Hz
ppm
Integral
3.0337
3.0364
1.0501
1.0041
3.0804
2.0660
2.0081
1.0204
1.0316
1.0315
2.0511
2.0455
0.9887
1.0902
1.0070

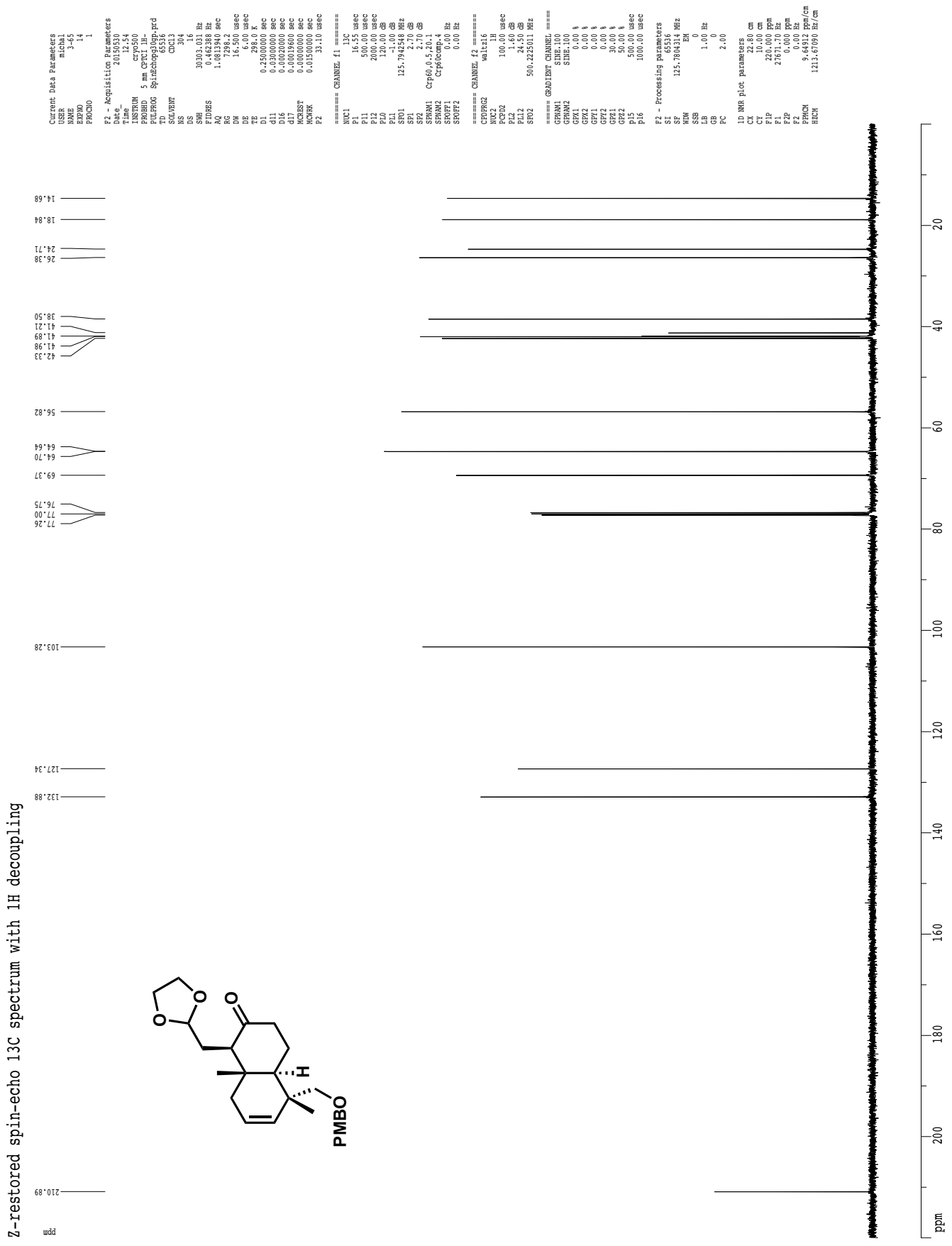
Z-restored spin-echo 13C spectrum with 1H decoupling
PMBO
O
O
O
H
ppm
210.89
132.88
127.34
103.28
77.26
77.00
76.75
69.37
64.70
64.64
56.82
42.33
41.98
41.89
41.21
38.50
26.38
24.71
18.84
14.68
20
40
60
80
100
120
140
160
180
200
ppm

1H spectrum

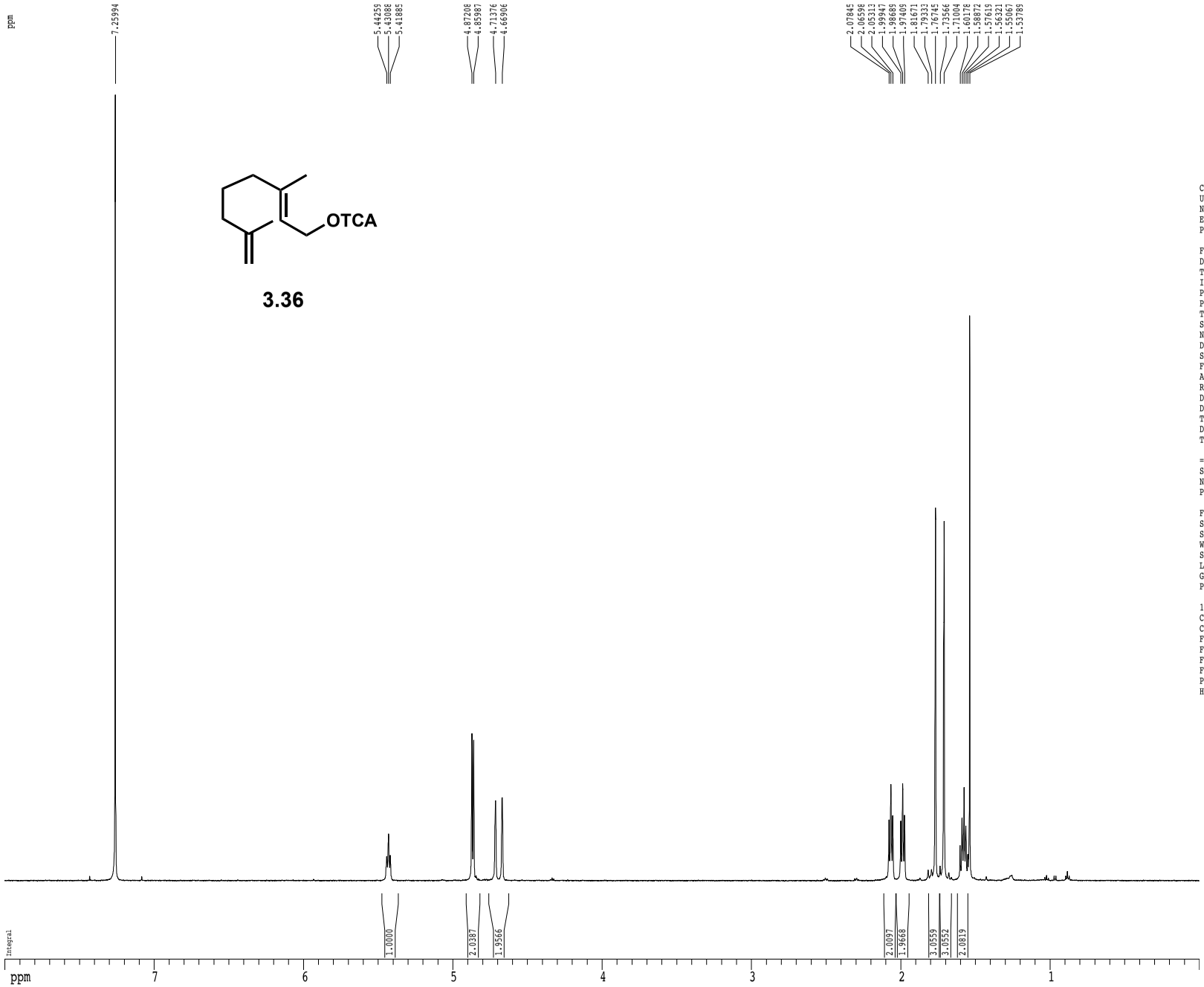


```
Current Data Parameters
USER                michal
NAME                 3-298
EXPNO                    3
PROCNO                   1

F2 - Acquisition Parameters
Date_             20160926
Time                 18.38
INSTRUM              av600
PROBHD   5 mm CPBBO BB-
PULPROG               zg30
TD                   38460
SOLVENT              CDCl3
NS                       8
DS                       0
SWH              9615.385 Hz
FIDRES           0.250010 Hz
AQ               1.9999700 sec
RG                    28.5
DW                52.000 usec
DE                13.70 usec
TE                298.0 K
D1             0.10000000 sec
TD0                      1

======== CHANNEL f1 ========
SFO1          600.1342009 MHz
NUC1                    1H
P1                 12.00 usec

F2 - Processing parameters
SI                   65536
SF            600.1300354 MHz
WDW                     EM
SSB                      0
LB                  0.30 Hz
GB                       0
PC                    1.00

1D NMR plot parameters
CX                   22.80 cm
CY                   15.00 cm
F1P                  8.000 ppm
F1                 4801.04 Hz
F2P                  0.000 ppm
F2                   0.00 Hz
PPMCM             0.35088 ppm/cm
HZCM            210.57196 Hz/cm
```

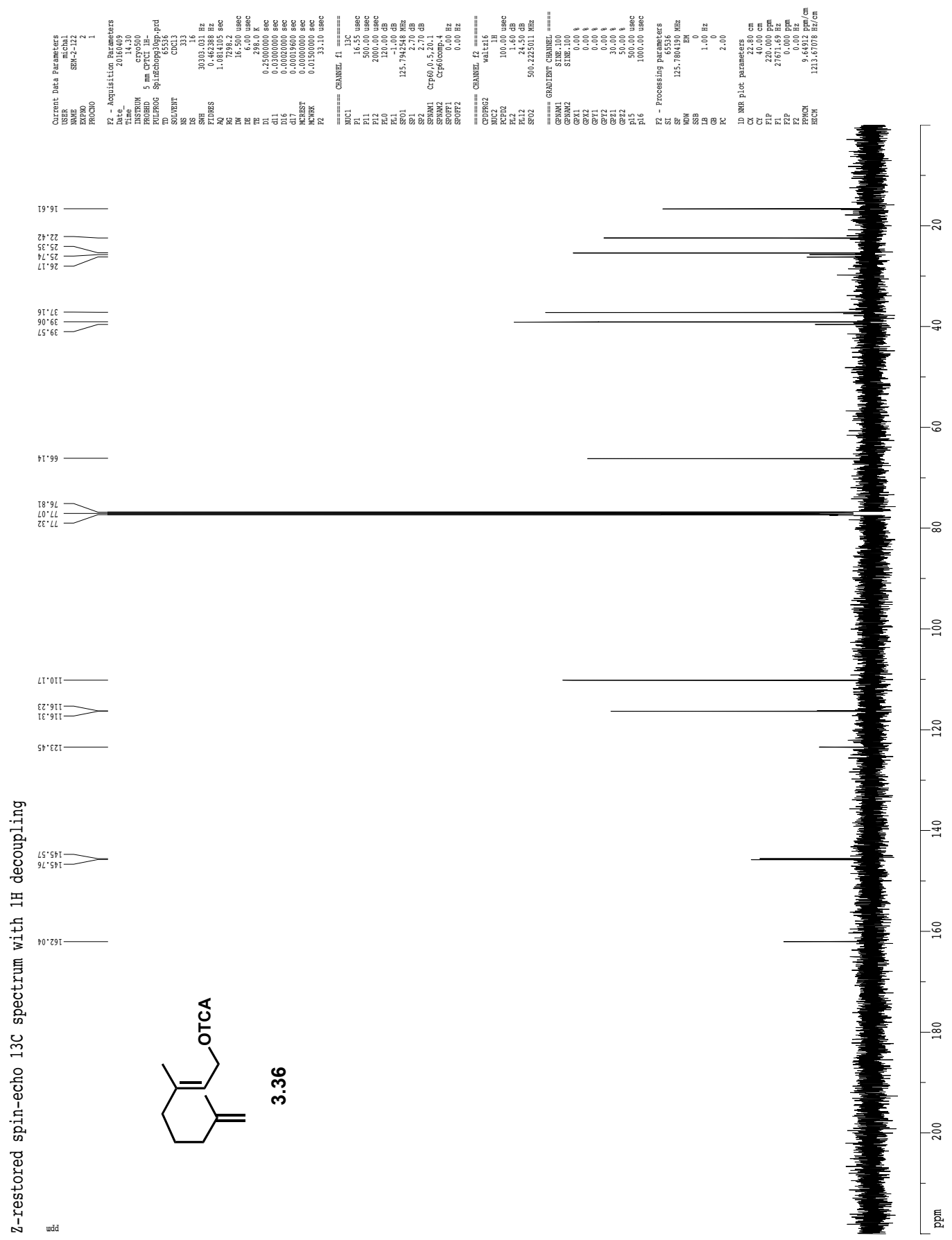
Z-restored spin-echo 13C spectrum with 1H decoupling
ppm
OTCA
3.36
Current Data Parameters
USER michal
NAME SEM-2-122
EXPNO 2
PROCNO 1
F2 - Acquisition Parameters
Date_ 20161019
Time 14.10
INSTRUM cryo500
PROBHD 5 mm CPTCI 1H-
PULPROG SpinEchopp30gp.prd
TD 65536
SOLVENT CDCl3
NS 333
DS 16
SWH 30303.031 Hz
FIDRES 0.462388 Hz
AQ 1.0814105 sec
RG 7298.2
DW 16.500 usec
DE 6.00 usec
TE 298.0 K
D1 0.25000000 sec
D11 0.03000000 sec
D16 0.00020000 sec
d17 0.00015600 sec
MCREST 0.00000000 sec
MCWRK 0.01500000 sec
P2 33.10 usec
======= CHANNEL f1 =======
NUC1 13C
P1 16.55 usec
P11 500.00 usec
P12 2000.00 usec
PL0 120.00 dB
PL1 -1.00 dB
SFO1 125.7942548 MHz
SP1 2.70 dB
SP2 2.70 dB
SPNAM1 Crp60,0.5,20.1
SPNAM2 Crp60comp.4
SPOFFS1 0.00 Hz
SPOFF2 0.00 Hz
======= CHANNEL f2 =======
CPDPRG2 waltz16
NUC2 1H
PCPD2 100.00 usec
PL2 1.60 dB
PL12 24.50 dB
SFO2 500.2225011 MHz
===== GRADIENT CHANNEL =====
GPNAM1 SINE.100
GPNAM2 SINE.100
GPX1 0.00 %
GPX2 0.00 %
GPY1 0.00 %
GPY2 0.00 %
GPZ1 30.00 %
GPZ2 50.00 %
p15 500.00 usec
p16 1000.00 usec
F2 - Processing parameters
SI 65536
SF 125.7804190 MHz
WDW EM
SSB 0
LB 1.00 Hz
GB 0
PC 2.00
1D NMR plot parameters
CX 22.80 cm
CY 40.00 cm
F1P 220.000 ppm
F1 27671.69 Hz
F2P 0.000 ppm
F2 0.00 Hz
PPMCM 9.64912 ppm/cm
HZCM 1213.67078 Hz/cm
16.61
22.42
25.35
25.74
26.17
37.16
39.06
39.57
66.14
76.81
77.07
77.32
110.17
116.23
116.31
123.45
145.57
145.76
162.04
ppm
20
40
60
80
100
120
140
160
180
200

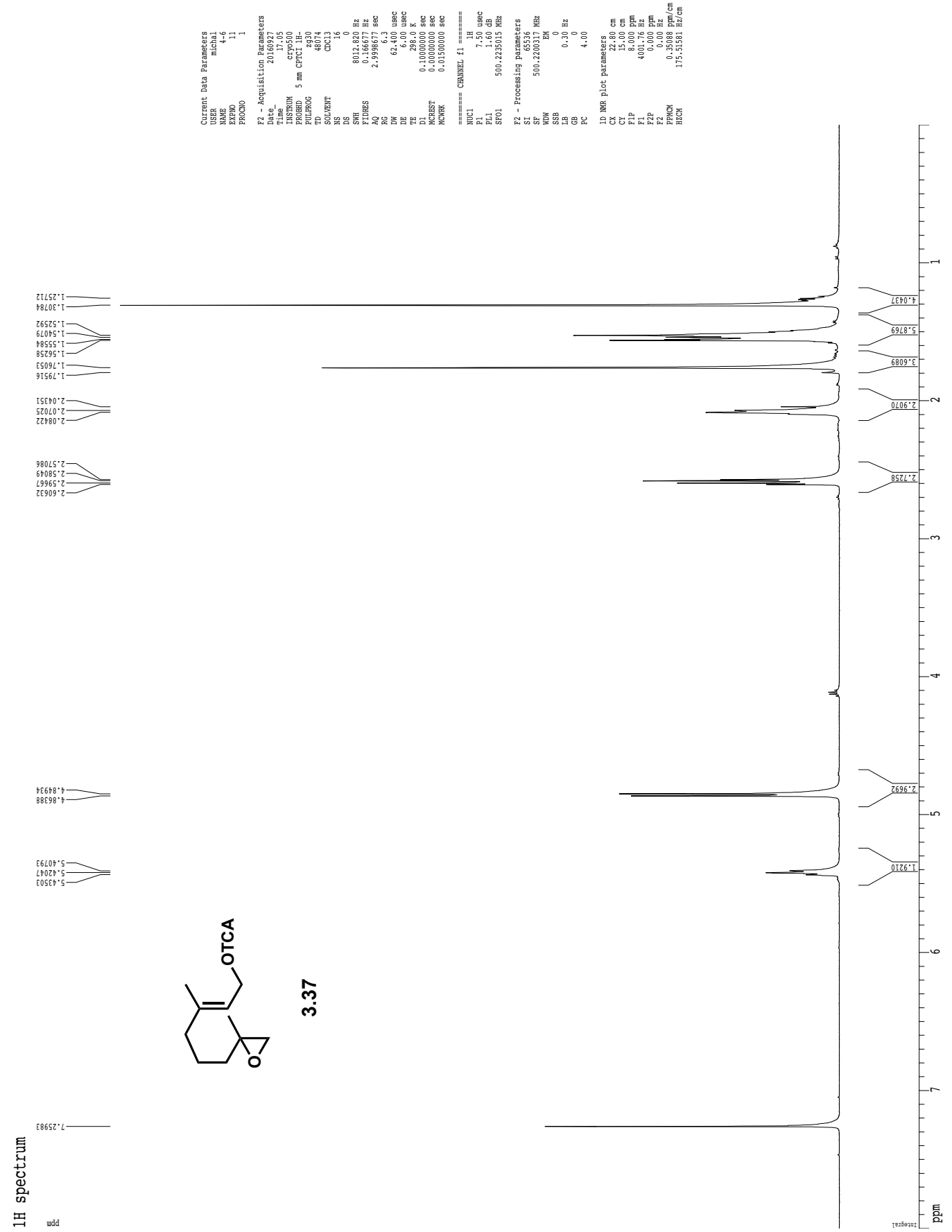
1H spectrum
ppm
Integral
OTCA
O
3.37
Current Data Parameters
USER michal
NAME 4-6
EXPNO 11
PROCNO 1
F2 - Acquisition Parameters
Date_ 20160927
Time 17.05
INSTRUM crp500
PROBHD 5 mm CPTCI 1H-
PULPROG zg30
TD 48074
SOLVENT CDCl3
NS 16
DS 0
SWH 8012.820 Hz
FIDRES 0.166677 Hz
AQ 2.9998677 sec
RG 6.3
DW 62.400 usec
DE 6.00 usec
TE 298.0 K
D1 0.10000000 sec
MCREST 0.00000000 sec
MCWRK 0.01500000 sec
======== CHANNEL f1 ========
NUC1 1H
P1 7.50 usec
PL1 1.60 dB
SFO1 500.2235015 MHz
F2 - Processing parameters
SI 65536
SF 500.2200317 MHz
WDW EM
SSB 0
LB 0.30 Hz
GB 0
PC 4.00
1D NMR plot parameters
CX 22.80 cm
CY 15.00 cm
F1P 8.000 ppm
F1 4001.76 Hz
F2P 0.000 ppm
F2 0.00 Hz
PPMCM 0.35088 ppm/cm
HZCM 175.51581 Hz/cm
7.25983
5.43503
5.42047
5.40793
4.86388
4.84934
2.60632
2.59667
2.58049
2.57086
2.08422
2.07025
2.04351
1.79516
1.76053
1.56258
1.55584
1.54079
1.52592
1.30784
1.25712
4.0437
5.8769
3.6089
2.9070
2.7258
2.9692
1.9210

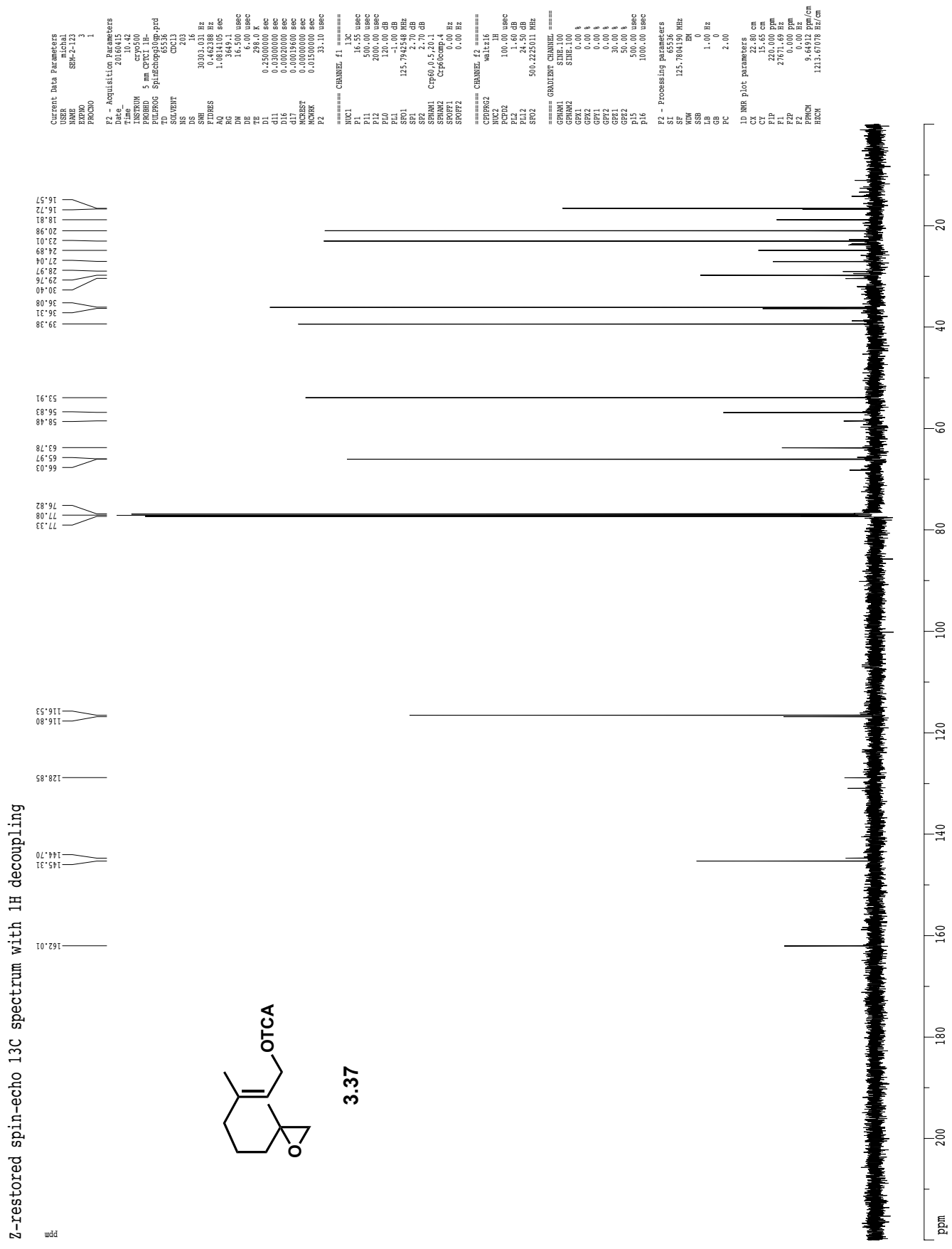
Z-restored spin-echo 13C spectrum with 1H decoupling
ppm
OTCA
O
3.37
Current Data Parameters
F2 - Acquisition Parameters
INSTRUM crypo500
PROBHD 5 mm CPTCI 1H-
PULPROG SpinEchopg30gp.prcl
SOLVENT CDCl3
F2 - Processing parameters
1D NMR plot parameters
77.33
77.08
76.82
66.03
65.97
63.78
58.48
56.83
53.91
39.38
36.31
36.08
30.40
29.76
28.97
27.04
24.89
23.01
20.98
18.81
16.72
16.57
128.85
116.80
116.53
162.01
145.31
144.70
ppm

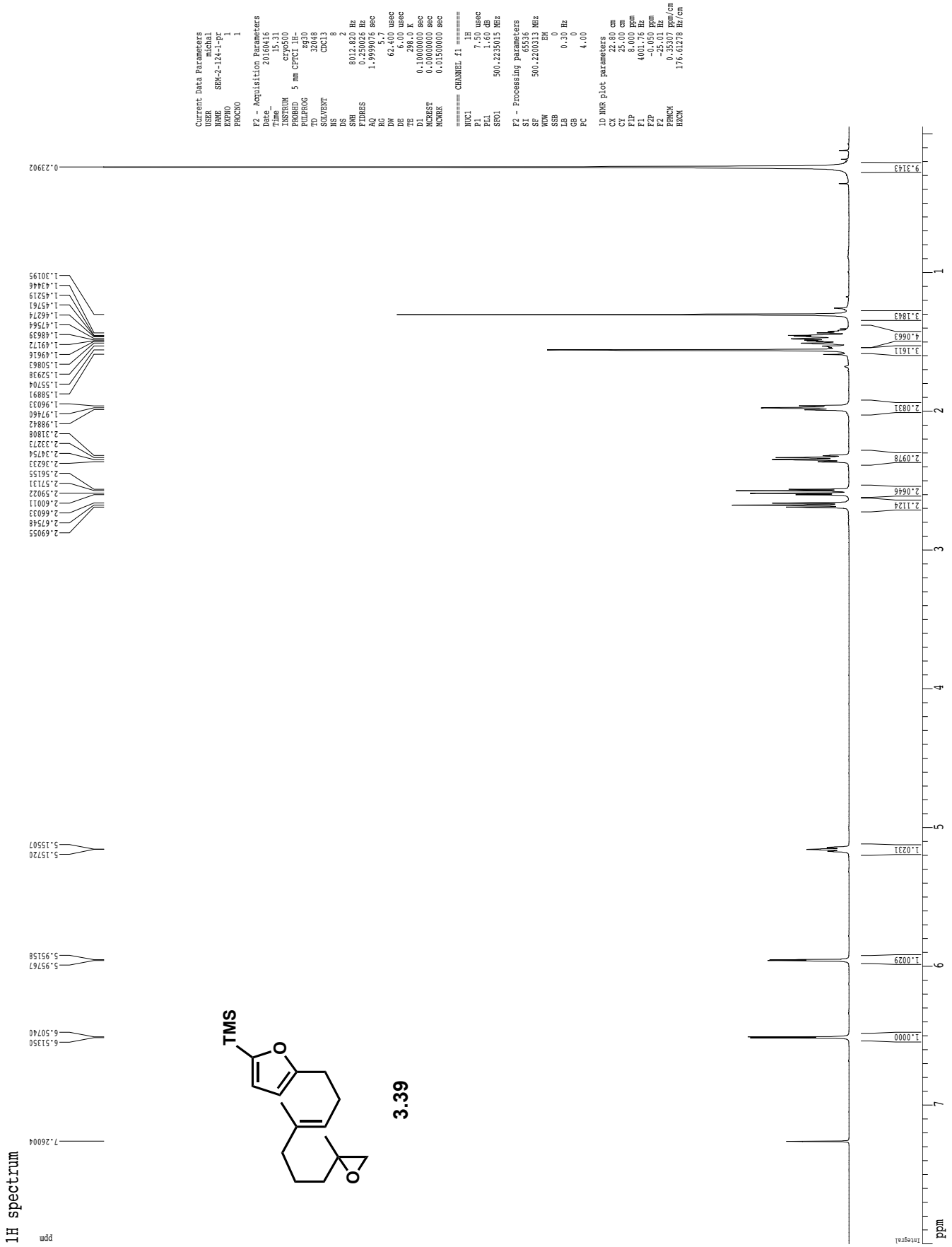
1H spectrum
3.39
TMS

Z-restored spin-echo 13C spectrum with 1H decoupling

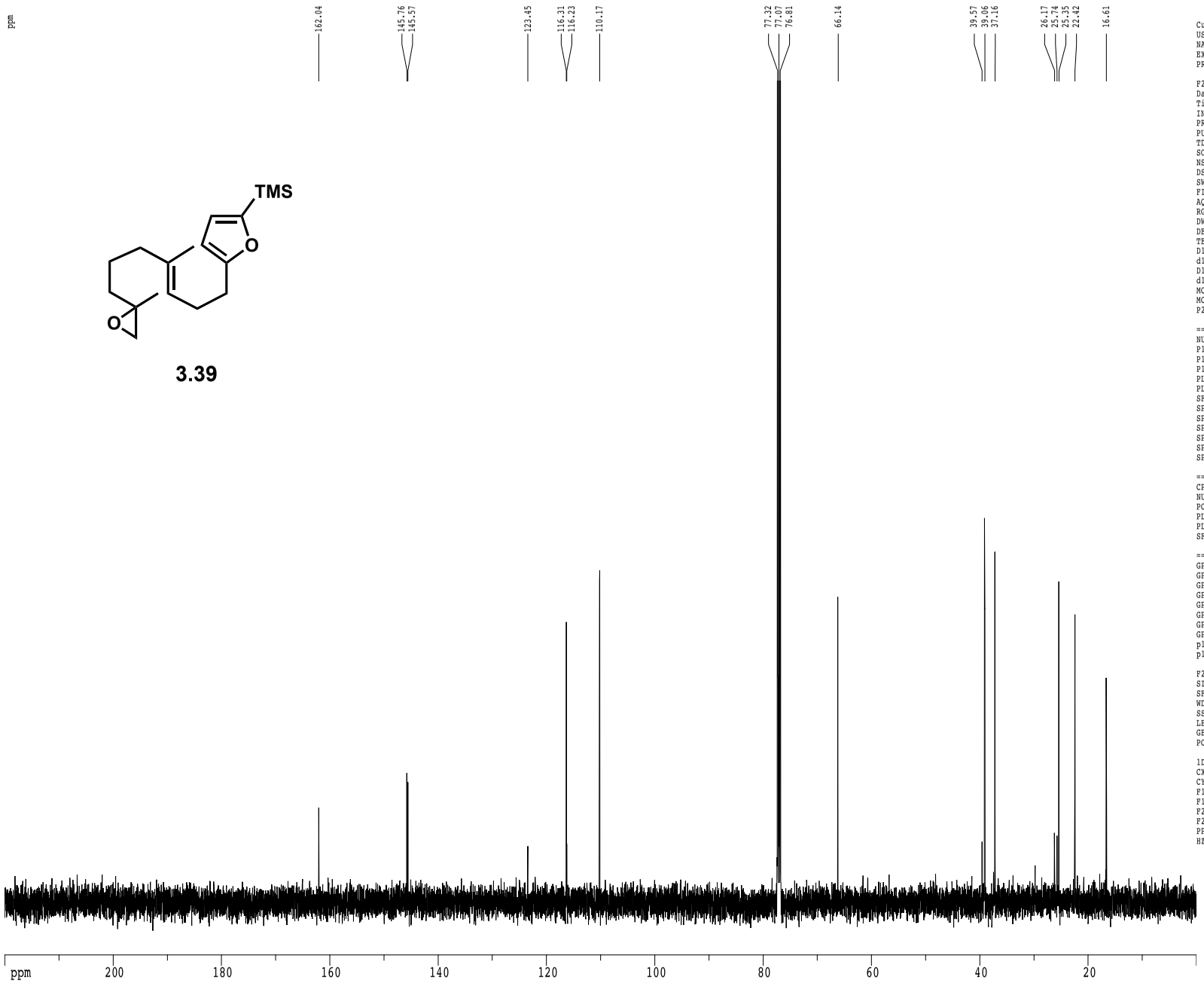

Current Data Parameters
USER michal
NAME SEM-2-122
EXPNO 2
PROCNO 1

F2 - Acquisition Parameters
Date_ 20160409
Time 14.30
INSTRUM cryo500
PROBHD 5 mm CPTCI 1H-
PULPROG SpinEchopg30gp.prd
TD 65536
SOLVENT CDCl3
NS 333
DS 16
SWH 30303.031 Hz
FIDRES 0.462388 Hz
AQ 1.0814105 sec
RG 7298.2
DW 16.500 usec
DE 6.00 usec
TE 298.0 K
D1 0.25000000 sec
d11 0.03000000 sec
D16 0.00020000 sec
d17 0.00019600 sec
MCREST 0.00000000 sec
MCWRK 0.01500000 sec
P2 33.10 usec

======= CHANNEL f1 =======
NUC1 13C
P1 16.55 usec
P11 500.00 usec
P12 2000.00 usec
PL0 120.00 dB
PL1 -1.00 dB
SFO1 125.7942548 MHz
SP1 2.70 dB
SP2 2.70 dB
SPNAM1 Crp60,0.5,20.1
SPNAM2 Crp60comp.4
SPOFF1 0.00 Hz
SPOFF2 0.00 Hz

======= CHANNEL f2 =======
CPDPRG2 waltz16
NUC2 1H
PCPD2 100.00 usec
PL2 1.60 dB
PL12 24.50 dB
SFO2 500.2225011 MHz

===== GRADIENT CHANNEL ====
GPNAM1 SINE.100
GPNAM2 SINE.100
GPX1 0.00 %
GPX2 0.00 %
GPY1 0.00 %
GPY2 0.00 %
GPZ1 30.00 %
GPZ2 50.00 %
p15 500.00 usec
p16 1000.00 usec

F2 - Processing parameters
SI 65536
SF 125.7804190 MHz
WDW EM
SSB 0
LB 1.00 Hz
GB 0
PC 2.00

1D NMR plot parameters
CX 22.80 cm
CY 40.00 cm
F1P 220.000 ppm
F1 27671.69 Hz
F2P 0.000 ppm
F2 0.00 Hz
PPMCM 9.64912 ppm/cm
HZCM 1213.67078 Hz/cm

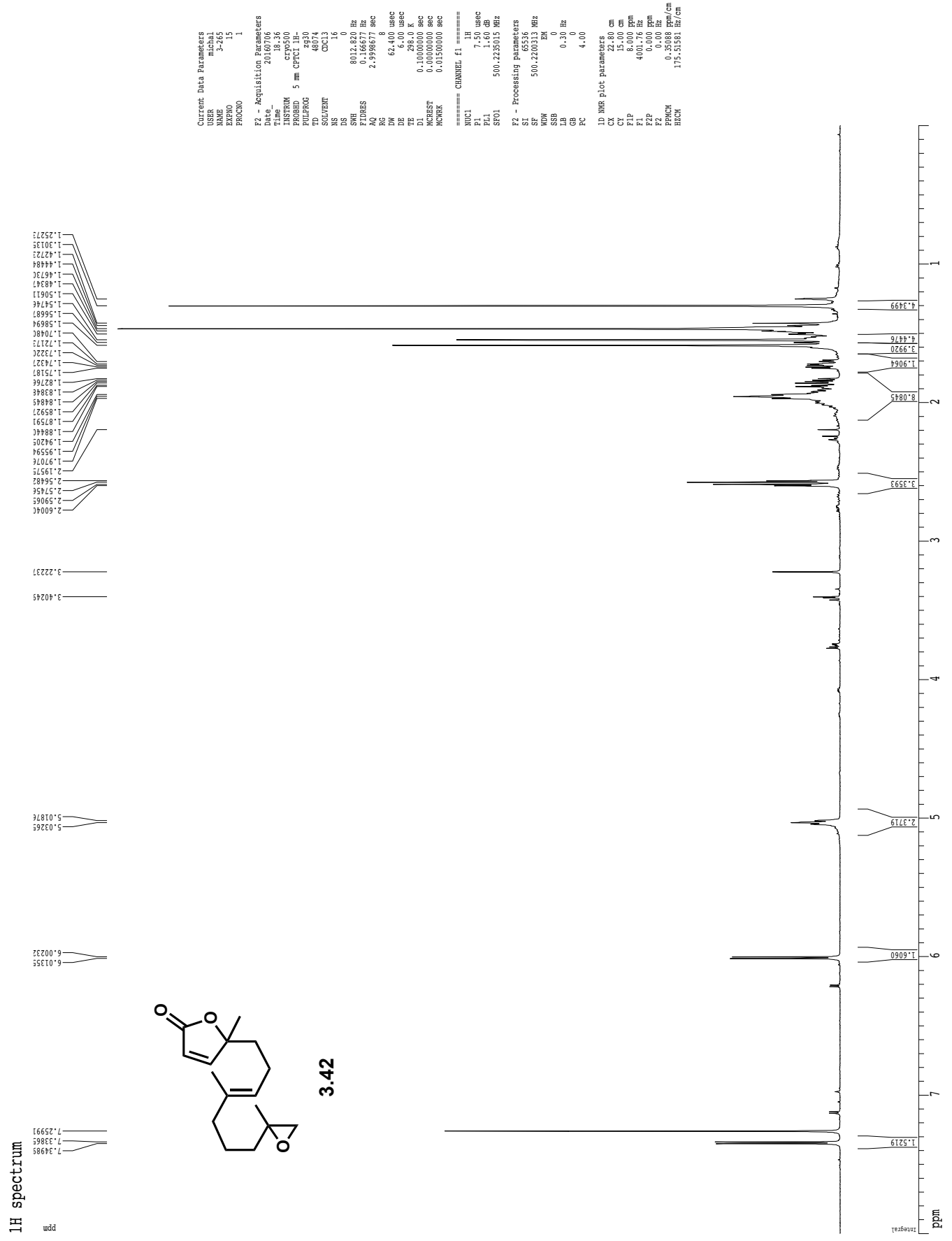
1H spectrum
3.42

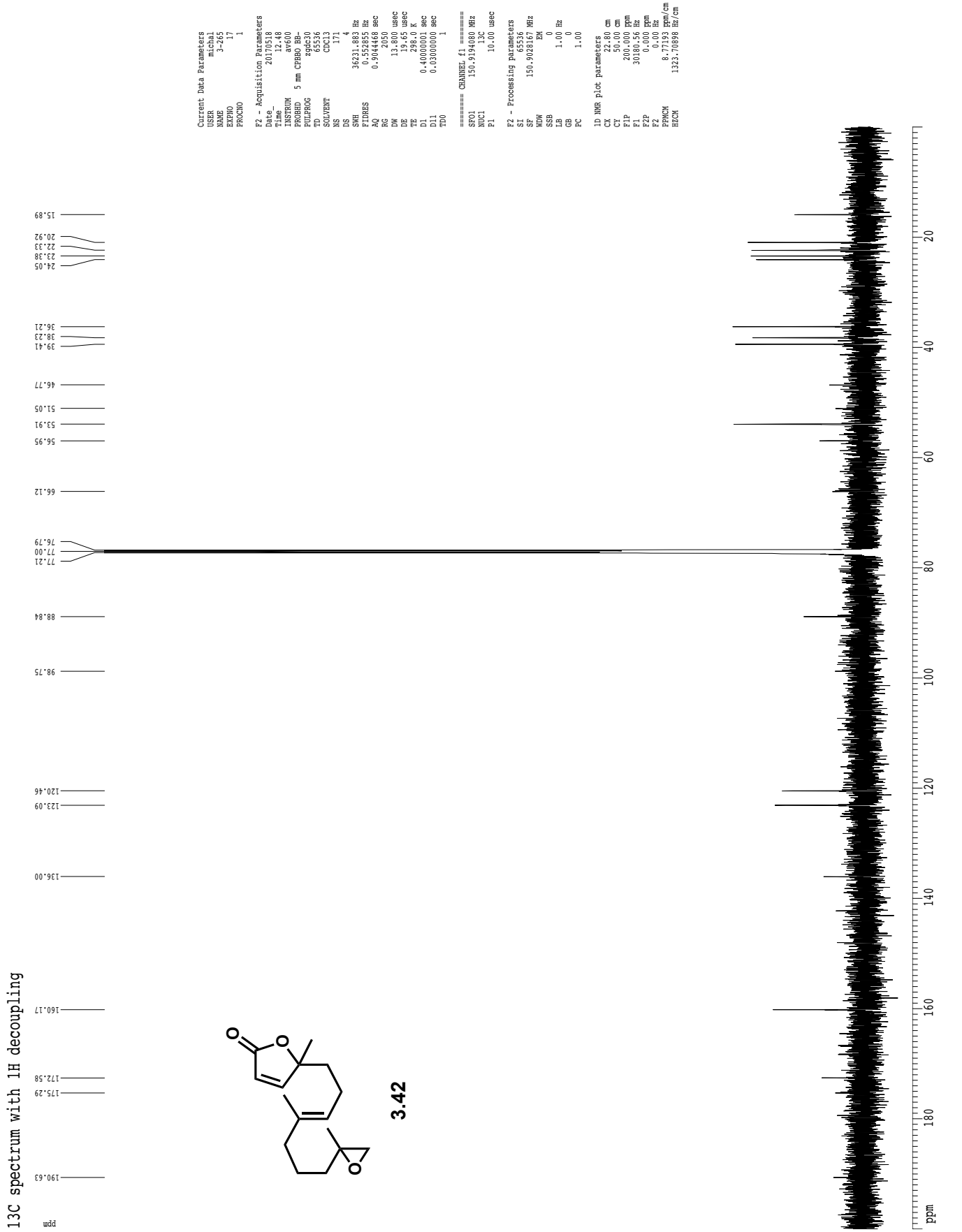
13C spectrum with 1H decoupling
Current Data Parameters
USER michal
NAME 3-265
EXPNO 17
PROCNO 1
F2 - Acquisition Parameters
Date_ 20170518
Time_ 12.48
INSTRUM av600
PROBHD 5 mm CPBBO BB-
PULPROG zgdc30
TD 65536
SOLVENT CDCl3
NS 171
DS 4
SWH 36231.883 Hz
FIDRES 0.552855 Hz
AQ 0.9044468 sec
RG 2050
DW 13.800 usec
DE 19.65 usec
TE 298.0 K
D1 0.40000001 sec
D11 0.03000000 sec
TD0 1
======== CHANNEL f1 ========
SFO1 150.9194080 MHz
NUC1 13C
P1 10.00 usec
F2 - Processing parameters
SI 65536
SF 150.9028167 MHz
WDW EM
SSB 0
LB 1.00 Hz
GB 0
PC 1.00
1D NMR plot parameters
CX 22.80 cm
CY 50.00 cm
F1P 200.000 ppm
F1 30180.56 Hz
F2P 0.000 ppm
F2 0.00 Hz
PPMCM 8.77193 ppm/cm
HZCM 1323.70898 Hz/cm
15.89
20.92
22.33
23.38
24.05
36.21
38.23
39.41
46.77
51.05
53.91
56.95
66.12
76.79
77.00
77.21
88.84
98.75
120.46
123.09
136.00
160.17
172.58
175.29
190.63
ppm
3.42

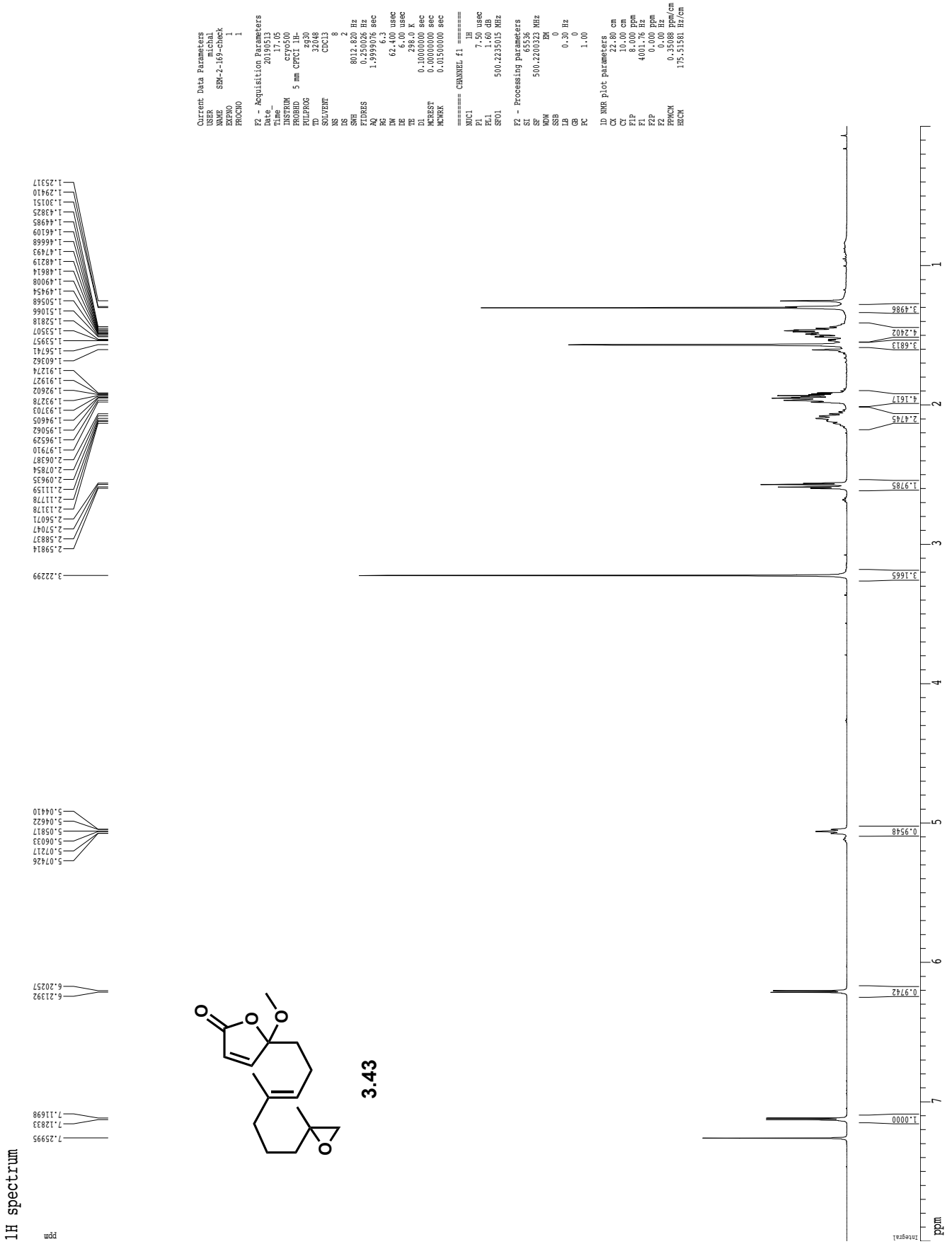
1H spectrum
Current Data Parameters
USER michal
NAME SBM-2-169-check
EXPNO 1
PROCNO 1
F2 - Acquisition Parameters
Date_ 20190513
Time 7.65
INSTRUM cryo300
PROBHD 5 mm CPTCI 1H-
PULPROG zg30
TD 32048
SOLVENT CDCl3
NS 8
DS 2
SWH 8012.820 Hz
FIDRES 0.250026 Hz
AQ 1.9999076 sec
RG 6.3
DW 62.400 usec
DE 6.00 usec
TE 298.0 K
D1 0.10000000 sec
MCREST 0.00000000 sec
MCWRK 0.01500000 sec
======== CHANNEL f1 ========
NUC1 1H
P1 7.50 usec
PL1 1.60 dB
SFO1 500.2235015 MHz
F2 - Processing parameters
SI 65536
SF 500.2200323 MHz
WDW EM
SSB 0
LB 0.30 Hz
GB 0
PC 1.00
1D NMR plot parameters
CX 22.80 cm
CY 10.00 cm
F1P 8.000 ppm
F1 4001.76 Hz
F2P 0.000 ppm
F2 0.00 Hz
PPMCM 0.35088 ppm/cm
HZCM 175.51581 Hz/cm
7.25995
7.12833
7.11698
6.21392
6.20257
5.07426
5.07217
5.06033
5.05817
5.04622
5.04410
3.22299
2.59814
2.58837
2.57047
2.56071
2.13178
2.11778
2.11159
2.09635
2.07854
2.06387
1.97910
1.96529
1.95062
1.94605
1.93703
1.93278
1.92602
1.91927
1.91274
1.60362
1.56741
1.53957
1.53507
1.52818
1.51066
1.50568
1.49454
1.49008
1.48614
1.48219
1.47493
1.46668
1.46109
1.44985
1.43825
1.30151
1.29410
1.25317
3.43
3.4986
4.2402
3.6813
4.1617
2.4745
1.9785
3.1665
0.9548
0.9742
1.0000
Integral
ppm
1
2
3
4
5
6
7
ppm

Z-restored spin-echo 13C spectrum with 1H decoupling

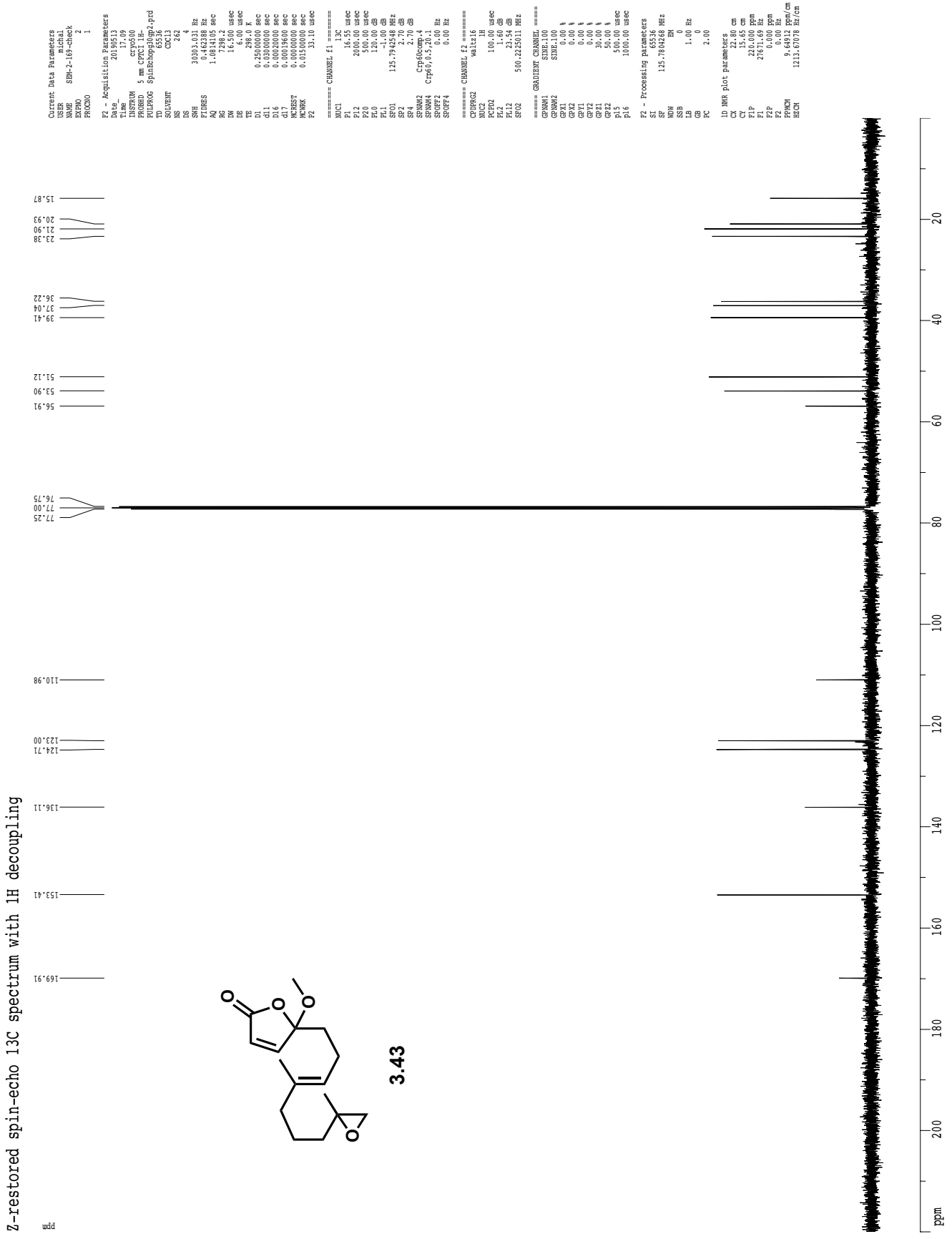

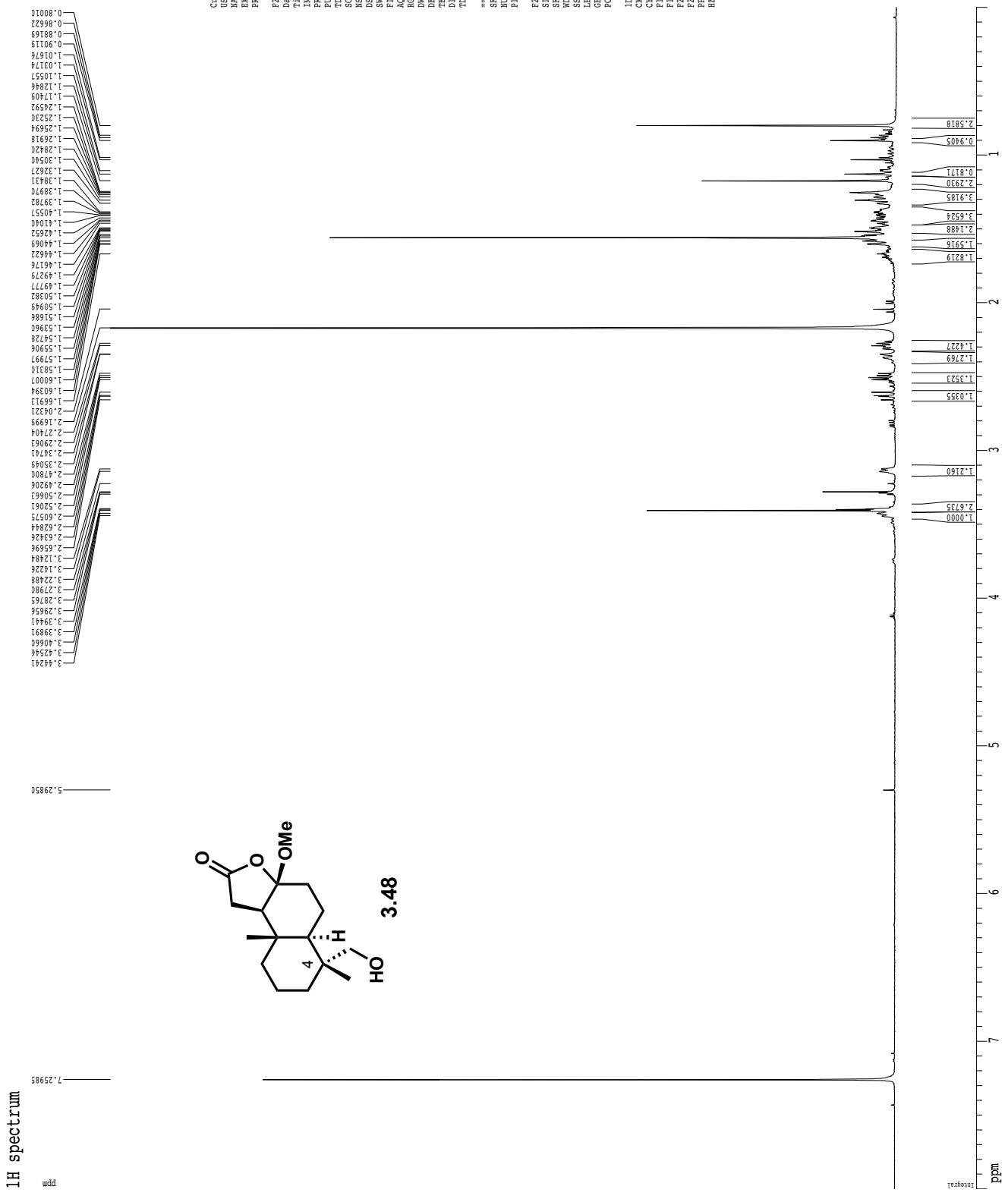
1H spectrum
Current Data Parameters
USER michal
NAME SEM-2-163-fr1
EXPNO 2
PROCNO 1
F2 - Acquisition Parameters
Date_ 20160709
Time_ 18.17
INSTRUM av600
PROBHD 5 mm CPBBO BB-
PULPROG zg30
TD 38460
SOLVENT CDCl3
NS 32
DS 2
SWH 9615.385 Hz
FIDRES 0.250010 Hz
AQ 1.9999700 sec
RG 20.2
DW 52.000 usec
DE 13.70 usec
TE 298.0 K
D1 0.10000000 sec
TD0 1
======== CHANNEL f1 ========
SFO1 600.1342009 MHz
NUC1 1H
P1 12.00 usec
F2 - Processing parameters
SI 65536
SF 600.1300355 MHz
WDW EM
SSB 0
LB 0.30 Hz
GB 0
PC 1.00
1D NMR plot parameters
CX 22.80 cm
CY 40.000 cm
F1P 8.0000 ppm
F2P 4001.444 Hz
F1 1.000 ppm
F2 0.00 ppm
PPMCM 0.35088 ppm/cm
HZCM 210.57196 Hz/cm
OMe
H
HO
4
3.48
ppm
Integral

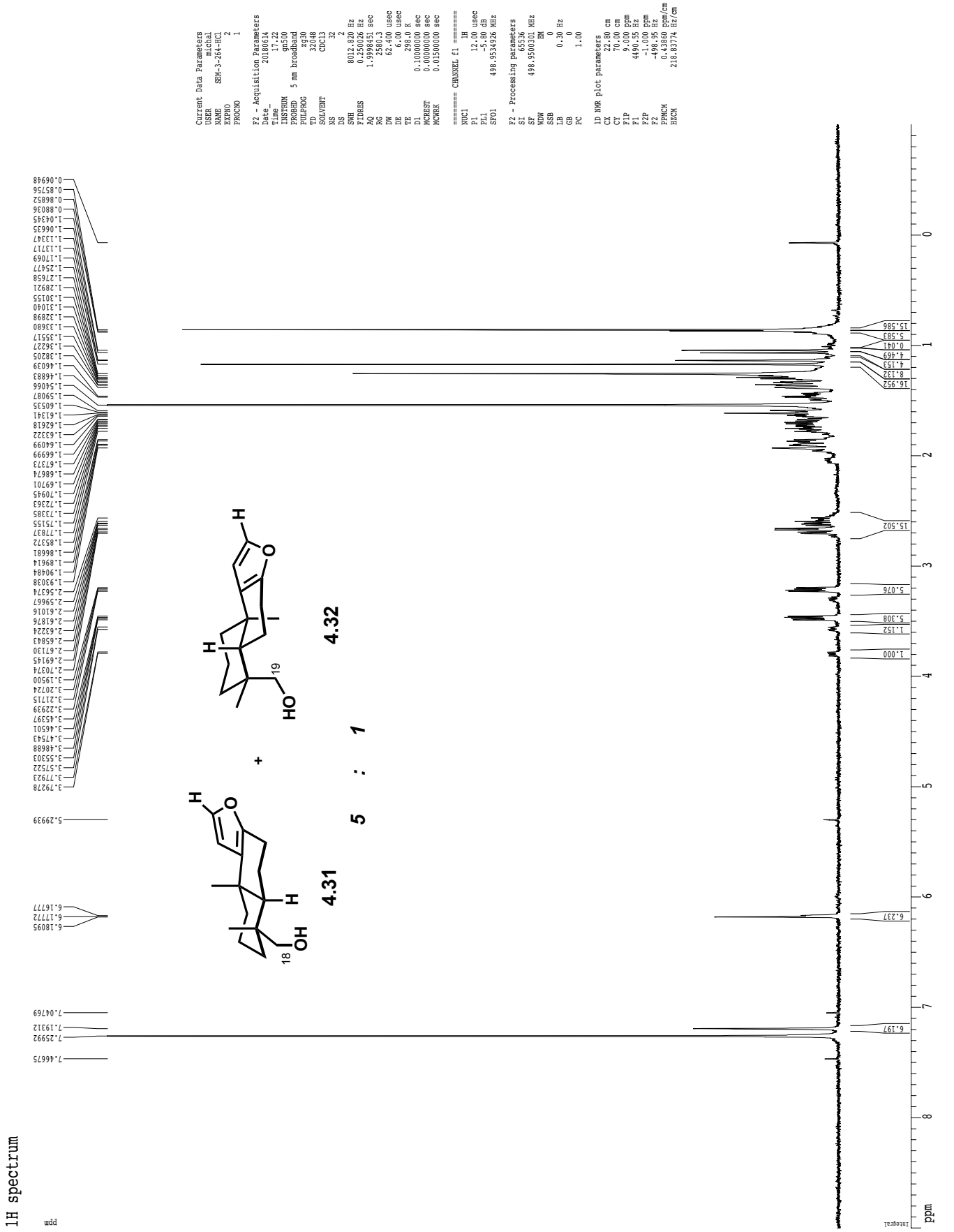
1H spectrum
Current Data Parameters
USER michal
NAME SEM-3-264-HCl
EXPNO 2
PROCNO 1
F2 - Acquisition Parameters
Date_ 20180614
Time 17.22
INSTRUM qnp500
PROBHD 5 mm broadband
PULPROG zg30
TD 32048
SOLVENT CDCl3
NS 32
DS 2
SWH 8012.820 Hz
FIDRES 0.250026 Hz
AQ 1.9998451 sec
RG 2580.3
DW 62.400 usec
DE 6.00 usec
TE 298.0 K
D1 0.10000000 sec
MCREST 0.00000000 sec
MCWRK 0.01500000 sec
======== CHANNEL f1 ========
NUC1 1H
P1 12.00 usec
PL1 -5.80 dB
SFO1 498.9534926 MHz
F2 - Processing parameters
SI 65536
SF 498.9500301 MHz
WDW EM
SSB 0
LB 0.30 Hz
GB 0
PC 1.00
1D NMR plot parameters
CX 22.80 cm
CY 70.00 cm
F1P 9.000 ppm
F1 4490.55 Hz
F2P -1.000 ppm
F2 -498.95 Hz
PPMCM 0.43860 ppm/cm
HZCM 218.83774 Hz/cm
4.31
5 : 1
4.32
ppm
Integral

1H spectrum

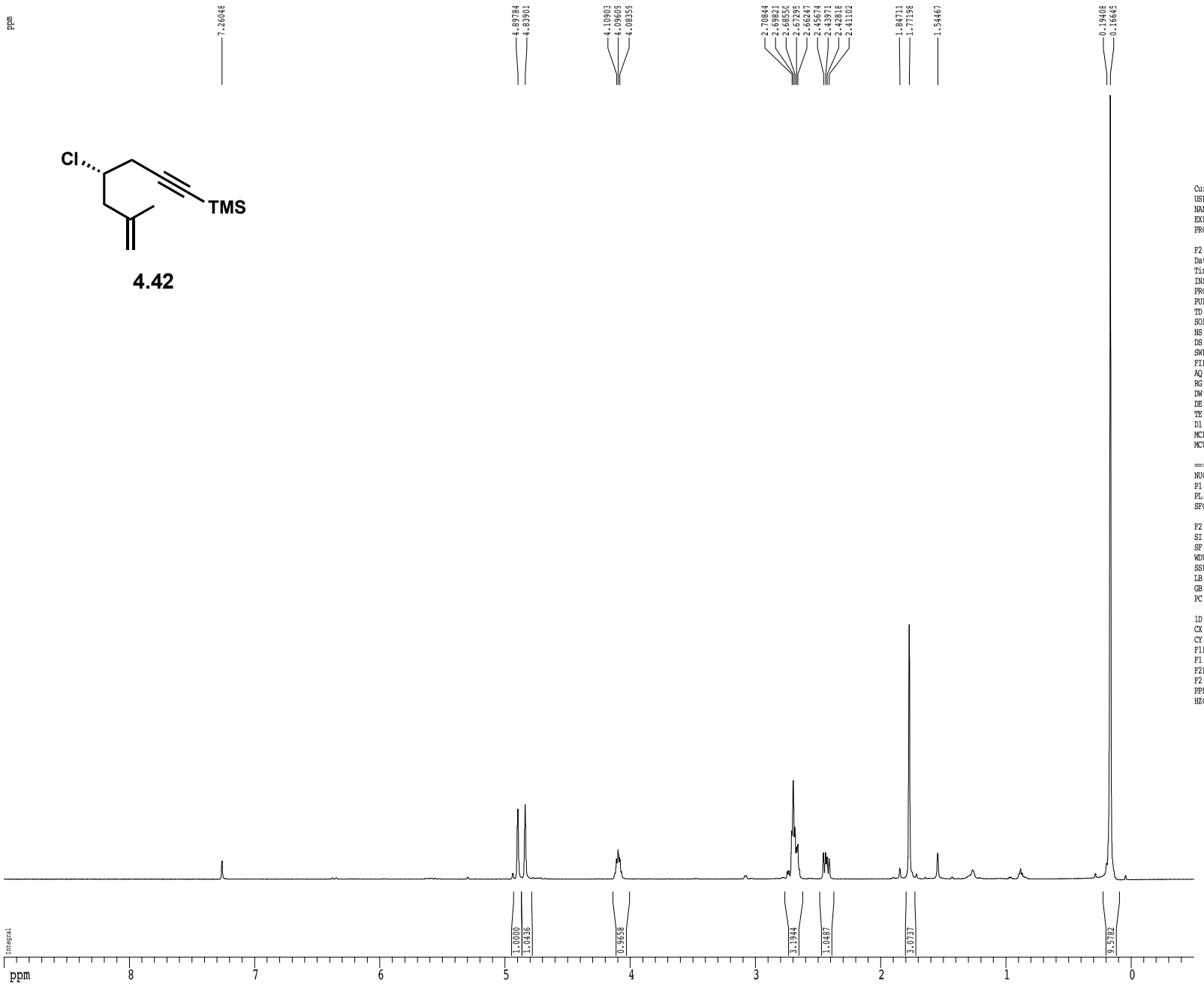

Current Data Parameters
USER michal
NAME SEM-2-241
EXPNO 2
PROCNO 1

F2 - Acquisition Parameters
Date_ 20161026
Time 18.49
INSTRUM gn500
PROBHD 5 mm broadband
PULPROG zg30
TD 32048
SOLVENT CDCl3
NS 8
DS 2
SWH 8012.820 Hz
FIDRES 0.250026 Hz
AQ 1.9998451 sec
RG 143.7
DW 62.400 usec
DE 6.00 usec
TE 298.0 K
D1 0.10000000 sec
MCREST 0.00000000 sec
MCWRK 0.01500000 sec

======= CHANNEL f1 =======
NUC1 1H
P1 12.00 usec
PL1 -5.80 dB
SFO1 499.0734935 MHz

F2 - Processing parameters
SI 65536
SF 499.0700320 MHz
WDW EM
SSB 0
LB 0.30 Hz
GB 0
PC 1.00

1D NMR plot parameters
CX 22.80 cm
CY 15.00 cm
F1P 9.000 ppm
F1 4491.63 Hz
F2P -0.500 ppm
F2 -249.53 Hz
PPMCM 0.41667 ppm/cm
HZCM 207.94586 Hz/cm

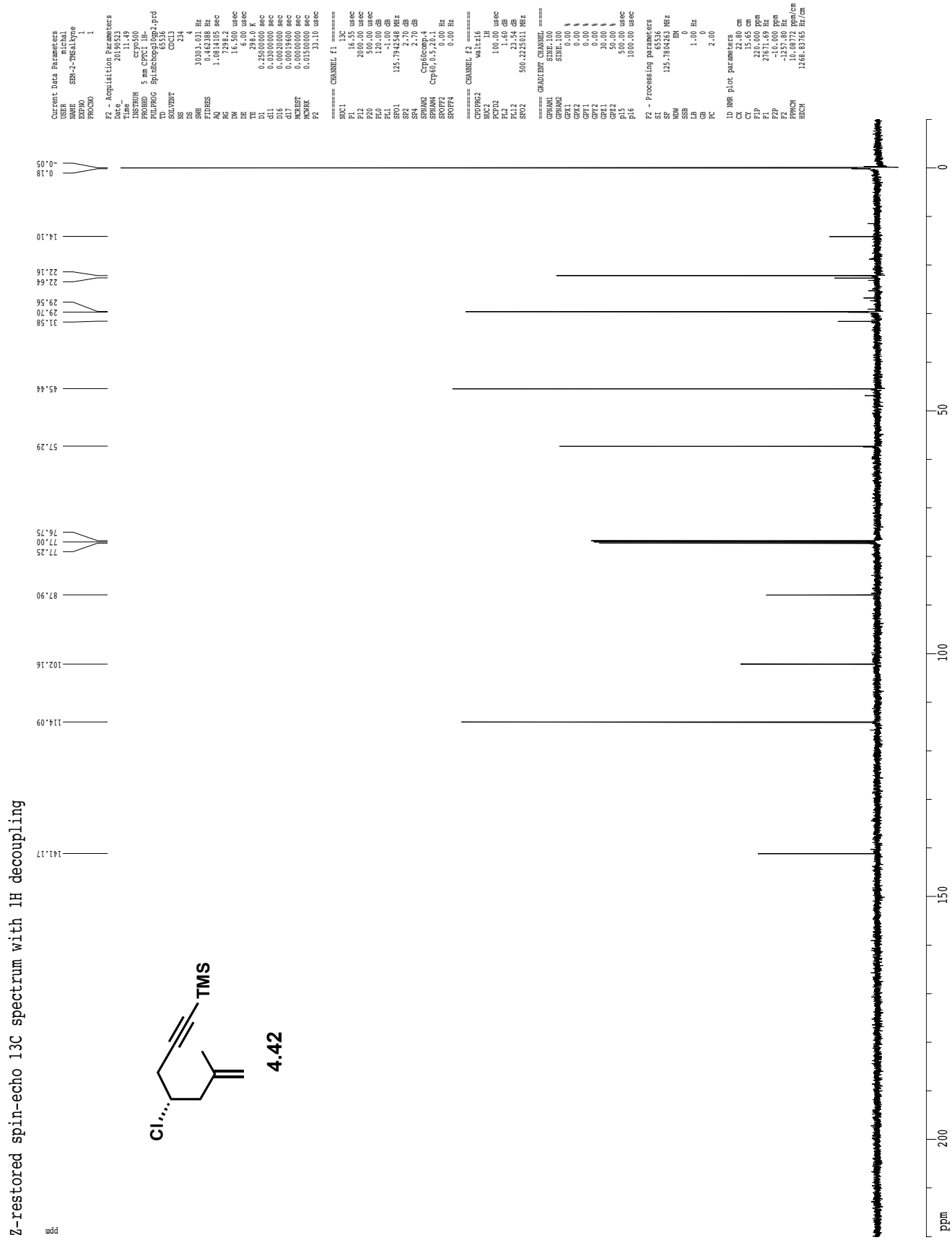
Z-restored spin-echo 13C spectrum with 1H decoupling
TMS
Cl
4.42
ppm
ppm

1H spectrum

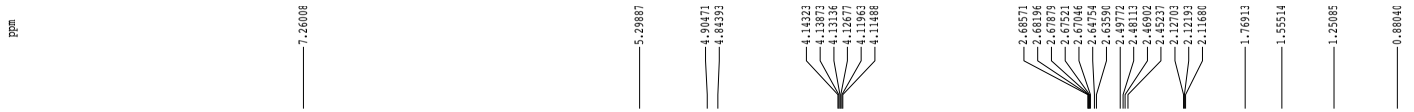

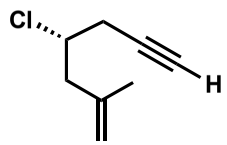

4-S1

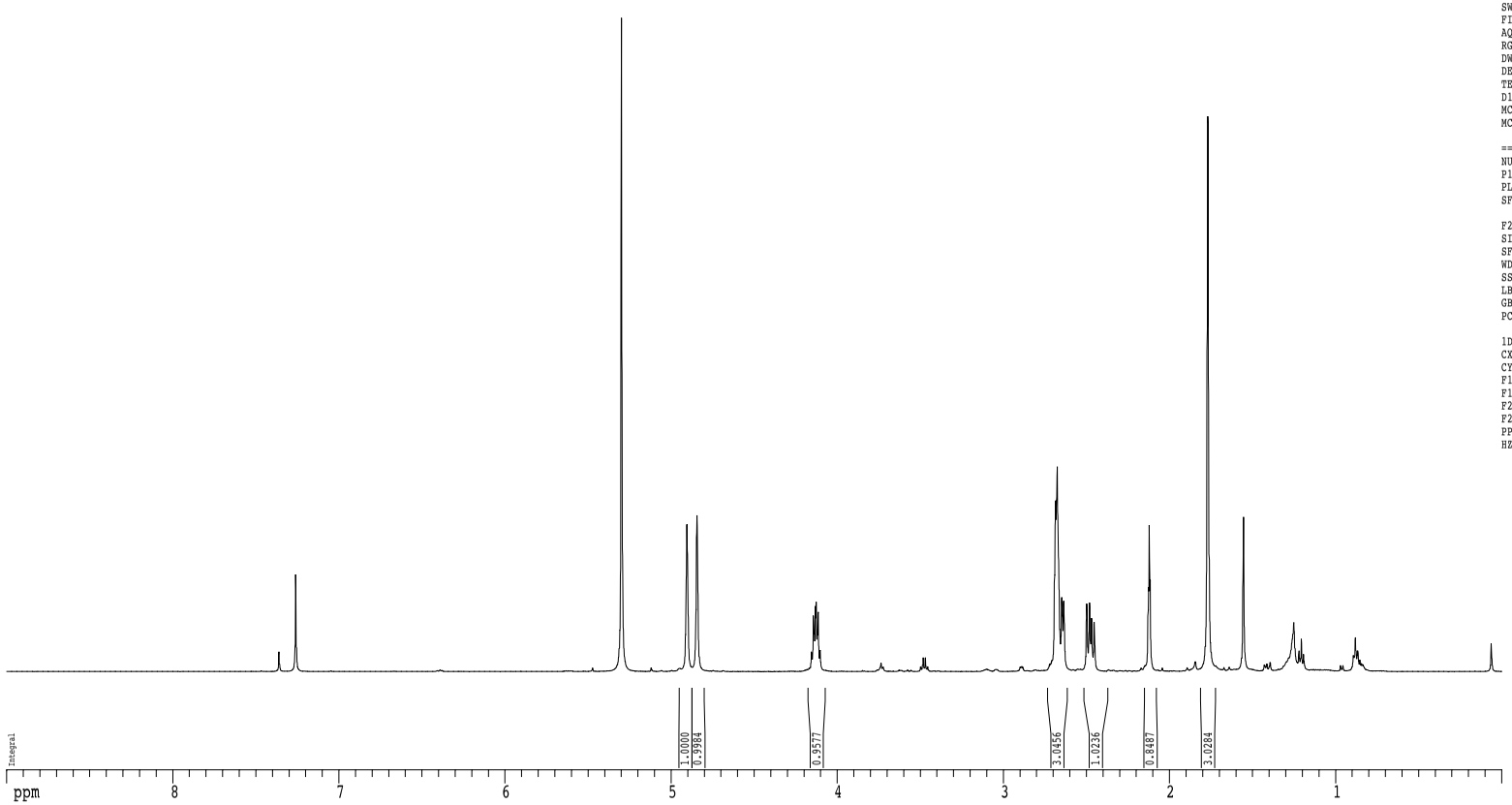


```
Current Data Parameters
USER              michal
NAME          SEM-2-223
EXPNO                 1
PROCNO                1

F2 - Acquisition Parameters
Date_          20160929
Time              19.51
INSTRUM         cryo500
PROBHD   5 mm CPTCI 1H-
PULPROG            zg30
TD                32048
SOLVENT           CDCl3
NS                   16
DS                    2
SWH            8012.820 Hz
FIDRES         0.250026 Hz
AQ             1.9998451 sec
RG                   5.7
DW                62.400 usec
DE                 6.00 usec
TE                298.0 K
D1           0.10000000 sec
MCREST       0.00000000 sec
MCWRK        0.01500000 sec

======== CHANNEL f1 ========
NUC1                 1H
P1                 7.50 usec
PL1                1.60 dB
SFO1        500.2235015 MHz

F2 - Processing parameters
SI                65536
SF          500.2200315 MHz
WDW                  EM
SSB                   0
LB                 0.30 Hz
GB                    0
PC                 4.00

1D NMR plot parameters
CX                22.80 cm
CY                10.00 cm
F1P               9.000 ppm
F1             4501.98 Hz
F2P               0.000 ppm
F2                0.00 Hz
PPMCM          0.39474 ppm/cm
HZCM          197.45528 Hz/cm
```

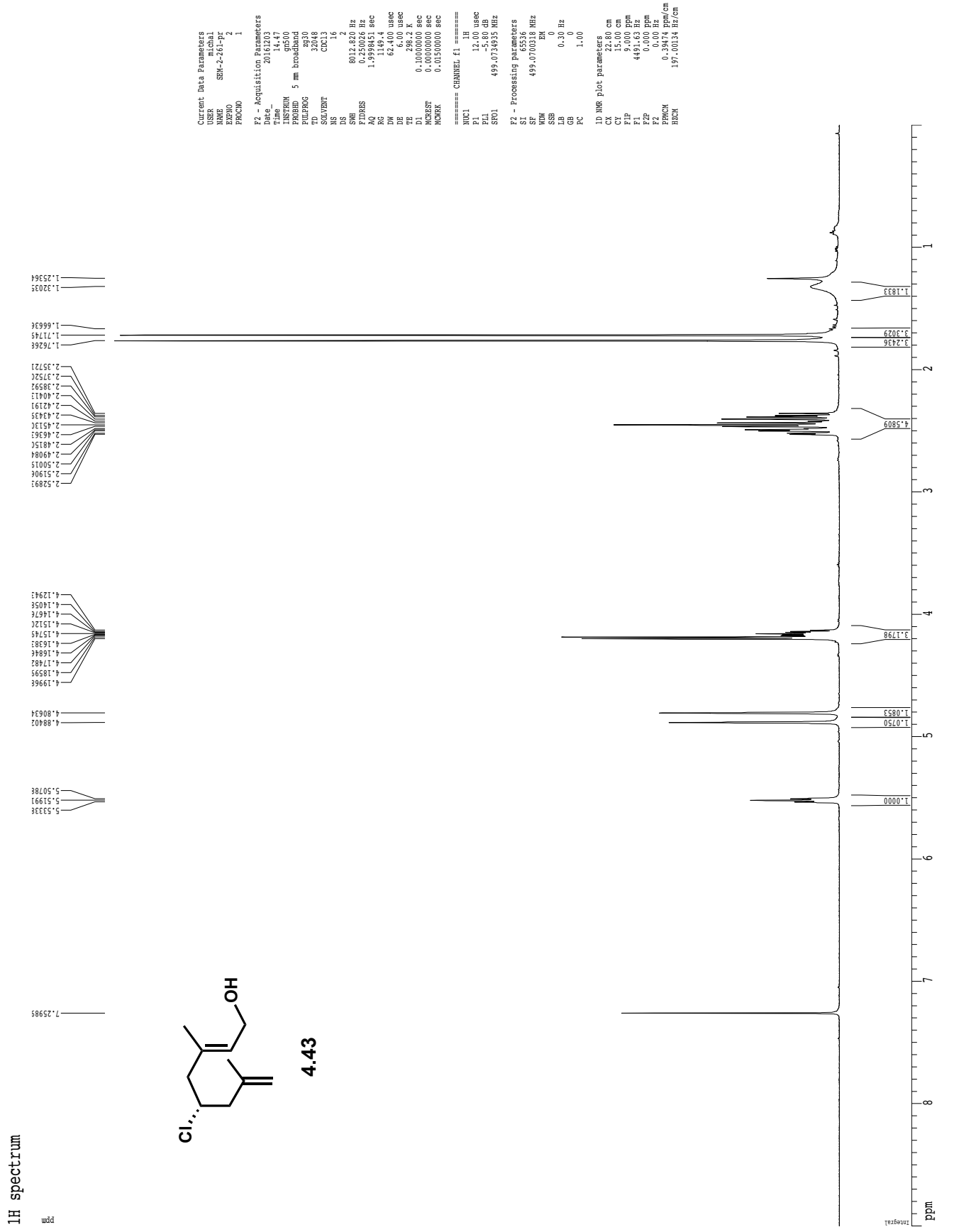
1H spectrum
Cl
OH
4.43

Z-restored spin-echo 13C spectrum with 1H decoupling

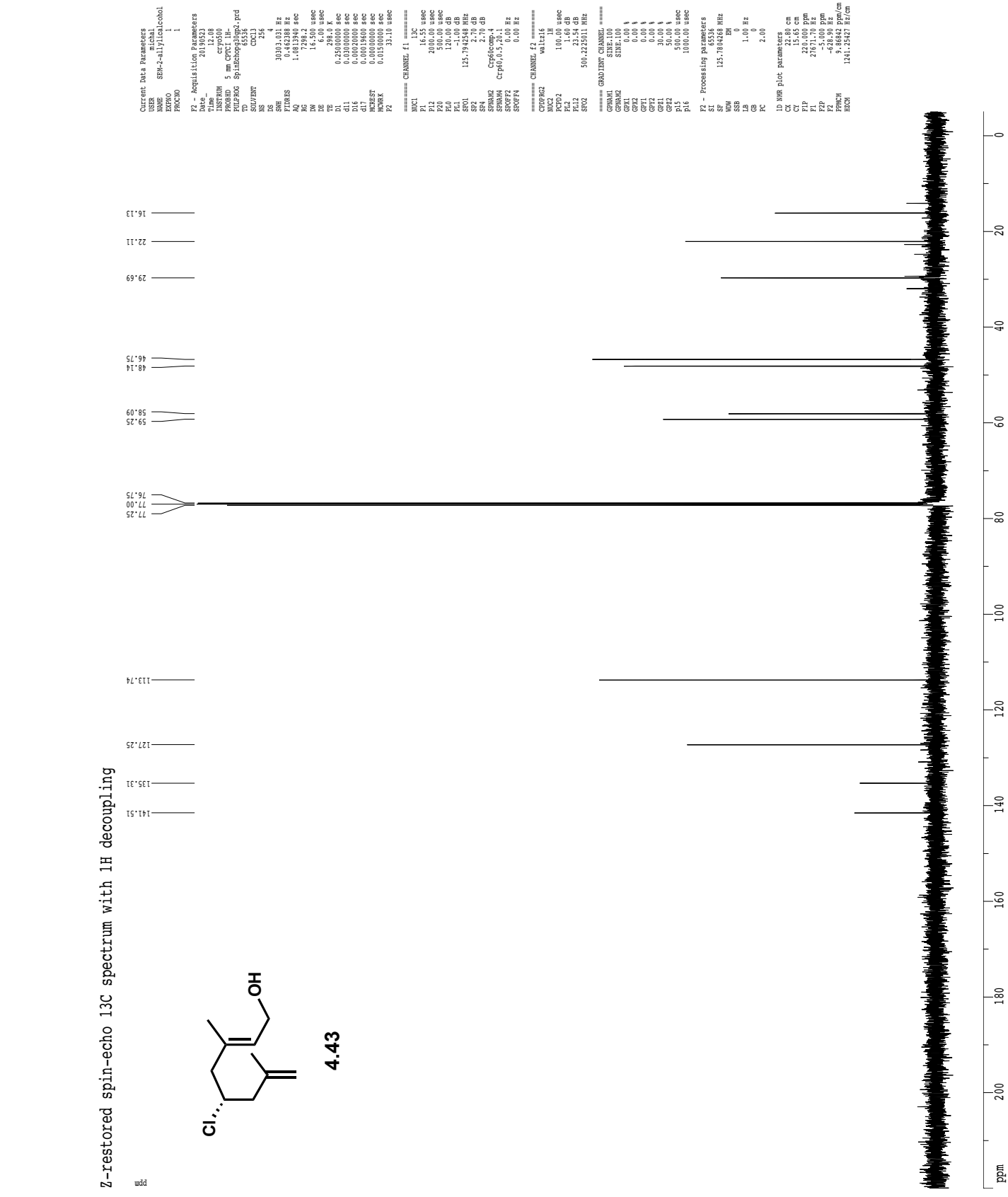

1H spectrum

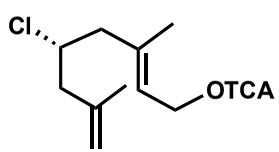

4-S2

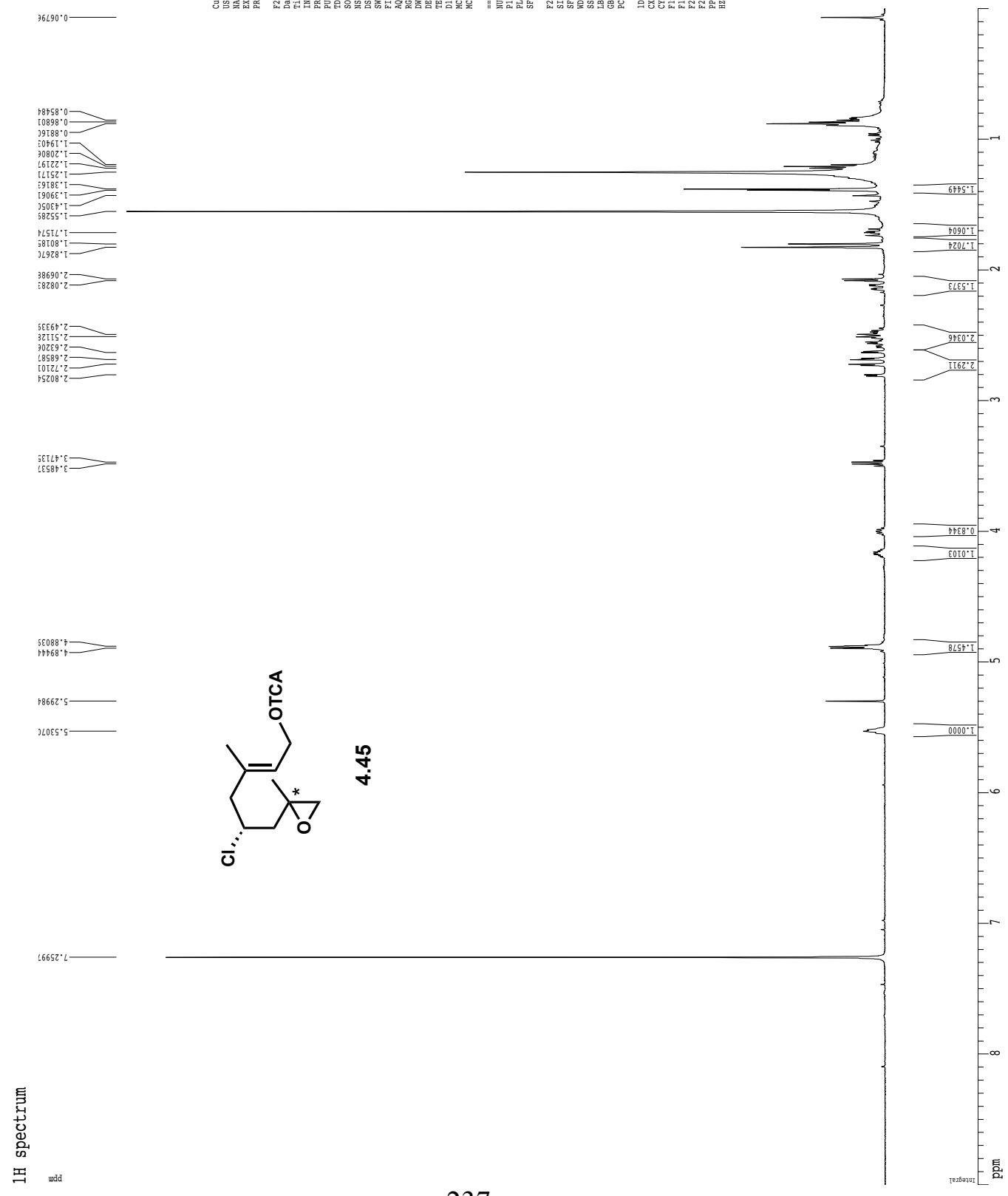
1H spectrum
Current Data Parameters
USER michal
NAME SEM-2-218
EXPNO 2
PROCNO 1
F2 - Acquisition Parameters
Date_ 20160924
Time_ 18.58
INSTRUM cryo500
PROBHD 5 mm CPTCI 1H-
PULPROG zg30
TD 32048
SOLVENT CDCl3
NS 24
DS 2
SWH 8012.820 Hz
FIDRES 0.250026 Hz
AQ 1.9998451 sec
RG 5.7
DW 62.400 usec
DE 6.00 usec
TE 298.0 K
D1 0.10000000 sec
MCREST 0.00000000 sec
MCWRK 0.01500000 sec
======= CHANNEL f1 =======
NUC1 1H
P1 7.50 usec
PL1 1.60 dB
SFO1 500.2235015 MHz
F2 - Processing parameters
SI 65536
SF 500.2200313 MHz
WDW EM
SSB 0
LB 0.30 Hz
GB 0
PC 4.00
1D NMR plot parameters
CX 22.80 cm
CY 15.00 cm
F1P 9.000 ppm
F1 4501.98 Hz
F2P 0.000 ppm
F2 0.00 Hz
PPMCM 0.39474 ppm/cm
HZCM 197.45528 Hz/cm
0.06796
0.85484
0.86801
0.88164
1.19403
1.20806
1.22197
1.25171
1.38163
1.39061
1.43050
1.55289
1.71574
1.80185
1.82670
2.06988
2.08283
2.49335
2.51126
2.63206
2.68587
2.72101
2.80254
3.46537
3.47135
4.88035
4.89444
5.29984
5.53070
7.25997
OTCA
4.45
Cl
O
1.5449
1.0604
1.7024
1.5373
2.0346
2.2911
0.8344
1.0103
1.4578
1.0000
integral
ppm
1
2
3
4
5
6
7
8

1H spectrum

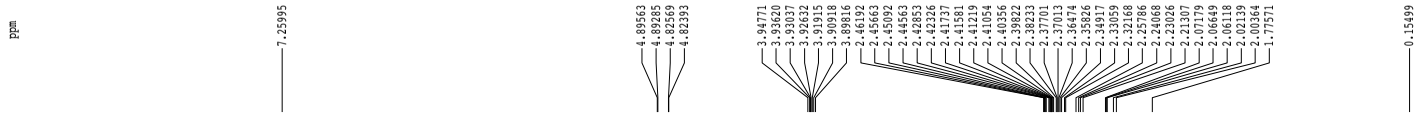

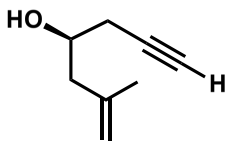

4.46

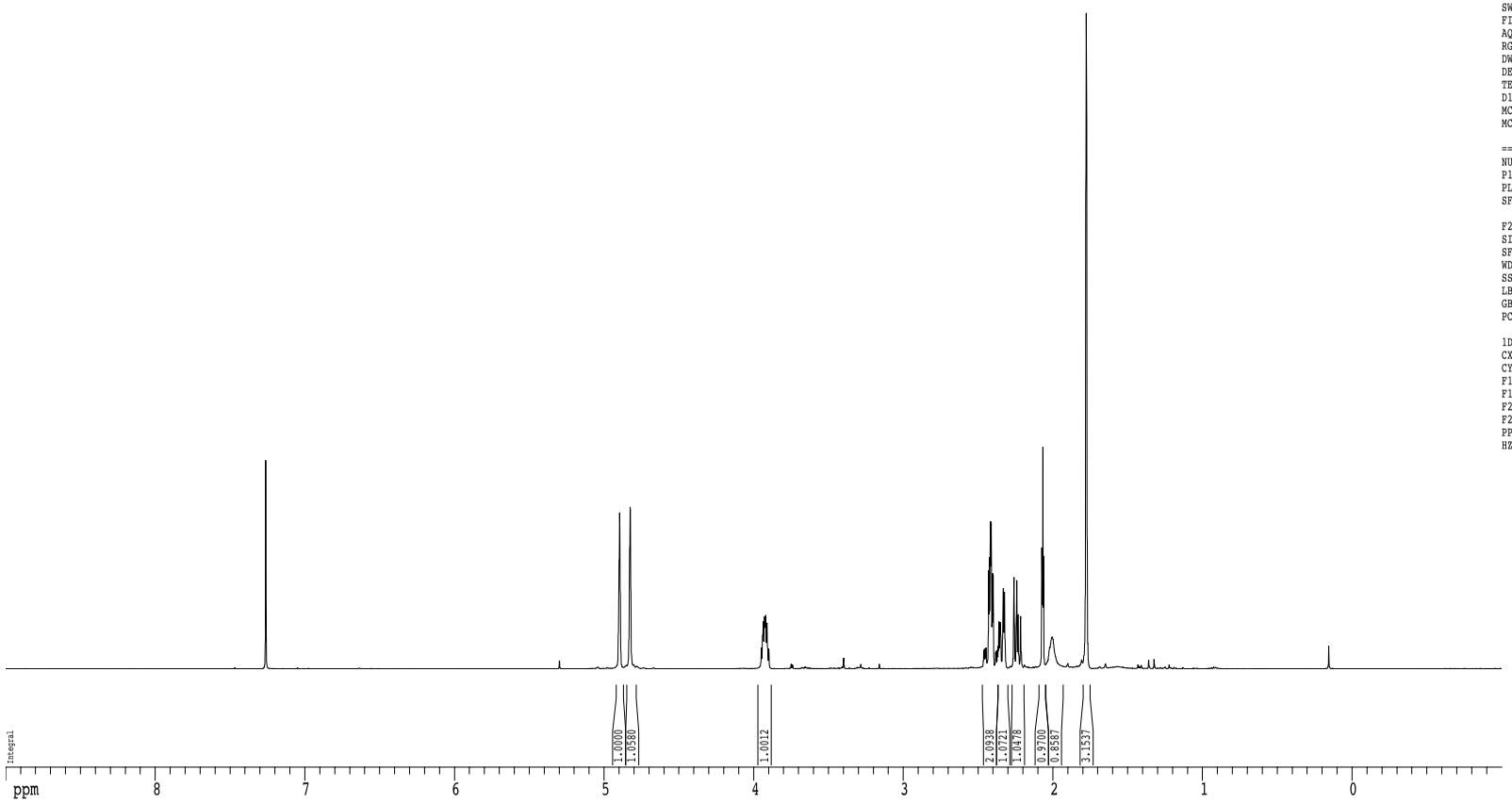

Current Data Parameters
USER michal
NAME SEM-4-41-2-pr
EXPNO 2
PROCNO 1

F2 - Acquisition Parameters
Date_ 20181211
Time 18.41
INSTRUM cryo500
PROBHD 5 mm CPTCI 1H-
PULPROG zg30
TD 32048
SOLVENT CDCl3
NS 8
DS 2
SWH 8012.820 Hz
FIDRES 0.250026 Hz
AQ 1.9998451 sec
RG 8
DW 62.400 usec
DE 6.00 usec
TE 298.0 K
D1 0.10000000 sec
MCREST 0.00000000 sec
MCWRK 0.01500000 sec

======== CHANNEL f1 ========
NUC1 1H
P1 7.50 usec
PL1 1.60 dB
SFO1 500.2235015 MHz

F2 - Processing parameters
SI 65536
SF 500.2200324 MHz
WDW EM
SSB 0
LB 0.30 Hz
GB 0
PC 1.00

1D NMR plot parameters
CX 22.80 cm
CY 10.00 cm
F1P 9.000 ppm
F1 4501.98 Hz
F2P -1.000 ppm
F2 -500.22 Hz
PPMCM 0.43860 ppm/cm
HZCM 219.39476 Hz/cm

Z-restored spin-echo 13C spectrum with 1H decoupling

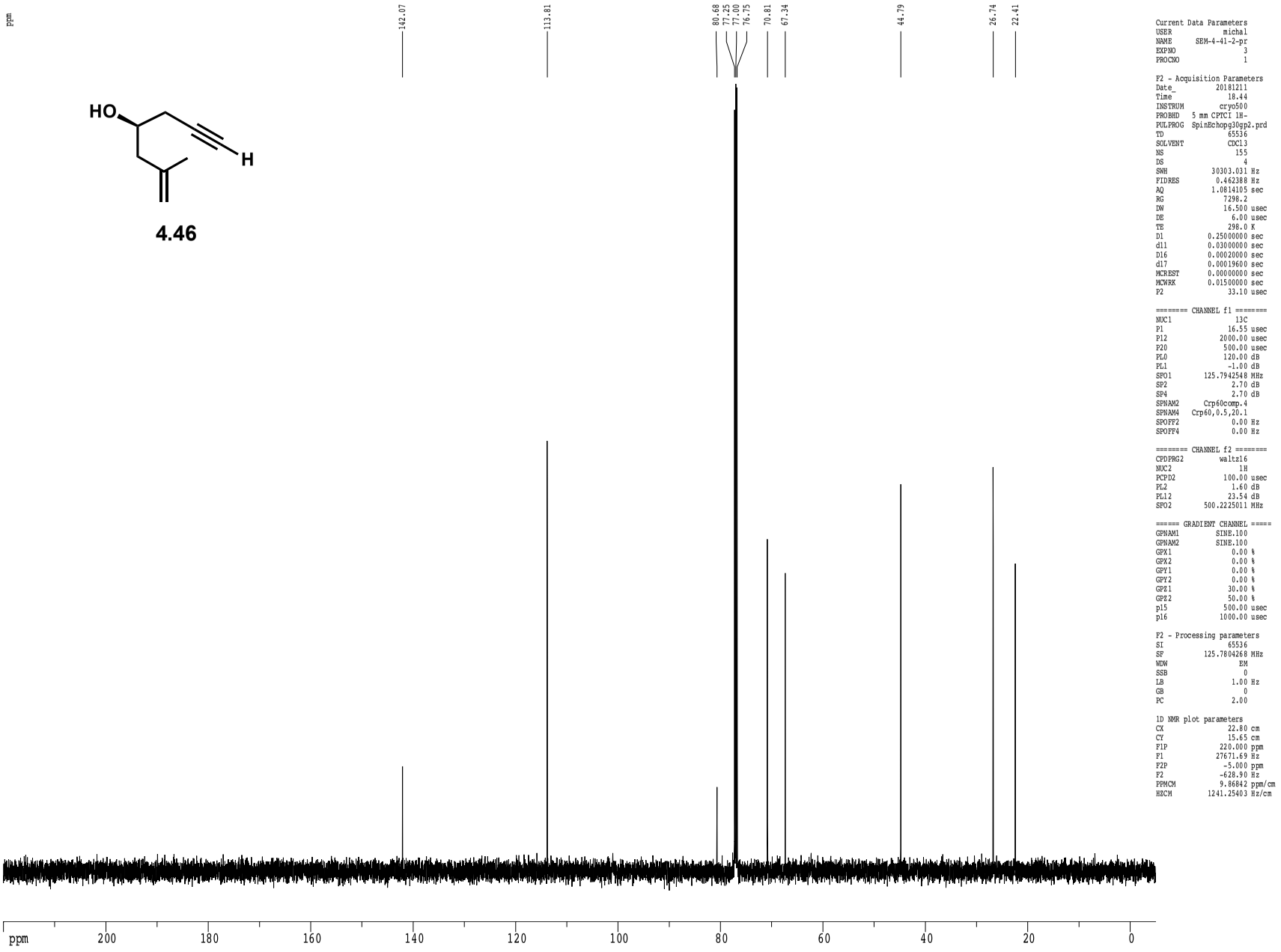

Current Data Parameters
USER michal
NAME SEM-4-41-2-pr
EXPNO 3
PROCNO 1

F2 - Acquisition Parameters
Date_ 20181211
Time 18.44
INSTRUM cryo500
PROBHD 5 mm CPTCI 1H-
PULPROG SpinEchopg30gp2.prd
TD 65536
SOLVENT CDCl3
NS 155
DS 4
SWH 30303.031 Hz
FIDRES 0.462388 Hz
AQ 1.0814105 sec
RG 7298.2
DW 16.500 usec
DE 6.00 usec
TE 298.0 K
D1 0.25000000 sec
d11 0.03000000 sec
D16 0.00020000 sec
d17 0.00019600 sec
MCREST 0.00000000 sec
MCWRK 0.01500000 sec
P2 33.10 usec

======= CHANNEL f1 =======
NUC1 13C
P1 16.55 usec
P12 2000.00 usec
P20 500.00 usec
PL0 120.00 dB
PL1 -1.00 dB
SFO1 125.7942548 MHz
SP2 2.70 dB
SP4 2.70 dB
SPNAM2 Crp60comp.4
SPNAM4 Crp60,0.5,20.1
SPOFF2 0.00 Hz
SPOFF4 0.00 Hz

======= CHANNEL f2 =======
CPDPRG2 waltz16
NUC2 1H
PCPD2 100.00 usec
PL2 1.60 dB
PL12 23.54 dB
SFO2 500.2225011 MHz

===== GRADIENT CHANNEL =====
GPNAM1 SINE.100
GPNAM2 SINE.100
GPX1 0.00 %
GPX2 0.00 %
GPY1 0.00 %
GPY2 0.00 %
GPZ1 30.00 %
GPZ2 50.00 %
p15 500.00 usec
p16 1000.00 usec

F2 - Processing parameters
SI 65536
SF 125.7804268 MHz
WDW EM
SSB 0
LB 1.00 Hz
GB 0
PC 2.00

1D NMR plot parameters
CX 22.80 cm
CY 15.65 cm
F1P 220.000 ppm
F1 27671.69 Hz
F2P -5.000 ppm
F2 -628.90 Hz
PPMCM 9.86842 ppm/cm
HZCM 1241.25403 Hz/cm

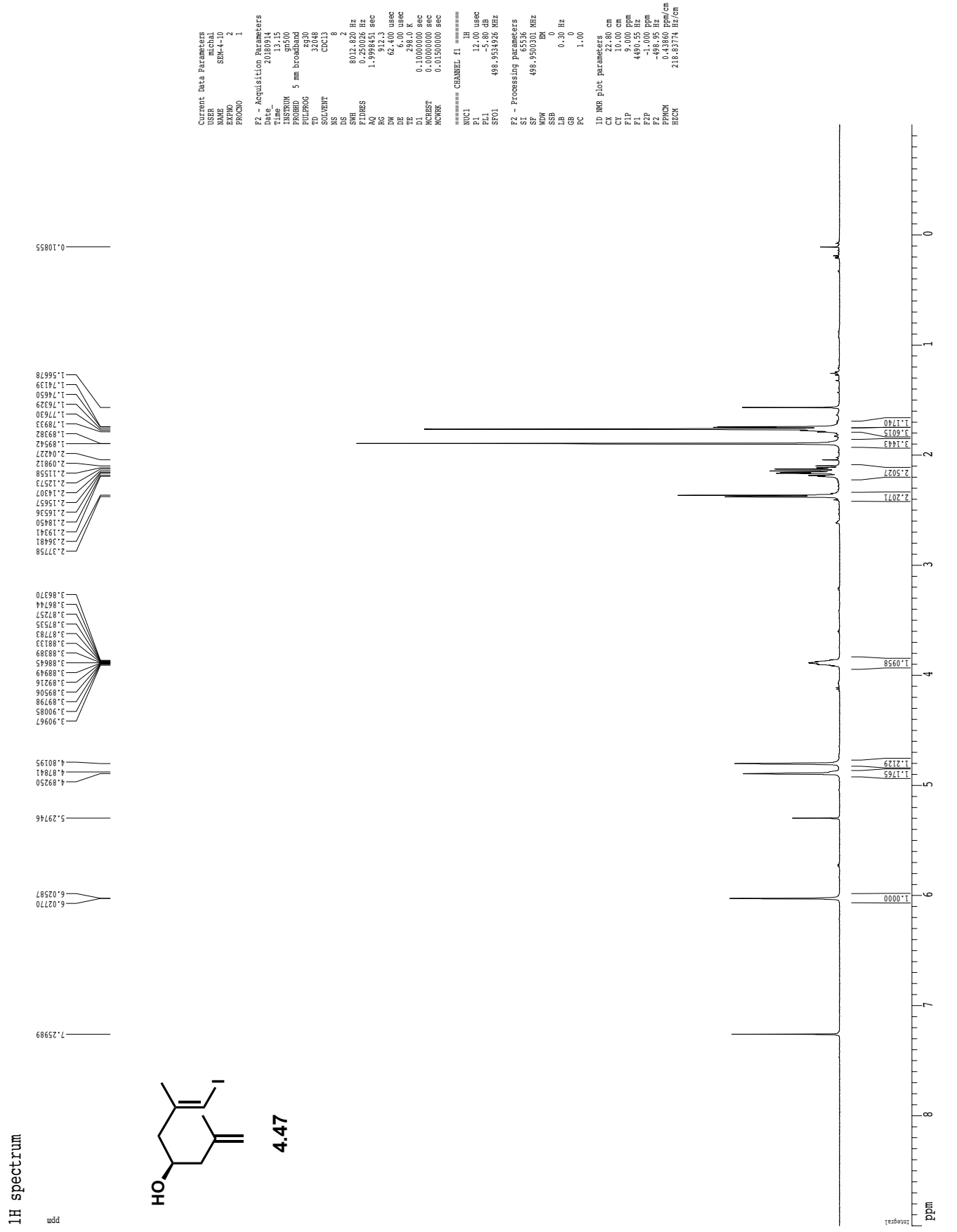
1H spectrum
4.47
HO
I
Current Data Parameters
USER michal
NAME SEM-4-10
EXPNO 2
PROCNO 1
F2 - Acquisition Parameters
Date_ 20160914
Time 13.15
INSTRUM cp500
PROBHD 5 mm broadband
PULPROG zg30
TD 32048
SOLVENT CDCl3
NS 8
DS 2
SWH 8012.820 Hz
FIDRES 0.250026 Hz
AQ 1.9998451 sec
RG 912.3
DW 62.400 usec
DE 6.00 usec
TE 298.0 K
D1 0.10000000 sec
MCREST 0.00000000 sec
MCWRK 0.01500000 sec
======== CHANNEL f1 ========
NUC1 1H
P1 12.00 usec
PL1 -5.80 dB
SFO1 498.9534926 MHz
F2 - Processing parameters
SI 65536
SF 498.9500201 MHz
WDW EM
SSB 0
LB 0.30 Hz
GB 0
PC 1.00
1D NMR plot parameters
CX 22.80 cm
CY 10.00 cm
F1P 9.000 ppm
F1 4490.55 Hz
F2P -1.000 ppm
F2 -498.95 Hz
PPMCM 0.43860 ppm/cm
HZCM 218.83774 Hz/cm
0.10855
1.56678
1.74139
1.74650
1.76329
1.77630
1.78933
1.89382
1.89542
2.04227
2.09812
2.11558
2.12573
2.14307
2.15657
2.16536
2.18450
2.19341
2.36481
2.37758
3.86370
3.86744
3.87257
3.87535
3.87783
3.88133
3.88389
3.88645
3.88949
3.89216
3.89506
3.89798
3.90085
3.90967
4.80195
4.87841
4.89250
5.29746
6.02587
6.02770
7.25989
1.1740
3.6015
3.1443
2.5027
2.2071
1.0958
1.2129
1.1765
1.0000
integral
ppm
0
1
2
3
4
5
6
7
8

Z-restored spin-echo 13C spectrum with 1H decoupling

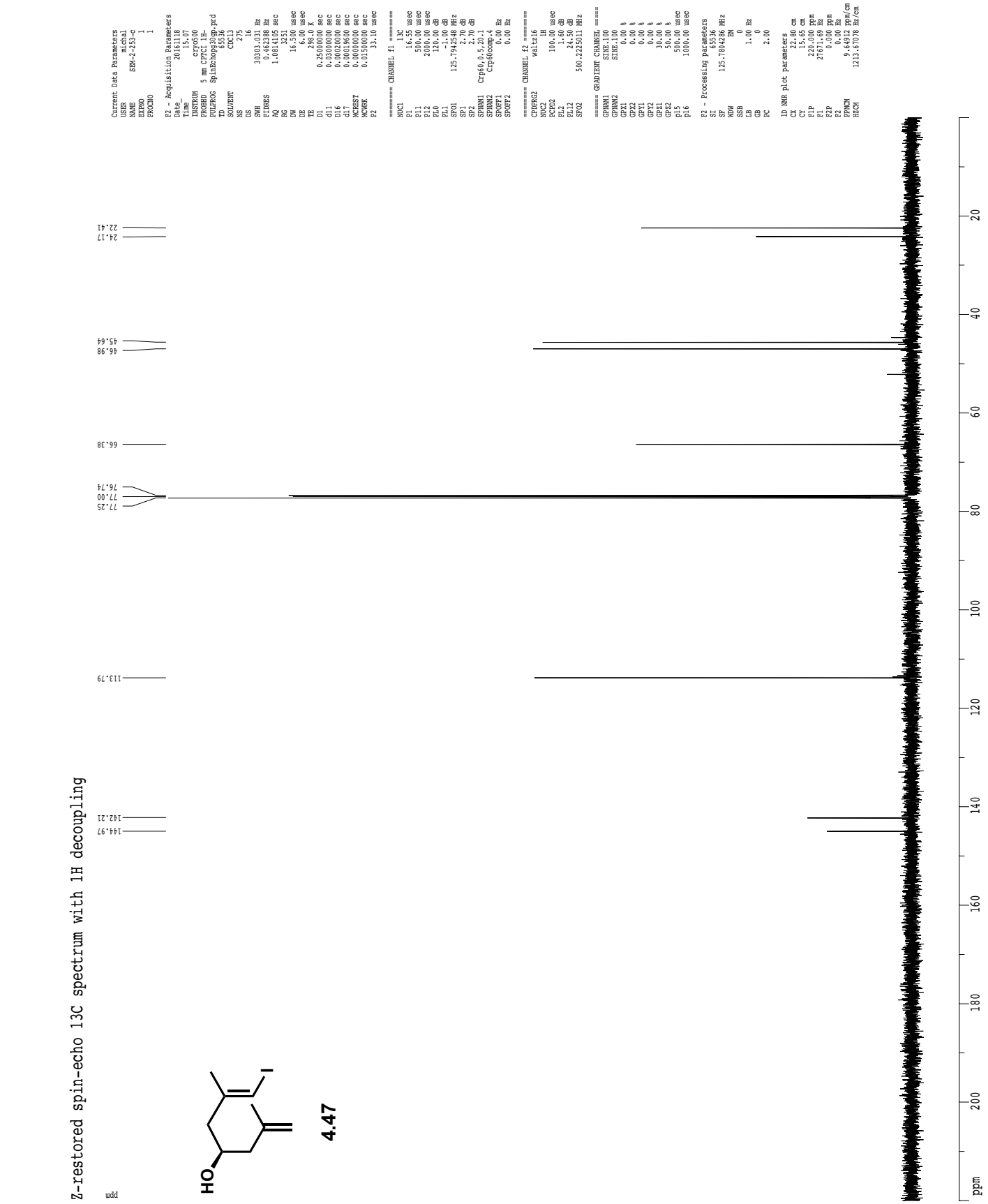

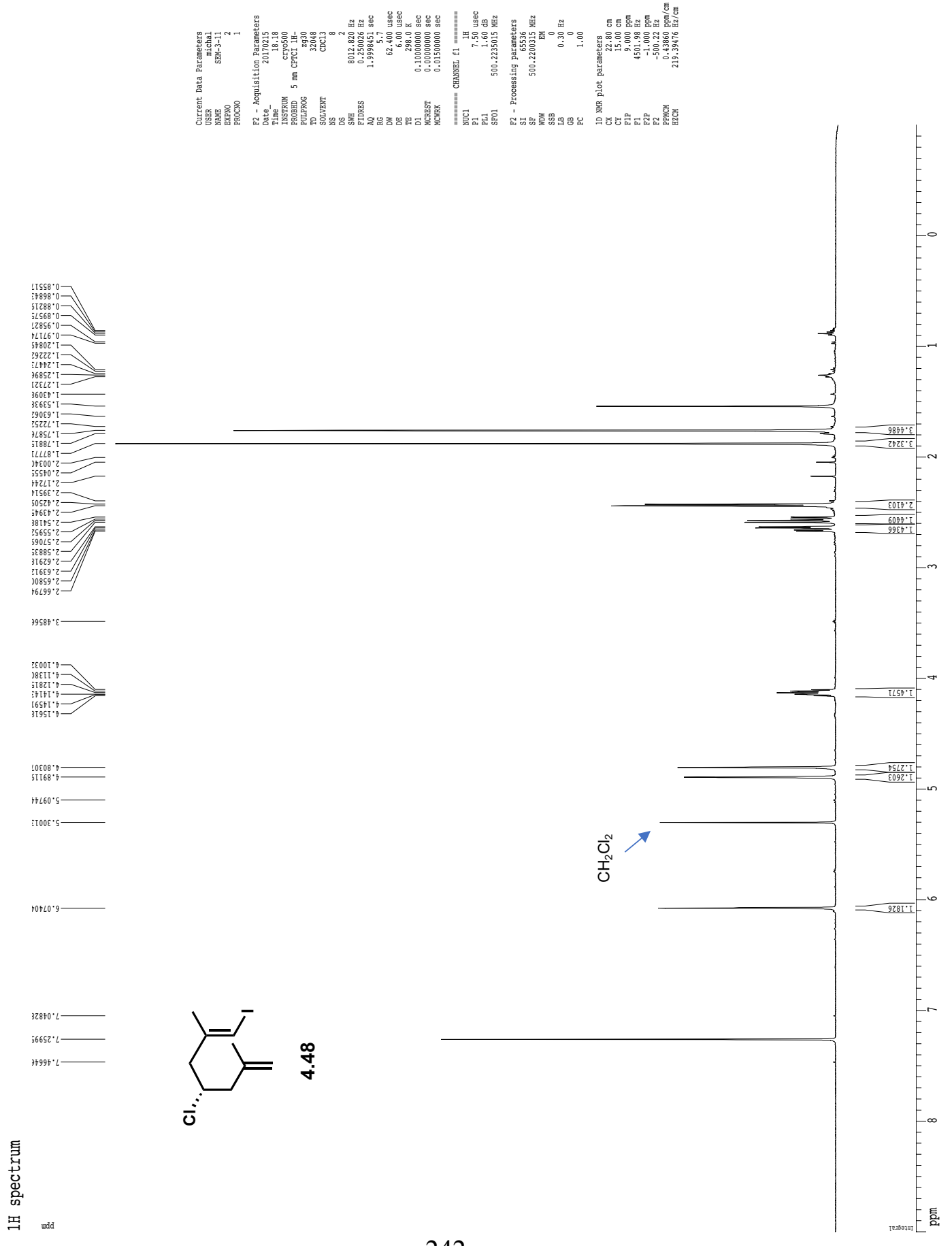
1H spectrum
Current Data Parameters
USER michal
NAME SEM-3-11
EXPNO 2
PROCNO 1
F2 - Acquisition Parameters
Date_ 20170215
Time 18.18
INSTRUM cryo500
PROBHD 5 mm CPTCI 1H-
PULPROG zg30
TD 32048
SOLVENT CDCl3
NS 8
DS 2
SWH 8012.820 Hz
FIDRES 0.250026 Hz
AQ 1.9998451 sec
RG 5.7
DW 62.400 usec
DE 6.00 usec
TE 298.0 K
D1 0.10000000 sec
MCREST 0.00000000 sec
MCWRK 0.01500000 sec
======== CHANNEL f1 ========
NUC1 1H
P1 7.50 usec
PL1 1.60 dB
SFO1 500.2235015 MHz
F2 - Processing parameters
SI 65536
SF 500.2200315 MHz
WDW EM
SSB 0
LB 0.30 Hz
GB 0
PC 1.00
1D NMR plot parameters
CX 22.80 cm
CY 15.00 cm
F1P 9.000 ppm
F1 4501.98 Hz
F2P -1.000 ppm
F2 -500.22 Hz
PPMCM 0.43860 ppm/cm
HZCM 219.39476 Hz/cm
7.46646
7.25995
7.04828
6.07404
5.30013
5.09744
4.89115
4.80307
4.15618
4.14543
4.14591
4.11380
4.12815
4.10032
3.48566
2.66794
2.65800
2.63912
2.62918
2.58835
2.57065
2.55952
2.54188
2.43946
2.42505
2.39514
2.17244
2.04555
2.00340
1.87771
1.78815
1.75874
1.72252
1.63062
1.55938
1.43098
1.27321
1.25894
1.24473
1.22262
1.20845
0.97174
0.95827
0.89575
0.88215
0.86843
0.85517
3.44486
3.32421
2.41031
1.44091
1.43661
1.45711
1.27541
1.26031
1.18261
CH2Cl2
Cl
I
4.48
ppm
Integral

13C spectrum with 1H decoupling

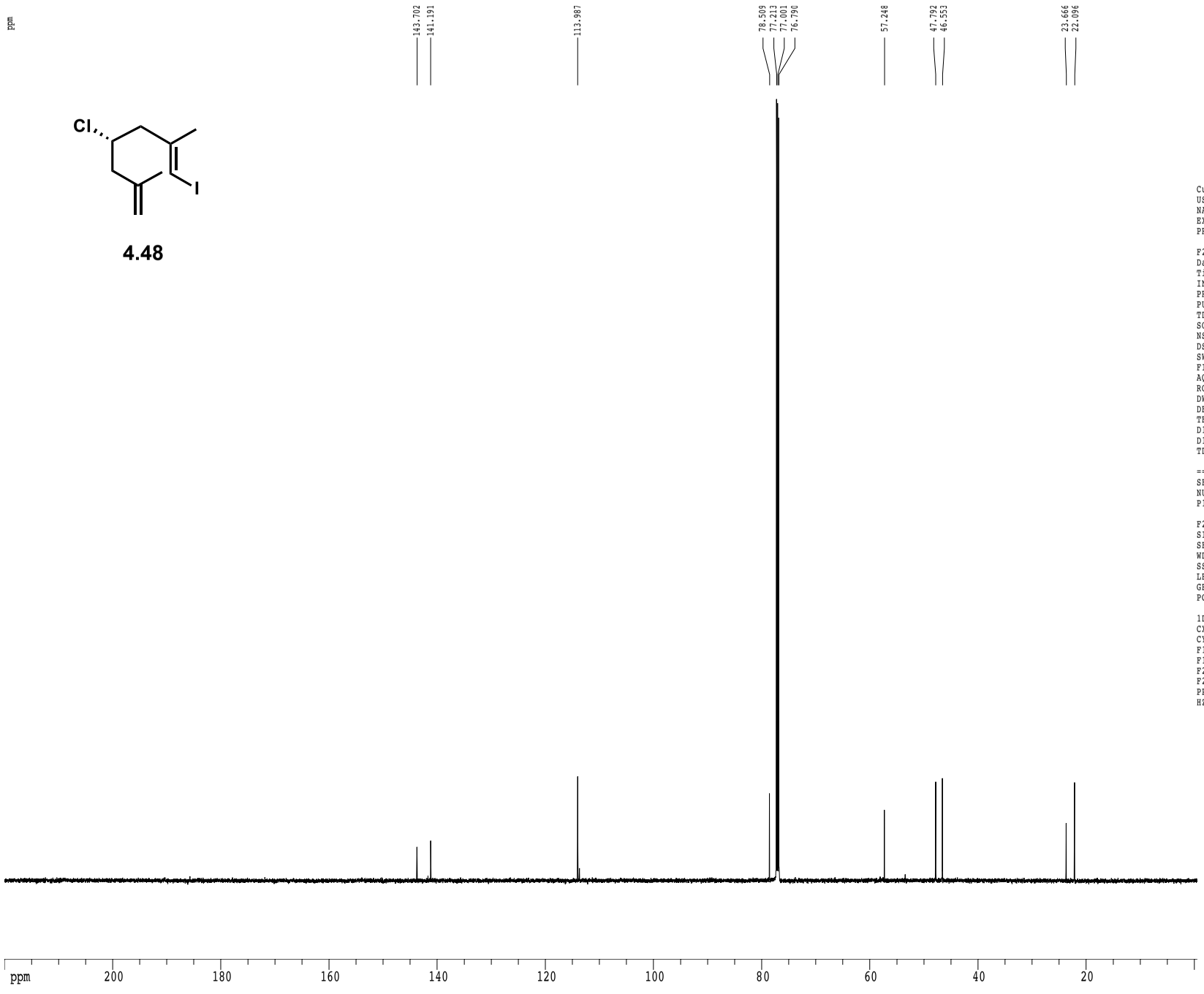

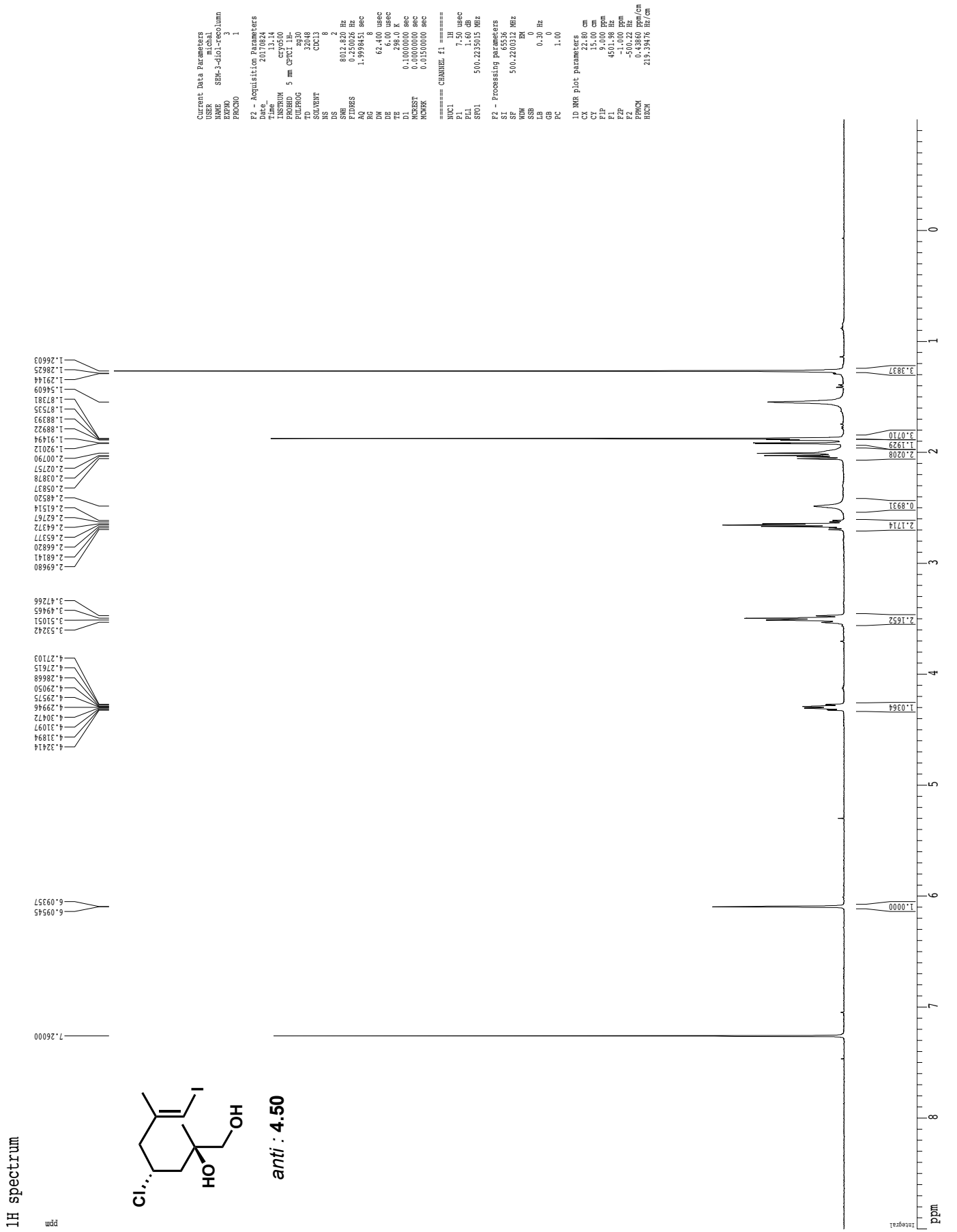
1H spectrum
anti : 4.50
Cl
I
OH
HO
ppm
integral
Current Data Parameters
USER michal
NAME SBM-3-diol-recolumn
EXPNO 3
PROCNO 1
F2 - Acquisition Parameters
Date_ 20170824
Time_ 13.14
INSTRUM cryo500
PROBHD 5 mm CPTCI 1H-
PULPROG zg30
TD 32048
SOLVENT CDCl3
NS 8
DS 2
SWH 8012.820 Hz
FIDRES 0.250026 Hz
AQ 1.9999451 sec
RG 8
DW 62.400 usec
DE 6.00 usec
TE 298.0 K
D1 0.10000000 sec
MCREST 0.00000000 sec
MCWRK 0.01500000 sec
======== CHANNEL f1 ========
NUC1 1H
P1 7.50 usec
PL1 1.60 dB
SFO1 500.2235015 MHz
F2 - Processing parameters
SI 65536
SF 500.2200312 MHz
WDW EM
SSB 0
LB 0.30 Hz
GB 0
PC 1.00
1D NMR plot parameters
CX 22.80 cm
CY 15.00 cm
F1P 9.000 ppm
F1 4501.98 Hz
F2P -1.000 ppm
F2 -500.22 Hz
PPMCM 0.43860 ppm/cm
HZCM 219.39476 Hz/cm
7.26000
6.09545
6.09357
4.32414
4.31894
4.31097
4.30472
4.29946
4.29575
4.29050
4.28668
4.27615
4.27103
3.53242
3.51051
3.49465
3.47266
2.69680
2.68141
2.66820
2.65377
2.64372
2.62767
2.61514
2.48520
2.05837
2.03878
2.02757
2.00790
1.92012
1.91494
1.89222
1.88393
1.87535
1.87381
1.54609
1.29144
1.28625
1.26603
1.000
1.0364
2.1652
2.1714
0.8931
2.0208
1.1929
3.0710
3.3837

Z-restored spin-echo 13C spectrum with 1H decoupling

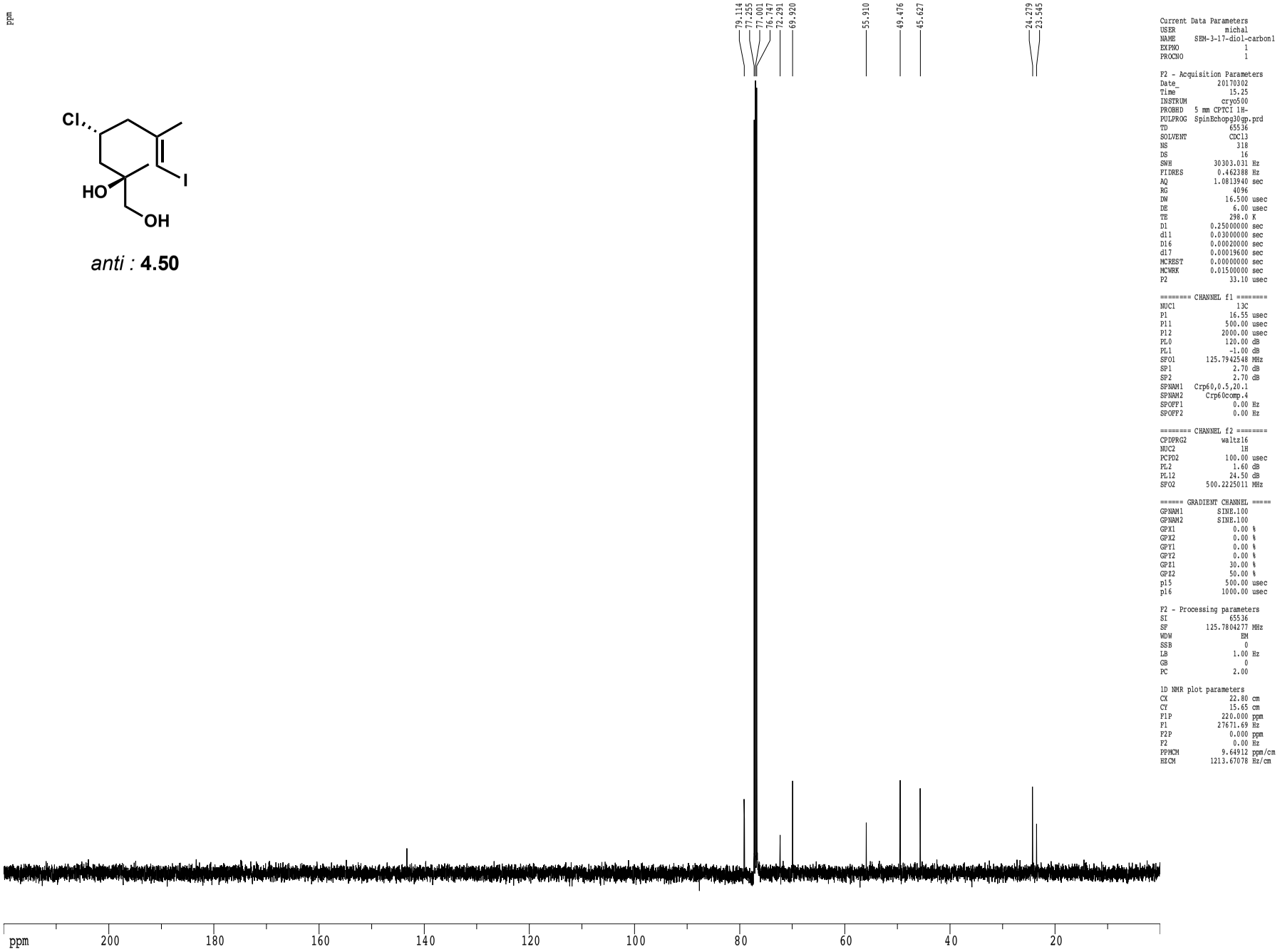

Current Data Parameters
USER michal
NAME SEM-3-17-diol-carbon1
EXPNO 1
PROCNO 1

F2 - Acquisition Parameters
Date_ 20170302
Time 15.25
INSTRUM cryo500
PROBHD 5 mm CPTCI 1H-
PULPROG SpinEchopg30gp.prd
TD 65536
SOLVENT CDCl3
NS 318
DS 16
SWH 30303.031 Hz
FIDRES 0.462388 Hz
AQ 1.0813940 sec
RG 4096
DW 16.500 usec
DE 6.00 usec
TE 298.0 K
D1 0.25000000 sec
d11 0.03000000 sec
D16 0.00020000 sec
d17 0.00019600 sec
MCREST 0.00000000 sec
MCWRK 0.01500000 sec
P2 33.10 usec

======== CHANNEL f1 ========
NUC1 13C
P1 16.55 usec
P11 500.00 usec
P12 2000.00 usec
PL0 120.00 dB
PL1 -1.00 dB
SFO1 125.7942548 MHz
SP1 2.70 dB
SP2 2.70 dB
SPNAM1 Crp60,0.5,20.1
SPNAM2 Crp60comp.4
SPOFF1 0.00 Hz
SPOFF2 0.00 Hz

======== CHANNEL f2 ========
CPDPRG2 waltz16
NUC2 1H
PCPD2 100.00 usec
PL2 1.60 dB
PL12 24.50 dB
SFO2 500.2225011 MHz

===== GRADIENT CHANNEL =====
GPNAM1 SINE.100
GPNAM2 SINE.100
GPX1 0.00 %
GPX2 0.00 %
GPY1 0.00 %
GPY2 0.00 %
GPZ1 30.00 %
GPZ2 50.00 %
p15 500.00 usec
p16 1000.00 usec

F2 - Processing parameters
SI 65536
SF 125.7804277 MHz
WDW EM
SSB 0
LB 1.00 Hz
GB 0
PC 2.00

1D NMR plot parameters
CX 22.80 cm
CY 15.65 cm
F1P 220.000 ppm
F1 27671.69 Hz
F2P 0.000 ppm
F2 0.00 Hz
PPMCM 9.64912 ppm/cm
HZCM 1213.67078 Hz/cm

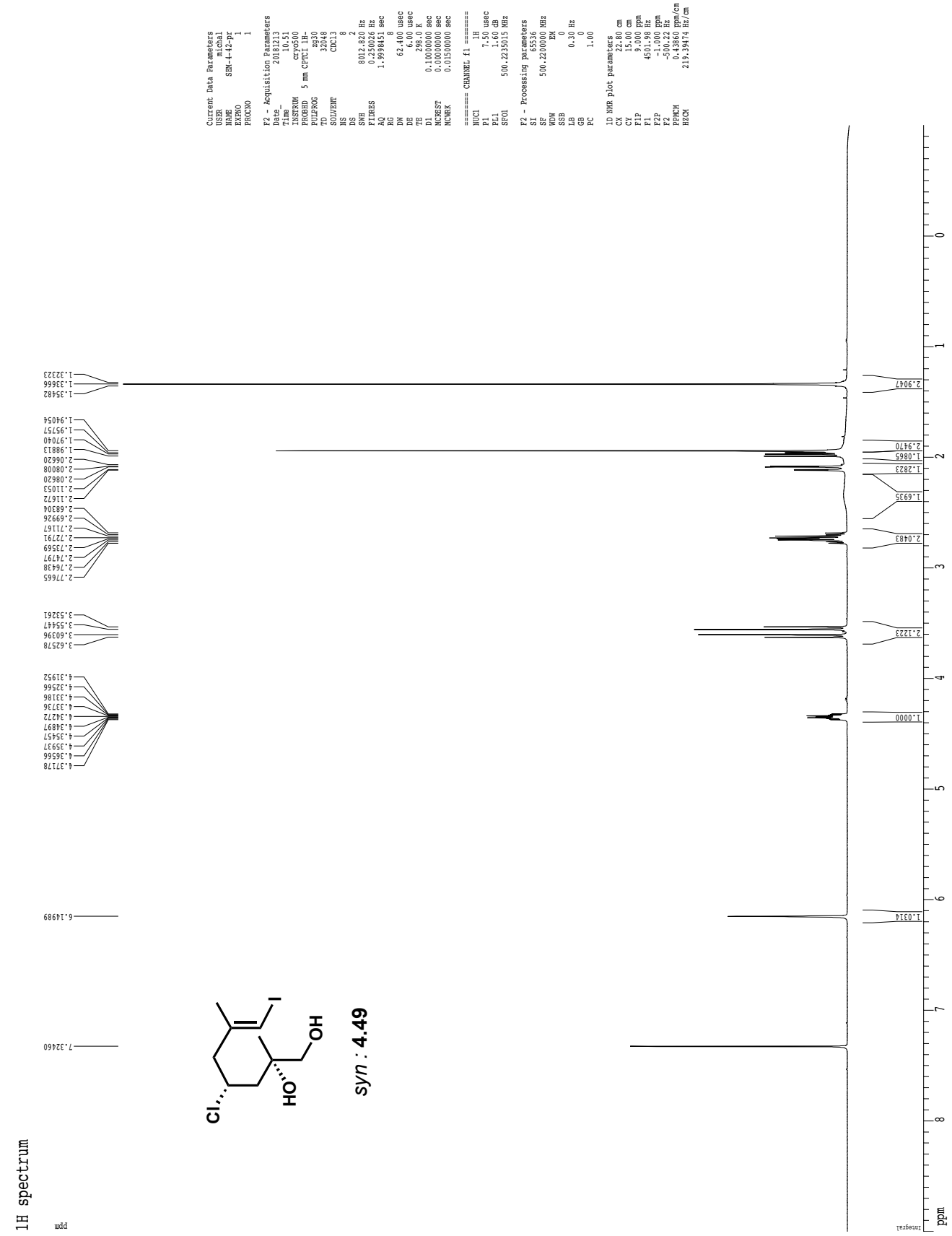
1H spectrum
ppm
Current Data Parameters
USER michal
NAME SRM-4-42-pr
EXPNO 1
PROCNO 1
F2 - Acquisition Parameters
Date_ 20181213
Time 10.51
INSTRUM cryo500
PROBHD 5 mm CPTCI 1H-
PULPROG zg30
TD 32048
SOLVENT CDCl3
NS 8
DS 2
SWH 8012.820 Hz
FIDRES 0.250026 Hz
AQ 1.9998451 sec
RG 8
DW 62.400 usec
DE 6.00 usec
TE 298.0 K
D1 0.10000000 sec
MCREST 0.00000000 sec
MCWRK 0.01500000 sec
======= CHANNEL f1 =======
NUC1 1H
P1 7.50 usec
PL1 1.60 dB
SFO1 500.2235015 MHz
F2 - Processing parameters
SI 65536
SF 500.2200000 MHz
WDW EM
SSB 0
LB 0.30 Hz
GB 0
PC 1.00
1D NMR plot parameters
CX 22.80 cm
CY 15.00 cm
F1P 9.000 ppm
F1 4501.98 Hz
F2P -1.000 ppm
F2 -500.22 Hz
PPMCM 0.43860 ppm/cm
HZCM 219.394774 Hz/cm
integral
ppm
1.32323
1.33666
1.35482
1.94054
1.95757
1.97040
1.98813
2.06620
2.08008
2.08620
2.11053
2.11672
2.68304
2.69926
2.71167
2.72791
2.73569
2.74797
2.76438
2.77665
3.52261
3.55447
3.60396
3.62578
4.31952
4.32566
4.33186
4.33736
4.34272
4.34897
4.35457
4.35937
4.36566
4.37178
6.14989
7.32460
1.0314
2.1223
1.0000
2.0483
1.6935
1.2823
1.0865
2.9470
2.9047
Cl
I
OH
HO
syn : 4.49

Z-restored spin-echo 13C spectrum with 1H decoupling

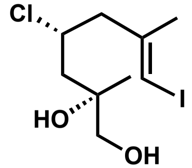

syn : **4.49**

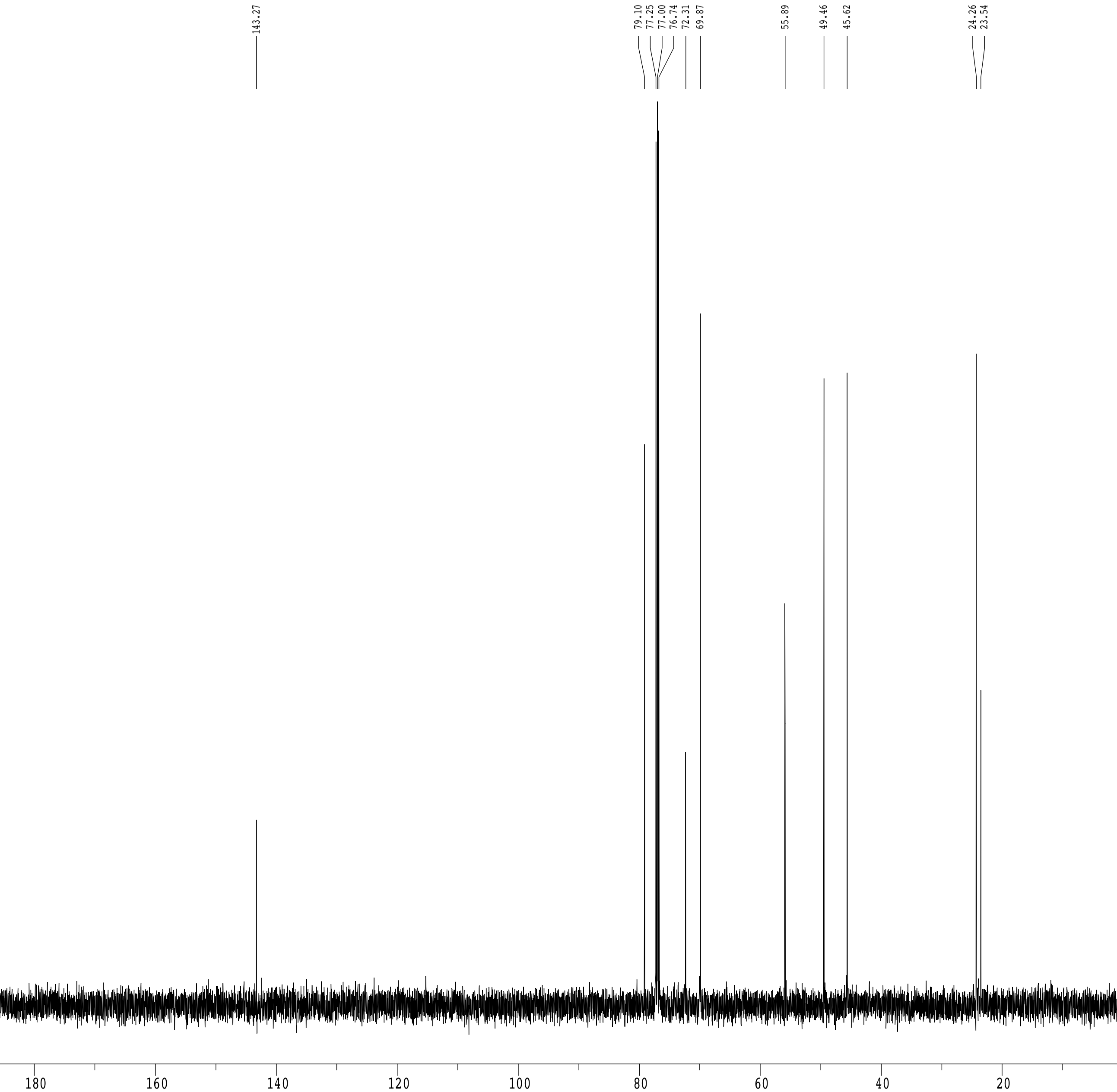

Current Data Parameters
USER michal
NAME SEM-3-17-diol-carbon2
EXPNO 1
PROCNO 1

F2 - Acquisition Parameters
Date_ 20170302
Time 15.36
INSTRUM cryo500
PROBHD 5 mm CPTCI 1H-
PULPROG SpinEchopg30gp.prd
TD 65536
SOLVENT CDCl3
NS 93
DS 16
SWH 30303.031 Hz
FIDRES 0.462388 Hz
AQ 1.0813940 sec
RG 2580.3
DW 16.500 usec
DE 6.00 usec
TE 298.0 K
D1 0.25000000 sec
d11 0.03000000 sec
D16 0.00020000 sec
d17 0.00019600 sec
MCREST 0.00000000 sec
MCWRK 0.01500000 sec
P2 33.10 usec

======== CHANNEL f1 ========
NUC1 13C
P1 16.55 usec
P11 500.00 usec
P12 2000.00 usec
PL0 120.00 dB
PL1 -1.00 dB
SFO1 125.7942548 MHz
SP1 2.70 dB
SP2 2.70 dB
SPNAM1 Crp60,0.5,20.1
SPNAM2 Crp60comp.4
SPOFF1 0.00 Hz
SPOFF2 0.00 Hz

======== CHANNEL f2 ========
CPDPRG2 waltz16
NUC2 1H
PCPD2 100.00 usec
PL2 1.60 dB
PL12 24.50 dB
SFO2 500.2225011 MHz

====== GRADIENT CHANNEL =====
GPNAM1 SINE.100
GPNAM2 SINE.100
GPX1 0.00 %
GPX2 0.00 %
GPY1 0.00 %
GPY2 0.00 %
GPZ1 30.00 %
GPZ2 50.00 %
p15 500.00 usec
p16 1000.00 usec

F2 - Processing parameters
SI 65536
SF 125.7804295 MHz
WDW EM
SSB 0
LB 1.00 Hz
GB 0
PC 2.00

1D NMR plot parameters
CX 22.80 cm
CY 15.65 cm
F1P 220.000 ppm
F1 27671.69 Hz
F2P 0.000 ppm
F2 0.00 Hz
PPMCM 9.64912 ppm/cm
HZCM 1213.67078 Hz/cm

X-ray crystal structure plots of diol **4.49** (2 molecules present in unit cell)

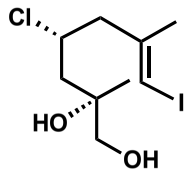

syn : **4.49**

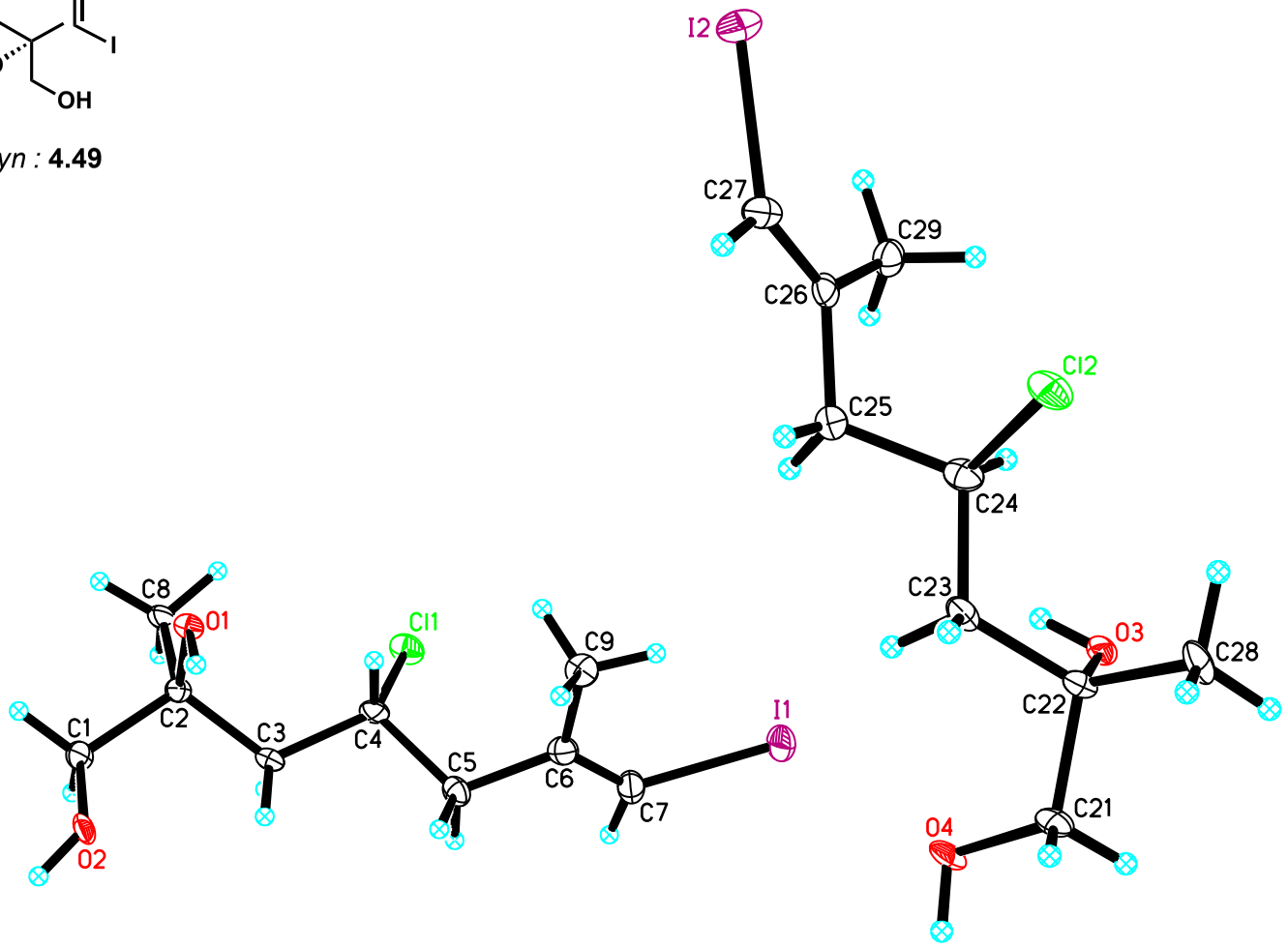

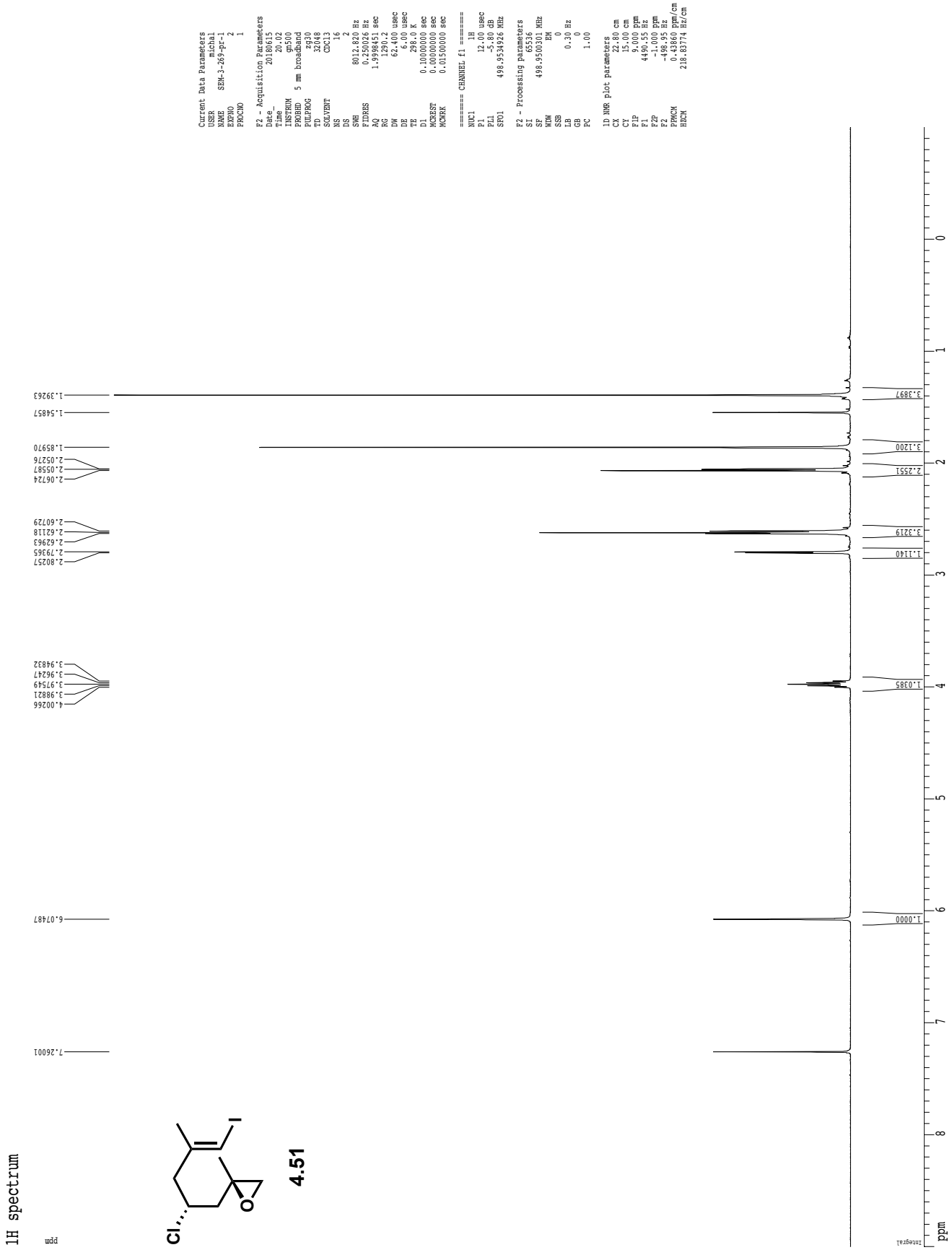
1H spectrum
4.51
Cl
I
O
Current Data Parameters
USER michal
NAME SEM-3-269-pr-1
EXPNO 2
PROCNO 1
F2 - Acquisition Parameters
Date_ 20180615
Time_ 20.02
INSTRUM qn500
PROBHD 5 mm broadband
PULPROG zg30
TD 32048
SOLVENT CDCl3
NS 16
DS 2
SWH 8012.820 Hz
FIDRES 0.250026 Hz
AQ 1.9998451 sec
RG 1290.2
DW 62.400 usec
DE 6.00 usec
TE 298.0 K
D1 0.10000000 sec
MCREST 0.00000000 sec
MCWRK 0.01500000 sec
======== CHANNEL f1 ========
NUC1 1H
P1 12.00 usec
PL1 -5.80 dB
SFO1 498.9534926 MHz
F2 - Processing parameters
SI 65536
SF 498.9500301 MHz
WDW EM
SSB 0
LB 0.30 Hz
GB 0
PC 1.00
1D NMR plot parameters
CX 22.80 cm
CY 15.00 cm
F1P 9.000 ppm
F1 4490.55 Hz
F2P -1.000 ppm
F2 -498.95 Hz
PPMCM 0.41650 ppm/cm
HZCM 218.83774 Hz/cm
7.26001
6.07487
4.00266
3.98821
3.97549
3.96247
3.94832
2.80257
2.79365
2.63118
2.62963
2.60729
2.06724
2.05587
2.05276
1.85970
1.54857
1.39263
1.0000
1.0385
1.1140
3.2319
2.2551
3.1200
3.3897
Integral
ppm
0
1
2
3
4
5
6
7
8

13C spectrum with 1H decoupling

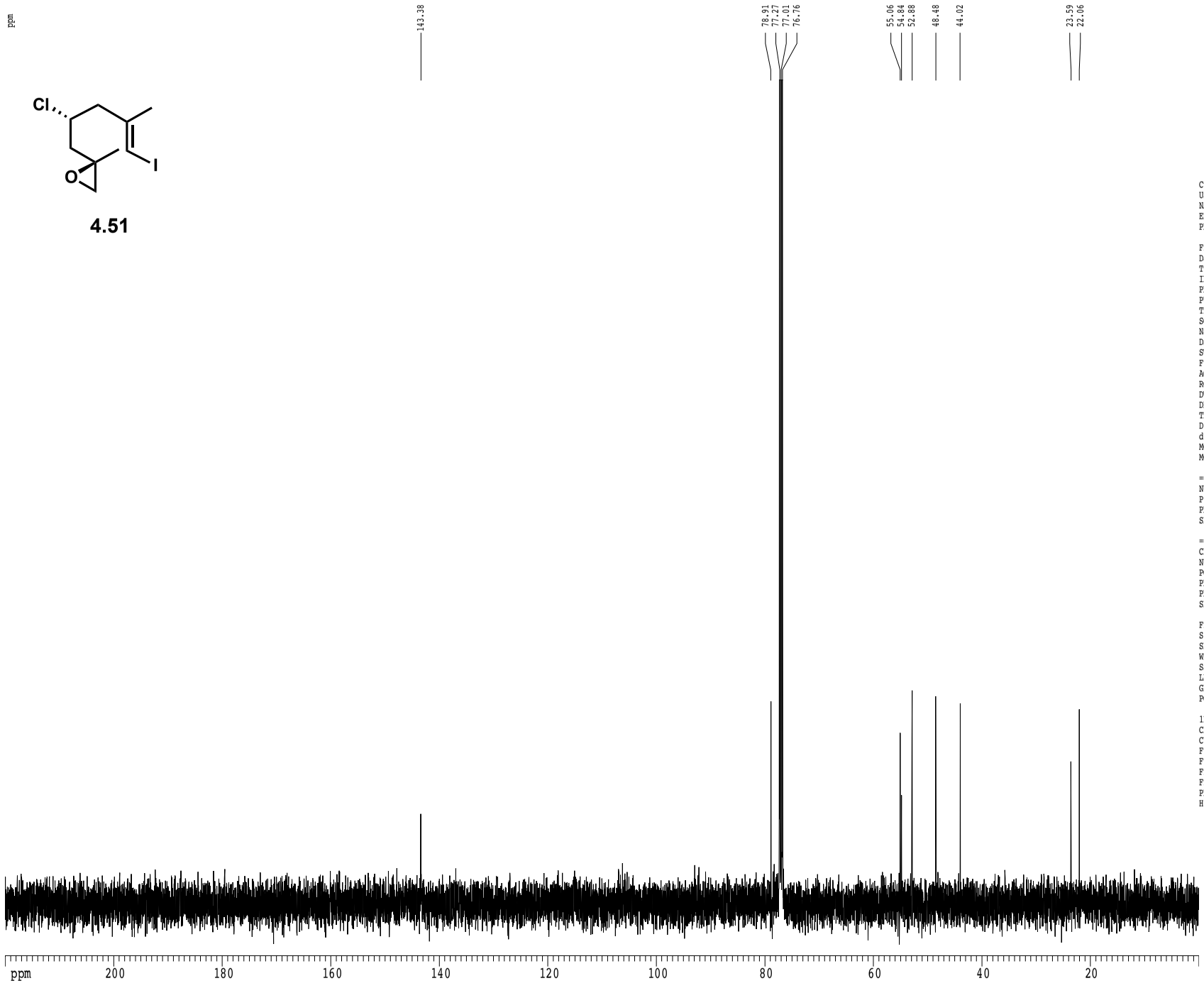


```
Current Data Parameters
USER                michal
NAME       SEM-3-269-pr-1
EXPNO                   3
PROCNO                  1

F2 - Acquisition Parameters
Date_            20180615
Time                20.06
INSTRUM             gn500
PROBHD   5 mm broadband
PULPROG           zgdc30
TD                 65536
SOLVENT            CDCl3
NS                   153
DS                     4
SWH           30303.031 Hz
FIDRES         0.462388 Hz
AQ             1.0814105 sec
RG                5792.6
DW                16.500 usec
DE                 4.50 usec
TE                298.0 K
D1            0.25000000 sec
d11           0.03000000 sec
MCREST        0.00000000 sec
MCWRK         0.01500000 sec

======== CHANNEL f1 ========
NUC1                 13C
P1                  9.00 usec
PL1                -0.60 dB
SFO1         125.4748777 MHz

======== CHANNEL f2 ========
CPDPRG2          waltz16
NUC2                 1H
PCPD2              80.00 usec
PL2                -3.00 dB
PL12               12.80 dB
SFO2         498.9524948 MHz

F2 - Processing parameters
SI                 65536
SF           125.4610830 MHz
WDW                  EM
SSB                   0
LB                 1.00 Hz
GB                    0
PC                 2.00

1D NMR plot parameters
CX                 22.80 cm
CY                 30.00 cm
F1P              220.000 ppm
F1             27601.44 Hz
F2P                0.000 ppm
F2                 0.00 Hz
PPMCM            9.64912 ppm/cm
HZCM          1210.58948 Hz/cm
```

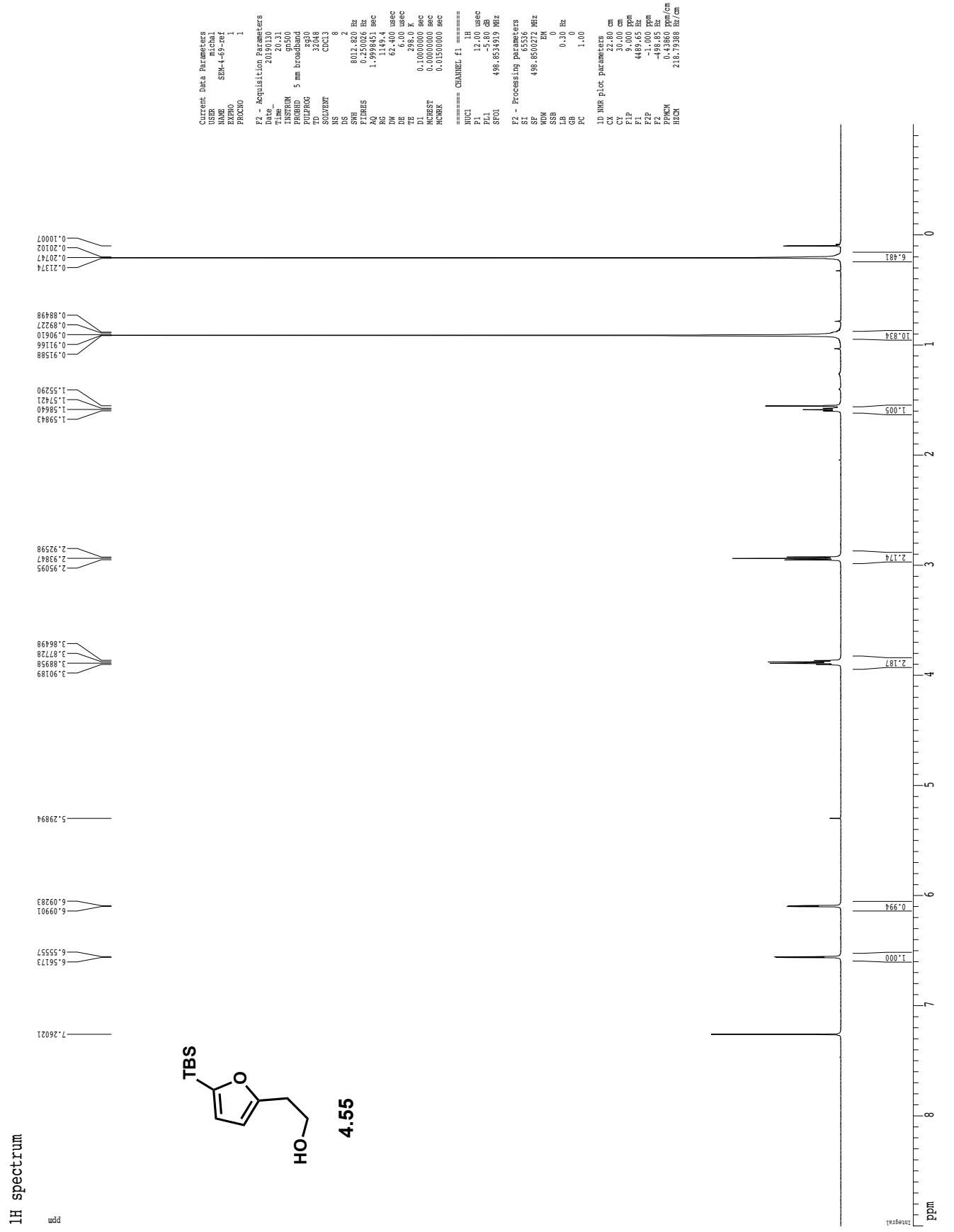
1H spectrum
TBS
O
HO
4.55
ppm
Integral
Current Data Parameters
USER michal
NAME SEM-4-69-ref
EXPNO 1
PROCNO 1
F2 - Acquisition Parameters
Date_ 20150130
Time 20.31
INSTRUM qnp500
PROBHD 5 mm broadband
PULPROG zg30
TD 32048
SOLVENT CDCl3
NS 8
DS 2
SWH 8012.820 Hz
FIDRES 0.250026 Hz
AQ 1.9998451 sec
RG 1149.4
DW 62.400 usec
DE 6.00 usec
TE 298.0 K
D1 0.10000000 sec
MCREST 0.00000000 sec
MCWRK 0.01500000 sec
======== CHANNEL f1 ========
NUC1 1H
P1 12.00 usec
PL1 5.80 dB
SFO1 498.0534919 MHz
F2 - Processing parameters
SI 65536
SF 498.0500272 MHz
WDW EM
SSB 0
LB 0.30 Hz
GB 0
PC 1.00
1D NMR plot parameters
CX 22.80 cm
CY 30.00 cm
F1P 9.000 ppm
F1 4489.65 Hz
F2P -1.000 ppm
F2 -498.85 Hz
PPMCM 0.43860 ppm/cm
HZCM 218.79388 Hz/cm
7.26021
6.56173
6.55557
6.09901
6.09283
5.29894
3.90189
3.88958
3.87728
3.86498
2.95095
2.93847
2.92598
1.59843
1.58640
1.57421
1.55290
0.91588
0.91166
0.90610
0.89227
0.88498
0.21374
0.20747
0.20102
0.10007
6.481
10.834
1.005
2.174
2.187
0.994
1.000

Z-restored spin-echo 13C spectrum with 1H decoupling

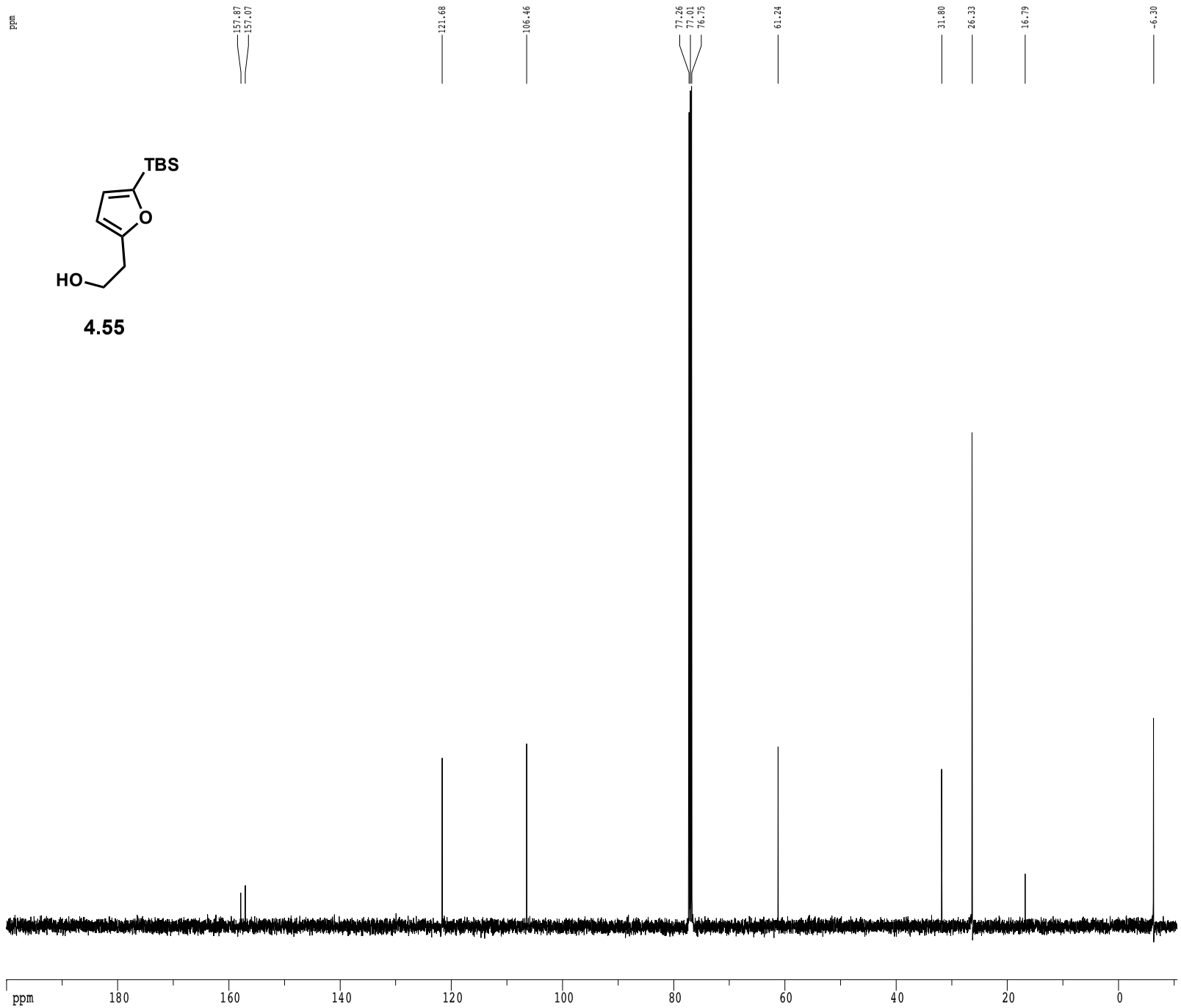

Current Data Parameters
USER michal
NAME SEM-3-59-2
EXPNO 3
PROCNO 1

F2 - Acquisition Parameters
Date_ 20170517
Time 17.34
INSTRUM cryo500
PROBHD 5 mm CPTCI 1H-
PULPROG SpinEchopg30gp.prd
TD 65536
SOLVENT CDCl3
NS 239
DS 16
SWH 30303.031 Hz
FIDRES 0.462388 Hz
AQ 1.0813940 sec
RG 4096
DW 16.500 usec
DE 6.00 usec
TE 298.0 K
D1 0.25000000 sec
d11 0.03000000 sec
D16 0.00020000 sec
d17 0.00019600 sec
MCREST 0.00000000 sec
MCWRK 0.01500000 sec
P2 33.10 usec

======== CHANNEL f1 ========
NUC1 13C
P1 16.55 usec
P11 500.00 usec
P12 2000.00 usec
PL0 120.00 dB
PL1 -1.00 dB
SFO1 125.7942548 MHz
SP1 2.70 dB
SP2 2.70 dB
SPNAM1 Crp60,0.5,20.1
SPNAM2 Crp60comp.4
SPOFF1 0.00 Hz
SPOFF2 0.00 Hz

======== CHANNEL f2 ========
CPDPRG2 waltz16
NUC2 1H
PCPD2 100.00 usec
PL2 1.60 dB
PL12 24.50 dB
SFO2 500.2225011 MHz

====== GRADIENT CHANNEL =====
GPNAM1 SINE.100
GPNAM2 SINE.100
GPX1 0.00 %
GPX2 0.00 %
GPY1 0.00 %
GPY2 0.00 %
GPZ1 30.00 %
GPZ2 50.00 %
p15 500.00 usec
p16 1000.00 usec

F2 - Processing parameters
SI 65536
SF 125.7804268 MHz
WDW EM
SSB 0
LB 1.00 Hz
GB 0
PC 2.00

1D NMR plot parameters
CX 22.80 cm
CY 15.65 cm
F1P 200.000 ppm
F1 25156.09 Hz
F2P -20.000 ppm
F2 -2515.61 Hz
PPMCM 9.64912 ppm/cm
HZCM 1213.67078 Hz/cm

1H spectrum

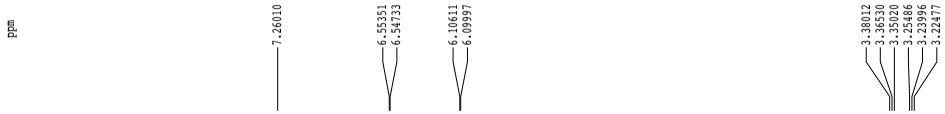

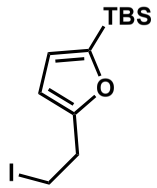

4.56

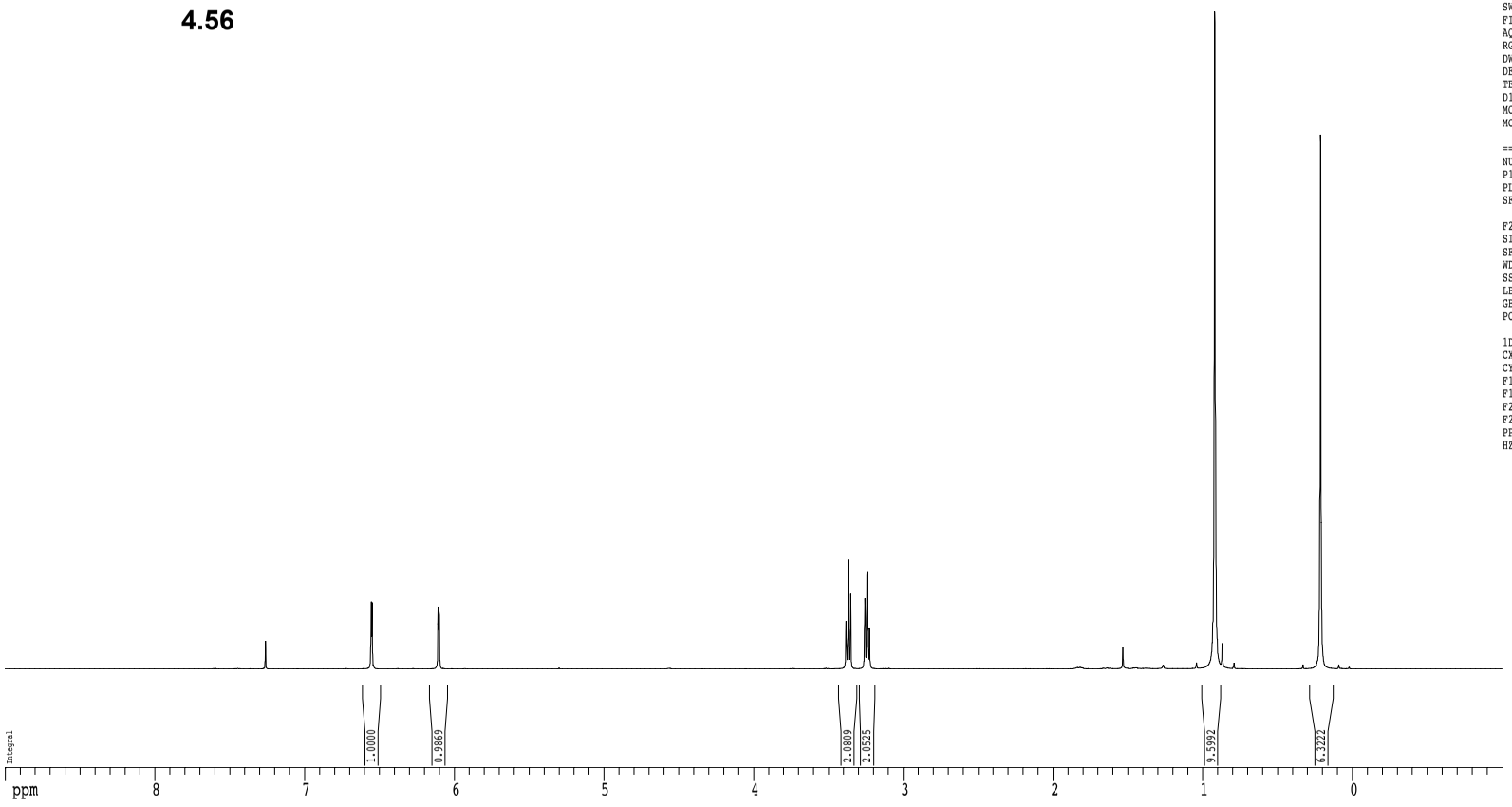


```
Current Data Parameters
USER              michal
NAME      SEM-4-73-proton
EXPNO                  1
PROCNO                 1

F2 - Acquisition Parameters
Date_           20190418
Time              15.34
INSTRUM         cryo500
PROBHD   5 mm CPTCI 1H-
PULPROG            zg30
TD                32048
SOLVENT           CDCl3
NS                    8
DS                    2
SWH            8012.820 Hz
FIDRES         0.250026 Hz
AQ             1.9998451 sec
RG                  5.7
DW                62.400 usec
DE                 6.00 usec
TE                298.0 K
D1           0.10000000 sec
MCREST       0.00000000 sec
MCWRK        0.01500000 sec

======= CHANNEL f1 ========
NUC1                  1H
P1                 7.50 usec
PL1                1.60 dB
SFO1        500.2235015 MHz

F2 - Processing parameters
SI                 65536
SF          500.2200327 MHz
WDW                   EM
SSB                    0
LB                  0.30 Hz
GB                     0
PC                  1.00

1D NMR plot parameters
CX                 22.80 cm
CY                 10.00 cm
F1P                9.000 ppm
F1               4501.98 Hz
F2P               -1.000 ppm
F2              -500.22 Hz
PPMCM           0.43860 ppm/cm
HZCM          219.39476 Hz/cm
```

Z-restored spin-echo 13C spectrum with 1H decoupling

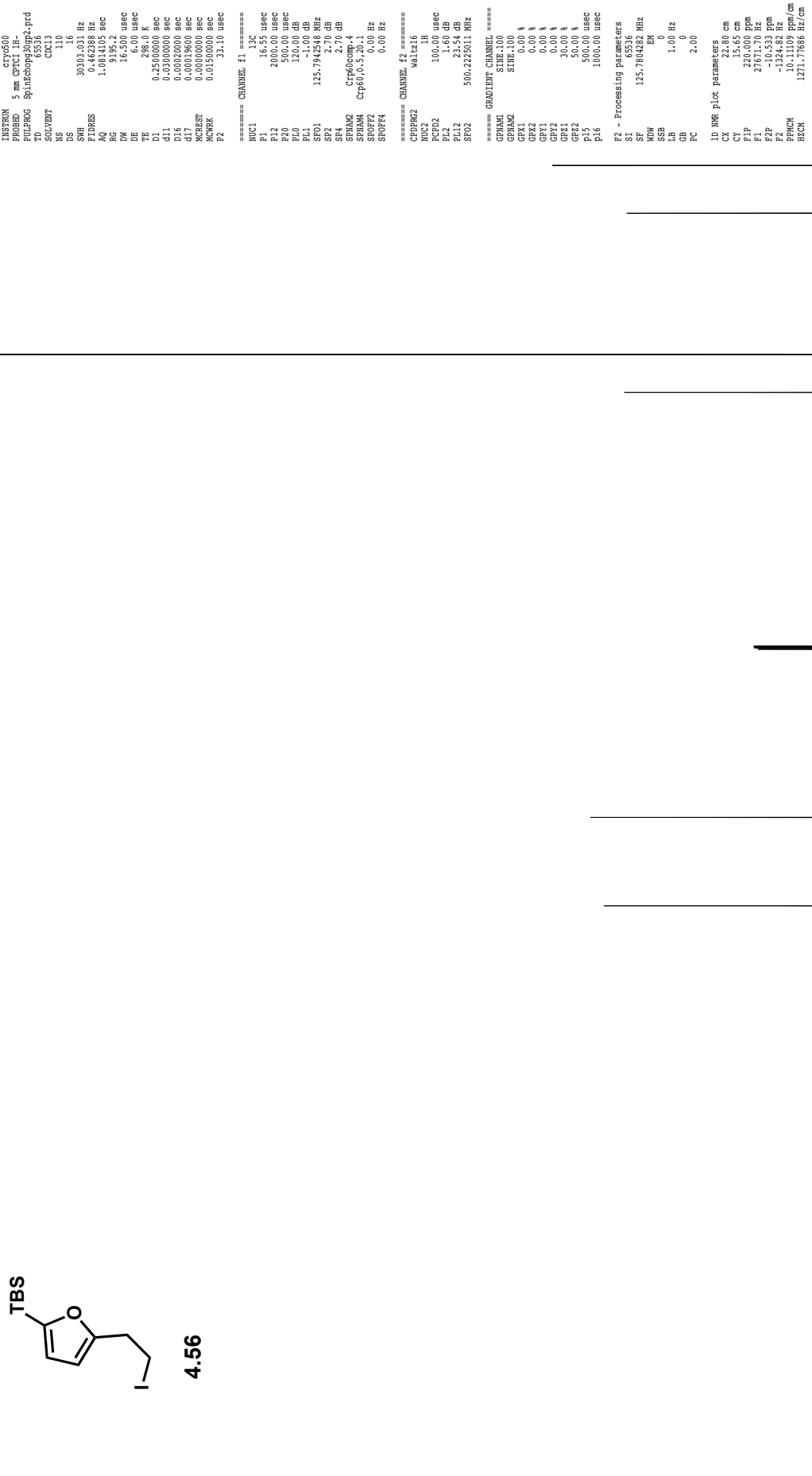

4.56

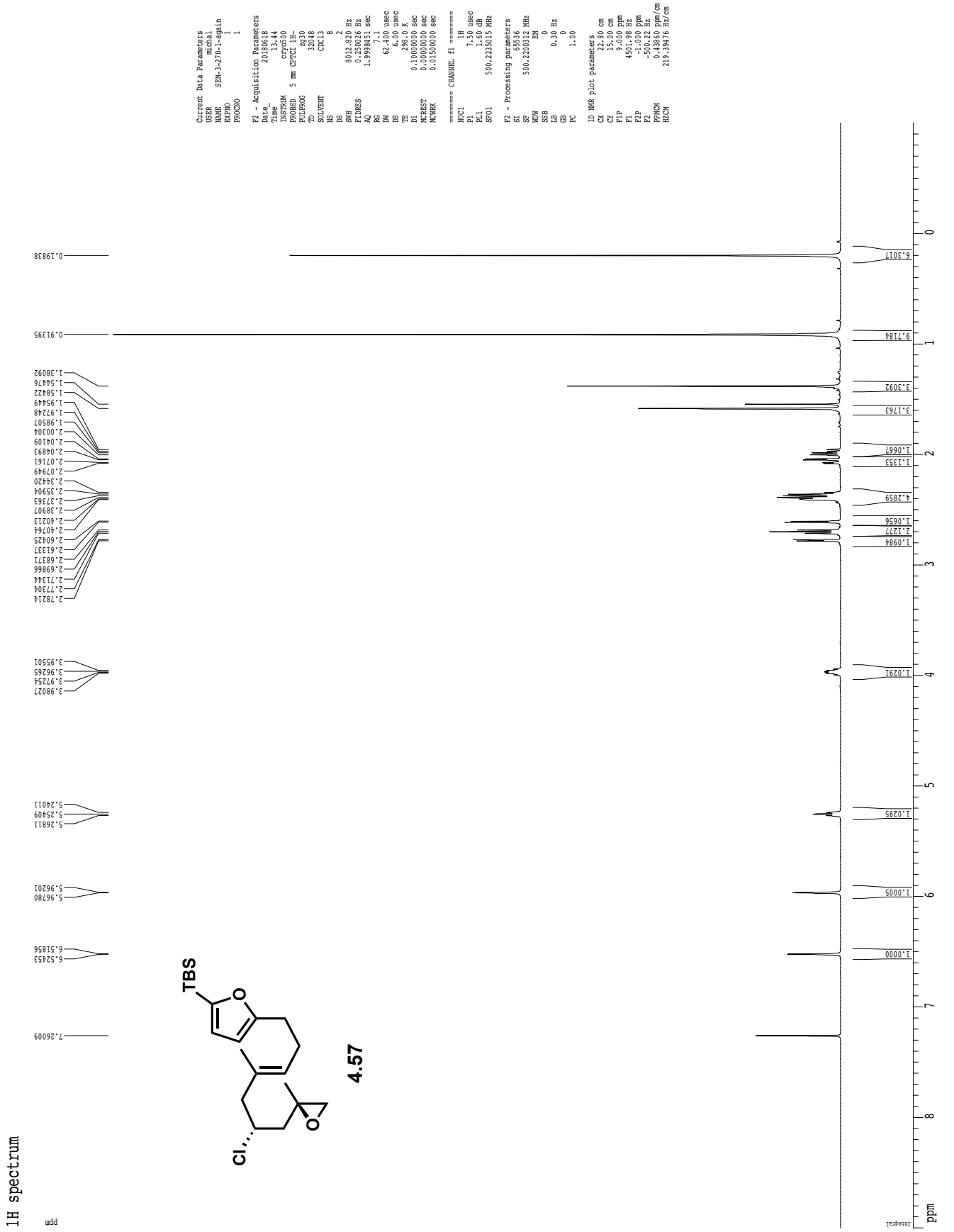
1H spectrum
TBS
O
O
Cl
4.57
Current Data Parameters
USER mlchal
NAME SBM-3-270-1-again
EXPNO 1
PROCNO 1
F2 - Acquisition Parameters
Date_ 20180618
Time 13.44
INSTRUM cryo500
PROBHD 5 mm CPTCI 1H-
PULPROG zg30
TD 32048
SOLVENT CDCl3
NS 8
DS 2
SWH 8012.820 Hz
FIDRES 0.250026 Hz
AQ 1.9998451 sec
RG 7.1
DW 62.400 usec
DE 6.00 usec
TE 298.0 K
D1 0.11000000 sec
MCREST 0.00000000 sec
MCWRK 0.01500000 sec
======== CHANNEL f1 ========
NUC1 1H
P1 7.50 usec
PL1 1.60 dB
SFO1 500.2235015 MHz
F2 - Processing parameters
SI 65536
SF 500.2200312 MHz
WDW EM
SSB 0
LB 0.30 Hz
GB 0
PC 1.00
1D NMR plot parameters
CX 22.80 cm
CY 15.00 cm
F1P 9.000 ppm
F1 4501.98 Hz
F2P -1.000 ppm
F2 -500.22 Hz
PPMCM 0.43860 ppm/cm
HZCM 219.39476 Hz/cm
0.19838
0.91395
1.38092
1.54476
1.58422
1.95449
1.97248
1.98507
2.00304
2.04109
2.04893
2.07161
2.07949
2.34420
2.35904
2.37363
2.38907
2.40213
2.40764
2.60425
2.61337
2.68371
2.69866
2.71344
2.77304
2.78214
3.95501
3.96265
3.97254
3.98027
5.24011
5.25409
5.26811
5.96201
5.96780
6.51856
6.52453
7.26009
6.3017
9.7184
3.3092
3.1763
1.0667
1.1353
4.2859
1.0656
2.1277
1.0984
1.0291
1.0295
1.0005
1.0000
ppm
Integral

Z-restored spin-echo 13C spectrum with 1H decoupling

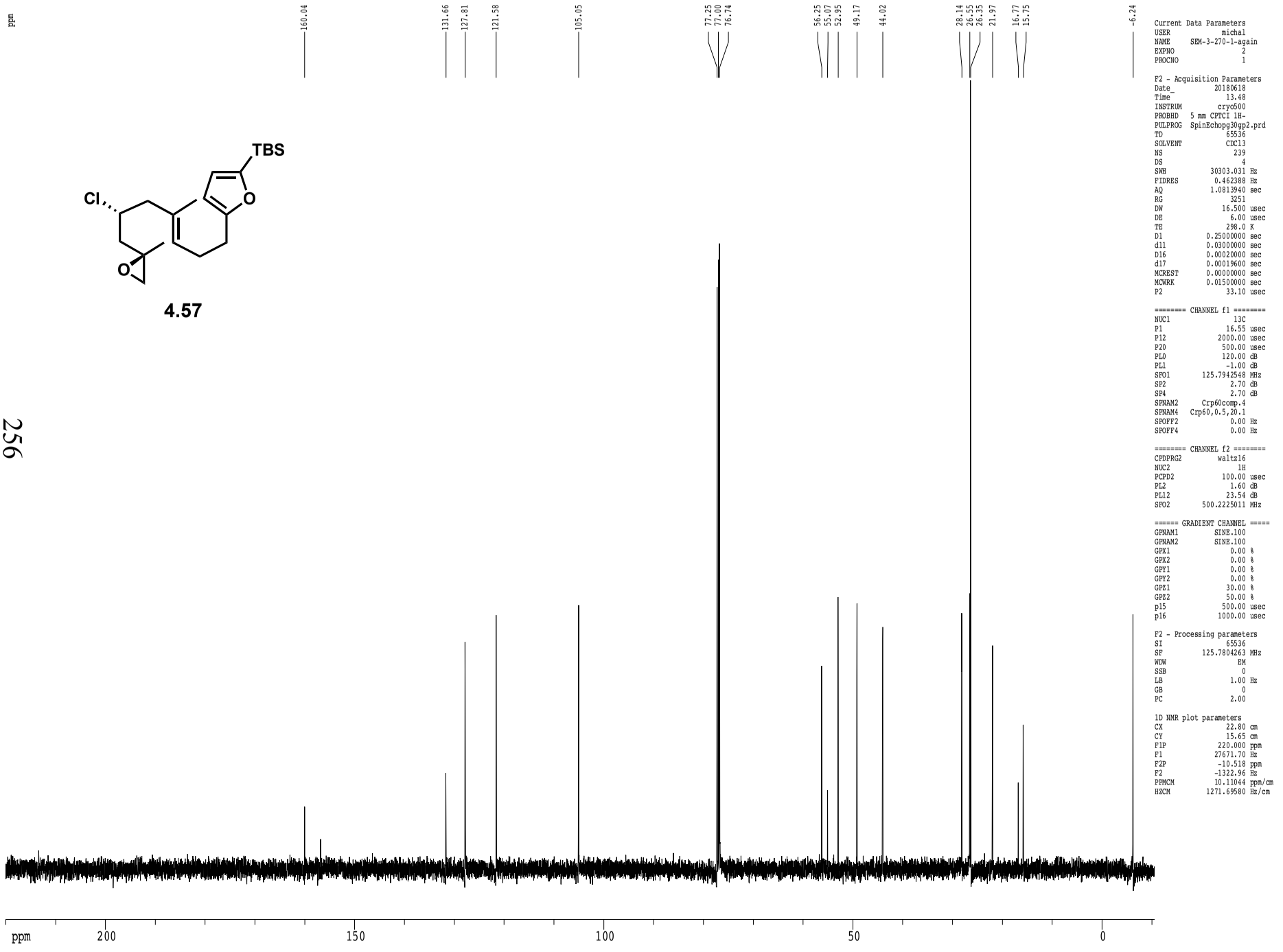

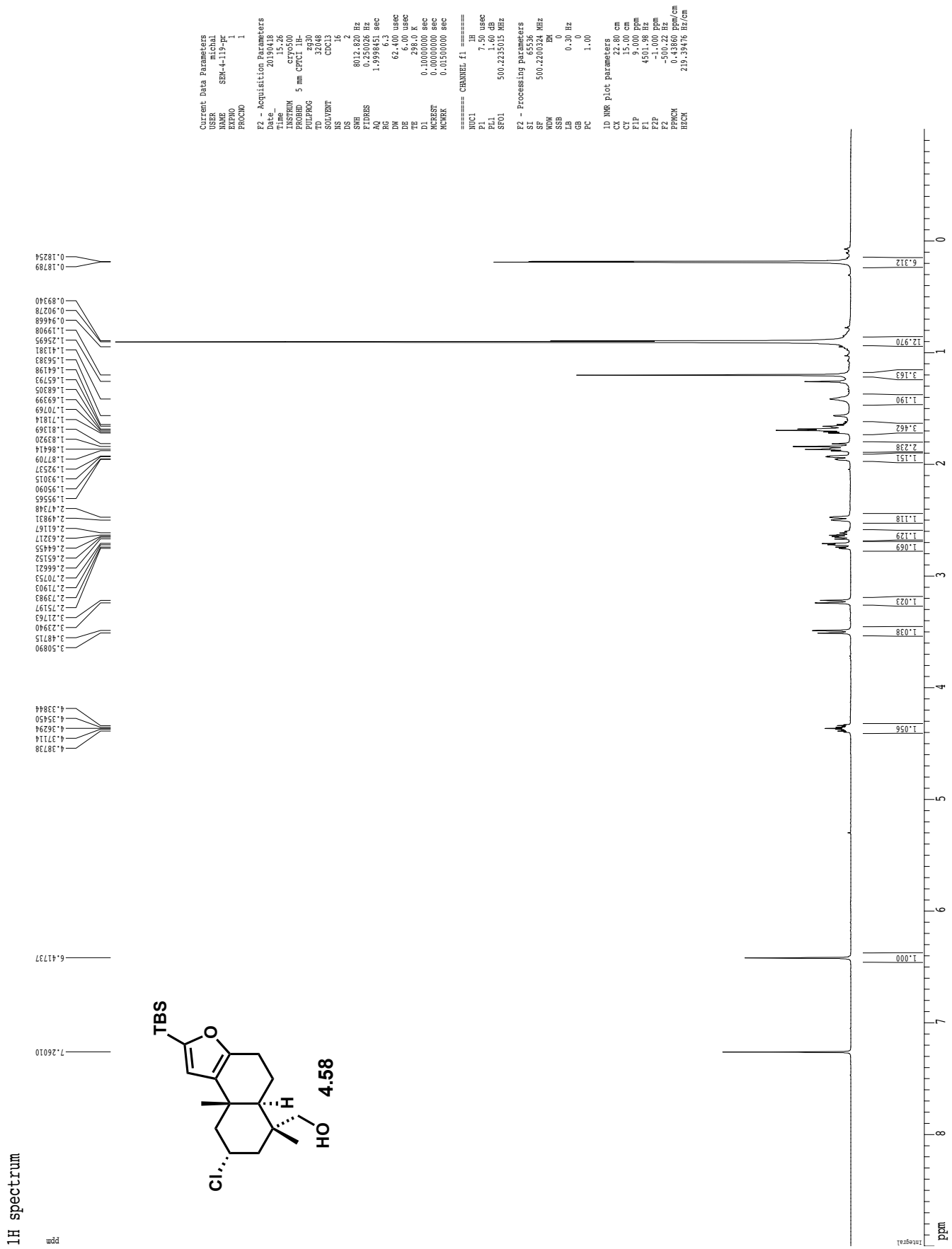
1H spectrum
TBS
O
H
HO
4.58
Cl
ppm
Integral

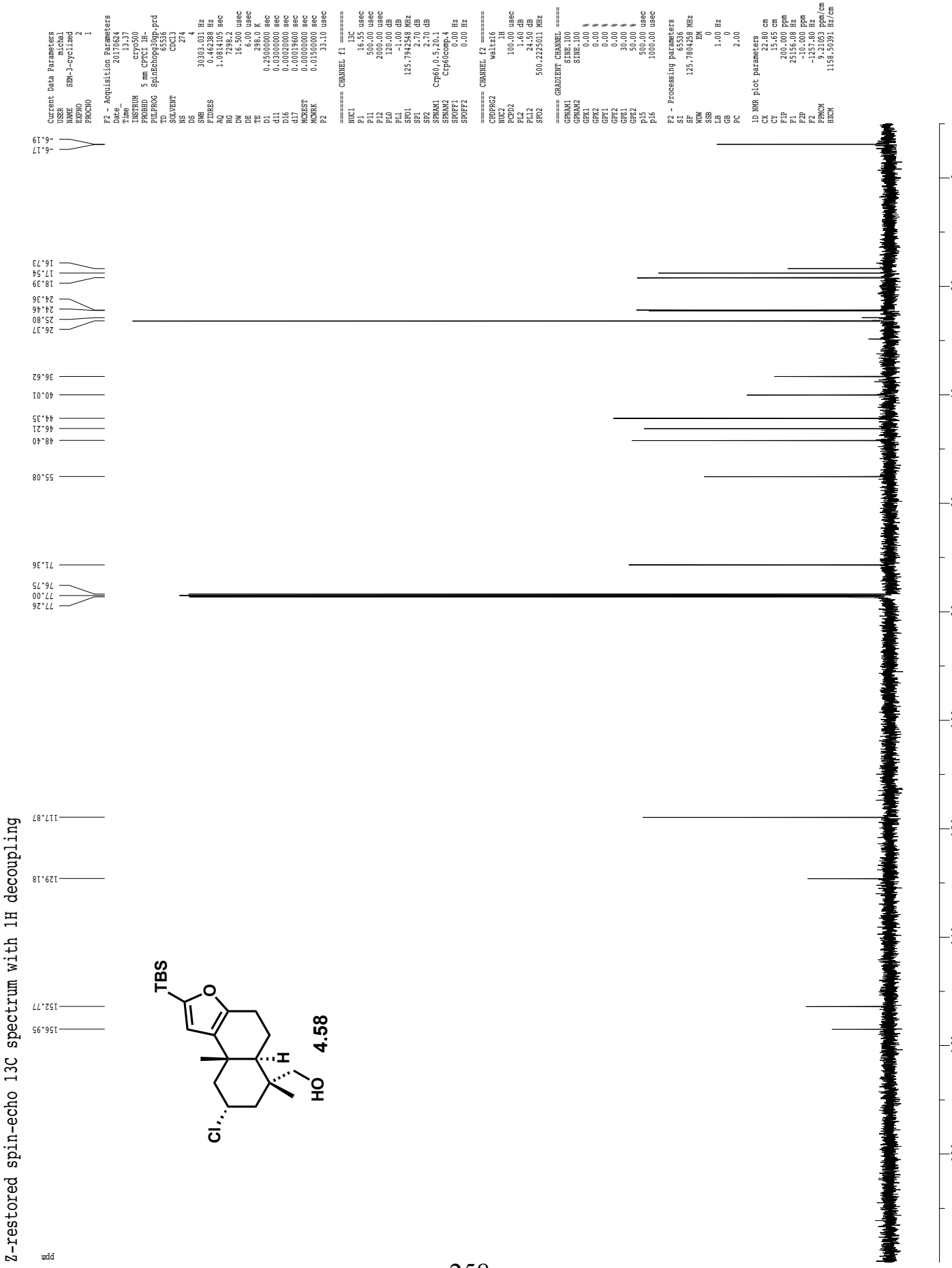
Z-restored spin-echo 13C spectrum with 1H decoupling
TBS
O
H
HO
4.58
Cl
ppm

gnoe

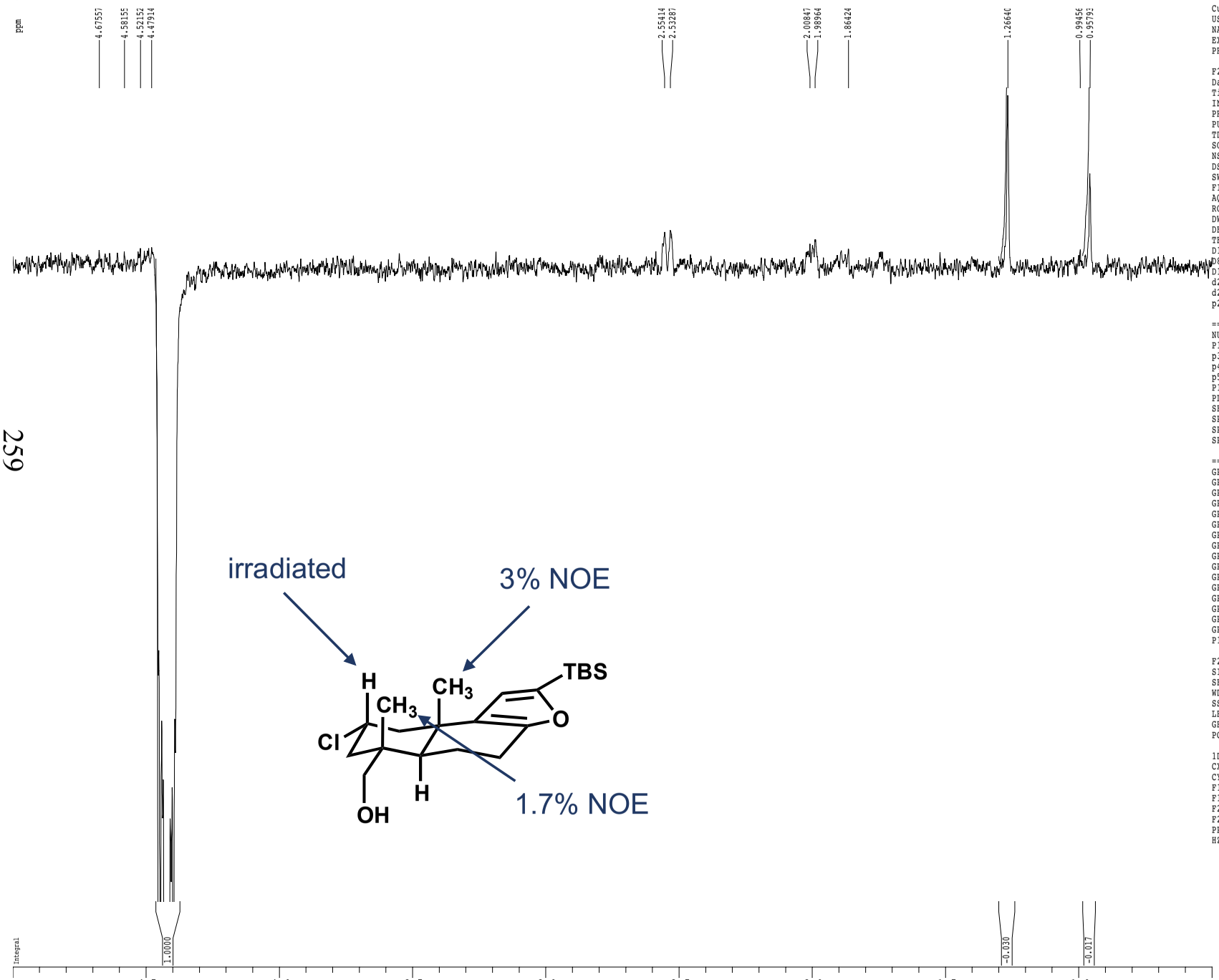

Current Data Parameters

USER	michal
NAME	SEM-3-33-2D
EXPNO	2
PROCNO	1

F2 - Acquisition Parameters

Date_	20170328
Time	18.32
INSTRUM	gn500
PROBHD	5 mm broadband
PULPROG	gnoelcc.wu
TD	65536
SOLVENT	CDCl3
NS	256
DS	8
SWH	8012.820 Hz
FIDRES	0.122266 Hz
AQ	4.0894966 sec
RG	4096
DW	62.400 usec
DE	6.00 usec
TE	298.0 K
D1	1.00000000 sec
D8	0.50000000 sec
D16	0.00020000 sec
d21	0.33374399 sec
d22	0.16399699 sec
p2	24.00 usec

======== CHANNEL f1 ========

NUC1	1H
P1	12.00 usec
p3	36.00 usec
p4	48.00 usec
p5	32.00 usec
P12	40000.00 usec
PL1	-5.80 dB
SFO1	499.0722064 MHz
SP1	53.60 dB
SPNAM1	gauss1.512
SPOFF1	0.00 Hz

====== GRADIENT CHANNEL =====

GPNAM1	sine.100
GPNAM2	sine.100
GPNAM3	sine.100
GPNAM4	sine.100
GPX1	0.00 %
GPX2	0.00 %
GPX3	0.00 %
GPX4	0.00 %
GPY1	0.00 %
GPY2	0.00 %
GPY3	0.00 %
GPY4	0.00 %
GPZ1	7.00 %
GPZ2	3.00 %
GPZ3	2.30 %
GPZ4	-2.30 %
P16	1000.00 usec

F2 - Processing parameters

SI	65536
SF	499.0700000 MHz
WDW	EM
SSB	0
LB	1.00 Hz
GB	0
PC	1.00

1D NMR plot parameters

CX	22.80 cm
CY	30.00 cm
F1P	5.000 ppm
F1	2495.35 Hz
F2P	0.500 ppm
F2	249.54 Hz
PPMCM	0.19737 ppm/cm
HZCM	98.50066 Hz/cm

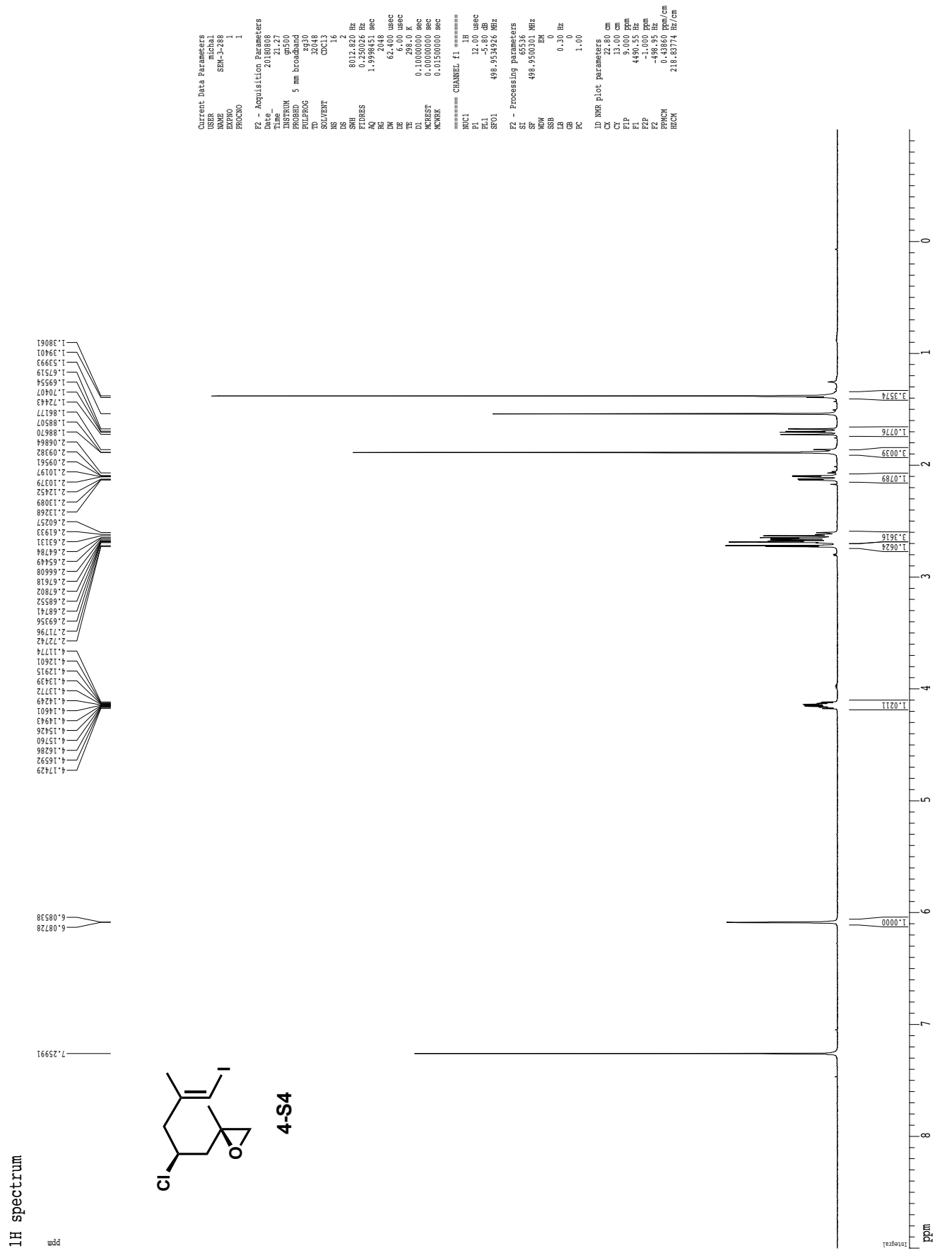
1H spectrum
4-S4
Cl
O
I
Current Data Parameters
USER michal
NAME SEM-3-288
EXPNO 1
PROCNO 1
F2 - Acquisition Parameters
Date_ 20180809
Time 21.27
INSTRUM qn500
PROBHD 5 mm broadband
PULPROG zg30
TD 32048
SOLVENT CDCl3
NS 16
DS 2
SWH 8012.820 Hz
FIDRES 0.250026 Hz
AQ 1.9998451 sec
RG 2048
DW 62.400 usec
DE 6.00 usec
TE 298.0 K
D1 0.10000000 sec
MCREST 0.00000000 sec
MCWRK 0.01500000 sec
======= CHANNEL f1 =======
NUC1 1H
P1 12.00 usec
PL1 -5.80 dB
SFO1 498.9534926 MHz
F2 - Processing parameters
SI 65536
SF 498.9500301 MHz
WDW EM
SSB 0
LB 0.30 Hz
GB 0
PC 1.00
1D NMR plot parameters
CX 22.80 cm
CY 13.00 cm
F1P 9.000 ppm
F1 4490.55 Hz
F2P -1.000 ppm
F2 -498.95 Hz
PPMCM 0.43860 ppm/cm
HZCM 218.83774 Hz/cm
7.25991
6.08728
6.08538
4.17429
4.16592
4.16286
4.15760
4.15426
4.14943
4.14601
4.14249
4.13772
4.13439
4.12915
4.12601
4.11774
2.72742
2.71796
2.69356
2.68741
2.68552
2.67802
2.67618
2.66608
2.65449
2.64784
2.63131
2.61933
2.60257
2.13268
2.13089
2.12452
2.10379
2.10197
2.09561
2.09382
2.06864
1.88670
1.88507
1.86177
1.72443
1.70407
1.69554
1.67519
1.53993
1.39401
1.38061
1.0000
1.0211
3.6616
1.0624
1.0789
3.0039
1.0776
3.3574
integral
ppm
0
1
2
3
4
5
6
7
8
ppm

13C spectrum with 1H decoupling

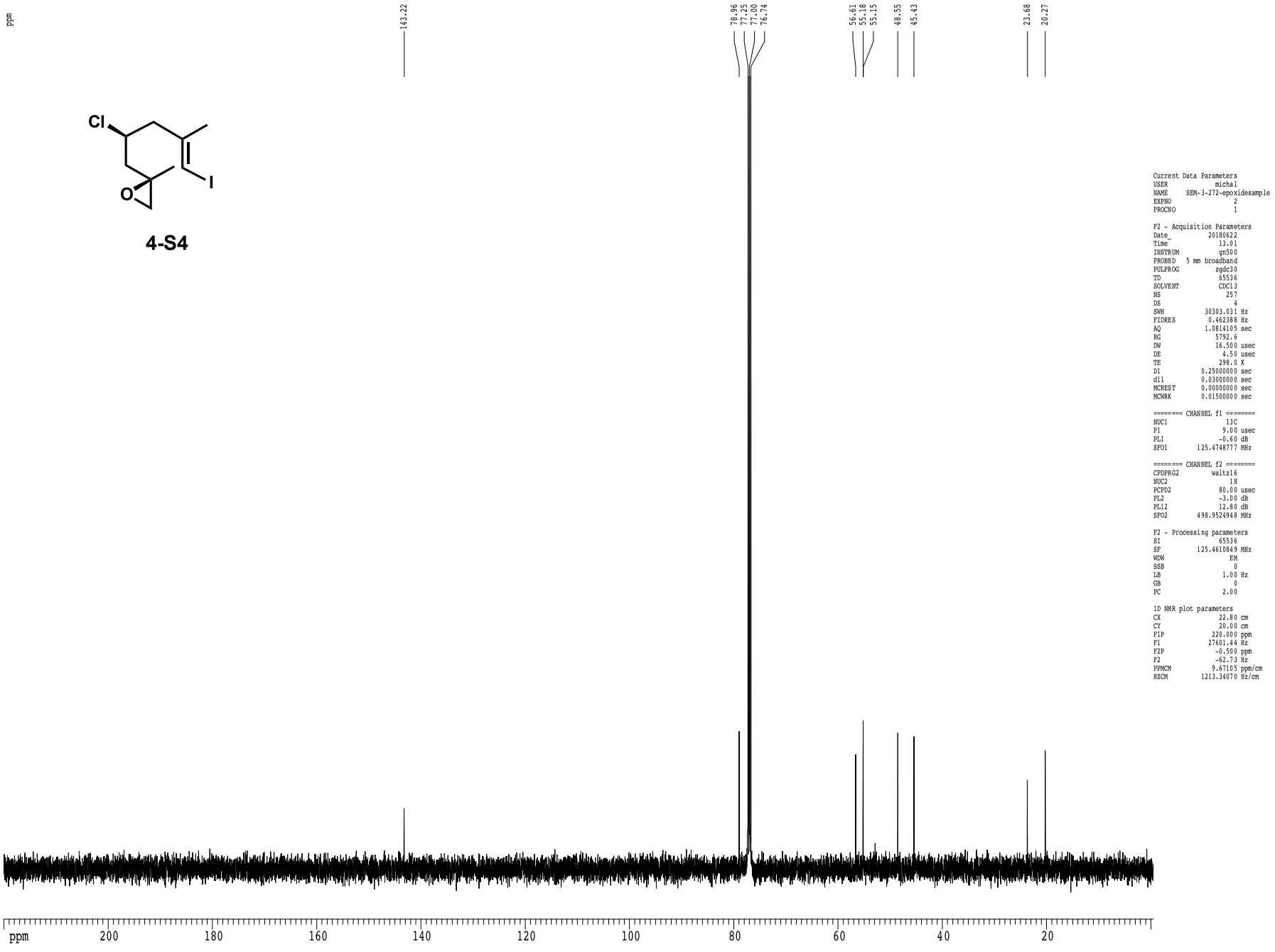

1H spectrum

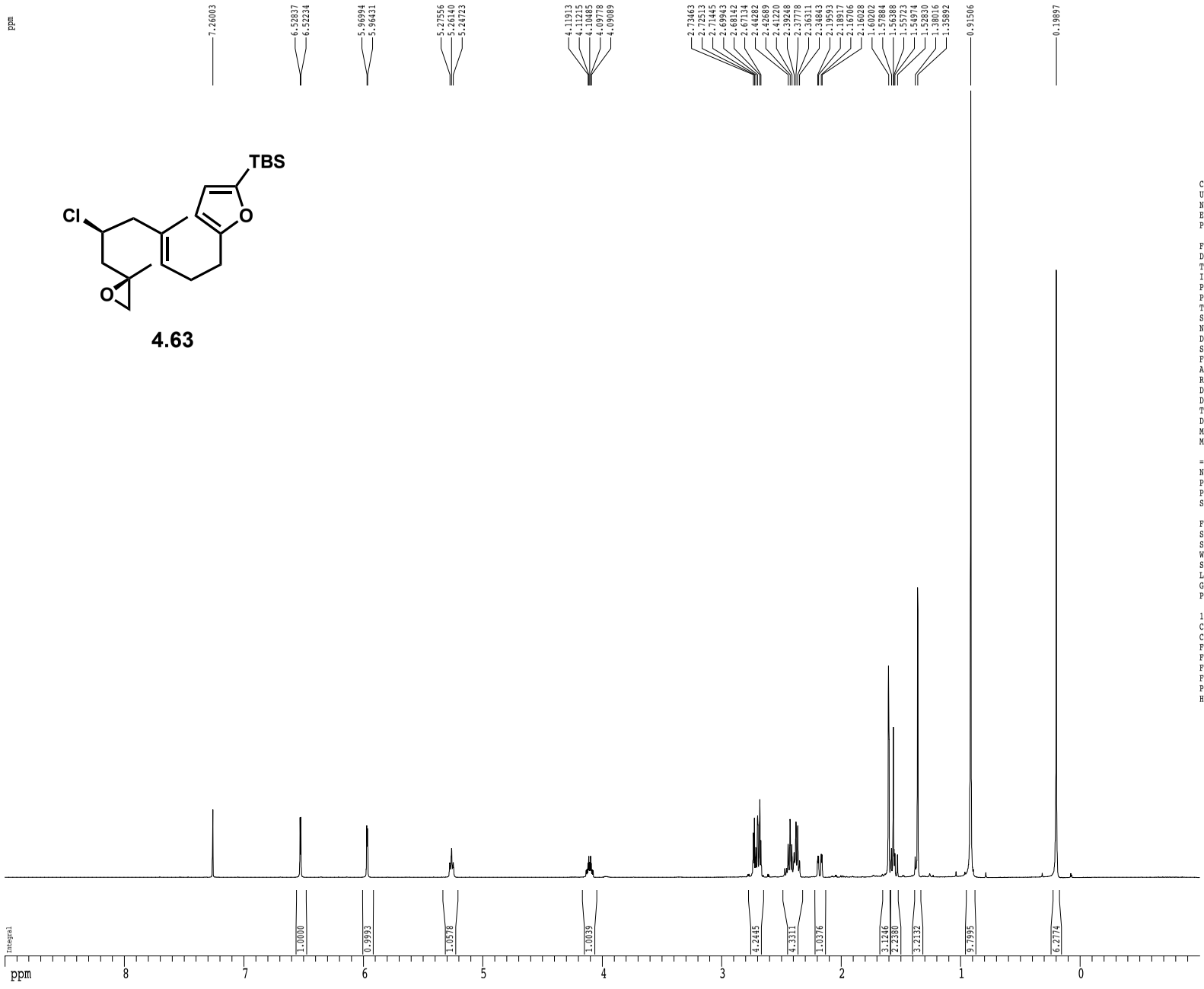

Current Data Parameters
USER michal
NAME SEM-3-292-pr
EXPNO 2
PROCNO 1

F2 - Acquisition Parameters
Date_ 20180821
Time 15.34
INSTRUM cryo500
PROBHD 5 mm CPTCI 1H-
PULPROG zg30
TD 32048
SOLVENT CDCl3
NS 8
DS 2
SWH 8012.820 Hz
FIDRES 0.250026 Hz
AQ 1.9998451 sec
RG 6.3
DW 62.400 usec
DE 6.00 usec
TE 298.0 K
D1 0.10000000 sec
MCREST 0.00000000 sec
MCWRK 0.01500000 sec

======== CHANNEL f1 ========
NUC1 1H
P1 7.50 usec
PL1 1.60 dB
SFO1 500.2235015 MHz

F2 - Processing parameters
SI 65536
SF 500.2200313 MHz
WDW EM
SSB 0
LB 0.30 Hz
GB 0
PC 1.00

1D NMR plot parameters
CX 22.80 cm
CY 15.00 cm
F1P 9.000 ppm
F1 4501.98 Hz
F2P -1.000 ppm
F2 -500.22 Hz
PPMCM 0.43860 ppm/cm
HZCM 219.39476 Hz/cm

Z-restored spin-echo 13C spectrum with 1H decoupling

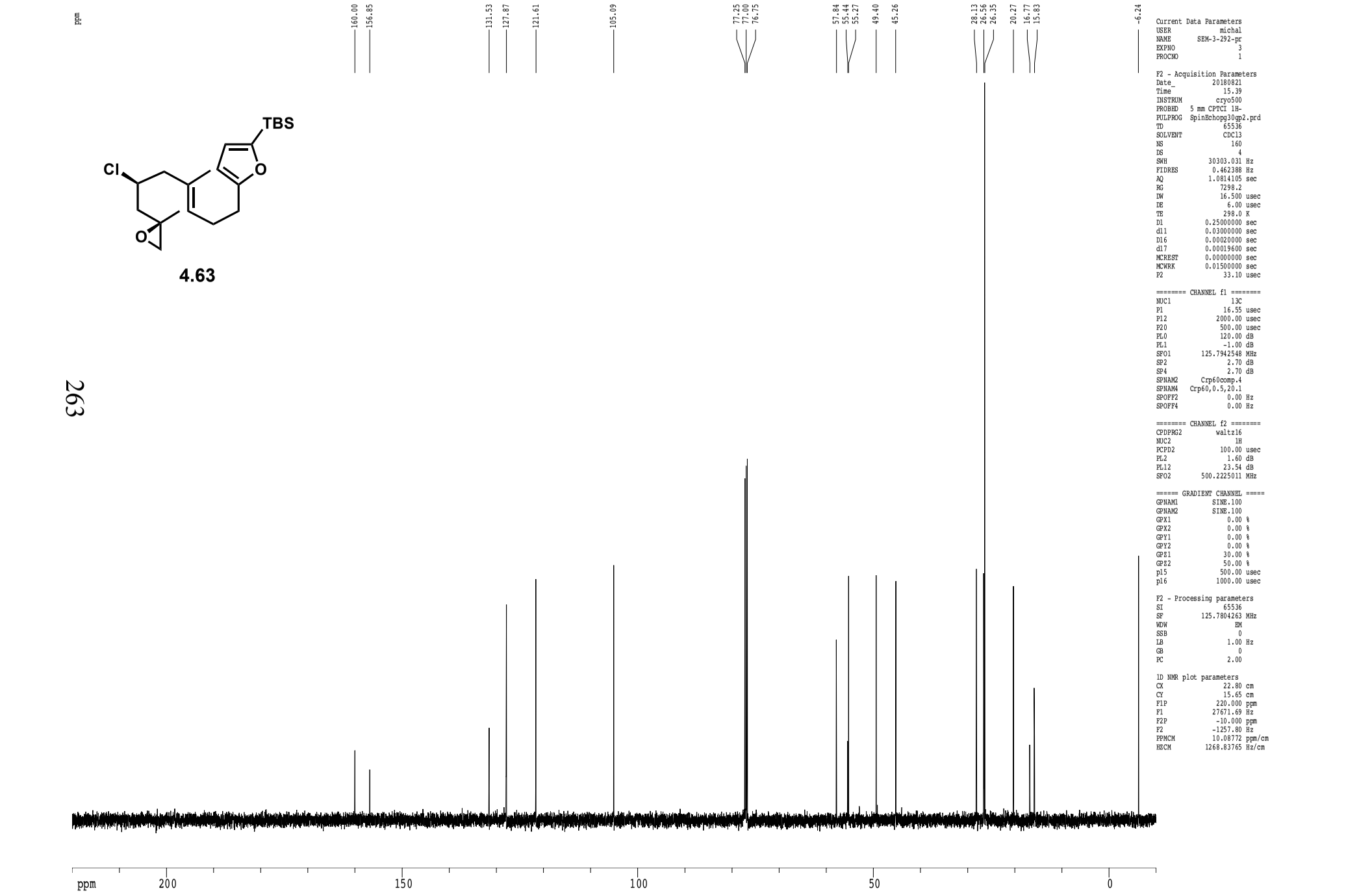

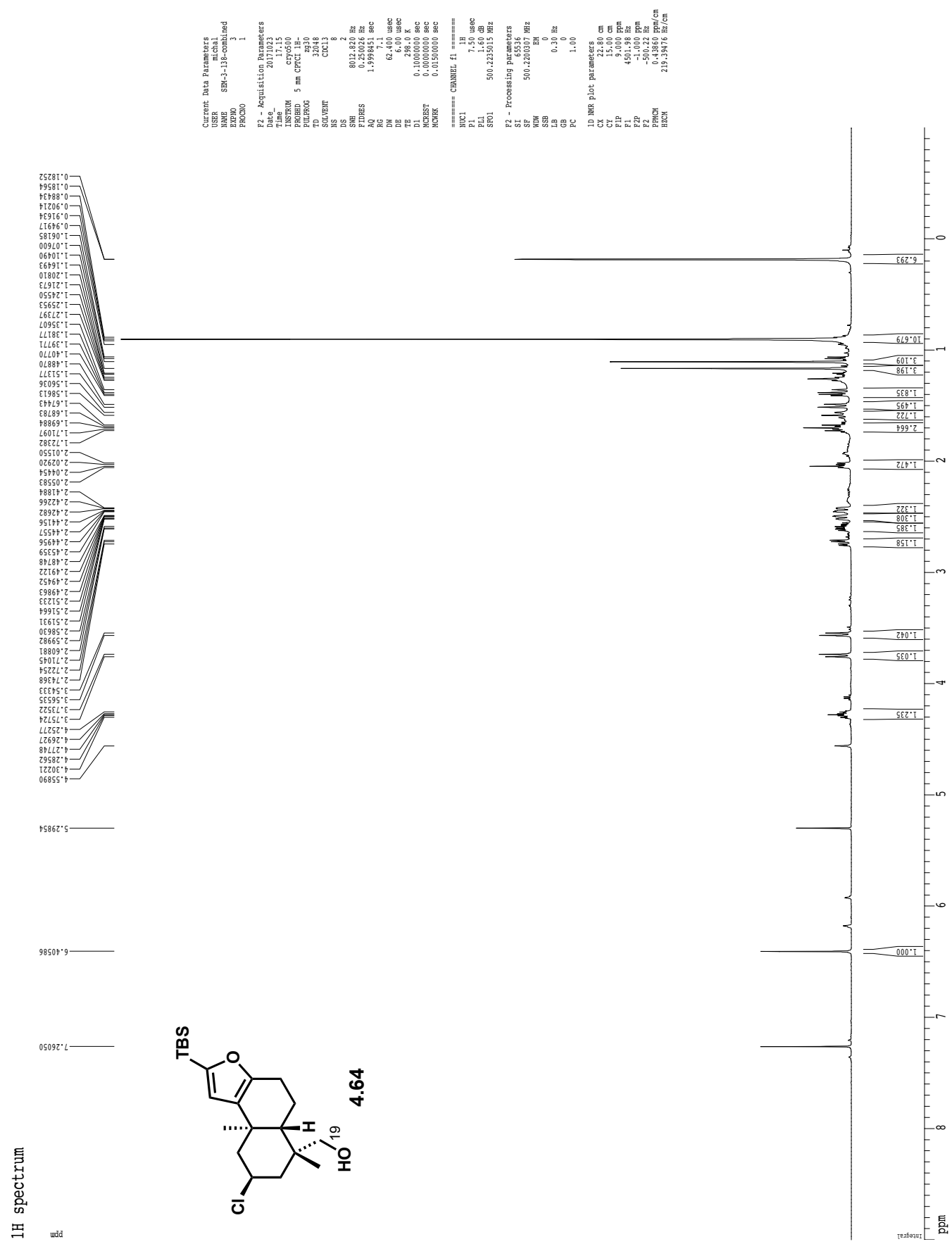
1H spectrum
TBS
O
H
HO
19
Cl
4.64
ppm
Integral

Z-restored spin-echo 13C spectrum with 1H decoupling

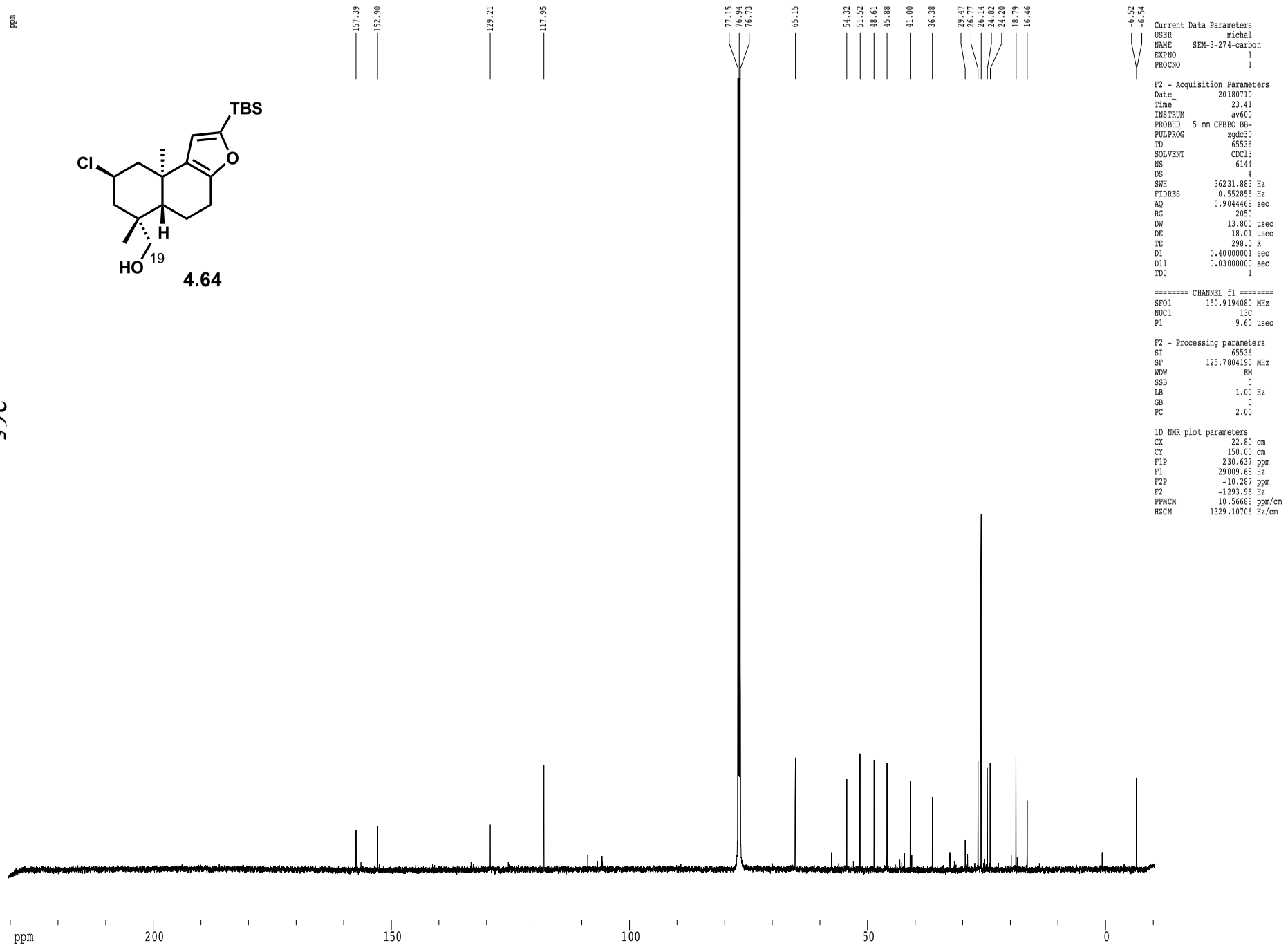

gnoe

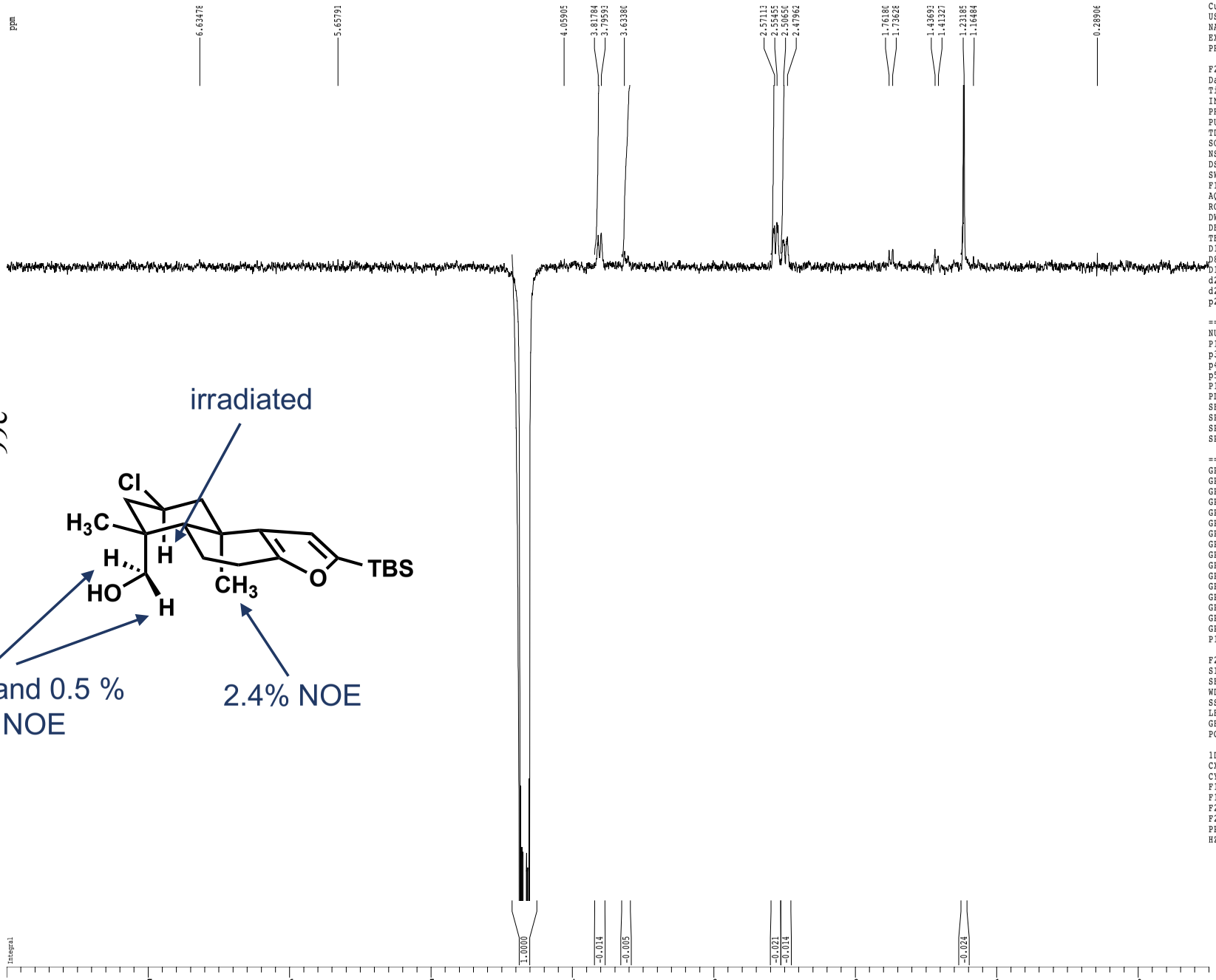

266

1.4 and 0.5 % NOE

2.4% NOE

Current Data Parameters
USER michal
NAME SEM-3-34-diast
EXPNO 2
PROCNO 1

F2 - Acquisition Parameters
Date_ 20170330
Time 11.38
INSTRUM gn500
PROBHD 5 mm broadband
PULPROG gnoelcc.wu
TD 65536
SOLVENT CDCl3
NS 256
DS 8
SWH 8012.820 Hz
FIDRES 0.122266 Hz
AQ 4.0894966 sec
RG 3649.1
DW 62.400 usec
DE 6.00 usec
TE 298.0 K
D1 1.00000000 sec
D8 0.50000000 sec
D16 0.00020000 sec
d21 0.33374399 sec
d22 0.16399699 sec
p2 24.00 usec

======== CHANNEL f1 ========
NUC1 1H
P1 12.00 usec
p3 36.00 usec
p4 48.00 usec
p5 32.00 usec
P12 40000.00 usec
PL1 -5.80 dB
SFO1 499.0721643 MHz
SP1 53.60 dB
SPNAM1 gauss1.512
SPOFF1 0.00 Hz

====== GRADIENT CHANNEL =====
GPNAM1 sine.100
GPNAM2 sine.100
GPNAM3 sine.100
GPNAM4 sine.100
GPX1 0.00 %
GPX2 0.00 %
GPX3 0.00 %
GPX4 0.00 %
GPY1 0.00 %
GPY2 0.00 %
GPY3 0.00 %
GPY4 0.00 %
GPZ1 7.00 %
GPZ2 3.00 %
GPZ3 2.30 %
GPZ4 -2.30 %
P16 1000.00 usec

F2 - Processing parameters
SI 65536
SF 499.0700000 MHz
WDW EM
SSB 0
LB 1.00 Hz
GB 0
PC 1.00

1D NMR plot parameters
CX 22.80 cm
CY 50.00 cm
F1P 8.000 ppm
F1 3992.56 Hz
F2P -0.500 ppm
F2 -249.54 Hz
PPMCM 0.37281 ppm/cm
HZCM 186.05681 Hz/cm

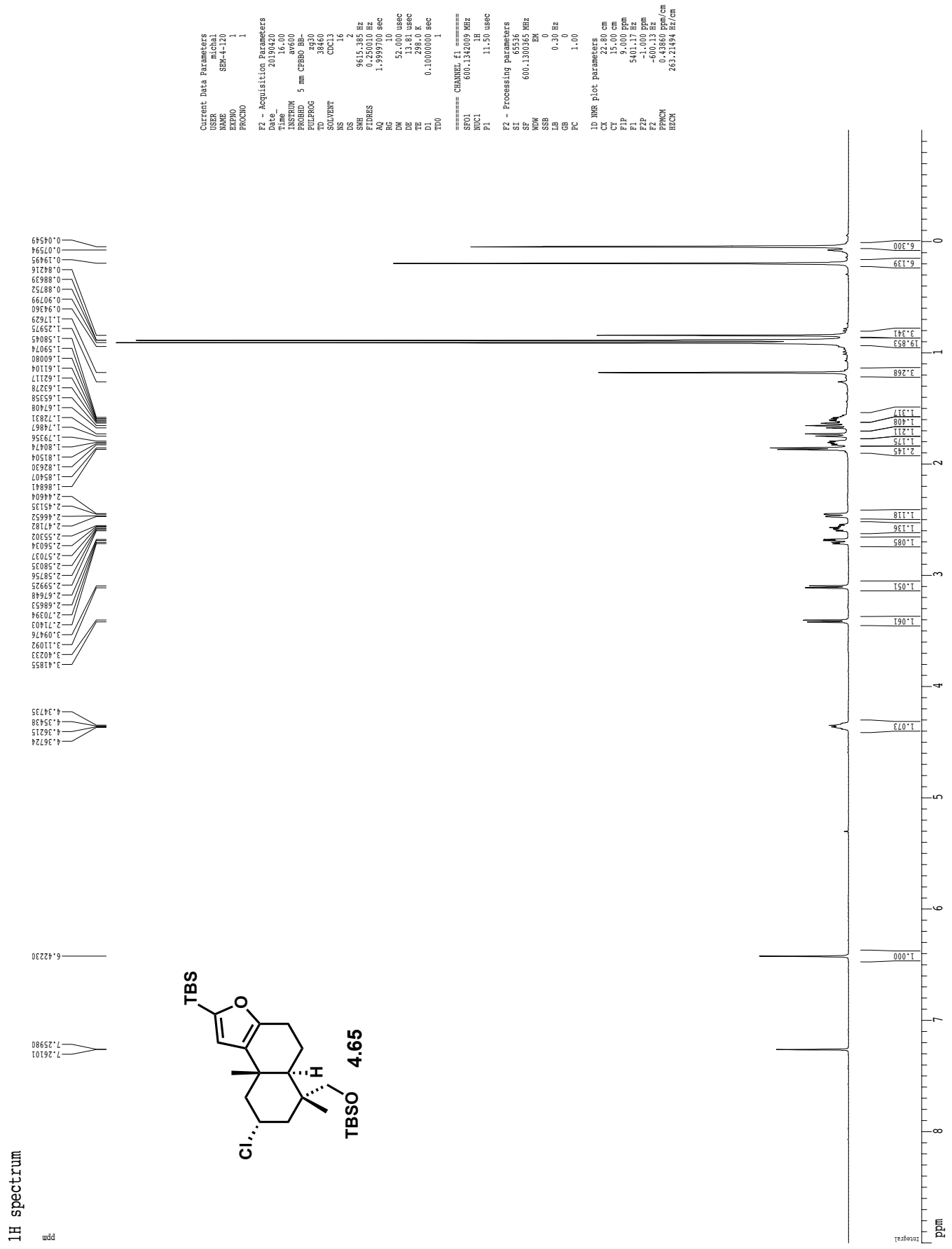
1H spectrum
TBS
O
H
TBSO
4.65
Cl
ppm

Z-restored spin-echo 13C spectrum with 1H decoupling

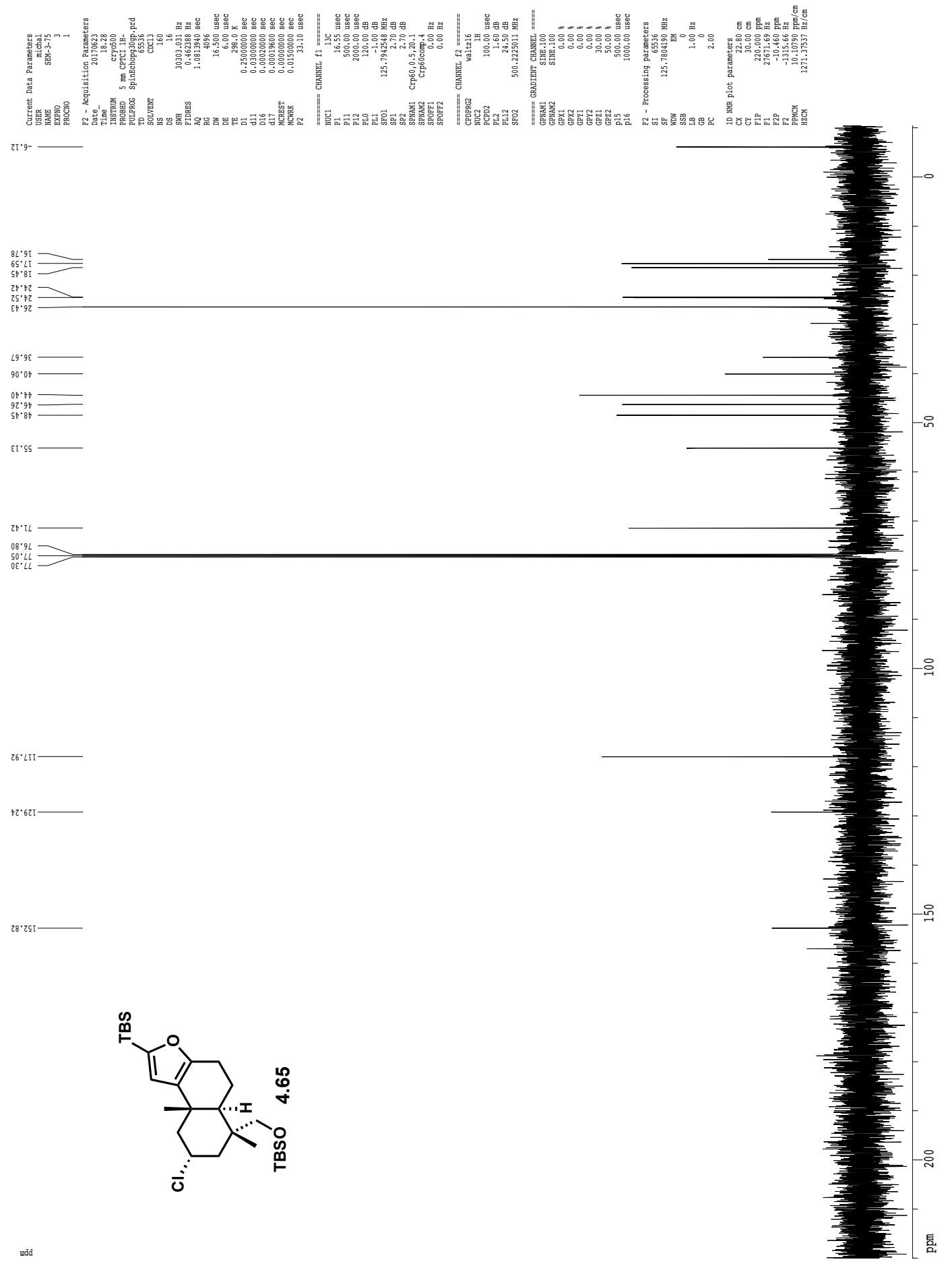

1H spectrum

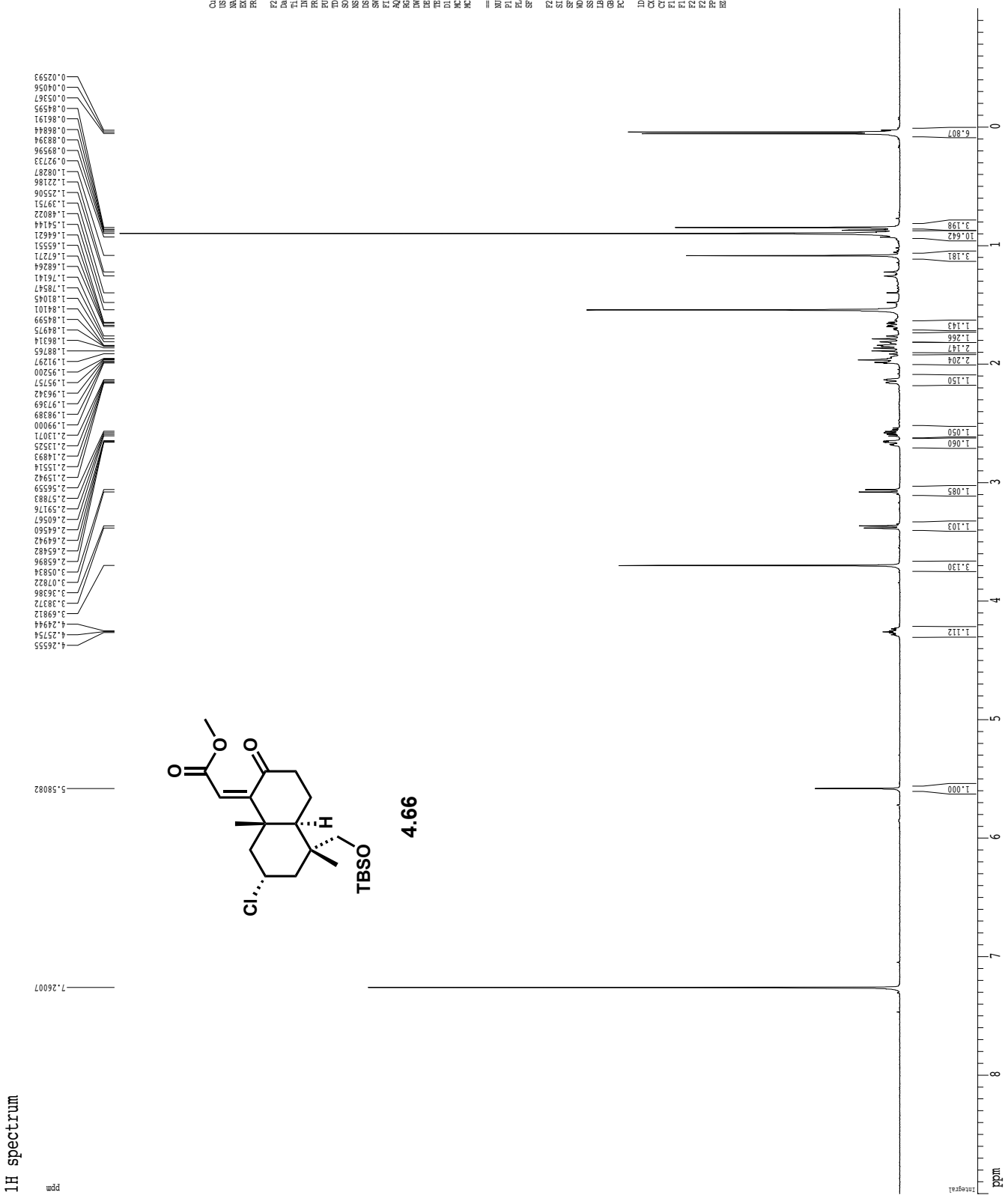
Current Data Parameters
USER michal
NAME SBM-3-178
EXPNO 2
PROCNO 1
F2 - Acquisition Parameters
Date_ 20180111
Time_ 14.41
INSTRUM cryo500
PROBHD 5 mm CPTCI 1H-
PULPROG zg30
TD 32048
SOLVENT CDCl3
NS 16
DS 2
SWH 8012.820 Hz
FIDRES 0.250026 Hz
AQ 1.9998451 sec
RG 6.3
DW 62.400 usec
DE 6.00 usec
TE 298.0 K
D1 0.10000000 sec
MCREST 0.00000000 sec
MCWRK 0.01500000 sec
====== CHANNEL f1 ======
NUC1 1H
P1 7.50 usec
PL1 1.60 dB
SFO1 500.2235015 MHz
F2 - Processing parameters
SI 65536
SF 500.2200313 MHz
WDW EM
SSB 0
LB 0.30 Hz
GB 0
PC 1.00
1D NMR plot parameters
CX 22.80 cm
CY 15.00 cm
F1P 9.000 ppm
F1 4501.98 Hz
F2P -1.000 ppm
F2 -500.22 Hz
PPMCM 0.43860 ppm/cm
HZCM 219.39476 Hz/cm
ppm
Integral
O
O
O
H
Cl
TBSO
4.66

Z-restored spin-echo 13C spectrum with 1H decoupling

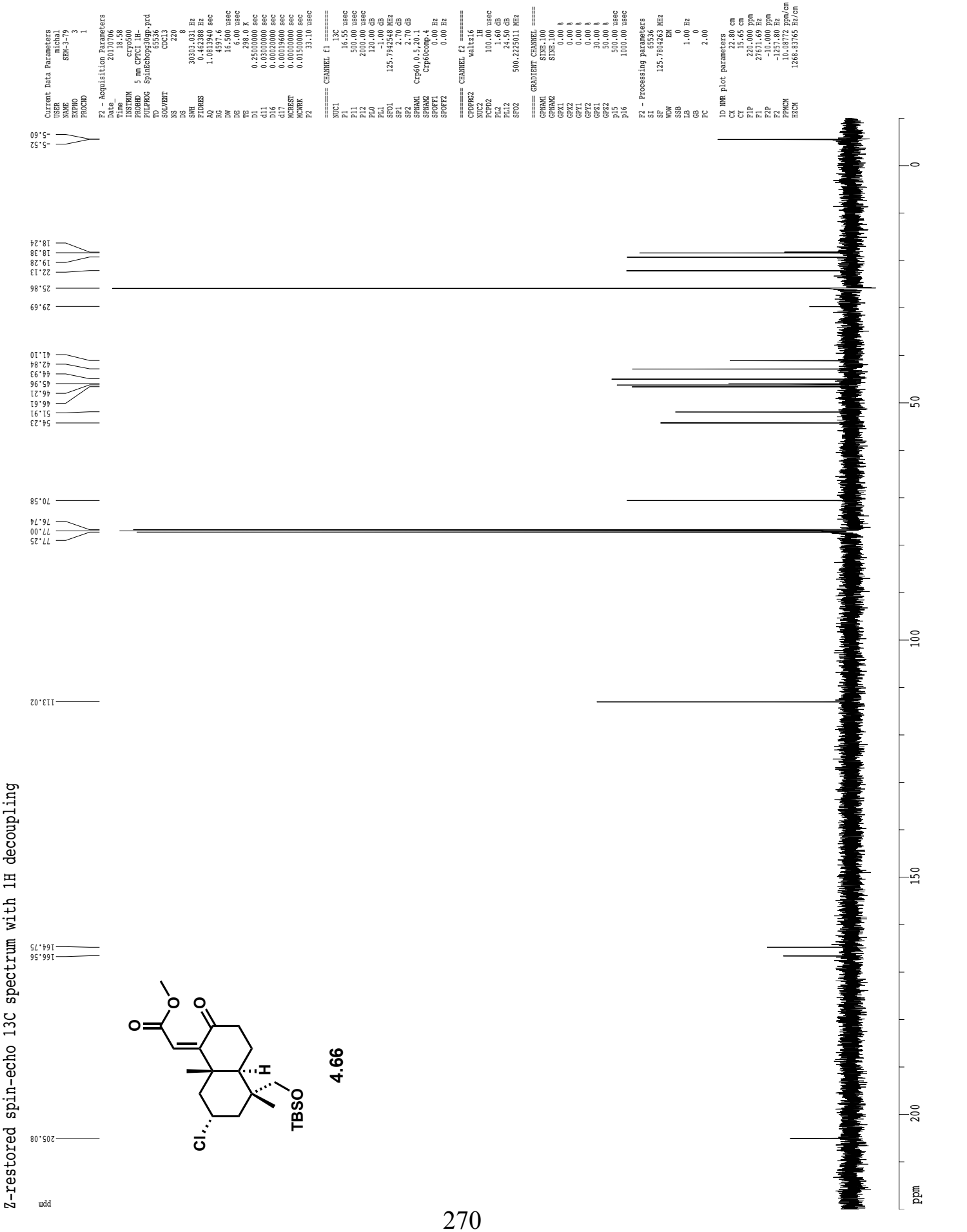

1H spectrum

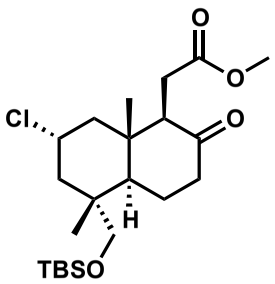

4.71

Z-restored spin-echo 13C spectrum with 1H decoupling

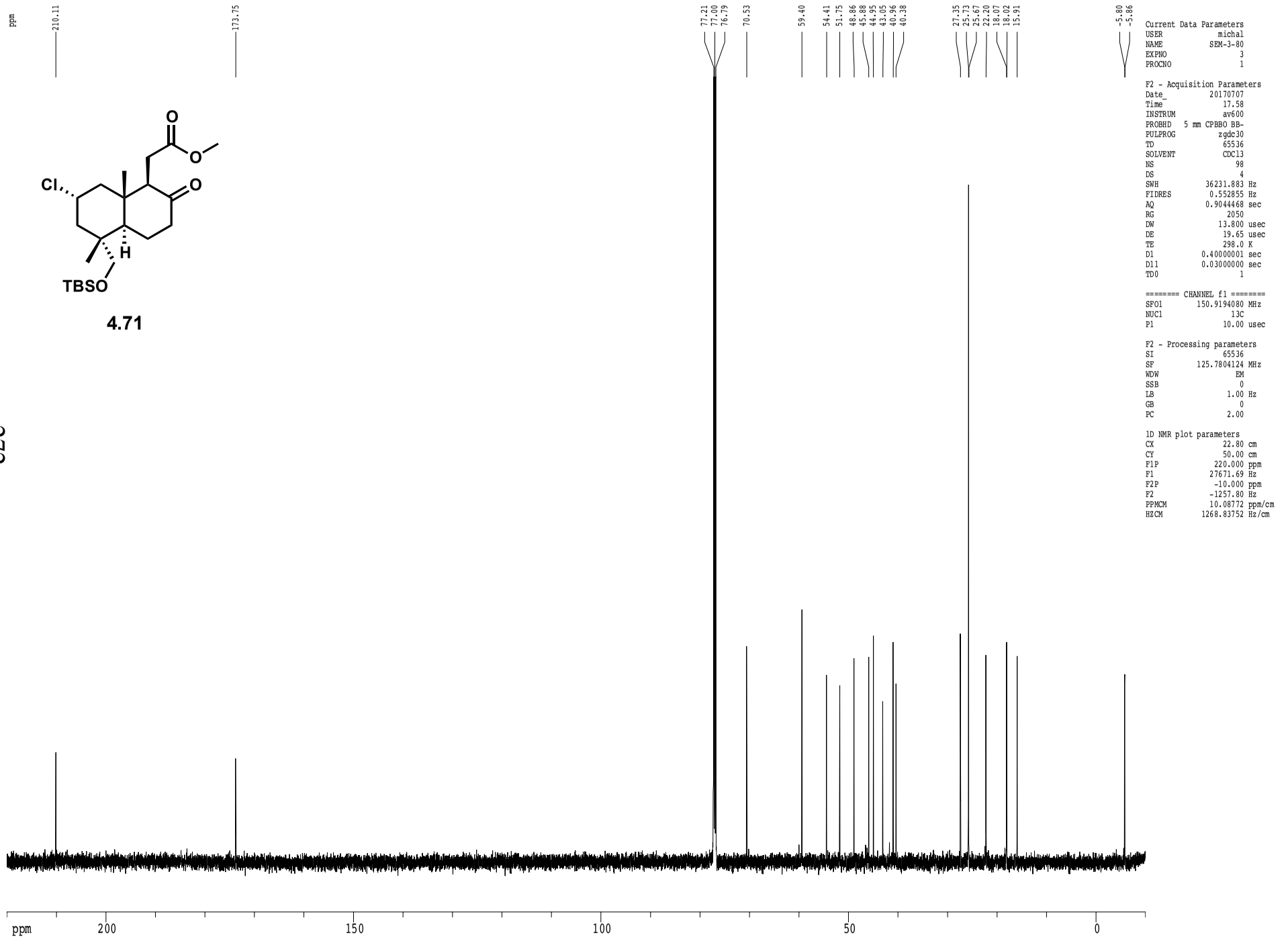

Current Data Parameters

USER	michal
NAME	SEM-3-80
EXPNO	3
PROCNO	1

F2 - Acquisition Parameters

Date_	20170707
Time	17.58
INSTRUM	av600
PROBHD	5 mm CPBBO BB-
PULPROG	zgdc30
TD	65536
SOLVENT	CDCl3
NS	98
DS	4
SWH	36231.883 Hz
FIDRES	0.552855 Hz
AQ	0.9044468 sec
RG	2050
DW	13.800 usec
DE	19.65 usec
TE	298.0 K
D1	0.40000001 sec
D11	0.03000000 sec
TD0	1

======= CHANNEL f1 =======

SFO1	150.9194080 MHz
NUC1	13C
P1	10.00 usec

F2 - Processing parameters

SI	65536
SF	125.7804124 MHz
WDW	EM
SSB	0
LB	1.00 Hz
GB	0
PC	2.00

1D NMR plot parameters

CX	22.80 cm
CY	50.00 cm
F1P	220.000 ppm
F1	27671.69 Hz
F2P	-10.000 ppm
F2	-1257.80 Hz
PPMCM	10.08772 ppm/cm
HZCM	1268.83752 Hz/cm

DEPTQ

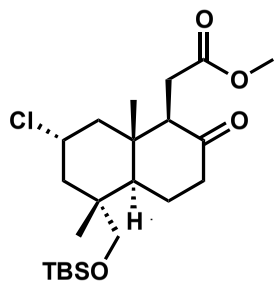

4.71


```
Current Data Parameters
NAME      SEM-3-146-DEPTQ
EXPNO                   1
PROCNO                  1

F2 - Acquisition Parameters
Date_           20171116
Time               11.37
INSTRUM            av600
PROBHD   5 mm CPBBO BB-
PULPROG         deptqgpsp
TD                 65536
SOLVENT             CDCl3
NS                    184
DS                      8
SWH             36231.883 Hz
FIDRES          0.552855 Hz
AQ              0.9043968 sec
RG                    322
DW                 13.800 usec
DE                 18.00 usec
TE                298.0 K
CNST2          145.0000000
CNST12           1.5000000
D1             2.00000000 sec
D2             0.00344828 sec
D12            0.00002000 sec
D16            0.00020000 sec
TD0                     1

======== CHANNEL f1 ========
SFO1          150.9194080 MHz
NUC1                    13C
P1                   10.00 usec
P13                2000.00 usec
PLW0     0 W
PLW1         64.00000000 W
SPNAM[5]     Crp60comp.4
SPOAL5             0.500
SPOFFS5  0 Hz
SPW5          9.96000004 W

======== CHANNEL f2 ========
SFO2          600.1330010 MHz
NUC2                    1H
CPDPRG[2          waltz16
P0                   18.00 usec
P3                   12.00 usec
P4                   24.00 usec
PCPD2                80.00 usec
PLW2         20.00000000 W
PLW12         0.36000001 W

====== GRADIENT CHANNEL =====
GPNAM[1]      SMSQ10.100
GPNAM[2]      SMSQ10.100
GPNAM[3]      SMSQ10.100
GPZ1                31.00 %
GPZ2                31.00 %
GPZ3                31.00 %
P16               1000.00 usec

F2 - Processing parameters
SI                  65536
SF            150.9028196 MHz
WDW                    EM
SSB      0
LB                  1.00 Hz
GB       0
PC                  1.00
```

gcosy60

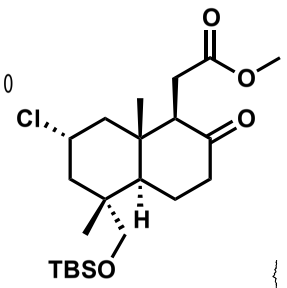

4.71


```
        Current Data Parameters
USER              michal
NAME      SEM-3-146-COSY
EXPNO                2
PROCNO               1

      F2 - Acquisition Parameters
Date_          20171114
Time              19.18
INSTRUM            gn500
PROBHD   5 mm broadband
PULPROG    cosygp60.prd
TD                2048
SOLVENT           CDCl3
NS                   2
DS                  16
SWH            4006.410 Hz
FIDRES         1.956255 Hz
AQ             0.2556404 sec
RG              5792.6
DW              124.800 usec
DE                6.00 usec
TE              298.0 K
d0           0.00000300 sec
D1           1.00000000 sec
d13          0.00000300 sec
D16          0.00025000 sec
IN0          0.00024960 sec

     ======== CHANNEL f1 ========
NUC1                 1H
P1                12.00 usec
PL1               -5.80 dB
SFO1        498.9520258 MHz

     ====== GRADIENT CHANNEL =====
GPNAM1          SINE.100
GPNAM2          SINE.100
GPX1               0.00 %
GPX2               0.00 %
GPY1               0.00 %
GPY2               0.00 %
GPZ1              17.00 %
GPZ2              17.00 %
P16             1000.00 usec

      F1 - Acquisition parameters
ND0                  1
TD                 256
SFO1           498.952 MHz
FIDRES        15.650040 Hz
SW             8.030 ppm
FnMODE              QF

      F2 - Processing parameters
SI                1024
SF          498.9500300 MHz
WDW               SINE
SSB                  0
LB                0.00 Hz
GB                   0
PC                1.00

      F1 - Processing parameters
SI                1024
MC2                 QF
SF          498.9500300 MHz
WDW               SINE
SSB                  0
LB                0.00 Hz
GB                   0

        2D NMR plot parameters
CX2              15.00 cm
CX1              15.00 cm
F2PLO             5.000 ppm
F2LO           2494.75 Hz
F2PHI             1.000 ppm
F2HI            498.95 Hz
F1PLO             5.000 ppm
F1LO           2494.75 Hz
F1PHI             1.000 ppm
F1HI            498.95 Hz
F2PPMCM        0.26667 ppm/cm
F2HZCM        133.05334 Hz/cm
F1PPMCM        0.26667 ppm/cm
F1HZCM        133.05334 Hz/cm
```

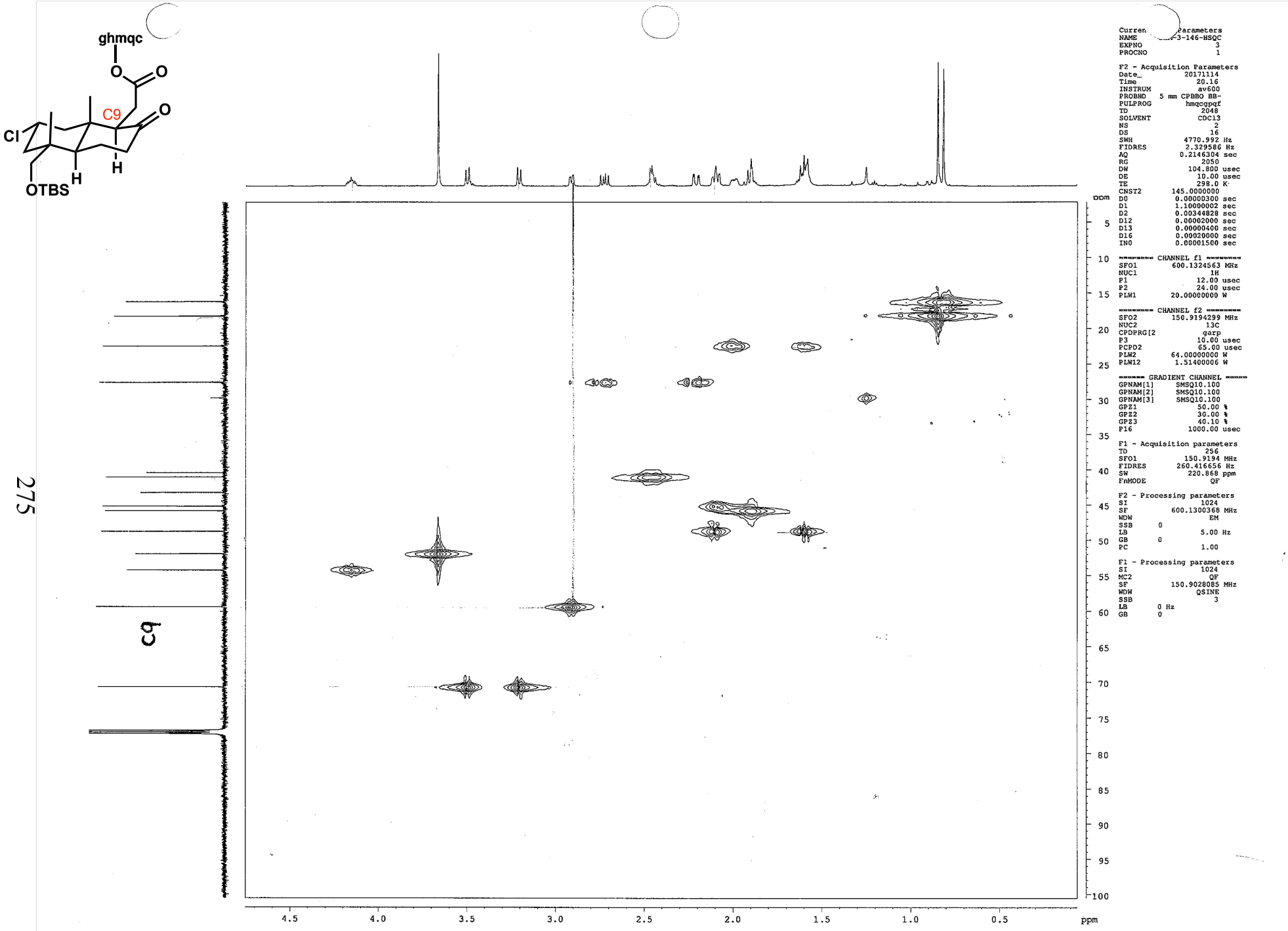
ghmqc
O
O
O
C9
O
Cl
H
H
OTBS
cq
4.5
4.0
3.5
3.0
2.5
2.0
1.5
1.0
0.5
ppm
5
10
15
20
25
30
35
40
45
50
55
60
65
70
75
80
85
90
95
100
Curren Parameters
NAME -3-146-HSQC
EXPNO 3
PROCNO 1
F2 - Acquisition Parameters
Date_ 20171114
Time 20.16
INSTRUM av600
PROBHD 5 mm CPBBO BB-
PULPROG hmqcgpqf
TD 2048
SOLVENT CDCl3
NS 2
DS 16
SWH 4770.992 Hz
FIDRES 2.329586 Hz
AQ 0.2146304 sec
RG 2050
DW 104.800 usec
DE 10.00 usec
TE 298.0 K
CNST2 145.0000000
D0 0.00000300 sec
D1 1.10000002 sec
D2 0.00344828 sec
D12 0.00002000 sec
D13 0.00000400 sec
D16 0.00020000 sec
IN0 0.00001500 sec
======== CHANNEL f1 ========
SFO1 600.1324563 MHz
NUC1 1H
P1 12.00 usec
P2 24.00 usec
PLW1 20.00000000 W
======== CHANNEL f2 ========
SFO2 150.9194299 MHz
NUC2 13C
CPDPRG[2 garp
P3 10.00 usec
PCPD2 65.00 usec
PLW2 64.00000000 W
PLW12 1.51400006 W
====== GRADIENT CHANNEL =====
GPNAM[1] SMSQ10.100
GPNAM[2] SMSQ10.100
GPNAM[3] SMSQ10.100
GPZ1 50.00 %
GPZ2 30.00 %
GPZ3 40.10 %
P16 1000.00 usec
F1 - Acquisition parameters
TD 256
SFO1 150.9194 MHz
FIDRES 260.416656 Hz
SW 220.868 ppm
FnMODE QF
F2 - Processing parameters
SI 1024
SF 600.1300368 MHz
WDW EM
SSB 0
LB 5.00 Hz
GB 0
PC 1.00
F1 - Processing parameters
SI 1024
MC2 QF
SF 150.9028085 MHz
WDW QSINE
SSB 3
LB 0 Hz
GB 0

gnoe

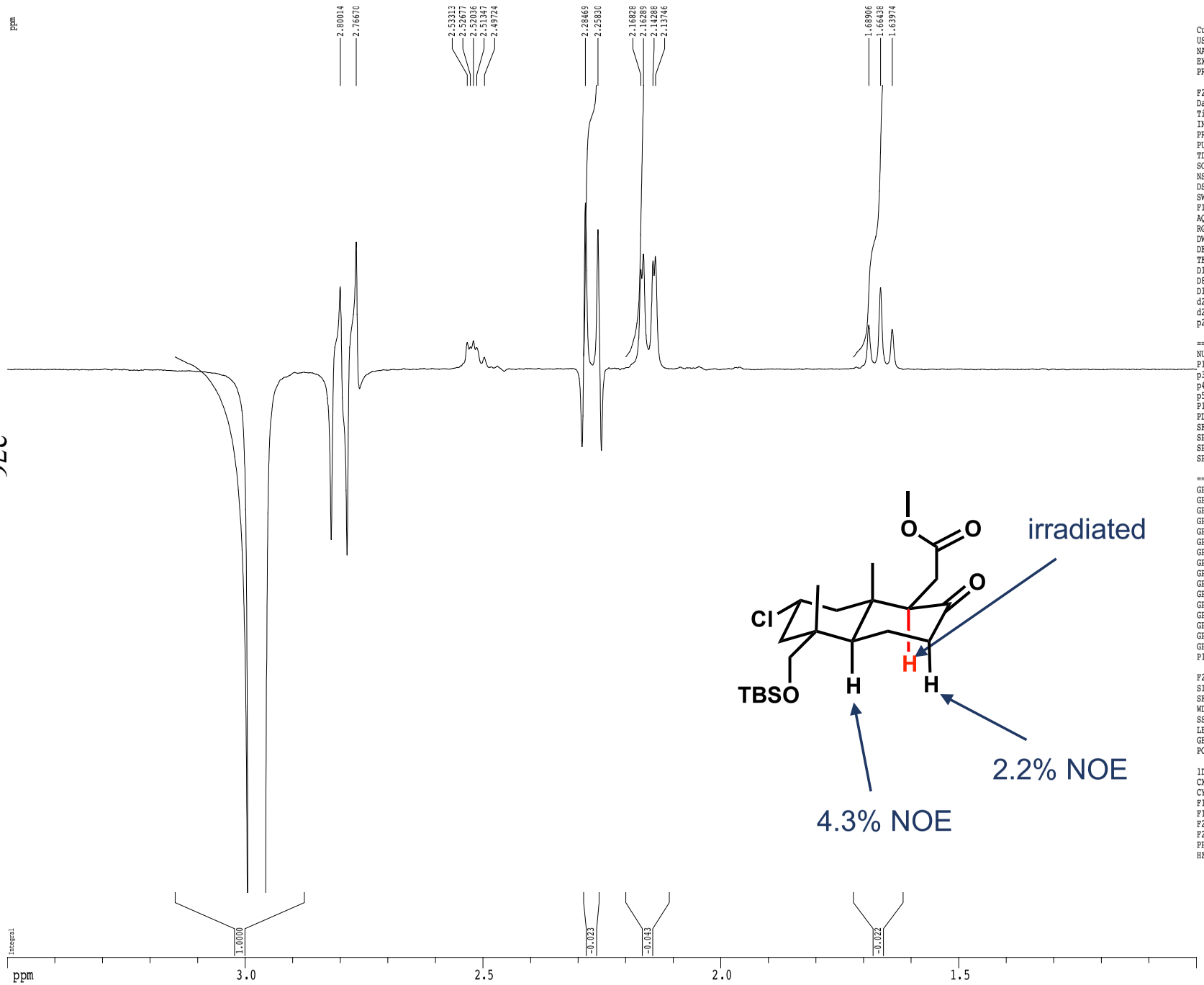

276

Current Data Parameters
USER michal
NAME SEM-3-146-NOE1
EXPNO 2
PROCNO 1

F2 - Acquisition Parameters
Date_ 20171116
Time 13.07
INSTRUM cryo500
PROBHD 5 mm CPTCI 1H-
PULPROG gnoelcc.wu
TD 65536
SOLVENT CDCl3
NS 256
DS 8
SWH 8012.820 Hz
FIDRES 0.122266 Hz
AQ 4.0894966 sec
RG 45.3
DW 62.400 usec
DE 6.00 usec
TE 298.0 K
D1 1.00000000 sec
D8 0.50000000 sec
D16 0.00020000 sec
d21 0.33376500 sec
d22 0.16399699 sec
p2 15.00 usec

======== CHANNEL f1 ========
NUC1 1H
P1 7.50 usec
p3 22.50 usec
p4 30.00 usec
p5 20.00 usec
P12 40000.00 usec
PL1 1.60 dB
SFO1 500.2214890 MHz
SP1 61.60 dB
SPNAM1 gauss1.512
SPOFF1 0.00 Hz

====== GRADIENT CHANNEL =====
GPNAM1 sine.100
GPNAM2 sine.100
GPNAM3 sine.100
GPNAM4 sine.100
GPX1 0.00 %
GPX2 0.00 %
GPX3 0.00 %
GPX4 0.00 %
GPY1 0.00 %
GPY2 0.00 %
GPY3 0.00 %
GPY4 0.00 %
GPZ1 7.00 %
GPZ2 3.00 %
GPZ3 2.30 %
GPZ4 -2.30 %
P16 1000.00 usec

F2 - Processing parameters
SI 65536
SF 500.2200000 MHz
WDW EM
SSB 0
LB 1.00 Hz
GB 0
PC 1.00

1D NMR plot parameters
CX 22.80 cm
CY 50.00 cm
F1P 3.500 ppm
F1 1750.77 Hz
F2P 1.000 ppm
F2 500.22 Hz
PPMCM 0.10965 ppm/cm
HZCM 54.84869 Hz/cm

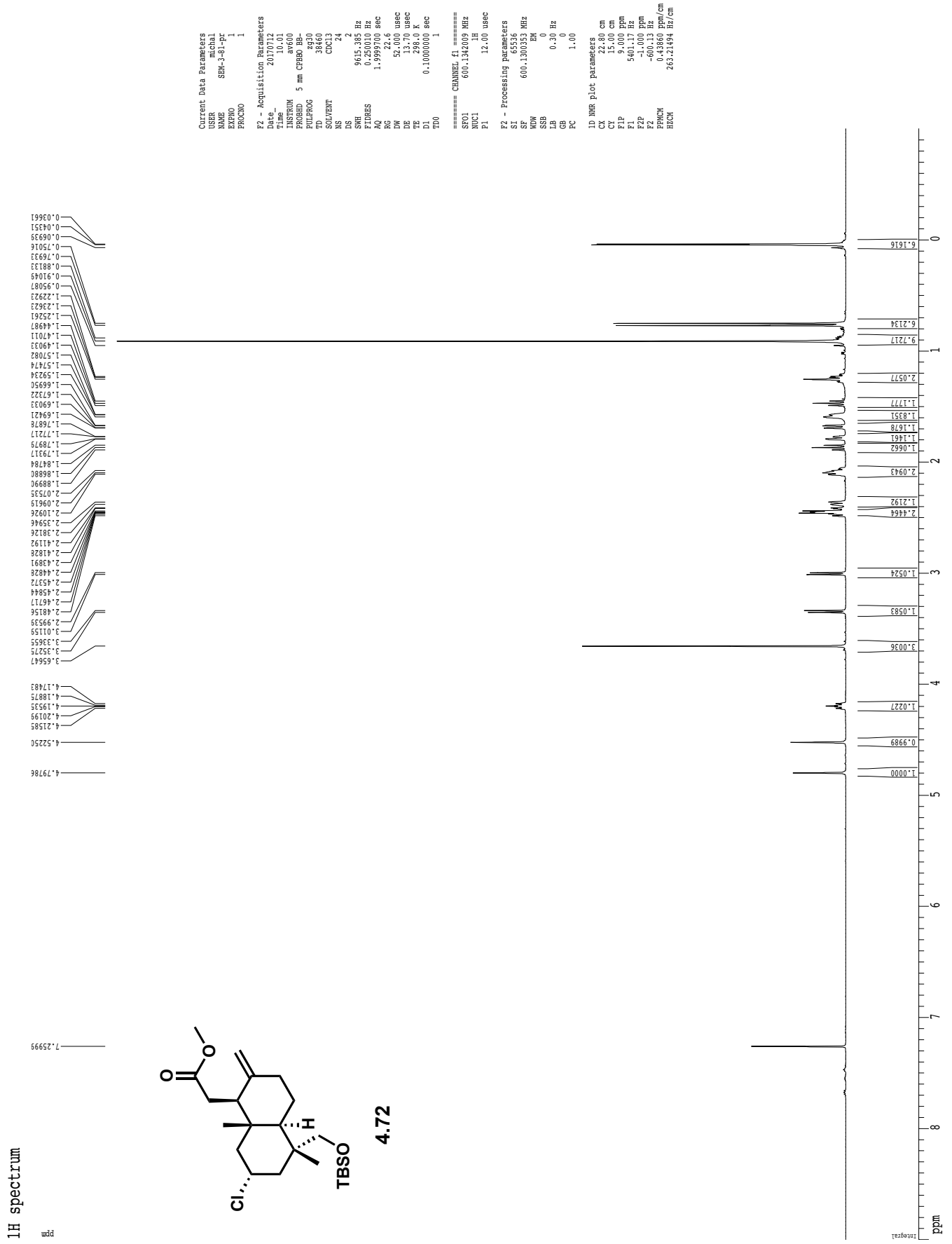
1H spectrum
ppm
Integral
Current Data Parameters
USER michal
NAME SEM-3-81-pr
EXPNO 1
PROCNO 1
F2 - Acquisition Parameters
Date_ 20170712
Time_ 10.01
INSTRUM av600
PROBHD 5 mm CPBBO BB-
PULPROG zg30
TD 38460
SOLVENT CDCl3
NS 24
DS 2
SWH 9615.385 Hz
FIDRES 0.250010 Hz
AQ 1.9999700 sec
RG 22.6
DW 52.000 usec
DE 13.70 usec
TE 298.0 K
D1 0.10000000 sec
TD0 1
======== CHANNEL f1 ========
SFO1 600.1342009 MHz
NUC1 1H
P1 12.00 usec
F2 - Processing parameters
SI 65536
SF 600.1300353 MHz
WDW EM
SSB 0
LB 0.30 Hz
GB 0
PC 1.00
1D NMR plot parameters
CX 22.80 cm
CY 15.00 cm
F1P 9.000 ppm
F1 5401.17 Hz
F2P -1.000 ppm
F2 -600.13 Hz
PPMCM 0.43860 ppm/cm
HZCM 263.21494 Hz/cm
7.25999
4.79786
4.52250
4.21585
4.20199
4.19535
4.18875
4.17483
3.65647
3.35275
3.33655
3.01155
2.99539
2.46156
2.46717
2.45844
2.45372
2.44828
2.43891
2.41892
2.41828
2.38126
2.35946
2.10926
2.09619
2.07535
1.88990
1.86880
1.84784
1.79317
1.78979
1.77217
1.76878
1.69421
1.69033
1.67322
1.66950
1.59234
1.57474
1.57082
1.49033
1.47011
1.44987
1.25261
1.23623
1.22923
0.95087
0.91049
0.88133
0.76933
0.75016
0.69039
0.04351
0.03661
6.1616
6.2134
9.7217
2.0577
1.1777
1.8351
1.1678
1.1461
1.0662
2.0943
1.2192
2.4464
1.0524
1.0583
3.0036
1.0227
0.9989
1.0000
O
O
H
Cl
TBSO
4.72

Z-restored spin-echo 13C spectrum with 1H decoupling

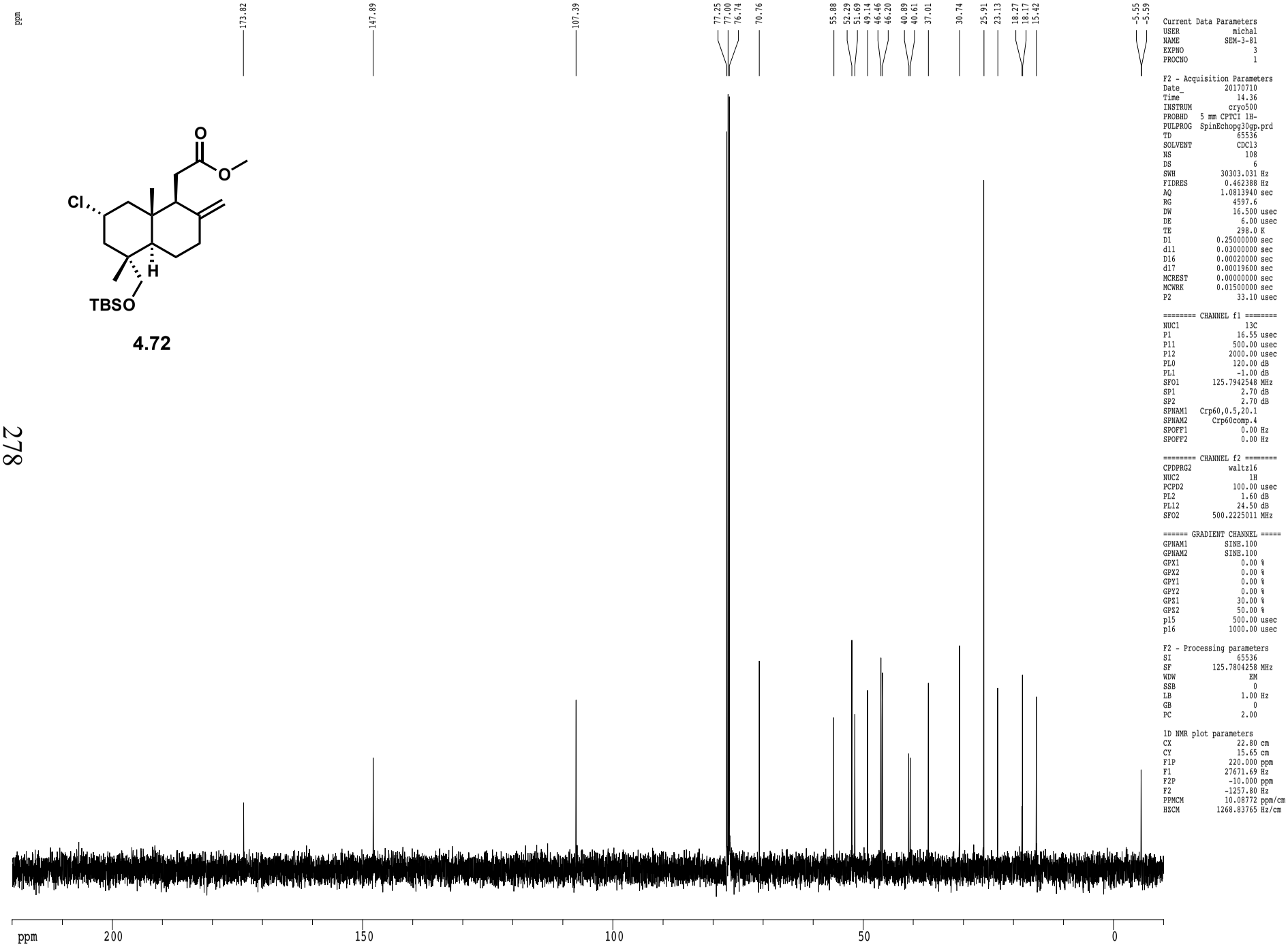

278

Current Data Parameters
USER michal
NAME SEM-3-81
EXPNO 3
PROCNO 1

F2 - Acquisition Parameters
Date_ 20170710
Time 14.36
INSTRUM cryo500
PROBHD 5 mm CPTCI 1H-
PULPROG SpinEchopg30gp.prd
TD 65536
SOLVENT CDCl3
NS 108
DS 6
SWH 30303.031 Hz
FIDRES 0.462388 Hz
AQ 1.0813940 sec
RG 4597.6
DW 16.500 usec
DE 6.00 usec
TE 298.0 K
D1 0.25000000 sec
d11 0.03000000 sec
D16 0.00020000 sec
d17 0.00019600 sec
MCREST 0.00000000 sec
MCWRK 0.01500000 sec
P2 33.10 usec

======== CHANNEL f1 ========
NUC1 13C
P1 16.55 usec
P11 500.00 usec
P12 2000.00 usec
PL0 120.00 dB
PL1 -1.00 dB
SFO1 125.7942548 MHz
SP1 2.70 dB
SP2 2.70 dB
SPNAM1 Crp60,0.5,20.1
SPNAM2 Crp60comp.4
SPOFF1 0.00 Hz
SPOFF2 0.00 Hz

======== CHANNEL f2 ========
CPDPRG2 waltz16
NUC2 1H
PCPD2 100.00 usec
PL2 1.60 dB
PL12 24.50 dB
SFO2 500.2225011 MHz

====== GRADIENT CHANNEL =====
GPNAM1 SINE.100
GPNAM2 SINE.100
GPX1 0.00 %
GPX2 0.00 %
GPY1 0.00 %
GPY2 0.00 %
GPZ1 30.00 %
GPZ2 50.00 %
p15 500.00 usec
p16 1000.00 usec

F2 - Processing parameters
SI 65536
SF 125.7804258 MHz
WDW EM
SSB 0
LB 1.00 Hz
GB 0
PC 2.00

1D NMR plot parameters
CX 22.80 cm
CY 15.65 cm
F1P 220.000 ppm
F1 27671.69 Hz
F2P -10.000 ppm
F2 -1257.80 Hz
PPMCM 10.08772 ppm/cm
HZCM 1268.83765 Hz/cm

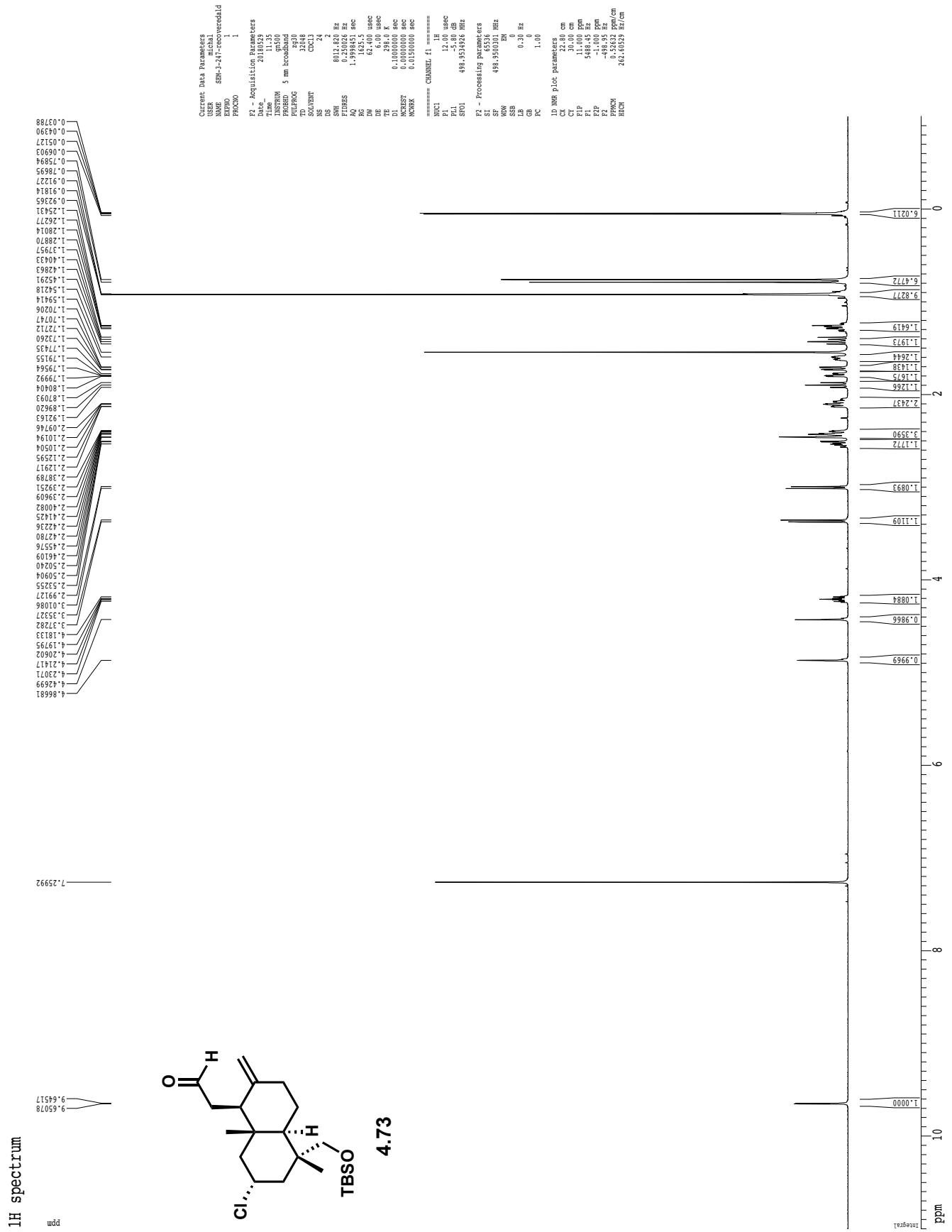
1H spectrum
4.73
TBSO
Cl
H
O
H
ppm
Integral

Z-restored spin-echo 13C spectrum with 1H decoupling

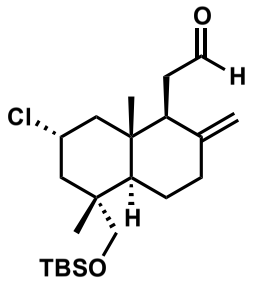

4.73

300

ppm

202.89 147.41 109.27 77.15 76.94 76.73 70.43 55.56 50.54 49.27 46.26 46.00 40.61 40.43 39.48 36.76 25.67 22.77 17.99 17.94 15.36 -5.90 -5.94

```
Current Data Parameters
USER              michal
NAME      SEM-3-227-recoveredcarbon
EXPNO                2
PROCNO               1

F2 - Acquisition Parameters
Date_          20180529
Time             12.48
INSTRUM          av600
PROBHD   5 mm CPBBO BB-
PULPROG          zgdc30
TD               65536
SOLVENT          CDCl3
NS                 417
DS                   4
SWH          36231.883 Hz
FIDRES       0.552855 Hz
AQ           0.9044468 sec
RG                2050
DW              13.800 usec
DE              18.01 usec
TE              298.0 K
D1           0.40000001 sec
D11          0.03000000 sec
TD0                  1

======== CHANNEL f1 ========
SFO1        150.9194080 MHz
NUC1               13C
P1                9.60 usec

F2 - Processing parameters
SI                65536
SF          125.7804190 MHz
WDW                  EM
SSB                  0
LB                1.00 Hz
GB                   0
PC                2.00

1D NMR plot parameters
CX               22.80 cm
CY              100.00 cm
F1P             220.000 ppm
F1              27671.69 Hz
F2P             -10.460 ppm
F2              -1315.66 Hz
PPMCM           10.10789 ppm/cm
HZCM          1271.37524 Hz/cm
```

ppm 200 150 100 50 0

1H spectrum

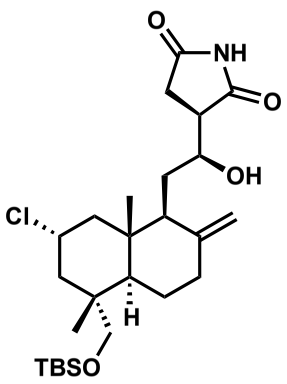

4.78

Current Data Parameters
USER michal
NAME SEM-4-107-2
EXPNO 4
PROCNO 1

F2 - Acquisition Parameters
Date_ 20190320
Time 13.47
INSTRUM cryo500
PROBHD 5 mm CPTCI 1H-
PULPROG zg30
TD 32048
SOLVENT CDCl3
NS 32
DS 2
SWH 8012.820 Hz
FIDRES 0.250026 Hz
AQ 1.9998451 sec
RG 10.1
DW 62.400 usec
DE 6.00 usec
TE 298.0 K
D1 0.10000000 sec
MCREST 0.00000000 sec
MCWRK 0.01500000 sec

======= CHANNEL f1 =======
NUC1 1H
P1 7.50 usec
PL1 1.60 dB
SFO1 500.2235015 MHz

F2 - Processing parameters
SI 65536
SF 500.2200319 MHz
WDW EM
SSB 0
LB 0.30 Hz
GB 0
PC 1.00

1D NMR plot parameters
CX 22.80 cm
CY 40.00 cm
F1P 9.000 ppm
F1 4501.98 Hz
F2P -1.000 ppm
F2 -500.22 Hz
PPMCM 0.43860 ppm/cm
HZCM 219.39476 Hz/cm

Z-restored spin-echo 13C spectrum with 1H decoupling

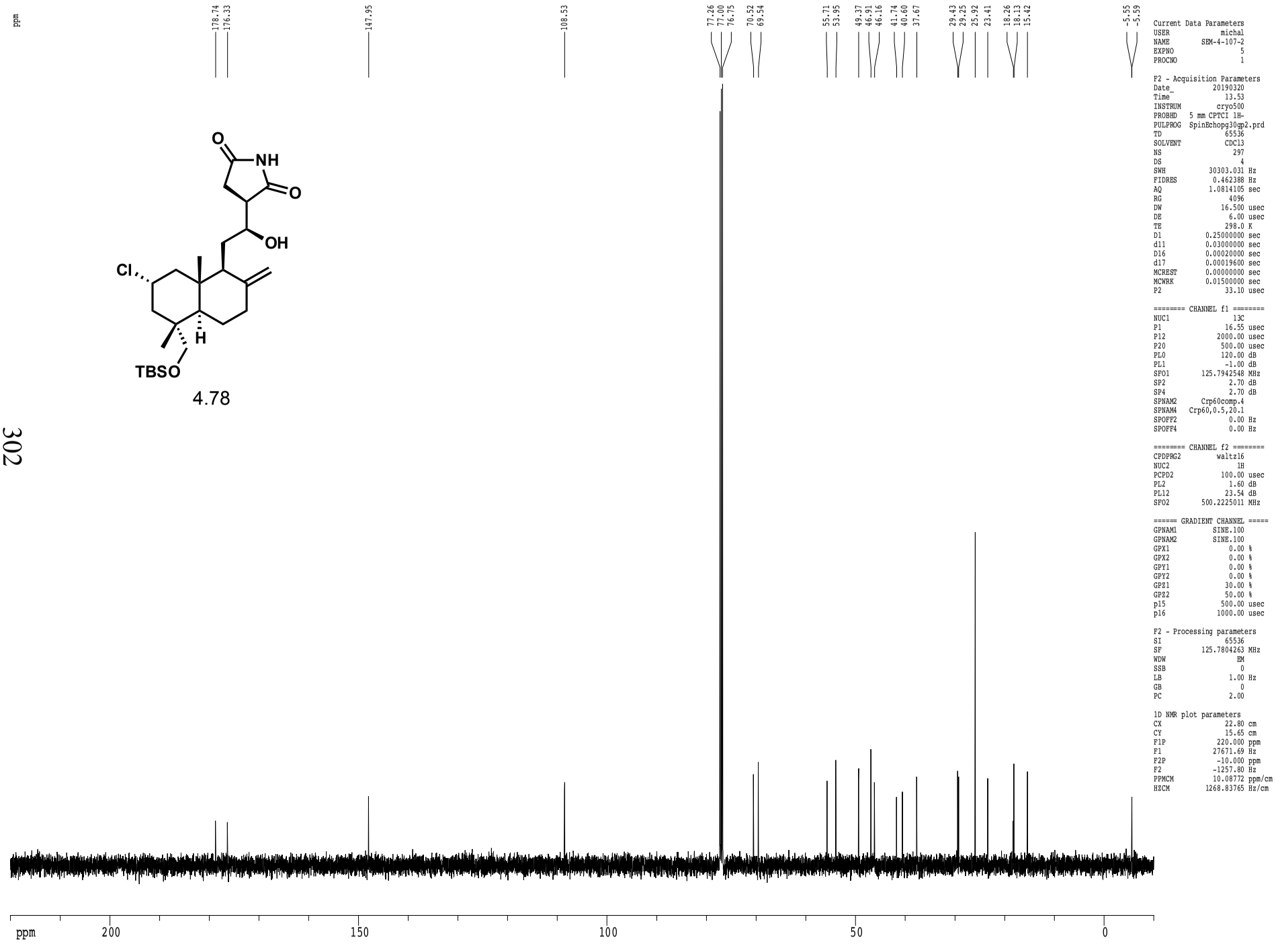

1H spectrum

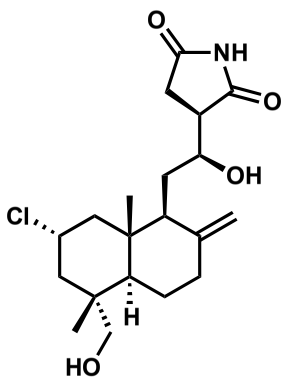

hatJ : 4.4

(in $CDCl_3$)


```
Current Data Parameters
USER                michal
NAME          SEM-4-108-2
EXPNO                   1
PROCNO                  1

F2 - Acquisition Parameters
Date_            20190321
Time                15.25
INSTRUM           cryo500
PROBHD   5 mm CPTCI 1H-
PULPROG               zg30
TD                   32048
SOLVENT              CDCl3
NS                      24
DS                       2
SWH               8012.820 Hz
FIDRES            0.250026 Hz
AQ                1.9999076 sec
RG                       9
DW                  62.400 usec
DE                   6.00 usec
TE                  298.0 K
D1              0.10000000 sec
MCREST          0.00000000 sec
MCWRK           0.01500000 sec

======== CHANNEL f1 ========
NUC1                    1H
P1                   7.50 usec
PL1                  1.60 dB
SFO1          500.2235015 MHz

F2 - Processing parameters
SI                   65536
SF            500.2200321 MHz
WDW                     EM
SSB                      0
LB                    0.30 Hz
GB                       0
PC                    1.00

1D NMR plot parameters
CX                   22.80 cm
CY                   15.00 cm
F1P                 10.000 ppm
F1                5002.20 Hz
F2P                  0.000 ppm
F2                   0.00 Hz
PPMCM             0.43860 ppm/cm
HZCM            219.39476 Hz/cm
```

Z-restored spin-echo 13C spectrum with 1H decoupling

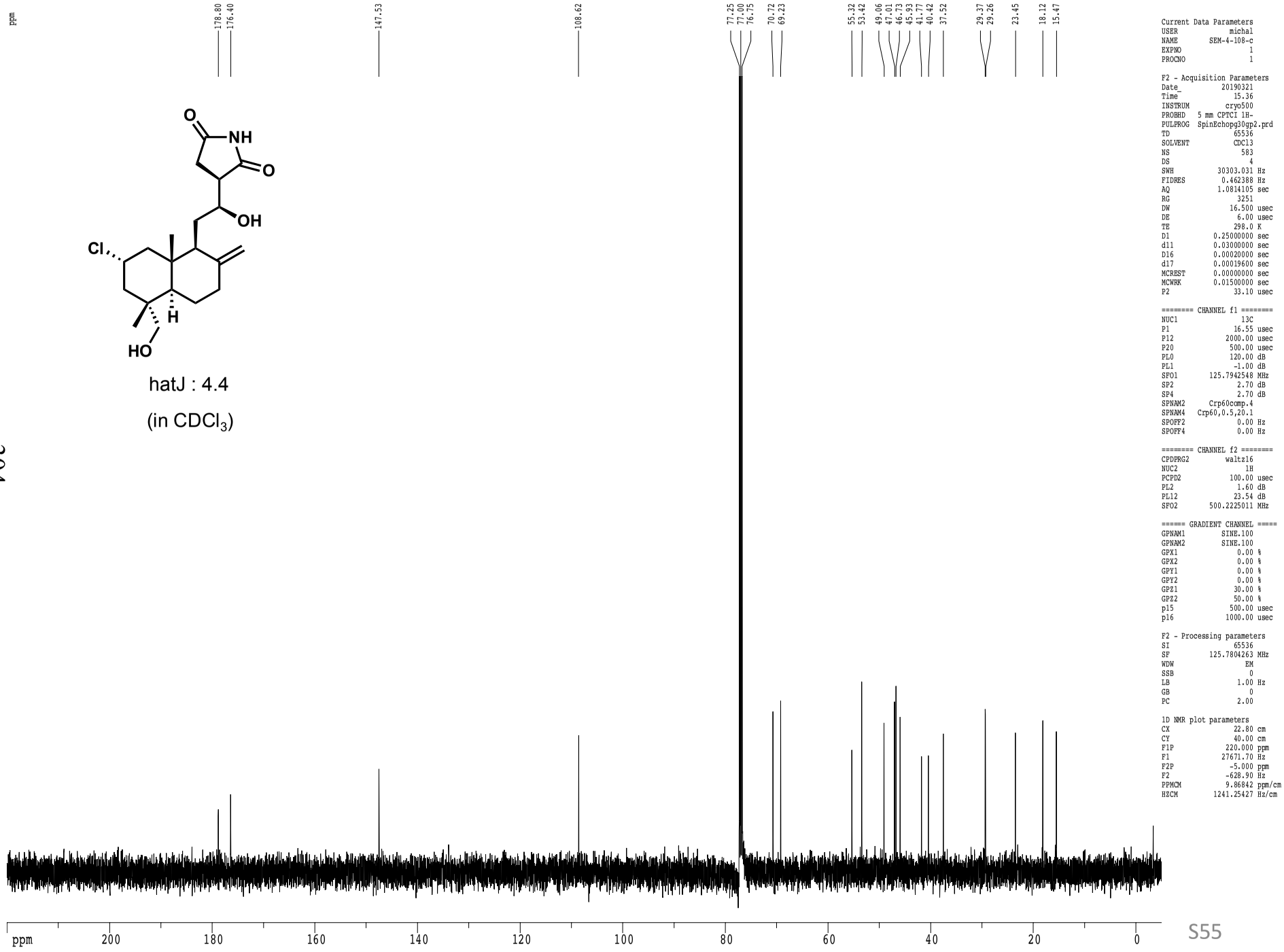

hatJ : 4.4

(in $CDCl_3$)

304

```
Current Data Parameters
USER              michal
NAME         SEM-4-108-c
EXPNO                   1
PROCNO                  1

F2 - Acquisition Parameters
Date_            20190321
Time                15.36
INSTRUM          cryo500
PROBHD    5 mm CPTCI 1H-
PULPROG   SpinEchopg30gp2.prd
TD                  65536
SOLVENT             CDCl3
NS                    583
DS                      4
SWH            30303.031 Hz
FIDRES         0.462388 Hz
AQ             1.0814105 sec
RG                   3251
DW                 16.500 usec
DE                  6.00 usec
TE                298.0 K
D1            0.25000000 sec
d11           0.03000000 sec
D16           0.00020000 sec
d17           0.00019600 sec
MCREST        0.00000000 sec
MCWRK         0.01500000 sec
P2                  33.10 usec

======== CHANNEL f1 ========
NUC1                13C
P1                16.55 usec
P12             2000.00 usec
P20              500.00 usec
PL0              120.00 dB
PL1               -1.00 dB
SFO1         125.7942548 MHz
SP2                2.70 dB
SP4                2.70 dB
SPNAM2      Crp60comp.4
SPNAM4    Crp60,0.5,20.1
SPOFF2             0.00 Hz
SPOFF4             0.00 Hz

======== CHANNEL f2 ========
CPDPRG2           waltz16
NUC2                 1H
PCPD2            100.00 usec
PL2                1.60 dB
PL12              23.54 dB
SFO2         500.2225011 MHz

====== GRADIENT CHANNEL =====
GPNAM1          SINE.100
GPNAM2          SINE.100
GPX1               0.00 %
GPX2               0.00 %
GPY1               0.00 %
GPY2               0.00 %
GPZ1              30.00 %
GPZ2              50.00 %
p15              500.00 usec
p16             1000.00 usec

F2 - Processing parameters
SI                  65536
SF           125.7804263 MHz
WDW                    EM
SSB                     0
LB                 1.00 Hz
GB                      0
PC                   2.00

1D NMR plot parameters
CX                 22.80 cm
CY                 40.00 cm
F1P              220.000 ppm
F1              27671.70 Hz
F2P               -5.000 ppm
F2               -628.90 Hz
PPMCM             9.86842 ppm/cm
HZCM          1241.25427 Hz/cm
```

1H spectrum

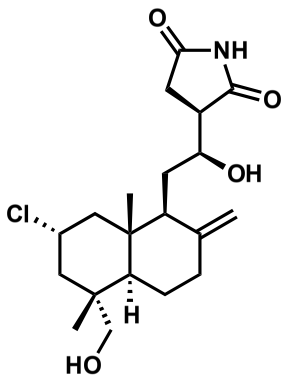

hatJ : 4.4

(in DMSO-d_6)

Z-restored spin-echo 13C spectrum with 1H decoupling

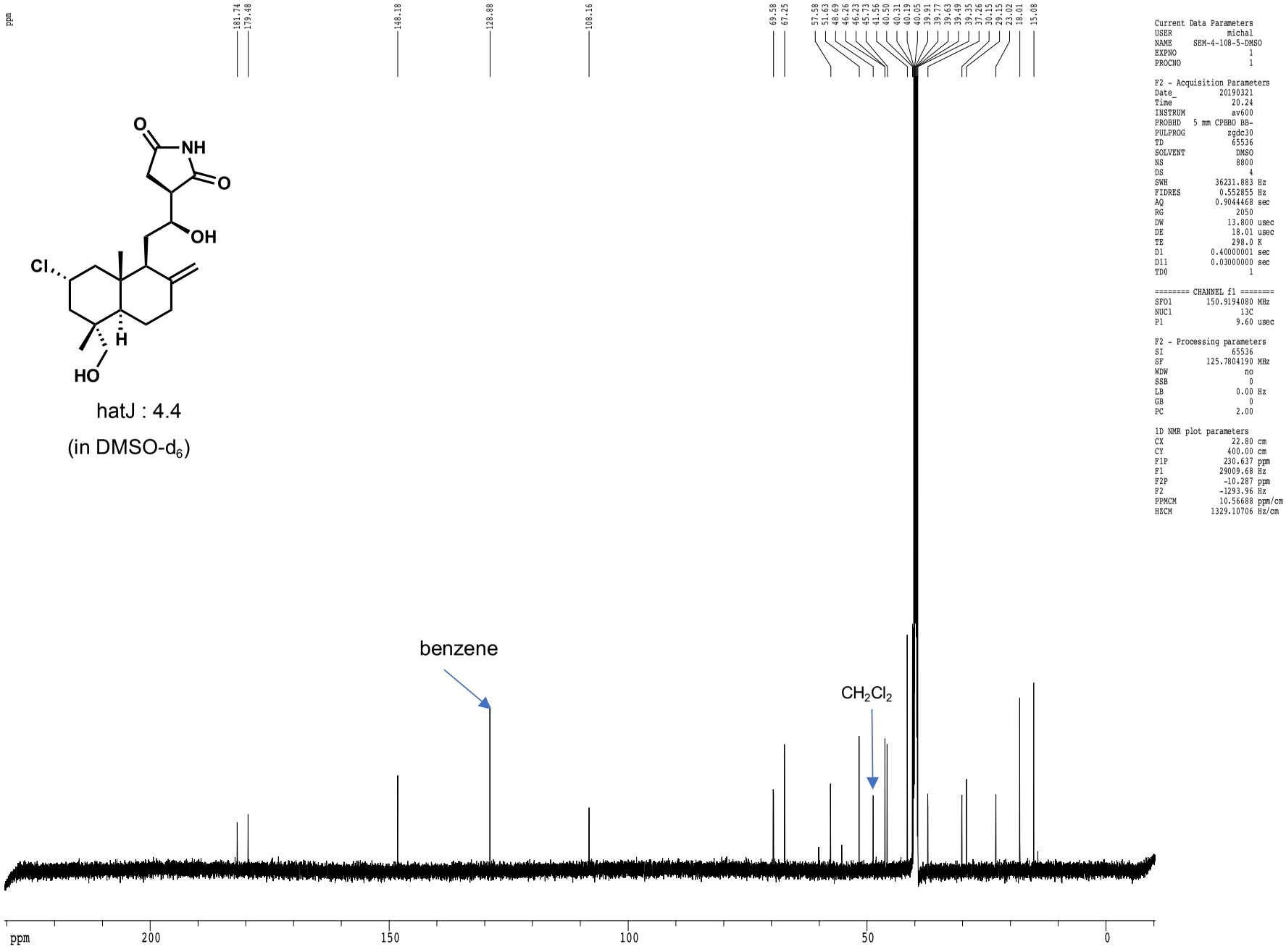

Current Data Parameters
USER michal
NAME SEM-4-108-5-DMSO
EXPNO 1
PROCNO 1

F2 - Acquisition Parameters
Date_ 20190321
Time 20.24
INSTRUM av600
PROBHD 5 mm CPBBO BB-
PULPROG zgdc30
TD 65536
SOLVENT DMSO
NS 8800
DS 4
SWH 36231.883 Hz
FIDRES 0.552855 Hz
AQ 0.9044468 sec
RG 2050
DW 13.800 usec
DE 18.01 usec
TE 298.0 K
D1 0.40000001 sec
D11 0.03000000 sec
TD0 1

======== CHANNEL f1 ========
SFO1 150.9194080 MHz
NUC1 13C
P1 9.60 usec

F2 - Processing parameters
SI 65536
SF 125.7804190 MHz
WDW no
SSB 0
LB 0.00 Hz
GB 0
PC 2.00

1D NMR plot parameters
CX 22.80 cm
CY 400.00 cm
F1P 230.637 ppm
F1 29009.68 Hz
F2P -10.287 ppm
F2 -1293.96 Hz
PPMCM 10.56688 ppm/cm
HZCM 1329.10706 Hz/cm

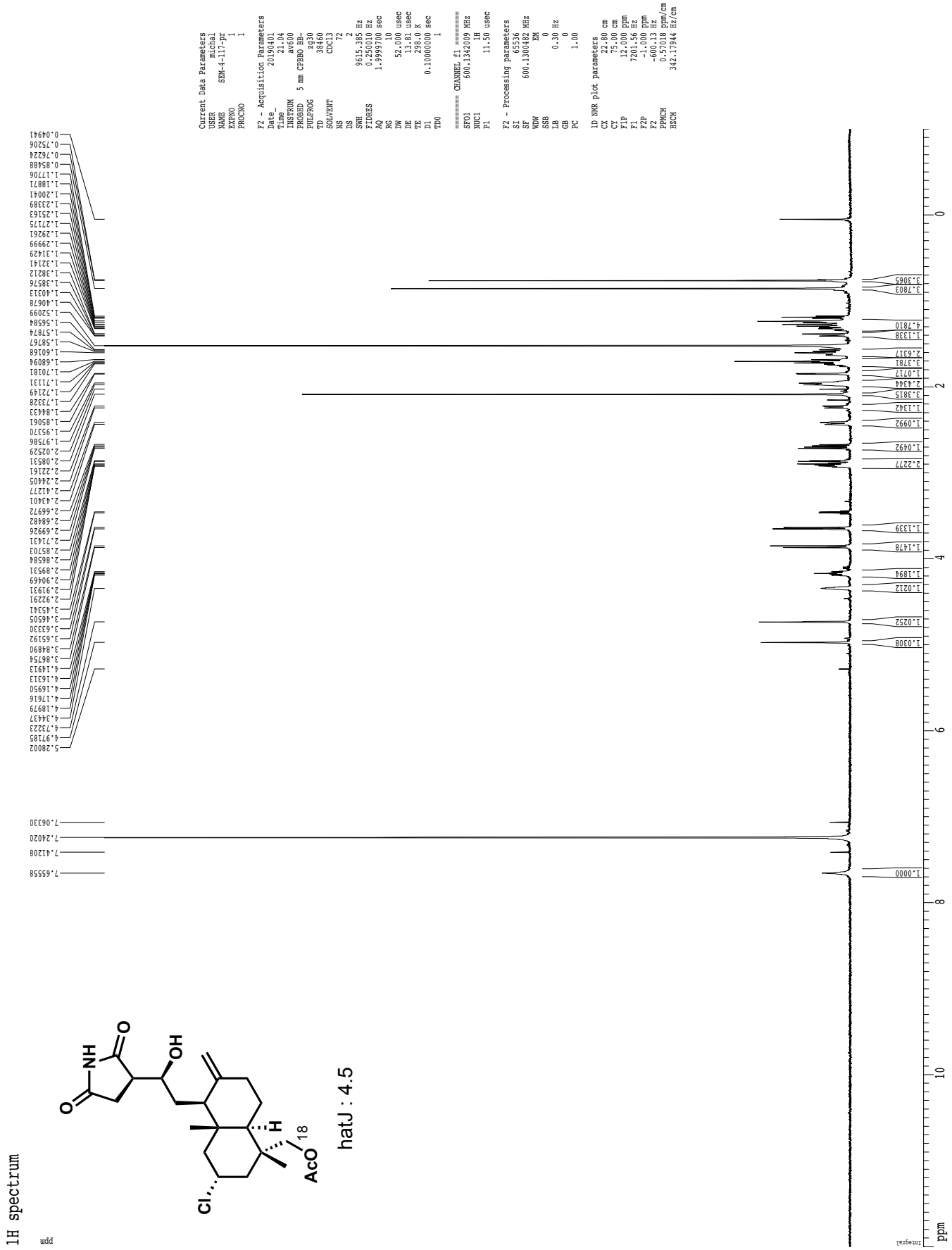
1H spectrum
ppm
integral
Current Data Parameters
USER michal
NAME SEM-4-117-pr
EXPNO 1
PROCNO 1
F2 - Acquisition Parameters
Date_ 20190401
Time 21.04
INSTRUM av600
PROBHD 5 mm CPBBO BB-
PULPROG zg30
TD 38460
SOLVENT CDCl3
NS 72
DS 2
SWH 9615.385 Hz
FIDRES 0.250010 Hz
AQ 1.9999700 sec
RG 10
DW 52.000 usec
DE 13.81 usec
TE 298.0 K
D1 0.10000000 sec
TD0 1
======== CHANNEL f1 ========
SFO1 600.1342009 MHz
NUC1 1H
P1 11.50 usec
F2 - Processing parameters
SI 65536
SF 600.1300482 MHz
WDW EM
SSB 0
LB 0.30 Hz
GB 0
PC 1.00
1D NMR plot parameters
CX 22.80 cm
CY 75.00 cm
F1P 12.000 ppm
F1 7201.56 Hz
F2P -1.000 ppm
F2 -600.13 Hz
PPMCM 0.57018 ppm/cm
HZCM 342.17944 Hz/cm
NH
O
O
OH
H
AcO
18
Cl
hatJ : 4.5

Z-restored spin-echo 13C spectrum with 1H decoupling

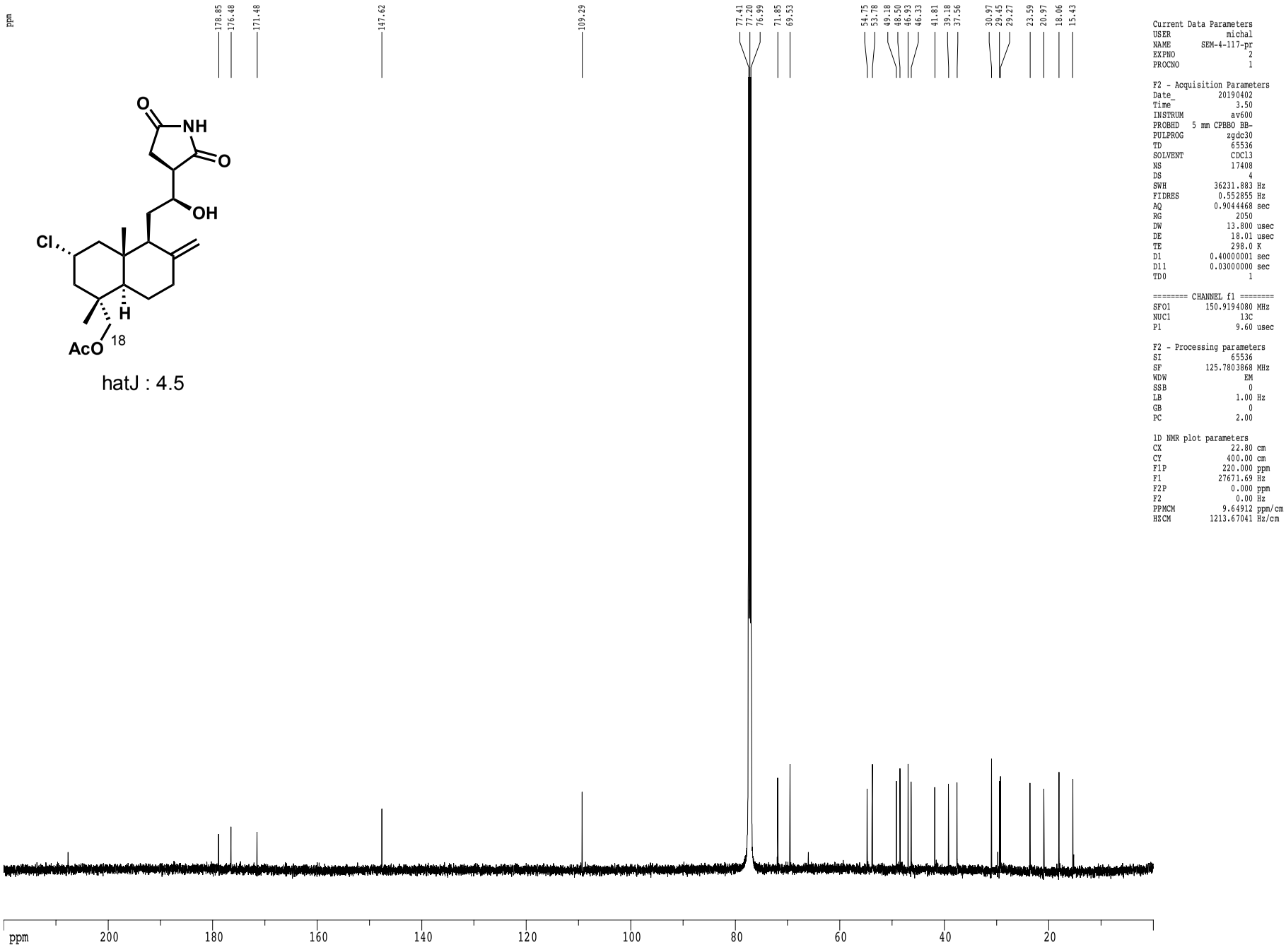

Current Data Parameters
USER michal
NAME SEM-4-117-pr
EXPNO 2
PROCNO 1

F2 - Acquisition Parameters
Date_ 20190402
Time 3.50
INSTRUM av600
PROBHD 5 mm CPBBO BB-
PULPROG zgdc30
TD 65536
SOLVENT CDCl3
NS 17408
DS 4
SWH 36231.883 Hz
FIDRES 0.552855 Hz
AQ 0.9044468 sec
RG 2050
DW 13.800 usec
DE 18.01 usec
TE 298.0 K
D1 0.40000001 sec
D11 0.03000000 sec
TD0 1

======== CHANNEL f1 ========
SFO1 150.9194080 MHz
NUC1 13C
P1 9.60 usec

F2 - Processing parameters
SI 65536
SF 125.7803868 MHz
WDW EM
SSB 0
LB 1.00 Hz
GB 0
PC 2.00

1D NMR plot parameters
CX 22.80 cm
CY 400.00 cm
F1P 220.000 ppm
F1 27671.69 Hz
F2P 0.000 ppm
F2 0.00 Hz
PPMCM 9.64912 ppm/cm
HZCM 1213.67041 Hz/cm

File :D:\MassHunter\GCMS\1\data\SEM\SEM-racemic chloride-method3.D
Operator :
Acquired : 06 Sep 2017 15:37 using AcqMethod racemic chloride 3.M
Instrument : GCMS
Sample Name:
Misc Info :
Vial Number: 6

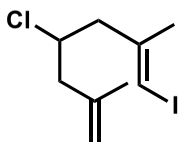

(±)-4.48

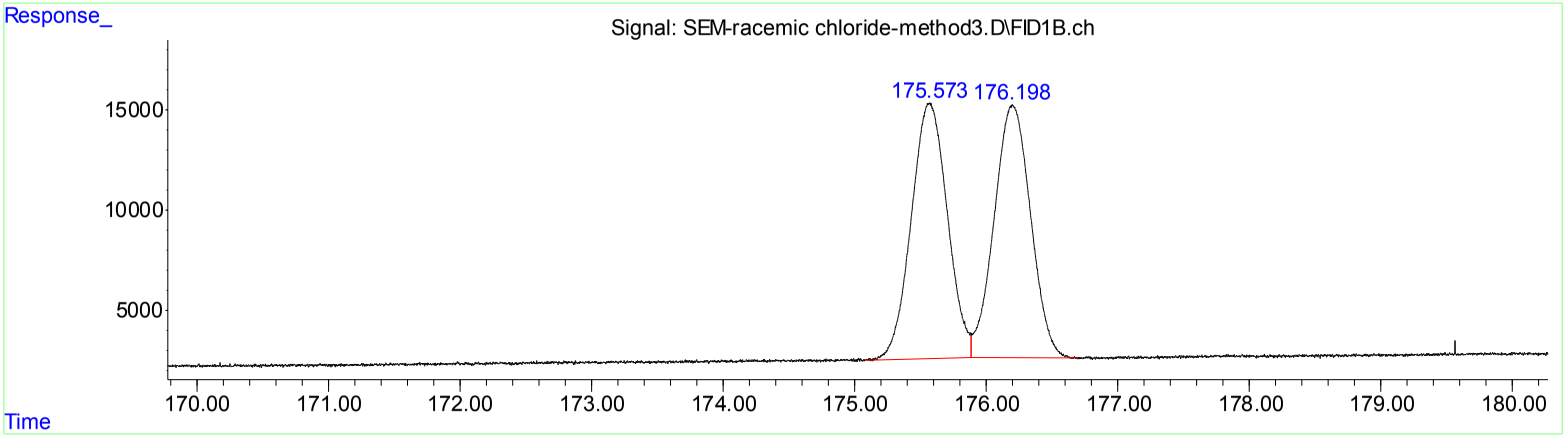

Data Path : D:\MassHunter\GCMS\1\data\SEM\
Data File : SEM-racemic chloride-method3.D
Signal(s) : Signal #1: FID1B.ch Signal #2: TST2A.ch
Acq On : 06 Sep 2017 15:37
Sample :
Misc :
ALS Vial : 6 Sample Multiplier: 1

Integration File signal 1: autoint1.e
Integration File signal 2: events2.e
Integration File signal 3: events3.e

Method : D:\MassHunter\GCMS\1\methods\SEM-3-252-method3.M
Title :

Signal #1 : FID1B.ch

peak #	R.T. min	Start min	End min	PK TY	peak height	peak area	peak % max.	% of total
1	175.573	175.080	175.885	M	12764	2436584	100.00%	50.046%
2	176.198	175.885	176.696	M	12632	2432085	99.82%	49.954%

Sum of corrected areas: 4868669

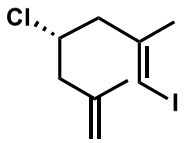

4.48

```
File       :D:\MassHunter\GCMS\1\data\SEM\SEM-racemic chloride-method4.D
Operator   :
Acquired   : 07 Sep 2017  10:47     using AcqMethod racemic chloride 4.M
Instrument :    GCMS
Sample Name:
Misc Info  :
Vial Number: 7
```

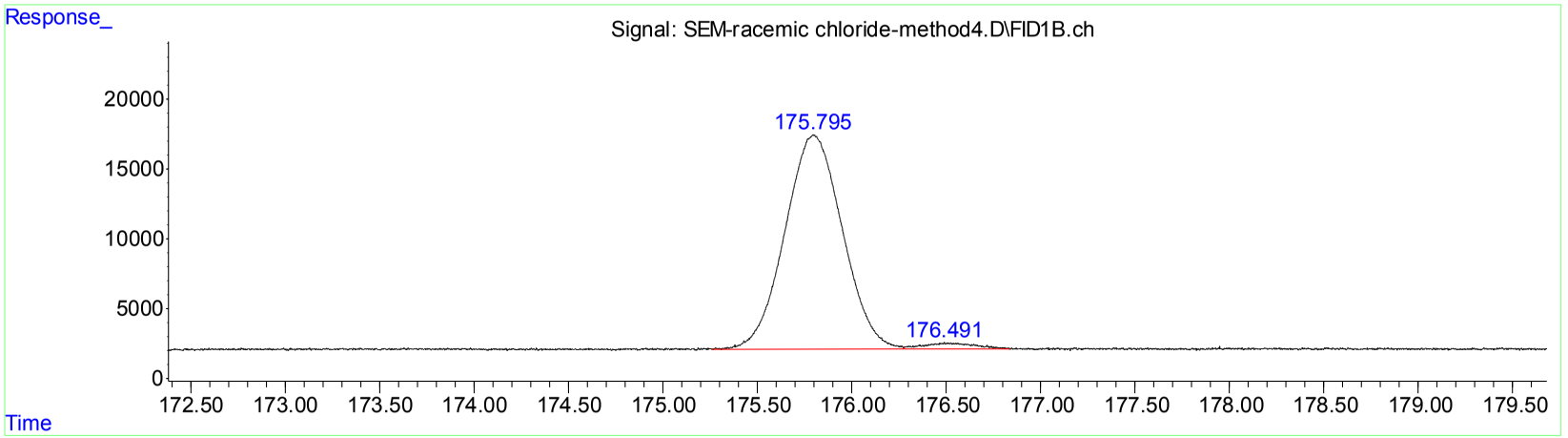

Area Percent Report

```
Data Path : D:\MassHunter\GCMS\1\data\SEM\
Data File : SEM-racemic chloride-method4.D
Signal(s) : Signal #1: FID1B.ch  Signal #2: TST2A.ch
Acq On    : 07 Sep 2017  10:47
Sample    :
Misc      :
ALS Vial  : 7   Sample Multiplier: 1

Integration File signal 1: autoint1.e
Integration File signal 2: events2.e
Integration File signal 3: events3.e

Method    : D:\MassHunter\GCMS\1\methods\Phenyl ethyl CA_ketone 5.M
Title     :

Signal #1 : FID1B.ch
```

peak #	R.T. min	Start min	End min	PK TY	peak height	peak area	peak % max.	% of total
1	175.795	175.258	176.277	M	15374	3248634	100.00%	97.553%
2	176.491	176.277	176.837	M	489	81478	2.51%	2.447%

Sum of corrected areas: 3330112

Dihydroxylation of **(±)-4.48** under Sharpless type conditions, with pyridine (no chiral ligand)

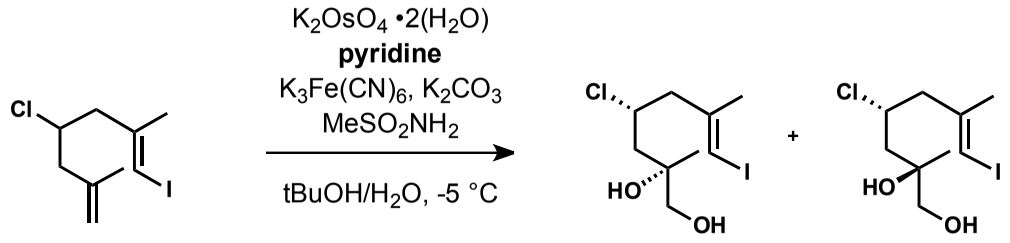

(±)-4.48

4.49
(racemic)

4.50
(racemic)

Sample Info : Chiralcel AS-H 1.0mL/min 98.5:1.5

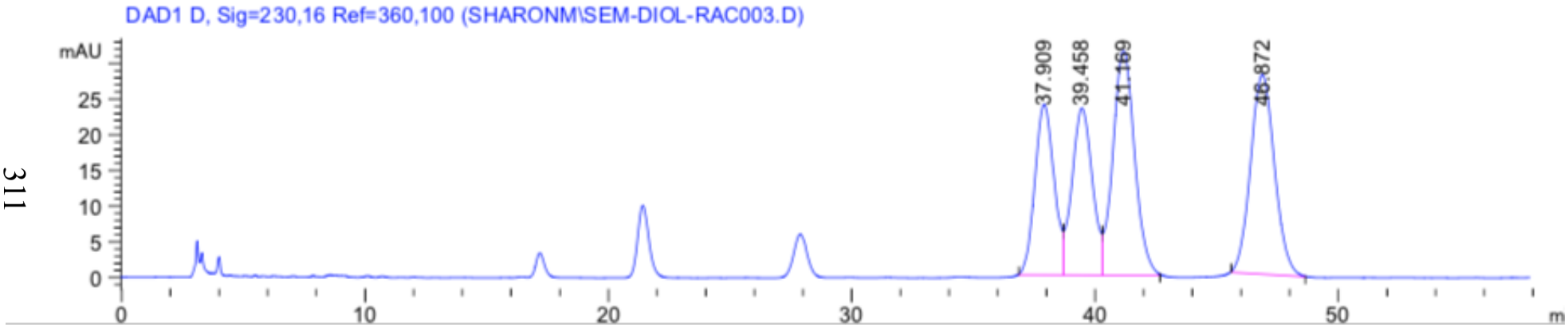

Signal 3: DAD1 D, Sig=230,16 Ref=360,100

Peak #	RetTime [min]	Type	Width [min]	Area [mAU*s]	Height [mAU]	Area %
1	37.909	BV	0.8413	1309.76855	23.90205	19.9768
2	39.458	VV	0.8819	1372.25671	23.40971	20.9299
3	41.169	VB	0.9481	1957.73877	31.54276	29.8598
4	46.872	BB	1.0578	1916.67896	27.95788	29.2335
Totals :				6556.44299	106.81241	

311

Dihydroxylation of **(±)-4.48** under Sharpless AD-mix β, $(DHQD)_2PHAL$ ligands

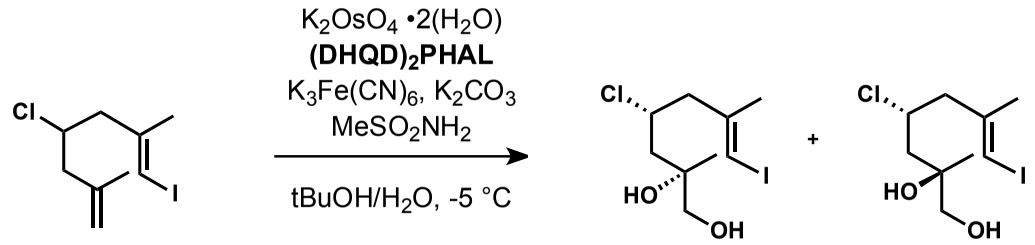

(±)-4.48

4.49
(low ee)

4.50
(low ee)

Sample Info : Chiralcel AS-H 1.0mL/min 98.5:1.5

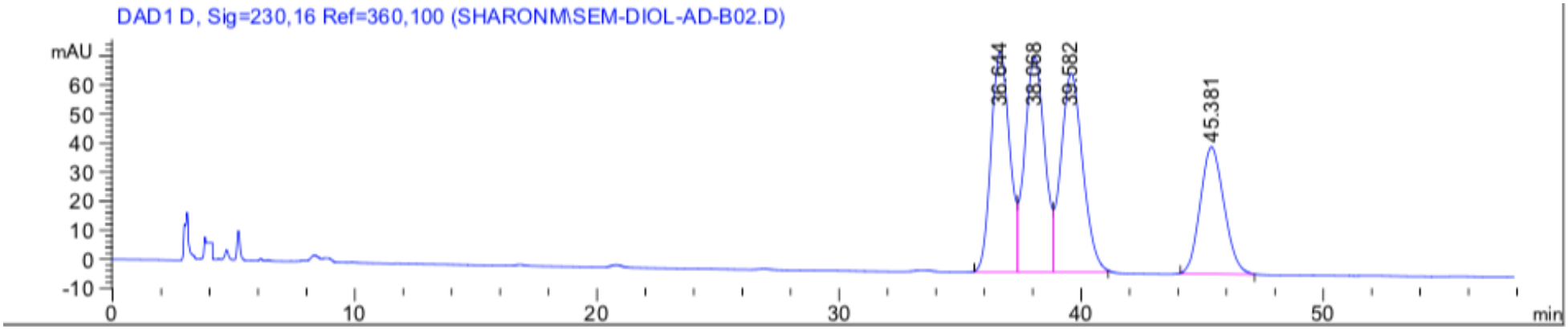

Signal 3: DAD1 D, Sig=230,16 Ref=360,100

Peak #	RetTime [min]	Type	Width [min]	Area [mAU*s]	Height [mAU]	Area %
1	36.644	BV	0.8240	4035.99487	75.94986	25.9398
2	38.068	VV	0.8807	4249.65820	74.14701	27.3131
3	39.582	VB	0.9491	4283.40723	68.35707	27.5300
4	45.381	BB	1.0486	2990.01416	43.68309	19.2172
Totals :				1.55591e4	262.13703	

Effects of Haterumaimide J and K on P388 cells

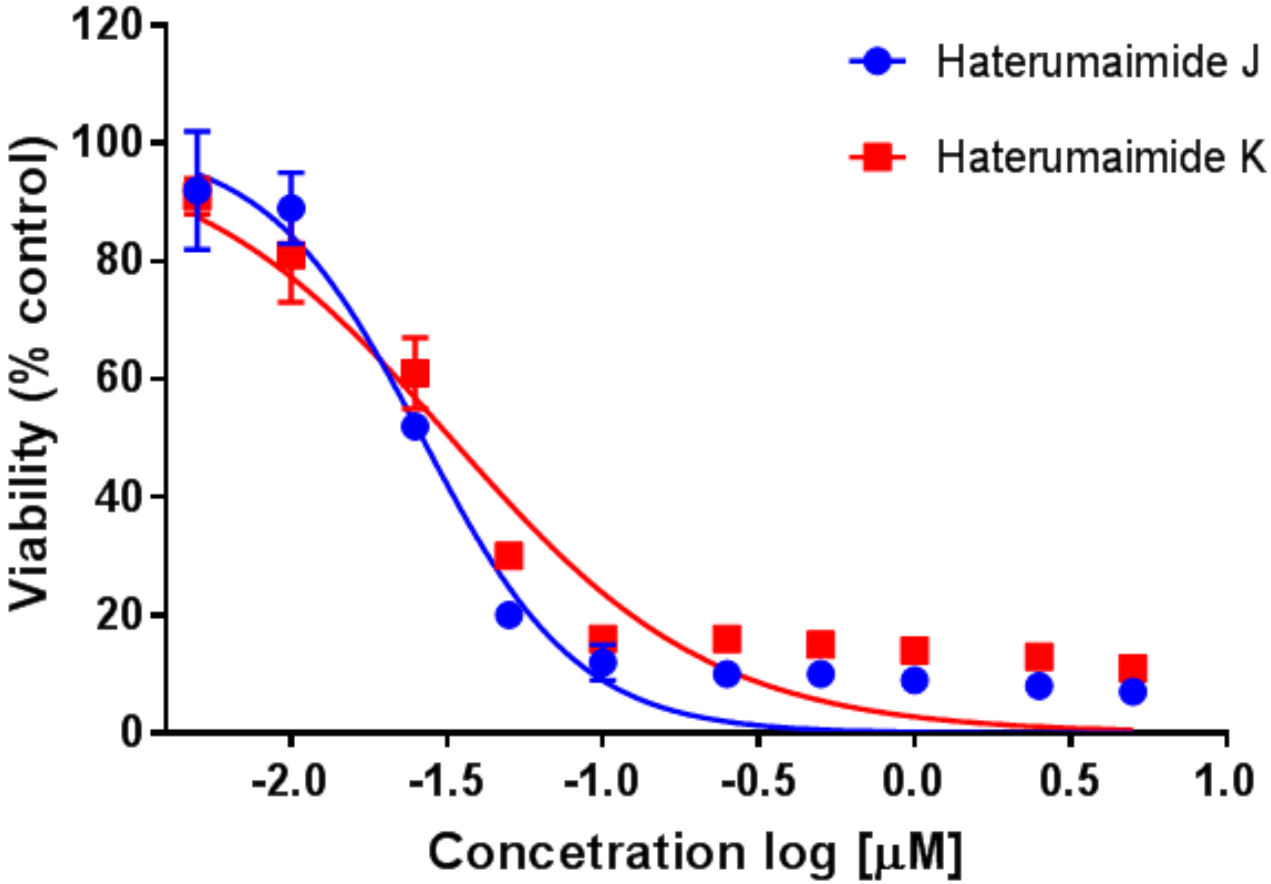

IC_{50} (μM)

Hat J = 0.026

Hat K = 0.033

Effects of Haterumaimide J and K on Hut78 cutaneous T-cell lymphoma cells

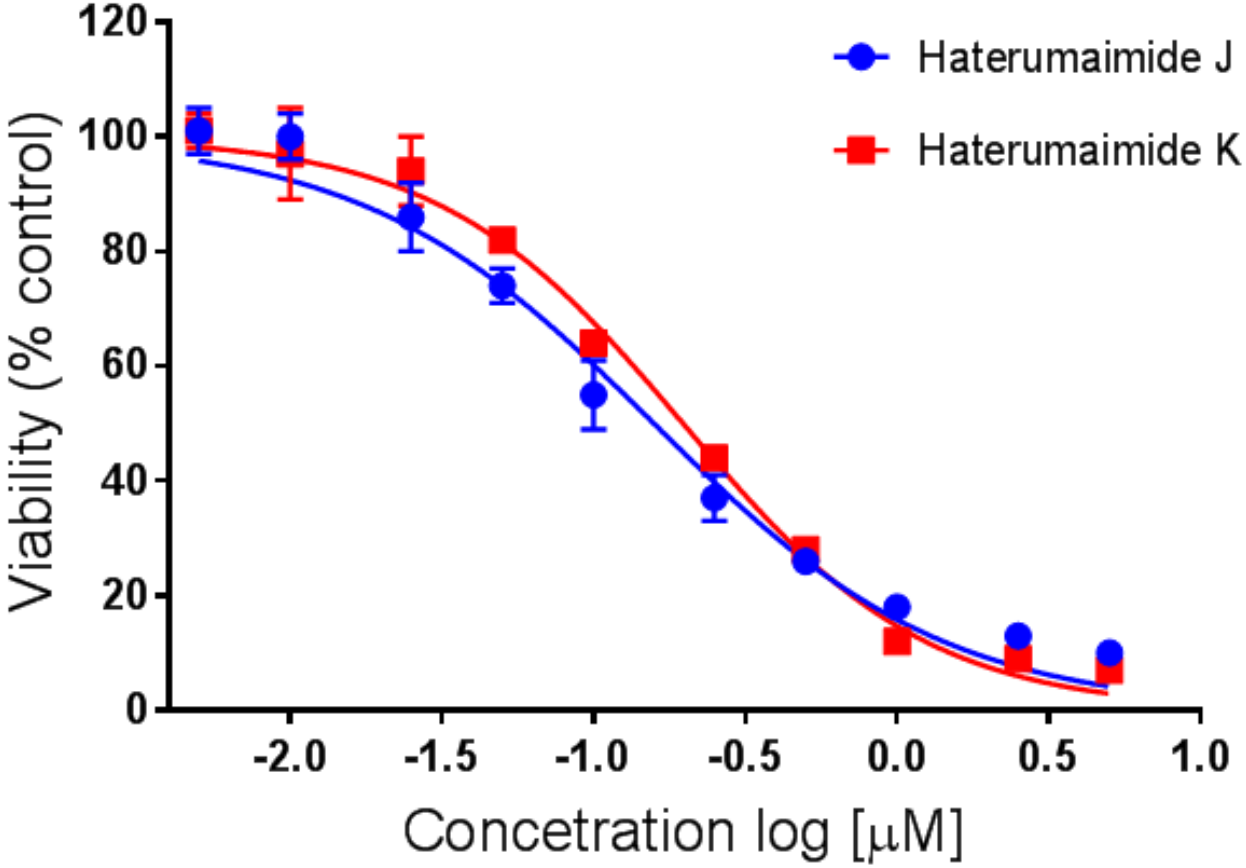

IC_{50} (μM)

Hat J = 0.16

Hat K = 0.2

Effects of Haterumaimide J and K on DU145 prostate cancer cells

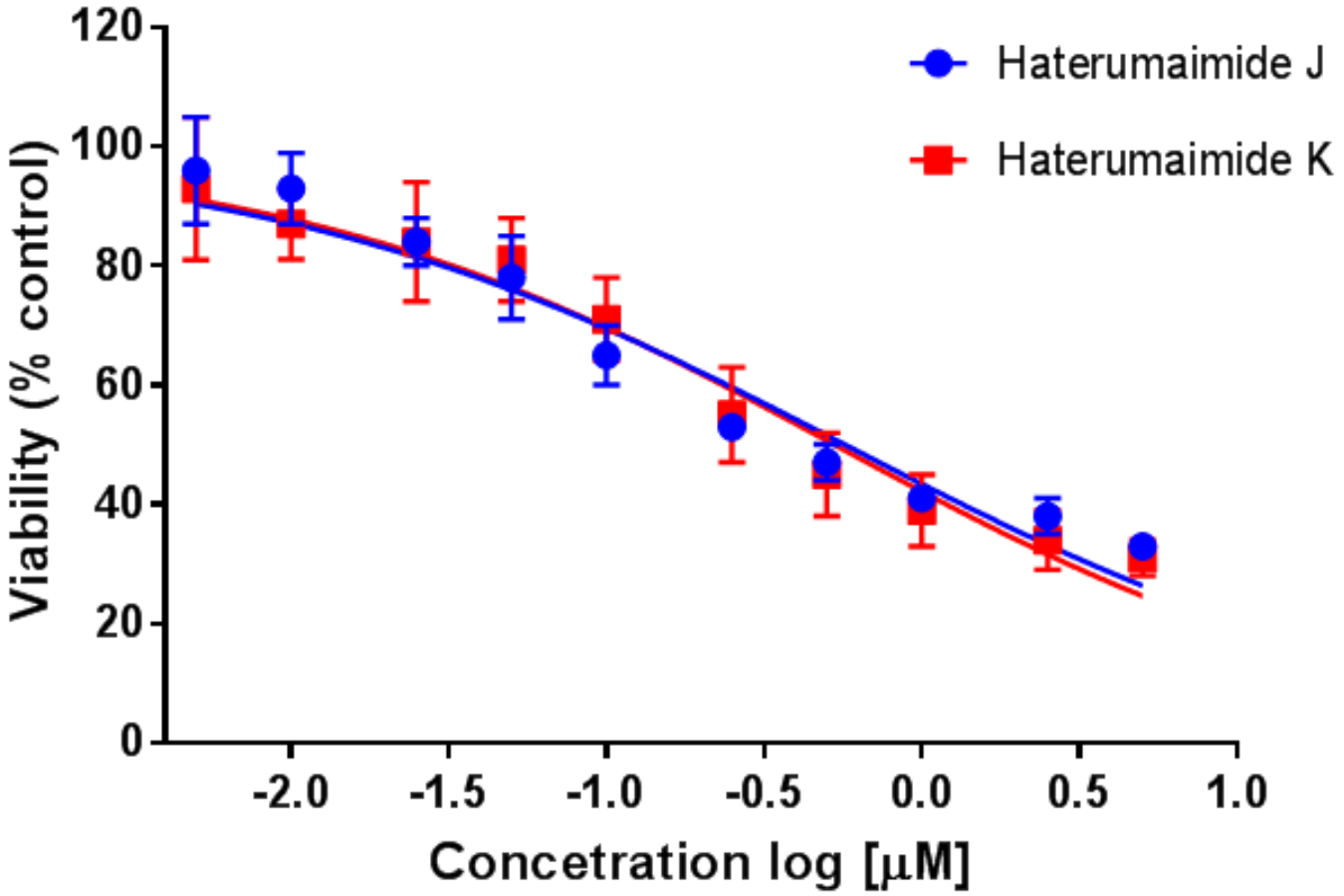

IC_{50} (µM)

Hat J = 0.57

Hat K = 0.53

Effects of Haterumaimide J and K on A2058 melanoma cells

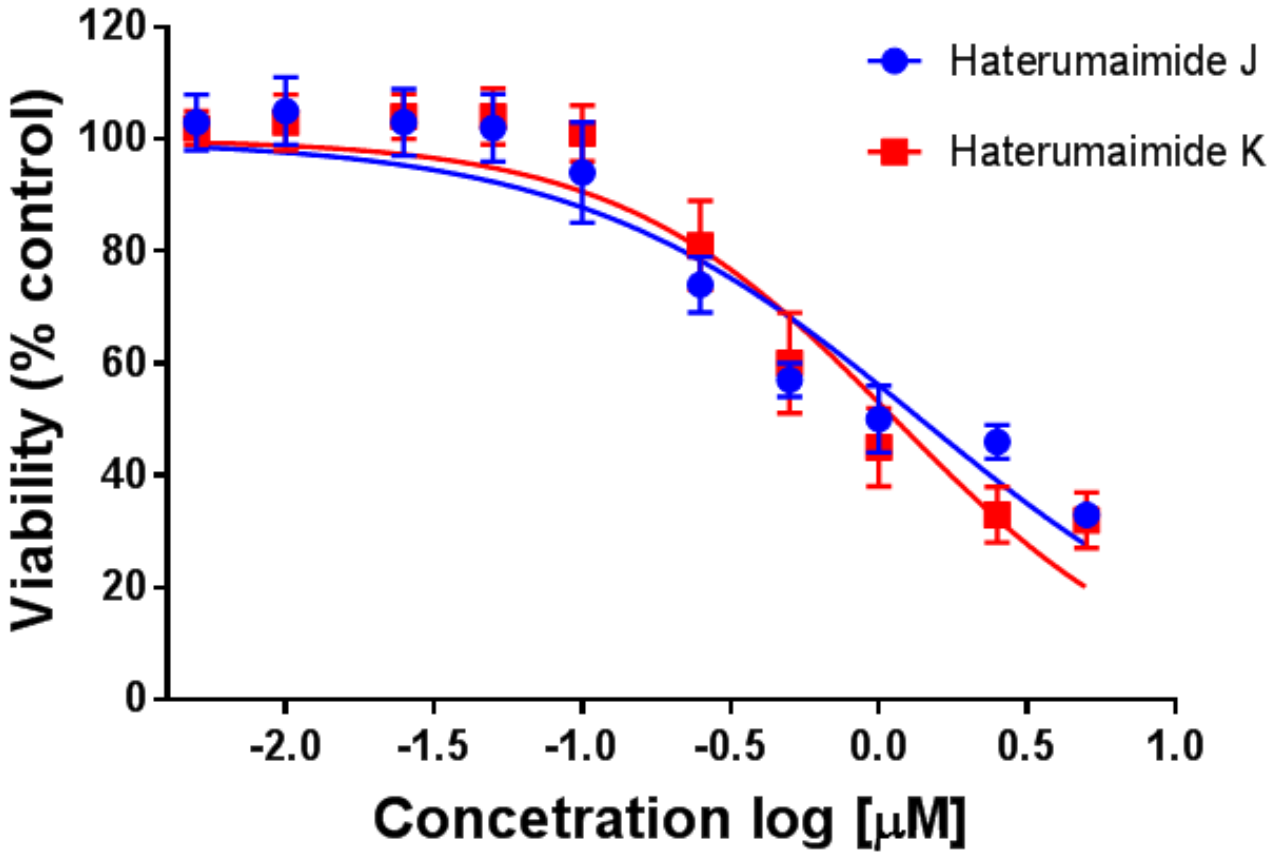

IC_{50} (μM)

Hat J = 1.4

Hat K = 1.1

1H spectrum

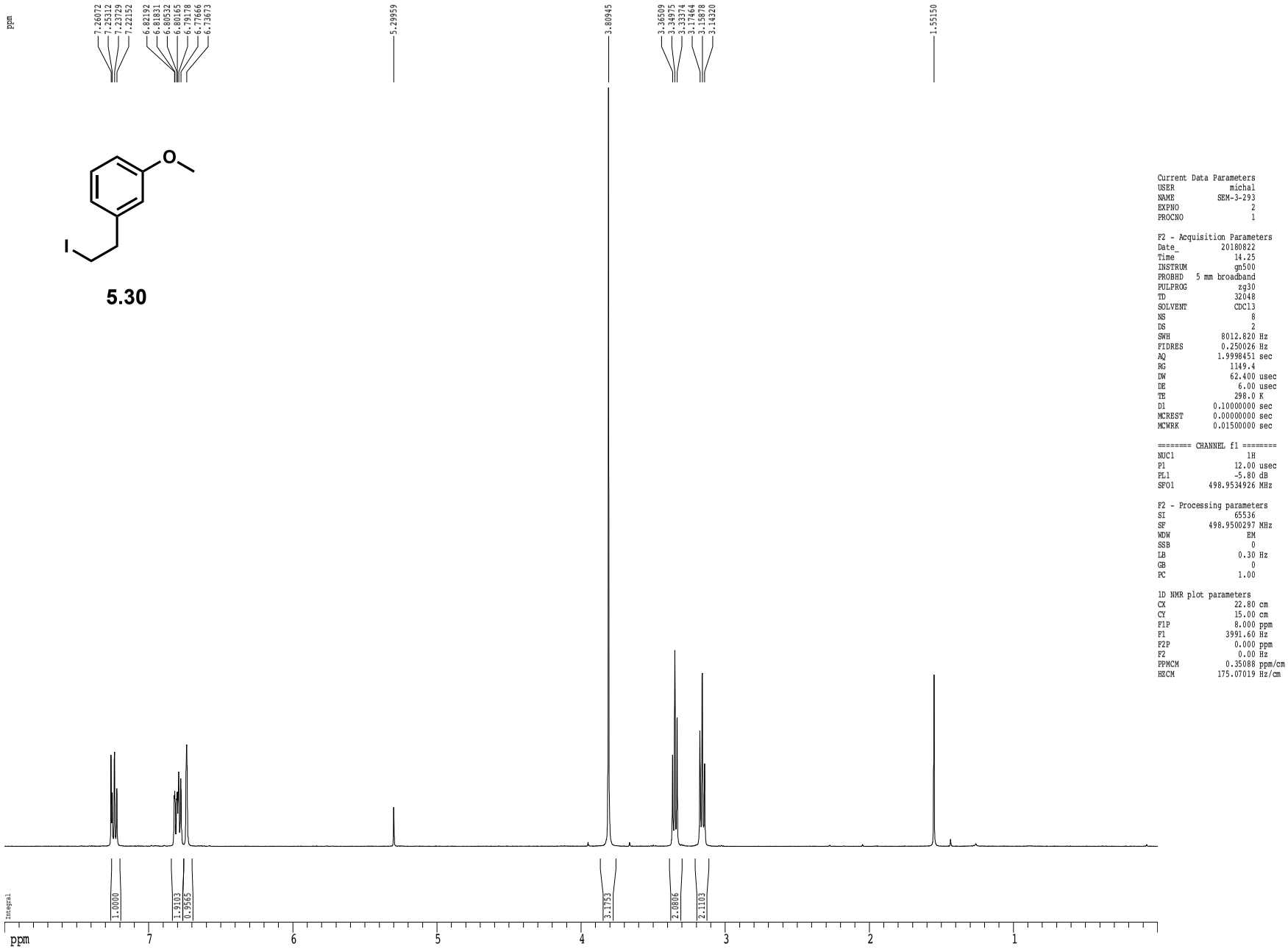
ppm
7.26072
7.25312
7.23729
7.22152
6.82192
6.81831
6.80532
6.80165
6.79178
6.77666
6.73673
5.29959
3.80945
3.36509
3.34975
3.33374
3.17464
3.15878
3.14320
1.55150
O
5.30
Current Data Parameters
USER michal
NAME SEM-3-293
EXPNO 2
PROCNO 1
F2 - Acquisition Parameters
Date_ 20180822
Time 14.25
INSTRUM gn500
PROBHD 5 mm broadband
PULPROG zg30
TD 32048
SOLVENT CDCl3
NS 8
DS 2
SWH 8012.820 Hz
FIDRES 0.250026 Hz
AQ 1.9998451 sec
RG 1149.4
DW 62.400 usec
DE 6.00 usec
TE 298.0 K
D1 0.10000000 sec
MCREST 0.00000000 sec
MCWRK 0.01500000 sec
======= CHANNEL f1 =======
NUC1 1H
P1 12.00 usec
PL1 -5.80 dB
SFO1 498.9534926 MHz
F2 - Processing parameters
SI 65536
SF 498.9500297 MHz
WDW EM
SSB 0
LB 0.30 Hz
GB 0
PC 1.00
1D NMR plot parameters
CX 22.80 cm
CY 15.00 cm
F1P 8.000 ppm
F1 3991.60 Hz
F2P 0.000 ppm
F2 0.00 Hz
PPMCM 0.35088 ppm/cm
HZCM 175.07019 Hz/cm
Integral
1.0000
1.9103
0.9565
3.1753
2.0806
2.1103
ppm
7
6
5
4
3
2
1

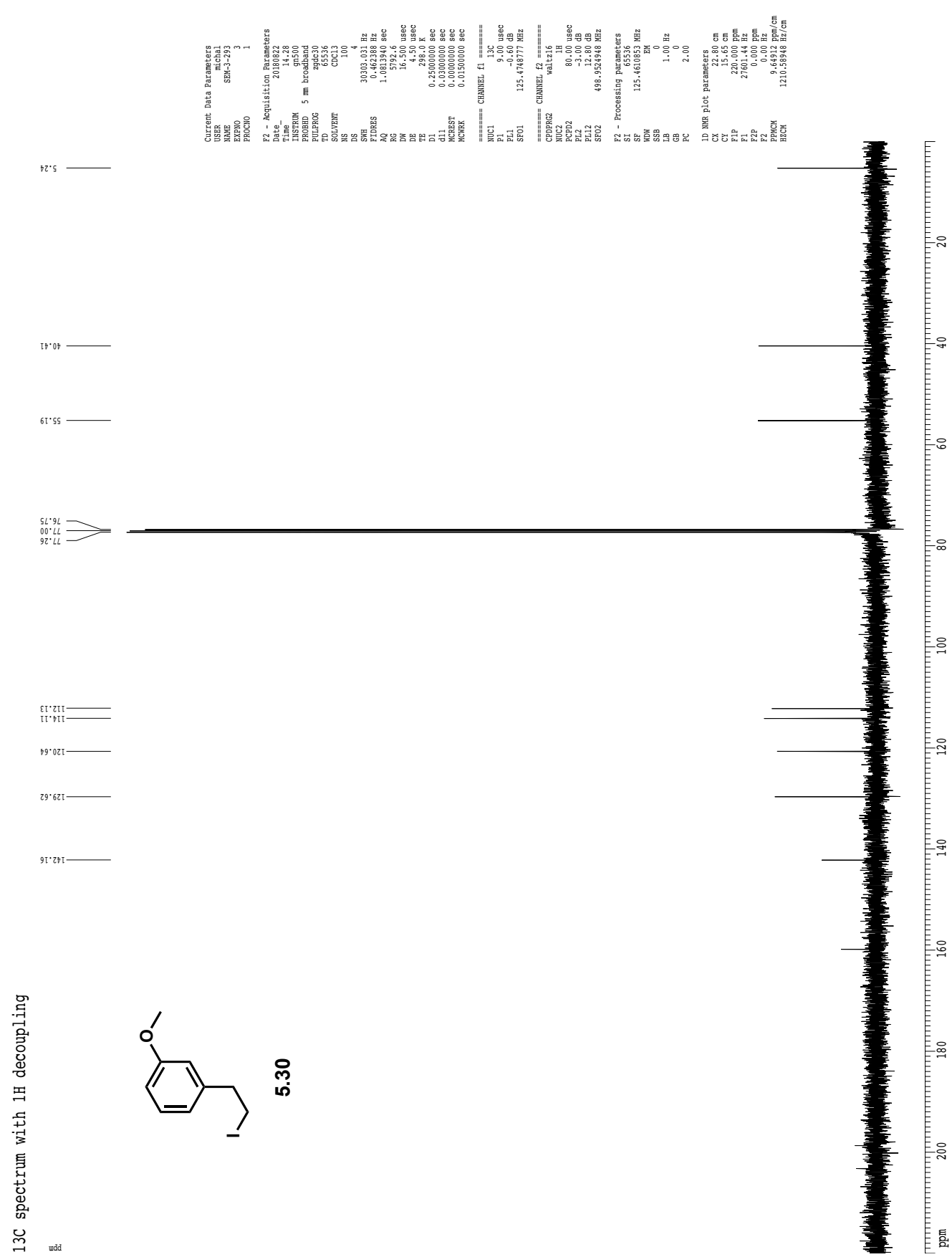
13C spectrum with 1H decoupling
ppm
5.30
Current Data Parameters
USER mlchal
NAME SEM-3-293
EXPNO 3
PROCNO 1
F2 - Acquisition Parameters
Date_ 20180822
Time 14.28
INSTRUM gn500
PROBHD 5 mm broadband
PULPROG zgpg30
TD 65536
SOLVENT CDCl3
NS 100
DS 4
SWH 30303.031 Hz
FIDRES 0.462398 Hz
AQ 1.0813940 sec
RG 5792.6
DW 16.500 usec
DE 4.50 usec
TE 298.0 K
D1 0.25000000 sec
d11 0.03000000 sec
MCREST 0.00000000 sec
MCWRK 0.01500000 sec
======== CHANNEL f1 ========
NUC1 13C
P1 9.00 usec
PL1 -0.60 dB
SFO1 125.4748777 MHz
======== CHANNEL f2 ========
CPDPRG2 waltz16
NUC2 1H
PCPD2 80.00 usec
PL2 -3.00 dB
PL12 12.80 dB
SFO2 498.9524948 MHz
F2 - Processing parameters
SI 65536
SF 125.4610853 MHz
WDW EM
SSB 0
LB 1.00 Hz
GB 0
PC 2.00
1D NMR plot parameters
CX 22.80 cm
CY 15.65 cm
F1P 220.000 ppm
F1 27601.44 Hz
F2P 0.000 ppm
F2 0.00 Hz
PPMCM 9.64912 ppm/cm
HZCM 1210.58948 Hz/cm
5.24
40.41
55.19
76.75
77.00
77.26
112.13
114.11
120.64
129.62
142.16
ppm

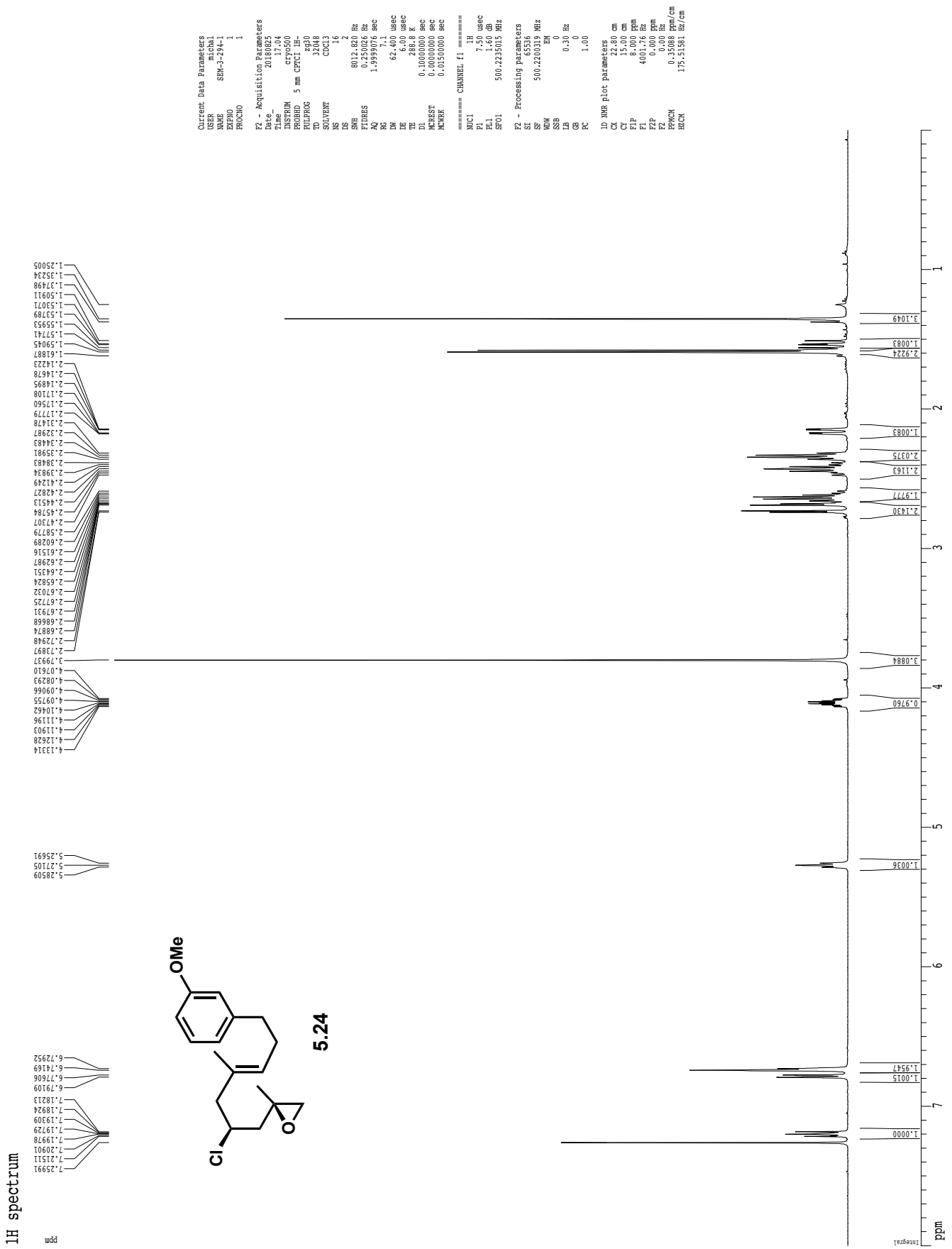
1H spectrum
Current Data Parameters
USER michal
NAME SEM-3-294-1
EXPNO 1
PROCNO 1
F2 - Acquisition Parameters
Date_ 20180825
Time 17.04
INSTRUM cryo500
PROBHD 5 mm CPTCI 1H-
PULPROG zg30
TD 32048
SOLVENT CDCl3
NS 16
DS 2
SWH 8012.820 Hz
FIDRES 0.250026 Hz
AQ 1.9999076 sec
RG 7.1
DW 62.400 usec
DE 6.00 usec
TE 298.1 K
D1 0.10000000 sec
MCREST 0.00000000 sec
MCWRK 0.01500000 sec
======= CHANNEL f1 =======
NUC1 1H
P1 7.50 usec
PL1 1.60 dB
SFO1 500.2235015 MHz
F2 - Processing parameters
SI 65536
SF 500.2200319 MHz
WDW EM
SSB 0
LB 0.30 Hz
GB 0
PC 1.00
1D NMR plot parameters
CX 22.80 cm
CY 15.00 cm
F1P 8.000 ppm
F1 4001.76 Hz
F2P 0.000 ppm
F2 0.00 Hz
PPMCM 0.35088 ppm/cm
HZCM 175.51581 Hz/cm
OMe
Cl
O
5.24
ppm
Integral

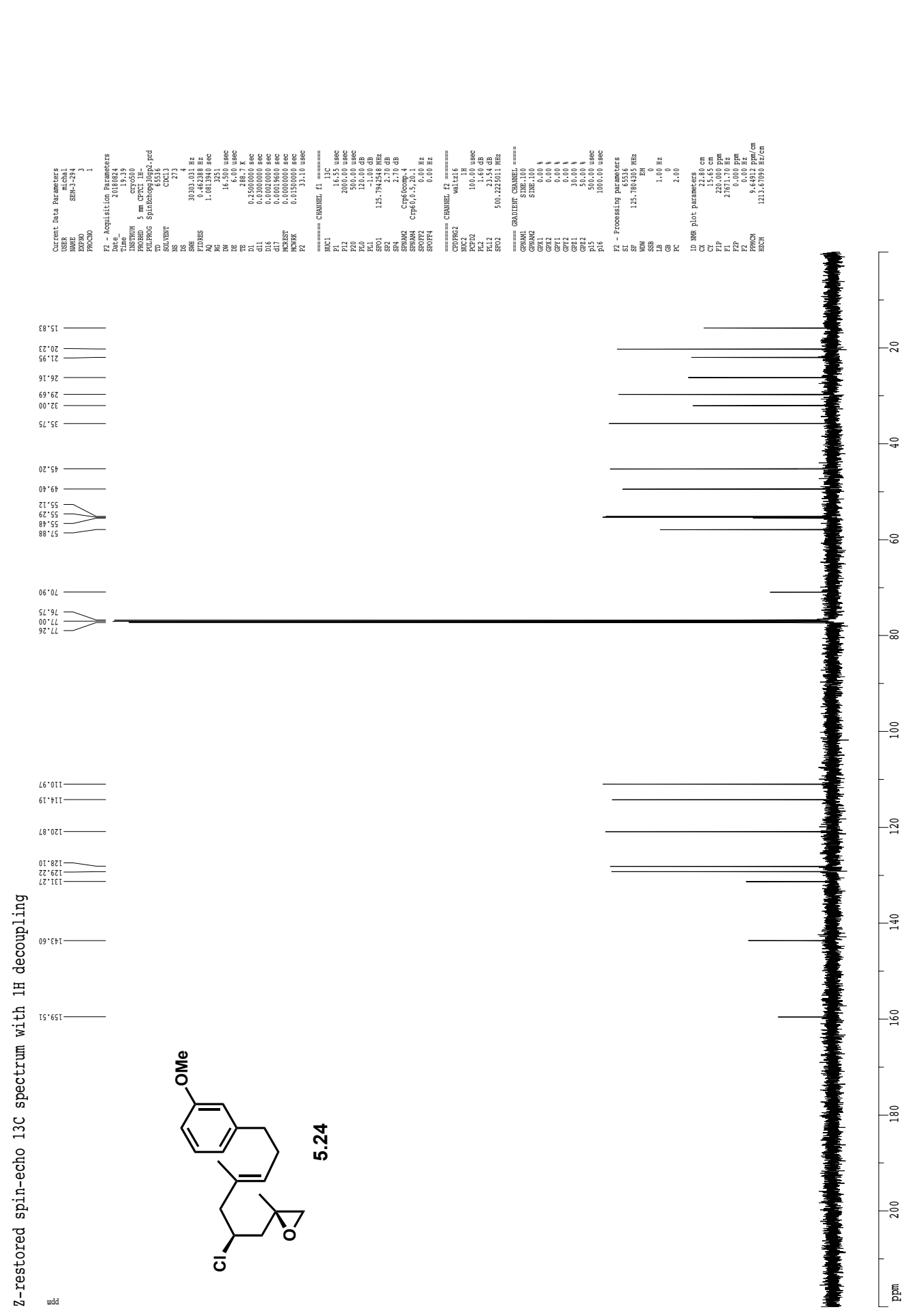
Z-restored spin-echo 13C spectrum with 1H decoupling
OMe
Cl
O
5.24
ppm

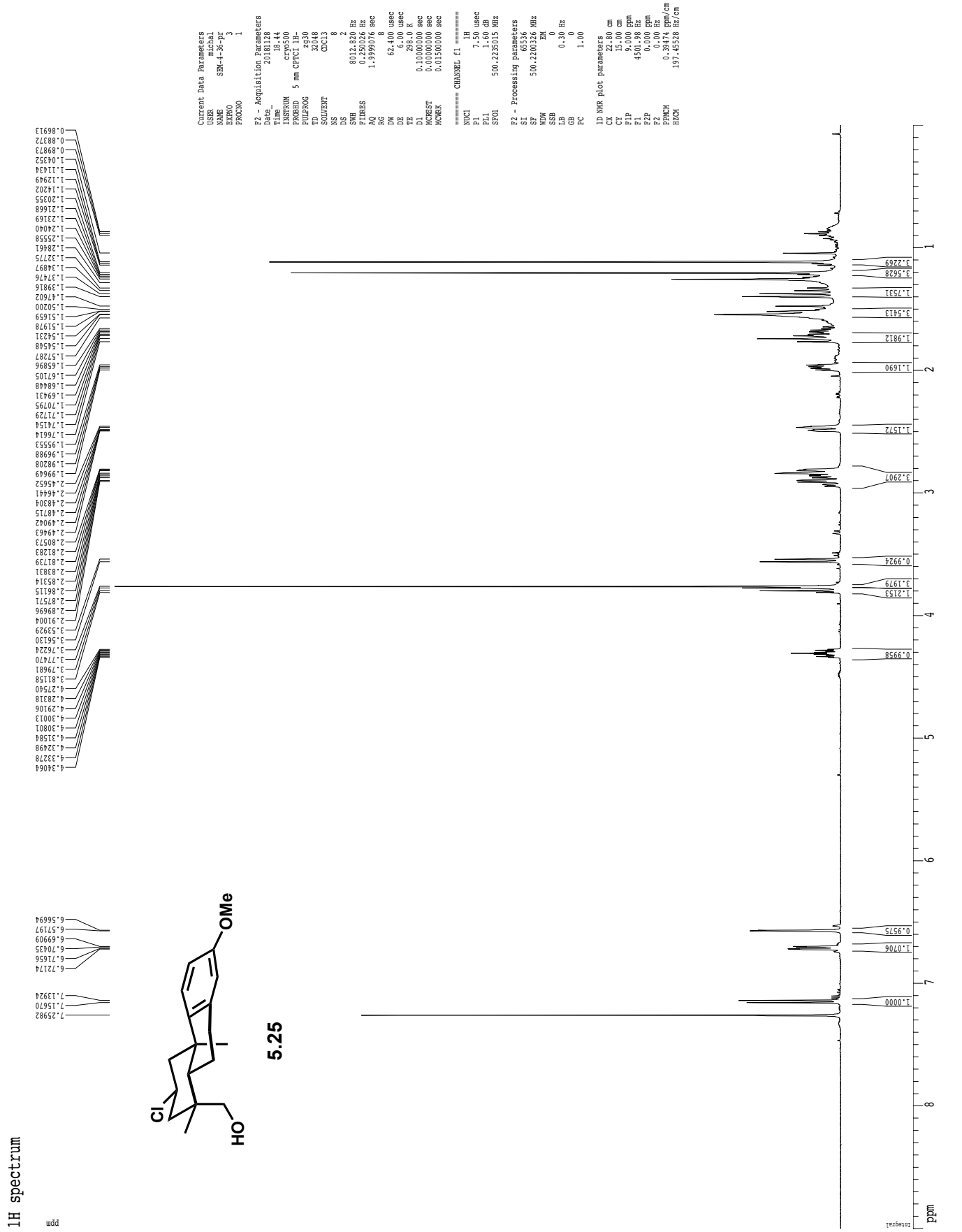
1H spectrum
Current Data Parameters
USER michal
NAME SBM-4-36-pr
EXPNO 3
PROCNO 1
F2 - Acquisition Parameters
Date_ 20181128
Time 18.44
INSTRUM cryo500
PROBHD 5 mm CPTCI 1H-
PULPROG zg30
TD 32048
SOLVENT CDCl3
NS 8
DS 2
SWH 8012.820 Hz
FIDRES 0.250026 Hz
AQ 1.9999076 sec
RG 8
DW 62.400 usec
DE 6.00 usec
TE 298.0 K
D1 0.10000000 sec
MCREST 0.00000000 sec
MCWRK 0.01500000 sec
======== CHANNEL f1 ========
NUC1 1H
P1 7.50 usec
PL1 1.50 dB
SFO1 500.2235015 MHz
F2 - Processing parameters
SI 65536
SF 500.2200326 MHz
WDW EM
SSB 0
LB 0.30 Hz
GB 0
PC 1.00
1D NMR plot parameters
CX 22.80 cm
CY 15.00 cm
F1P 9.000 ppm
F1 4501.98 Hz
F2P 0.000 ppm
F2 0.00 Hz
PPMCM 0.39474 ppm/cm
HZCM 197.45528 Hz/cm
OMe
Cl
HO
5.25
ppm
Integral

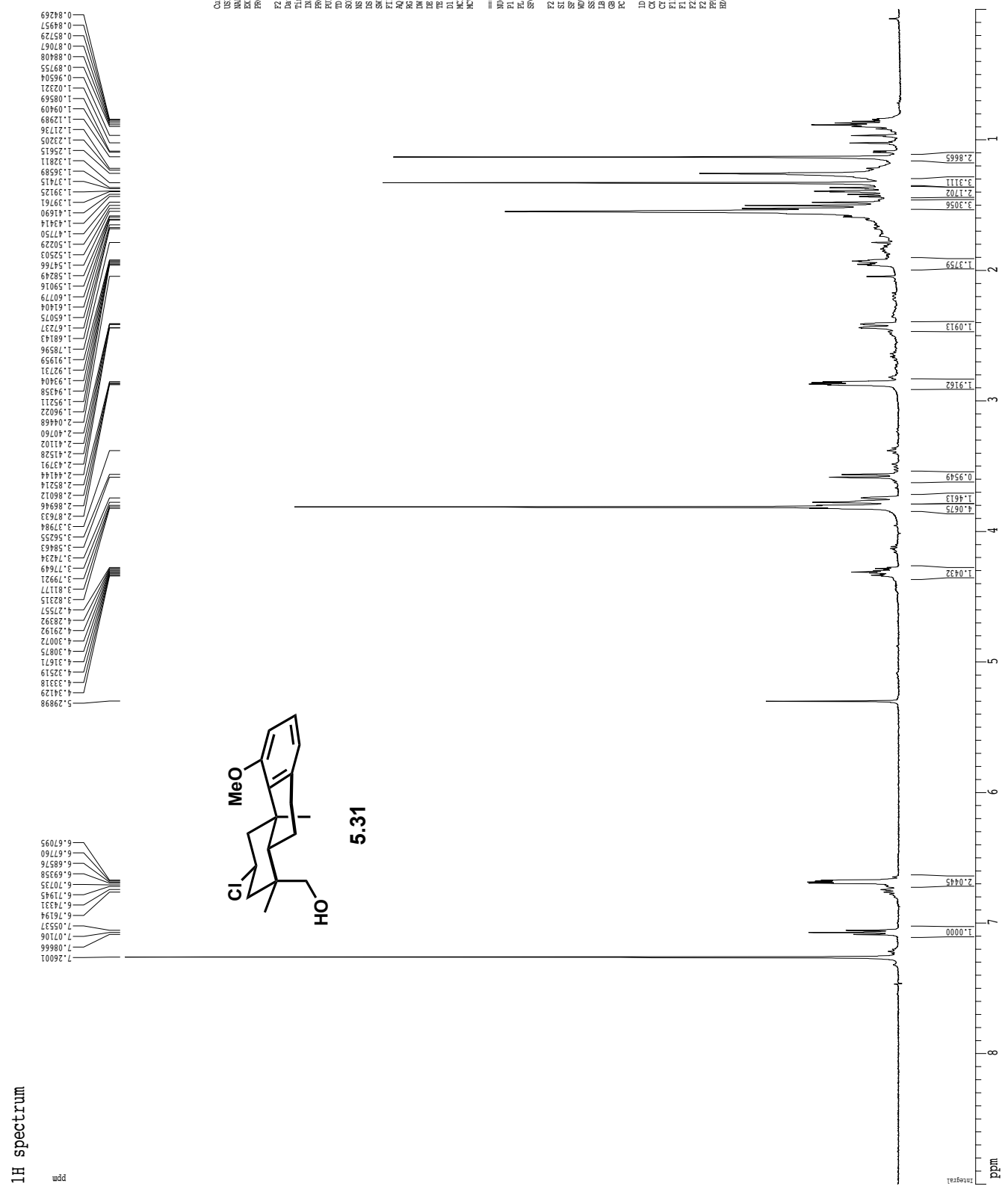
1H spectrum
Current Data Parameters
USER michal
NAME SEM-4-36-pr
EXPNO 2
PROCNO 1
F2 - Acquisition Parameters
Date_ 20181128
Time 18.40
INSTRUM cryo500
PROBHD 5 mm CPTCI 1H-
PULPROG zg30
TD 32048
SOLVENT CDCl3
NS 8
DS 2
SWH 8012.820 Hz
FIDRES 0.250026 Hz
AQ 1.9999076 sec
RG 8
DW 62.400 usec
DE 6.00 usec
TE 298.1 K
D1 0.10000000 sec
MCREST 0.00000000 sec
MCWRK 0.01500000 sec
======== CHANNEL f1 ========
NUC1 1H
P1 7.50 usec
PL1 1.60 dB
SFO1 500.2235015 MHz
F2 - Processing parameters
SI 65536
SF 500.2200326 MHz
WDW EM
SSB 0
LB 0.30 Hz
GB 0
PC 1.00
1D NMR plot parameters
CX 22.80 cm
CY 15.00 cm
F1P 9.000 ppm
F1 4501.98 Hz
F2P 0.000 ppm
F2 0.00 Hz
PPMCM 0.39474 ppm/cm
HZCM 197.45528 Hz/cm
MeO
Cl
I
HO
5.31
ppm
Integral

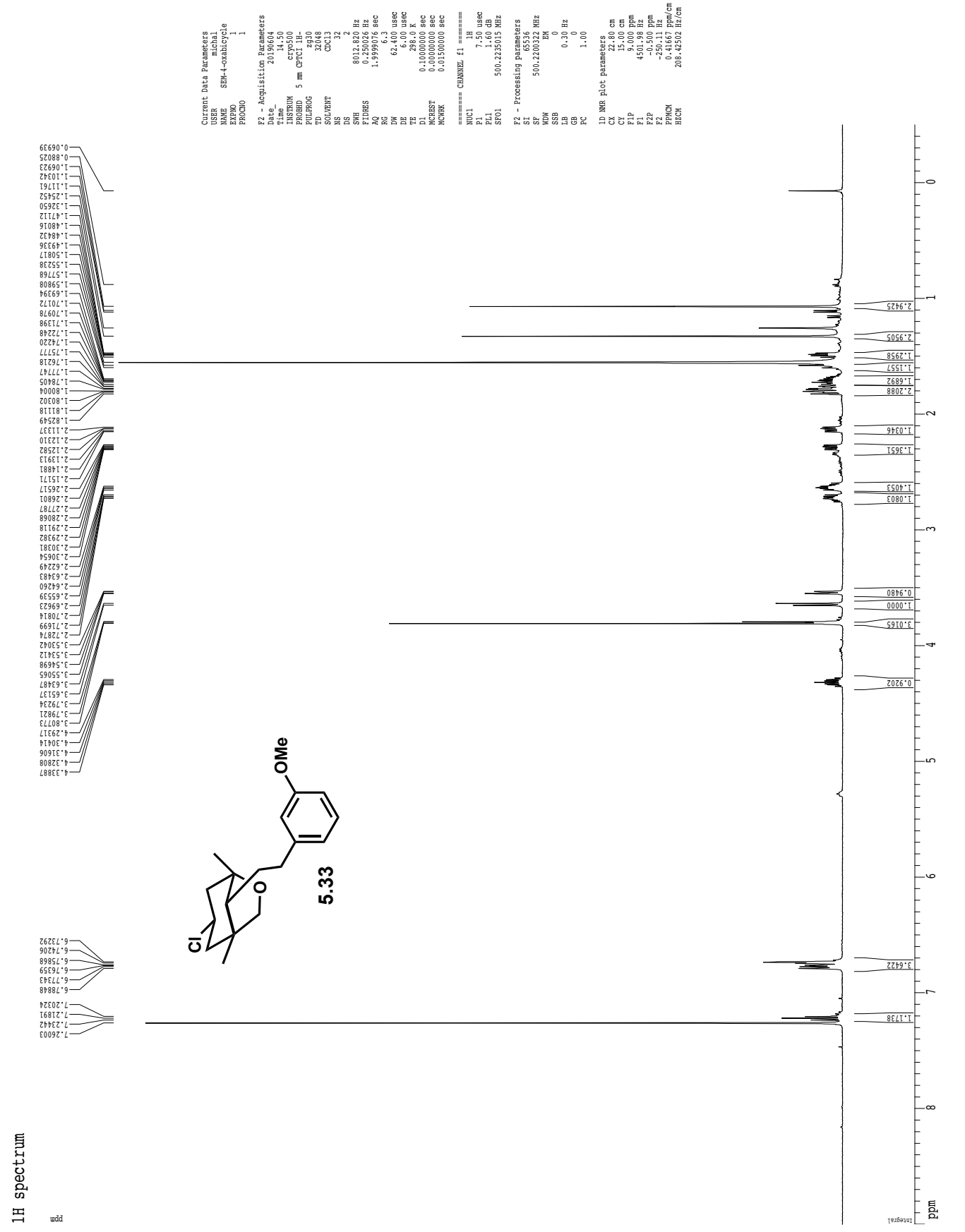
1H spectrum
ppm
integral
Current Data Parameters
USER michal
NAME SEM-4-oxabicycle
EXPNO 1
PROCNO 1
F2 - Acquisition Parameters
Date_ 20190604
Time 14:50
INSTRUM ccry500
PROBHD 5 mm CPTCI 1H-
PULPROG zg30
TD 32048
SOLVENT CDCl3
NS 32
DS 2
SWH 8012.820 Hz
FIDRES 0.250026 Hz
AQ 1.9999076 sec
RG 6.3
DW 62.400 usec
DE 6.00 usec
TE 298.0 K
D1 0.10000000 sec
MCREST 0.00000000 sec
MCWRK 0.01500000 sec
======== CHANNEL f1 ========
NUC1 1H
P1 7.50 usec
PL1 1.60 dB
SFO1 500.2235015 MHz
F2 - Processing parameters
SI 65536
SF 500.2200322 MHz
WDW EM
SSB 0
LB 0.30 Hz
GB 0
PC 1.00
1D NMR plot parameters
CX 22.80 cm
CY 15.00 cm
F1P 9.000 ppm
F1 4501.98 Hz
F2P -0.500 ppm
F2 -250.11 Hz
PPMCM 0.41667 ppm/cm
HZCM 208.42502 Hz/cm
OMe
Cl
O
5.33

1H spectrum

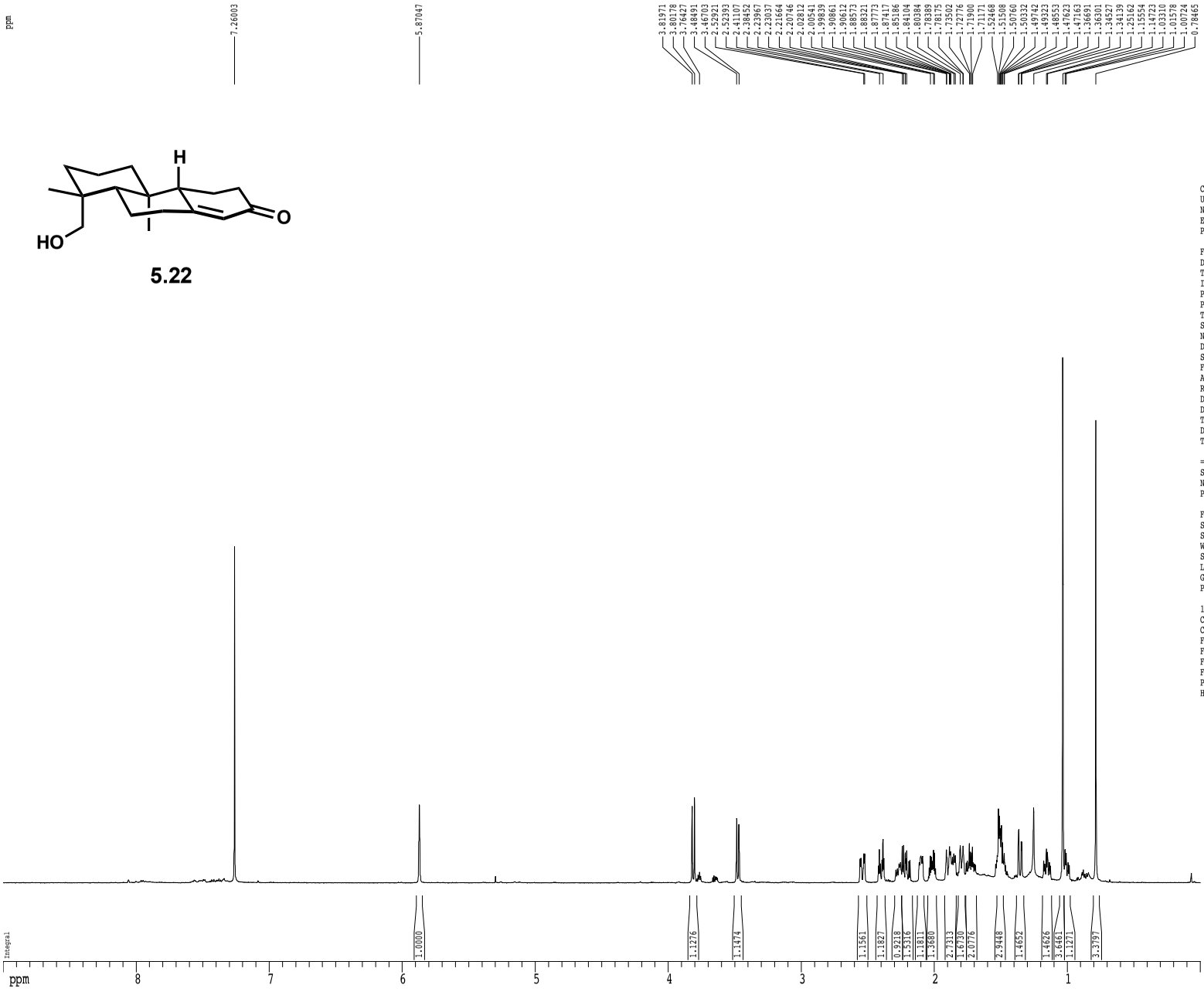
ppm
7.26003
5.87047
3.81971
3.80178
3.76427
3.48491
3.46703
2.52921
2.52393
2.41107
2.38452
2.23967
2.23037
2.21664
2.20746
2.02812
2.00541
1.99839
1.90861
1.90612
1.88573
1.88321
1.87773
1.87417
1.85186
1.84104
1.80384
1.78389
1.78175
1.73502
1.72776
1.71900
1.71171
1.52468
1.51508
1.50760
1.50332
1.49742
1.49323
1.48553
1.47623
1.47163
1.46691
1.36301
1.34527
1.34139
1.25162
1.15554
1.11723
1.03310
1.01578
1.00724
0.78465
H
O
HO
5.22
Current Data Parameters
USER michal
NAME SEM-4-121-pr
EXPNO 2
PROCNO 1
F2 - Acquisition Parameters
Date_ 20190424
Time 20.19
INSTRUM av600
PROBHD 5 mm CPBBO BB-
PULPROG zg30
TD 38460
SOLVENT CDCl3
NS 16
DS 2
SWH 9615.385 Hz
FIDRES 0.250010 Hz
AQ 1.9999700 sec
RG 18
DW 52.000 usec
DE 13.81 usec
TE 298.0 K
D1 0.10000000 sec
TD0 1
======== CHANNEL f1 =======
SFO1 600.1342009 MHz
NUC1 1H
P1 11.50 usec
F2 - Processing parameters
SI 65536
SF 600.1300362 MHz
WDW EM
SSB 0
LB 0.30 Hz
GB 0
PC 1.00
1D NMR plot parameters
CX 22.80 cm
CY 10.00 cm
F1P 9.000 ppm
F1 5401.17 Hz
F2P 0.000 ppm
F2 0.00 Hz
PPMCM 0.39474 ppm/cm
HZCM 236.89345 Hz/cm
Integral
1.0000
1.1276
1.1474
1.1561
1.1827
0.9218
1.5316
1.1811
1.3680
2.7313
1.6730
2.0776
2.9448
1.4652
1.4626
3.6461
1.1271
3.3797
ppm
8
7
6
5
4
3
2
1

Z-restored spin-echo 13C spectrum with 1H decoupling